GEOLOGY, STRUCTURE AND TIMING OF GOLD MINERALIZATION AT THE KIENA DEPOSIT, VAL D'OR, QUÉBEC

by

Suzanne Morasse

A thesis submitted to the Department of Geological Sciences in conformity with the requirements for the degree of Doctor of Philosophy

Queen's University
Kingston, Ontario, Canada
June 1998

the competency contrast between albitite dikes and mafic/ultramafic wall rocks. Albitization was followed by the formation of a crackle breccia and subsequently overprinted by main-stage carbonate-quartz-pyrite(pyrrhotite)-±albite-Au stockwork veins, carbonate-pyrite-Au replacement veins, albite-pyrite-chalcopyrite-scheelite-Au stockwork veins and breccias, and quartz-carbonate-biotite-albite±tourmaline-pyrite-chalcopyrite-Au veins. Stockwork veins show crustiform textures, whereas breccias locally show cockade infill-textures. Main-stage carbonate-quartz stockwork vein alteration is funnel-shaped, as are the host albitite dikes, but goes beyond the dikes to form an outer gold alteration halo. Carbonate-pyrite replacement veins and albite stockwork veins and breccia are confined to the core and upper part of the orebody. The lateral extent of vein-breccia mineralization decreases with each successive event, but more gold was introduced each time to form a sheet-like high-grade ore zone at the centre of the orebody. Kiena's alteration-mineralization sequence was subsequently interrupted by the intrusion of intermineral granodiorite and quartz-monzonite porphyry dikes, dismembering part of the orebody into gold-ore xenoliths. Concordant U-Pb ages of 2686 ±2 Ma for prismatic euhedral zircons from the intermineral granodiorite porphyry assign a minimum age to gold mineralization at Kiena. Porphyry dikes were then fractured and weakly mineralized by calcite-quartz-pyrite-Au stockwork veins, before being overprinted by late-stage vein sericite and biotite-magnetite veins, later replaced by chlorite. Vein chlorite is interpreted as the last hydrothermal event in the deposit's alteration-mineralization sequence, as it appears restricted to the orebody's outer gold alteration halo. During the regional synmetamorphic D_2 deformation (ca. 2677-2645 Ma), the orebody and the dikes were deformed by an asymmetric z-shaped fold and cut by an axial planar north-dipping schistosity (S_2), which was subsequently folded together with the ore-dike complex and overprinted by a gently northeast-dipping crenulation cleavage (S_3).

Gold-ore formation at Kiena is bracketed between ca. 2694 Ma, the age of the oldest pre-ore dikes emplaced after the tilting of volcanic strata in the Val d'Or-Malartic region, and 2686 Ma, the crystallization age of the deposit's intermineral granodiorite dike. As part of the geochronology study at Kiena, sharp-faceted euhedral zircon fractions from the nearby Snowshoe granodiorite stock yielded concordant U-Pb ages of 2693 ± 3 Ma, whereas $^{40}Ar/^{39}Ar$ dating of gold-related vein biotite yielded several disturbed spectra and only one plateau age of 2313 ± 15 Ma. As the firm lower age constraint of 2686 ± 2 Ma and the overprint of the regional S_2 schistosity on all pre-existing ore structures indicate that the timing of gold mineralization at Kiena is pre-metamorphic, shear zone-controlled and metamorphogenic models proposed for other Archean gold deposits (e.g. Sibson et al., 1988; Robert and Boullier, 1992; Groves, 1993) are not applicable to Kiena. Instead, relatively shallow emplacement levels for the deposit and a porphyry-style ore-forming process is suggested by: 1) an orebody predominantly hosted by a funnel-shaped albitite dike swarm, 2) intermineral porphyry dikes that link gold magmatic-hydrothermal activity to regional orogenic plutonism, 3) an upward and outwardly zoned, fracture-controlled alteration-mineralization sequence characterized by early feldspathization (albite), episodic gold mineralization, and late-stage chlorite alteration, and 4) open-space crystal growth in veins and breccias. Among the various types of porphyry ore systems, the geological setting of

Kiena more closely resembles that of the Cenozoic gold-rich end-member of this class of deposits (e.g. Santo Thomas II, Luzon, Phillipines). At the regional-scale, the Val d'Or plutonic belt, which formed along the southern margin of the Abitibi subprovince following the initial collision stage of the Abitibi-Pontiac orogen, is similar to present-day magmatic arcs developed at convergent plate margins and implies a possible tectonic control for pre-metamorphic magmatism and gold mineralization at Kiena. At the deposit-scale, Kiena's alteration-mineralization pattern is similar to that in more deeply eroded porphyry gold ore systems exposed in selected subvolcanic porphyry deposits. Based on deposit- and regional-scale similarities, Kiena is thus envisaged as a metamorphosed Archean analogue of Cenozoic gold-rich, and gold only, porphyry deposits encountered in discrete belts along Circum-Pacific orogens.

The demonstration in this study that early porphyry gold is linked to post-volcanic but pre-metamorphic magmatic events, a fact not previously recognized in this region of the Superior Province, opens the question whether similar relationships exist in other deposits of the Val d'Or plutonic belt. The hierarchy of structures, styles and patterns of alteration-mineralization, and the timing of gold-ore formation at the Canadian Malartic, Camflo, Orion Vein No.8, Goldex, Siscoe, Sigma-Lamaque No.2, and main Lamaque deposits were thus examined and compared to Kiena. Although the geology of Kiena is more akin to Malartic- than Sigma-type deposits, the comparison suggests that in spite of disparities styles of mineralization, the timing of gold-ore formation appears to be everywhere post-volcanic (ca. 2700 Ma) and pre-metamorphic (ca. 2677-2660 Ma). Mineralization in both types of deposits is thought to be coincident with the episode of post-accretionary calc-alkalic and alkalic plutonism (ca. 2694-2680 Ma) and implies a district-wide magmatic-hydrothermal connection among the deposits of the Val d'Or plutonic belt. The proposed concept is illustrated in a temporal-genetic model for gold mineralization in the Val d'Or-Malartic area, showing the evolution of Malartic and Sigma-type gold mineralization in relation to the Abitibi-Pontiac orogen.

RÉSUMÉ

La mine d'or Kiena est en opération depuis 1981. Elle est la propriété de 'Les Mines d'Or McWaters Incorporées' qui l'ont acquise de Placer Dome Canada en septembre 1997. Elle est située sur l'île Parker, dans la moitié sud du Lac de Montigny, Canton de Dubuisson, Québec. Kiena fait partie de la ceinture d'or archéenne de Val d'Or-Malartic, dans la partie sud de la ceinture de roches vertes de l'Abitibi. Il s'agit d'une suite de gisements d'or qui coincide avec un alignement d'intrusions épizonales de composition calc-alcaline et alcaline, datées entre ca. 2694-2680 Ma, auquel on a donné le nom de "ceinture plutonique de Val d'Or". Cette dernière est parallèle à la zone de contact entre les Sous-provinces géologiques de l'Abitibi et du Pontiac, située plus au sud. Le gisement repose dans une zone de transition plus ou moins bien définie entre les gisements de type Malartic, situés plus à l'ouest, lesquels sont charactérisés par des réseaux de veines de carbonate-quartz en stockwork accompagnées de sulfures disséminés (Couture et al., 1994), et les gisements de type Sigma, situés plus à l'est, qui sont constitués de filons aurifères de quartz-tourmaline-carbonate (Robert, 1994). En incluant les réserves actuelles, la quantité d'or contenu dans le gisement se chiffre à 1,690,444 onces, soit 52.5 tonnes d'or, faisant ainsi de Kiena le cinquième producteur de la ceinture d'or de Val d'Or-Malartic après Lamaque-Sigma-Lamaque No. 2 (280 t Au), Canadian-Barnat-East Malartic (165 t Au), Camflo-Malartic Hygrade (58 t Au), et Malartic Gold Field #2 (53 t Au).

Le gîte de la mine Kiena se compose d'une zone minéralisée principale, que l'on nomme zone S-50, et de deux autres zone minéralisées (zones Nord-Ouest et Nord) situées sur l'axe nord-sud et le flanc ouest, respectivement, d'un pli en "z" régional. La zone minéralisée principale suit plus ou moins le contact supérieur d'une coulée tholéiitique déversée et inclinée modérément vers l'ouest avec une coulée de basalte komatiitique altéré et schistosé appartenant à la Formation de Jacola du Groupe de Malartic (Imreh, 1984). Le minerai, qui est encaissé par un essaim de dykes d'albitite s'élargissant vers le haut, est recoupé par un dyke de granodiorite et un dyke de porphyre feldspathique. Les dykes d'albitite, appelés auparavant dykes de diorite, se sont mis en place au tout début de la phase de plutonisme orogénique régional (ca. 2694-2680 Ma). Les dykes se sont introduits subverticalement dans le toit de la faille de la mine Kiena, une faille subparallèle à la stratigraphie qui s'est formée pendant ou peu de temps après le déversement des strates volcaniques (D_1, ca. 2700-2694 Ma). Les albitites, que l'on reconnaît à leurs zones de trempe bleu-grises, leur texture aplitique et leur composition dioritique, sont des roches monominéraliques composées d'un assemblage d'albite pure (An_{0-1}) charactérisé par de l'albite microgrenue non mâclée, et des gerbes d'albite dentritique allant vers des assemblages d'intercroissances micrographiques à myrmékitiques d'albite et quartz. Même si les albitites sont nettement des roches intrusives, la très faible calcicité des albites suggèrent qu'elles ont été affectées par des processus hydrothermaux.

Le corps minéralisé de Kiena est constitué d'un système de veines en stockwork, brèches, et veines de remplacement, développé de façon épisodique. Il est zoné et centré sur les dykes

d'albitite pré-minéralisation. L'albitisation est la première phase d'altération de la séquence d'altération-minéralisation du gisement. Cette altération ressemble à l'altération en feldspath potassique des systèmes de porphyre cuprifère. Elle émane et va au-delà des dykes d'albitite pour ainsi transformer les encaissants tholéiitiques et komatiitiques en roches à texture aplitique formées d'albite. L'albitisation a probablement contrôlé le processus de minéralisation par fracturation qui pris place par la suite, en rehaussant la différence de compétence entre les albitites et l'encaissant mafique/ultramafique. L'albitisation fut suivie par le développement d'une brèche par fissuration (crackle breccia), laquelle fut empreinte successivement par les phases principales de la minéralisation. Celles-ci comprennent, de la plus ancienne à la plus jeune, des veines de carbonate-quartz-pyrite-(pyrrhotine)±albite-or en stockwork, des veines de remplacement à carbonate-pyrite-or, des brèches et veines d'albite--pyrite-chalcopyrite-scheelite-Au en stockwork, et des veines à quartz-carbonate-biotite-albite±tourmaline-pyrite-chalcopyrite-or. Les veines en stockwork montrent des textures de remplissage en croûte (crustiform textures), tandis que les brèches montrent localement des textures en cocarde. Parmi les altérations qui composent la minéralisation principale, le réseau de veines de carbonate-quartz en stockwork est celui qui possède la plus grande portée. Il a une forme en entonnoir similaire à celle de l'essaim de dykes d'albitite qui l'encaisse, mais il se poursuit au-delà des dikes créant ainsi un halo externe d'altération en or autour du gisement. Quant à elles, les veines de remplacement à carbonate-pyrite et les brèches et veines en stockwork à albite se situent au centre du corps minéralisé et sont confinées à la partie supérieure du gisement. L'étendue de la minéralisation de types veine-brèche diminue avec chaque événement minéralisateur successif, cependant il semble qu'une plus grande quantité d'or ait été introduite à chaque épisode de minéralisation, créant ainsi une colonne de minerai à forte teneur au coeur du gisement. La séquence d'altération-minéralisation de Kiena est ensuite interrompue par la mise en place de dykes de porphyres interminéralisation de granodiorite et quartz monzonite. Ceux-ci, en recoupant le gisement, ont formé de grandes enclaves de minerai. Les âges U-Pb concordants de 2686 ± 2 Ma, obtenus à partir de prismes automorphes de zircons provenant du dyke interminéralisation de granodiorite, donnent un âge minimum au minerai de Kiena. Les dykes de porphyre sont ensuite fracturés et faiblement minéralisés avant d'être subséquemment recoupés, d'abord par des veinules de séricite, puis par des veines de biotite-magnétite, qui seront remplacées plus tard par de la chlorite. L'altération en chlorite est interprétée comme le dernier événement hydrothermal de la séquence d'altération-minéralisation du gisement, parce qu'elle semble confinée au halo externe d'altération en or du gisement. Lors de la déformation synmétamorphique régionale D_2 (ca. 2677-2645 Ma), le corps minéralisé et les dykes furent déformés par un pli asymétrique en "z" et recoupé par une schistosité de plan axial (S_2) inclinée vers le nord. La schistosité et le complexe minerai-dykes furent ensuite plissés et empreints d'un clivage de crénulation (S_3) incliné faiblement vers le nord-est.

La mise en place de l'or à Kiena est survenue entre ca. 2694 Ma, i.e. l'âge des dykes les plus anciens à être mis en place après le déversement des strates volcaniques dans la région de Val d'Or-Malartic, et ca. 2686 Ma soit l'âge de cristallisation du dyke interminéralisation de granodiorite du gisement. L'étude géochronologique de Kiena a également produit, à partir

de fraction de zircons automorphes à facettes bien développées, les âges U-Pb concordants de 2693 ± 2 Ma pour le stock granodioritique avoisinant de Snowshoe. L'analyse isotopique par la méthode $^{40}Ar/^{39}Ar$ de biotites filoniennes liées à la minéralisation n'a engendré, cependant, qu'un seul âge plateau de 2313 ± 15 Ma et plusieurs spectres d'âges perturbés. La contrainte rigide d'un âge minimum de 2686 ± 2 Ma pour la minéralisation et l'empreinte de la schistosité régionale S_2 sur toutes structures aurifères pré-existantes, signifient que la formation du minerai à Kiena est pré-métamorphique. Ainsi, le modèle de zones de cisaillement et les modèles métamorphogéniques proposés pour expliquer la genèse d'autres gisements d'or Archéens (e.g. Sibson et al., 1988; Robert et Boullier, 1992; Groves, 1993) ne s'appliquent pas à Kiena. Au lieu de cela, la mise en place du gisement à faible profondeur et sa genèse par un processus de minéralisation de style porphyre, sont suggérés par: 1) un corps minéralisé encaissé par un essaim de dykes d'albitite, 2) des dykes de porphyres interminéralisation qui font le lien entre l'activité magmatique-hydrothermal aurifère et le plutonisme orogénique régionale, 3) une séquence d'altération-minéralisation contrôlée par la fracturation montrant une zonation vers le haut et vers l'extérieur, qui se charactérise par un stade de feldspathisation (albite) précoce, une minéralisation épisodique, et une altération tardive en chlorite, et 4) la croissance de cristaux en fracture ouverte dans les veines et les brèches. Parmi les divers type de système porphyre, la géologie de Kiena ressemble de plus près à celle des gîtes riche en or d'âge Cénozoique appartenant à cette classe gisements (e.g. Santo Thomas II, Luzon, Phillipines). A l'échelle régionale, la ceinture plutonique de Val d'Or, qui s'est formée en marge de la Sous-province de l'Abitibi lors de la phase initiale de l'orogène Abitibi-Pontiac, est comparable aux arcs magmatiques modernes qui se développent aux abords des plaques tectoniques convergentes et implique la possibilité d'un contrôle tectonique sur le magmatisme et la minéralisation pré-métamorphique de Kiena. A l'échelle du gisement, le patron d'altération-minéralisation de Kiena est similaires à celui des gîtes de porphyres aurifères sub-volcaniques plus profondément érodés. Ainsi donc, en se basant sur des similarités à l'échelle du gisement et à l'échelle régionale, Kiena est perçu comme l'analogue Archéen métamorphosé des gisements Cénozoique riche en or, ou uniquement minéralisé en or, de type porphyre que l'on retrouve en ceintures discrètes le long des zones orogéniques du Circum-Pacific.

Puisqu' un lien entre minéralisation aurifère précoce de style porphyre et activité magmatique post-volcanique mais pré-metamorphique est démontré dans cette étude, un fait préalablement ignoré dans cette région de la Province du Supérieur, la question se pose à savoir si de tels liens existent parmi d'autres gisements de la ceinture plutonique de Val d'Or. Ainsi donc, la hiérarchie des structures, le style de minéralisation, les patrons d'altération-minéralisation, et la chronologie de la mise en place de l'or aux gisements Canadian Malartic, Camflo, Orion Vein No. 8, Goldex, Siscoe, Sigma-Lamaque No. 2, et Lamaque ont été examinés et comparés à Kiena. Même si la géologie de Kiena ressemble de plus près à celle des gisements de type Malartic qu'à celle des gisements de type Sigma, cette comparaison montre qu'en dépit de différences dans le style de minéralisation, l'or semble partout s'être mis en place après le volcanisme (ca. 2700 Ma) et avant le métamorphisme (ca. 2677-2660 Ma). On pense que ces deux types de minéralisation coincident avec l'épisode de plutonisme calc-alcalin et

alcalin (ca. 2694-2680 Ma) survenu suite à l'amorce du processus d'accrétion entre l'Abitibi et le Pontiac, impliquant ainsi une affiliation magmatique-hydrothermale d'ordre régionale pour tous les gisements de la ceinture plutonique de Val d'Or. Ce concept est illustré dans un modèle temporel-génétique de la mise en place de l'or dans la région de Val d'Or-Malartic, montrant l'évolution entre la minéralisation de type Malartic et de type Sigma en relation avec l'orogène Abitibi-Pontiac.

ACKNOWLEDGEMENTS

This research was made possible by the financial support of Placer Dome Inc. (PDI) (now Placer Dome Canada Limited) and Les Mines d'Or Kiena Limitée who provided access to the mine and kindly shared their human and technical resources for the benefit of this project. I particularly wish to thank Mr. Michel Cormier, chief geologist of the Kiena Mine from 1987 to 1997, for inviting me to do this study and Mr. Henry Brehault, former manager of PDI mining operations for Canada, who gave the "green light" for the project. I also wish to thank PDI's project supervisors, Mr. John Morganti, former exploration manager for Eastern Canada, and Mr. Ed Kimura, former exploration manager for Canada. Thanks are also extended to former Kiena mine manager, Mr. Michel Rodrigue, for financial support and the interest he took in the study. The new owners of Kiena, Les Mines McWatters Inc., and the new chief geologist, Mr. Michel Crevier, are also acknowledged for graciously printing the sets of maps and diagrams appearing in this thesis.

I wish to extend my gratitude to my principal thesis advisor, Dr. Herwart (Herb) Helmstaedt. I particularly want to thank him for his intellectual support and financial assistance. I thank him also for the advice he provided while visiting me several times in the field, for always so generously making time to discuss various aspects of the research, and for carefully reviewing abstracts, papers, and this thesis manuscript. I am also indebted to Herb and his wife Mrs. Audrey Helmstaedt for kindly offering me to stay with them on several occasions while I resided off-campus.

I sincerely thank my thesis co-advisor, Dr. Robert Mason, for his diligent advice while visiting me in the field, the many thought-provoking discussions, and for allowing me to participate in the 1993 MINEX field trip. Having the opportunity to visit epithermal and porphyry deposits throughout the Southwest U.S. and Mexico has, undoubtedly, benefitted this study.

Special thanks are extended to Dr. Hardolph Wasteneys for the high quality U-Pb zircon dates he has produced for this study during his post-doctorate fellowship at the Royal Ontario Museum in Toronto. Dr. Wasteneys has supplied also the scanning electron photomicrograph of zircons and the U-Pb Concordia diagram appearing in Chapter 6. His contributions to this study are gratefully acknowledged.

At Kiena, I thank my collaborator and friend, Mr. Cormier for his guidance, his openness to receive new ideas, and his unconditional support. I am also indebted to the Kiena Mine employees for their kind help and cooperation during field work and several subsequent visits to the mine. Special thanks go to Mr. Serge Tremblay, former draftsman at Placer Dome Inc. exploration offices in Val d'Or, for having so diligently produced the AutoCad drawings featured in this thesis. His dedication to this study is gratefully acknowledged.

Many people in the Department of Geological sicences of Queen's University brought

contributions to this study. Dr. Ed Farrar is thanked for the use of his geochronology laboratory. Dr. Doug Archibald and Mr. Jerry Grant assisted with the preparation of biotite separates. Dr. Sandra McBride step-heated the biotite samples and produced the corresponding $^{40}Ar/^{39}Ar$ age spectra. Dr. Heather Jamieson and Mr. Dave Kempson provided assistance with the electron microprobe work. Dr. Noel James is thanked for the use of his microscope and photographic equipment. Dr. Dugald Carmichael provided assistance with his APL 'MINERAL' software. Dr. Alan H. Clark is thanked for several insightful discussions and for providing an early version of Arancibia and Clark (1996). Mr. Jerze Advent, Mr. Roger Innes and Mr. Walter Morales made thin sections and two or three rock slabs out of very difficult material. Mr. Yvon Boudreault of Chicoutimi made the first set of thin and polished thin sections. Ms. Nancy Thomas assisted with computer drafting. Ms. Ella Rusak gave advice on rock photography. Thanks are also extended to Rob Renaud for his assistance in solving various computer and printer problems. All the personnel in the department's main office, Mrs. Aria Karvinen, Ms. Linda Anderson, Ms. Joan Charbonneau, as well as Mrs. Hanne Sherboneau and Mrs. Larke Zarichny, offered assistance and logistical support throughout my stay at Queen's University.

Thanks are also due to the School of Graduate Studies and Research for providing two travel grants while at Queen's. Additional miscellaneous research expenses were covered by NSERC operating grants to Dr. H. Helmstaedt.

I would also like to thank Dr. Richard H. Sillitoe for graciously setting time aside during Queen's University Giant Ore Deposit I seminar, to discuss Kiena geology and intermineral dikes.

The french version of the thesis abstract has benefitted from comments by Ms. Chantal Dussault, Ministère Énergie Ressources du Québec district geologist in Val d'Or.

For all the good times and stimulating geological discussions, I sincerely thank my fellow students Mr. Alexis Anastas, Mr. Paul Johnston, Ms. Adrienne Laroque, Ms. Annette McIlroy, Mr. Mike Muir, Mr. Mike Orobona, Mr. Rob Penzak and Mr. Bruce Wilson. Special thanks go to my friend Annette for sharing her apartment and good company during the last stages of this study.

Finally, I want to offer my heartfelt thanks to my parents, Mrs. Irma and Mr. Philippe Morasse, my dearest godmother Ms. Rita Morasse, my uncle Mr. Simon Morasse, and especially my husband Vicente Palma for their love and support and for all their encouragements through the trials and tribulations of this study.

REMERCIEMENTS

Cette recherche fut rendue possible grâce au soutien financier de Placer Dome Inc. (PDI) (maintenant Placer Dome Canada Limited) et Les Mines d'Or Kiena Limitée, qui ont facilité l'accès à la mine et aimablement partagé leurs ressources humaines et techniques pour le bénéfice de ce projet. Je tiens particulièrement à remercier M. Michel Cormier, géologue-en-chef à la mine de 1987 à 1997, pour m'avoir invitée à participer à ce projet de recherche, ainsi que M. Henry Brehault, ancien directeur des opérations minières de PDI au Canada pour avoir authorisé le projet. Je souhaite également remercier les superviseurs du projet, M. John Morganti ancien directeur de l'exploration de PDI pour l'Est du Canada, ainsi que M. Ed Kimura, ancien directeur de l'exploration de PDI pour le Canada. Je tiens aussi à remercier l'ancien directeur de la mine Kiena, M. Michel Rodrigue pour son aide financière ainsi que pour l'intérêt qu'il a porté envers le projet. Je suis également reconnaissante au nouveau propriétaire de la Mine Kiena, Les Mines McWatters Incorporées, et au nouveau géologue-en-chef, M. Michel Crevier, pour avoir gracieusement imprimé la série de cartes et diagrammes apparaissant dans cette thèse.

Je tiens à offrir toute ma gratitude à mon directeur de thèse, le Dr. Herwart (Herb) Helmstaedt. Je le remercie sincèrement pour son soutien intellectuel et son aide financière. Je le remercie également pour tous les conseils qu'il m'a prodigués lors de ses nombreuses visites sur le terrain, pour toujours si généreusement trouver le temps de discuter de divers aspects de la recherche, ainsi que pour avoir révisé avec soin les résumés, articles, et ce manuscrit de thèse. Je lui suis également reconnaissante, ainsi qu'à son épouse Mme Audrey Helmstaedt, de m'avoir aimablement offert de rester avec eux à plusieurs occasions lorsque je résidais hors campus.

Je remercie très sincèrement mon co-directeur de thèse, le Dr. Robert Mason, de m'avoir prodigué tant de pertinents conseils sur le terrain et pour s'être engagé dans tant de discussions stimulantes. Je lui suis également reconnaissante de m'avoir permise de participer à l'excursion MINEX de 1993. La visite opportune de gîtes épithermaux et de type porphyre à travers le Sud-Ouest américain et le Mexique n'a su que bénéficier ce projet de recherche.

Je tiens spécialement à remercier le Dr. Hardolph Wasteneys pour la haute qualité des dates U-Pb sur zircons produites pour le bénifice de cette étude lors de son séjour comme étudiant au post-doctorat au Musé Royal de l'Ontario. Le Dr. Wasteneys a également fourni la microphotographie de zircons prise au microscope à balayage ainsi que diagramme Concordia apparaissant au Chapitre 6. Je lui suis reconnaissante des contributions qu'il a apportées à cette étude.

A Kiena, je remercie mon collègue et ami Mr. Cormier, pour ses conseils judicieux, son ouverture d'esprit, et son soutien inconditionnel. J'ai également une dette de reconnaissance envers les employés de la Mine Kiena qui m'ont si gentiment offert leur collaboration lors de

mes travaux sur le terrain ainsi que lors de plusieurs visites subséquentes à la mine. Je tiens tout spécialement à remercier M. Serge Tremblay, ancien dessinateur au bureau d'exploration de Placer Dome Inc. à Val d'Or, pour avoir produit avec ardeur et dévouement les dessins Autocad apparaissant dans ce manuscrit de thèse. Je lui suis reconnaissante de s'être montré aussi consciencieux.

Plusieurs personnes du 'Department of Geological Sciences' de l'Université Queen's ont apporté leurs contributions à ce projet de recherche. Le Dr. Ed Farrar est remercié pour avoir permis l'utilisation de son laboratoire de géochronologie. Le Dr. Doug Archibald et M. Jerry Grant ont offert leur assistance à la préparation de fractions de biotite. Le Dr. Sandra McBride a procédé au réchauffement par étapes des échantillons de biotite et préparé les spectres d'âge $^{40}Ar/^{39}Ar$ correspondants. Le Dr. Heather Jamieson et M. Dave Kempson ont offert leur assistance aux travaux d'analyse à la microsonde électronique. Le Dr. Noel James a gracieusement offert l'utilisation de son microscope et équipement photographique. Le Dr. Dugald Carmichael a offert son assistance avec l'utilisation de son logiciel APL 'MINERAL'. Le Dr. Alan H. Clark est remercié pour ses commentaires perspicaces ainsi que pour m'avoir procuré une épreuve de l'article de Arancibia et Clark (1996). M. Jerze Advent, M. Roger Innes, et M. Walter Morales ont préparés des sections minces et deux ou trois morceaux d'échantillons à surface polie particulièrement difficiles à réussir. M. Yvon Boudreault à Chicoutimi a préparé la première série de lames minces et lames minces polies. Mme Nancy Thomas a offert son assistance avec le dessin par ordinateur. Mme Ella Rusak a prodigué des conseils sur la photographie d'échantillons de roche. Je remercie également M. Rob Renaud pour avoir trouvé solution à tous mes problèmes d'ordinateur et d'imprimante. Tout le personnel du bureau de réception du département, soit Mme Aria Karvinen, Mme Linda Anderson, Mme Joan Charbonneau, ainsi que Mme Hanne Sherboneau et Mme Larke Zarichny, ont offert leur assistance et soutien logistique tout au long de mon séjour à l'Université Queen's.

Je me dois également de remercier l'École des Étude Graduées et de la Recherche (School of Graduate Studies and Research) pour avoir reçu deux bourses pour frais de déplacement (travel grants) lors de mon séjour à Queen's. Les dépenses additionnelles liées à ce projet de recherche ont été couvertes par les bourses du CRSNG (NSERC) émises au Dr. H. Helmstaedt.

J'aimerais aussi remercier le Dr. Richard H. Sillitoe pour m'avoir gracieusement offert de son temps lors de sa visite à l'Université Queen's pendant la tenue du séminaire Giant Ore Deposits I, pour discuter de la géologie de Kiena et m'éclairer sur la nature des dykes interminéralisation.

Le résumé en français de la thèse a bénéficié des commentaires pertinents de Mme Chantal Dussault, géologue résidente du Ministère Énergie et Ressources du Québec à Val d'Or.

Pour tous les bons moments ainsi que toutes les stimulantes discussions à caractère

géologique, je remercie mes compagnons d'étude M. Alexis Anastas, M. Paul Johnston, Mme Adrienne Larocque, Mme Annette McIlroy, M. Mike Muir, M. Mike Orobona, M. Rob Penzak et M. Bruce Wilson. Je remercie tout spécialement Annette pour m'avoir fait partagé son appartement et sa compagnie lors des dernières phases du projet.

Enfin, je tiens à offrir mes plus sincères remerciements et toute ma gratitude envers mes parents, Mme Irma Morasse et M. Philippe Morasse, ma chère marrainne Mme Rita Morasse, mon oncle M. Simon Morasse, et tout particulièrement mon mari M. Vicente Palma pour leur affection et leur soutien ainsi que pour tous les encouragements prodigués lors des moments difficiles à traverser au cours de ce périple.

TABLE OF CONTENTS

LIST OF CONTENTS IN BACK POCKET

LIST OF FIGURES

LIST OF TABLES

CHAPTER 1 INTRODUCTION

1.1 PURPOSE OF RESEARCH

This study of the Kiena Mine originated in part from the controversy existing over the nature of its orebody, a massive carbonate-rich and silica-poor "breccia body" (S-50 Zone) atypical of Archean greenstone belt gold deposits, and in part from the need to synthesize geological information accumulated over sixteen years of mine production. Kiena is located approximately halfway between the Val d'Or and Malartic mining camps, in a 25-km-long by 1- to 7-km-wide segment of the southern Abitibi greenstone belt, occupied by no less than 8 large (> 30 tonnes Au) and 19 smaller gold deposits, as well as by 1 large (Louvicourt Mine) and 4 smaller polymetallic massive sulphide deposits. Kiena is the largest of several gold deposits situated in and around Lac de Montigny, an ill-defined transition zone between two end members of vein- type gold deposits: (1) quartz-tourmaline-carbonate lode gold veins or "Sigma-type" vein deposits to the east, and (2) networks of carbonate-quartz stockwork veins with auriferous sulphide disseminations or "Malartic-type" vein deposits to the west (Sauvé et al., 1993; Couture et al., 1994; Robert, 1994). Although in recent years Kiena became the most important gold producer in the Val d'Or area, geological accounts of the deposit remained fragmentary and did not incorporate geological information from the deepest part of the mine. A need thus arose to re-examine the geological setting of the entire mine to characterize the composite nature of the orebody, and in doing so, determine its affinities with either one of the afore mentioned vein-type gold deposits.

Accordingly, the study of the Kiena Mine has two main objectives:

1) formulate a geological model to explain the genesis of the orebody and,
2) view the deposit in a broader, more regionally oriented context, in order to ascertain the link, if any, between Kiena and other deposits of the Val d'Or-Malartic gold belt.

1.2 LOCATION AND ACCESS

The Kiena Mine gold deposit is located in the Val d'Or gold camp, Québec, in the southeastern part of the Abitibi Subprovince of the Superior Province (**Figure 2.1**). The mine site lies on Parker Island, in the southern half of Lac De Montigny in Dubuisson Township (77°55'W, 48°07'N), between the cities of Val d'Or (10 km to the east) and Malartic (15 km to the west), two historically important mining centres in northwestern Québec (**Figure 2.2**). The mine is easily reached by highway 117, which passes along the south side of Lac de Montigny, and a small dirt road turning north from highway 117, approximately 2.5 kilometres west of the Thompson River (**Figures 2.2** and **3.1**). The mine property, which is mostly covered by the waters of Lac De Montigny, is at the end of a 1-kilometre-long causeway linking the dirt road to Parker Island.

1.3 EXPLORATION AND PRODUCTION HISTORY OF THE KIENA MINE

1.3.1 Introduction

As for many other mines in the district, the exploration history leading to the discovery of the Kiena Mine spans several decades with alternating periods of activity and inactivity. Causes for this include: the Second World War, the low price of Au in post-war periods, limitations of past mining techniques and, cyclical episodes of disbelief in the economic viability of the prospect. Fortunately, the price of gold almost doubled in 1972 (35.00 to 68.00 $ US/oz.) (Boyle, 1987) and, as faith was also restored from the results of geological and geophysical surveys, company managements were convinced to take more risks. As for many other ore deposit discoveries, much good fortune assisted at Kiena in finding the "golden needle" in the "greenstone haystack".

The section below is a description of the early discovery of the gold prospect found on Parker Island until the discovery of the "S-50" orebody, followed by an account of Kiena's

production history.

1.3.2 Early exploration: discovery of the "S-21 Zone" and "S-50 Zone"

Discovery outcrop

The first record of exploration along the shores of what was known then as Lac Kienawisik, dates back to 1911-1914 when prospector Barney Parker reported the discovery of native-gold-bearing quartz veins on a little outcrop at the northwestern end of the island that now bears his name (Cormier, 1986b). Martin Gold Mines and Parker Island Gold Mines did some follow-up work on the discovery outcrop between 1922 and 1927 and tested five quartz veins with trenches and drill holes (Robinson, 1962). Soon afterward, gold was also discovered in the "Wisik vein" on the eastern shore of Mocassin Island, the largest of two nearby islands located east of Parker Island (see **Figure 3.1**). Because the price of gold had such an important role to play in the making of the Kiena Mine, it should be mentioned that during this early exploration phase the price of gold was fluctuating somewhat around an average of 20.00 $US/oz. It remained such until 1934, when it was raised by the U.S. Treasury to 34.00 $US/oz. (Boyle, 1987).

Exploration by Ventures Limited

A "gold rush" was initiated in the Lac De Montigny area in 1929, following the beginning of mining operations at the Siscoe Mine (see **Figure 2.2**), the first mine in Québec to produce exclusively gold (Trudel, 1985b). Exploration activities were also intensified by the beginning of gold production at two other mines located on the eastern and southern shores of Lac de Montigny respectively, the Sullivan Mine in 1934 and the Shawkey Mine in 1936 (see **Figure 2.2**) (Trudel, 1985c; Trudel, 1985a). A very important moment in the history of the Kiena deposit occurred in 1936, when Kiena Gold Mines Limited was created. The latter, under the control of Ventures Ltd., immediately initiated a major surface and exploration program on

the property which resulted in the sinking of Parker Shaft at the western end of the island (Cormier, 1986b). Shaft sinking to a depth of 455 feet (-138 metres) was followed by the development of exploration drifts at the -130, -230, -330, and -430 feet levels, in an effort to test the surface showing, but the discovery veins were found to be of limited extent (Cormier, 1986b). Meanwhile, Wisik Gold Mines Limited, who had acquired the "Wisik vein" property, also sank a 325 feet (-114 metres) shaft on Mocassin Island and developed exploration drifts at -200 and -300 feet levels.

Discovery of the "S-21 Zone"

Shortly after the Geological Survey of Canada sent Duncan R. Derry on a mapping survey of the area in 1937, Ventures Ltd. initiated a stratigraphic drilling program which led, in 1938, to the discovery of the "S-21 Zone" (later called the "North Zone", see **Figure 3.1**). A crosscut was excavated toward the "S-21 Zone" and intersected four mineralized veins (Robinson, 1962). Unfortunately, mining operations ceased in 1940, due to limited ore reserves and wartime difficulties, and exploration activities were suspended for twenty years (Cormier, 1986b). During this exploration hiatus, the price of gold remained fixed at 35.00 $US/oz. (Boyle, 1987).

Discovery of the "S-50 Zone"

Ventures Ltd., who controlled the 1958 joint venture between Kiena Gold Mines Ltd. (KGWL) and Wisik Gold Mines Ltd. (WGML), carried out a magnetometer and geological mapping survey on KGML and WGML's combined claim block. A diamond drill program of 13 drill holes was proposed on the basis of favourable recommendations from these surveys, but R.W. Robinson (1961) cut this proposal down to only 3 drill holes. In 1961, targeting the "nose of a fold" and a "magnetic low that could represent a siliceous intrusive", the third and last drill hole (S-50) of this exploration program intersected 7.54 g/t Au over 15 metres of core, at approximately 245 metres below surface (Salt, 1960; Robinson, 1961b;

Cormier, 1986a).

Following the discovery of the "S-50 Zone", Falconbridge took over the management of Kiena Gold Mines Ltd. and its Kiena-Wisik property, and financed the subsequent underground exploration. Based on 24,000 metres of drilling from the surface, original ore reserves of the S-50 Zone were estimated as 4.5 million tonnes averaging 6.34 g/t Au of possible ore. In 1963, Shaft No. 1 was collared approximately 250 metres east of the Parker Shaft and sunk to a depth of 403 metres. Extensive underground exploration and a definition diamond drill program outlined ore reserves of 1.4 million tonnes grading 8.78 g Au/t above level 27 (270 metres below surface) (Cormier, 1986a).

1.3.3 Production history

In 1965, a feasibility study on the S-50 orebody suggested that mining would not be economic due to high mining costs resulting from adverse rock mechanic properties of the host rocks (gold was still at 35.00 $US/oz.) (Cormier, 1986b; Boyle, 1987). The property was placed under a care and maintenance program, leaving the S-50 orebody dormant for the next fourteen years.

In 1979, Falconbridge re-evaluated the property and, at last, recommended to bring it into production. The successful transition from an advanced exploration project to a mine operation, which officially started in October of 1981, partially coincided with a new record high in gold price (620.00 $ US/oz. in 1980) (Boyle, 1987), but was mostly attributed to the ingenuity of skilled geologists and mining engineers who proposed an innovative mine design and stope geometry for the necessary primary ground support (Cormier, 1986a). Trackless room-and-pillar stoping methods were employed, and custom milling of the ore was done at the nearby Teck's Lamaque mill for the first three years of production, until Kiena's own C.I.P. (Carbon-in-Pulp) mill was operational in September of 1984. Today's ore production originates from cut-and-fill and long-hole stoping, and from pillar recovery (Cormier, 1986a).

1.3.4 Ownership transfers

In January 1986, Campbell Red Lake Mines became the major shareholder of the Kiena Mine when it purchased Falconbridge's 56.7 % interest in the company (Cormier, 1986a). Following the amalgamation in 1987 of Placer Development Limited, Dome Mines Limited and Campbell Red Lake Mines Limited, Placer Dome Inc. of Vancouver, became the owner and operator of the Kiena Mine (Leggatt, 1989). On January 1st 1994, Placer Dome Inc. changed its name to Placer Dome Canada Limited. The company then sold the mine (along with the neighbouring Sigma Mine) to Les Mines d'Or McWatters Incorporées, who officially became the new owner and operator of Kiena on September 12, 1997.

1.3.5 Ore reserves

According to the size definition of volcanic-hosted Archean lode gold deposits (Hodgson et al., 1993) and the production figures shown in **Table 1.1**, the Kiena Mine classifies as a "large" gold deposit (total gold reserves between 6 and 60 tonnes of Au (Laznicka, 1983). On average, the mine has produced 445,585 tonnes of ore grading 5.23 g/t Au annually for the past 17 years. Regionally, and by comparison to other past and present gold producers in the Val d'Or and Malartic mining camps, Kiena's minimum gold content of 52 tonnes of Au ranks fifth behind those of the giant Lamaque-Sigma-Lamaque No.2 (280 tonnes Au) and Canadian-Barnat-East Malartic (165 tonnes Au) Mines, and those of the Camflo-Malartic Hygrade (~ 58 tonnes) and Malartic Gold Field #2 (53 tonnes Au) Mines (see **Figure 2.2**) (Trudel and Sauvé, 1992; Hodgson et al., 1993, Martin Bourgoin, Chief geologist Sigma-Lamaque No.2, personal communication).

1.4 PREVIOUS GEOLOGICAL STUDIES AND RESEARCH

Over the years, the geology of the Kiena Mine was the subject of several company and academic studies. Research topics included mapping surveys, geological compilations,

Table 1.1 Production history of the Kiena Mine 1981-1998

Production Year	*Ounces Au*	*Tonnes of Au*	*Tonnes of ore milled*	*Average grade g/t Au*
1981	15,018	0.4671	101,231	5.14
1982	63,038	1.9607	287,916	7.34
1983	61,193	1.9033	307,661	6.71
1984	66,658	2.0763	378,014	5.94
1985	70,035	2.1783	381,376	5.89
1986	72,694	2.2610	453,793	5.19
1987	67,113	2.0874	478,752	4.55
1988	58,219	1.8108	477,947	3.97
1989	66,235	2.0601	470,705	4.55
1990	65,953	2.0514	473,602	4.51
1991	71,112	2.2118	486,217	4.75
1992	81,195	2.5254	501,827	5.25
1993	79,034	2.4582	496,410	5.25
1994	83,044	2.5829	504,873	5.34
1995	86,375	2.6865	534,330	5.22
1996	84,609	2.6316	608,701	4.51
1997	93,169	2.8978	631,606	4.81

• Data compiled from Les Mines d'Or Kiena Limitée annual reports between 1981-1998.

Total production 1981-1997: 7,574,961 t at 5.23 g/t
1,184,962 oz. Au
36.8506 t Au

Mineral inventory:
January 1st, 1998: 3,527,000 at 4.46 g/t
505,752 oz. Au
15.730 t Au

Minimum tonnage: **11,101,961 t**
Minimum Au content: **1,690,444 oz. Au**
52.5806 t Au

geochemical, petrographic, and structural studies. The following section is an appraisal of those previous geological studies, with an emphasis on their main contributions and conclusions. These findings and other pertinent observations are summarized in Appendix A.

Ventures Ltd. commissioned the first geological synthesis of the Kiena Mine property to G.K. Polk in the summer of 1960 (Robinson, 1961a). Polk re-mapped the discovery outcrops, studied the old exploration records, and compiled a new geological map of the property (Polk, 1960). He concluded that the most prominent geological feature on the property was the presence of a large "dragfold" combined with "strike-slip fractures/shear zones". He also recognized the importance of mineralized dikes on the property that he termed "ore zone andesite" dikes. The dikes were not described in great detail, but were characterized as dioritic intrusive rocks with variable concentrations of white quartz stringer veins with albite and pyrite alteration, that are cut, in turn, by younger porphyritic granodiorite dikes (Polk, 1960). Polk's recommendations for the delineation of exploration targets were based on his observation that gold mineralization occurred where: 1) the concentration of white quartz stringer veins was greatest, 2) where structure was "composite", i.e.comprised of more than one generation of veins, 3) where fold noses were combined with intense alteration, and 4) where "ore zone andesite" and granodiorite dikes occurred together with "composite" veins.

A second synthesis of the mine geology was attempted by Clark (1963), who assembled a northwest-southeast composite cross-section based on selected diamond drill holes located in the vicinity of the discovery outcrop (see Kiena Mine Composite Section 11 in back pocket). His study of the various rock and alteration-mineralization types encountered in drill core marks a turning point in the understanding of the geology of the deposit, and many of his conclusions still hold true today. Clark established a crude stratigraphy and orebody geometry similar to those represented, thirty years later, on sections **12438.4 N** and **12514.6 N** (see Composite Section 11 and schematic 1:250 cross sections in back pocket), and his

description of the footwall rock succession is an account of what is known today as the "Jacola Triad" (see Chapter 2) (Imreh, 1984). Perhaps his most important contribution to the understanding of the geological setting of Kiena's orebody, and a lesson in observation, is his description of a felsic dike complex associated with the ore and his recognition of the combined role of faulting, felsic magmatism and plagioclase metasomatism, in Kiena's ore genesis. Clark observed the presence of three distinct felsic dikes and determined their relative time of emplacement as follows: 1) a pre-ore and mineralized dike which he termed "grey diorite" dike, 2) a "monzonite porphyry" and 3) a later "syenite porphyry". He was the first to detect the presence of a potassic alteration halo over the ore zone (biotite) and to make the distinction between what he called a "green diorite", a dark green and coarse-grained andesitic/basaltic flow, and a "grey diorite", a greyish and medium-grained sill or dike composed predominantly of plagioclase which occurred in contact with, or near the ore zone. Clark's main conclusions were as follows: 1) "grey diorite" dikes, "monzonite" and "syenite porphyries", as well as plagioclase metasomatism, are all genetically related, 2) intense igneous diking and gold alteration-mineralization are likely related to a parent intrusion at depth, 3) as suggested by the high density of "grey diorite" dikes (felsic dike swarm?) north of Parker Island (see **Figure 2.2**), this parent intrusion may lie in that area and, 4) a distinction between the effects of plagioclase metasomatism from those of quartz-carbonate alteration may indicate the proximity of an ore zone.

J.E. Muir (1979; 1981) performed an invaluable petrographic study and geochemical synthesis of drill core samples collected in the mine and its surroundings (Cloutier, 1979). Based on the statistical analysis of gold values obtained from his samples, Muir (1979) identified three populations of gold concentrations: an average population of 32-562 ppb Au, and two smaller populations of gold values < 32 ppb and >562 ppb, respectively. His most important conclusions were that, 1) the ore protolith is a S-, Na_2O-, and carbonate-enriched iron tholeiite, (2) the granodiorite porphyry and S-50 orebody are chemically similar to felsic dikes and "diorite" ores in the Malartic camp and that, (3) gold mineralization is micro-fracture-controlled. Detailed petrography also allowed Muir to recognize a persistent

sequence of alteration in Kiena's ore-dike complex from, main-stage carbonate-pyrite mineralization, to biotite-sericite alteration, followed by a chlorite alteration overprint. He suggested that Kiena's "breccia body" was a stratabound and epigenetic orebody.

Two years into gold production, C. Roy (1983) studied the geology of the deposit based on drill core, whole rock and REE geochemistry, and partial mapping of underground development. His main contribution to the understanding of Kiena's geological setting was to further refine the mine sequence of events as follows: (1) intrusion of pre-ore "dioritic" dikes, (2) pre-ore albite alteration, (3) main stage gold mineralization, (4) intrusion of granodioritic and feldspar porphyry dikes, (5) boudinage of the ore zone, and (6) development of an east-west schistosity. Roy concluded that the ore was stratabound and suggested that its genesis was synchronous with, and controlled by, the development of a conjugate fracture system during a protracted regional deformation event.

Based essentially on drill core, Bourget (1986) later mapped the distribution of high-strain rocks and alteration types in and around Kiena and tried to identify Au, As and Sb anomalies around the deposit. His findings are summarized as follows: 1) the S-50 orebody is enclosed in a "***mylonite zone***", 2) the "mylonite zone" consists of several lensoid bodies of ore, composed essentially of albite-carbonate-quartz-pyrite-pyrrhotite-Au, surrounded by highly strained and altered mafic-ultramafic volcanic rocks and felsic intrusions, 3) the "***mylonite zone***" is coincident with a ***biotite alteration zone*** which extends up to 20 metres in the footwall mafic volcanic rocks and 100-140 metres in the hangingwall ultramafic volcanic rocks of the S-50 orebody. Based on the statistical treatment of his geochemical data, Bourget estimated regional background Au and As content of mafic volcanic rocks at 3.2 ppb and 2.3 ppm, respectively. He also identified a zonation pattern in gold alteration-mineralization consisting, from the S-50 orebody (>5400 ppb Au) outward, of an inner alteration halo grading an average 197 ppb Au, through to an outer alteration halo grading 13-60 ppb Au, coinciding with the boundary of the "mylonite zone". Bourget concluded that the S-50 Zone was stratabound and hosted by an albite-altered "quartz diorite" dike, and

suggested that gold mineralization was synchronous with, and therefore controlled by, the development of a north-south shear zone (i.e. "mylonite zone").

The most recent geological study at Kiena was a structural study by Quirion (1988) who mapped the ore zones of the S-50 orebody at mine level 33, and subdivided Kiena's rock types into non-deformed, massive facies, and into mylonitic, non-mineralized and mineralized facies. She proposed the following mine sequence of events to explain the formation, and subsequent deformation, of the orebody: (1) emplacement of the Malartic Group mafic-ultramafic volcanic flows, (2) intrusion of "micro-diorite" dikes, (3) greenschist regional metamorphism, (4) formation of brittle-ductile faults, (5) hydrothermal fracturing and mineralization of "micro-diorite" dikes, (6) coeval gold mineralization and shear zone development, and (7) further shearing causing the boudinage of mineralized "micro-diorite" dikes. Quirion concluded that gold mineralization at Kiena was syntectonic, epigenetic and shear-zone-controlled (north-south "mylonite zone" of Bourget (1986)).

In spite of over thirty years of cumulative geological knowledge, our understanding of the genesis of Kiena's orebody remains fragmentary and rather disjointed because past geological observations focused mainly on the structural setting of the orebody. However, this approach fails to take into account the possible role of magmatism and related hydrothermal activity in the ore formation process. Recurring observations pertinent to the compounded effects of calc-alkalic intrusive igneous activity, sodic and potassic metasomatism on gold mineralization, have been stressed in the past (Clark, 1963), but systematically ignored later because of a bias towards theories stipulating that gold mineralization occurred late in the development of the Abitibi greenstone belt, and was related to the formation of shear zones in mid- to lower-crustal environments (e.g. Colvine (1988); Robert (1990); Hanes (1992); Groves (1993); Kerrich (1994)).

1.5 LOGISTICS, METHOD OF INVESTIGATION AND THESIS ORGANIZATION

1.5.1 Mapping and sampling

During this study, the logistics of detailed geological mapping at Kiena posed a problem. The combined effects of mining methods to optimize ground stability with a mining schedule designed to yield maximum profits, meant that the massive "breccia body" of the S-50 Zone was nearly mined out and back-filled when this study commenced, and access to the earlier mine workings was limited to non existent. The mining schedule indicated that selective mining of other existing ore zones ("C", "J", "K" and "L", see **Figure 3.2**), including the remaining pillars of the "breccia body", would be scattered over a 36 months period. Hence, field work was spread over the months of April to September of 1990, May to September of 1991, March and May to August of 1992, in addition to March and June of 1993, at time intervals dictated by the advances of mining. To insure maximum mine coverage, in view of time limitations imposed by active mining operations, extensive and detailed geological mapping was carried out on mine levels 38, 41, and 43, covering mostly ore zones "B" and "C". As for ore zones "A", "D", "J", "K", "L" and lower "C", geological mapping was restricted to selected "windows" into the ore on mine levels 27, 33, 36, 46, 57, and 64. Field observations were recorded on 1:250 scale geological plan maps (see Kiena Mine Index Geological Maps in back pocket) supplemented by photographs, structural logs, and the collection of hand specimens and drill core samples.

1.5.2 Methodology and analytical procedures

In order to achieve a breakthrough in the understanding of the geological setting of the deposit, Kiena geology was updated and compiled on selected mine levels and sections to show variations across the orebody. Geological information was drawn from the following sources: 1) early geological plan maps at 1:250 and 1:500 scale, 2) sets of partially interpreted geological sections at 1:500 scale, and 3) from detailed 1:250 scale geological plan maps

realized in the course of this study. The geological constraints essential to the interpretation of the compilation maps and sections were implemented by the ongoing observation of field relations, aided by the systematic evaluation of the gold content of rock samples collected during mapping. The resulting plan maps and sections were subsequently digitized and drafted using the Autocad computer software (see Kiena Mine schematic plan maps and cross-sections in back pocket), with plans to realize the first interactive 3D computer model of the orebody. Additional data related to the geology of Kiena were acquired by applying various analytical techniques (petrography, whole rock geochemistry, microprobe analysis, U-Pb age dating of zircons, $^{40}Ar/^{39}Ar$ age dating of biotites) to a collection of 273 rock samples gathered in the field, their corresponding polished rock slabs, supplemented by 281 thin and polished thin sections. The combined results of geological mapping and analytical work were subsequently utilized to reconstruct the deposit time sequence (Figure 7.1).

To further achieve the geological synthesis of Kiena's orebody, it was necessary to view the deposit in a regional geological context. Hence, close attention was given to the preparation of a regional compilation map (Figure 2.2), in conjunction with that of a detailed regional time sequence (Regional Sequence of Events diagram in back pocket), combining factual cross-cutting field relations gathered from the literature, and from personal observations at several gold deposit localities throughout the area, with a collection of mineral isotopic age dates. This combined exercise led to a re-appraisal of the geological history of the Val d'Or-Malartic area, following which the geology of the mine was compared to that of other gold mines.

1.5.3 Thesis organization

Unravelling the geological evolution of the Kiena Mine orebody coincided with a "quiet revolution" in the understanding of the geological setting of the Val d'Or-Malartic area. Under the rigid constraints of precise U-Pb zircon dating of selected volcanic and plutonic rocks, regional stratigraphic, structural and Archean gold metallogenic concepts had to be

updated, or rejuvenated. This thesis is thus, not only about the description of the geological setting of the Kiena Mine, but also about its impact on the geological history of the Val d'Or-Malartic area and the timing of gold mineralization across the entire district.

The first chapter of this thesis focuses on the history of the deposit, and summarizes the cumulative geological knowledge gathered before this study was undertaken. Abbreviated overviews of the Superior Province of the Canadian Shield, the southern part of the Abitibi greenstone belt, and of the geology of the Val d'Or-Malartic area, are presented in Chapter 2. This section accounts for the recent revisions to the local geological history with an emphasis on the timing of gold mineralization, the timing of regional deformation and metamorphism and, the structural evolution of regional- and deposit-scale shear zones. Chapter 3 is primarily concerned with the stratigraphic relations of the rock units found in the mine and by the internal geometry of the orebody. This section includes a description of the intermediate to felsic dike complex temporally-, and possibly genetically-, related to the ore. The deposit's alteration-mineralization sequence and zoned alteration pattern are characterized in Chapter 4, whereas the hierarchy of pre-, -syn, and post-ore structures is described in Chapter 5. The latter also profiles the "shear zone-hosted" character of the deposit based on a qualitative evaluation of strain partitioning across the zoned orebody. Results from the geochronological study of the deposit are presented in Chapter 6. Precise U-Pb zircon dating of an intermineral granodiorite dike assigns a minimum age of 2686 ± 2 Ma for main-stage gold mineralization at Kiena, whereas the neighbouring granodiorite Snowshoe stock is dated as 2693 ± 2 Ma. Biotites from a gold-bearing pegmatitic vein and late-stage biotite-chlorite-magnetite stringer veins yielded disturbed $^{40}Ar/^{39}Ar$ age spectra but one plateau age of 2313 ± 15 Ma, suggesting that gold-related hydrothermal biotites are thermally reset. Chapter 6 also features a regional time sequence setting the age of gold mineralization at Kiena in relation to other geological events in the Val d'Or-Malartic area. Gold-ore formation at Kiena is bracketed between ca. 2694-2686 Ma, post-dating the overturning of volcanic strata and Bourlamaque sills (ca. 2700 Ma), but pre-dating regional synmetamorphic deformation (ca. 2680-2660 Ma). Chapter 7 is a partial synthesis of this

study advocating a pre-metamorphic, intrusion-related origin for Kiena. The pre-metamorphic timing of gold-ore formation is supported by the absolute minimum age of 2686 ± 2 Ma for mineralization, the overprint of penetrative deformation on all preexisting ore structures, and the timing of peak synmetamorphic deformation in the regional time sequence (ca. 2680-2660 Ma). The proposed intrusion-related origin for the deposit is based on a comparison between Kiena and selected porphyry ore deposits. It shows that Kiena shares many features of magmatic-hydrothermal ore systems emplaced at relatively shallow depth, including: the upward-flaring geometry of the ore, a zoned alteration-mineralization sequence characterized by the early feldspathization of an intrusive centre, stockwork fracturing, brecciation, intermineral diking, biotite-magnetite and late chlorite alterations. Based on deposit- and regional-scale similarities, Kiena is also envisaged as a metamorphosed Archean analogue of Cenozoic gold-rich, porphyry-style deposits occurring in discrete belts along Circum-Pacific orogens. Chapter 8 is an attempt to show that "Malartic-" and "Sigma-type" deposits may share a Kiena-like, pre-metamorphic, magmatic-hydrothermal origin. The geology of the Canadian Malartic, Camflo, Orion Vein No. 8, Goldex, Siscoe, Sigma-Lamaque No. 2 and main Lamaque deposits is reviewed and compared to Kiena. A temporal-genetic model for gold mineralization in the Val d'Or-Malartic area is then proposed to explain the consistent overprint of gold-ore by regional penetrative structures and zonation of alteration-mineralization sequences characterized by early, inner feldspathization. A synopsis of the main contributions of this research follows in Chapter 9.

CHAPTER 2 GEOLOGICAL SETTING OF THE SOUTHEASTERN ABITIBI GREENSTONE BELT WITH SPECIAL EMPHASIS ON THE VAL D'OR-MALARTIC AREA

2.1 INTRODUCTION

This chapter is historical and bibliographic in nature. Its aim is to document the geological framework in which the problems posed, and the results achieved by this study, ought to be considered. Volcanic and plutonic rocks at the Kiena Mine belong to the southeastern Abitibi greenstone belt of the Abitibi Subprovince, located in the southeastern Superior Province of the Canadian Shield (**Figures 2.1** and **2.2**). The following is a synopsis of the geological evolution of the diverse rock assemblages of the Abitibi Subprovince with particular emphasis on the southern Abitibi greenstone belt. This review is necessary because of the acquisition of new geochronological (e.g. Corfu (1993)), structural (e.g. LITHOPROBE, Clowes (1993); Jackson (1995); Verpaelst (1995)), and metamorphic (e.g. Powell (1995a)) data across the southern Abitibi Subprovince bringing about new constraints on the formation and evolution of the Abitibi belt and the timing of gold mineralization.

2.1.1 Defining the Abitibi Subprovince

The Archean Superior Province of the Canadian Shield consists of an assemblage of fault-bounded, geologically distinctive domains which form the remnant of a formerly more extensive craton now surrounded and truncated by Early Proterozoic orogens (Card, 1990; Thurston, 1990). The Abitibi Subprovince, a Neoarchean granite-greenstone-gneiss terrain[1] that developed between 2.8 and 2.6 Ga, lies in the southeast corner of the Superior Province

---

[1] Throughout this thesis, "terrain" refers to a type of geologic region, without tectonic connotations, by contrast with "terrane" which refers to a fault-bounded package of strata that is allochthonous to, and has a geological history distinct from, adjoining geologic units (e.g. Howell, 1989 p. 214).

Figure 2.1 - *Simplified geological map of the Superior Province of the Canadian Shield showing the distribution of its plutonic, volcano-plutonic and metasedimentary subprovinces. The study area is highlighted by the red rectangle located at the contact between the Abitibi and Pontiac Subprovinces.*

Carte géologique simplifiée montrant la distribution des sous-provinces plutoniques, volcano-plutoniques et méta-sedimentaires de la Province du Supérieur du bouclier Canadien. La région à l'étude est représentée par le rectangle rouge situé au contact entre les sous-provinces de l'Abitibi et du Pontiac.

SUPERIOR PROVINCE

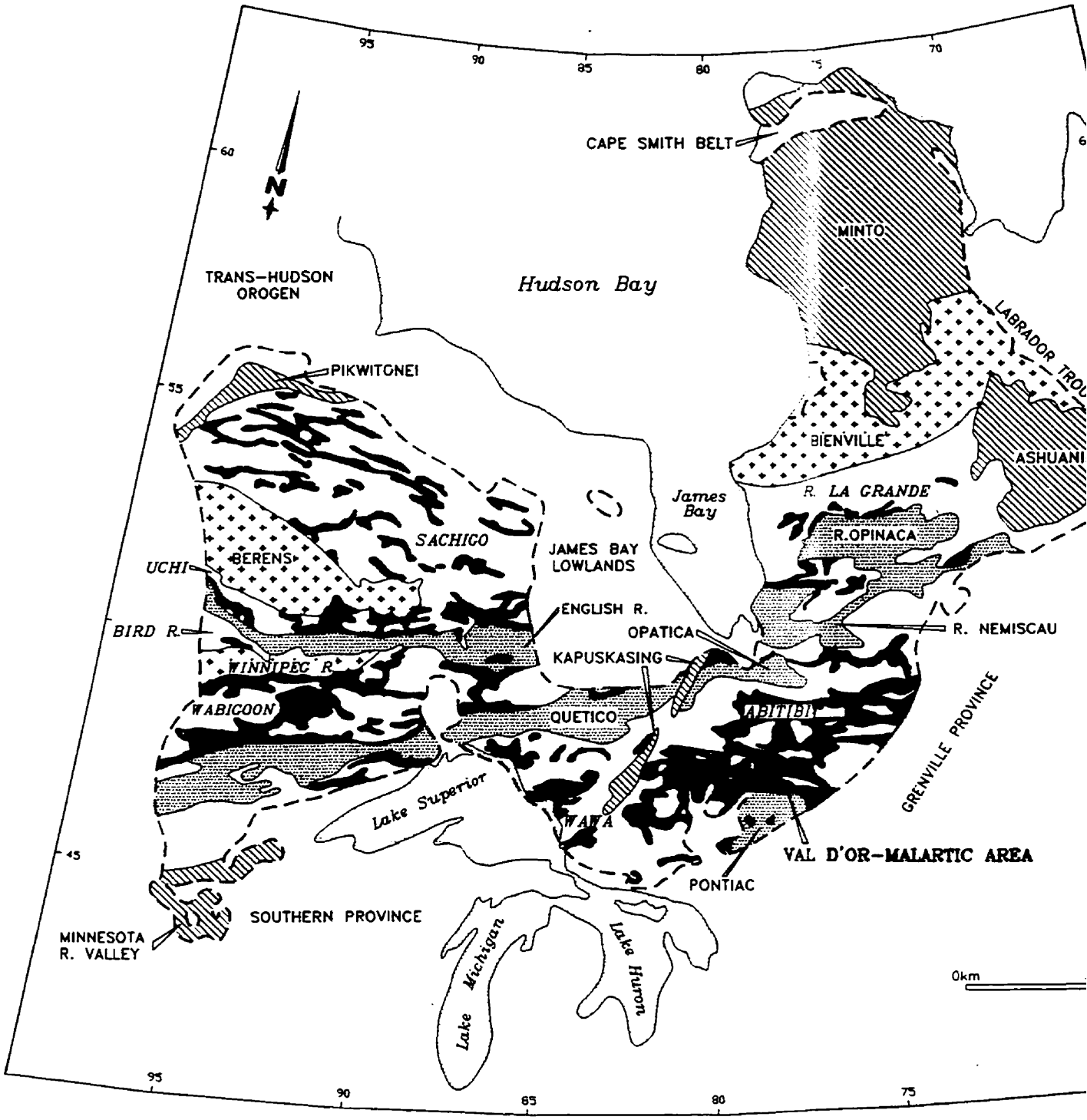

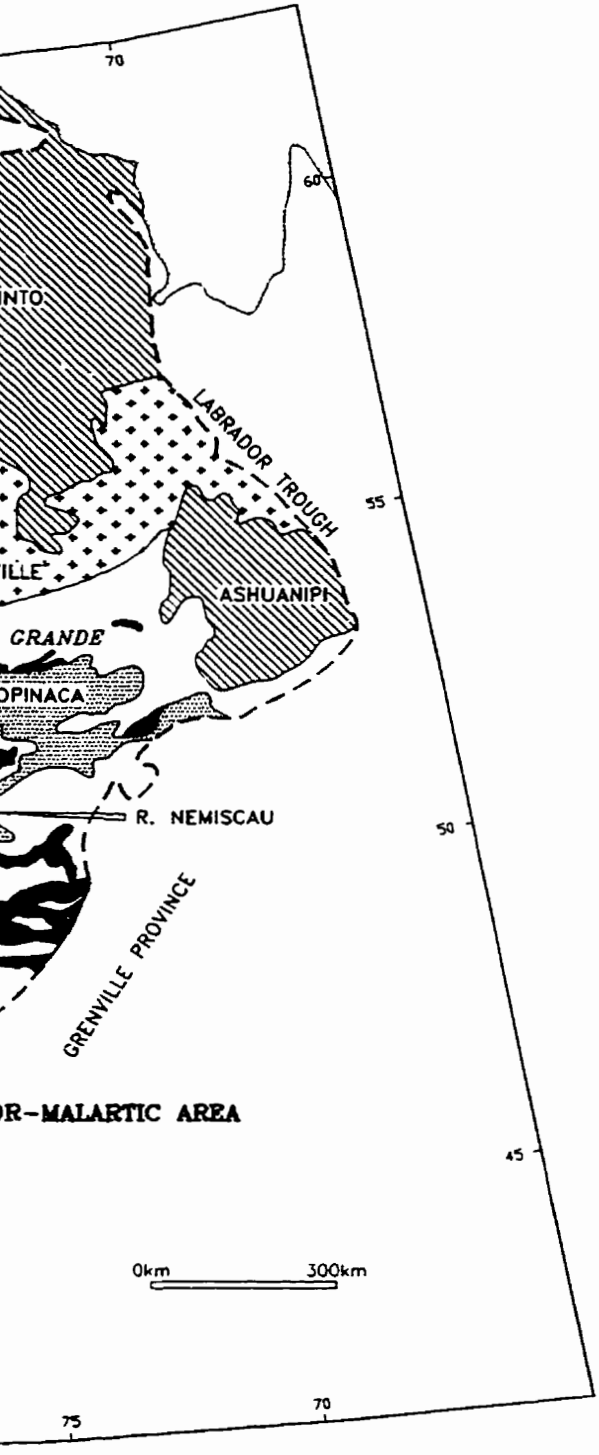

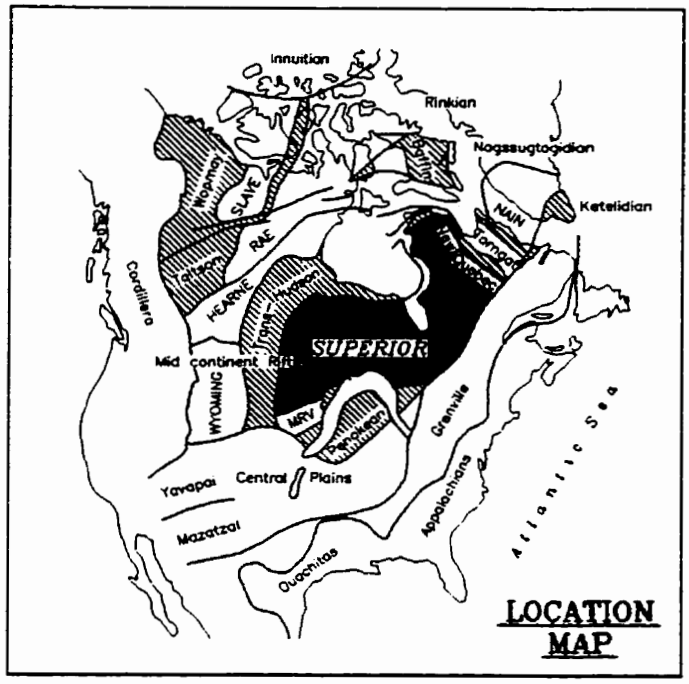

LEGEND

SUBPROVINCE TYPE

- *PLUTONIC*
- *VOLCANO–PLUTONIC*
- *METASEDIMENTARY*
- *HIGH–GRADE GNEISS*
- *LIMIT OF SUPERIOR PROVINCE*

LES MINES D'OR KIENA LTEE.

Figure 2.1

SUBPROVINCES OF SUPERIOR PROVINCE

DATE : 04/20/94

MODIFIED AFTER : Card & Ciesielski, 1986 ; Hoffman, 1988

COMPUTER DRAFTING BY : S. Tremblay

Table 2.1 Geotectonic divisions of the Abitibi Subprovince and the Abitibi greenstone belt

SOUTHEASTERN SUPERIOR PROVINCE	FORELAND GNEISS BELT (North)	QUETICO BELT	OPATICA GRANITE-GNEISS TERRANE	OPATICA METASEDIMENTARY SUBPROVINCE	OPATICA SUBPROVINCE	
ABITIBI OROGENIC BELT (Ontario and Quebec)	*Volcanogenic facies Northern complex*	*Internal Zone (Hinterland)*	*Northern Volcanic Zone*	ABITIBI VOLCANO-PLUTONIC SUBPROVINCE (ABITIBI BELT)	*Northern Volcanic Zone (NVZ)*	*Polycyclic volcanic segment* / *Monocyclic volcanic segment*
	Axial zone of orogen	*External Zone*	*Central granite-gneiss zone*			
	Volcanogenic facies Southern complex		*Southern Volcanic Zone*		*Southern Volcanic Zone (SVZ)*	
	Flyschoid-type sediments / *FORELAND GRANITIC-GNEISS BELT (South)*	*BELLECOMBE BELT*	*SOUTHERN GRANITE-GNEISS ZONE (PONTIAC)*	*PONTIAC METASEDIMENTARY SUBPROVINCE*	*PONTIAC SUBPROVINCE*	
PROPOSED GEOTECTONIC MODEL	*Intracratonic orogen between two spreading sialic forelands*	*Evolution of volcano-plutonic arc (autochtonous volcanic sequence)* / *Bellcombe belt underthrusting Abitibi belt*	*Microterrane accretion* / *(allochtonous fragments)*		*Arc-arc collision* / *(SVZ with NVZ)*	
SOURCE	*Goodwin and Ridler, 1970*	*Dimroth et al., 1982*	*Ludden et al., 1986*	*Card and Ciesielski, 1986 (Douglas, 1973)*	*Chown et al., 1992*	

• *Modified after Chown et al., 1992.*

(**Figure 2.1**). It was initially subdivided by Goodwin and Ridler (1970) into three lithotectonic domains: (1) a northern foreland gneiss belt, (2) a central granite-greenstone-gneiss domain, named the Abitibi Orogenic Belt, and (3) a southern foreland granitic-gneiss belt (**Table 2.1**). Based on a recent redefinition of lithotectonic subdivisions of the Superior Province, the northern and southern gneiss belts, were respectively renamed the Opatica and Pontiac metasedimentary Subprovinces, whereas the central granite-greenstone-gneiss domain was renamed the Abitibi volcano-plutonic Subprovince (**Figure 2.1, Table 2.1**) (Douglas, 1973; Card and Ciesielski, 1986). The Abitibi Subprovince is approximately 900-km-long and 75 to 300-km-wide and consists of elongate and anastomosing belts of metavolcanic and metasedimentary rock assemblages cut by syn- to post-orogenic granitic intrusions and surrounded by batholitic gneiss complexes. It is bounded to the west by the Kapuskasing Structural Zone (KSZ), a discontinuous, 500-km-long, partly fault-bounded, northeast-trending zone of granulite-grade gneiss, and to the east by the Grenville Front Tectonic Zone (GFTZ), a laterally extensive (4,000-km-long) deformation zone composed of northeast-trending shear zones and northwest-directed Proterozoic thrust faults, located at the boundary between the Superior and the Grenville Province (see **Figure 2.1**) (Percival and Card, 1983; Hoffman, 1988; Card, 1990). The northern boundary of the Abitibi Subprovince is shared by orthogneiss and plutonic rocks with remnant enclaves of greenstone rocks from the Abitibi belt, and by the fault-bounded para- and orthogneiss of the Opatica Subprovince (Card, 1990; Benn et al., 1992; Davis et al., 1995). At the southern edge of the Abitibi Subprovince, metavolcanic sequences are in fault contact with metasedimentary rocks of the Pontiac Subprovince through the Cadillac Tectonic Zone (CTZ), a steeply north-dipping, 200-km-long and 1-km-wide, high-strain zone (**Figure 2.2**) (Imreh, 1976a; Robert, 1989; Green et al., 1990). The southwestern boundary of the Abitibi Subprovince is outlined by an unconformity between Archean rocks and Early Proterozoic sediments of the Huronian Supergroup and Middle Proterozoic volcanic and sedimentary rocks of the Keweenawan rift sequence (see **Figure 2.1**)(Card, 1990).

2.1.2 Defining the Abitibi belt

Recent advances in understanding the evolution of the Archean Abitibi greenstone belt, indicate that the rocks within the belt formed between ca. 2750 and 2650 Ma (Chown et al., 1992; Corfu, 1993). Based on common volcanic, plutonic and deformational histories, the Abitibi belt has been divided into an older (ca. 2730-2686 Ma) Northern Volcanic Zone (NVZ) separated from a younger (ca. 2720-2670 Ma) Southern Volcanic Zone (SVZ) by a series of east-west faults (e.g. the Destor-Porcupine and Manneville Faults; **Table 2.1**) (Jackson and Fyon, 1991; Chown et al., 1992; Daigneault and Labbé, 1992; Daigneault et al., 1994). The northern part of the Abitibi belt (or NVZ) is characterized by abundant tonalite-trondhjemite-granodiorite intrusions, large anorthosite complexes, a paucity of ultramafic flows, and greenschist facies metamorphism (Dimroth et al., 1982; Dimroth et al., 1983a; Dimroth et al., 1983b). The southern part of the Abitibi belt (or SVZ), is characterized by fewer tonalite-trondjemite-granodiorite intrusions, abundant ultramafic flows and by subgreenschist to greenschist facies metamorphism (Jolly, 1978; Dimroth et al., 1982; Dimroth et al., 1983a; Dimroth et al., 1983b; Jackson and Fyon, 1991; Corfu, 1993; Powell et al., 1995a). The following overview is concerned with the southern part of the Abitibi belt.

2.1.2.1 Volcanism (ca. 2720-2677 Ma)

The volcanic successions of the southern Abitibi belt comprise several major volcanic cycles, typically subdivided into three sequences on the basis of their geochemical composition and paleo-geomorphology: a lower ultramafic-mafic sequence, a middle tholeiitic basalt sequence, and an upper bi-modal, tholeiitic-to-calc-alkalic sequence (Dimroth et al., 1982). Locally, alkalic-to-shoshonitic volcanic rocks, interbedded with an assemblage of fluviatile sandstones, polymictic conglomerates, and minor turbidites, form the uppermost volcanic cycle which unconformably overlies the older volcanic rocks (Timiskaming Group in the Kirkland Lake area of Ontario e.g. Cooke (1969); Hyde (1980); Jackson (1991)). These volcanic sequences have been interpreted as representing three distinct paleogeographic environments of

deposition: 1) deep to shallow submarine lava plains, represented by interlayered peridotitic, pyroxenitic komatiites and basaltic Mg- and Fe-rich tholeiites with minor felsic tuffs and chert, 2) submarine to subaerial central volcanic complexes, forming shield volcanoes or several coalescing volcanoes, represented by tholeiitic and calc-alkalic sequences with subaqueous to subaerial felsic pyroclastic rocks, and 3) either pull-apart or forearc basins represented by alkalic volcanic flows ranging in composition from trachyte and trachyandesite, to leucitite and mugearite, interbedded with molasse-facies sedimentary rocks (Cooke and Moorhouse, 1969; de Rosen-Spence, 1976; Hyde, 1980; Gélinas and Ludden, 1984; Imreh, 1984; Piché, 1984; Dimroth et al., 1985; Picard and Piboule, 1986; Hodgson and Hamilton, 1989; Card, 1990; Thurston, 1990; Corfu, 1991; Mueller and Donaldson, 1992). According to Corfu (1993), major pre-tectonic[2] magmatism in the southern Abitibi greenstone belt occurred between 2720 and 2700 Ma and gradually tapered off until the emplacement of a Timiskaming alkalic volcanic unit near Larder Lake, which marked the cessation of volcanism at around 2677 ± 2 Ma.

2.1.2.2 Plutonism (ca. 2720-2645 Ma)

Felsic intrusions found throughout the belt have been subdivided into "pre-tectonic", "syntectonic[3]" and "late- to post-tectonic" suites, based on their lithological associations, geochemistry, structural and metamorphic characteristics and precise U-Pb zircon ages (Rive et al., 1990; Corfu, 1993; Sutcliffe et al., 1993). ***"Pre-tectonic" intrusions*** range in age from

---

[2] Throughout this thesis, the term "pre-tectonic" refers to a geologic process or event that occurred before the pre-metamorphic regional deformation event D_1 postulated by Dimroth et al., (1983). In the southern Abitibi belt, D_1 has been bracketed between ca. 2700-2688 Ma by Corfu (1993), and at ca. 2700-2686 Ma by Morasse and Wasteneys (1994). This time interval has now been narrowed down to ca. 2700-2694 Ma (see chapters 6 and 7).

[3] Throughout this thesis, the term "syntectonic" and "late-tectonic" are used to describe a geologic process or event that occurred during the combined time interval of D_1 and D_2, as defined by Dimroth et al. (1983), Corfu (1993) and Powell (1994), i.e. between ca. 2700-2645 Ma. By extension, the term "post-tectonic" refers to a post-D_2 geologic process or event that occurred after 2645 Ma.

ca. 2720-2700 Ma, and are represented by large, multiphase subvolcanic intrusions composed of several, high-level, sill-like intrusions or plugs, located at the core of volcanic complexes (e.g. Flavrian/Powell pluton in Rouyn-Noranda and Bourlamaque sills in Val d'Or) (Campiglio and Darling, 1976; Goldie, 1979; Verpaelst et al., 1995). The low-K, tholeiitic to calc-alkaline, dioritic to tonalitic intrusions are surrounded by weak contact metamorphic aureoles which are generally retrograded during regional tectono-dynamic metamorphism (Goldie, 1978); "pre-tectonic" intrusions are commonly cut by younger felsic dyke swarms (e.g. the ca. 2694 Ma Sigma-Lamaque Mines feldspar porphyry dikes cross-cutting the ca. 2704 Ma porphyritic diorite). ***"Syntectonic" intrusions*** consist of small, calc-alkalic plutons and porphyry dikes of granodioritic and tonalitic composition (e.g. Round Lake batholith near Kirkland Lake, Timmins and Val d'Or porphyries) ranging in age between ca. 2696-2688 Ma (Corfu, 1993) . ***"Late-tectonic" intrusions*** consist of alkalic intrusions of monzonitic and syenitic composition ranging in age between 2685 and 2680 Ma (e.g. Camflo stock near Val d'Or, Otto stock near Kirkland Lake, Aldermac stock near Rouyn-Noranda) (Corfu et al., 1989; Jemielita et al., 1990; Zweng, 1991). Syn- to late-tectonic intrusions, commonly have been fractured, altered, and gold-mineralized prior to being variously foliated, folded, deformed by shear zones and metamorphosed (e.g. Sansfaçon (1990)). Hornfels and calc-silicate contact metamorphic assemblages that occur around late-tectonic intrusions, appear to have been retrograded to actinolite-epidote-chlorite-bearing assemblages (see Zweng (1993) and Powell (1995a)). ***"Post-tectonic" intrusions*** consist of peraluminous monzogranites (S-type granites, see Sutcliffe (1993)) containing biotite-muscovite-garnet (e.g. Lacorne pluton, Boily (1990)) ranging in age between ca. 2645-2632 Ma (Feng and Kerrich, 1991b). Contact metamorphic aureoles of post-tectonic monzogranites overprint regional metamorphic fabrics and show no evidence of a regional retrograde event (Powell et al., 1995a).

2.1.2.3 Sedimentation (ca. 2700-2677 Ma)

In the southern Abitibi belt, metasedimentary assemblages occur in east-west-trending belts,

and two types of sedimentary rock sequences are recognized: (1) an older sequence (ca. 2700-2688 Ma), which is conformable with the pre-Timiskaming volcanic rocks, and (2) a younger sequence (ca. 2686-2676), which is unconformably overlying older sediments and volcanic rocks. The older sedimentary sequence consists of oxide-sulphide-carbonate facies ironstone, chert, mudstone and turbidites, and is thought to have been deposited on submarine lava plains (Dimroth et al., 1982). Turbiditic sediments comprising conglomerate, wacke and siltstone, were deposited in the periphery of central volcanic complexes. Conglomerates are either rich in volcanic debris or in plutonic clasts, presumably derived from synvolcanic intrusions (Card et al., 1981; Mueller and Donaldson, 1992). The younger sequences consist of alluvial-fluvial metasedimentary rocks locally interbedded with alkalic and shoshonitic volcanic flows and breccias, that unconformably overly the older volcanic and sedimentary sequences and are associated with regional-scale faults (e.g. Destor-Porcupine and Kirkland Lake-Larder Lake-Cadillac faults). One such sequence, referred to as the Timiskaming Group, occurs in the Kirkland Lake-Larder Lake area and is characterized by clast-supported conglomerates containing distinctive syenite, red chert (jasper) and "green carbonate" (Bass, 1961) clasts, interbedded with trachyte flows, tuffs and agglomerates (Jackson and Fyon, 1991). Clasts of alkalic intrusions and detrital zircons have yielded U-Pb ages of 2685-2679 Ma, suggesting a close temporal association between deposition of the Timiskaming-type sediments and alkalic magmatism (Cooke and Moorhouse, 1969; Corfu, 1993).

2.1.2.4 The "Kenoran orogeny": deformation and metamorphism (ca. 2700-2645 Ma)

Polyphase deformation affecting supracrustal rock assemblages of the southern Abitibi belt is attributed to the "Kenoran orogeny", a sequence of deformation events (D_1, D_2) including folding and faulting, accompanied by plutonism and polyphase metamorphism (Stockwell, 1982; Dimroth et al., 1983a; Dimroth et al., 1983b; Card, 1990; Thurston and Chivers, 1990; Corfu, 1993; Mason, 1995). The deformation sequence consists of an early, pre-cleavage deformation, followed by two episodes of folding which have been designated as D_1 and D_2 (Dimroth et al., 1983a; Dimroth et al., 1983b). Early deformation is characterized by

thrusting and imbrication (Daigneault and Labbé, 1992), a deformation style which has been referred to as "thin-skinned" (Thurston, 1990; Lacroix and Sawyer, 1995). This was broadly coeval with a first episode of regional folding (D_1) characterized by large, shallowly plunging domal antiforms (F_1), commonly cored by granitic batholiths (e.g. La Motte-Vassan anticline, **Figure 2.2**), and by synforms occupied by thick volcanic sequences (e.g. Blake River Group, Dimroth (1983a); Card (1990)). This older episode of folding was locally accompanied by the development of a penetrative planar fabric (e.g. S_1, La Motte Vassan anticline). It predates the deposition of Timiskaming-type sediments and has been bracketed between 2700-2688 Ma by Corfu (1993) and 2700-2686 Ma by Morasse and Wasteneys (1994), who later modified this time interval to 2700-2694 Ma (Morasse et al., 1995b , see Chapter 7 and Regional Sequence of Events diagram in back pocket). The second episode of folding (D_2), which affects Timiskaming-type sediments, is a multiphase deformation event characterized by the steepening of early F_1 folds into tight sub-vertical isoclinal folds and upright asymmetric "S"- and "Z"-shaped fold (F_2), accompanied by the development of syn-metamorphic axial planar foliation/schistosity (S_2) and east-plunging lineation (L_2), locally overprinted by crenulation cleavage (S_3) (Dimroth et al., 1983a; Robert, 1989; Card, 1990; Powell et al., 1995a). The last major deformation event to affect the southern Abitibi belt is the development of transcurrent east-west, southeast-, and northeast-trending brittle-ductile faults and shear zones (Card, 1990; Daigneault and Labbé, 1992). They form laterally extensive, narrow structural domains in which metasedimentary and metavolcanic rock assemblages are affected by high strain and intense hydrothermal alteration. It is postulated that some of these major faults or "breaks" initially formed as synvolcanic, normal listric or dip-slip faults, which were reactivated into thrust faults and dextral transcurrent faults during the terminal collision stage of the Kenoran orogeny (Dimroth et al., 1982; Hodgson and Hamilton, 1989; Robert, 1989; Green et al., 1990; Jackson and Fyon, 1991).

Three types of pre-"Kenoran" (pre-D_1) metamorphism were recognized by Dimroth *et al.* (1983b) in the rocks of the southern Abitibi belt: (1) sea-floor metamorphism, (2) thermal contact metamorphism, and (3) localized hydrothermal alteration related to the deposition of

volcanogenic massive sulfides. "Kenoran" regional thermo-dynamic metamorphism, which is related to the second episode of folding (D_2, F_2), is coeval with the development of a regional east-west-trending schistosity (S_2), and has affected the volcanic strata, a suite of syenitic intrusions (e.g. Aldermac, Otto and Camflo stocks), and the Timiskaming-type sedimentary rocks (Jackson and Fyon, 1991; Trudel and Sauvé, 1992; Corfu, 1993; Powell et al., 1995a). Metamorphic grade ranges from subgreenschist prehnite-pumpellyite facies to greenschist facies, except around post-D_2 granitic intrusions where upper greenschist to lower amphibolite conditions have been reached (Jolly, 1978; Dimroth et al., 1982; Powell et al., 1995a). Throughout the southern Abitibi belt, the age of metamorphism has either been dated directly on metamorphic minerals, or constrained by the ages of pre- and post-metamorphic intrusions. In the Kirkland Lake and Destor areas, regional metamorphism and fabric development have been dated directly as 2665 ± 4 Ma (U-Pb, yellow titanite Murdock Creek syenite, Kirkland Lake area, Wilkinson *et al.* (1993)), and as 2657 ± 3 Ma ($^{40}Ar/^{39}Ar$ biotite, Cléricy syenite, Destor area, Powell (1994)). Because dynamothermal metamorphism post-dates regional calc-alkalic and alkalic magmatism occurring at ca. 2694-2680 Ma (Corfu, 1993), these radiometric ages suggest that peak metamorphic conditions were reached in the interval 2680-2660 Ma (Powell et al., 1995b). A pre-metamorphic felsic dike cross-cutting Timiskaming sediments in the Kirkland Lake area dated as 2677 ± 3 Ma (Corfu, 1993) and a post-metamorphic S-type granite of the Lacorne batholith dated as 2643 ±4 Ma (Feng and Kerrich, 1991b), also bracket regional metamorphism with U-Pb radiometric ages at 2677-2643 Ma (Powell et al., 1993). In the Val d'Or area, the age of regional metamorphism is less well constrained and appears to be older. It has been dated directly as 2671 ± 17 Ma on amphiboles from the porphyritic diorite of the Sigma Mine (Hanes et al., 1992), and as 2684 ± 7 Ma on a rutile found in the Colombière "rhyolite" (Wong et al., 1991). However, Powell *et al.* (1995a) suggested that these older ages may have resulted from the thermal effects of contact metamorphism associated with late-tectonic plutonism at ca. 2685-2680 Ma, rather than regional metamorphism (see Regional Sequence of Events diagram in back pocket).

2.1.2.5 Types of mineralization with emphasis on base-metal and gold deposits

The southern Abitibi belt contains a variety of mineral deposits, including volcanogenic base metal sulfide (VMS) deposits, komatiite-associated Ni-Cu-PGE deposits, "mesothermal" gold deposits, and quartz-molybdenum and rare metal (Li-Cs-Be-Ta-Sn-U-Th) pegmatite deposits (Fyon et al., 1992; Poulsen et al., 1992). The following is a brief overview of the main attributes of VMS and gold deposits found throughout the belt.

Archean VMS deposits are interpreted to have formed in calderas (e.g. Noranda cauldron structure) contemporaneously with voluminous eruptions of pyroclastic rocks (Franklin et al., 1981; Gibson and Watkinson, 1990; Péloquin et al., 1996). They are typically subdivided into a "Noranda-type" and a "Mattabi-type" (Morton and Franklin, 1987). "Noranda-type" VMS deposits are characterized by bimodal submarine volcanic host rocks and well-defined, discordant, chloritic alteration pipes (e.g. Millenbach, Amulet). They are Cu-rich orebodies interpreted to have formed at water depth in excess of 500 metres (Morton and Franklin, 1987). By contrast, "Mattabi-type" VMS deposits occur in subaerial to shallow submarine mafic flows and pyroclastic rocks and are characterized by ill-defined alteration pipes which grade laterally into iron-carbonate-, and chloritoid-andalusite-kyanite-bearing alteration zones (e.g. Kidd Creek, Timmins). A third type of VMS deposit, reminiscent of present shallow submarine hot spring systems in the Western Pacific (Hannington, 1993), has recently been identified by Faure *et al.* (1990) and Larson and Hutchinson (1993) in the northern Abitibi belt. Exemplified by the Selbaie deposit, this VMS-deposit-type is characterized by Cu-Zn epithermal-style vein mineralization paragenetically linked to more conventional massive-sulphide-type ore. Gold grades of VMS deposits vary from camp to camp, but a number of deposits in the Noranda camp such as the Horne and Quémont Mines with average gold grades of 6.1 g Au/t and 4.5 g Au/t, respectively (Chartrand and Cattalani, 1990), classify as gold-rich VMS deposits.

Archean gold deposits consist of three main types: (1) syngenetic, volcanogenic-massive-

sulphide-related gold deposits, (2) porphyry-style Cu-Mo-Au and Cu-Au-Ag deposits, and (3) epigenetic, shear zone-hosted gold (± Ag) deposits related to various vein systems otherwise known as "mesothermal" gold deposits (Roberts, 1988; Fyon et al., 1992; Poulsen et al., 1992; Hutchinson, 1993; Laznicka, 1993). VMS-associated gold deposits, commonly referred to as "pyritic" or "sulfidic schist" deposits, are characterized by base metal or polymetallic sulphide mineralization, paraconcordant within their host volcano-sedimentary sequences, overprinted by quartz ± carbonate-sulfide-Au vein mineralization (e.g. Mobrun, Bousquet, Donald J. LaRonde Mines). Gold concentration in this deposit type is interpreted as pre-tectonic, presumably synvolcanic, remobilized later by metamorphic processes into discordant, synkinematic structures (Hutchinson, 1993; Larocque et al., 1993; Tourigny et al., 1993).

Porphyry-style Cu-Mo-Au and Cu-Au-Ag deposits occur in and around pipe-like felsic intrusions and breccia bodies characterized by strong mineral and chemical zonations grading from inner potassic (Cu, K-spar, biotite, sericite) to outer propylitic (carbonate-chlorite-albite-epidote) alteration zones (e.g. Don Rouyn Mine, Noranda, Goldie (1979)). They are also characterized by the presence of pre-, intra, and post-mineral felsic dikes, by sulphide disseminations (py, cpy, sph, po) and by micro-fracture- to stockwork-vein-controlled alteration/mineralization (Kirkham et al., 1995). As a result of controversial interpretations of field relations, the relative timing of gold-ore formation in this deposit type is equivocal. At the Hollinger-McIntyre (Timmins) and Lac Troilus deposits (Northern Abitibi belt), for example, the regional dynamothermal metamorphic assemblages and penetrative planar and linear fabrics have been interpreted to overprint the felsic dike complexes and gold alteration-mineralization by Mason and Melnik (1988) and Fraser (1993), whereas Burrows and Spooner (1986), Wood *et al.* (1986), Magnan (1993), and Burrows *et al.* (1993) concluded that gold mineralization in these deposits overprints regional schistosities and related metamorphic assemblages. However, in the Rouyn-Noranda area, where such gold deposits (e.g. Don Rouyn Mine) are related to syn- and late-volcanic tonalite-trondhjemite-granodiorite intrusions (ca. 2701-2694 Ma), part of the mineralization is thought to be

synvolcanic in origin (Jébrak et al., 1991; Couture and Verpaelst, 1994).

The most abundant type of Archean gold deposit, the epigenetic-type, is characterized by vein systems ranging from quartz-tourmaline-carbonate-Au±scheelite lode or fissure veins, to carbonate-quartz stockwork veins with pyrite (± pyrrhotite, arsenopyrite) disseminations and replacement zones. Although individual epigenetic gold deposits differ widely, they share the following features: they occur in structures distributed around major regional fault zones, and they are associated with small, syn- to late-tectonic felsic intrusions which cut across, but are also cut by, mineralization (Hodgson and MacGeehan, 1982; Trudel, 1985; Card, 1990; Sansfaçon and Hubert, 1990; Corfu, 1993; Pilote et al., 1993). The metamorphogenic model, the preferred genetic model proposed to explain the origin of this class of Archean gold deposits, suggests that they are "mesothermal" hydrothermal deposits controlled by the development of shear zones and the migration of auriferous hydrothermal fluids by seismic pumping ((Sibson et al., 1988; Robert, 1990; Hodgson et al., 1993). At deposits where gold mineralization has been dated on hydrothermal minerals that are thought to have precipitated with the gold, $^{40}Ar/^{39}Ar$ ages of muscovite (Hanes et al., 1989), Sm-Nd ages of scheelite (Anglin, 1990), U-Pb ages of rutile and titanite (Jemielita et al., 1989; Zweng and Mortensen, 1989; Zweng et al., 1993) range between ca. 2625-2579 Ma., suggesting that gold mineralization is late i.e. 55-100 m.y. younger than metamorphism (ca. 2680 Ma in Val d'Or area); however, "hydrothermal" zircons[4] of quartz-tourmaline veins from the Sigma and Bras d'Or Mines in Val d'Or (see **Figure 2.2**) have been dated as 2682 ±8 Ma by Claoué-Long *et al.* (1990) and as 2693 ± 2 Ma and 2688 ± 8 Ma by Kerrich and Kyser (1994) respectively, suggesting that mineralization may be pre-metamorphic (see section 6.3, Chapter 8, and

---

[4] Until recently, the hydrothermal nature of vein zircons analyzed by Claoué-Long et al. (1990) has been disputed by Corfu and Davis (1991) and by Hanes et al. (1992). However, the likelihood of there being hydrothermal vein zircons in gold-bearing quartz-tourmaline veins from selected Val d'Or mines distinct from magmatic zircons found in igneous host rocks, has been clarified by Claoué-Long et al. (1992), Kerrich and King (1993), and Kerrich (1994), on the basis of mineral paragenesis and fluid inclusion morphology, composition and gold inclusion content.

Regional Sequence of Events diagram in back pocket). On the other hand, and in support of this observation, at deposits where gold mineralization was constrained by U-Pb zircon ages of cross-cutting felsic intrusions the absolute minimum age of gold-ore formation ranges between ca. 2692-2686 Ma (Morasse et al., 1993; Pilote et al., 1993; Couture et al., 1994).

Recent overviews of the style and timing of gold mineralization in the southern Abitibi belt (Couture et al., 1994; Couture and Verpaelst, 1994; Robert, 1994; Robert et al., 1995) suggest that the relative timing of gold mineralization is polarized in two distinct time intervals: 1) a synvolcanic VMS- and porphyry-related period at ca. 2720-2694 Ma (e.g. Home and Don Rouyn Mines), and 2) a late- to post-tectonic and post-metamorphic period at ca. < 2685-2579 Ma, resulting from the remobilization of "early" gold from high-level stockwork vein mineralization systems into "late" "metamorphogenic" hydrothermal systems (e.g. Sigma Mine; Powell (1995b)). However, this pattern of time versus gold-mineralization-type has not yet been confirmed by mineralization that has been dated directly; hence, gold mineralization at the Norlartic Mine, which has been dated as >2692 ± 2 Ma (Pilote et al., 1993), is of "inferred" synvolcanic origin (Desrochers et al., 1994), whereas gold mineralization at the Kiena Mine, which has been dated as >2686 ± 2 Ma is neither synvolcanic nor post-metamorphic (Morasse and Wasteneys, 1994; Morasse et al., 1995b).

2.1.2.6 Geotectonic models

Two types of tectonodynamic evolutionary models, based on analogy with modern plate tectonic processes in effect since Proterozoic times, have been proposed to explain the present geometry of supracrustal assemblages and the sequence of geological events in the southern Abitibi belt: an ensialic rift model, and island-arc models. The ensialic rift model (Hodgson, 1986) suggests that the southern Abitibi greenstone belt formed on pre-existing sialic crust during protracted rifting and mantle diapirism, that evolved from ensialic to ensimatic. The presumed extensional tectonic regime, which caused komatiitic to tholeiitic and subsequent calc-alkalic volcanism, was followed by a compressional tectonic regime

inferred to be caused by both rising granitoid batholiths, and crustal shortening. Hodgson (1986) suggested that Timiskaming assemblages and regional shear zones formed during this compressional phase. Shear zones were intruded by felsic porphyry dyke swarms and stocks, which were subsequently altered and gold mineralized.

The first island-arc model was formulated by Dimroth *et al.* (1982; 1983a; 1983b) (**Table 2.1**) who inferred the construction of an island-arc system over a north-dipping subduction zone. The arc formed over a pre-existing oceanic crust, and volcanism in the arc-trench system evolved from komatiitic lava plains to calc-alkalic central volcanic complexes. Dimroth *et al.* (1983a) suggested that diapirism of granodioritic batholiths was coeval with the construction of the calc-alkalic volcanic edifices to explain the emergence and erosion of parts of the arc complex. They also suggested that the metasedimentary rocks of the Pontiac Subprovince, to the south, were deposited in a fore-arc basin environment. They interpreted the Pontiac Subprovince terrain to have been overthrust by the southern Abitibi greenstone belt island-arc assemblage during protracted north-south compression.

An alternative island-arc model was proposed by Ludden *et al.* (1986), who suggested that the southern Abitibi belt formed in a series of rift basins, which dissected a pre-existing continental-arc complex represented by the northern Abitibi belt or "northern volcanic zone" (**Table 2.1**). The arc and rifted-arc complexes were presumed to develop above a south-dipping subduction zone. Ludden *et al.* (1986) suggested that komatiitic to tholeiitic volcanic sequences represented subaqueous volcanic plateaus, which were subsequently amalgamated during an accretionary regime. This was followed by rifting of the assemblage of oceanic suspect terranes, which led to the eruption of calc-alkalic lavas to form central volcanic edifices cored by subvolcanic granodioritic intrusion complexes (Desrochers et al., 1993a). Following a transition from a north-south compressive tectonic regime to a transpressional regime, wrench-fault tectonic mechanisms are invoked to further explain the structural complexities of the belt (Hubert et al., 1984; Ludden and Hubert, 1986; Ludden et al., 1986).

Hodgson and Hamilton (1989) proposed a different version of the island-arc model formulated by Dimroth *et al.* (1983a), maintaining that island-arc rock assemblages formed above a north-dipping subduction zone, over pre-existing oceanic crust. They envisaged the metasedimentary assemblages of the Pontiac Subprovince to the south, as part of a foreland basin, which collided with the metavolcanic rock sequences of the southern Abitibi greenstone belt to the north during protracted north-south compression. They postulated that overthrusting of the Abitibi belt over the Pontiac Subprovince caused the formation of molasse-type deposits represented by Timiskaming and Timiskaming-like linear belts of polymictic conglomerates along collisional suture zones (i.e. Larder Lake-Cadillac tectonic zone). Hodgson and Hamilton (1989) further suggested that geologic processes active at the lower crust-mantle boundary during the terminal stages of collision, were responsible for the broadly coeval emplacement of syn- to post-deformational felsic intrusions, intense carbonate alteration, and widespread gold alteration-mineralization in the greenstone belt.

Yet another island-arc model, supported by precise U-Pb geochronology and deep seismic reflexion data, was proposed by Jackson and Fyon (1991), and refined by Mortensen and Card (1993) and Jackson (1994). These authors have suggested that the Abitibi greenstone belt, a region composed of oceanic microplates, formed at ca. 2750-2670 Ma (Corfu, 1993) between two large convergent masses: the Minnesota River Valley gneiss terrane (ca. 3.5 to 2.8 Ga, Sims *et al.* (1980)) to the south, and the Uchi Subprovince (ca. 3.0 to 2.7 Ga) (Stott and Corfu, 1992) and previously accreted metasedimentary and metavolcanic terrains to the north (see **Figure 2.1**). Corfu (1993) indicated that pre-orogenic komatiitic, tholeiitic and calc-alkalic magmatism was essentially coeval, and compared this geologic and geochemical evolution trend to that of paired, active arc and back-arc systems. Collision began at approximately 2700 Ma and caused thrusting and folding, followed by the emplacement of felsic intrusions in the microplate region between 2700-2688 Ma (Corfu, 1993). During the terminal stages of the subduction-collision process, between ca. 2681-2676 Ma (Corfu, 1993), magmatism became predominantly alkalic and was accompanied by the deposition of alluvial-fluvial metasedimentary rocks to form the Timiskaming Group and Timiskaming-like

rock assemblages. Jackson and Fyon (1991) postulated that the southern Abitibi greenstone belt was thrusted over the turbiditic deposits of the Pontiac Subprovince (Green et al., 1990), and suggested that the latter may represent an accretionary wedge. However, Mortensen and Card (1993) showed that volcanic and sedimentary sequences in the Pontiac Subprovince, dated as 2689-2682 Ma and as < 2683 Ma, respectively, were younger than similar sequences in the Abitibi belt, but broadly synchronous with Timiskaming sequences. They have suggested that rock assemblages of the Pontiac Subprovince may represent small volcanic arcs isolated in a large turbidite basin, and inferred that they could represent an accretionary prism derived from, amalgamated with, and overthrust by the Abitibi belt by subduction-driven accretion in the late stages of the Kenoran orogeny. Alkalic volcanism in the southern Abitibi greenstone belt, together with volcanism and sedimentation in the Pontiac Subprovince, was followed by renewed compression that caused polyphase folding and thrusting, and subgreenschist, to greenschist and amphibolite facies metamorphism accompanied by the development of a syn-metamorphic regional planar fabric between ca. 2680-2660 Ma (Powell et al., 1995a). This model presumes that regional shear zones, such as the Larder Lake-Cadillac tectonic zone and the Destor-Porcupine fault zone, may represent major suture zones between the Abitibi greenstone belt and the Pontiac Subprovince, and between the southern and northern part of the Abitibi belt, respectively (Green et al., 1990; Chown et al., 1992; Daigneault et al., 1994). This model also associates gold mineralization with lower crustal metamorphic processes and the development of shear zones between ca. 2630-2580 Ma (Corfu, 1993; Zweng et al., 1993).

Despite their differences, geotectonic models summarized herein have one thing in common: they all stipulate that epigenetic gold mineralization occurred late in the evolution of the southern Abitibi belt, and was structurally controlled by the formation of shear zones, during or after peak regional synmetamorphic deformation.

2.2 GEOLOGY OF THE VAL D'OR-MALARTIC AREA

We are at a point in the study of the Val d'Or-Malartic area where stratigraphic and structural notions of the past five decades (1940's-1990's) are challenged by the progressive stratigraphic, structural and metallogenic notions of modern plate tectonics applied to Archean rock assemblages. Terms such as "accreted terranes" are replacing earlier terms such as "alpine-type eugeosynclinal rock succession" in the jargon of the initiated geologists concerned with the geological history of this area. Increments in the geological knowledge of the Val d'Or-Malartic area will undoubtedly modify the evolutionary geological models of the past, but caution must be exercised when applying complex, and still evolving, plate-tectonic concepts to Archean greenstone belts. The accumulation of precise U-Pb zircons dates in the Val d'Or-Malartic area since 1989 and the recent acquisition of LITHOPROBE seismic reflection profiles (lines 12, 12a, 14 and 17; Green *et al.* (1990), Clowes (1993), Calvert *et al.*, (1995)) are not only changing our old perceptions of Archean crustal assembly in this part of the Abitibi greenstone belt, but are also adding time, and new structural and stratigraphic constraints to evolutionary geological models. The following is an abbreviated historical and descriptive review of the geology of the Val d'Or-Malartic area, introducing geochronological data where they are available.

2.2.1 Introduction

Lithostratigraphic subdivisions for the Val d'Or-Malartic area originate from the work of Gunning and Ambrose (1940), who mapped in detail parts of Cadillac, Malartic and Fournière Townships (area of Lac Fournière and Malartic on **Figure 2.2**) between 1934 and 1937. They outlined the "***Cadillac Syncline***" and subdivided the succession of alternating volcanic and sedimentary sequences into four groups: (1) the volcanic ***Malartic Group***, overlain by (2) the sedimentary Kewagama Group, (3) the volcanic Blake River Group, and (4) the sedimentary Cadillac Group (**Table 2.2**). The sedimentary rock assemblages of the Kewagama Group, located on the south limb of the "Cadillac Syncline" (now, the Pontiac

Figure 2.2 - *Simplified geological compilation map of the Val d'Or-Malartic area showing the distribution of volcanic, sedimentary and intrusive rocks, as well as the occurrence of gold and volcanogenic massive sulphide deposits. Stratigraphic and structural subdivisions are modified from Campliglio and Darling (1976), Imreh (1984), Gaudreau et al. (1986), Rocheleau et al. (1990), Robert (1989; 1990) and Sauvé et al. (1993). Radiometric zircon ages of volcanic, intrusive and sedimentary rocks, and those of hydrothermal minerals spatially associated with Au mineralization are shown for locations where data are available (see also* ***Table 7.3*** *for age dating authorship). The lake on which Kiena (deposit No. 10) is located is lake De Montigny.*

Carte géologique simplifiée de la région de Val d'Or-Malartic montrant la distribution des différents assemblages de roches volcaniques, sédimentaires et intrusives, ainsi que celle des divers gisements d'or et de sulfures massifs volcanogènes. Les subdivisions stratigraphiques et structurales sont modifiées d'après Campiglio et Darling (1976), Imreh (1984), Gaudreau et al. (1986), Rocheleau et al. (1990), Robert (1989; 1990) and Sauvé et al. (1993). Les âges radiométriques obtenus à partir de zircons provenant de roches volcaniques, plutoniques ou sédimentaires, ainsi que ceux obtenus de mineraux hydrothermaux en contact avec la minéralisation aurifère, apparaissent aux localités où ces âges ont été déterminés (voir ***Tableau 7.3*** *pour obtenir la référence des âges isotopiques). Le plan d'eau entourant Kiena (gisement N0. 10) est le lac De Montigny.*

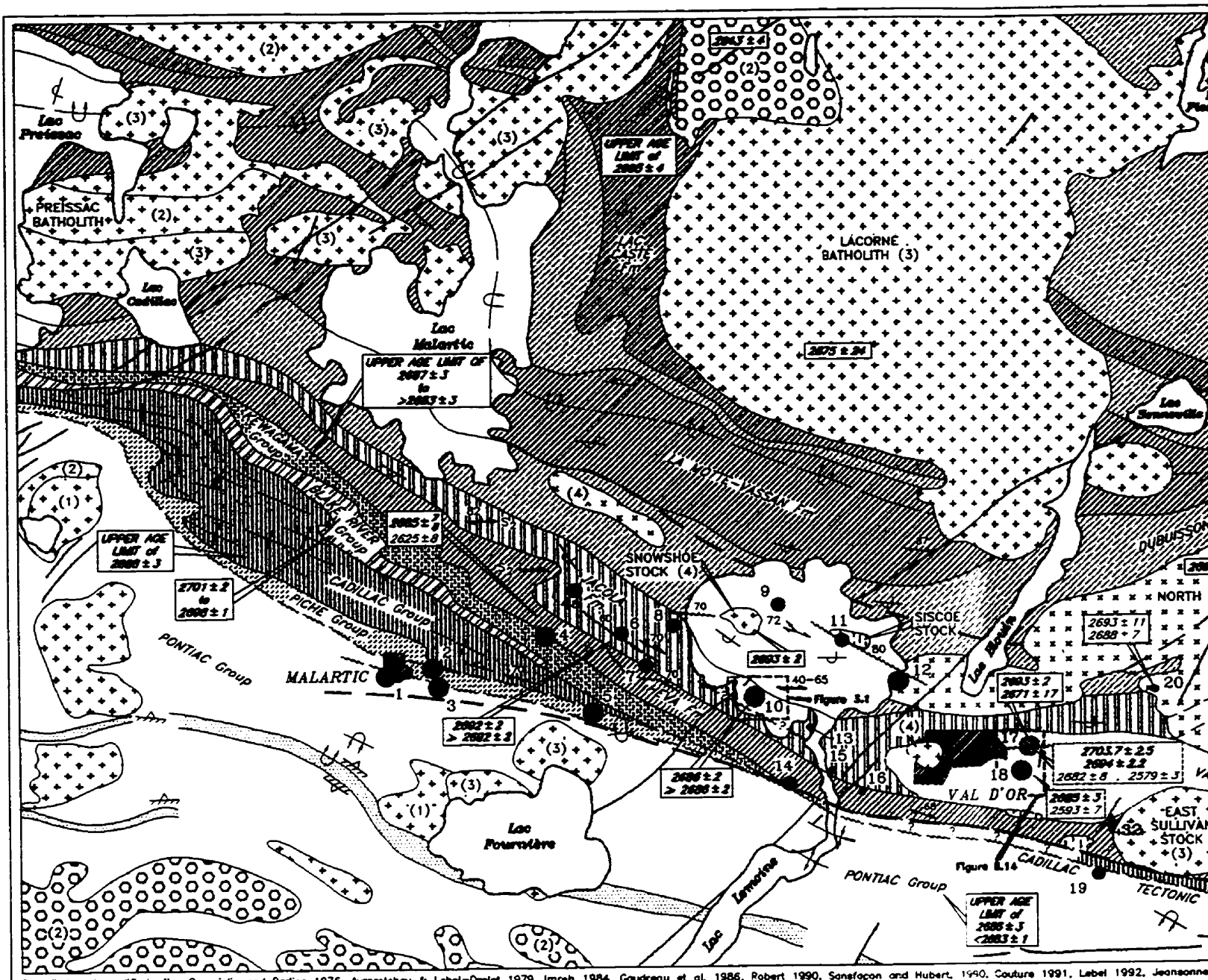

Compiled and modified after Campiglio and Darling 1976, Avramtchev & Label-Drolet 1979, Imreh 1984, Gaudreau et al. 1986, Robert 1990, Sansfaçon and Hubert, 1990, Couture 1991, Label 1992, Jeanson

2686 ± 2 — Radiometric age of intrusion,volcanic or sedimentary rock formation (Ma)

2579 ± 3 — Radiometric age of minerals associated with Au mineralization (Ma)

2686 ± 2 — Minimum age of Au mineralization (Ma)
Precise U/Pb zircon age of cross-cutting intrusion

2684 ± 7 — Radiometric age of "metamorphic" minerals (Ma)

META-VOLCANIC ROCKS

- BLAKE RIVER GROUP : pillow basalt
- PICHE Group : basalts , komatiite ultramafic flows
- LA MOTTE - VASSAN Fm : komatiitic ultramafic flows
- DUBUISSON Fm : basalts , komatiitic ultramafic flows
- JACOLA Fm : repetitive cycle of komatiite , basalt and basaltic breccia
- VAL D'OR Fm : massive and volcaniclastic basalts - andesite flows
- HEVA Fm : volcaniclastic and massive andesites - basalt flows
- VILLEBON GROUP : basalt , andesite and ultramafic flows and breccia
- PONTIAC GROUP : Komatiitic , Ultramafic flows

META-SEDIMENTARY ROCKS

- CADILLAC GROUP : graywacke , pelitic schists , polymictic con
- KEWAGAMA Fm : graywacke and volcanosedimentary rocks
- LAC CASTE Fm : graywacke
- TRIVIO GROUP : conglomerate , graywacke , sandstone , muds basalt and andesite flows and volcanoclastic roc
- PONTIAC GROUP : graywacke , rare komatiite ultramafic flows

INTRUSIVE ROCKS

- Diabase dikes
- Gabbro , diorite , granophyre (peridotite)
- Pre - tectonic suite
- Syn - to - late - tectonic suite
- Post-tectonic suite

(1) Monzonite , quartz monzonite with pyroxene
(2) Biotite and/or muscovite monzogranite, granitic pegmatite dike
(3) Monzodiorite , hornblende and biotite monzodiorite
(4) Tonalite , leucotonalite , granodiorite
(*) Central Bourlamaque "batholith" : metadiorite-trondhjemite suit

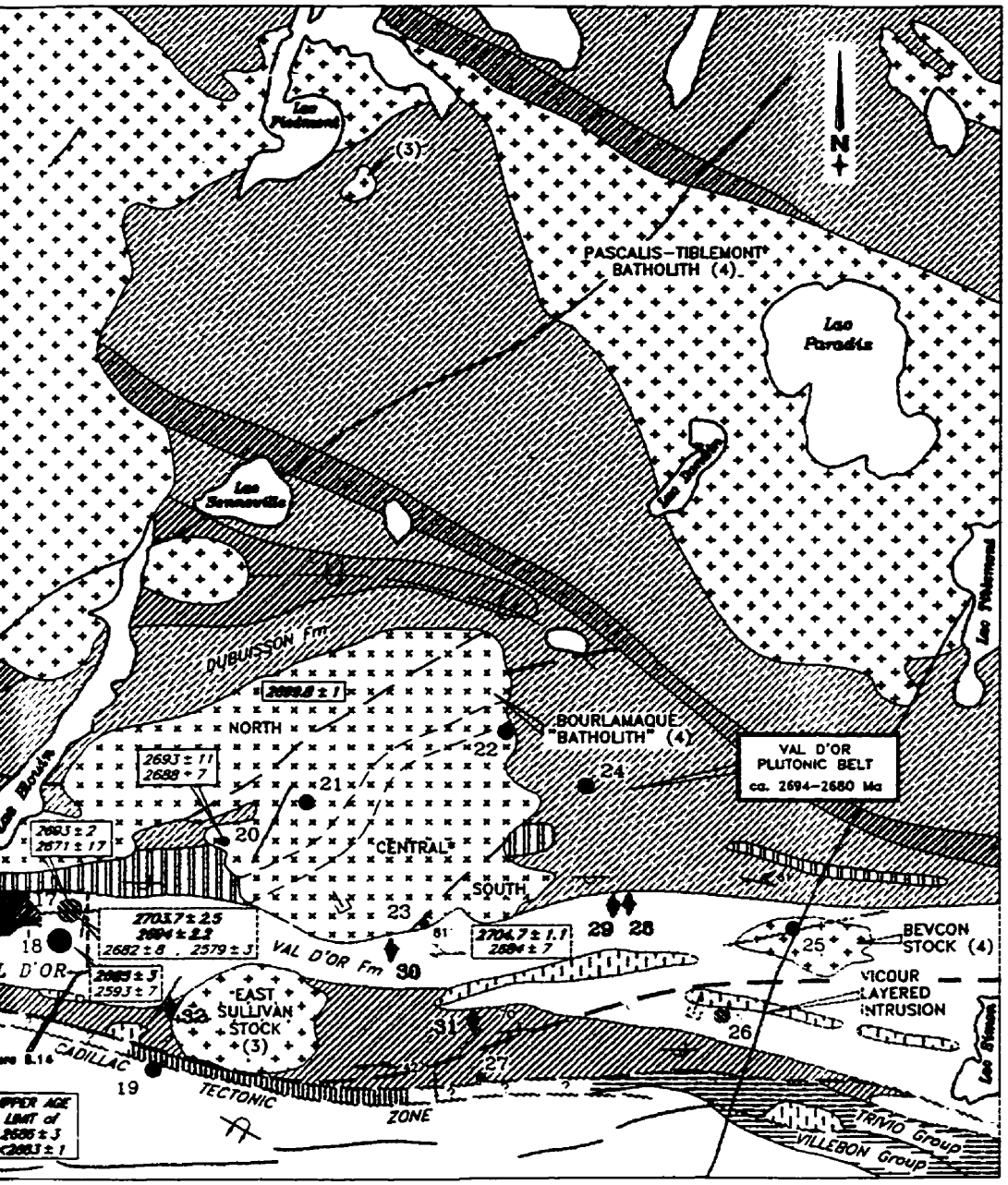

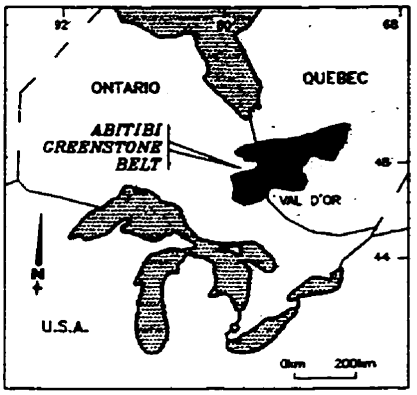

GOLD AND VOLCANOGENIC MASSIVE SULPHIDE DEPOSITS (PAST AND PRESENT * PRODUCERS)

- < 3 Tonnes Au
- 3–30 Tonnes Au
- > 30 Tonnes Au

1 Canadian Malartic
2 Barnat – Sladen
3 East Malartic
4 Camflo * – Malartic Hygrade
4a Orion Vein # 8
5 Malartic Gold Fields #2
6 Norlartic – First Canadian (Kierens)
7 Marban
8 Callahan
9 Wesdome (Western Quebec)
10 **KIENA** *
11 Siscoe
12 Sullivan
13 Shawkey
14 Quebec Explorer
15 Goldex
16 Joubi #1 *
17 Sigma* – Lamaque No. 2
18 Lamaque (main)
19 Orenada Zone 4
20 Bras d'Or (Dumont) *
21 Ferderber (Belmoral) *
22 Perron
23 Wrightbar
24 L.C. Beliveau (New Pascalis) *
25 Bevcon
26 Sigma #2 *
27 Akasaba
28 **Louvicourt (Cu–Zn) ***
29 **Louvem (Cu–Zn)**
30 **Manitou–Barvue (Zn–Ag–Cu)**
31 **Dunraine (Cu)**
32 **East Sullivan (Cu–Zn–Ag)**

0, Couture 1991, Label 1992, Jeansonne 1993, Sauvé et al., 1993.

See Table 5.2 for radiometric age dating authorship

, pelitic schists , polymictic conglomerate
nd volcanosedimentary rocks

, graywacke , sandstone , mudstones
esite flows and volcanoclastic rocks
, rare komatiite ultramafic flows

(peridotite)

suite

with pyroxene
nzogranite, granitic pegmatite dikes
d biotite monzodiorite
odiorite
h" : metadiorite–trondhjemite suite

STRUCTURAL SYMBOLS

- Fault, Deformation/Alteration Zone
- Presumed sill contact
- Internal sill layering contact
- Lithological contacts
- Bedding and stratigraphic top
- 70 Overturned bedding and dip
- 75 Regional schistosity
- 40–65 Penetrative spaced cleavage KIENA mine, level 27
- 42 schistosity and streching lineation
- Synform
- Antiform
- Overturned anticline
- Stratigraphic top of layered intrusion
- Bedding and stratigraphic top of ultramafic flow with spinifex texture

LES MINES D'OR KIENA LTEE.

SIMPLIFIED GEOLOGICAL COMPILATION MAP OF THE VAL D'OR – MALARTIC AREA

COMPILED BY : S. Morasse
DATE : 08/18/96
COMPUTER DRAFTING BY : S. Tremblay

SCALE 1 : 250 000
0m 2.5km 5.0km 7.5km 10.0km

Figure 2.2

Table 2.2 Evolution of the lithostratigraphic and lithotectonic nomenclature applied to the geology of the Val d'Or-Malartic area represented on Figure 2.2*

NORTH				KINOJEVIS**			MANNEVILLE THRUST***
	PREISSAC-LACORNE BATHOLITH	PREISSAC-LACORNE BATHOLITH	PREISSAC-LACORNE BATHOLITH	PREISSAC-LACORNE BATHOLITH	PREISSAC-LACORNE BATHOLITH	PREISSAC-LACORNE BATHOLITH	PREISSAC-LACORNE BATHOLITH
		Kewagama Group	Kewagama Group	Garden Island Group	(north limb) Lac Caste Fm Dubuisson Fm	GARDEN ISLAND TECTONIC ZONE	Lac Caste Fm
KEEWATIN	SYNCLINE — MALARTIC GROUP	MALARTIC GROUP	SYNCLINE — MALARTIC GROUP	ABITIBI SUPERGROUP — MALARTIC GROUP	LA MOTTE-VASSAN ANTICLINE — "MALARTIC GROUP"	VAL D'OR DOMAIN	"MALARTIC COMPOSITE BLOCK"
			LOWER MALARTIC		La Motte-Vassan Fm	Dubuisson Fm (base)	Northern Domain Vassan Domain
					Dubuisson Fm		
			UPPER MALARTIC		VAL D'OR COMPLEX		Central Domain
					Jacola Fm Val d'Or Fm (Bourlamaque "batholith")	Jacola Fm Val d'Or Fm	Val d'Or Domain (Bourlamaque "batholith")
					(south limb) Héva sud Fm	Héva Fm (top)	Southern Domain
	Kewagama Group Blake River Group	Kewagama Group Blake River Group	Kewagama Group Blake River Group		Kewagama Group Blake River Group		Kewagama Group
	SYNCLINE — Cadillac Group	Cadillac Group	SYNCLINE — Cadillac Group		Cadillac Group		
	CADILLAC "BREAK"	CADILLAC "BREAK"	CADILLAC "BREAK"	CADILLAC "BREAK"	CADILLAC TECTONIC ZONE Chlorite-talc schists and komatiite of upper	CADILLAC TECTONIC ZONE Trivio Structural	CADILLAC TECTONIC ZONE (CTZ) Piché & Cadillac
	CADILLAC — Blake River (Gunning	Blake River (Gunning	MALARTIC — Blake River (Gunning				

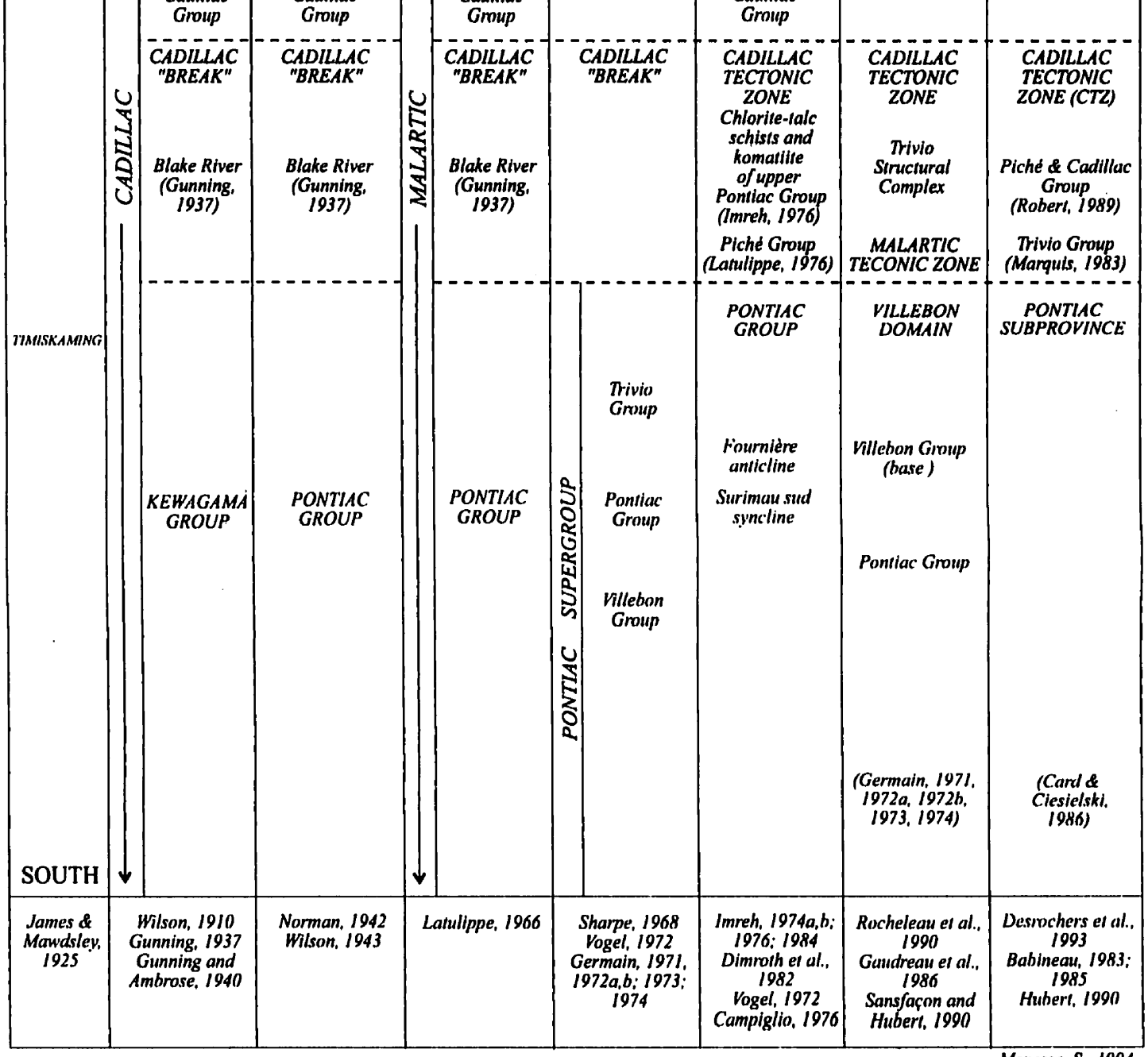

* *No correlation among the lithostratigraphic and lithotectonic subdivisions of the authors, the units in each column are systematized as they appear on a traverse from north to south on Fig.2.*

** *Part of the Abitibi Supergroup of Germain (1971; 1972 a,b; 1973; 1974) but not represented on Fig.2.*

*** *Daigneault and Labbé, 1992*

- - - *Documented fault contact*

Inferred fault contact

Group), were separated from the stratigraphic units located on the north limb by the ***Cadillac "Break"***, a zone of chlorite and talc schist that was thought to have been derived from the mafic and ultramafic rocks of the Blake River Group (Gunning and Ambrose, 1940). Other mapping surveys conducted by Norman in the Val d'Or-Malartic area and further east in the Louvicourt Township resulted in series of annotated maps between 1941 and 1947 (Norman, 1941; Norman, 1942; Norman, 1943; Norman, 1946; Norman, 1947b; Norman, 1947a). Norman (1941) determined on the basis of stratigraphic top determinations that in the rock succession east of Malartic, the sedimentary rocks of the Kewagama Group overlie the volcanic rocks of the Blake River Group, as opposed to the Blake River Group overlying the Kewagama Group in the "Cadillac syncline" to the west. Norman doubted the existence of the synclinal structure because the order of rock successions between the Blake River and Kewagama Groups on the north limb was different from that in the south limb. He also pointed out that volcanic rocks of the Blake River Group were cut to the south by the Cadillac Break and questioned whether any rock units could be correlated across the fault zone. The stratigraphic subdivision of the area was refined by Latulippe who subdivided the volcanic rocks of the Malartic Group into a northern ***"Lower Malartic"*** sub-group, dominated by ultramafic flows and related intrusions, and a southern ***"Upper Malartic"*** sub-group, dominated by mafic and felsic flows with abundant pyroclastic rocks intruded by dioritic to granodioritic intrusions (Latulippe, 1966). He also renamed the "Cadillac Syncline" of Gunning and Ambrose (1940), the ***"Malartic Syncline"*** (**Table 2.2**). Geological units of the Val d'Or-Malartic area were later subdivided into two large lithostratigraphic assemblages: the ***Abitibi Supergroup*** to the north (Germain, 1971; Germain, 1972b; Germain, 1972a; Germain, 1973; Germain, 1974), overlain by the ***Pontiac Supergroup*** to the south (Vogel, 1972). The Abitibi Supergroup is composed, from the oldest to the youngest, of the volcanic rocks of the Kinojevis Group, the sedimentary rocks of the Garden Island Group, and the volcanic rocks of the Malartic Group, whereas the Pontiac Supergroup is composed of the ultramafic and mafic volcanic rocks of the Villebon Group overlain by the sedimentary and volcano-sedimentary rocks of the Pontiac and Trivio Groups, respectively (**Table 2.2**).

Having demonstrated that ultramafic and ultrabasic rocks of the La Motte, Vassan and Dubuisson Townships were flows rather than intrusions, as previously thought, Imreh used cooling textures such as komatiitic pillow flow top breccias, zones of spinifex and polygonal fractures to outline a large anticlinal structure, which he termed the ***"La Motte-Vassan Anticline"*** (**Figure 2**)(Imreh, 1974c; Imreh, 1974a; Imreh, 1974b; Imreh, 1976b; Imreh, 1976a). Imreh then proposed a revision of the early lithostratigraphic subdivisions of Gunning and Ambrose (1940) based on the succession of volcano-sedimentary sequences located on the south limb of the "La Motte-Vassan Anticline", which he compared to an "alpine-type" ultramafic-basaltic eugeosynclinal succession (**Table 2.2**)(Imreh, 1976b; Imreh, 1984).

As illustrated in **Figure 2.2**, eight major lithologically distinctive assemblages of supracrustal rocks were recognized by Imreh (1984) that were regrouped, from the oldest to the youngest, into the ***"Malartic Group"*** which Imreh (1976) restricted to oceanic lava-plain-type ultramafic and mafic volcanic flows of the LaMotte-Vassan and Dubuisson Formations, the ***"Val d'Or Volcanic Complex"***, composed of the Jacola, Val d'Or, and Héva Formations, and the ***Kewagama***, ***Blake River*** and ***Cadillac Groups*** (**Table 2.2**). Following the discovery of narrow bands of ultramafic and mafic volcanic rocks further south in the metasedimentary Pontiac Group (see **Figure 2.2**), Imreh (1976) re-interpreted the chlorite-talc schists of the Blake River Group, located in the Cadillac "Break" west of Val d'Or (Gunning and Ambrose, 1940), as highly strained and altered ultramafic and mafic flows of the Pontiac Group. However, Latulippe (1976) attributed the ultramafic-mafic protoliths of the same chlorite-talc schist to the Piché Group, arguing that the latter was more akin to the volcanic rocks of the "Malartic Group", and could therefore no longer be correlated with the felsic volcanic and pyroclastic rocks of the Blake River Group (**Table 2.2**). Imreh (1976) also renamed the Cadillac "Break" of Gunning and Ambrose (1940) the ***"Cadillac Tectonic Zone"***.

Since the work of Babineau (1983; 1984), Hubert (1984), Ludden *et al.*(1986) and Sansfaçon and Hubert (1990), this simple lithostratigraphic succession, younging south toward the

Cadillac Tectonic Zone, has been questioned and re-examined by Gaudreau *et al.* (1986), Rocheleau *et al.* (1990), and Desrochers *et al.* (1992; 1993b; 1996). Gaudreau *et al.* (1986) and Rocheleau *et al.* (1990) were the first to introduce the concept of lithotectonic domains east of Val d'Or, by subdividing sedimentary and volcanic rock formations into high-strain and lower-strain rock domains. High-strain domains form narrow, elongated belts of highly strained and faulted metasedimentary rock assemblages, which are thought to coincide with major crustal discontinuities (i.e. Garden Island Tectonic Zone and Trivio Structural Complex; **Figure 2.2, Table 2.2**). The ***"Trivio Structural Complex"***, a zone of highly deformed and anastomosing blocks of metasedimentary and metavolcanic rocks of mixed origin, was interpreted as the extension of the "Cadillac Tectonic Zone" by Marquis (1983) and Rocheleau *et al.* (1990). By contrast, lower-strain domains which are juxtaposed to high-strain domains, form the large areas of weakly deformed metavolcanic and metasedimentary rock successions of the Val d'Or and Villebon Domains, respectively (**Table 2.2**). Germain (1971; 1972b; 1972a; 1973; 1974) noted the presence of "minor fault zones at various lithological contacts", but did not observe major structural discontinuities across the stratigraphic sequences of the Val d'Or and Villebon Domains.

Desrochers *et al.* (1993a; 1994; 1996) proposed to group the volcanic and sedimentary rock assemblages of the Val d'Or-Malartic area into one large tectonic block, called the ***"Malartic Composite Block"*** (**Table 2.2**). The latter extends north to the Manneville fault* at the northern edge of the Lacorne batholith, east to the "Grenville Tectonic Zone"*, south to the "Cadillac Tectonic Zone", and west to the Parfouru Lake fault (* not shown on **Figure 2.2**). Based on rock type association, geochemical composition, and deformation style, the Malartic Composite Block is subdivided into six mafic-ultramafic and one calc-alkaline lithotectonic domains: the Northern, Central, Southern, Vassan, de Montigny, Baie Carpentier and Val d'Or Domains, respectively (**Table 2.2**) (Desrochers et al., 1993a; Desrochers and Hubert, 1996). Fault-bounded komatiitic and tholeiitic lithotectonic domains are characterized by complex deformation patterns and the presence of two penetrative planar fabrics (S_1, S_2). By contrast, calc-alkaline volcanic and intrusive rocks of the Val d'Or domain are characterised

by a single penetrative planar fabric (S_2) and the discordant intrusive contact of the Bourlamaque "batholith" with mafic-ultramafic rocks of adjacent lithostratigraphic domains. These are thought to represent fault blocks, or fragments of "exotic" oceanic plateaus, sequentially accreted from north to south during a D_1 deformation event and sutured by the imbrication of volcanic and sedimentary layers (Central Domain) which are compared to small-scale accretionary complexes (Ludden and Hubert, 1986; Desrochers et al., 1993a; Hubert and Ludden, 1994). Post-accretionary calc-alkaline volcanism and plutonism related to a local extensional tectonic event, followed by the superimposition of a common D_2 penetrative deformation during a later collisional event, are invoked to explain the discordant Bourlamaque intrusive contact and the present geometry of penetrative deformation structures (Desrochers et al., 1993a).

In the following section, rock successions found across the Val d'Or-Malartic area are described in a stratigraphic order younging from north to south, as proposed by Imreh (1976; 1984), moving broadly from west to east on the regional map of **Figure 2.2**. Although some authors may not agree with this stratigraphic layout, it is adopted here to enable the reader to evaluate the early lithostratigraphic and latest lithotectonic models invoked to explain the formation of this complexly deformed and metamorphosed package of Archean rocks. The Lac Caste Formation, located in the north central part of the map of **Figure 2.2**, will be described first, because its stratigraphic position is still uncertain at this time.

2.2.2 Volcanic and sedimentary rock successions

2.2.2.1 Lac Caste Formation

The Lac Caste Formation (Dimroth et al., 1983a) is an intra-volcanic metasedimentary unit that outcrops approximately 10 km north of the Kiena Mine. It is located on the northern limb of the La Motte-Vassan anticline in the ultramafic-mafic Dubuisson Formation and it is cut by the Lacorne batholith (**Figure 2.2**). This northwest-striking metasedimentary rock

sequence, which is isoclinally folded and overturned to the southwest, is chiefly composed of feldspathic graywackes and argillites displaying graded bedding and, locally interbedded with pebble conglomerate and rare iron formation (Dimroth et al., 1982). The pebbles found in the conglomerates are commonly composed of rounded and flattened fragments of felsic volcanic and intrusive rocks (Gaudreau et al., 1986). The contact between the Lac Caste and Dubuisson Formations has not been observed by Gaudreau *et al.* (1986) east of Val d'Or, but west of Val d'Or, Dimroth *et al.* (1982) has suggested that fault breccias cutting the Dubuisson Formation "*merge with mass-flow conglomerate whose composition proves derivation from the Dubuisson Formation*", and that locally, the conglomerate interfingers with komatiitic flows of the Dubuisson. Preliminary $^{207}Pb/^{206}Pb$ age determinations of detrital zircons from the Lac Caste Formation by Feng and Kerrich (1991a) suggest an ***upper age limit of 2695 Ma*** for the depositional age of this unit, which was recently correlated with the Garden Island Formation of Bell and Bell (1932) by Gaudreau *et al.* (1990) (see **Table 2.2** and **Figure 2.2**).

2.2.2.2 Malartic Group

From the core of the "La Motte-Vassan Anticline" outward (**Figure 2.2**), and at the base of Imreh's stratigraphic succession, is the "Malartic Group" which has been subdivided into two formations: (1) the La Motte-Vassan Formation and (2) the Dubuisson Formation. These volcanic rock formations are described below.

La Motte-Vassan Formation

The La Motte-Vassan Formation (Imreh, 1976b) outcrops immediately north of Lac De Montigny and consists of a northwest- to east-west-striking assemblage of serpentinized komatiitic flows and tholeiitic basalts, folded into a southerly overturned anticline (Imreh, 1984) and later cut by the Lacorne batholith (**Figure 2.2**). The lower section of the La Motte-Vassan Formation is composed predominantly of peridotitic komatiite flows (up to

33.87 % MgO) grading into picritic basalts (20.43 % MgO), and tholeiitic basalts (7.99 % MgO), in the upper part of the section (Imreh, 1976a). At the base of the section, ultramafic flows are commonly massive with well developed spinifex zones, whereas the olivine-rich and tholeiitic basalts are pillowed and usually without vesicles (Imreh, 1976a). The transition between the La Motte-Vassan and overlying Dubuisson Formations is marked by the predominance of tholeiitic basalt flows over komatiitic flows (Imreh, 1984). Imreh (1984) and Dimroth *et al.* (1982) interpreted the ultramafic La Motte-Vassan Formation as a deep (> 2000 m) oceanic, fissural-type of volcanic rock assemblage, however, the common occurrence of "mega" pillows (0.5-10 metres) with brecciated fringes within komatiitic flows (Imreh, 1974c; Imreh, 1976b; Imreh, 1976a) suggests that they may have been erupted in shallow water.

Dubuisson Formation

The upper part of the "Malartic Group", the Dubuisson Formation (Imreh, 1976b), underlies the mafic-ultramafic rock assemblage hosting Kiena's orebody, and is host to gold mineralization at the Siscoe Mine and Wesdome deposit (**Figure 2.2**). It consists of a 2-km-thick sequence of northwesterly- to westerly-striking and steeply north-dipping komatiite and tholeiite flows, with south-facing stratigraphic tops (Imreh, 1984). West of Val d'Or, the Dubuisson Formation is characterized by tholeiitic flows with subordinate intercalations of serpentinized picritic basalts, locally overlain by a thick horizon of felsic volcaniclastic rocks (Imreh, 1976b). East of Val d'Or, the unit is dominated by basaltic flow breccias (45 %) and massive tholeiite flows (35 %) with lesser tholeiitic pillow flows (20 %) (Imreh, 1976b; Gaudreau et al., 1986). Tholeiitic pillow flows of the Dubuisson Formation have a unique alteration feature in the form of a whitish and sphere-shaped epidote alteration assemblage displayed in positive relief at the core of individual pillows. This tholeiitic facies is locally referred to as the "epidote sphere" horizon (Imreh, 1976a). Imreh (1984) and Dimroth *et al.* (1982) have interpreted the volcanic rock assemblages of the Dubuisson Formation as having formed in a deep oceanic lava-plain environment.

2.2.2.3 Val d'Or Volcanic Complex

According to Imreh (1984), the central "Val d'Or Volcanic Complex" which is composed from the base to the top of the Jacola, Val d'Or and Héva Formations, occurs stratigraphically above the lava-plain ultramafic-mafic rock assemblages of the "Malartic Group". It is the economically most important volcanic rock sequence of the area; the Val d'Or Formation is host to the supergiant Sigma-Lamaque Mines (~258 t Au) and to all the polymetallic volcanogenic massive sulfide mines of the Val d'Or camp, whereas the Jacola and Héva Formations host all of the volcanic- and felsic intrusion-hosted vein-type gold deposits north of the Cadillac Tectonic Zone but the Wesdome deposit (**Figure 2.2**).

Jacola Formation

The Jacola Formation (Imreh, 1976b) is host to several gold mines in the area, the most important of which is the Kiena Mine located in the southwestern corner of Lac De Montigny (see deposit labelled **10** on **Figure 2.2**). It consists of a south- to southwest-facing homoclinal sequence of northwest-southeast to east-west-striking and steeply north-dipping Fe- and Mg-rich tholeiitic basalts interbedded with pyroxenitic komatiite flows (Polk, 1960; Cloutier, 1979; Imreh, 1984). The "Jacola Triad", is a repetitive volcanic cycle composed from the base to the top of: (1) a serpentinized pyroxenitic komatiite flow, (2) a tholeiitic basaltic flow accompanied by a flow top breccia and, (3) a basaltic agglomerate with minor hyaloclastic material (Imreh, 1976b; Imreh, 1976a; Imreh, 1984). The Jacola Formation has been cut by several small granodioritic to tonalitic stocks, and by several intermediate to felsic dike swarms. Most of these intrusions, which range from albitite and quartz-diorite dikes, to granodiorite and tonalite porphyries, do not outcrop at surface but at shallow depth within the local mines (e.g. Kiena, Norlartic, Marban, Callahan, Shawkey, Goldex). Imreh (1984) regarded the volcanic rock sequence of the Jacola Formation as a transitional unit, representing a facies change between the ultramafic-mafic volcanism of oceanic lava plain environments, envisaged for the "Malartic Group", and the calc-alkaline central volcanism,

more typical of island arc environments, envisaged for the Val d'Or Formation.

Val d'Or Formation

The Val d'Or Formation (Imreh, 1976b; Imreh, 1976a; Imreh, 1984), economically the most important volcanic rock formation of the Val d'Or camp, overlies the Kiena Mine volcanic rock assemblage. This band of calc-alkaline flows and pyroclastic debris, which stretches east of Val d'Or, hosts the largest polymetallic volcanogenic massive sulfide deposit discovered in Canada in the past 10 years, the Louvicourt VMS deposit (24 million tons grading 3.9% Cu, 2% Zn, 31 g/t Ag and 1 g/t Au; Econ. Geol. V. 88, No. 6, frontispiece), and the Sigma-Lamaque Mines (~130.2 t Au and 21.2 t Ag; ~140.9 t Au; see deposits labelled **28**, **17** and **18** on **Figure 2.2**). It consists of an east-west-striking, steeply north-dipping sequence of basaltic and andesitic flows, pyroclastic breccias (or agglomerate with andesitic and dioritic porphyry fragments ranging from 1 to 30 cm in diameter), polymictic lapillis and crystal tuffs, overturned to the south (Imreh, 1984; Gaudreau et al., 1986; Taner and Trudel, 1991). One of its members, the Colombière "rhyolite" (highly Si-altered andesite; J. Hanes, personal communication), has been dated as ***2704.9 ± 1.1 Ma*** by Wong *et al.* (1991) (**Figure 2.2**; see also **Table 7.3** and Regional Sequence of Events diagram in back pocket). The volcanic edifice of the Val d'Or Formation is in conformable contact with the co-magmatic, calc-alkaline Bourlamaque sill complex (Campiglio, 1974; Campiglio and Darling, 1976; Latulippe, 1976; Campiglio, 1977; Taner and Trudel, 1989; Tessier et al., 1990) dated as ca. 2700 Ma by Wong *et al.* (1991) (see footnote in section 2.2.3.1). Based on the geochemical evolution of the volcanic rock sequence and the distribution of its pyroclastic deposits, Imreh (1984) inferred that the centre of emission of the Val d'Or Formation was located about the city of Val d'Or. More recently, Taner and Trudel (1991) and Taner (1993) based on a detailed survey of gold distribution in the Val d'Or Formation, have postulated that a gold-rich fossil geothermal field was located at the core of the "Val d'Or Volcanic Complex", i.e. over the zoned granodiorite-diorite intrusion of the main Lamaque Mine (deposit # 18 on **Figure 2.2**, **Figure 8.27**) (see also Karvinen (1985), p. 29 and Taner (1996b). However, field relations and

geochronological data do not support Taner's contention that this intrusion was ever a centre of volcanic activity. The Lamaque intrusion, dated as ca. 2685 Ma (Jemielita et al., 1989), was emplaced some 15 m.y. after cessation of calc-alkaline volcanism (ca. 2701-2698, Mortensen (1987) and Corfu *et al.* (1989)) into volcanic strata of the Val d'Or Formation that were overturned to the south between ca. 2700-2694 Ma (Morasse et al., 1995b; Morasse et al., 1996) (see also Regional Sequence of Events diagram in back pocket).

Héva Formation

The Héva Formation (Imreh, 1984), the uppermost member of the "Val d'Or Volcanic Complex", outcrops south of Val d'Or and south of Lac De Montigny, where it is in contact with the Jacola Formation of the Kiena Mine (**Figure 2.2**). Imreh (1984) informally subdivided this bi-modal, southerly overturned and east-west- to northwest-southeast-striking sequence of volcanic rocks into a "Lower" and "Upper" Héva Formation. The tholeiitic, lower part of the section is located between Lac Malartic and the city of Val d'Or and is characterized by an assemblage of massive (magnetite rich), but predominantly pillowed (vesicular), basaltic flows. The calc-alkaline, upper part of the section is located east of Val d'Or and is composed of pillowed, but predominantly brecciated andesitic and rare dacitic flows interlayered with lenses of pyroclastic debris and minor basaltic flows (Imreh, 1984; Gaudreau et al., 1986). Noting that sedimentary intercalations were common, Imreh (1976) attributed the Héva Formation to a transition between the dominant volcanic regime of the "Malartic Group" and "Val d'Or Volcanic Complex", and the sediment- dominated regime of the Pontiac Group, further south (**Figure 2.2**).

2.2.2.4 Kewagama Group

The Kewagama Group (Gunning, 1937) is a northwest-trending metasedimentary belt located west of Kiena (**Figure 2.2**). It consists of a sequence of graywacke and mudstones interbedded with "minor horizons of conglomerate" and iron formation, and it is host to the

monzonitic Camflo stock and its gold mineralization. The lower section of the Kewagama Group is characterized by the presence of a polymictic conglomerate with pebble-size fragments of andesite, dacite and sericite schist, in contact with an iron formation (Trudel and Sauvé, 1992). The southern contact between the Kewagama Formation and Blake River Group is particularly complex (Trudel, 1990); it has been interpreted as an interdigitation of two concordant units by Dimroth *et al.* (1982), and as a transposed faulted contact by Tourigny and Hubert (1986). Single grains of detrital zircons from the Kewagama Group graywackes have yielded ages as young as 2687 ± 3 Ma (Davis, 1991), indicating a possible upper age limit of deposition at ca. 2687 Ma. However, the Camflo monzonite stock which cross-cuts the Kewagama sediments has been U-Pb zircon dated as ca. 2685 $\pm ^{7}$ Ma by Zweng and Mortensen (1989) and as 2683 ± 3 Ma by Jemielita *et al.* (1990). Accordingly, the timing of deposition of the Kewagama Group may be constrained informally between ***ca. 2687-2683 Ma.*** Sediments of the Kewagama Group have been compared to those of the Timiskaming Group (Couture, 1991; Mortensen, 1993) because they are cut by alkaline intrusions (i.e. Camflo monzonite and the Clericy syenite further west in the Rouyn-Noranda area), and because they show a dacitic pebble-bearing conglomerate at the base of the formation. However, Mueller and Donaldson (1992) have clearly contrasted the depositional environments of the Kewagama and Timiskaming Groups as deep-water facies rock association containing flysch-type deposits and fluvial to shallow-water marine sedimentary deposits, respectively. They also pointed out that younger alluvial-fluvial sedimentary sequences such as the Timiskaming (main phase at ca. 2681-2676 Ma, Corfu (1993), Mortensen (1993)), are preferentially deposited in older sedimentary basins such as that occupied by the Kewagama Group turbidites and resedimented conglomerates (ca. 2687-2683 Ma)(Dimroth et al., 1982; Corfu et al., 1991; Mueller and Donaldson, 1992). Their age, distinct plutonic and volcanic rock associations and contrasting conditions of deposition, indicate that the Kewagama and Timiskaming Groups are two sedimentologically different sequences.

2.2.2.5 Blake River Group

The easternmost part of the Blake River Group (Gunning, 1937; de Rosen-Spence, 1976; Dimroth et al., 1982; Péloquin et al., 1990; Péloquin et al., 1995; Péloquin et al., 1996), outcrops north of the Malartic gold camp (**Figure 2.2**) and stretches west to the Cadillac gold camp. Mineral deposits found at the eastern end of the Blake River Group are as economically important and diverse (VMS and Au deposits) as those found at the western end (i.e. VMS and Au deposits of the Noranda cauldron). Deformed and metamorphosed "pyritic" gold deposits occur at the Bousquet and Donald J. LaRonde (former Dumagami Mine) Mines, and intrusion-related gold mineralization occurs at the Doyon Mine and Mic Mac and Mouska deposits (Savoie et al., 1991; Marquis et al., 1992; Tourigny et al., 1992; Trudel and Sauvé, 1992; Tourigny et al., 1993; Belkabir et al., 1994; Hoy et al., 1994). In the Malartic area, the Blake River Group consists of a northwest-striking, steeply north-dipping and southerly overturned sequence of alternating basaltic-andesitic and rhyolitic flows of tholeiitic and calc-alkaline affinities. This sequence has been subdivided, from north to south, as follows: 1) a massive to pillowed tholeiitic flow (Mic Mac Mine), 2) a sodic quartz porphyritic rhyolite, 3) an andesitic blocky tuff (Doyon and Bousquet Mines) with minor quartz-muscovite schists (Doyon No. 1), and 4) a rhyodacitic to rhyolitic flow (Donald J. LaRonde Mine) (Trudel and Sauvé, 1992). The volcanic rock assemblage is perceived as the lateral extension of the bi-modal volcanic sequence of the "Eastern Sector", as defined by Péloquin *et al.* (1990), which overlies the central volcanic complex of the Noranda cauldron. On the basis of isotopic age dating of volcanic rocks apparently lower in the Blake River Group sequence (Rouyn-Noranda area) than those of the Malartic area, Mortensen (1987) and Corfu *et al.* (1989) have bracketed this episode of volcanism between ***ca. 2701-2698 Ma.*** According to Marquis and Hubert (1989), volcanic rocks of the Blake River Group are in fault contact with the metasedimentary rocks of the Cadillac Group to the south.

2.2.2.6 Cadillac Group

The Cadillac Group of Gunning (1937) and Gunning and Ambrose (1940), outcropping west of Kiena (**Figure 2.2**), is a complexly folded metasedimentary sequence composed predominantly of graywacke and pelitic schists (70 %), with lenticular intercalations of polymictic conglomerate, minor tuff, volcaniclastic rocks, sandstone and iron formation (Dimroth et al., 1982). A thin band of metasedimentary rocks situated east of Val d'Or, has been assigned to the Cadillac Group by Robert (1989) based on its lithological assemblage, magnetic map patterns (GSC, 1981) and the composition of its southernmost conglomeratic unit. This metasedimentary rock assemblage consists mostly of graywacke and siltstone, with less abundant mudstone, sandstone and clast-supported polymictic conglomerate. The latter is characterized by pebbles of feldspar porphyry (up to 70%) and by fragments of black chert and fuschite (Bouchard, 1980); Gorman, 1986 #368; Trudel, 1990 #303]. The magnetite-bearing iron formations are associated with chlorite schist zones hosting the Wood Cadillac and Central Cadillac Mines (Trudel and Sauvé, 1991). Preliminary isotopic U-Pb age determination of single zircons from the Cadillac Group graywackes, suggest an ***upper age limit of sedimentation as ca. 2688 ± 3 Ma*** (Davis, 1991) (**Table 7.3** and Regional Sequence of Events diagram in back pocket). Based on the occurrence of a granite pebble-rich conglomeratic unit and its distribution along the Cadillac Tectonic Zone, rocks of the Cadillac Group have been correlated with those of the Granada and LaBruère Formations, farther west in the Rouyn-Noranda area, and with the Timiskaming Group sediments of the Kirkland Lake area (Goulet, 1978; Dimroth et al., 1982; Couture, 1991). However, Mueller and Donaldson (1992) pointed out that, although lithologically similar and in proximity to a major east-trending fault (Cadillac Tectonic Zone), coarse-clastic and turbiditic sediments of the Cadillac Group are older (ca. 2700-2688 Ma) than the alluvial-fluvial Timiskaming-type sediments (ca. 2681-2676 Ma, Corfu (1993)).

2.2.2.7 Piché Group

The Piché Group (Gunning and Ambrose, 1940), outcrops predominantly west of Kiena (**Figure 2.2**), but has been traced to the Cadillac Tectonic Zone east of Val d'Or, by Robert (1989). It consists of a complexly folded sequence of graywackes, conglomerate lenses, pyritic chert, and graphitic schists interbedded with tholeiitic and andesitic basaltic volcanic flows in the Cadillac area (Trudel and Sauvé, 1992), and of a highly deformed rock sequence composed of hydrothermally altered and mineralized komatiitic and minor basaltic flows (now metamorphosed to talc-chlorite-carbonate schists), in the Malartic area (Sansfaçon and Hubert, 1990). The Piché Group is host to the former O'Brien, Thompson Cadillac, Pandora and Lapa Cadillac Mines of the Cadillac mining district, and the former, more economically important, Malartic Gold Fields, Barnat, East-Malartic, Canadian Malartic and Sladen Mines (Sansfaçon and Hubert, 1990; Trudel and Sauvé, 1992). The conglomeratic unit of the O'Brien Au-Ag-As mine (west of Cadillac), located approximately 60 metres south of the Cadillac Tectonic Zone, consists predominantly of pancake-shaped microporphyritic dacitic pebbles (Trudel, 1990; Trudel et al., 1992), indicating that volcano-sedimentary rocks of the Piché Group have been severely flattened in a non-rotational stress regime.

2.2.2.8 Trivio Group

The Trivio Group (Sharpe, 1968), located east of Kiena and south of the Val d'Or volcanic complex (**Figure 2.2**), is a structurally complex sedimentary-volcanic rock assemblage composed of coarse clastic sediments, turbidites, tholeiitic and calc-alkaline volcanic flows and pyroclastic rocks (Gaudreau et al., 1986). Sedimentary rocks consist of clast-supported polymictic conglomerate, graywacke, mudstone and iron formation, whereas volcanic and pyroclastic rocks consist of massive to pillowed magnesian, tholeiitic and andesitic basalts and andesites, graphitic andesitic crystal and lapilli tuff, respectively (Gaudreau et al., 1986). Rocheleau *et al.* (1990) renamed the Trivio Group of Sharpe (1968), the "Trivio Structural Complex" (see **Table 2.2**), which they characterized as a lithotectonic block based on

complex fault contact relations between various sedimentary and volcanic rocks of mixed origin.

2.2.2.9 Villebon Group

The metavolcanic Villebon Group (Vogel, 1972) outcrops east of Kiena and south of the "Trivio Structural Complex" (**Figure 2.2**). It consists of massive, pillowed and brecciated volcanic flows ranging from serpentinized komatiites, to Mg-rich (picritic) basalts, to tholeiitic basalts and andesites (Gaudreau et al., 1986). Rocheleau *et al.* (1990) have included the lithostratigraphic Villebon Group into the Villebon lithotectonic Domain (see **Table 2.2**), where it has been inferred to be stratigraphically below the Pontiac Group (Vogel, 1972; Gaudreau et al., 1986). To the north, stratigraphic relations between the Villebon Group and "Trivio Structural Complex" are obscured by their faulted contact (Rocheleau et al., 1990).

2.2.2.10 Pontiac Group

The metasedimentary Pontiac Group (Wilson, 1910), which is exposed south of the Kiena Mine and the Cadillac Tectonic Zone, consists of a sequence of turbiditic graywacke and argillite (90%), with minor monomictic and polymictic conglomerate, iron formation and graphitic schist (Dimroth et al., 1982; Mortensen and Card, 1993). Sedimentary rocks of the Pontiac Group form much of the northern part of the Pontiac Subprovince, but also occur extensively in the "Belleterre Volcanic Zone" farther south (Dimroth et al., 1982; MERQ-OGS, 1983). The northern belt of Pontiac Group sediments (**Figure 2.2**) is in contact with the granitic intrusion-, pegmatite- and paragneiss-complex of the "Decelles batholith" to the south (Rive et al., 1990), with the Grenville Front Tectonic Zone to the east, and the early Proterozoic Huronian sediments to the west (MERQ-OGS, 1983). The latter occupy a north-trending trough that may cover a major fault, juxtaposing the metasedimentary rocks of the Pontiac Group (east) with Abitibi volcanic rocks (west) (Kalliokoski, 1987). Thin ultramafic to mafic volcanic flows (chemically similar to those of the Dubuisson Formation)

are present at or near the inferred base of the sequence (see **Figure 2.2** and **Table 2.2**, Imreh (1976b); Rocheleau *et al.* (1990)). Monomictic conglomerate are composed of graywacke pebbles, whereas polymictic conglomerate contain volcanic, plutonic and sedimentary clasts (Mortensen and Card, 1993). Pontiac Group sediments are characterized by their higher grade of metamorphism than adjacent Abitibi greenstone belt rocks, ranging form their contact southward from the biotite zone of the greenschist facies, through garnet, hornblende, staurolite and sillimanite-kyanite zones of the amphibolite facies (Jolly, 1978). U-Pb dates on single detrital zircons by Gariepy *et al.* (1984) and Davis (1991), as old as ca. 3000 Ma and as young as 2686 ± 3 Ma, suggest that Pontiac sediments were derived mainly from erosion of Abitibi greenstone belt supracrustal rocks (< 2686 Ma), but also in part from older volcano-plutonic rocks (>2750 Ma, Davis, 1991). However, a recent study by Mortensen and Card (1993) suggests that, for the most part, this erosion occurred after 2683 ± 3 Ma, following volcanism in the Abitibi belt to the north (ca. 2720-2698 Ma), but coeval with volcanism in the Baby and Belleterre volcanic zones (ca. 2689-2682 Ma) further south in the Pontiac Subprovince.

2.2.3 Plutonic rocks

Based on their spatial, mineralogical, chemical and temporal characteristics, plutonic rocks of the Val d'Or-Malartic area have been subdivided by Rives (1990) and Robert (1990) into pre-orogenic, syn- to late-orogenic and post-orogenic suites in relation to volcanism, episodes of regional folding and faulting, and synmetamorphic planar fabrics. These respective plutonic suites are characterized below with special emphasis on intrusions of economic importance.

2.2.3.1 Pre-orogenic intrusions (ca. 2705-2700 Ma)

Pre-orogenic intrusions were emplaced during, or shortly after, volcanism (ca. 2705 Ma-2698 Ma) and before the onset of an early, pre-metamorphic regional folding and faulting event

(D_1) as defined by Dimroth *et al.* (1983b). They consist of irregular polyphase intrusions which lack a contact metamorphic aureole and which have been folded together with their enclosing volcanic and sedimentary rocks. They have been metamorphosed to the greenschist facies and commonly display a strongly developed regional foliation at their contact margins, which becomes progressively weaker toward the core of the intrusion complex. In the Val d'Or-Malartic area, pre-orogenic intrusions occur predominantly in the upper units of the stratigraphic sequence (Val d'Or and Héva Formations) and consist of two compositionally distinct suites: (1) a tholeiitic suite, including homogeneous and layered igneous bodies ranging in composition from gabbro, to diorite and granophyre, and (2) a calc-alkaline suite, including sill complexes and stocks, ranging in composition from granodiorite, to trondhjemite, and tonalite (**Figure 2.2**). The tholeiitic suite is represented by the gabbroic Siscoe stock (Tessier et al., 1990) and Vicour layered sill (gabbro to granophyre) (Sauvé et al., 1993), which are host to the Siscoe and Sigma #2 gold deposits, respectively (deposits 11 and 26 on **Figure 2.2**). The calc-alkaline suite is exemplified by the Bourlamaque metadiorite-trondhjemite ***sills*** (Campiglio, 1974; Campiglio and Darling, 1976; Taner and Trudel, 1989; Tessier et al., 1990; Jébrak et al., 1991; Morasse et al., 1996; Taner, 1996b), and by the porphyritic granodiorite (termed "C" porphyry) of the Sigma-Lamaque Mines. The composite Bourlamaque sills are dated as ***2700 ± 1 Ma***[5], whereas the Sigma Mine ***"C" porphyry*** is dated as ***2704 ± 2.5 Ma*** (Wong et al., 1991). The Bourlamaque intrusive complex contains many of the local gold deposits (**Figure 2.2**), including the Bras d'Or (Dumont), Ferderber (Belmoral), Perron, Sullivan and Wrightbar Mines (Belkabir, 1990; Tessier, 1990; Belkabir et al., 1993; Sauvé et al., 1993). Layered intrusions such as the Vicour and central sill of the Bourlamaque, display a well defined, in the case of the Vicour sill, and cryptic, in the case of the Bourlamaque sill, south-facing igneous layering (see **Figure**

---

[5] Taner and Trudel (1989) have also dated the Bourlamaque intrusion as 2710 (+4/-5) Ma. However, the age of 2700 ± 1 Ma is considered a more accurate age because the zircon fractions from the *main intrusion* analyzed by Wong *et al.* (1991) *are concordant*, whereas the zircon fractions from *ultramafic xenoliths* dated as 2710 (+4/-5) Ma by Taner and Trudel (1989) *are highly discordant* (see Wong *et al.* (1991), Taner (1996) and Morasse *et al.* (1996).

2.2; Campiglio (1976); Tessier (1990); Sauvé (1993)) which is structurally concordant with their co-magmatic and southerly-overturned, enclosing volcanic rocks. Mafic to felsic igneous layers of the Bourlamaque central sill have also been deformed by an S-shaped fold (**Figure 2.2**), suggesting that the south-facing layered sill must have been overturned before it was subjected to folding (Campiglio and Darling, 1976; Morasse and Wasteneys, 1994).

2.2.3.2 Syn- to late-orogenic intrusions (ca. 2694-2680 Ma) - Val d'Or plutonic belt

Before precise U-Pb zircon dates were obtained on several intrusions of the Val d'Or-Malartic area, the latter were informally classified as syn-orogenic calc-alkalic intrusions and late-orogenic alkalic intrusions based on chemical composition and deformation features recorded in the rocks (Robert, 1990; Sauvé et al., 1993; Taner, 1996a). Syn- to late-orogenic intrusions typically form small elliptical plutons and dike swarms that have been commonly micro-fractured and mineralized, variously affected by folds, faults and shear zones, and locally transposed by the dominant northwest-southeast to east-west regional foliation (S_2) (Jenkins et al., 1989; Sansfaçon and Hubert, 1990; Morasse et al., 1993; Sauvé et al., 1993; Couture et al., 1994). Small plutons are accompanied by metamorphic contact aureoles of limited lateral extent (< 3 km) (e.g. Bevcon and Camflo stocks) that appear to have been retrograded to greenschist metamorphic assemblages (e.g. Camflo stock) (Sauvé et al., 1993; Zweng et al., 1993; Powell et al., 1995a). Massive to foliated felsic dikes are commonly emplaced in fault planes sub-parallel to axial planes of early F_1 folds and display narrow chilled margins (Sansfaçon and Hubert, 1990; Zweng et al., 1993; Morasse et al., 1995a). These observations suggest that syn- to late-orogenic intrusions were emplaced after the tilting, folding and faulting of the volcanic and sedimentary strata during an early episode of deformation (D_1), but before the onset of the main regional deformation event responsible for the development of the regional syn-metamorphic foliation (D_2, S_2) (Sansfaçon and Hubert, 1990; Sauvé et al., 1993; Morasse and Wasteneys, 1994; Morasse et al., 1995b).

Syn- to late-orogenic intrusions predominantly occur at shallow depth in the local gold mines.

They are distributed along an east-west curvilinear trend subparallel to, and partly coincident with, the Malartic and Cadillac tectonic zones (**Figure 2.2**). The array of variously mineralized and deformed intrusions is herein referred to as the "Val d'Or plutonic belt". The belt is composed of a prominent northern segment comprised of intrusions located north of the Malartic-Cadillac tectonic zones, separated from a cluster of dike swarms and small stocks straddling the Malartic tectonic zone to the southwest by a wedge of sedimentary rocks belonging to the Kewagama and Cadillac Groups (**Figure 2.2**). Intrusions from the northern segment of the Val d'Or plutonic belt cut across the southerly-overturned volcanic rocks of the Dubuisson, Jacola, Héva and Val d'Or Formations and Bourlamaque sills (Camflo to Bevcon Mines), whereas the Malartic cluster of intrusions cut the southerly-overturned volcanic and sedimentary strata of the Piché and Pontiac Groups, respectively (Malartic to Quebec Explorer Mines). The Val d'Or plutonic belt is composed of a calc-alkalic suite of intrusions comprised of diorite, granodiorite, and tonalite dated as ca. 2694-2685 Ma (e.g. Sigma Mine feldspar porphyry dikes and Kiena Mine intermineral dikes), and of a more alkalic suite of intrusions comprised of monzo-syenite dated as ca. 2685-2680 Ma (e.g. Camflo mine monzonite stock) (see **Table 6.2** and Regional Sequence of Events chart in back pocket). Malartic intrusions have not been directly dated, but their post-$D_1(S_1)$ and pre-$D_2(S_2)$ time of emplacement (Sansfaçon and Hubert, 1990) suggests that they are similar in age to Kiena's albitite and intermineral porphyry dikes (see Chapters 6, 7 and 8).

All the intrusions of the Val d'Or plutonic belt are metamorphosed to the greenschist facies (Trudel and Sauvé, 1992; Sauvé et al., 1993; Taner, 1996a) and overprinted by regional penetrative structures (see Chapter 8). Since regional peak metamorphic conditions are estimated to have occurred in the interval 2680-2660 Ma (Powell et al., 1995a), the upper age limit of regional synmetamorphic deformation of 2680 Ma is thus interpreted as the possible minimum age of late-orogenic plutonism in the Val d'Or plutonic belt.

The Val d'Or plutonic belt is interpreted as a deep-seated regional fault zone for the following reasons: 1) granitoid stocks and dikes were emplaced into folded strata along a series of

discrete fractures predominantly developed at lithological contacts (see Chapter 8), 2) the array of intrusive bodies parallels a regional fault lineament coinciding with the Abitibi-Pontiac terrane boundary suggesting a tectonic control for the emplacement of the syn- to late-orogenic intrusions and, 3) xenocrystic zircons from Kiena's intermineral dikes and magmatic zircons from the neighbouring Snowshoe stock are of similar age (see Chapter 6), suggesting that these individual intrusions may share a common magmatic source concealed at depth (Morasse et al., 1993).

2.2.3.3 Post-orogenic intrusions (ca. 2643-2632 Ma)

Post-orogenic plutons commonly form large, irregular zoned intrusions, accompanied by amphibolite-grade metamorphic aureoles which overprint the regional east-west to northwest-southeast S_2 foliation (Feng and Kerrich, 1991a; Sutcliffe et al., 1993; Powell et al., 1995a). Post-orogenic intrusions thus post-date the main regional synmetamorphic D_2 deformation (ca. 2680-2660 Ma, Powell *et al.* (1995a)). They are more abundant in the metasedimentary Pontiac Subprovince than in the Abitibi greenstone belt, where they are represented by the Preissac-Lacorne batholith (**Figure 2.2**) (Boily et al., 1990; Powell et al., 1995a; Bédard and Ludden, 1997). Post-orogenic intrusions commonly range in composition from an outer muscovite monzogranite to an inner biotite-muscovite monzogranite cut by rare element- and molybdenum-bearing pegmatitic dikes (Dawson, 1966; Boily et al., 1989; Boily et al., 1990; Rive et al., 1990; Bédard and Ludden, 1997). The outer monzodiorite-monzonite-granodiorite and inner garnet-muscovite granite intrusive phases of the Lacorne batholith are dated as ca. 2675 ± 24 Ma and ***2643 ± 4 Ma***, respectively (Feng and Kerrich, 1991c) (see **Figure 2.2**, **Table 6.2** and Regional Sequence of Events chart in back pocket).

Northeast- and east-west-trending Proterozoic diabase dikes are the youngest post-orogenic intrusions in the area. The dikes, which average 30 to 80 metres in width, cut primary volcanic, igneous and sedimentary structures, fold axes (F_1, F_2), schistosities (S_1, S_2), fault zones, gold orebodies, as well as the earlier monzonite-granite post-orogenic intrusions. They

are unaffected by regional greenschist to amphibolite metamorphism, and commonly contain unaltered olivine, augite and labradorite (Trudel, 1990). Northeast-trending Preissac and Lac de Montigny diabase dikes are probably similar in age to northeast-trending Abitibi dikes of Lake Abitibi, near Munro Township to the west, dated by Hanes and York (1979) as ca. 2150 ± 25 Ma.

2.2.4 Structures

Polyphase deformation and the alternation of large, low-strain rock domains with regionally extensive but narrow high-strain domains, characterizes the structural style of the Val d'Or-Malartic region. The orientation and geographic distribution of structures related to the deformation history of this area are ascribed to two main folding-faulting episodes: an early pre-metamorphic folding event, designated as D_1, followed after a 17-20 m.y. hiatus by a multiphase dynamothermal event accompanied by greenschist-lower amphibolite facies metamorphism, designated as D_2 (Dimroth *et al.*, 1983). The chronology of these regional deformation events is summarized in **Table 2.3** and charted in a Regional Sequence of Events diagram located in one of the back pockets accompanying this thesis.

D_1 is represented by northeast-southwest, locally southerly-facing recumbent F_1 folds, observed in weakly strained sections of the Cadillac and Pontiac Group metasediments located north and south of the Malartic Tectonic Zone (**Figure 2.2**; Sansfaçon and Hubert (1990)). Locally, F_1 folds are cut by an east-west- to northwest-southeast-striking and shallowly to moderately north-dipping (20-60°) axial planar S_1 schistosity (**Table 2.3**). The latter is commonly parallel to the set of brittle faults hosting the felsic dykes and sills encountered in the Malartic Tectonic Zone gold mines (Sansfaçon and Hubert, 1990). The most important F_1 fold structure of the area, the La Motte-Vassan anticline (**Figure 2.2**), was recognized just north of Kiena by Imreh (1984) and Dimroth *et al.* (1983a) based on polarity reversals observed in the ultramafic La Motte-Vassan Formation and the presence of a crenulated northeast-striking S_1 flow cleavage defined by chlorite in the hinge zone of the

Table 2.3 Chronology of deformation and metamorphic

Time (Ma)	Deformation event	Folds	Planar and linear fabrics	
ca. 2700-2694	**D_1**	NE-SW southerly recumbent F_1 folds	**S_1** N240-280, 20-60N (N315-340, 20-70 N) Brittle fractures // to **S_1** Felsic intrusions // **S_1**	
ca. 2694-2680				
ca. 2680-2645	**D_2, M_2 (main phase)** Peak metamorphic conditions reached at ca. 2660 Ma	Refolded F_1 folds into upright, bedding-parallel EW to NW-SE **F_2** folds and asymmetric "S" or "Z"-shaped **F_2** folds (Camflo and Kiena deposits, Bourlamaque central sill)	**S_2** EW, 80-85 N Synmetamorphic: chlorite, seritcite, biotite **L_2** N085-090, 30-45 E (mineral or down-dip streching lineation)	**M_2-** Gr Sta Po
? > 2645	Incremental phase of **D_2**	Intrafolial sheath folds **F_3** asymmetric z-folds of S_2 shallowly-plunging E , W. or doubly plunging	EW steeply north-dipping S_2schistosity folded by F_3 S_3 NE-SW, 60-80 SE	
ca. 2645-2632				wi or
ca. 2150 ± 25				

* *See Table 2.6 and Chapter 8 for more detail of standard setting of gold*

and metamorphic events in the Val d'Or-Malartic area

ear	Metamorphism	Gold*	Locality / References
50N 70 N) o S_1 / S_1		Syn- to post-S_1 but pre-$F_2(S_2)$	**Malartic, Val d'Or** Sanfaçon and Hubert, 1990 a, b; Robert and Brown, 1986; Wong et al. 1991; Morasse et al., 1995
	M_1- Local thermal metamorphism District-wide calc-alkalic and alkalic plutonism: small stocks accompanied by contact metamorphic aureoles	Syn-M_1 pre-$D_2(S_2)$	**Bevcon and Camflo deposits** Sauvé et al., 1993; Zweng, 1993
N ic: iotite 45 E -dip on)	M_2- Regional dynamothermal metamorphism Greenschist to amphibolite facies in rocks assemblages of the Abitibi belt Staurolite to garnet-sillimanite zones in rock assemblages of the Pontiac Group Possible regional subhorizontal isograd (?)	Pre-S_2^* Syn-S_2^* Post-S_2^*	**Malartic, Val d'Or** Imreh, 1984; Gaudreau et al., 1986; Hanes et al., 1989; Sansfaçon and Hubert, 1990; Robert, 1990; Claoué-Long et al., 1990; King and Kerrich, 1993; Wilkinson et al., 1993; Powell, 1995
dipping / 3 0 SE		Pre-S_2^* Pre-F_3^*	**Cadillac and Malartic** **Tectonic Zones** Sansfaçon and Hubert, 1990; Robert, 1990; Robert et al., 1990; Robert et al., 1994
	M_3- Local thermal metamorphism S-type granites with contact metamorphic aureole overprint onto earlier greenschist-amphibolite facies regional metamorphic assemblages		**2 micas granite phase** **of the** **Lacorne batholith** Feng and Kerrich, 1991; Powell et al., 1995 a
	M_4- Shield-wide thermal event NE-trending Proterozoic diabase dikes		**Preissac dikes** Hanes and York, 1979

fold. The early, pre-metamorphic D_1 deformation event is postulated to have occurred in the interval 2700-2694 Ma (**Table 2.3**; Regional Sequence of Events chart in back pocket). The upper age is the U-Pb zircon age of the pre-D_1 Bourlamaque sills (Campiglio and Darling, 1976; Wong et al., 1991), whereas the lower age is the U-Pb zircon age of the post-D_1 dioritic dikes of the Sigma-Lamaque mines (Robert and Brown, 1986a; Wong et al., 1991).

D_2 is represented by refolded F_1 folds into upright, bedding-parallel, east-west to northwest-striking isoclinal F_2 folds, observed north and south of the Cadillac and Malartic Tectonic Zones (Dimroth et al., 1983a; Imreh, 1984), and by map-scale asymmetric "S"- and "Z"-shaped F_2 folds, observed in the Pontiac Group metasediments of the Malartic Tectonic Zone (Sansfaçon and Hubert, 1990) and at the Camflo-Malartic Hygrade and Kiena Mines west of Lac de Montigny, respectively (Imreh, 1984; Sauvé and Makila, 1987; Robert, 1990; Morasse et al., 1995b) (**Figure 2.2** and **Table 2.3**). F_2 folds are accompanied by the development of an east-west to southeast-striking and northerly-dipping syn-metamorphic axial planar S_2 schistosity, generally defined by the alignment of chlorite, sericite and biotite, overprinted by a steeply-plunging elongation lineation (Dimroth et al., 1983a; Robert, 1990). As clearly stated by Dimroth *et al.* (1983a), S_2 is a regional schistosity, and most penetrative strain is related to it. Its intensity is a function of both, regional rock strain and rock type; S_2 is a crenulation cleavage in lower strained, incompetent rocks, where the S_1 schistosity is present (Sansfaçon and Hubert, 1990), and becomes increasingly more penetrative in highly strained and altered rocks (Sauvé et al., 1993; Powell et al., 1995a). West of Kiena, in the Malartic area, Babineau (1983) observed an early northwest-southeast schistosity locally overprinted by "Z" folds and their east-west axial planar schistosity, but Sauvé *et al.* (1993) indicated that cross-cutting relationships between schistosities are ambiguous and that in most cases variations in orientation from east-west to west-northwest in a single schistosity are observed. They suggested that the change in orientation of the regional structural grain (S_0, S_2) and the complex fold patterns observed west of Val d'Or could be related to the presence of a large number of syn-orogenic intrusions located about Lac de Montigny. The S_2 schistosity is locally deformed by asymmetric north-easterly plunging folds of S_2 with related S_3 crenulation

cleavages as commonly observed in the Cadillac Tectonic Zone (see below). Synmetamorphic D_2 deformation across the southern Abitibi belt is bracketed between 2677 and 2643 Ma (Powell et al., 1995a) (**Table 2.3**; Regional Sequence of Events diagram in back pocket). The upper age is the U-Pb zircon age of a post-D_1 and pre-D_2 felsic dike (Corfu et al., 1991), whereas the lower age is the U-Pb zircon age of the post-D_2 garnet-muscovite intrusion of the Lacorne batholith (Feng and Kerrich, 1991c).

In the Val d'Or-Malartic area, early F_1 folds and related faults have been overprinted by ***two types*** of ***shear zones***: ***"regional shear zones"*** and ***"deposit-scale shear zones"*** (**Figure 2.2**). Examples of regional shear zones include the Malartic and Cadillac Tectonic Zones (**Table 2.4**), whereas deposit-scale shear zones are represented by the Norbenite, Marbenite and "K" zones of the Norlartic, Marban and Siscoe Mines, respectively (**Table 2.5**). The Malartic and Cadillac Tectonic Zones are two segments of a continuous northwest-striking and steeply north-dipping structure, cutting across the boundaries of the Cadillac, Pontiac, and Piché Groups to the west, and confined to the Piché and Cadillac Groups to the east (Gunning and Ambrose, 1940; Imreh, 1976b; Robert, 1989; Robert, 1990; Sansfaçon and Hubert, 1990). Recent LITHOPROBE seismic reflexion surveys across the Cadillac Tectonic Zone further west, in the Rouyn-Noranda area (Lines 14, 14a, 14b), display this major regional fault zone as the trace of a "non-reflective" plane dipping approximately 70° north, down to a depth of 10-12 km, cross-cutting the numerous shallowly north-dipping reflectors north and south of it (Green et al., 1990; Clowes, 1993). At surface, the Malartic Tectonic Zone is bound to the north and south by the Malartic and Sladen Faults, respectively, and consists of three sets of brittle-ductile faults oriented at N280°, N320°, and N305,° and a fourth minor set oriented at N065°, that have affected the gold-bearing volcanic, sedimentary and intrusive rocks confined to it (see **Table 2.4**)(Sansfaçon and Hubert, 1990). Primary mineral assemblages are metamorphosed to upper greenschist- or lower amphibolite-facies assemblages and form numerous anastomosing lozenge-shaped, high-strain rock domains cut by the brittle-ductile faults. Within the Malartic Tectonic Zone, gold mineralization occurs in association with altered and deformed bodies of diorite and monzonite and their enclosing mafic and ultramafic schists or sedimentary rocks. According to Sansfaçon and Hubert (1990), most of the gold recovered from the Malartic camp gold mines originated from schists

Table 2.4 Regional-scale "shear-zones" of the

Gold-bearing deformation zones	*Attitude Relative sense of motion*	*Dimensions*	*Faults and Fractures Folds and Schistosities**	*Host rocks*
Malartic Tectonic Zone *(Malartic Mines) See Fig. 2.2: deposits 1,2,3*	*N320 to N280 70-85°N*	*900 m x 7.0 km depth: 10 km*	*1. Regional F_1 folds (south-facing recumbent folds)* *2. S_1 schistosity: N315-340 20-60°NE; N240-280 20-60°NW* *3. Felsic intrusions emplaced in S_1 // fractures* *4. "Cooling joints" in monzonite* *5. S_1 // auriferous veins* *6. Auriferous stockwork veins (Qz-Cb-Py-Au)* *7. Folds in gold-bearing veins, Sladen Mine orebody (fold plunging 45-50°E)* *8. S_2 schistosity: N110 90* *S_2 // faults* *Dextral and senestral strike slip faults (N270, N240)* *Malartic fault: N260-280 75°N* *Sladen fault: N090-100 70-90°S* *Baenat fault: N305-320 80°NE* *Other faults: N065 70°SE* *9. Late fractures: N030, N070, N090*	*Cadillac, Piché, Pontiac Groups* *Tc-Chl-Cb schis* *Deformed mafic and felsic intrus*
Cadillac Tectonic Zone *(Orenada Zone 4 and Zone 2) see Fig. 2.2: deposit 19 and Fig. 2.3*	*N290 70-80° N Normal (?); Dextral trancurrent shear (1)*	*1 km x 200 km depth: 10-12 km*	*1. Cadillac tectonic zone(?): N110 70-80°N (Abitibi / Pontiac Terrane boundary)* *2. Regional F_1 folds (?) S_1 (?)* *3. "Porphyritic felsic schist" (?): (Ab-Qz) - possible porphyry dikes?* *4. "Concordant" veins: Tm-Ab-Qz veins with auriferous Aspy halos (see Fig. 3)* *5. Regional isoclinal F_2 folds: S_2 :N090-110 80°N; Boudins and Qz tension veins across auriferous "concordant" veins (N-S compression across CTZ)* *6. Assymetric Z-folds: zone 2 and zone 4 orebodies plunge of Z-fold = plunge of orebodies: 45°E or W; Assymetric intrafolial (S_2) F_3 folds of boudinaged auriferous veins (plunge: 30-35°E); S_3 (N270 55°S) spaced cleavage axial planar to F_3 folds. (Dextral transcurrent movement across the CTZ).* *7. Late strike-slip faults: N120 85°SW; N250 70°NW*	*Cadillac and Pic Groups* *Tc-Chl-Cb schist* *Chl-Ab-Cb-Qz sc* *Ser-Chl-Qz-Ab-C schist* *Ser schist* *"Porphyritic (Ab- felsic schist"*

Key: Ab: albite; Au: gold; Bo: biotite; Cb: carbonate; Cc: calcite; Chl: chlorite; Cpy: chalcopyrite; Il: ilmenite; Po: pyrrhotite; QFP: quartz-fe

Sigma - Lamaque Mines 'shear' and 'flat' veins: Qz-Tm-Cb ± Sch-Py-Cpy-Po-Au

* *Structures are listed in relative chronological order based on cross-cutting relationships documented by the authors cited in the reference lis*

le "shear-zones" of the Val d'Or-Malartic area

	Host rocks	Type of intrusions and their structural attributes	Au mineralization in relation to intrusions, fractures and planar fabrics	Reference
mbent folds) *y* *ractures* *Py-Au)* *Mine orebody* *s (N270, N240)*	*Cadillac, Piché, Pontiac Groups* *Tc-Chl-Cb schists;* *Deformed mafic and felsic intrusions*	*Dismembered, folded and foliated sills and dikes including: diorite, lamprophyre, monzonite, albitite, and pegmatite*	*Episodic* *1. Post - F_1 (3)* *2. Post- diorite dikes (3)* *3. Pre- and post- monzonite porphyry dikes (5)* *4. Syn- to post- S_1 but pre- S_2 (3,5)* *5. Pre- folds (Sladen Mine) (3,5)* *6. Pre- S_2 and S_2 // faults (3)* *7. Pre- MTZ faults and late fractures (3)* *(2): Reference number*	*1. Gunning & Ambrose, 1942* *2. Eakins, 1962* *3. Sansfaçon & Hubert, 1990* *4. Greene et al., 1990* *5. Trudel & Sauvé, 1992*
80°N *s with* *)-110 80°N; auriferous across CTZ)* *t orebodies s: 45°E or W; f boudinaged* *l planar to ment across*	*Cadillac and Piché Groups* *Tc-Chl-Cb schist* *Chl-Ab-Cb-Qz schist* *Ser-Chl-Qz-Ab-Cb schist* *Ser schist* *"Porphyritic (Ab-Qz) felsic schist"*	*Dismembered porphyry dikes(?) transposed along S_2 (main ore zone at Orenada zone 4)*	*1. Post- CTZ (1)* *2. Post- F_1 and S_1 (?)* *3. Post- porphyry dikes (?) (2)* *4. Pre- F_2 and S_2 (5)* *Pre- assymetric Z-fold (2)* *Pre- intrafolial F_3 fold and S_3 (2)* *5. Pre- strike-slip faults (2)* *(2): Reference number*	*1. Robert, 1984* *2. Robert et al., 1990* *3. Robert, 1990* *4. Greene et al., 1990* *5. Robert et al., 1994* *(see also Figure 2.3)*

ite; Po: pyrrhotite; QFP: quartz-feldspar-porphyry; Qz: quartz; Sch: scheelite; Stwk: stockwork; Tc: talc; Tm: tourmaline

he authors cited in the reference list.

Table 2.5 Deposit-scale "shear zones" across the Val d

Gold-bearing deformation zones	*Attitude Relative sense of motion*	*Dimensions*	*Faults and Fractures Folds and Schistosities**	*Host rocks*
Callahan Mine *see Figure 2: deposit 8*	*N270 60-80°N (Main)* *Sigmoidal shear zones:* *N290 60-80°N* *N270 60-80°N*	*30 m x 220 m* *depth 285 m*	*1. Regional F_1 folds (?) S_1 (?)* *2. S_1 // fractures (?)* *3. Diorite, tonalite - trondhjemite dikes: N040 90° (?)* *4. Banded Qz-Tm-Py-Au veins:* *Sigmoidal folds in auriferous veins* *(N225 75°NW and N090 90°)* *5. Tonalite - trondhjemite dikes* *Dismembering of mineralized dikes by shear zones:* *N290 60-80°NE* *N315 65-80°N*	*NE quartz-diorite dil (ore host Callahan zone 4)* *Dubuisson Fm* *Komatiite / tholeiite*
Norbenite (Norlartic Mine) *see Figure 2: deposit 6*	*N300 60°NE* *Normal, dextral (2,3)* *Reverse, dextral (6)*	*500 m x 3 km (8 km)* *depth: 300 m*	*1. Regional F_1 folds (?) S_1 (?)* *2. S_1 // fractures (?)* *3. Microdiorite (albitite?) dike swarm: N300 60°NE* *4. Auriferous stockwork veins Cb-Qz-Ab-Py-Cpy* *5. Tonalite dikes: N300 60°NE* *6. NE- to E- plunging S-fold of North Zone and Z-fold of Main ore zone* *Regional S_2 schistosity (?)* *7. Qz-Tm-Py-Au veins (?)* *8. Late faults: N220 80°NW, N090 50-60°S, N270 80°N*	*Chl-Cb-Ab-Py-Po-Cpy-Bo schist* *(main ore zone)* *Jacola Fm* *Komatiite / tholeiite*
Marbenite (Marban Mine) *see Figure 2: deposit 7*	*N310-to N270 70°NE (Z-fold)* *Dextral (2)*	*300 m x 370 m* *depth: 275 m*	*1. Regional F_1(?), S_1(?)* *2. Concealed intrusion (magnetic surveys) 100 m north of Marban Mine shaft (?)* *3. Cb-Qz-Au stockwork veins* *4. Qz-Cb-Py-Po-Au stockwork veins* } *(?)* *5. Regional S_2(?) N270-285 75°N* *6. Marbenite shear zone (MSZ)* *7. F_2 Z-fold of MSZ: N310 to N270 70°NE* *F_3 Z-fold of S_2* *En echelon disposition of 'C'-'L'-'J'-'F'-'D' ore zones (?)*	*Chl-Cb-Py-Po-Il-Bo schist* *Jacola Fm* *Komatiite / tholeiite*

Key: Ab: albite; Au: gold; Bo: biotite; Cb: carbonate; Cc: calcite; Chl: chlorite; Cpy: chalcopyrite; Il: ilmenite; Po: pyrrhotite; QFP: quartz-feldsp

Sigma - Lamaque Mines 'shear' and 'flat' veins: Qz-Tm-Cb ± Sch-Py-Cpy-Po-Au

* *Structures are listed in relative chronological order based on cross-cutting relationships documented by the authors cited in the reference list.*

zones" across the Val d'Or-Malartic area

	Host rocks	Type of intrusions and their structural attributes	Au mineralization in relation to intrusions, fractures and planar fabrics	Reference
40 90° (?) r zones:	NE quartz-diorite dike (ore host Callahan zone 4) Dubuisson Fm Komatiite / tholeiite	Z-fold Callahan Zone 1 intrusion (diorite - tonalite - trondhjemite) S-fold in post-ore dike (zone 4) (1)	1. Post- F_1 (?), S_1 (/) 2. Post- S_1 // fractures (?) 3. Post- felsic intrusions (1,2,3) 4. Pre- sigmoidal folds of auriferous veins and orebodies (3) 5. Pre- shear zones dismembering orebodies (1) (1): Reference number	1. Beaudoin et al., 1987 2. Jenkins et al., 1989 3. Sauvé et al., 1993
0 60°NE -Cpy and N270 80°N	Chl-Cb-Ab-Py-Po-Cpy-Bo schist (main ore zone) Jacola Fm Komatiite / tholeiite	Z-fold microdiorite (Albite?) Main ore zone, North zone (4,5) Foliated, intermineral tonalite dikes (2692±2 Ma)	Episodic 1. Post- F_1 (?), S_1 (?) 2. Post- S_1 // fractures (?) 3. Post- microdiorite (albitite?) dikes but pre- tonalite dike (5,6) 4. Pre- NE-plunging S-fold (North Zone) and Z-fold (Main ore zone) S_2 schistosity (4,5) 5. Post- tonalite dikes (5) (Qz-Tm-Cb-Py-Au veins) 6. Pre- faults (1) (1): Reference number	1. Mannard, 1986 2. Trudel and Sauvé, 1989 3. Lebel, 1989 4. Sauvé et al., 1993 5. Pilote et al., 1993 6. Desrochers et al., 1993 7. This study
100 m D'	Chl-Cb-Py-Po-Il-Bo schist Jacola Fm Komatiite / tholeiite	Concealed intrusion 100 north of Marban Mine shaft	Episodic 1. Post- F_1 (?), S_1 (?) 2. Post- S_1 // fractures (?) 3. Post- intrusion (?) 4. Pre-, syn-, post- S_2 (?) 5. Pre-, syn-, or post- Marban shear zone (?) (1): Reference number	1. Méthot and Trudel, 1987 2. Sauvé et al., 1993

; Po: pyrrhotite; QFP: quartz-feldspar-porphyry; Qz: quartz; Sch: scheelite; Stwk: stockwork; Tc: talc; Tm: tourmaline

e authors cited in the reference list.

Table 2.5 continued...

Gold-bearing deformation zones	*Attitude Relative sense of motion*	*Dimensions*	*Faults and Fractures Folds and Schistosities**	*Host rocks*
'K' Zone *(Siscoe Mine)* *see Figure 2: deposit 11*	*N295 80°NE* *Normal, senestral (3)* *Reverse, vextral (1,2,5,6)*	*20 m x 1.5 km (5 km)* *depth: 750 m*	*1. Regional F_1 folds (?), S_1 (?)* *2. S_1 // fractures (?)* *3. Quartz gabbro Siscoe stock or sill(?): N290 70°N* *4. **Main ore zone** and Horse Tail zone: Qz-<Tm-<Py-dark native Au from N015 60°SE to N045 to N090 45°S* *Siscoe Vein: from N015 to N070 to N090 35-80° S-SE* *5. **Albitite dikes: N225 85°NW (Siscoe stock)*** *N290 80°NE ('K' zone)* ***Andesite dike: N360 75°E (Siscoe stock)*** *Diorite dike: N260 40°NW* *Feldspar porphyry dikes: N290 80°NE ('K' zone)* *6. **'C' vein (N215 40NW)** and veins N °27, 608, 610: Qz-Tm-Py < Sch or Tm-Qz-Py < Sch, pale native Au* *7. Post-'C' vein carbonate veins* *8. Regional F_2 NW-SE fold and coeval **S_2 schistosity (N285-290° 90°)*** *Transposition of Siscoe stock, Main Ore Zone/Horse Tail Zone, Albitite dike and 'C' vein(?) into **'K' Zone: N295 80°NE*** *9. 'K' Zone boudins of albitite dikes - folds and deformation of auriferous quartz veins chlorite stringer veins(?)*	*Tc-Chl-Cb-Ab schist* *Dubuisson Fm Komatiite/tholeiite* *Actinolite schist* *Sericite schist* *Microdiorite, feldspar porphyry, albitite and dioritic dikes*
Sigma Mine North and South Shears *Lamaque Mine Thrust faults* *see Figure 2: deposits 17, 18*	*N265 85°N Normal Sigma Mine 'shear veins': reverse* *Lamaque Mine thrust faults: (host to 'shear veins') N270 20-70°S*	*2 m x 1.5 km depth: 1-2 km* *Sigma Mine 'shear veins': 2-9 m x 600 m depth: 200-1800 m* *Lamaque Mine 'shear veins': 2-9 m x 600 m depth: 300m*	*1. Porphyritic diorite: "C" porphyry 2704±2 Ma* *2. Regional F_1 folds but S_1 (?)* *3. S_1 // fractures (?)* *4. Feldspar prophyry dike swarm: "G" dikes, 2694 Ma* *5. QFP dikes (Lamaque Mine): N300 to N270 to N300* *6. Diorite-tonalite plugs (Lamaque Mine): 2683±3 Ma* *7. "Shear" veins: N085-092 70-75°S Qz-Tm-(Cb-Chl-Py-Po-Sch-Au) veins "Flat" veins: N180-194 10-33°W Qz-Tm or Tm-Qz (Cb-Chl-Py-Po-Sch-Au) veins "Dike stringer" veins: N085 75°S 'en echelon' crack-and-seal Qz-Tm veins* *8. Intermineral (?), tourmaline-cemented breccia (Sigma)* *9. "Shear" veins (Sigma)* *10. EW Regional S_2 schistosity axial planar to buckled "Flat" veins (see Fig. x); Vertical extension and boudinage along sub-vertical "shear" veins; EW schistosity in diorite-tonalite plug, foliation in intermineral (?) tourmaline breccia; Z-fold, QFP dikes (Lamaque); F_2 fold of 'shear' vein with axial-planar EW spaced cleavage (Lamaque); North and south shears* *11. Late strike-slip and oblique-slip faults: N265 85°N, N245 40°NW*	*Porphyritic diorite ('C' porphyry)* *Val d'Or Fm andesite* *Feldspar porphyry dike swarm ('G' dikes)*

Key: Ab: albite; Au: gold; Bo: biotite; Cb: carbonate; Cc: calcite; Chl: chlorite; Cpy: chalcopyrite; Il: ilmenite; Po: pyrrhotite; QFP: quartz-feldspar-

Sigma - Lamaque Mines 'shear' and 'flat' veins: Qz-Tm-Cb ± Sch-Py-Cpy-Po-Au

* *Structures are listed in relative chronological order based on cross-cutting relationships documented by the authors cited in the reference list.*

	Host rocks	Type of intrusions and their structural attributes	Au mineralization in relation to intrusions, fractures and planar fabrics	Reference
N290 70°N Qz-<Tm-<Py- 045 to N090 45°S 90 35-80° S-SE stock)) ck) E ('K' zone) 7, 608, 610: pale native Au S, schistosity ore Zone/Horse) into 'K' Zone: ds and s	Tc-Chl-Cb-Ab schist Dubuisson Fm Komatiite/tholeite Actinolite schist Sericite schist Microdiorite, feldspar porphyry, albitite and dioritic dikes	Foliated Siscoe Stock (quartz gabbro) Deformed (boudinaged, foliated) intermineral dikes: microdiorite, feldspar porphyry, albitite and diorite dikes	Episodic 1. Post-F_1 (?), S_1 (?) 2. Post-S_1 // fractures (?) 3. Post-Siscoe stock or sill but pre-albitite, andesite, diorite, and feldspar prophyry dikes (4,5,7,8) 4. Post-albitite, andesite, diorite and feldspar porphyry dikes (4,5,7,8) 5. Pre-S_2 (8) 6. Pre-'K' Zone (1) Partly syn-'K' Zone (?) (7) (1): Reference number	1. Moss, 1939 2. Asbury, 1942 3. Hawley, 1942 4. Auger, 1947 5. Trudel, 1985 6. Tessier et al., 1990 7. Sauvé et al., 1993 8. Pilote et al., 1993
04 ±2 Ma ikes, 2694 Ma N270 to N300): 2683±3 Ma -Au) veins ins d breccia (Sigma) nar to buckled ng sub-vertical g, foliation in nar EW spaced s:	Porphyritic diorite ('C' porphyry) Val d'Or Fm andesite Feldspar porphyry dike swarm ('G' dikes)	Overturned and foliated 2704± 2 Ma porphyritic diorite (2,4,5) 2694±2 Ma EW feldspar porphyry dike swarm // S containing fractured and deformed auriferous Py with Cb-Qz-Au pressure shadows(3) Sigma Mine Boudinaged 'shear' veins(6) N-S horizontal stylolitic peaks in 'shear' veins (6) Buckling of 'flat' veins (3,6) Recrystallized Au-bearing Py (3) Lamaque Mine Z-folded QFP dikes (2,4) (younger than 'G' dikes, older than 'Main plug') Schistose 2683±3 Ma (2,4) 'Main diorite-tonalite plug' Z-folded 'shear veins' N°1,13,39 cross-cutting 'Main plug' exhibiting spaced cleavage and stylolites (4)	Episodic 1. Post-F_1 folds (S_1 ?) (3) 2. Post-porphyritic diorite (3,4,5) 3. Post-feldspar porphyry dikes (3,4,5) 4. Post-QFP dikes (2,4) 5. Post-diorite/tonalite plugs (2,4) 6. Pre-F_2 fold and EW axial-planar spaced cleavage (4) (Pre-S_2) (4) 7. Partly syn-F_2 (S_2) as local Au remobilization in fractured porphyroblastic auriferous Py and pressure shadows to deformed auriferous Py. (3) Partly syn-North and South shears(?) (1): Reference number	1. Robert et al., 1983 2. Daigneault et al., 1983 3. Robert and Brown, 1984 4. Karvinen, 1985 5. Robert and Brown, 1986a,b 6. Boullier and Robert, 1993 7. Sauvé et al., 1993 8. Robert, 1994 9. This study (see Figures 2.4, 2.5, and 2.6)

ite; Po: pyrrhotite; QFP: quartz-feldspar-porphyry; Qz: quartz; Sch: scheelite; Stwk: stockwork; Tc: talc; Tm: tourmaline

he authors cited in the reference list.

Table 2.6 Hierarchy of pre- to post-ore structures in gold-bearing deformation zones of the Val d'Or-Ma

	MTZ* (MALARTIC MINES)	CTZ** (ORENADA ZONE 4, ZONE 2)	CALLAHAN MINE	NORBENITE ZONE (NORLARTIC MINE)	M
PRE-ORE STRUCTURES EXERTING CONTROL OVER MINERALIZATION	1. Southerly-recumbent F_1 folds S_1 schistosity S_1 // fractures 2. Diorite, albite and monzonite dikes 3. "Cooling joints" in monzonite	1. CTZ 2. Regional F_1 folds, S (?) 3. "Porphyritic felsic schist" (possible porphyry dikes) (ore host Orenada Zone 4)	1. Regional F_1 folds (?) S_1 (?) 2. S_1 // fractures (?) 3. Diorite, tonalite - trondhjemite dikes	1. Regional F_1 folds (?). S_1 (?) 2. S_1 // fractures (?) 3. "Microdiorite" dike swarm (albitite dikes?)	1. 2. 3.
SYN-ORE STRUCTURES	Stwk veins: (Qz-Cb-Py-Au)	"Concordant" veins: (Tm-Ab-Qz-Aspy-Au)	Banded Stwk veins: (Qz-Tm-Py-Au)	Stwk veins: (Cb-Qz-Ab-Py-Cpy-Au) "Sheeted " veins (?): (Qz-Tm-Au)	Stwk (Cb- (Qz-
INTERMINERAL STRUCTURES EXERTING CONTROL OVER MINERALIZATION	Monzonite porphyry dikes (?)			Tonalite dike (2692 ± 2 Ma)	
POST-ORE STRUCTURES MODIFYING GEOMETRY OF ORE STRUCTURES	1. NE-plunging F_2 folds of Sladen Mine orebody Regional EW-SE S_2 schistosity S_2 // fractures 2. Malartic, Sladen and Barnat faults 3. Late strike-slip faults	1. Regional EW S_2 schistosity Boudins and Qz tension veins across auriferous veins 2. NE-plunging F_2 Z-fold of main ore zones NE-plunging, assymetric interfolial F_3 folds (S_2) of boudinaged auriferous veins (see Fig.3) S_3 spaced cleavage of F_3 3. Late strike-slip faults	1. Sigmoidal shapes of auriferous veins Sigmoidal shape of mineralized tonalite-trondhjemite dikes (Callahan Zone 1) 2. S-shape F_2 fold in post-ore dike 3. EW shear zones	1. NE-plunging F_2 S-fold of North Zone NE-plunging F_2 Z-fold of main ore body Regional EW S_2 schistosity (?) 2. Late faults	1. 2. 3.
REFERENCES:	Sansfaçon and Hubert, 1990; Trudel and Sauvé, 1992.	Robert, 1989; Robert et al., 1990; Robert, 1990; This study.	Imreh, 1984; Beaudoin et al., 1987; Jenkins et al., 1989; Sauvé et al., 1993.	Sauvé et al., 1993; Pilote et al., 1993.	Ma Sa

*Structures listed in chronological order. * Malartic Tectonic Zone ** Cadillac Tectonic Zone*
Key: Ab: Albite: Aspy: Arsenopyrite: Au: Gold: Bo: Biotite: Cb: Carbonate: Chl: Chlorite: Cpy: Chalcopyrite: Mt: Magnetite: Py: Pyrite: Po: Pyrrhotite: QFP: Qz-felds
Data from Tables 2.4 and 2.5.

ıtion zones of the Val d'Or-Malartic area as inferred from the literature and personal observations

NORBENITE ZONE (NORLARTIC MINE)	MARBENITE ZONE (MARBAN MINE)	KIENA MINE FAULT ZONE	'K' ZONE (SISCOE MINE)	NORTH & SOUTH SHEARS (SIGMA MINE) E-W THRUST FAULTS (LAMAQUE MINE)
1. Regional F_1 folds (?), S_1 (?) 2. S_1 // fractures (?) 3. "Microdiorite" dike swarm (albitite dikes?)	1. Regional F_1 folds (?), S_1 (?) 2. S_1 // fractures (?) 3. Concealed intrusion (magnetic surveys) 100m north of Marban Mine shaft	1. Southwesterly-recumbent regional F_1 folds, S_1 (?) 2. Bedding - parallel fault zone: Kiena Mine Fault Zone 3. Upward-flaring albitite dike swarm	1. Regional F_1 folds (?), S_1 (?) 2. S_1 // fractures (?) 3. Quartz - gabbro Siscoe stock (sill?) Microdiorite, feldspar porphyry and albitite dikes 4. Southern Siscoe stock/ mafic volcanic rocks contact: precursor to "K" zone (?)	Sigma Mine: 1. Porphyritic diorite or "C" porphyry 2704±2 Ma 2. Regional F_1 folds, S_1(?) 2700 - 2694 Ma 3. S_1 // fractures (?) 4. Feldspar prophyry ("G") dike swarm: 2694 ± 2 Ma Lamaque Mine: 1.; 2.; 3.; 4.; 5. QFP dikes 6. Diorite-Tonalite plugs: 2685 ± 3 Ma
Stwk veins: (Cb-Qz-Ab-Py-Cpy-Au) "Sheeted " veins (?): (Qz-Tm-Au)	Stwk veins: (Cb-Qz-Au) (Qz-Cb-Py-Po-Au)	Stwk veins: (Cb-Qz-Ab-Py-Po-Au) Replacement veins: (Cb-Py-Au) Stwk veins and breccias: (Ab-Py-Cpy-Sch-Au) Pegmatitic veins: (Cb-Bo-Qz-Py-Tm-Sch-Au) Phyllosilicate stwk veins:	Lode-gold veins: Qz-Tm-Py-Sch-Au ±Cpy±Po	Lode-gold veins: Qz-Tm-Chl-Py-Po-Sch-Au "Dike stringers": (Cb-Qz-Py-Au) Tourmaline stwk veins and tourmaline-cemented breccias: cross-cutting Au-bearing veins and cut by
Tonalite dike (2692 ± 2 Ma)		Granodiorite and feldspar porphyry dikes. 2686 ± 2 Ma (xenocrystic zircons 2697 ± 2 Ma)	Albitite dikes	Sigma Mine tourmaline-cemented breccia (see Fig. 8.18 to 8.23)
1. NE-plunging F_2 S-fold of North Zone NE-plunging F_2 Z-fold of main ore body Regional EW S_2 schistosity (?) 2. Late faults	1. Regional F_2 folds (?) EW S_2 schistosity (?) 2. Marbenite shear zone (?) 3. F_3 intrafolial (S_2) folds in Marbenite shear zone (?)	1. Main, N-dipping cleavage/schistosity (S_2) 2. NW-plunging regional z-shaped fold (F_2) 3. NE-dipping crenulation cleavage (S_3) 4. Late-stage, NW-dipping oblique-slip faults	1. Buckle folds cut by axial planar S_2 schistosity - Stylolites 2. "K" shear zone: penetrative planar fabric, folds, and boudinage 3. Late faults	Regional S_2 schistosity Sigma Mine: 1. Deformation of 'G' dikes and their Au-bearing Py. (Robert & Brown, 1984 p.396). 2. Boudins and stylolites in 'shear' veins. Buckle folds in 'flat' veins. Foliation in intermineral (?) Tm breccia. Lamaque Mine: 1. Z-fold of QFP dikes F_2 folds of 'shear' veins with axial planar EW spaced cleavage. Stylolites in 'shear' veins.
Sauvé et al., 1993; Pilote et al., 1993.	Méthot and Trudel, 1987; Sauvé et al., 1993.	This study.	J.E. Gill in Moss (1939) and Asbury (1941); Auger, 1947; Trudel, 1985; Tessier et al., 1990; Sauvé et al., 1993; Pilote et al., 1993; Sauvé et al., 1993 This study.	Daigneault et al., 1983; Robert & Brown, 1984; Karvinen, 1985; Robert & Brown, 1986 Boullier & Robert, 1993; Morasse & Wasteneys, 1994; This study.

: Pyrite: Po: Pyrrhotite: QFP: Qz-feldspar porphyry: Qz: quartz: Sch: Scheelite: Ser: Sericite: Stwk: stockwork: Tm: Tourmaline.

zones and alteration envelopes associated with early sets of brittle fractures related to S_1 schistosities, which were deformed by F_2 folds and subsequently cut by brittle-ductile faults of the Malartic Tectonic Zone. This observation suggests, at least in the Malartic gold camp, that gold mineralization is syn- to post-F_1 folds and -S_1 schistosities (D_1), but pre-dates F_2 folds (D_2) (see **Tables 2.4,2.6** and Chapter8). This in turn, suggests that gold mineralization across the Malartic camp has not been controlled by the formation of shear zones, but overprinted by them (see Chapter 8 and the Regional Sequence of Events diagram in back pocket).

The Cadillac Tectonic Zone is located at the boundary between the Malartic and Pontiac Groups (**Figure 2.2**) and consists of anastomosing lenticular-shaped and highly strained rock assemblages characterized by the presence of an intensely developed east-west and steeply north-dipping, penetrative S_2 foliation, intrafolial F_2 sheath folds, asymmetric "Z"-shaped F_3 folds and their northeast-striking, moderately to steeply southeast-dipping S_3 axial planar spaced cleavage (Robert, 1990). The main S_2 foliation corresponds to a strong schistosity, a compositional layering and the flattening of conglomerate pebbles and is systematically oblique in strike to the boundaries of the Cadillac Tectonic Zone (Robert, 1989). Based on the orientation of principal stresses deduced from strain markers, Robert (1990) interpreted the Cadillac Tectonic Zone as a zone of transpression resulting from an initial north-south compressional event, later evolving into a dextral transcurrent deformation event causing the formation of asymmetric "Z"-shaped folds (F_3) of the regional S_2.

In the Cadillac Tectonic Zone, gold mineralization is exemplified by the Orenada Zone 4 deposit. Gold occurs in association with tourmaline-albite-quartz veins that are parallel to the main regional S_2 schistosity that Robert (1989) termed "concordant" veins[6]. Figure 2.3 is an

---

[6] Penetrative foliation and elongation lineation within the Cadillac Tectonic Zone were originally interpreted as S_1 and L_1 by Robert (1989) and Robert *et al.* (1990). However, the same structural features of the Cadillac Tectonic Zone have been re-interpreted as S_2 and L_2 by Robert (1990) and Robert *et al.* (1994) because of their similarity with the predominant regional S_2 (L_2) schistosity.

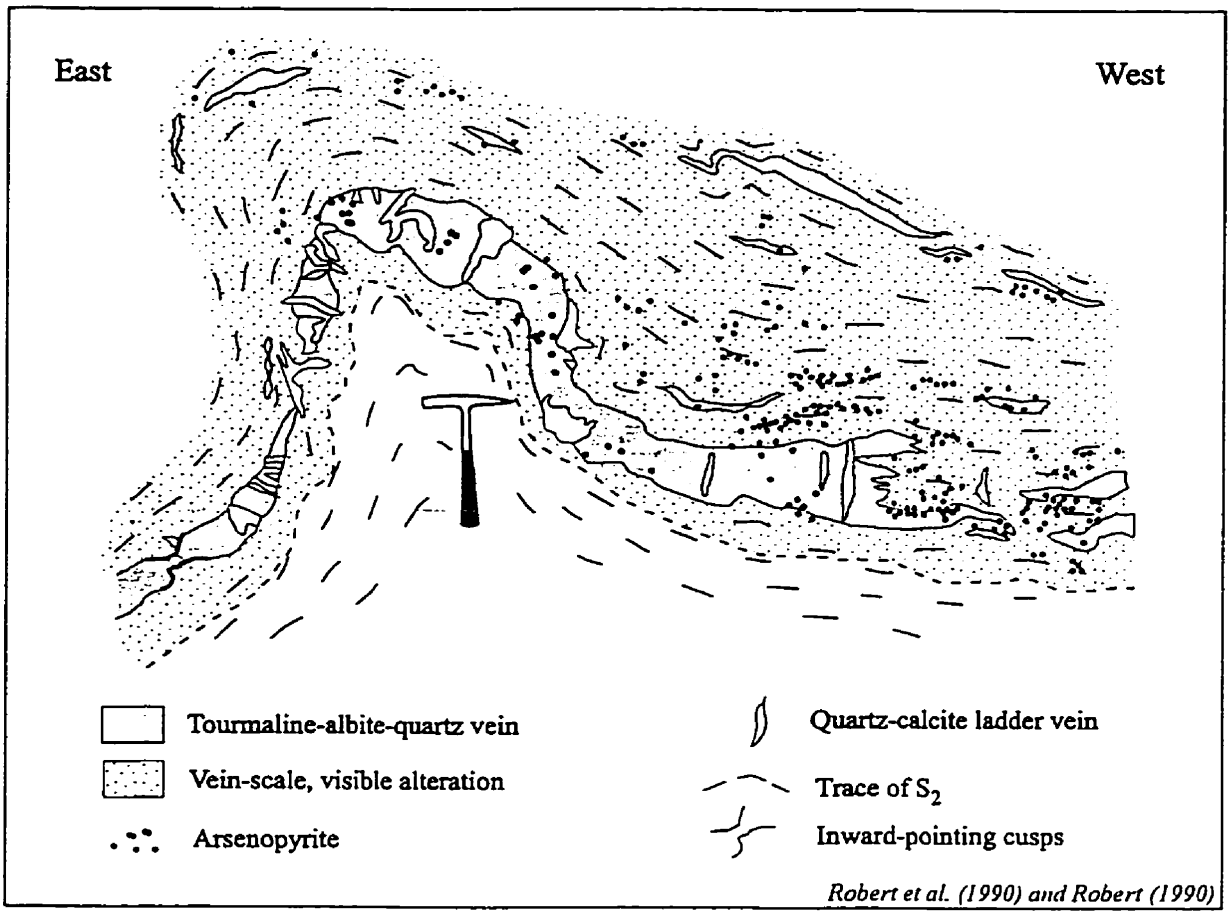

*Figure 2.3 - Detailed geological map of drift wall at the 800' level of the Orenada Zone 4 deposit of the Cadillac Tectonic Zone (deposit #19, **Figure 2.2**) modified after Robert et al. (1990) and Robert (1990). Asymmetric F_3 fold affecting a tourmaline-albite-quartz-arsenopyrite-Au vein ("concordant" veins of Robert et al. (1990)) and the regional S_2 schistosity. The distribution of quartz tension veins across the main gold-bearing vein suggests that extension of the vein occurred prior to folding. Inward-pointing cusps and tension veins perpendicular to S_2 further indicate that boudinage and the development of S_2 were broadly coeval. These observations thus suggest that the regional D_2 (S_2) deformation overprints a pre-existing gold-bearing vein.*

*Carte géologique détaillée du mur d'une galerie du niveau 800' du gisement Orenada Zone 4 de la Zone Tectonique de Cadillac (gisement # 19, **Figure 2.2**) modifiée d'après Robert et al. (1990) and Robert (1990). Plis asymétriques F_3 affectant une veine à tourmaline albite-quartz-arsénopyrite-Au (veine "concordante" de Robert et al. (1990)) ainsi que la foliation régionale S_2. La distribution des veines de tension à quartz le long de la veine aurifère suggère que l'étirement de la veine a précédé son plissement. Les formes en croissant (cusps) tournées vers l'intérieur de la veine ainsi que les veines de tension à quartz perpendiculaires à S_2 appuient également l'hypothèse du développement simultané de S_2, des boudins et des veines de tension. Cette interprétation suggère que la déformation régionale D_2 (S_2) a affecté une veine aurifère pré-existante.*

illustration of a deformed "concordant" vein interpreted by Robert (1990) to have formed coevally or shortly after the development of S_2. However, the radial distribution of quartz extension veinlets in the nose of the folded auriferous vein suggests that extensional strain occurred prior to folding. Quartz extension veins set perpendicular to S_2 also indicate that boudinage causing the formation of inward-pointing cusps in the auriferous quartz-tourmaline veins was probably coeval with the development of S_2 (see (Talbot and Sokoutis, 1992)). The present geometry of quartz tension veins in relation to gold-bearing veins and S_2 alternatively suggests that Orenada Zone 4 auriferous veins were formed prior to S_2. This interpretation allows for the extension of the auriferous tourmaline-albite-quartz veins, and concomitant development of quartz tension veins, to occur during the development of the regional penetrative S_2 schistosity followed by the folding of boudinaged auriferous veins and S_2 into asymmetric F_3 folds. Hence, gold vein formation in the Cadillac Tectonic Zone may have preceded regional syn-metamorphic deformation (D_2, S_2), in agreement with the relative timing of gold mineralization observed in the Malartic Tectonic Zone to the west (**Tables 2.4** and **2.6**; see also Chapter 8).

Deposit-scale shear zones occur in many of the local gold mines of the Val d'Or district, and are as structurally complex as their regional Cadillac and Malartic counterparts. Some gold-bearing shear zones, such as the "K" zone of the Siscoe Mine, are mappable on a regional scale (Sauvé et al., 1993), but most of them are restricted to the strike-length of the hosted gold deposit (**Table 2.5**). Deposit-scale shear zones should be more appropriately termed "composite" deformation zones, as they typically consist of an amalgam of structural elements including faults, fractures, sills, dikes, veins, folds, penetrative planar and linear fabrics, ranging in age from pre-, to syn-, and post-mineral (Sauvé et al., 1993 , Table 2.6). They usually consist of steeply-dipping zones of highly altered and schistose mafic to ultramafic volcanic rocks associated with folded and mylonitized felsic intrusions and vein-type gold mineralization (**Table 2.5**). Deposit-scale deformation zones share the same orientation as the regional-scale shear zones i.e. parallel to the regional S_2 schistosity, but their internal fractures, dikes and veins systems are frequently set at high angles to

S_2 (see as an example the strike of the Siscoe deposit albitite dikes and main ore zone in relation to that of the "K" shear zone and regional S_2 schistosity in **Table 2.5**; see also Figures 2 and 4 of Auger (1947)). According to Trudel and Sauvé (1992) and Sauvé *et al.* (1993), timing of gold mineralization in most deposit-scale deformation zones of the area is ambiguous and unresolved, but these authors recognized that mineralization generally post-dates the emplacement of small calc-alkalic to alkalic intrusions. Hydrothermal fluids have usually filled sets of fractures in competent host rocks rather than shear zones[7]. These authors also stressed another important characteristic of gold-bearing or deposit-scale deformation zones in the Val d'Or-Malartic region: alteration zones around mineralization do not cause a metamorphic overprint in the rock. Instead, alteration and gold-vein mineralogy vary with the regional metamorphic grade indicated by the host rock mineral assemblage. Alternatively, the above observation maysuggest that alteration, gold-vein and host-rock mineralogy vary sympathetically because gold mineralization may have been pre-metamorphic and re-equilibrated some time later during regional synmetamorphic deformation.

If the pre-metamorphic timing of gold mineralization in regional- and deposit-scale shear zones holds, the Sigma-Lamaque No.2 deposit (deposit No. 17 on **Figure 2.2**) is presumed to be an exception (Robert, 1996). Mineralization there is interpreted as syn- to post-shear zone development and metamorphism based on the following arguments: 1) gold-bearing quartz-tourmaline veins are predominantly hosted by seemingly undeformed feldspar porphyry dikes in the upper part of the deposit (Robert and Brown, 1986a; Robert, 1994), 2) hydrothermal alteration mineral assemblages in the halos of gold-bearing veins appear to overprint upper greenschist (biotite zone) to amphibolite facies mineral assemblages in adjacent volcanic and igneous rocks (Robert and Brown, 1984; Robert and Brown, 1986b; Taner et al., 1986; Powell et al., 1995a), and 3) foliation-parallel trails of rutile grains adjacent

---

[7] "..., les aquifères formés par la fracturation des roches cassantes ont été beaucoup plus importants que le transport hydrothermal par voie des zones de cisaillement" Sauvé *et al.* (1993), p.172.

to a shear vein are overgrown by gold-related tourmaline crystals (Robert, 1996). However, additional field observations and isotopic age dating causes this line of evidence to become equivocal. For example, the presence of disseminated auriferous pyrite grains fringed by carbonate-gold pressure shadows in the feldspar porphyry dikes (Robert and Brown, 1984) not only suggests that host intrusions subparallel to the regional S_2 schistosity are deformed along with mineralization, but that part of the primary gold mineralization may have been remobilized during deformation. Similarly, the possible post-ore remobilization in and around "shear veins" may explain the overgrowth of foliation by a second generation of metamorphic tourmaline (Morasse et al., 1996). At depth, field relations reveal that the Sigma deposit may have a Kiena-like magmatic-hydrothermal character based on the occurrence of a zoned alteration- mineralization pattern overprinted by penetrative deformation (Morasse et al., 1996, see also Chapter 8). This observation thus suggests that the apparent overprint of gold vein alteration halos onto metamorphic mineral assemblages may alternatively represent the overprint of gold mineralization onto early alteration zones all metamorphosed sometime later. In fact, the U-Pb zircon age of 2694 ± 2 Ma obtained for the feldspar porphyry dikes (Wong et al., 1991), that of ca. 2682 Ma obtained for gold mineralization (Claoué-Long et al., 1990; Corfu and Davis, 1991; Claoué-Long et al., 1992; Kerrich and King, 1993), in addition to the time interval of ca. 2680-2660 estimated for regional peak deformation/metamorphic conditions (Corfu et al., 1989; Wilkinson et al., 1993; Powell et al., 1995a) are all compatible with a pre-metamorphic timing for gold mineralization at Sigma.

2.2.5 Metamorphism

Field and geochronological evidence in the Val d'Or-Malartic region is consistent with four metamorphic events after the regional overturning of volcano-sedimentary strata, or D_1 (**Table 2.3**). *"M_1"* was a thermal metamorphic event related to the emplacement of the numerous calc-alkaline and alkaline granitoid dike swarms and stocks forming the Val d'Or plutonic belt (see section 2.2.3.2). M_1 metamorphism thus coincided with regional orogenic plutonism bracketed between ca. 2694-2680 Ma (Burrows and Spooner, 1991; Morasse et

al., 1995b). *"M_2"* was a sub-province-wide low to medium-grade (250°C and < 3.3 kbar, Powell (1995a)) dynamothermal metamorphic event that produced the prevalent regional S_2 foliation across the Val d'Or-Malartic area (Jolly, 1978; Dimroth et al., 1983a; Powell et al., 1994; Powell et al., 1995a). $^{40}Ar/^{39}Ar$ ages of 2693-2672 Ma obtained for metamorphic amphiboles from the Sigma deposit porphyritic diorite (Hanes et al., 1989; Hanes et al., 1992), as well as U-Pb age of 2684 ± 7 Ma obtained for metamorphic rutiles from volcanic rocks of the Val d'Or Formation (Wong et al., 1991), were initially interpreted as the ages of regional metamorphism. However, these ages have been re-interpreted as the probable isotopic signature of district-wide tonalitic to monzonitic plutonism (Powell et al., 1995a; Powell et al., 1995b). U-Pb zircon age dating of pre- and post-metamorphic intrusions constrain the M_2 metamorphic event to the time interval of ca. 2677-2645 Ma. The maximum age of 2677 Ma is provided by a deformed and foliated quartz-feldspar porphyry dike cutting a Timiskaming sandstone unit south of Larder Lake (Corfu et al., 1991), whereas the minimum age is provided by the $^{207}Pb/^{206}Pb$ zircon age of 2643 ± 4 Ma for the garnet-muscovite granite phase of the Lacorne batholith[8] (Feng and Kerrich, 1991a). The M_2 metamorphism has been directly dated as 2665 ± 4 Ma by Wilkinson *et al.* (1993) on metamorphic titanites from the Murdock Creek syenite (ca. 2673 Ma) located in the Larder Lake-Cadillac tectonic zone, and as 2657 ± 3 Ma by Powell (1994) on biotites from the Clériсy syenite (ca. 2682 Ma) located in the Parfouru fault zone, northeast of Rouyn-Noranda. Base on these radiometric ages, in addition to the U-Pb titanite age of 2660 ± 6 Ma obtained for the Lac Opasatica orthogneiss (Machado et al., 1991) located further south in the Pontiac Subprovince, Powell (1995a) estimates that peak regional metamorphic conditions were reached simultaneously throughout the southern Abitibi and Pontiac Subprovinces at ca. 2660 Ma. *"M_3"* was a thermal metamorphic event related to the up-rise of S-type granitoids (Powell et al., 1994; Powell et al., 1995a) across the Abitibi and Pontiac Subprovinces between ca. 2645-2611 Ma (Feng and Kerrich, 1991a; Bédard and Ludden,

---

[8] Mineral assemblages of the contact aureole to the garnet-muscovite granite of the Lacorne batholith overprint the staurolite-biotite schist derived from the Lac Caste greywackes and show no evidence of a regional retrograde event (Powell, 1994).

1997). Thermobarometric studies of mineral assemblages in the contact aureole of the Preissac-Lacorne peraluminous granite, suggest that low pressure conditions (410-450°C and 2.5-4 kbar) were in effect during this metamorphic event (Feng and Kerrich, 1990; Powell, 1994). *"M_4"* was a shield-wide thermal event related to the emplacement of late Archean to Proterozoic diabase dikes between ca. 2450-2150 Ma (Stockwell, 1964; Hanes and York, 1979; Heaman, 1988; Mason, 1995).

North of the Cadillac and Malartic Tectonic Zones, mineral assemblages are generally indicative of greenschist facies metamorphism (chlorite-calcite-epidote-pale green actinolite-albite-quartz±stilpnomelane), although locally, in and around gold mines, upper greenschist assemblages of the biotite zone are reported (Sauvé et al., 1993)[9]. At the Sigma and Camflo Mines, the metamorphic grade is reported to increase with depth from greenschist to lower amphibolite facies (Grant, 1986; Robert and Brown, 1986a; Zweng et al., 1993), suggesting the presence of regional sub-horizontal metamorphic isograds (Sauvé et al., 1993; Powell et al., 1995b). At the Sigma Mine, the changes in metamorphic grade with depth range from greenschist facies assemblages (albite-chlorite-muscovite-epidote-quartz-calcite) between 0-800 metres, to upper greenschist facies assemblages (oligoclase-biotite-chlorite-epidote-quartz-calcite-muscovite) between 800-1500 metres, to lower amphibolite facies assemblages (andesine-hornblende-biotite-chlorite-quartz-<epidote-< calcite) from 1500 metres downward (Grant, 1986). South of the Cadillac and Malartic Tectonic Zones in the Pontiac Group metasediments, regional metamorphic grade progressively increases southward from the staurolite, to the garnet-sillimanite zone of the amphibolite facies (Imreh, 1984; Trudel and Sauvé, 1992).

As most of gold deposits are "shear zone-hosted", time relationships between gold

---

[9] It should be noted that the assessment of the metamorphic origin of biotites has usually been made without reporting the mode of occurrence of the biotites. The existence of pre-metamorphic hydrothermal biotites can be demonstrated at Kiena, suggesting that other biotite occurrences in the district may be part of a gold-related alteration assemblage (see Morasse *et al.*, 1996).

mineralization and metamorphism closely follow that between gold mineralization and shear zones. In the case of the Sigma deposit, metamorphism has affected all rock types in the mine from the host andesitic volcanic rocks, to the porphyritic diorite ("C" porphyry), and feldspar porphyry dikes ("G" dikes) as well as gold-bearing veins and related alteration halos (Sauvé et al., 1993 , p. 53). According to Sauvé *et al.* (1993) all the silicate minerals present in gold-bearing veins, apart from tourmaline, are observed in the selvages at some distance from the veins. Taner's (1986)observation that biotites from gold vein alteration halos have the same composition as those from the host porphyritic diorite, away from the veins,is also compatible with a pre-metamorphic origin for mineralization at Sigma (see section on Sigma-Lamaque No. 2 deposits in Chapter 8). Deformed porphyroblastic pyrite, in feldspar porphyry dikes, exhibits globular inclusions of gold with carbonate-gold-filled pressure shadows (Robert and Brown, 1984) which suggests that there may be two generation of gold associated with the pyrite: primary globular gold and secondary, possibly remobilized (?), gold in pressure shadows to the pyrite. All these observations are in agreement with the effects of deformation on Sigma-Lamaque No.2 Mines gold mineralization reviewed in the previous section, suggesting that at least part of the mineralization is pre-metamorphic.

2.4. SUMMARY

In summary, the geologic history of the Val d'Or-Malartic area as envisaged herein is consistent with that which has been documented for the southwestern (Kirkland Lake area) and south central (Rouyn-Noranda area) segments of the southern Abitibi belt, except for the timing of gold mineralization. The region is characterized by broadly coeval komatiitic-tholeiitic and tholeiitic-calc-alkaline volcanism at ca. 2720-2700, quickly followed by a first phase of uplift and sedimentation synchronous with sporadic but evolving orogenic plutonism at ca. 2694-2680 Ma. A regional low- to medium-grade metamorphism accompanied by fabric development prevailed throughout the entire region and reached its peak at ca. 2680-2660 Ma. However, contrary to the previously accepted view stipulating that late Archean gold mineralization is either syn- to post-regional deformation, this overview of the geology

of the Val d'Or-Malartic area suggests that mineralization is pre-metamorphic (see also Chapter 8). It is predominantly hosted by fractures developed in syn- to late-orogenic, pre-ore intrusions and penetrative deformation affects all preexisting ore structures. According to Powell (1995a), low-pressure conditions continued throughout the region during the post-tectonic emplacement of the two mica Preissac-Lacorne monzogranite. The 20 m.y. duration of low-pressure conditions characterizing the final stages of the Kenoran orogeny (ca. 2665-2645 Ma), has prompted Powell (1995a) to suggest that post-metamorphic up-lift and erosion, in this part of the southern Abitibi greenstone belt, were not very significant.

CHAPTER 3 GEOLOGICAL SETTING OF THE KIENA MINE

3.1 GEOLOGY OF THE KIENA MINE PROPERTY

The Kiena Mine property occupies the southwestern corner of Lac de Montigny (**Figure 2.2**) and, apart from the presence of several small islands, is mostly covered by the waters of this lake (**Figure 3.1**). The geology of the property is known from surface mapping of the islands and peninsulas by Polk (1960) and Cloutier (1979), numerous drilling surveys (Gagnon, 1987; Lebel, 1987; Lebel, 1988b; Lebel, 1988a; Lebel, 1989; Lebel, 1990; Lebel, 1992), several ground magnetic surveys (performed from the icy surface of the lake), and from underground mapping and drilling at the Kiena Mine (Jeansonne, 1992) and the Wisik deposit (Lebel, 1991)(**Figure 3.1**). The property boundaries[1] straddle, from north to south, rock units of the Dubuisson[2], Jacola and Héva Formations. The section of ***Dubuisson Formation*** encountered on the property consists of a thick sequence of massive, foliated to schistose tholeiitic basalts, with rare komatiitic intercalations. This volcanic rock assemblage has been cut by the ***Snowshoe stock*** (**Figure 3.1**), a sub-circular and weakly deformed granodioritic to tonalitic (locally monzonitic, < 5% quartz) intrusion dipping 70° north, which is associated with a swarm of northwest-southeast, moderately to steeply south-dipping tonalite and quartz diorite porphyry dikes (north of **Figure 3.1**) (Gardiner, 1988; Sauvé, 1988; Sauvé et al., 1993).

The rocks of the Snowshoe stock have a granitoid texture and are composed of albite and quartz with lesser microcline (0-10 %), hornblende, biotite, epidote and trace amounts of

---

[1] Property boundaries reported on **Figure 3.1** do not represent the actual outline of the Kiena Mine claim block, following the loss of several claims, in the fall of 1992. Negotiations to regain control of the lost claims and to restore the former mining claim block (# 1707-01) to its previous configuration, are underway (Cormier M., personal communication 1994).

[2] The contact between the Jacola and Dubuisson Formations appearing on the geological compilation map of Lebel (1992), has been shifted north on the map of **Figure 3.1**, to match the geological contact previously proposed by Imreh (1984).

Figure 3.1 - *Simplified geological map of the Kiena Mine property below the waters of Lac de Montigny, showing the surface projections of the "S-50" Zone and other gold mineralization occurrences. Stratigraphic and structural data compiled and modified from surface mapping by Polk (1960) and Cloutier (1978; 1986), underground drilling and mapping by Jeansonne (1993), drilling surveys by Gagnon (1987) and Lebel (1987-1992), and from several ground magnetic surveys. Southwesterly-facing homoclinal volcanic sequence is cut by granodiorite, tonalite and "diorite" dikes, and by the Snowshoe stock. Attitude and inferred horizontal component of movement of main deformation zones are interpreted from drill core.*

Carte géologique simplifiée de la propriété de la Mine Kiena telle que perçue sous les eaux du Lac de Montigny, montrant la projection à la surface de la Zone "S-50" et autres zones minéralisées. Les données stratigraphiques et structurales ont été compilées et modifiées à partir des cartes géologiques de surface de Polk (1960) et Cloutier (1978; 1986), de cartes géologiques sous-terrainnes de Jeansonne (1993), de levés de sondage par Gagnon (1987) et Lebel (1987-1992), ainsi qu'à partir de levés magnétique de surface. La séquence homoclinale de roches volcaniques déversées vers le sud-ouest est recoupée par des dykes de composition granodioritique à tonalitique, dykes de "diorite" et, par le stock de Snowshoe. L'attitude et la direction de la composante horizontale de mouvement des zones de déformation sont interprétées à partir de données de sondage.

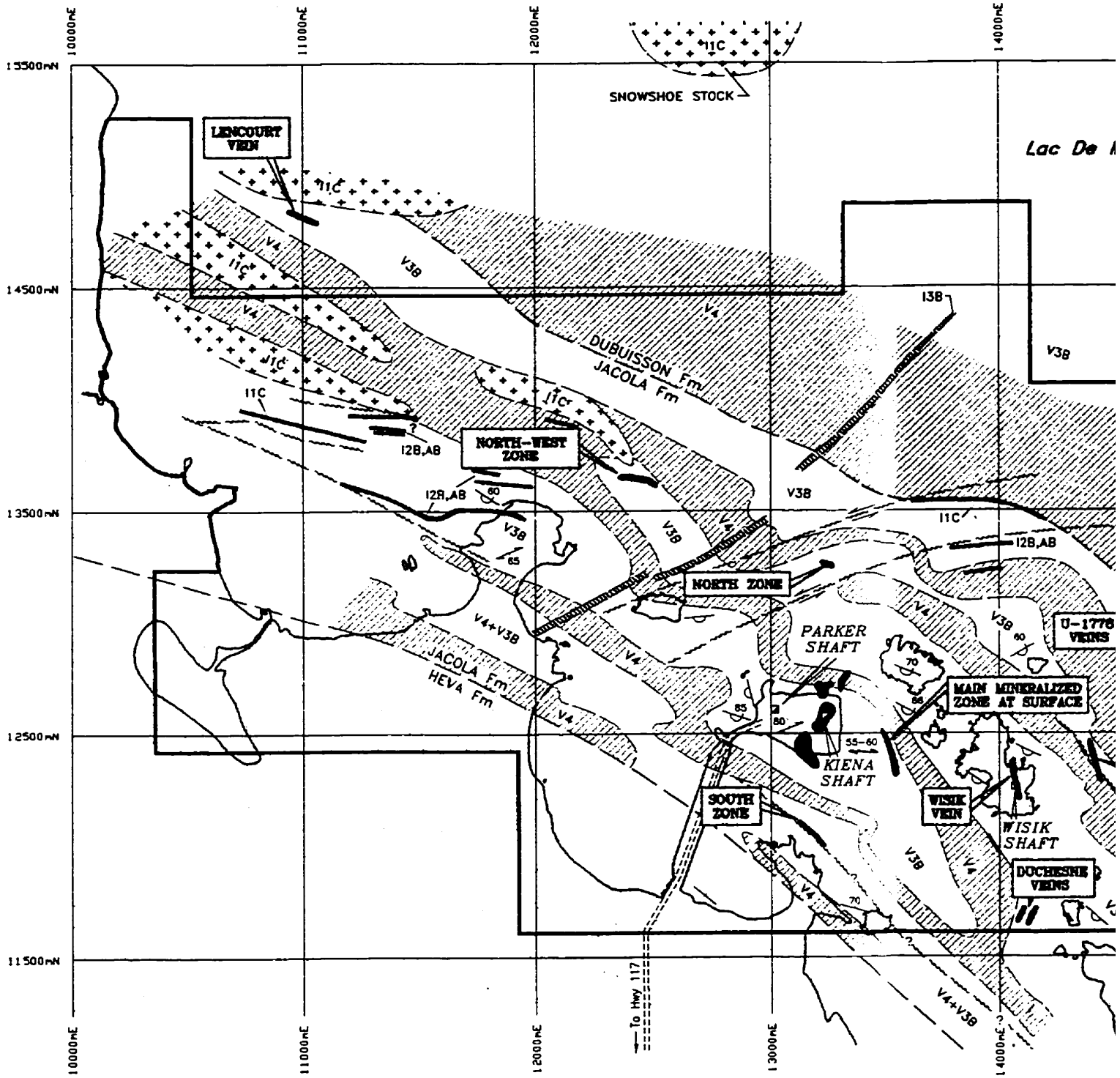
10000mE
11000mE
12000mE
13000mE
14000mE
13500mN
14500mN
13500mN
12500mN
11500mN
SNOWSHOE STOCK
LENCOURT VEIN
NORTH-WEST ZONE
NORTH ZONE
SOUTH ZONE
DUBUISSON Fm
JACOLA Fm
HEVA Fm
V4+V38
PARKER SHAFT
KIENA SHAFT
WISIK VEIN
WISIK SHAFT
MAIN MINERALIZED ZONE AT SURFACE
DUCHESNE VEINS
To Hwy 117
Lac De

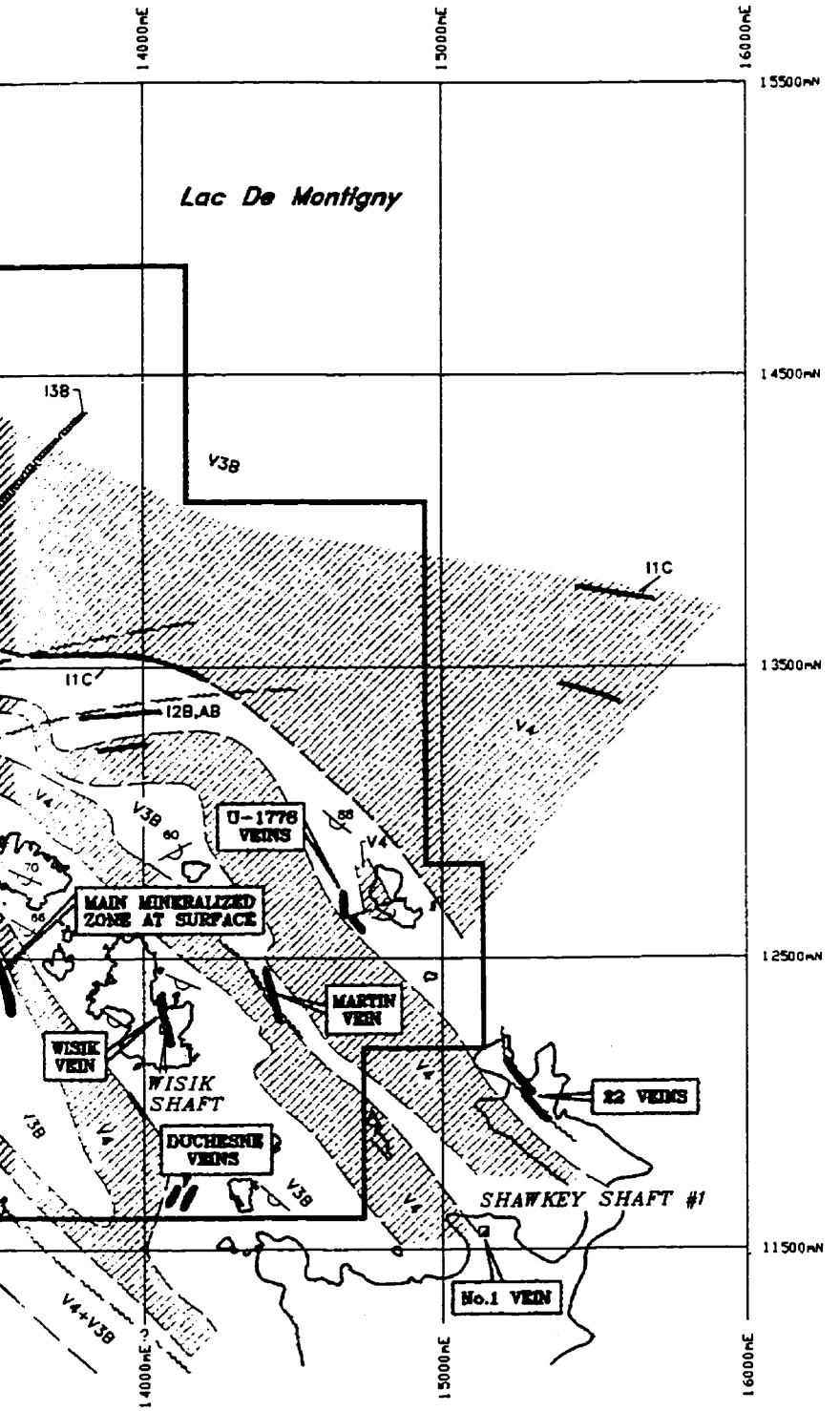

N

LEGEND

VOLCANIC ROCKS

- V4 — Komatiite
- V3B — Tholeiitic basalt

INTRUSIVE ROCKS

- I1C — Granodiorite/Tonalite sills and stocks
- I3B — Diabase dike
- I2B (AB) — Diorite dikes (possibly including some albitite dikes)

SYMBOLS

- Au-mineralized veins
- S-50 Zone at mine level 33
- Presumed stratigraphic contact
- Faults and deformation zones
- Horizontal component of movement
- 60 — Overturned bedding and dip
- 60 — Bedding and dip, vertical
- Regional schistosity
- 55-60 — Main schistosity (Sn) KIENA Mine, level 27

LES MINES D'OR KIENA LTEE.

Figure 3.1

SIMPLIFIED GEOLOGICAL MAP OF THE KIENA MINE AREA

COMPILED BY : S. Morasse
DATE : 06/15/94

MODIFIED AFTER Polk 1960, Cloutier 1978; 1986, Lebel 1990; 1992, Jeansonne, 1993
COMPUTER DRAFTING BY : S. Tremblay

SCALE 1 : 25 000
0m 250m 500m

chlorite, ilmenite and sphene (Sauvé, 1987). Albite grains show inclusions of clinozoizite and are replaced by white mica, suggesting that the original plagioclase of the Snowshoe stock were more calcic. Biotite and hornblende are replaced by chlorite, epidote, carbonate, quartz and sphene, whereas ilmeno-hematite and magnetite show coronas of sphene and epidote, respectively, suggesting that primary mineral assemblages have been metamorphosed to the greenschist facies. Basalts of the Dubuisson Formation have also been metamorphosed to the greenschist facies and consist of fine-grained, massive, foliated to schistose rocks composed of albite, chlorite, epidote, and carbonate with minor biotite, hornblende, magnetite, ilmenite, rutile and sphene (Sauvé, 1988).

The ***Jacola Formation*** which hosts Kiena's orebody, consists of alternating peridotitic/basaltic komatiites and iron and magnesian tholeiites, with rare intercalated thin layers of tuffaceous rocks of intermediate composition (Sauvé, 1988). Strongly magnetic peridotitic and basaltic komatiites form massive to schistose rocks composed mainly of serpentine and talc with lesser tremolite-actinolite, carbonate, chlorite, fine-grained magnetite and ± biotite, containing between 30% MgO and >18% MgO, respectively (Sauvé, 1988; Lebel, 1991). Iron tholeiites (Fe_2O_3 total/MgO > 2; SiO_2 < 54 %) have a microcrystalline texture showing plagioclase microlites in a matrix composed mainly of chlorite and hornblende with lesser carbonate, quartz and green stilpnomelane (Sauvé, 1988). Magnesian basalts (Fe_2O_3 total/MgO < 1.5; MgO > 8%; SiO_2 < 54 %) are microporphyritic rocks composed of chlorite, carbonate, clinozoisite and albite replacing primary olivine and calcic plagioclase microphenocrysts, in a rock matrix composed of albite microlites, actinolite and quartz (Sauvé, 1988). Volcanic rocks of the Jacola Formation have been cut by fine-grained gabbroic sills that are not easily distinguished from the coarse-grained tholeiitic basalts ("green diorites" of Clark, 1963). Gabbroic sills have been cut by numerous granodiorite to tonalite porphyries and "dioritic" dikes (albitite dikes ?) (see **Figure 3.1**). ***Granodioritic to tonalitic dikes*** vary in texture from medium-grained equigranular to microporphyritic, to schistose, and consist mainly of albite and quartz, with lesser carbonate, "streaks" of chlorite, sericite, clinozoizite, pyrite (< 5%), and traces of tourmaline, ilmenite, sphene, chalcopyrite

and sphalerite (Muir, 1979; Sauvé, 1988). Whole rock analyses of these rocks show elevated CaO, Na_2O and K_2O contents, as well as gold values ranging from 0.25 to 1.91 g/t Au, indicating that they have been altered and weakly mineralized (Sauvé, 1988; Lebel, 1991). "***Dioritic***" dikes, also known as "grey diorite" dikes (Clark, 1963) and as "sodic microdiorite" dikes (Sauvé, 1988) because of their elevated Na_2O content (9 %), consist of light to dark grey rocks with microporphyritic to fine-grained granitic textures. They are composed mainly of albite with lesser hornblende and carbonate, and minor quartz, epidote, chlorite, magnetite, biotite and green stilpnomelane (Sauvé, 1988). Sauvé (1988) reported prismatic, green-brown hornblende microphenocrysts in "sodic microdiorite" dikes which are least affected by carbonate alteration, and indicated that these hornblendes are distinct from the blue-green hornblendes observed in metamorphosed basalts. Carbonate-altered "sodic microdiorite" dikes, on the other hand, lack hornblende and epidote, and in addition to albite are characterized by the presence of chlorite, magnetite, biotite, and green stilpnomelane. However, Sauvé (1988) has not indicated the mode of occurrence of the latter mineral assemblage (veinlets ?), nor the relationships between biotite, chlorite, and stilpnomelane (successive overprint ?).

The contact between the Jacola and the lower Héva Formations is outlined by a sharp magnetic contrast delineating the contact between the southernmost ultramafic komatiitic flow of the Jacola Formation and a calc-alkaline pyroclastic flow unit of the Héva Formation (Lebel, 1991). The mine property encompasses a section of the ***Héva Formation*** characterized by an abundance of mafic volcaniclastic rocks chiefly composed of massive to foliated andesitic agglomerate, feldspar crystal tuff and blocky tuffs, intercalated with tholeiites and local dacites (Sauvé, 1988; Lebel, 1989).

The Dubuisson, Jacola and Héva Formations form a steeply northeast-dipping (70°) and southerly overturned, northwest-striking (N290-310°) homoclinal volcanic sequence (**Figure**

3.1)[3]. However, the main orebody of the Kiena Mine and its volcanic wall-rocks strike north-south (N190°), are overturned to the west, and dip moderately to the west (**Figure 3.1** and **Table 3.1**). Volcanic rocks of the Kiena Mine property show only weak penetrative strain but local high-strain zones, marked by a penetrative schistosity defined by talc, chlorite, and biotite. These narrow deformation zones occur around the various gold showings and deposits, as well as around the contacts of granodiorite, tonalite and "dioritic" dikes[4] (**Figure 3.1**). Overturned volcanic strata, altered and sheared gold orebodies and felsic dikes have been subsequently cut by a subvertical northeast-trending Proterozoic diabase dike (**Figure 3.1**, Regional Sequence of Events Chart in back pocket).

---

[3] Based on previous geological mapping by Polk (1960), Cloutier (1979) and Imreh (1984) the rock units in and around the Kiena Mine were interpreted as a weakly deformed, south- southwesterly-facing and northeast-dipping homoclinal volcanic rock sequence. Since then, Desrochers et al. (1993 b, map 2 of 2) reported stratigraphic polarity reversals and a penetrative schistosity striking north-northwest in tholeiitic pillow flows outcropping on the islands east of the mine. Accordingly, the volcanic rock assemblage of Lac de Montigny was re-interpreted as a tightly, isoclinally folded sequence exhibiting closely spaced (λ = 200-400 m) antiforms and synforms with sub-vertical axial planes oriented N315°. This interpretation is not supported by the very low strain state of deformation observed in the pillow flows forming the islands. Pillow structures are characteristically undeformed, show consistent younging to the south-southwest and lack the regional NW-SE S_2 schistosity.

[4] Two narrow, northwest-striking and steeply north-dipping deformation zones were discovered in drill core at the "South" Zone and west of the westernmost peninsula, respectively (see **Figure 3.1**). They have been interpreted as two segments of a single and extensive high-strain zone, representing the possible eastern extension of the "Norlartic" shear zone (Lebel, 1991; see **Figure 2.2**). As field evidence supporting this interpretation is still lacking, this deformation zone may not extend far beyond the segments originally confirmed by drilling.

Table 3.1 Main structures of the Kiena Mine property *(see Figure 3.1)*

Structure	*Orientation*	*Younging direction*	*Location*	*Comments*	*Source*
Bedding (Folds)	N290-310 70-80°NE	overturned to the southwest	Across property	"z"-fold structure over North Zone (?)	Polk (1960); Cloutier (1978); Lebel (1991)
Schistosity	—		Across property	Not observed in weakly strained pillow flows 200 m away from Kiena	This study; Polk (1960)
Extension (?) fractures	N040-050 90°		Across property	Perpendicular to bedding in weakly strained pillow flows	This study; (Polk, 1960)
Bedding (Folds)	N190 25-40° W	overturned to the west	Parker Island area	"z"-folded orebody	Polk (1960); Kiena Mine
Schistosity	N270 55-60° N		Parker Island area	—	Kiena Mine
Main shear zone	N190 80° SW		Parker Island area	< 200 m on either side of the island	Polk (1960); Bourget (1986); Kiena Mine
Faults and minor shear zones	N115 80° SW N225-240 78° NW N260-270 80° NE N290 80° NE		Across property	—	Polk (1960)
Granodiorite/ tonalite dikes	N270-290 70° N (?) < N330 ?		Across property	Folded, foliated, laced with gold-bearing carbonate stockwork veins: 0.25-1.91 g/t Au; < 5% Py	Polk (1960) Lebel (1989; 1991)
Microdiorite (albitite?) dikes	N290-315 70-80° NE N190 30° W		Across property Parker Island area	Pre-granodiorite, folded, foliated laced with gold-bearing carbonate stockwork veins: 0-1 g/t Au	Lebel (1991); Kiena Mine
Lamprophyre dikes	N260 70° N		SW komatiite unit	—	Polk (1960)
Diabase dikes	N045 90°		Across property	Post-microdiorite, post-granodiorite, post-ore	Lebel (1991); Kiena Mine

3.2 ORE TYPES AND INTERNAL GEOMETRY OF OREBODY

Pre-existing data and problems

At the time this study commenced, a crude vertical zonation of the orebody from a core of breccia ore ("S-50" zone) enclosed by, and grading downward into, a shear zone-type of ore ("J", "K", "L", and "C" zones) had been recognized (**Figure 3.2**). Mine geologists knew also of the existence of two felsic porphyry dikes intruding the mine's wall-rock sequence. However, the geologic relations between the two ore types and the porphyries were unclear and, although geological plan maps of mine levels 17 to 43 had been partially compiled, plan maps below level 43 and geological sections across the entire vertical extent of the orebody, were not available. One fundamental and unresolved aspect of Kiena geology was thus the internal geometry of the entire ore-dike complex. Other unanswered questions included the following: what caused the zonation of the ore, what is the origin of the high-grade breccia, do felsic porphyry dikes play a role in the mineralization process and, what are the controls on, and timing of, gold-ore mineralization?

Technical approach

To remedy the situation, selected geological sections and plan maps were updated and compiled at 1:500 and 1:250 scale to establish the geometry of the orebody and ascertain cross-cutting relationships. The assembly of Kiena geology is based on underground mapping executed for this research project (see set of Index maps in back pocket) and the study of pre-existing maps and boreholes[5]. The resulting sections and maps, which were subsequently digitized and scaled to 1:2500 using the Autocad drafting software, are located in the back

---

[5] The average grade of individual ore zones shown on either sections or plan maps, has been calculated from mineralized borehole intersections; it does not reflect the average grade calculated from the tons of ore recovered by mining in any given ore zone, on any given section or mine level.

pocket of this thesis (see also **Figure 3.2**). From this point on, these schematic plan maps and sections will serve as a reference framework to assist the characterization of Kiena geology throughout the remainder of this thesis.

Internal geometry

For the purpose of mining, Kiena geologists had subdivided the orebody into seven individual ore zones, based on the attitude of the ore, its composition and the presence of a granodiorite dike. These ore zones can be regrouped as follows: a high-grade core consisting of the "A", "B", "D" zones and lower part of the "C" zone, and a lower-grade ore shell comprised of the "J", "K", "L" zones and upper part of the "C" zone (**Figures 3.2** and **4.22**). Two small gaps appear on the longitudinal section of **Figure 3.2**. One is located between the "L", "K", "J" and "B" ore zones and indicates the presence of the deposit's intermineral dike which partly dismembers the orebody (see section **12636.5 N** and **33 Level Map**, back pocket). The other gap is situated between the "B" and "C" ore zones. It coincides with the southern hinge of a z-shaped fold which affects the orebody between levels 33 and 54 (see sections **12438.4 N** and **12514.6 N**, back pocket). The Kiena orebody is composed of three ore types which are referred to, from the oldest to the youngest, as: "Stwk Cb-Qz-Py(Po)±Ab Au" vein, "Breccia 1" and "Breccia 2" ore types. The ***Stwk Cb-Qz-Py(Po)±Ab-Au*** vein ore type consists of a funnel-shaped body of carbonate-quartz stockwork veins with auriferous alteration halos composed chiefly of albite and disseminated pyrite and/or pyrrhotite. It is overprinted by the ***Breccia 1*** ore type which forms a more restricted, lensoid body of mineralized rocks, essentially composed of irregular carbonate(ankerite)-pyrite-Au replacement veins[6]. This ore type is overprinted in turn by the ***Breccia 2*** ore type which forms a sheet-like body of stockwork veins and breccias composed mainly of albite with disseminated pyrite, chalcopyrite, scheelite and gold (see **41 Level Map** in back pocket). The high-grade core of

---

[6] Throughout this thesis auriferous carbonate-pyrite replacement veins are termed "breccia" to avoid confusion with pre-existing terminology in use at the mine. This ore type is not a breccia sensu stricto (see section 4.2.3.2).

Figure 3.2 - *North-south longitudinal section of the Kiena Mine orebody, looking east, showing the distribution of ore types across the deposit. Kiena's orebody is composed of three ore types which are referred to, from the oldest to the youngest, as "Stwk Cb-Qz-Py(Po)±Ab-Au" vein, "Breccia 1" and "Breccia 2" ore types. The "Stwk Cb-Qz-Py(Po)±Ab-Au" vein ore type is the most extensive and consists of a network of carbonate-quartz stockwork with alteration halos composed of albite, disseminated pyrite (and/or pyrrhotite) and gold. "Breccia 1" and "Breccia 2" ore types are restricted to the centre and upper part of the deposit. "Breccia 1" ore consists of carbonate-pyrite-gold replacement veins, whereas "Breccia 2" ore consists of albite stockwork veins and breccias with disseminated pyrite, chalcopyrite, scheelite, and gold. The best ore grades are obtained at the core of the deposit from the "Stwk Cb-Qz-Py(Po)±Ab-Au" vein ore type at lower mine levels and from the "Breccia 1" and "Breccia 2" ore types at upper mine levels (see Figure 4.22 for details on the zonation of the ore). Vertical lines across the orebody and highlighted mine levels indicate the position of schematic sections and plan mapslocated in the back pocket of this thesis.*

Section longitudinale de la mine Kiena orientée nord-sud, avec regard vers l'est, illustrant la distribution des types de minerai à travers le gisement. Le gisement se compose de trois types de minerai auxquels l'on réfère, du plus ancient au plus récent, par les acronymes suivants: minerai de type "Stwk Cb-Qz-Py(Po)±Ab-Au", "Breccia 1" et "Breccia 2". Le minerai de type "Stwk Cb-Qz-Py(Po)±Ab-Au" est celui qui possède la plus grande portée. Il consiste en un réseau de veines de carbonate-quartz en stockwork accompagnées par des halos d'altération composés d'albite, pyrite (et/ou pyrrhotite) et or disséminés. Les minerais de type brèche se situent au centre et dans la partie supérieure du gisement. Le minerai de type "Breccia 1" consiste en veines de remplacement à carbonate-pyrite-or, tandis que le minerai de type "Breccia 2" consiste en veines d'albite et brèche à matrice filonienne d'albite avec pyrite, chalcopyrite, scheelite et or disséminés. Les meilleures teneurs proviennent du coeur du gisement et sont issues du minerai de type "Stwk Cb-Qz-Py(Po)±Ab-Au" aux niveaux inférieurs de la mine et des minerais de type brèche aux niveaux supérieurs de la mine (voir la Figure 4.22 afin d'obtenir des détails sur la zonation du minerai). Les lignes verticales tirées à travers le gisement ainsi que les plans niveau dont le nom est accentué en marge du gisement, indiquent la position des sections et plans schématiques situés en pochette.

Abbreviations: **Stwk Cb-Qz-Py(Po)±Ab-Au** = carbonate-quartz stockwork veins with albite-pyrite (pyrrhotite)-Au gold alteration haloes (1st ore type); **Breccia 1** = ankerite(dolomite)-pyrite-Au replacement veins (2nd ore type); **Breccia 2** = albite-pyrite-chalcopyrite-scheelite-Au stockwork veins and breccias (3rd ore type).

Abréviations: **Stwk Cb-Qz-Py(Po)±Ab-Au** = veines de carbonate-quartz en stockwork avec halos d'altération à albite-pyrite(pyrrhotite)-Au (1er type de minéralisation); **Breccia 1** = veine de remplacement à ankérite(dolomie)-pyrite-Au (2ième type de minéralisation); **Breccia 2** = veines en stockwork et brèches à albite-pyrite(Au)-chalcopyrite-scheelite-Au (3ième type de minéralisation).

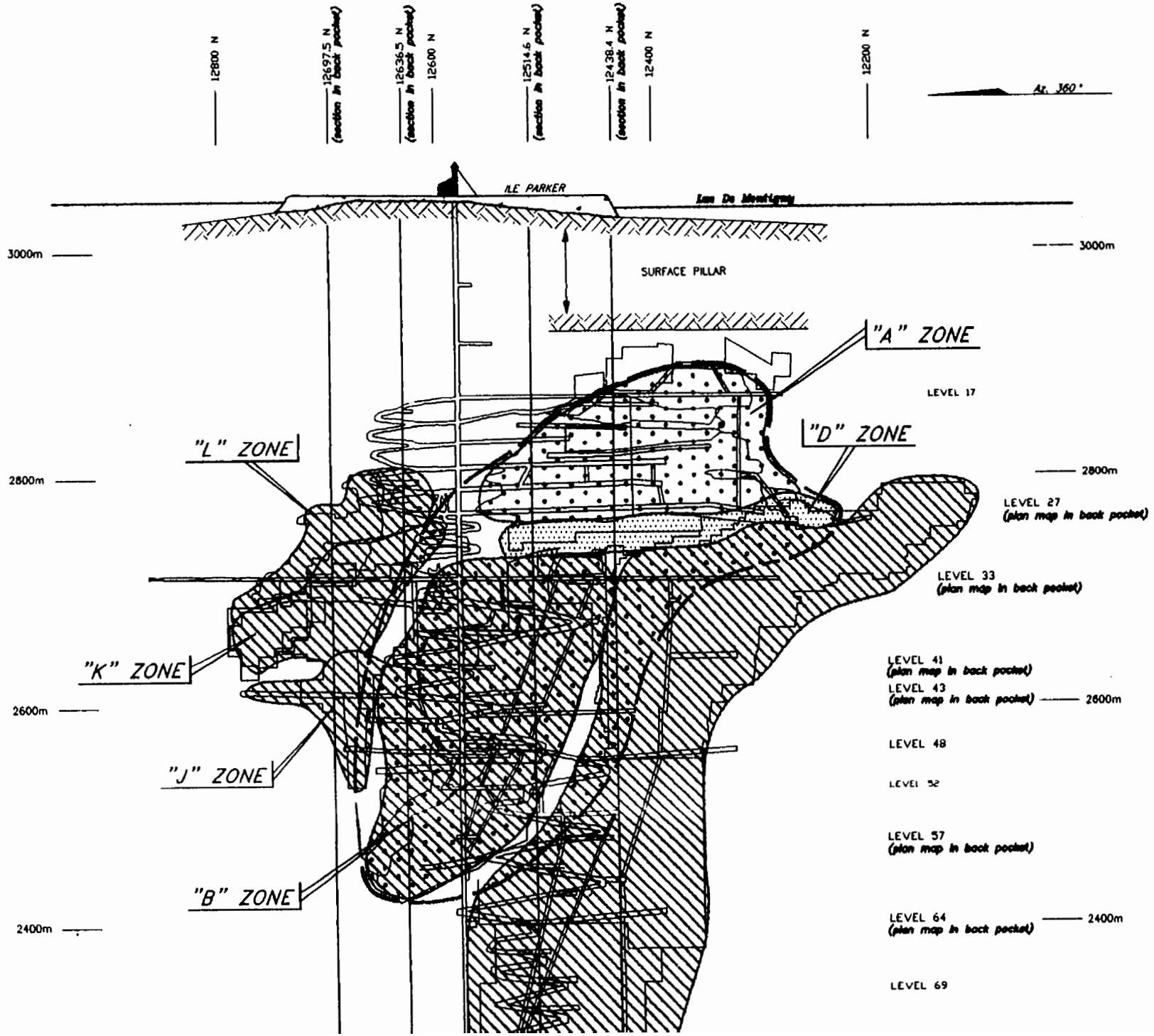
12800 N
12697.5 N
(section in back pocket)
12636.5 N
(section in back pocket)
12600 N
12514.6 N
(section in back pocket)
12438.4 N
(section in back pocket)
12400 N
12200 N
Az. 360°
ILE PARKER
Lac De Montigny
3000m
SURFACE PILLAR
"A" ZONE
LEVEL 17
"D" ZONE
"L" ZONE
2800m
LEVEL 27
(plan map in back pocket)
LEVEL 33
(plan map in back pocket)
"K" ZONE
LEVEL 41
(plan map in back pocket)
LEVEL 43
(plan map in back pocket)
2600m
"J" ZONE
LEVEL 48
LEVEL 52
LEVEL 57
(plan map in back pocket)
"B" ZONE
LEVEL 64
(plan map in back pocket)
2400m
LEVEL 69

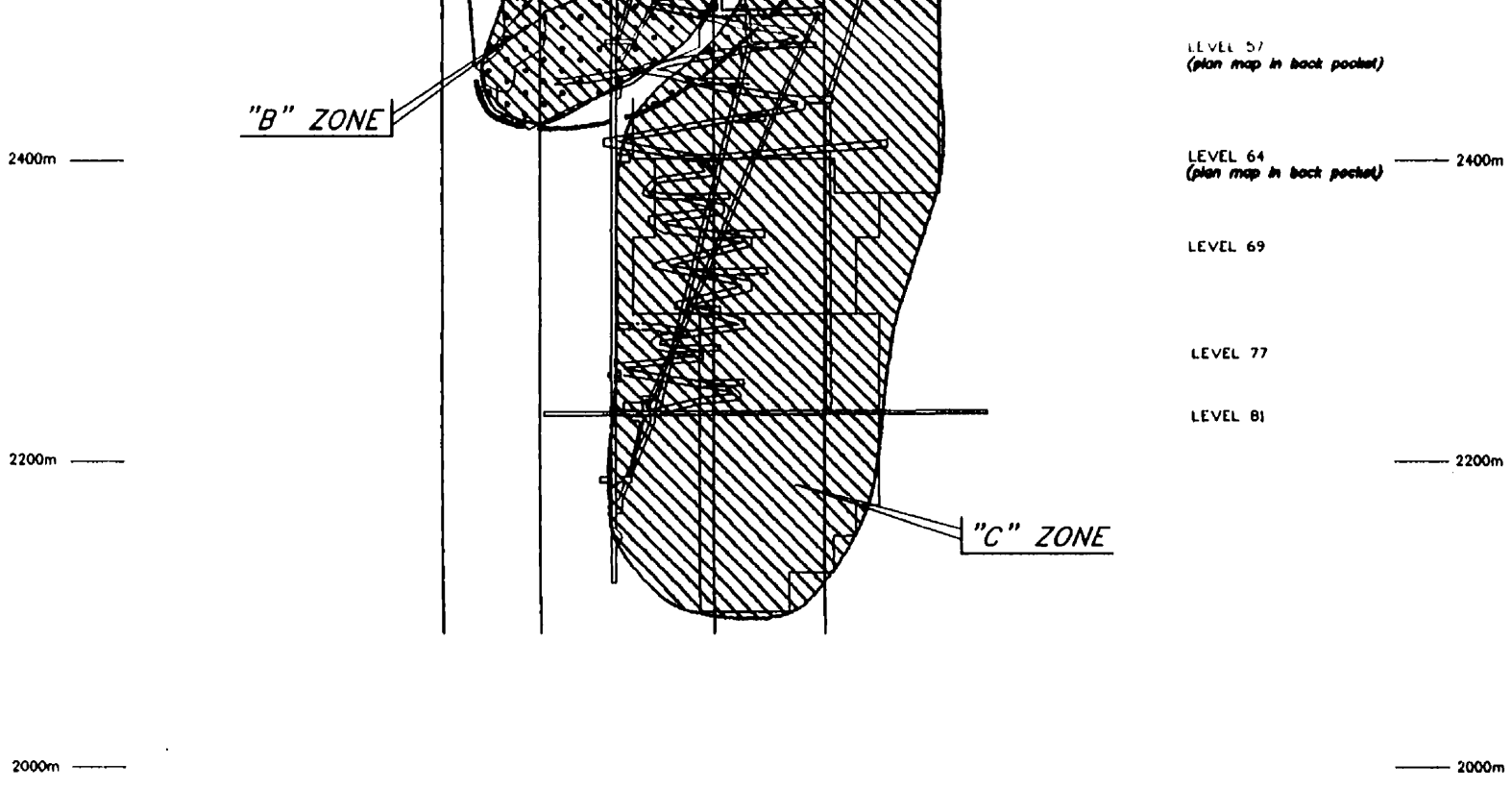

LEGEND

- Stwk Cb-Qz-Py(Po) ± Ab-Au (10%) Breccia 1 (15%) BRECCIA 2 (75%)
- Stwk Cb-Qz-Py(Po)±Ab-Au (20%) BRECCIA 1 (35%) BRECCIA 2 (45%)
- Stwk Cb-Qz-Py(Po)±Ab-Au (35%) BRECCIA 1 (40%) Breccia 2 (25%)
- STWK CB-QZ-PY(PO)±AB-AU (80%) Breccia 1 (10-15%) Breccia 2 (5%)
- **"S-50" ZONE**
- Stopes Outlines

* *See Sections and Level Maps located in the back pocket*

LES MINES D'OR KIENA LTEE.

Figure 3.2

LONGITUDINAL SECTION

COMPILED BY : S. Morasse
DATE : 04/20/94

COMPUTER DRAFTING BY : S. Tremblay

SCALE 1 : 5 000
0m 50m 100m

the deposit chiefly consists of Breccia 2 and lesser Breccia 1 ore types at upper mine levels, and exclusively consists of "Stwk Cb-Qz-Py(Po)±Ab-Au" vein ore type at lower mine levels (see **Figure 4.22**). By contrast, the lower-grade ore shell is restricted to upper mine levels and predominantly consists of "Stwk Cb-Qz-Py(Po)±Ab-Au" vein ore type with minor "Breccia 1" and "Breccia 2" ore types (**Figure 4.22**). Breccia-type ores are thus restricted to upper mine levels and change toward stockwork vein ore type occurs progressively with depth.

The following is an overview of the Kiena deposit ore-dike system based on the study of schematic geological plan maps and sections (in back pocket) prepared during field work:

1. The volcanic wall-rock sequence east of the orebody consists, from the oldest to the youngest of a basaltic flow breccia, an iron tholeiite and a carbonate-chlorite-talc-± quartz schist (or meta-basaltic komatiite), whereas that west of the orebody consists of a carbonate-talc-chlorite-sericite-±albite schist, and a magnesian tholeiite (sections **12438.4 N** and **12514.6 N**).

2. Kiena's gold-ore forms a thin and continuous orebody sub-parallel to bedding. It varies between 225 and 600 metres in length, between 10 and 50 metres in width, and has a vertical extent which varies between 250 and a 1000 metres.

3. The main host rock of the Kiena deposit consists of an anastomosing albitite dike swarm. The eastern iron tholeiite forms a secondary and minor ore host.

4. The orebody is comprised of three ore types which consist, from the oldest to the youngest, of carbonate-quartz stockwork veins accompanied by albite-pyrite(pyrrhotite)-Au alteration halos or Stwk Cb-Qz-Py(Po)±Ab-Au vein ore type, of carbonate (ankerite)-pyrite-Au replacement veins or "Breccia 1" ore type, and of albite stockwork veins and breccias with disseminated pyrite, chalcopyrite, scheelite, and gold or "Breccia 2" ore type (**41 Level Map**).

5. The orebody shows a clear upward and outward zonation pattern (see **Figure 4.22**) consisting of a high-grade core enclosed, at upper mine levels, by a lower-grade ore shell. The high-grade core (5-25 g/t Au) is defined by a narrow "root zone" (lower "C" ore zone) consisting of albitite dikes essentially mineralized by the "Stwk Cb-Qz-Py(Po)-±Ab-Au" vein ore type (e.g. **64 Level Map**), progressing upward into a broader "apical zone" ("A", "D" and "B" ore zones) consisting of albitite dikes and contiguous mafic volcanic flows almost entirely obliterated by the

Breccia 1 and Breccia 2 ore types (e.g. **33 Level Map**). The lower-grade ore shell (3-5 g/t Au) consists of mafic volcanic flows predominantly mineralized by the "Stwk Cb-Qz-Py(Po)-±Ab-Au" vein ore type ("J", "K", "L", and upper "C" ore zones), and grades into the deposit's outer gold alteration halo (0.34-3 g/t Au) with the progressive decrease in carbonate-quartz stockwork veins away from the ore. Pyrrhotite is the predominant sulfide at depth, whereas pyrite is the main sulfide at upper mine levels (see **Figure 4.22**).

6. Breccia ore types do not occur beyond mine level 62 at a depth greater than 620 metres below surface (sections **12514.6 N** and **12636.5 N**).

7. The orebody is associated with an intermediate to felsic dike complex composed of pre-mineral albitite dikes and intermineral granodiorite and feldspar porphyry dikes. Cross-cutting relationships indicate that the feldspar porphyry dike is the youngest intrusion at Kiena (section **12636.5 N** and **57 Level Map**).

8. The intermineral granodiorite dike is xenolithic and contains large fragments of gold ore (section **12696.5 N**) and of mineralized albitite dikes (section **12696.5 N**, **33** and **41 Level Maps**).

9. Kiena's orebody was initially deformed by an asymmetric z-shaped fold, and refolded later into a broad open fold plunging 30-40° to the north-northwest. The z-fold, visible in plan view (e.g. **41** and **43 Level Maps**), is associated with a moderately north-dipping axial planar schistosity. The ore-dike complex and the main schistosity are deformed by the north-northwest-plunging fold (e.g. sections **12438.4 N** and **12514.6 N**) and overprinted by the deposit's east-dipping crenulation cleavage (e.g. **43** and **64 Level Maps**).

10. Removing the effects of folding restores the narrow Kiena ore-dike complex to a northwest-striking, bedding-parallel fault zone cutting across the southerly-overturned Jacola volcanic rock sequence (**Figure 3.1**, section **12514.6 N**).

11. The progressive tightening of the anastomosed albitite dike pattern between mine levels 57 and 64 suggests that penetrative strain increases with depth.

12. Penetrative planar fabrics overprinting the ore and intermineral dikes are cut by late-stage, steeply northwest-dipping, oblique-slip faults.

In summary, information gathered from the internal geometry of the orebody and its relationship to the country rocks may already point out to geological controls, details of ore-forming processes, and timing of gold ore formation at Kiena. Mineralization is partially

controlled by a pre-ore, bedding-parallel fault zone and by the successive overprint of episodic veining and brecciation events. Albitite dikes exert a strong control over the distribution of mineralization suggesting a possible genetic relation between these intrusions and the ore. The lateral and vertical extent of mineralization diminishes with each successive vein mineralizing event, but more gold appears to be introduced (partly remobilized ?) each time. As seen in the longitudinal section of **Figure 3.2**, coalescing breccias in the upper part of the deposit suggests that brittle structures flare upwards with ascending hydrothermal fluids. Events occurring after main-stage gold mineralization include the emplacement of intermineral granodiorite and feldspar porphyry dikes, deformation of the ore-dike complex by folds and related penetrative planar fabrics, and later overprint by oblique-slip faults. Accordingly, these events suggest that the deposit is not controlled, but overprinted, by regional synmetamorphic deformation.

3.3 STRATIFORM ROCKS EAST OF THE "S-50" ZONE

3.3.1 Introduction

The objective of this section is to characterize the mine's volcanic rock sequence. Because there is reason to believe that the rocks were steep when the ore was emplaced, and because the rocks are folded i.e. hangingwall changes (sections **12438.4 N** and **12514.6N**, back pocket), it is more useful to describe the rock sequence hosting the Kiena deposit as stratiform rocks "***east of the S-50 zone***" and stratiform rocks "***west of the S-50 zone***".

At the time this study was undertaken, the stratigraphic order of the Kiena Mine wall-rock sequence remained unclear for two main reasons: 1) previous younging directions were not considered reliable as a result of the high variability of sizes among the spinifex structures of komatiites, and 2) advances in mining did not provide cuts of tholeiitic pillowed flows permitting to read flow top directions (Cormier M., personal communication). However, the discovery of a basaltic flow top breccia at level 41 during the course of mapping (**41 Level**

Map and Index geological maps 4138/4105), in conjunction with top determinations recorded in the pillowed volcanic rocks outcropping at surface (see **Figure 3.1**), suggests that the rock succession enclosing the mine is facing west to southwest (see also Kiena Mine 33 Level Map at 1:5000 in back pocket). Based on this interpretation, the volcanic rock sequence "east of the S-50 zone" consists, from the oldest to the youngest, of a basaltic flow top breccia, overlain by a massive iron tholeiite, which in turn, is locally overlain by a basaltic komatiite, now altered and metamorphosed to a carbonate-talc-chlorite-±quartz schist. Descriptions of these rock units are presented below.

3.3.2 Basaltic flow top breccia (marker unit)

The easternmost rock unit exposed by mine workings at Kiena is a light green and weakly schistose volcanic rock (**41 Level Map**, back pocket) of tholeiitic composition (**Tables C.1 and C.2, Appendix C**). The latter has been difficult to map because it is rarely cut by bore holes, and is only sporadically exposed by mining development. The distribution of this rock type is not fully known at this time, but with distinctive mesoscopic features such as its pillow flow breccia character and its light green color, this rock unit should be easily traced in the earlier mining and drilling records and used as a marker unit in the mine volcanic sequence.

This rock unit consists of sub-rounded and highly vesicular basaltic fragments, varying in length between 2 and 10 centimetres, set in a fine-grained brecciated basaltic matrix composed of an assemblage of plagioclase microlites with relics of plagioclase and mafic phenocrysts. The volcanic fragments are easily recognized by their light green to beige color, which contrasts with the greyish-green color of the rock matrix. The core of the fragments is generally light green and displays a porphyritic texture which grades into a dark green aphanitic rim. The larger of these fragments are reminiscent of small pillow structures, suggesting that this rock type may represent a brecciated pillow flow (**Figure 3.3**). To the west, the brecciated tholeiitic rock is in contact with a massive and coarse grained iron

Figure 3.3 - *Underground exposure of the schistose basaltic flow top breccia, east of the "S-50" zone. Vertical cross-section view, looking to the northeast.*

Access drift 4105, north of "C" zone, Kiena Mine level 41.

Affleurement de la brèche de sommet d'une coulée basaltique coussinée, située à l'est de la zone "S-50". Vue sur une section verticale avec regard vers le nord-est.

Galerie d'accès 4105, au nord de la zone "C", niveau 41 Mine Kiena.

tholeiite. The contact is sharp and is marked by a sudden change in color from light green to dark grey, by the disappearance of feldspar phenocrysts and by a decrease in both, the density of carbonate-quartz-filled fracture planes and schistosity planes. It is therefore interpreted as a stratigraphic contact. Primary bedding planes measured in the brecciated tholeiitic rock unit east of the "C" Zone (**41 Level Map** and Index geological map 4105, back pocket) indicate that this unit of volcanic rocks strikes north-south and with an apparent dip of 25-30° west[7]. A southwesterly-younging direction is suggested by the southward succession of a massive, coarse-grained basalt, followed by a pillowed basalt and the pillow flow top breccia as mapped in drill core by Jeansonne (1993) at level 33 (see Kiena Mine 33 Level Map at 1:5000 in back pocket). Pillow fragments commonly display fine carbonate-quartz-filled stockwork fractures and have been flattened, as indicated by their long axis set parallel to the main schistosity. The basaltic rock matrix surrounding the pillow fragments contains plagioclase phenocrysts partly replaced by sericite and mafic phenocrysts replaced by calcite, chlorite and epidote in a felty groundmass composed of plagioclase microlites, chlorite and calcite.

3.3.3 Tholeiitic basalt (iron tholeiite)

A massive mafic volcanic flow overlies the basaltic flow top breccia and is in contact with the main orebody between mine levels 38 and 46 (e.g. **41** and **43 Level Maps** in back pocket). Compositions of the least-altered samples of this rock type (**Tables C.3 and C.4, Appendix C**) reveal that this rock unit is an iron tholeiite (see Jensen cation plot on **Figure 3.4**) confirming the earlier findings of Muir (1981).

The iron tholeiite is a massive to schistose, coarse-grained to aphanitic rock characterized by a dark grey to greyish-green color, the presence of carbonate-quartz (py-po) stockwork veins, and by finely disseminated magnetite grains. Several compositional and textural changes

---

[7] However,schematic cross-section 12438.4 N shows that at level 41, all rock units are steeply west-dipping.

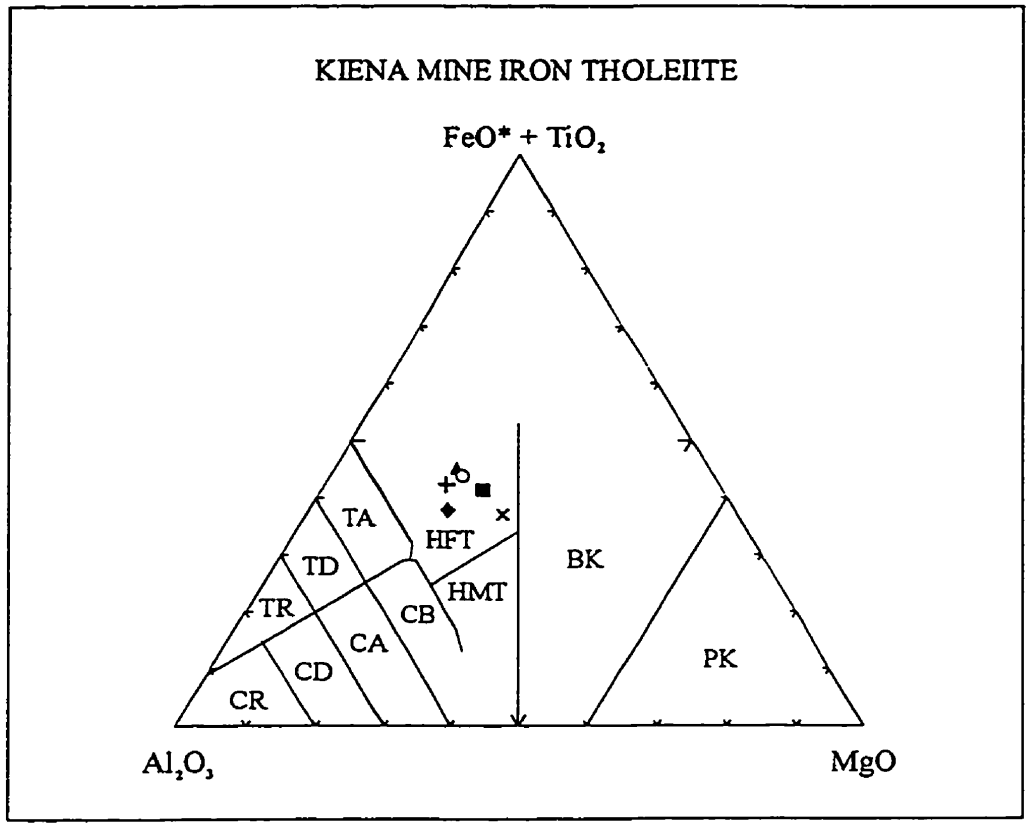

Figure 3.4 *Compositions of the least-altered iron tholeiite east of the "S-50" zone reported on a Jensen (1976) cation plot. Total iron recalculated as FeO (Newpet, 1993). See Appendix C to obtain the composition of the iron tholeiite samples used in this plot.*

Compositions de la tholéiite ferrifère située à l'est de la zone "S-50", reportées sur un diagramme ternaire cationique de Jensen (1976). Le fer total a été recalculé sous forme de FeO (Newpet, 1993). Se référer à l'Appendice C afin de consulter la composition des échantillons de tholéiite ferrifère utilisés dans ce diagramme.

Abbreviations: ***PK - peridotitic komatiite; BK - basaltic komatiite; HFT - high iron tholeiite; HMT - high magnesian tholeiite; TA - tholeiitic andesite; TD - tholeiitic dacite; TR - tholeiitic rhyolite; CB - calc-alkalic basalt; CA - calc-alkalic andesite; CD - calc-alkalic dacite; CR - calc-alkalic rhyolite.***

Samples: ***o K92-3002-237; × K92-3033-247; + K92-3841-252; ▲ K92-4346-254; ◆ K92-6401-245; ■ K92-6467-246.***

Abréviations: ***PK - komatiite péridotitique; BK - komatiite basaltique; HFT - tholéiite hautement ferrifèrel; HMT - tholéiite hautement magnésienne; TA - andésite tholéiitique; TD - dacite tholéiitique; TR - rhyolite tholéiitique; CB - basalte calc-alkalin; CD - dacite calc-alkaline; CR - rhyolite calc-alkaline.***

Échantillons: ***o K92-3002-237; × K92-3033-247; + K92-3841-252; ▲ K92-4346-254; ◆ K92-6401-245; ■ K92-6467-246.***

observed in the iron tholeiite when approaching the ore zone, led to the recognition of three distinct alteration facies based on color, texture, magnetism, vein alteration and deformation. They are as follows: 1) weakly deformed and least altered tholeiite (**Figure 3.5**), 2) variously deformed, stockwork vein-altered and weakly gold-bearing tholeiite (**Figure 3.6**), and 3) weakly to highly deformed mineralized tholeiite (**Figure 3.7**). The "first alteration facies" occurs 10 to 25 metres away from the ore zone and is characterized by a massive, coarse-grained, magnetic, dark grey rock (**Figure 3.5**). Magnetism is caused by the presence of disseminated magnetite grains along fine chlorite stringer veins which cut the tholeiite. As the density of chlorite-magnetite veinlets is low, rock magnetism is sporadic and may not be detected[8]. This facies is further characterized by the local presence of carbonate stockwork veinlets and by a widely-spaced cleavage (2-10 cm; **Figure 3.5**). The "second alteration facies" forms part of the orebody's alteration envelope shown on the schematic geological plan maps and cross-sections (in back pocket). It is characterized by an abundance of variously deformed carbonate-quartz stockwork veins accompanied by albite-pyrite-±pyrrhotite alteration halos (grading 0.3-3.0 g/t Au), the green color of the intervening volcanic rock, and by a notable increase in the intensity of spaced cleavage development (**Figure 3.6**). The "third alteration facies" consists of a greyish-green rock characterized by the presence of coalescing albite stockwork veins and breccias which hosts a mosaic of angular wall-rock fragments (main ore zone, **Figure 3.7**). The mineralized iron tholeiite is further characterized by the presence of fine chlorite-biotite-magnetite stringer veins, locally altered to stilpnomelane, and by the development of a north-dipping schistosity affecting both, the altered iron tholeiite, and the veins (**Figure 3.7**). All the samples of iron tholeiite collected in the mine have been variously altered by albite, carbonate-quartz-pyrite(Po) and chlorite-biotite-magnetite stringer veins and exhibit various degrees of deformation. The least-altered and -deformed iron tholeiite consists of a mineral assemblage comprised of feldspar and mafic phenocrysts replaced by calcite and epidote, set in a granoblastic quartzo-feldspathic groundmass partially replaced by chlorite, calcite, epidote and actinolite. The iron

---

[8] Magnetometer (K-2) readings for this facies of iron tholeiite facies vary between 1.0 and 4.7 x 10^{-5} cgs units.

Figure 3.5 - *Photograph of the least-altered and least-deformed iron tholeiite east of the S-50 zone, showing a weakly developed north-dipping (to the left) spaced cleavage.*

Access drift 4105, level 41 Kiena Mine.

Photo du faciès le moins altéré et le moins déformé de la tholéiite ferrifère située à l'est de la zone S-50, montrant un clivage d'espacement pendant vers le nord (à gauche).

Galerie d'accès 4105, niveau 41 Mine Kiena.

Figure 3.6 - *Photograph of the carbonate-quartz stockwork vein-altered iron tholeiite east of the S-50 zone, characteristic of the gold alteration envelope enclosing the main orebody (see Figure 4.22). The strong discoloration observed along vein selvages consists of an assemblage of albite and disseminated pyrite. The deposit's main schistosity dips north-northwest (to the left) and is axial planar to the weakly mineralized stockwork veins.*

Access drift 3810 to "B" zone, Kiena Mine level 38.

Photo de la tholeiite ferrifère située à l'est de la zone S-50, altérée par des veinules de carbonate-quartz en stockwork; ce facies de la tholeiite est charactéristique de l'enveloppe d'altération aurifère développée autour du gisement (voir Figure 4.22). Le blanchiment qui est observé autour des veines est formé d'un assemblage d'albite et de pyrite disséminée. La schistosité principale du gisement pend vers le nord-nord-ouest (vers la gauche) et est plan axial des plis affectant les veines minralisles en stockwork..

Galerie d'accès 3810 de la zone "B", niveau 38 Mine Kiena.

Figure 3.5

Figure 3.6

Figure 3.7 - *Photo mosaic showing the mineralized and deformed iron tholeiite forming part of the "S-50" zone. The outcrop is laced with albite-pyrite-chalcopyrite-scheelite-Au stockwork veins which coalesce locally into pods of mosaic breccia (Breccia 2 ore). The altered wall-rock, the veins, and the breccia are cut by the deposit's main schistosity which dips moderately to the north-northwest (to the left).*

"B" zone, ore drift 4117, Kiena Mine level 41.

Collage photographique montrant la tholéiite ferrifère minéralisée et déformée de la zone "S-50". L'affleurement est recoupé par des veines d'albite-pyrite-chalcopyrite-scheelite-Au en stockwork, qui s'amalgament localement pour former des zones irrégulières de brèche (minerai de type Breccia 2). Les épontes de tholéiite altérée, les veines ainsi que la brèche, sont affectées d'une schistosité à pendage modéré vers le nord-nord-ouest (vers la gauche).

Zone "B", galerie à minerai 4117, niveau 41 Mine Kiena.

tholeiite samples have been analyzed for a suite of trace elements commonly found in copper/molybdenum porphyry and precious metal epithermal deposits, but only very small quantitites of Cu, Hg, and Zn have been detected (see **Appendix C**).

3.3.4 Carbonate-talc-chlorite± quartz-albite schist (meta-basaltic komatiite)

A lenticular unit of light greyish-green and highly schistose rock is in contact with the orebody east of the S-50 zone in the upper levels of the mine (e.g. section 12514.6 N, back pocket). The schist, which pinches out towards the main ore zone at level 38, re-appears at level 46 (Index geological map 4613, back pocket), but it was not possible to determine if these two schist zones form a single rock unit or two separate lenticular units. Occasional relics of komatiitic texture seen in this section suggest that the protolith of this schistose rock was probably a basaltic komatiite. This former volcanic rock, which has been variously altered and weakly mineralized, forms part of the gold alteration envelope enclosing the orebody when its gold content ranges between 0.34 g/t Au and the cut-off grade of 3.0 g/t Au.

Textural and compositional variations are also observed in the schist when approaching the contact with the ore zone. Away from the ore, the schist is a dark green rock exhibiting relics of spinifex texture consisting of parallel arrangements of radiating talc and chlorite with an interstitial assemblage of fine-grained albite and lesser quartz (**Figure 3.8**). The fabric is moderately schistose, and characteristically cut by various amounts of fine, folded and boudinaged carbonate-quartz±albite-pyrite veins. Closer to the ore, the schist becomes a strongly schistose greyish-green rock characterized by the presence of a particularly high density of carbonate-quartz-(pyrite) veins (up to 40%; **Figure 3.9**). This schistose rock is chiefly composed of carbonate, talc and chlorite, with lesser quartz, albite and ilmenite. Where the density of carbonate-quartz stockwork veins is the greatest, the fabric of the rock is gneissic and characterized by the alternation of lensoid assemblages of carbonate grains with talc-chlorite-rich bands (**Figure 3.10**).

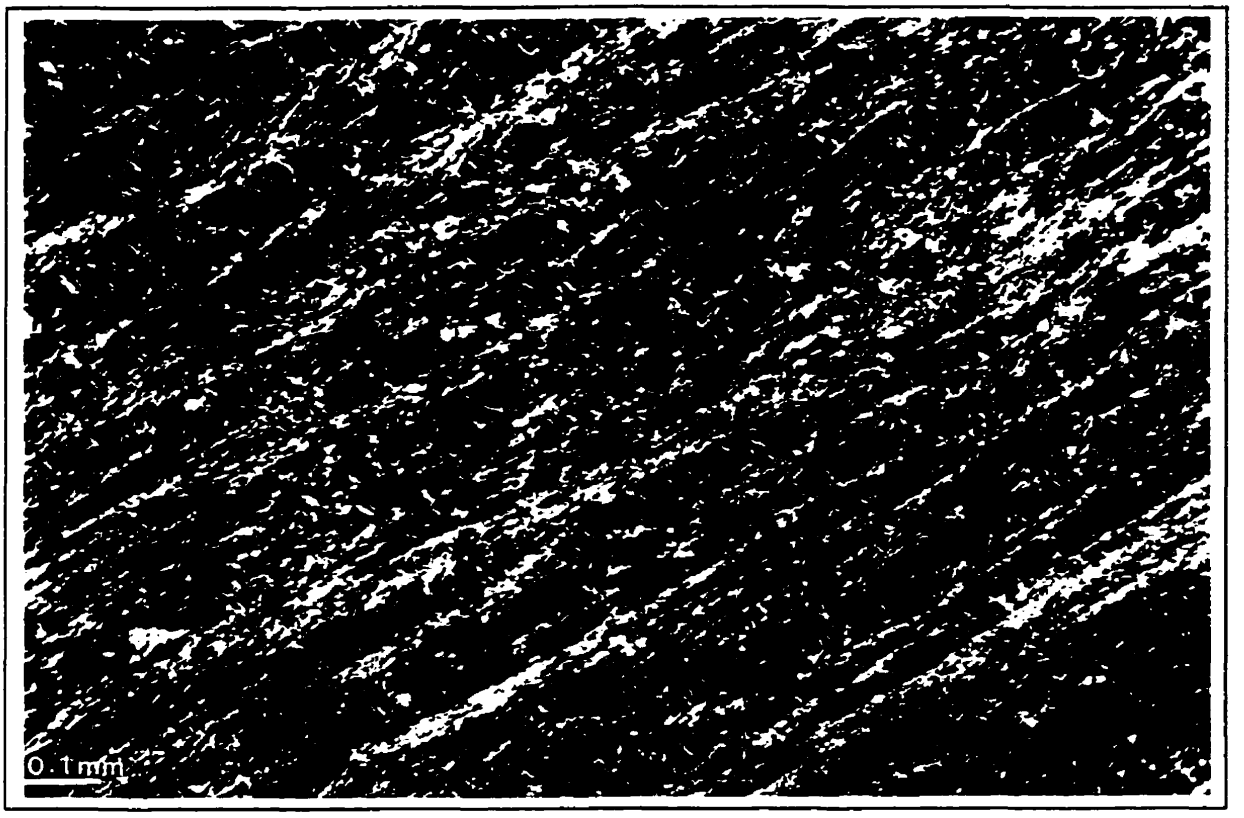

Figure 3.8 *- Photomicrophotograph of a carbonate-talc-chlorite±quartz-albite schist, east of the S-50 zone. The blade-like microstructure is defined by a parallel arrangement of talc and chlorite with an intersticial microcrystalline assemblage of quartz and albite. It is interpreted as a relic spinifex texture.*

Sample K92-3033-247, crossed polars. Ramp of the Kiena Mine, levels 30-33.

Microphotographie du schiste à carbonate-talc-chlorite±quartz-albite situé à l'est de la zone S-50. Le schiste est charactérisé par sa microstructure lamellaire composée de feuillets de talc et chlorite disposés en bandes parallèles, avec quartz et albite en interstice. Cette fabrique est interprétée comme étant une relique de texture en spinifex.

Échantillon K92-3033-247, nicols croisés. Rampe de la Mine Kiena, niveaux 30-33.

Figure 3.9 - *Photograph of the carbonate-talc-chlorite-±quartz-albite schist east of the S-50 zone in contact with the main orebody. The schist is laced with carbonate-quartz-stockwork veins, which have been deformed and cut by the main north-northeast-dipping (to the left) schistosity. This alteration facies is typical of the carbonate-talc-chlorite-±quartz-albite schists forming part of the orebody's gold alteration envelope.*

"B" zone, ore drift 4613, Kiena Mine level 43.

Photo du schiste à carbonate-talc-chlorite-±quartz-albite, situé à l'est de la zone S-50, au contact du minerai. Le schiste est recoupé par un réseau de veinules à carbonate-quartz en stockwork. Celles-ci ont été déformées puis recoupées par la schistosité à pendage modéré vers le nord-nord-ouest (vers la gauche). Ce faciès d'altération est typique du schiste à carbonate-talc-chlorite-±quartz-albite partiellement inclus dans l'enveloppe d'altération aurifère du gisement.

Zone "B", galerie à minerai 4613, niveau 46 Mine Kiena.

Figure 3.10 - *Photomicrograph of the carbonate-talc-chlorite-±quartz-albite schist represented in Figure 3.9, showing the alternation between carbonate- and talc-rich layers. Note in the talc-rich band, the presence of stylolitic dissolution cleavage set perpendicular to schistosity. Cb= carbonate, Tc= talc.*

Sample K92-4613-193, "B" zone, transmitted light, crossed Nicols. Ore drift 4613, Kiena Mine level 46.

Microphotographie du schiste à carbonate-talc-chlorite-±quartz-albite représenté à la Figure 3.9, montrant l'alternance de bandes riches en carbonate et riches en talc. Notez la présence de clivages de dissolution de type stylolitique (perpendiculaire à la schistosité)au sein de la bande riche en talc, . Cb= carbonate, Tc= talc.

Échantillon K92-4613-193, microscope à lumière transmise, Nicols croisés. Zone "B", galerie à minerai 4613, niveau 46 Mine Kiena.

Figure 3.9

Figure 3.10

Another basaltic komatiite rock unit was discovered in contact with the orebody at mine level 64 in the course of this mapping, but its distribution is not known. Away from the ore zone, this rock unit consists of a massive dark green rock characterized by a mineral assemblage chiefly composed of radiating, feathery blueish-green amphibole (actinolite) grains distributed along blade-like microstructures, with interstitial quartz and coarse-grained skeletal magnetite grains. This fabric is interpreted as a relic spinifex texture (**Figure 3.11**). The rosettes of actinolite which mimic somewhat the arrangement of crystals in a spinifex texture (i.e. "pseudo-spinifex" texture) are probably metamorphic in origin. Closer to the ore zone, relics of primary ultramafic igneous textures have been destroyed and replaced by an assemblage chiefly composed of microcrystalline albite and poikiloblastic hornblendes, with lesser quartz and disseminated relics of skeletal magnetite (**Figure 3.12**).

Figure 3.11

Figure 3.12

3.4 STRATIFORM ROCKS WEST OF THE "S-50" ZONE

3.4.1 Introduction

Underground exposure of the volcanic sequence west of the S-50 zone is very limited due to the advance of mining, which generally takes place from the wall-rock sequence east of the S-50 Zone towards the main orebody (see section 12514.6 N, back pocket). At the time this study was undertaken, most of the mine workings previously available west of the orebody, had been either too severely oxidized for mapping, condemned as a result of wall-rock instability, or flooded. However, Clark (1963) has depicted the volcanic sequence west of the S-50 zone at upper mine levels on a composite section, and has shown that the orebody is mostly in contact with a magnesian tholeiite and is locally interdigitated with thin, lenticular meta-komatiitic flows (Kiena Mine Composite Section 11, back pocket). Two main rock types located west of the S-50 zone were mapped between mine levels 36 and 64 in the course of this study: a massive, porphyritic-to schistose, basaltic volcanic rock and several varieties of schists. The descriptions of these rock types are featured in the following sections.

3.4.2 Glomero-porphyritic basalt (magnesian tholeiite)

This weakly mineralized volcanic rock is in contact with the orebody and forms part of the alteration envelope. It consists of a greyish-green and strongly porphyritic (10-15%) rock, laced with albite-carbonate-pyrite stockwork veins (**Figure 3.13**). The distribution of this basaltic rock is not fully known at this time, but judging from its stratigraphic position it may coincide with the magnesian tholeiite described by Clark (1963) and Muir (1979; 1981). The basaltic rock has been weakly foliated and displays a relic glomero-porphyritic texture consisting of clusters of albite phenocrysts set in a microcrystalline groundmass composed of equigranular and commonly untwinned albites marked by highly serrated (sutured) grain boundaries (i.e. albitized volcanic rock, see **Figure 3.4**). This albite-altered rock has been cut and weakly mineralized by albite-carbonate-pyrite stockwork veins, overprinted in turn by

Figure 3.13 - *Photograph of the magnesian tholeiite west of the S-50 zone at the contact with the orebody. The rock, which displays a strongly porphyritic fabric, is laced with albite-carbonate-pyrite stockwork veins (Cb). The latter are overprinted by chlorite (biotite)-magnetite stringer veins (Chl). The basalt is deformed as indicated by the folded stockwork veins as well as by the weakly developed foliation axial planar to the folds (dashed line), which is defined by the alignement of the long axis of albite phenocrysts (Ab). Note that the deformed chlorite stringer veins are also subparallel to foliation.*

Sample K90-4313-062, ore drift 4313, Kiena Mine level 43.

Photo du basalte magnésien situé à l'ouest de la zone S-50, en contact avec la zone minéralisée. L'échantillon illustre la texture densément porphyritique du basalte, laquelle est lacérée par des veines d'albite-carbonate-pyrite en stockwork (Cb). Ces dernières ont été recoupées par des veinules de chlorite (biotite)-magnétite (Chl). Le basalte est déformé tel que l'indique les plis qui affectent les veines en stockwork ainsi que la faible foliation développéee dans le plan axial des plis (ligne pointillée). Celle-ci est représentée par l'alignement des axes long des phénocristaux d'albite (Ab). Notez que les veinules de chlorite, qui sont également déformées, sont subparallèles à la foliation.

Échantillon K90-4313-062, galerie à minerai 4313, niveau 43 Mine Kiena.

Figure 3.14 - *Photomicrograph of the glomero-porphyritic basalt represented on Figure 3.13, showing fractured and chlorite-altered albite phenocrysts (Ab) in a microcrystalline groundmass composed of untwinned albite grains (Ab), chlorite and calcite. The fabric is cut by albite-carbonate veinlets, that are cut, in turn, by chlorite-magnetite (Chl) stringer veins.*

Sample K90-4313-062, crossed-polars. "B" Zone, ore drift 4313, Kiena Mine level 43.

Microphotographie du basalte glomérо-porphyrique représenté à la Figure 3.13, montrant des phénocristaux fracturés et chloritisés d'albite (Ab) baignant dans une matrice microgrenue composée de cristaux d'albite non maclés (Ab), de chlorite et de calcite. Cette fabrique est recoupée par des veinules à albite- carbonate, qui sont elle-même recoupées par des veinules à chlorite-magnétite (Chl).

Échantillon K90-4313-062, microscope à lumière transmise, Nicols croisés. Zone "B", galerie à minerai 4313, niveau 43 Mine Kiena.

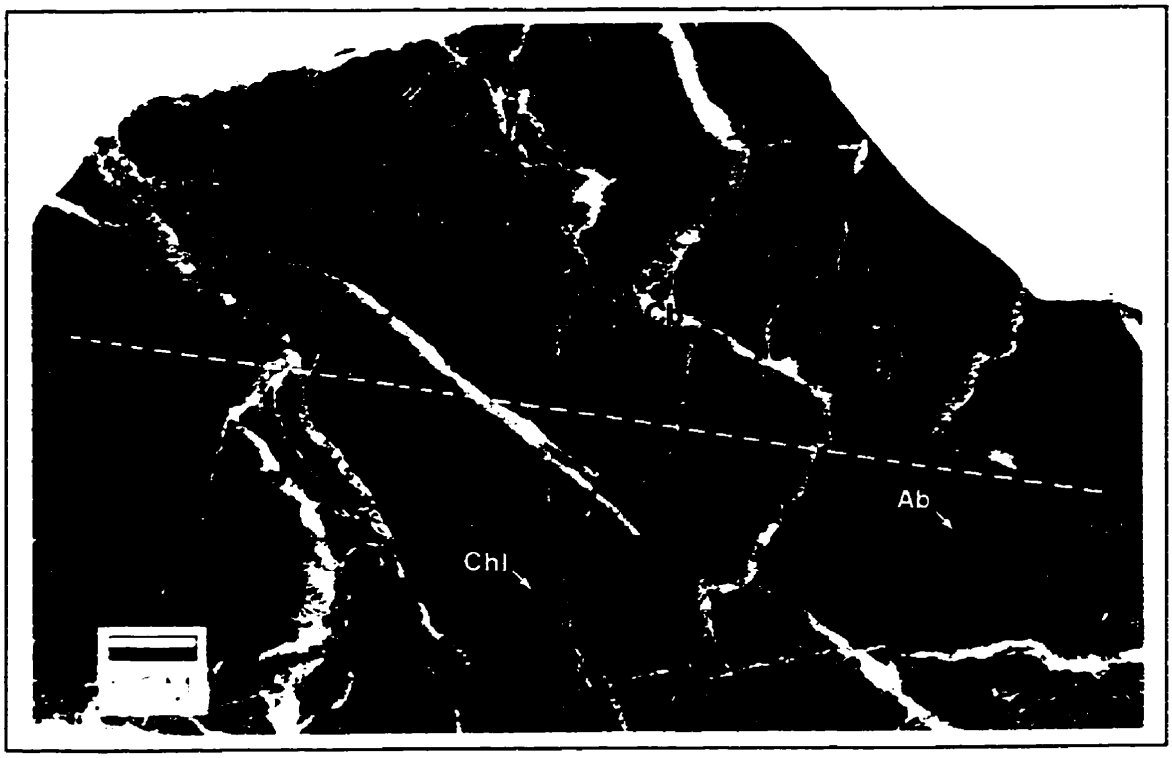

Figure 3.13

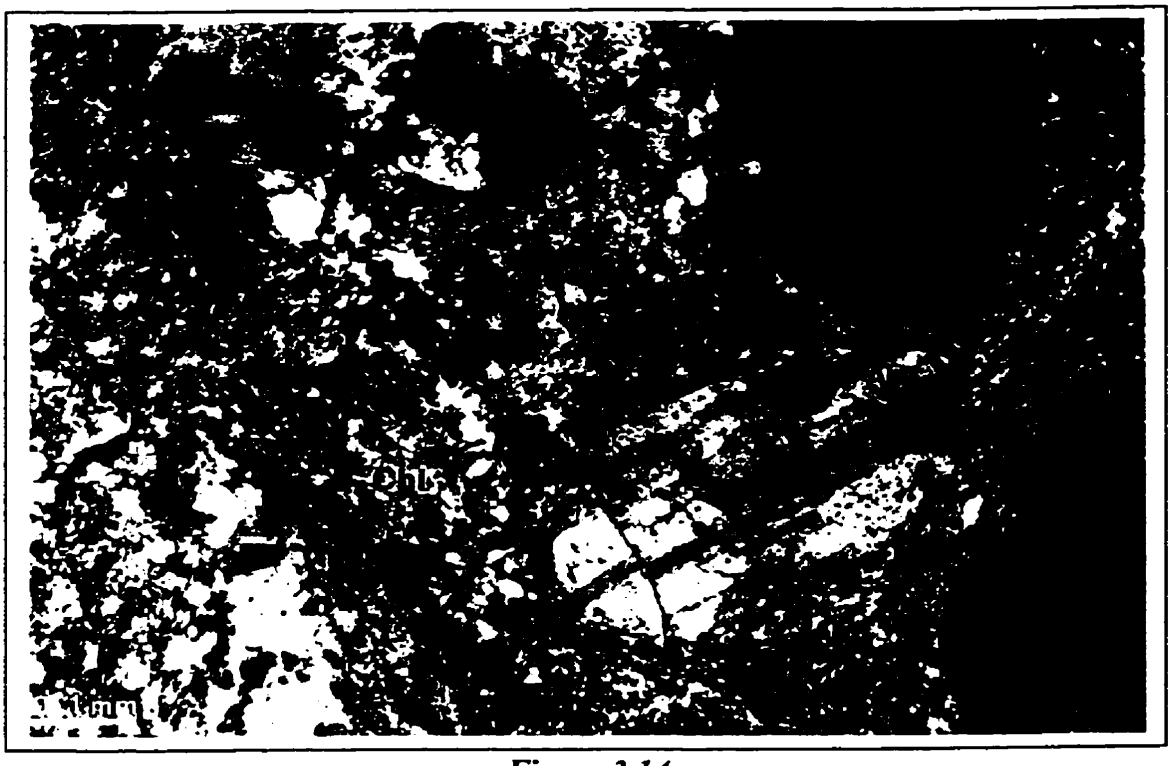

Figure 3.14

chlorite-biotite-magnetite stringer veins. Penetrative strain is exhibited by folded albite-carbonate-pyrite veins, anastomosing chlorite-biotite-magnetite stringer veins, and a weak mineral lineation defined by albite phenocrysts (**Figure 3.13**). This suggests that the porphyritic volcanic rock in contact with the S-50 Zone was first weakly mineralized and then deformed.

3.4.3 Schist zones

Two schist zones are observed at the western contact of the main orebody: a carbonate-chlorite-sericite-quartz schist, which forms a minor alteration/deformation zone around the intermineral granodiorite dike, and a carbonate-talc-chlorite-sericite-±albite schist which is interpreted as a highly altered and strongly deformed meta-komatiite. These two schists are characterized below.

3.4.3.1 Carbonate-chlorite-sericite-quartz schist in contact with the intermineral granodiorite dike

A schist zone, ranging approximately 1 to 2 metres in width, locally occurs at the interface between the intermineral granodiorite dike (see section 3.5.2 for description) and the main ore zone (e.g. **64 Level Map** and Index geological map 6446, back pocket). It consists of a light green-grey and highly schistose rock, cut by strongly deformed carbonate-quartz stockwork veins (**Figure 3.15**). The schist is characterized by a protomylonitic gneissic texture defined by lensoid granular assemblages of carbonate alternating with relics of strongly boudinaged chlorite-sericite stringer veins (**Figures 3.15** and **3.16**). Locally, both the intermineral granodiorite dike and its adjacent schist have been folded and overprinted by a sub-horizontal crenulation cleavage.

3.4.3.2 Carbonate-talc-chlorite-sericite-±albite schist (meta-komatiite?)

This is the rock unit most commonly observed at the contact with the orebody *west of the S-*

50 zone. It is characterized by the presence of large fragments of albitite dikes (**Figure 3.17**; see also **41 Level Map** in back pocket) but as the dikes are highly altered, deformed and strongly affected by penetrative strain (particularly in the lower part of the deposit), they may be difficult to distinguish from the schist at depth. This schistose rock unit is characterized by a mylonitic (**Figure 3.18**) fabric consisting of an augen- or gneissic-textured matrix composed of carbonate and talc, cut by carbonate-quartz veinlets, which are overprinted in turn by chlorite-sericite-magnetite stringer veins. Both vein sets are deformed: carbonate-quartz stockwork veins have been folded whereas chlorite-sericite stringer veins have been boudinaged into strings of wispy chlorite and sericite (**Figure 3.19**). Parts of the schist in contact with the fragments of albitite dikes are pervasively albite altered (**Figure 3.17**). These rocks are composed of a microcrystalline assemblage of albite with lesser carbonate and talc and characterized by the partitioning of penetrative strain across the fabric of the schist (**Figure 3.20**). Intense alteration and deformation have obliterated primary textures, however, this schistose rock bears resemblance with the altered and weakly mineralized carbonate-talc-chlorite±albite schist unit in contact with the ore east of the S-50 zone (see section 3.3.4). Hence, by analogy with the latter, the protolith of this schistose rock may have also been a komatiitic volcanic rock.

Figure 3.15 - *Photograph of the carbonate-chlorite-sericite-quartz schist in contact with the intermineral granodiorite dike. The ribboned and protomylonitic texture of the rock is illustrated by the alternation of carbonate-rich bands (Cb) with dark, patchy chlorite-rich bands (Chl). The main carbonate-quartz vein has been tightly folded and boudinaged. Note the well preserved open-space infill-texture exhibited by the branching vein located in the lower right of the photograph (arrow).*

Sample K90-41092-040, ore drift 4139, Kiena Mine level 41.

Photo du schiste à carbonate-chlorite-séricite-quartz en contact avec le dyke de granodiorite interminéralisation. La texture rubannée et protomylonitique de cette roche est illustrée par l'alternance de bandes riches en carbonate (Cb) avec bandes riches en petits lambeaux de veinules de chlorite (Chl). La veine de carbonate-quartz la plus saillante de l'échantillon est à la fois plissée et boudinée. Notez la texture relique de remplissage en fracture ouverte qui est toujours visible au sein de la veine située dans le coin inférieur droit de la photo (flèche).

Échantillon K90-41092-040, galerie à minerai 4139, niveau 41 Mine Kiena.

Figure 3.16 - *Photomicrograph of the carbonate-chlorite-sericite-quartz represented on Figure 3.15, showing the ribboned protomylonitic texture of the schist. Note the wispy habit of chlorite (Chl) as a result of the extension of former chlorite-sericite stringer veins.*

Sample K90-41092-040, plane-polarized transmitted light. Ore drift 4139, Kiena Mine level 41.

Microphotographie du schiste à carbonate-chlorite-séricite-quartz représenté à la Figure 3.15, montrant la texture rubannée et protomylonitique du schiste. Notez l'aspect "échevelé" de la chlorite (Chl), créé par l'extension de veinules réticulées de chlorite-séricite lors de la déformation.

Échantillon K90-41092-040, microscope à lumière transmise, lumière naturelle. Galerie à minerai 4139, niveau 41 Mine Kiena.

Figure 3.15

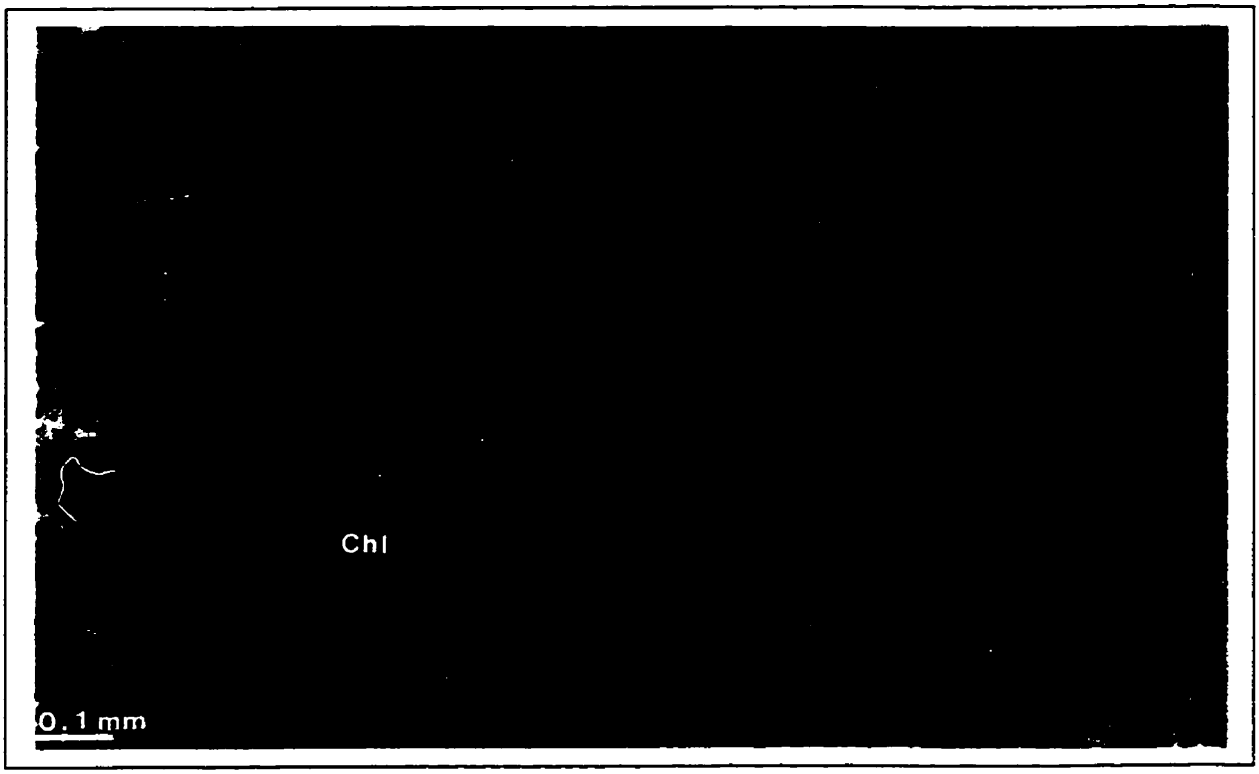

Figure 3.16

Figure 3.17 - *Photograph of the carbonate-chlorite-talc-sericite-±albite schist (or meta-komatiite) west of the S-50 zone, showing a large, sub-angular fragment of weakly mineralized albitite dike outlined by a thin chilled margin (arrow). The deposit's main schistosity, dipping moderately to the north (to the right), cuts the albitite dike fragment. The schistosity and the albitite dike fragment are both cut by quartz-tourmaline-carbonate extension veins.*

"C" ore zone, ore drift 4138, Kiena Mine level 41.

Photo du schiste à carbonate-chlorite-talc-séricite-±albite (ou meta-komatiite) situé à l'ouest de la zone S-50, montrant un large fragment sub-angulaire de dyke d'albitite faiblement minéralisée, lequel est souligné par une mince bordure de trempe (flèche). Le fragment de dyke d'albitite est recoupé par la schistosité principale du gisement, laquelle pend modérement vers le nord (vers la droite). Le schiste et le fragment d'albitite sont tous deux affectés de veines d'extension à quartz-tourmaline-carbonate.

Zone "C", Galerie à minerai 4138, niveau 41 Mine Kiena.

Figure 3.18 - *Close-up view of the carbonate-chlorite-talc-sericite-±albite schist represented on Figure 3.17, showing a strongly developed ribbonned texture consisting of bands of carbonate-quartz veins alternating with bands of chlorite-talc-sericite. The main schistosity (S_n), which dips moderately to the north (to the left), is overprinted by a gently, east-dipping (to the right) crenulation cleavage (S_{n+1}).*

"C" ore zone, ore drift 4138, Kiena Mine level 41.

Vue détaillée du schiste à carbonate-chlorite-talc-séricite-±albite représenté à la Figure 3.17, montrant la texture rubannée du schiste tel que définie par l'alternance de veines de carbonate-quartz avec bandes riche en chlorite-talc et séricite. La schistosité principale (S_n) pend modérément vers le nord (vers la gauche). Elle est déformée par un clivage de crénulation (S_{n+1}) pendant faiblement vers l'est (vers la droite).

Zone "C", Galerie à minerai 4138, niveau 41 Mine Kiena.

Figure 3.17

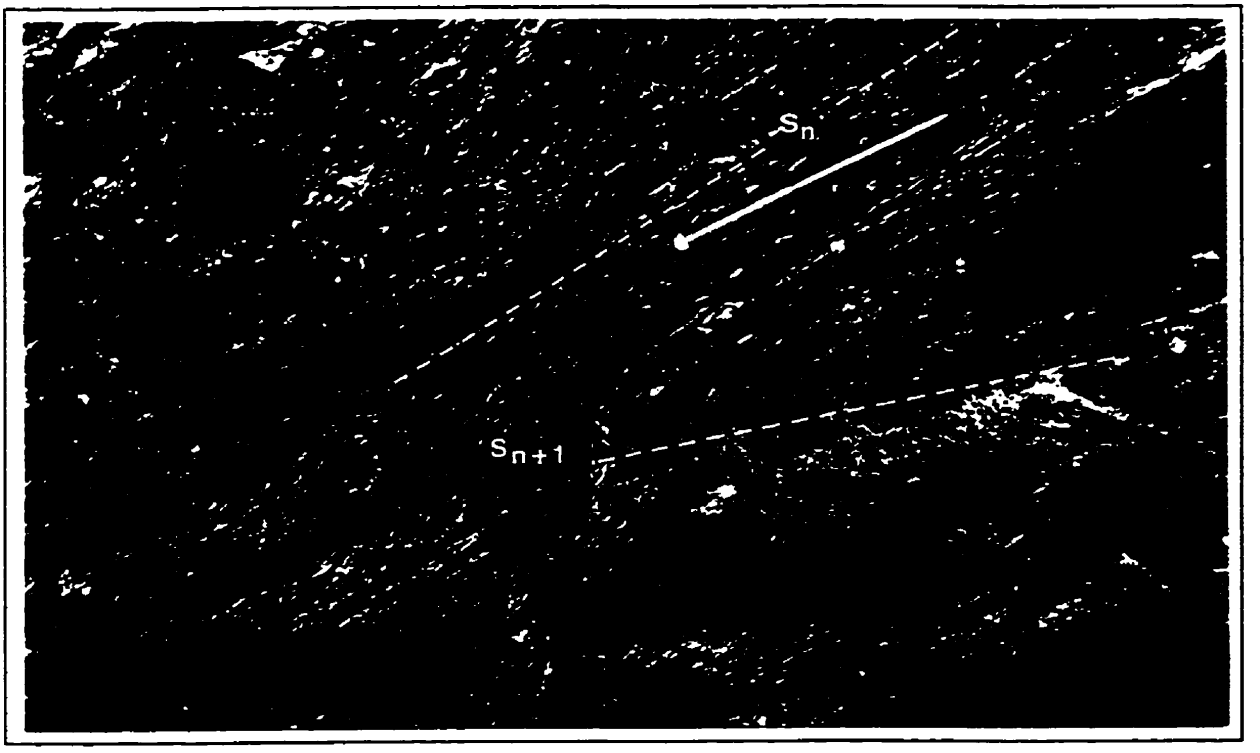

Figure 3.18

Figure 3.19 - *Photomicrograph of carbonate-chlorite-talc-sericite-±albite schist, west of the S-50 zone, showing a protomylonitic fabric defined by the alternation of carbonate-rich bands with chlorite-talc-sericite-magnetite rich bands.*

Sample K92-2752-201, plane-polarized transmitted light. Ore drift 2752, Kiena Mine level 27.

Photographie de section mince du schiste à carbonate-chlorite-talc-séricite-±albite, situé à l'ouest de la zone S-50, prise au microscope polarisant, montrant sa fabrique protomylonitique. Cell-ci est illustrée par l'alternance de bandes riche en carbonate avec bandes riche en chlorite-talc-séricite-magnétite.

Échantillon K92-2752-201, microscope à lumière transmise, lumière naturelle. Galerie à minerai 2752, niveau 27 Mine Kiena.

Figure 3.20 - *Photomicrograph illustrating the effects of strain partitioning across the fabric of the carbonate-chlorite-talc-sericite-±albite schist located west of the S-50 zone. The carbonate vein (Cb) is boudinaged and overprinted by quartz (Qz) extension veins. The albite (Ab) assemblage is weakly foliated, whereas the chlorite stringer vein (Chl) is schistose (S_n) and overprinted by a crenulation cleavage (S_{n+1}).*

Sample K91-3025-112, transmitted light, crossed Nicols. Ore drift 3025, Kiena Mine level 30.

Photographie de section mince du schiste à carbonate-chlorite-talc-séricite-±albite situé à l'ouest de la zone S-50, prise au microscope polarisant, montrant les effets de la déformation sur la fabrique du schiste. La veine de carbonate (Cb) est boudinée et affectée par le développement de veinules d'extension à quartz (Qz); l'assemblage de grains d'albite (Ab) par contre, est faiblement folié, tandis que la veine de chlorite (Chl) est schistosée (S_n) et recoupée d'un clivage de crénulation (S_{n+1}).

Échantillon K91-3025-112, microscope à lumière transmise, Nicols croisés. Galerie à minerai 3035, niveau 30 Mine Kiena.

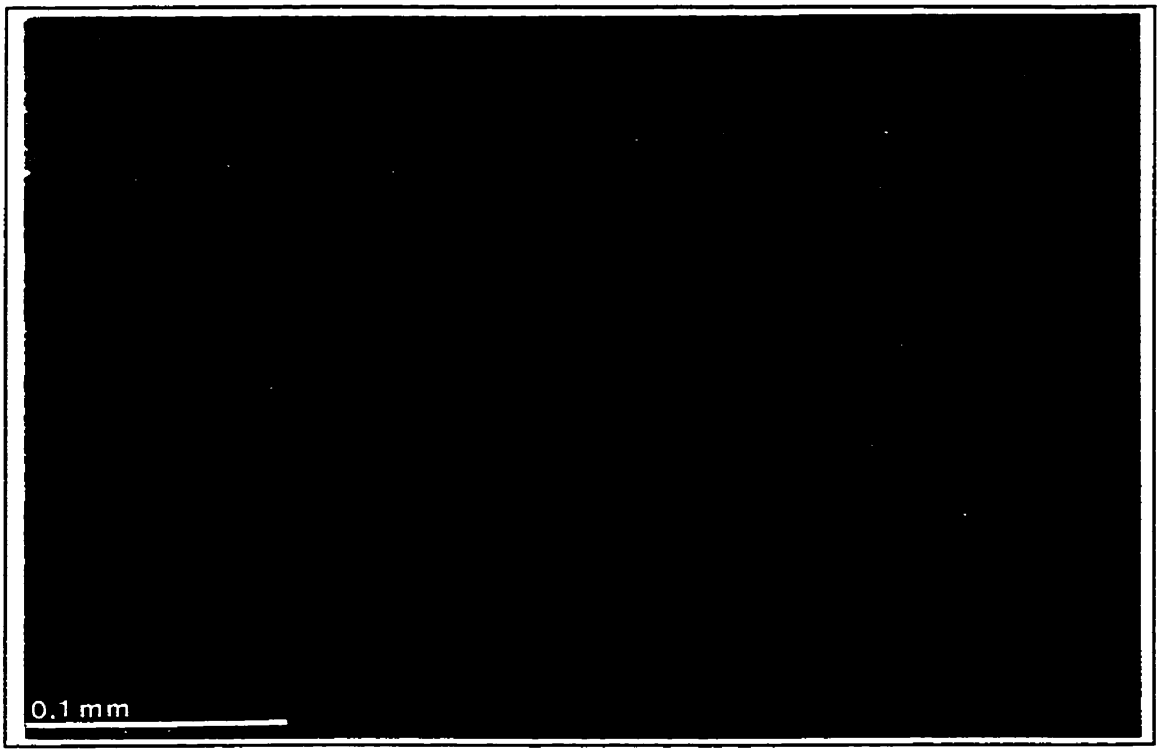

Figure 3.19

Figure 3.20

3.5 INTRUSIVE ROCKS

3.5.1 Introduction

Kiena's orebody is spatially associated with an intermediate to felsic dike complex composed of pre-ore albitite dikes and intermineral granodiorite and feldspar porphyry dikes. Although the presence of these dikes had been reported routinely by previous workers (see **Appendix A**), little was known prior to this study about their distribution, relative time of emplacement, and their relations to alteration-mineralization and deformation. These concerns are addressed in the section below.

3.5.2 Pre-ore albitite ("ore zone andesite"/"grey diorite") dikes

Albite dikes, also known as "*ore zone andesite*" (Polk, 1961), "*grey diorite*" (Clark, 1963), "*diorite*" (Roy, 1983), "*quartz diorite*" (Bourget, 1986) or "*microdiorite*" (Quirion, 1988) dikes, consist of a holocrystalline, medium to light grey rock showing distinct dark blueish-grey chilled margins at the dike/wall-rock contacts[9] (**Figure 3.21**). The dikes are characterized by a "sugary" aplitic texture and the presence of fine carbonate-quartz albite stringer to stockwork veins with disseminated pyrite, ± pyrrhotite and gold (**Figure 3.22**). They form narrow, discontinuous dikes of variable width (0.3-10 m) and limited strike-length (25-100 m). They predominantly occur within the altered basaltic komatiite located west of the S-50 zone, and locally cut across the iron tholeiite east of the S-50 zone. Albitite dikes are commonly observed in contact with the granodiorite porphyry dike, but they are also cut by the dike and locally occur as xenoliths in the granodiorite porphyry (e.g. **41 Level Map**, back pocket). Albitite dikes are intimately related to the ore, and are a major host to the ore. At upper mine levels, weakly mineralized dikes are usually observed as a cluster of narrow, isoclinally-folded intrusions located within the lower-grade ore shell west of the S-50 zone

---

[9] At depth (i.e. below level 48) however, chilled margins to albitite dikes are strongly attenuated by penetrative deformation.

(**Figure 3.21,** see Index map 2752 in back pocket). The intense hydrothermal alteration and brecciation in high-grade ore at these levels appears to have obscured the albitite protolith. At mid-mine levels (300-500 m below surface) the albitite dikes host, and are clearly cut by, high-grade mineralization (**Figure 3.23**). At these levels, they occur as xenoliths in the granodiorite porphyry dike (e.g. **41** and **43 Level Map**, back pocket) and as boudinaged and weakly foliated remnants of dikes in the lower-grade ore shell surrounding the high-grade ore (**Figure 3.17**). At lower mine levels, albitite dikes are usually restricted to the ore zone (e.g. **57** and **64 Level Maps**, back pocket) and form an anastomosing network of strongly foliated to schistose dikes (**Figure 3.24**) which appear to host all the economic gold mineralization recovered from these levels.

Unmineralized albitite dikes are essentially monomineralic rocks of dioritic composition (**Appendix C**) consisting of an assemblage of pure albite[10] with lesser quartz. Several distinctive textures characterize the fabric of this unusual intrusive rock. The predominant texture is granular and composed of interlocking subhedral albite (An_{0-1}) grains with prominent polysynthetic twinning (**Figure 3.25 A**). This texture locally grades into anhedral sections of albite (An_{0-1}) characterized by intergrown and highly serrated grain boundaries and less twinning, through to euhedral microcrystalline grains free of twins. The least prominent but most distinctive textures however, consist of linear arrays of radiating, plumose to dendritic albite (An_{0-1}) grains (**Figure 3.25 B**) grading into clusters of micrographic to myrmekitic albite (An_{0-1}) and quartz (**Figures 3.25 C**). The dendritic albite texture is reminiscent of fan-shaped aggregates of "cleavelandite", a leafy variety of pure albite formed as a late-stage mineral in pegmatites and replacing other minerals (AGI Glossary of Geology, p. 117). In addition, the cores of several albite crystals are characteristically sieved by numerous sub-microscopic aqueous fluid inclusions oriented along crystallographic axes **Figure 41 D**). Chilled margins, granitoid textures and the presence of myrmekitic

---

[10] Samples of albitite dikes were stained with a sodium cobaltinitrite solution, but revealed a lack of potassium feldspar, whereas microprobe analysis of several albite grains indicate $Ca/Na+Ca+K_2O$ ratios of 0 to 1.

intergrowths suggest that albitite dikes are of igneous origin. However, the extreme low calcicity of the albites and the high density of fluid inclusions suggest that these rocks may in part be of hydrothermal origin[11]. Characteristics of albite assemblages in albitite dikes, including crystal habit, low-calcicity and fluid inclusions, are also the trademark of albite assemblages observed in the selvages of gold-bearing carbonate-quartz stockwork veins (**Figure 4.3**) and ore-forming breccias (see Chapter 4). This is interpreted as another indication to the hydrothermal origin of albitite dikes. As a result of intense alteration of all albitites encountered, the primary igneous composition of the dikes is not known (**Figure 3.26**).

In **Table 3.2**, Kiena's albitite dikes are compared to albitite intrusions occurring in other gold deposits of Archean, Jurassic and Cretaceous greenstone belts. The results of this comparative survey of albitite dike occurrences reveal that albite-rich intrusions commonly occur as dike swarms distributed in linear arrays set paralell to regional fault zones which delineate terrane boundaries. The dikes, which are usually narrow and of limited lateral extent, are frequently emplaced into a folded and deformed sequence of mafic-ultramafic volcanic rocks. Albitite dikes are igneous rocks characterized by compositions ranging from diorite (Kiena, Malartic, Kerr-Addison-Chesterville, Hollinger McIntyre), to granodiorite-tonalite (Malartic, Bralorne-Pionner), to granite (Mother Lode belt), and exhibit elevated Na_2O contents but anomalously low K_2O contents. Accordingly, albitite dikes of dioritic composition usually show remnants of primary sub-ophitic mineral assemblages, whereas

---

[11] "The absence of any glassy rocks corresponding with granite very rich in albite is important in connection with the tendency of recent investigators to refer albite-rich rocks to a replacement process. One would expect glassy rocks of such composition if there were magmas of corresponding composition. On the other hand, if the richness in albite is the result of a secondary process of impregnation of a solid rock with albite circulating aqueous solutions, we should not expect glassy rocks rich in the albite molecule. Such solutions would be incapable of consolidating in toto, a process which is necessary for the formation of a glassy rock. The absence of glassy rocks rich in the albite molecule is thus to be taken as confirmatory of the concept that albite-rich rocks are formed by a process of replacement, probably in all cases.", Bowen (1928, p. 132).

Figure 3.21 - *Photograph of an isoclinally folded albitite dike cross-cutting the carbonate-chlorite-talc-sericite-±albite schist, west of the S-50 zone. Notice how the limbs of the folded dike appear unaffected by the penetrative planar fabric of the schist; however, the highly competent albitite dike is penetratively deformed as indicated by the presence of spaced cleavages in the nose of the fold.*

Access drift 27-03, Kiena Mine level 27.

Photo d'un dyke d'albitite recoupant le schiste à carbonate-chlorite-talc-séricite-±albite situé à l'ouest de la zone S-50, formant un pli isoclinal. Notez comme la portion de dyke située dans le flanc du pli ne parait pas être affectée par la schistosité développée dans la roche hôte qui lui est adjacente; cependant, en dépit de sa forte compétence, le dyke d'albite est déformé pénétrativement tel qu'en atteste la présence de clivages d'espacement dans la charnière du pli.

Galerie d'accès 27-03, niveau 27 Mine Kiena.

Figure 3.22 - *Photograph of a polished hand specimen of unmineralized albitite dike exhibiting a "sugary" aplitic texture. The fabric is composed of an assemblage of pure albite (An_{0-1}) and minor quartz. The fine carbonate veins criss-crossing the sample are accompanied by fine-grained disseminated pyrite.*

Sample K92-2752-200, access drift to ore drift 2752, Kiena Mine level 27.

Photographie de la surface polie d'un échantillon d'albitite non minéralisé, montrant une texture microgrenue, ou aplitique. La fabrique de l'échantillon est composée principalement d'un assemblage de pure albite (An_{0-1}) avec un peu de quartz. Les veinules de carbonate découpant la fabrique de l'albitite sont accompagnées de fine pyrite disséminée.

Échantillon K92-2752-200, accès de galerie à minerai 2752, niveau 27 Mine Kiena.

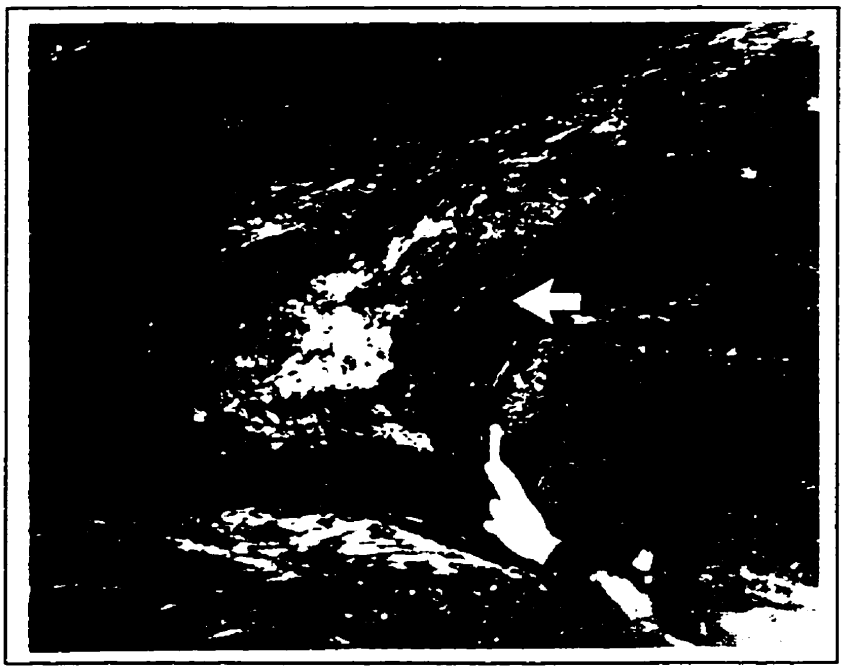

Figure 3.21

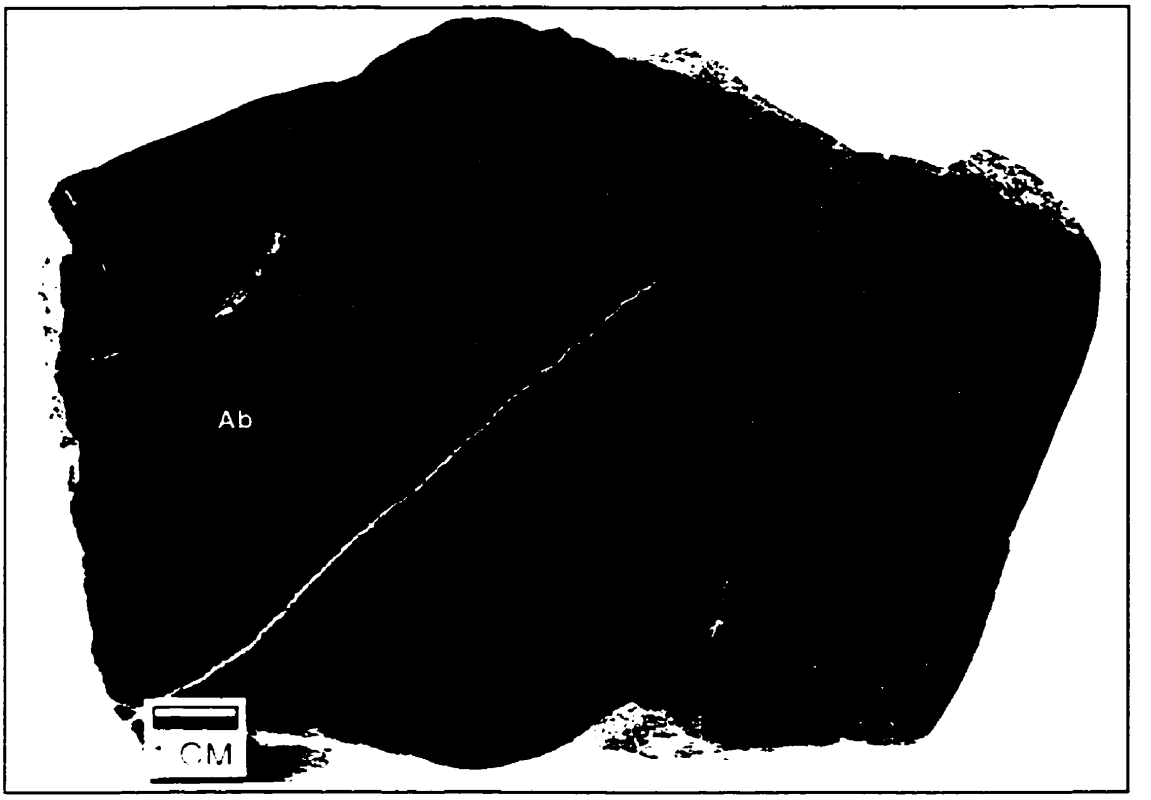

Figure 3.22

Figure 3.23 - Photograph of a mineralized albitite dike at upper mine levels exhibiting a mosaic-textured breccia cemented by vein albite (Ab). The large and sub-angular fragments (dark grey) have been partly replaced by albite (light grey area) along their margins. The large rock fragments are surrounded by several much smaller fragments (light grey) that have been entirely metasomatised by hydrothermal vein albite, which gives a partly mottled appearance to the breccia. Pyrites are partly recrystallized but frequently exhibit remnants of complex, squeletal-like forms (see Figures 4.11 and 4.16).

Sample K91-4117-160, "B" zone, ore drift 4117, Kiena Mine level 41.

Photo d'un dyke d'albitite minéralisé provenant des niveaux supérieurs de la mine, montrant une brèche de type mosaique cimentée par de l'albite filonienne (Ab). Les bordures des gros fragments sub-angulaires (gris fonçé) ont été partiellement remplacées par de l'albite (gris clair). Les grands fragments de roche sont entourés de plusieurs plus petits fragments (gris clair) entièrement métasomatisés par l'albite hydrothermale, ce qui donne à la brèche un aspect bigarré. Les pyrites sont partiellement recrystallisées mais elles montrent communément les reliques de textures squelettiques (voir Figures 4.11 et 4.16).

Échantillon K91-4117-160, Zone "B", galerie à minerai 4117, niveau 41 Mine Kiena.

Figure 3.24 - Photograph of mineralized and schistose albitite at lower mine levels. The fabric is outlined by trails of highly strained pyrite (Py) and pyrrhotite (Po) as well as by sub-parallel carbonate-quartz (Cb) and chlorite-magnetite (Chl) veins.

Sample K92-6446-214, "C" zone, ore drift 6446, Kiena Mine level 64.

Photo d'un dike d'albitite minéralisé provenant des niveaux inférieurs de la mine. La fabrique est soulignée par les chapelets de grains de pyrite (Py) et de pyrrhotine (Po) étirés le long de la schistosité, ainsi que par des veines sub-parallèles de carbonate-quartz (Cb) et de chlorite-magnétite (Chl).

Échantillon K92-6446-214, zone "C", galerie à minerai 6446, niveau 64 Mine Kiena.

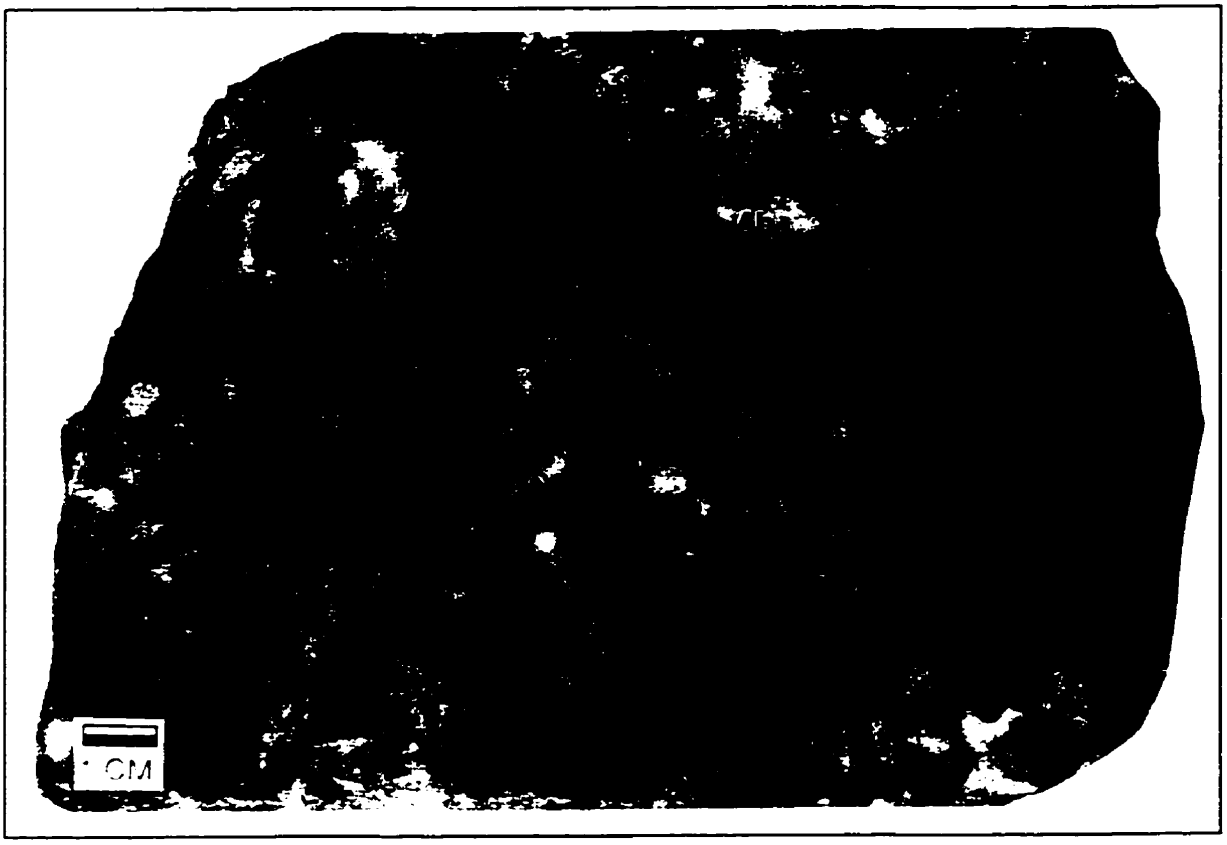

Figure 3.23

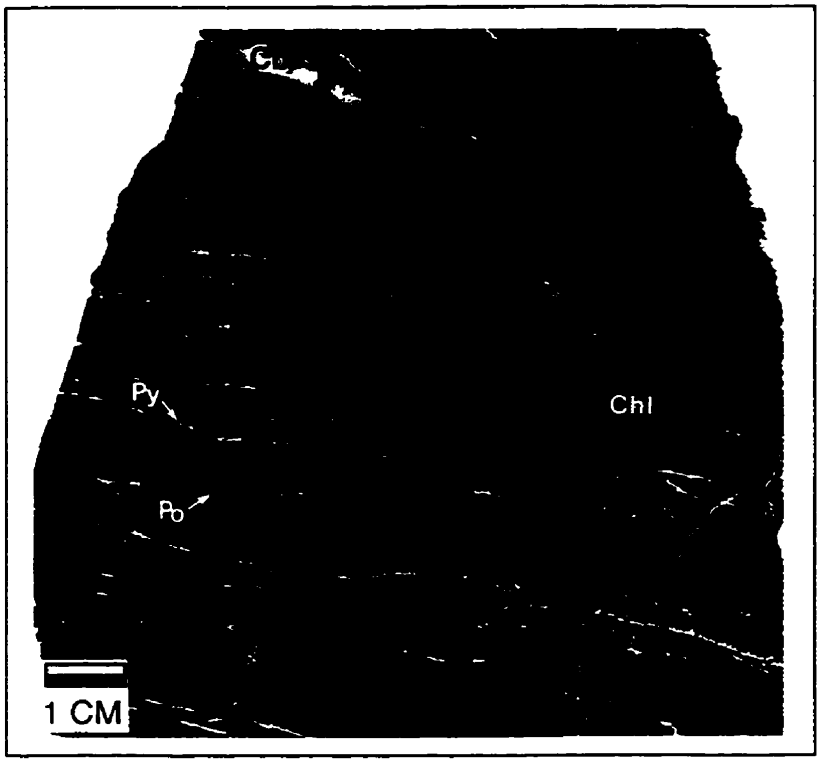

Figure 3.24

Figure 3.25 - Photomicrographs of albitite dikes illustrating the variety of distinctive textures which characterize this type of intrusion.

A - Granular texture composed of subhedral albite grains with interstitial carbonate (Cb). Note the highly serrated grain boundaries and the irregular twinning, indicating post-albitite dike deformation.

Sample K91-3828-168, transmitted light, crossed Nicols. "K" zone, ore drift 3828, Kiena Mine level 38.

Texture microgrenue composée d'un assemblage de cristaux hypidiomorphes d'albite avec carbonate (Cb) en interstice. Les grains d'albite montrent des bordures dentelées ainsi que des mâcles très irrégulières, attestant que ce dyke d'albite est déformé.

Échantillon K91-3828-168, microscope à lumière transmise, Nicols croisés. Zone "K", galerie à minerai 3828, niveau 38 Mine Kiena.

B - Complex arrangement of radiating, plumose to dendritic albite (Ab) crystals with a composition of An_{0-1}. Notice how this mineral assemblage can be subdivided in groups of crystals sharing the same optical orientation. The composition and crystal habit of these albite grains is reminiscent of fan-shaped aggregates of "cleavelandite", a leaf-like variety of pure albite formed as a late-stage mineral in pegmatites and replacing other minerals (AGI Glossary of Geology, 1990). Cb= carbonate.

Sample K92-2752-200, transmitted light, crossed Nicols. "A" zone, ore drift 2752, Kiena mine level 27.

Assemblage de cristaux dendritiques d'albite (Ab) de composition An_{0-1}, disposés selon un patron en éventail. Remarquez comment cet assemblage de cristaux d'albite se subdivise en petits groupes de cristaux ayant la même orientation optique. La composition et l'habitus de ces cristaux d'albite rapellent ceux d'aggrégats de "cleavelandite", une variété d'albite arborescente formée durant les derniers stages de cristallisation de pegmatites et qui remplace d'autres minéraux (AGI Glossary of Geology, 1990). Cb= carbonate.

Échantillon K92-2752-200, microscope à lumière transmise, Nicols croisés. Zone "A", galerie à minerai 2752, niveau 27 Mine Kiena.

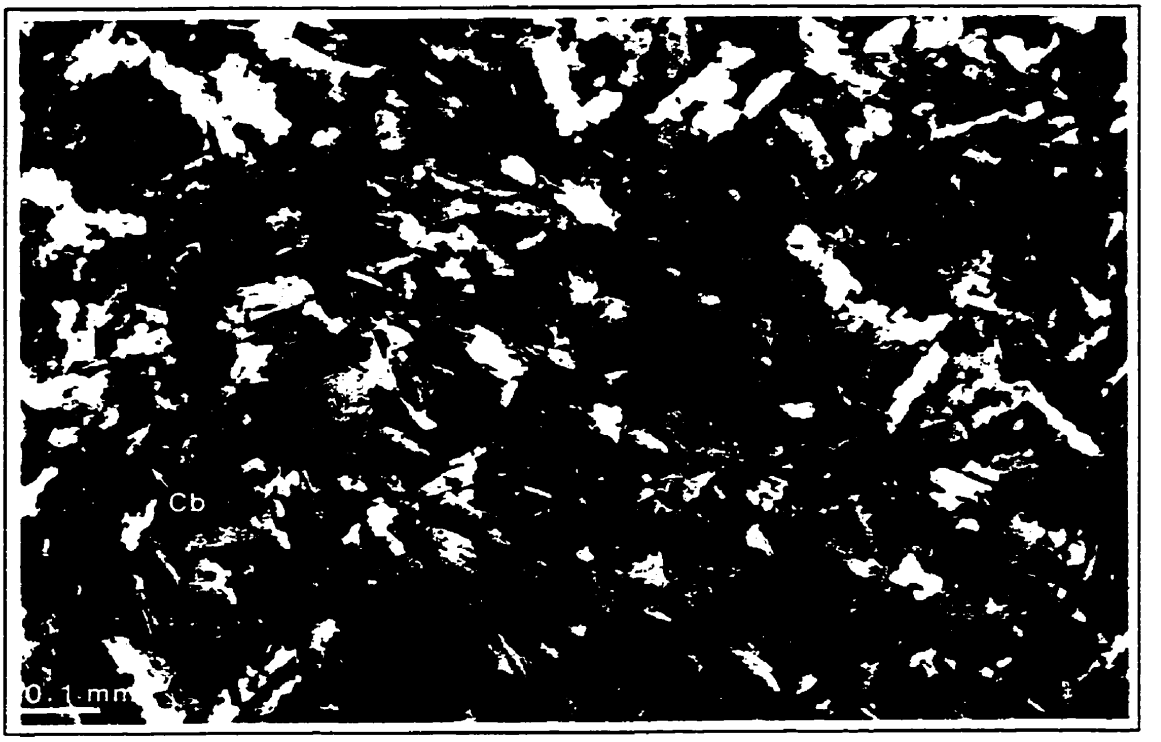

Figure 3.25 A

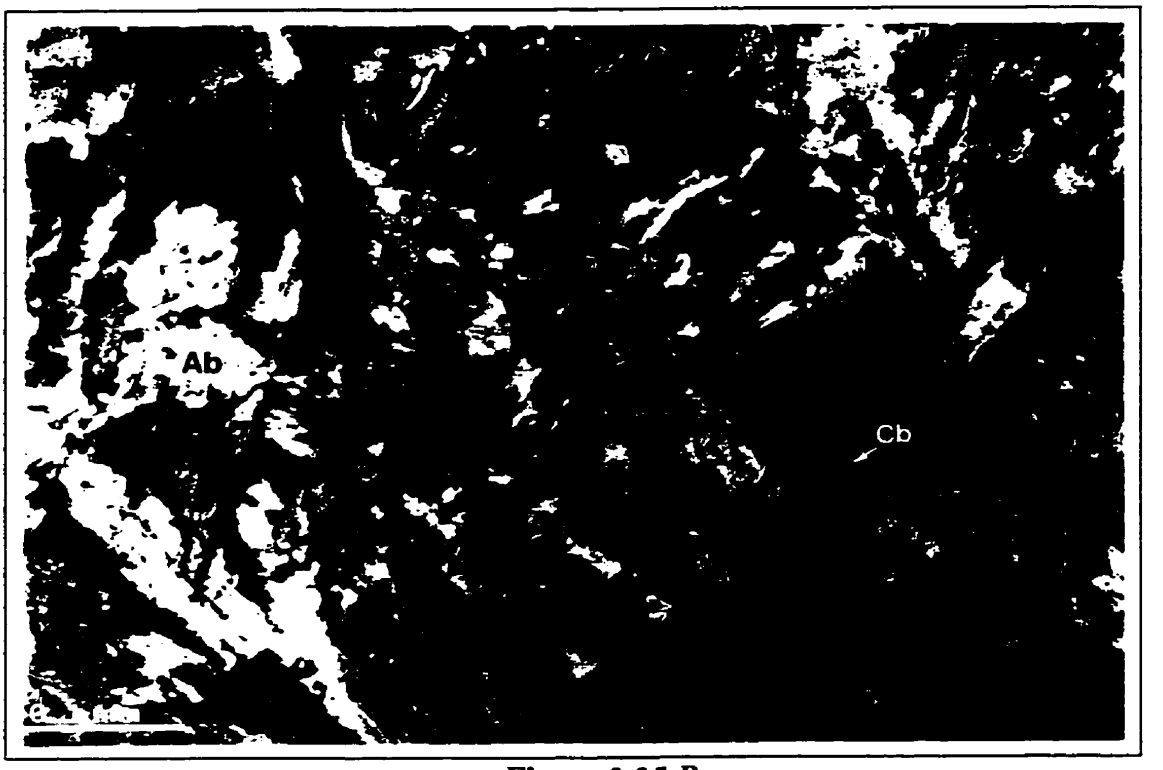

Figure 3.25 B

Figure 3.25 continued...

C - Granular albite assemblage exhibiting a cluster of grains characterized by micrographic to myrmekitic albite-quartz intergrowths. Note the highly serrated grain boundaries so characteristic of deformation in albite-rich rocks at Kiena.

Sample K91-3828-168, transmitted light, crossed Nicols. "K" zone, ore drift 3828, Kiena Mine level 38.

Assemblage microgrenu d'albite montrant plusieurs grains charactérisés par l'intercroissance micrographique à myrmékitique d'albite et quartz. Notez la bordure fortement dentelée des grains d'albite qui est si charactéristique de la déformation des roches fortement albitisées de Kiena.

Échantillon K93-3628-267, microscope à lumière transmise, Nicols croisés. Zone "K", galerie à minerai 3628, niveau 36 Mine Kiena.

D - Close-up view of a pure albite grain, fringed by micrographic to myrmekitic albite-quartz intergrowths. As for many other albite crystals in albitite dikes, this albite is sieved by numerous fluid inclusions preferentially oriented along crystallographic axes.

Sample K91-3828-168, transmitted light, crossed Nicols. "K" zone, ore drift 3828, Kiena Mine level 38.

Vue rapprochée d'un grain de pure albite, auréolé d'une couronne d'intercroissances d'albite et quartz. Il est fréquent d'observer une multitude d'inclusions fluides au sein des cristaux d'albite formant les dikes d'albitite, lesquelles sont généralement orientées le long d'axes cristallographiques.

Échantillon K91-3828-168, microscope à lumière transmise, Nicols croisés. Zone "K", galerie à minerai 3828, niveau 38 Mine Kiena.

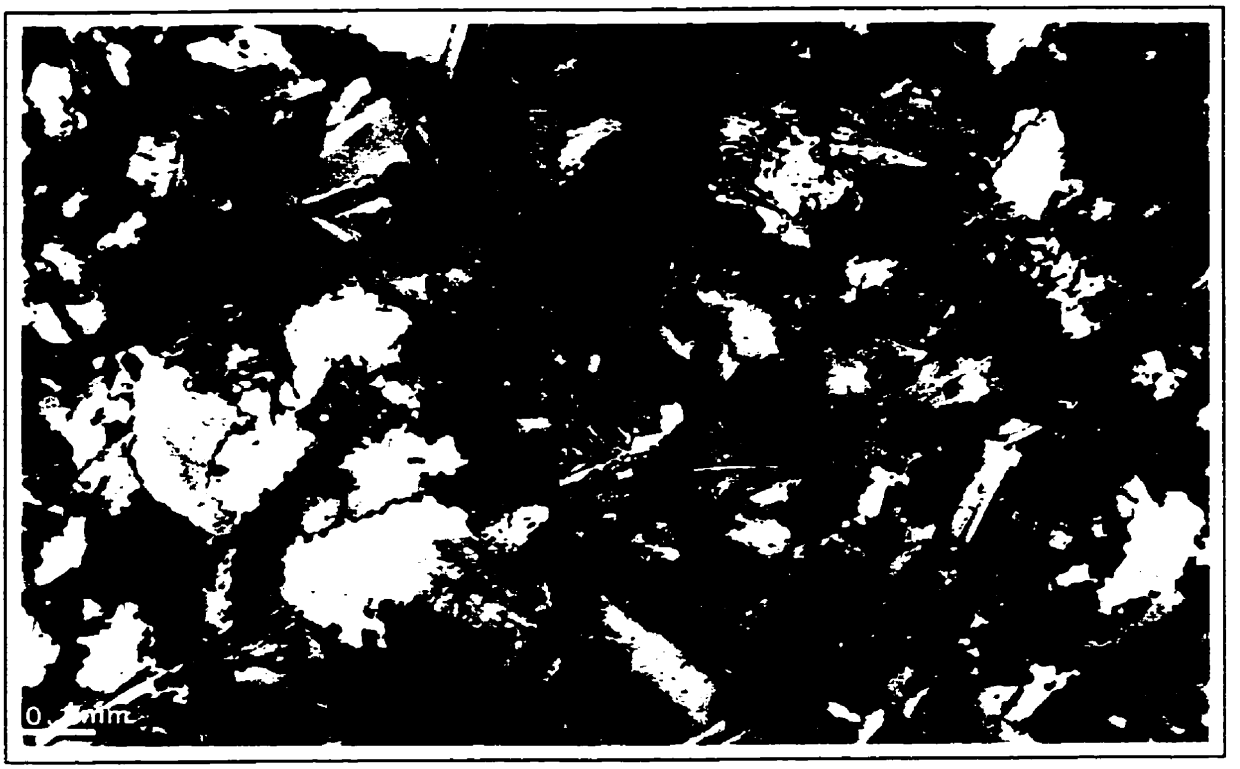

Figure 3.25 C

Figure 3.25 D

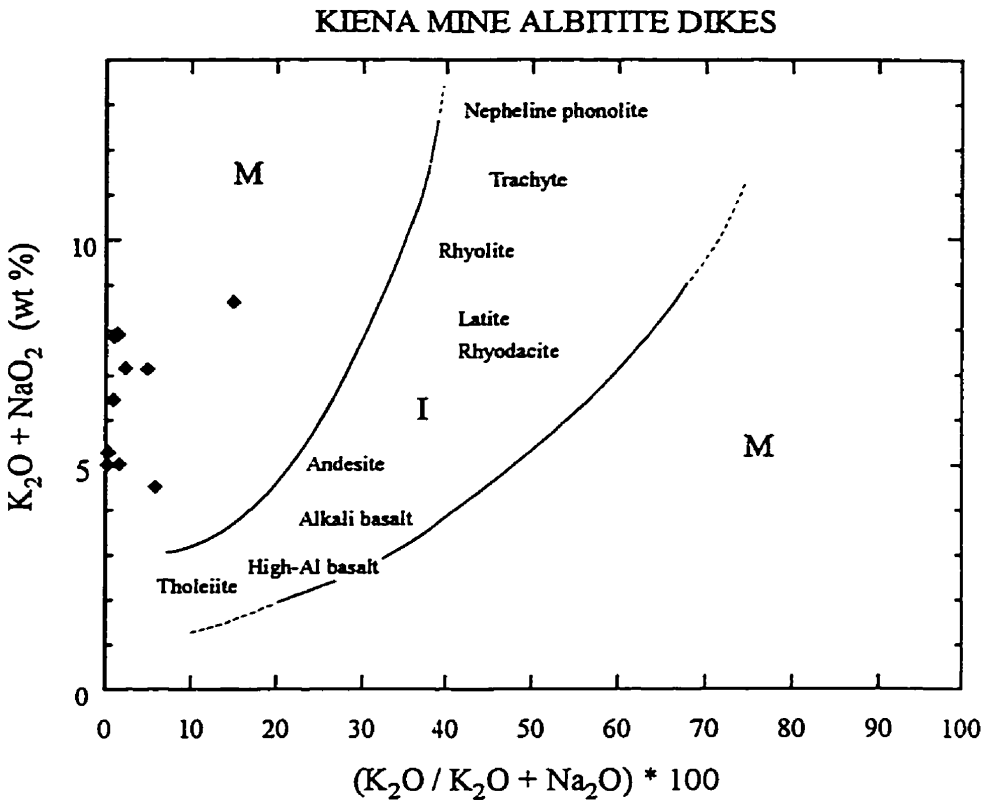

*Figure 3.26 - Compositions of the Kiena Mine albitite dikes reported on a Hughes (1973) diagram. All data points lie outside the "igneous spectrum" suggesting that these rocks have acquired their present mineralogy by sodic metasomatism (albitite dikes are characteristically deficient in K_2O). See **Appendix C** to obtain the compositions of albitite dikes used in this diagram. I= field of primary igneous rocks compositions; M= field of igneous rock compositions modified by alkali-metasomatism.*

*Compositions de dykes d'albitite de la mine Kiena reportées sur un diagramme de Hughes (1973). Tous les points d'analyse se situent à l'extérieur du "spectre igné" ce qui suggère que la minéralogie originale de ces roches a été modifiée par métasomatisme sodique (les dykes d'albitite sont charactérisés par une déficience en K_2O). Se reférer à l'**Appendice C** afin de pouvoir consulter la composition des albitites utilisées dans ce diagramme. I= aire incluant la composition originelle d'une suite de roches ignées; M= aire reflétant la composition de roches ignées modifiée par métasomatisme alkalin.*

Table 3.2 Comparative characterization of albitite intrusions reported at selected gold deposit localities.

	Kiena Mine Val d'Or, Québec Abitibi greenstone belt	Malartic mining district Malartic, Québec Abitibi greenstone belt
Chemical Composition		
1. SiO_2	1. 50.72 n=10	1. 62.23 n=5 47.35 n=3
2. Al_2O_3	2. 15.53	2. 16.29 "grey 13.27 "diorites"
3. Fe_2O_3	3. 8.91	3. 1.69 porphyry" 5.91
4. FeO	4. 7.25	4. 1.92 9.36
5. MgO	5. 5.31	5. 1.49 5.82
6. CaO	6. 4.23	6. 3.19 8.27
7. Na_2O	7. 6.25	7. 6.03 4.49
8. K_2O	8. 0.28	8. 2.81 0.45
9. TiO_2	9. 0.75	9. 0.50 1.34
10. P_2O_5	10. 0.24	10. 0.38 0.12
11. MnO	11. 0.12	11. 0.03 0.19
12. LOI	12. 6.14	12. 2.68 1.47
Au (ppb)	1471.00	---- ----
S (%)	0.80	0.42 0.39
Cu (ppm)	90.10	----- -----
Mo (ppm)	N.d.	----- -----
Ni (ppm)	52.30	----- -----
Zn (ppm)	74.10	----- -----
Mineralogy	Mostly albite (An_{0-1}) and minor quartz Vein Cc-Qz-Ab-Py-Po-Au Vein Bo-Mt-Chl	Mostly albite (An_{0-3}) with lesser hornblende and quartz (Ep + Sphene) (Mt + Ap) Pigeonite hornblende Hornblende sodic amphibole
Magmatic-hydrothermal Textures* *All albitite dikes are lined with chilled margins	Aplitic, anhedral albite assemblage Micrographic to myrmekitic Ab-Qz intergrowths Fluid inclusion-rich albite grains Plumose to dendritic albite grains (cleavelandite)	Aplitic (relic porphyritic texture) Mosaic of anhedral albite grains exhibiting highly serrated grain boundaries Relic ophitic texture
Relation to alteration-mineralization	Pre-ore: 1. Overprinted by main-stage Au 2. Overprinted by Bo-Mt-Chl-Ser vein alteration	Pre-ore: 1. Overprinted by Bo-Mt alteration 2. Overprinted by main-stage Au 3. Overprinted by vein biotite 4. Overprinted by vein actinolite 5. Chloritization 6. Overprinted by quartz veins
Type of Au mineralization	Intrusion-related	Intrusion-related (?) (5)
Style of Au mineralization	Fracture-controlled: Stockwork veins and breccias	Fracture-controlled: Stockwork veins and breccias
Age of mineralization	Archean ca. 2694-2686 Ma	Archean ca. 2694-2680 Ma (?) (5)
Estimated depth of emplacement	Epizonal: 1- 5 km	Epizonal: ? (5)
Relation to syn-metamorphic regional deformation	Post-D_1 and pre-D_2 Pre-metamorphic	Post-D_1 and pre-D_2 (4) Pre-metamorphic
Structures and Textures assigned to post-intrusion deformation	Regional NW-plunging, z-fold North-dipping schistosity outlined by pre-existing Bo-Mt-Chl stringer veins Highly serrated (almost stylolitic) albite grain boundaries	Regional, NE-plunging folds Common boudinage Regional NW-SE to E-W foliation Subparallel sericitic spaced cleavage
Mode of occurence	Swarm of narrow dikes with limited lateral extent (300-500 m)	
Comments	1. Emplaced in tilted, mafic-ultramafic volcanic rock sequence along plutonic belt north of Abitibi-Pontiac terrane boundary (Cadillac Tectonic Zone) 2. Apparent genetic relation to gold mineralization 3. Temporally-related to granodiorite and quartz monzonite porphyry dikes	1. Spatially- and temporally- related to quartz -feldspar porphyry dikes 2. Emplaced along Abitibi-Pontiac terrane boundary (Cadillac Tectonic Zone)
References	Morasse et al. (1995) This study	1. Gunning (1937) 2. Gunning and Ambrose (1942) 3. Eakins (1962) 4. Sansfaçon and Hubert (1990) 5. This study (see Chapter 8)

Table 3.2. continued...

	Kerr-Addison-Chesterville Mines Virginiatown, Ontario Abitibi greenstone belt	Hollinger-McIntyre Mines Timmins, Ontario Abitibi greenstone belt
Chemical Composition 1. SiO_2 2. Al_2O_3 3. Fe_2O_3 4. FeO 5. MgO 6. CaO 7. Na_2O 8. K_2O 9. TiO_2 10. P_2O_5 11. MnO 12. LOI	1. 44.93 n=8 2. 11.00 3. 8.06 4. ----- 5. 7.79 6. 7.14 7. 4.88 8. 0.40 9. 0.70 10. 0.45 11. 0.15 12. 12.63	1. 48.35 n=2 2. 11.70 3. 6.70 4. ----- 5. 7.44 6. 7.74 7. 3.60 8. 0.49 9. 0.55 10. 0.26 11. 0.14 12. -----
Au (ppb) S (%) Cu (ppm) Mo (ppm) Ni (ppm) Zn (ppm)	1492 0.73 97.25 N.d. N.d. 73.87	----- 0.04 ----- ----- 140 -----
Mineralogy	Mostly **albite** and minor quartz Vein Cb-Py-Au Mica and rutile	Mostly **albite** (An_{0-1}) with lesser quartz and Bo (Chl) Relic hornblende ? Irregular microstockwork
Magmatic-hydrothermal Textures* *All albitite dikes are lined with chilled margins	Massive (Aplitic ?) **Xenolithic:** mixed suite of xenoliths including fragments of mineralized albitite dike and Qz-Py vein fragments	**Aplitic** **Xenolithic:** well rounded to angular granitoid xenoliths ("Goose eggs") **Relic sub-ophitic texture** Myrmekitic Ab-Qz
Relation to alteration-mineralization	**Pre-ore** **Intermineral** **Late-stage**	**Pre-ore:** 1. Overprinted by main-stage Cu-Au 2. Overprinted by hematite 3. Overprinted by Ser + Py (phyllic)
Type of Au mineralization	Intrusion-related	Intrusion-related (2)
Style of Au mineralization	**Fracture-controlled:** Stockwork veins, replacement veins and breccias	**Fracture-controlled:** Stockwork veins and vein swarms
Age of mineralization	Archean	Archean post - 2673 $^{+6}_{-2}$ Ma
Estimated depth of emplacement	Epizonal: ?	Epizonal: 1-3 km (2)
Relation to syn-metamorphic regional deformation	Syn- to post-D_2 ?	Post-D_1 and pre-D_2 (2) Pre-metamorphic
Structures and Textures assigned to post-intrusion deformation	Regional, NE-plunging S-shaped fold Folding, flattening and boudinage Foliation Post-ore displacement on dextral 'Kerr' fault "En echelon" fractures	Post-mineralization penetrative deformation Discontinuous spaced cleavage defined by flattening of pre-existing chloritic microstockwork veins (2)
Mode of occurence	Swarm of narrow dikes with limited lateral extent (300-500 m)	
Comments	1. Emplaced along Abitibi-Pontiac Subprovince boundary (Larder Lake-Cadillac Break) into an overturned sequence of mafic-ultramafic volcanic rocks	1. Spatially- and temporally- related to Pearl Lake porphyry 2. Emplaced in tilted Mg- and Fe- tholeiitic volcanic rock sequence along fold axis of "Central Tisdale" anticline
References	Buffam and Allen (1948) Smith et al. (1990) Smith (1992)	1. Burrows and Spooner (1986) 2. Melnik-Proud (1992)

Table 3.2 continued...

	Bardoc-Kalgoorlie mining districts Menzies-Kambalda greenstone belt, Western Australia	Mother Lode Gold Belt Sierra Nevada Foothills metmorphic belt, California	Bralorne-Pionner Mine Bridge River mining camp, Southwerstern British Columbia
Chemical Composition 1. SiO_2 2. Al_2O_3 3. Fe_2O_3 4. FeO 5. MgO 6. CaO 7. Na_2O 8. K_2O 9. TiO_2 10. P_2O_5 11. MnO 12. LOI Au (ppb) S (%) Cu (ppm) Mo (ppm) Ni (ppm) Zn (ppm)	1. 66.90 n=3 2. 16.40 3. 0.78 4. 1.02 5. 1.04 6. 1.18 7. 9.21 8. 0.19 9. 0.33 10. 0.15 11. 0.02 12. 0.82 ----- ----- 35 ----- 16 17	1. 67.53 n=1 2. 18.57 3. 1.13 4. 0.08 5. 0.24 6. 0.55 7. 11.50 8. 0.10 9. 0.07 10. 0.11 11. ----- 12. 0.46 ----- ----- ----- ----- ----- -----	1. 63.31 n=4 2. 16.76 3. 4.00 4. ----- 5. 1.47 6. 3.47 7. 7.08 8. 0.86 9. 0.40 10. 0.17 11. 0.09 12. 2.71 ----- ----- ----- ----- ----- -----
Mineralogy	Albite (An_{0-2}); no quartz vein and disseminated Mv-Bo-Chl-Cb-Sulfides Vein actinolite	Mostly albite (An_{0-5}) with various amounts of fibrous riebeckite or anhedral prisms of aegirene-augite; disseminated Py and Pz stockwork veins	Mostly albite with lesser quartz and remnants of hornblende with accessory rutile, ilmenite (leucoxene) and zircon
Magmatic-hydrothermal Textures* *All albitite dikes are lined with chilled margins	**Porphyritic and aplitic:** 1. Grain size and texture variable at thin section level 2. K-spar phenocrysts - chess-board albite 3. Hornblende phenocryst - sodic amphibole 4. "Recrystallization" of porphyry dike groundmass into monomineralic mosaic of anhedral granular albite	**Aplitic and porphyritic** Allotriomorphic granular aggregate of albite * Riebeckite replaces aegirine	**Porphyritic** Symplectic Qz-Ab intergrowths in core areas of dikes
Relation to alteration-mineralization	**Pre-ore (ca. 2684-2662 Ma):** 1. Replacement of magnesio-hornblende by actinolite 2. Replacement of actinolite by magnesio-arfedsonite to -riebeckite (also in veins) 3. Overprint by Bo-Ser-Cb- sulfide mineralization 4. Chloritization	**Pre-ore**	**Pre-ore:** 1. Overprinted by main-stage Au
Type of Au mineralization	Intrusion-related ? Metamorphogenic ?	Intrusion-related ? Metamorphogenic ?	Intrusion-hosted
Style of Au Mineralization	**Fracture-controlled:** Sheeted and stockwork vein systems (breccias)	**Fracture-controlled:** lode quartz veins and stockwork veins and replacement orebodies (ankerite-Au)	**Fracture-controlled:** fault-hosted veins and breccias; sulphide-bearing microstock-work in quartz veins
Age of mineralization	Archean	Late Jurassic-early Cretaceous	Cretaceous ca. 90-85 Ma
Estimated depth of emplacement	?	?	5-7 km
Relation to syn-metamorphic regional deformation	Syn- to post-D_2 ; post-metamorphic (Witt and Swager, 1989)	Syn-orogenic (Nevada orogeny ca. 160-140 Ma); plutonism? Post-Nevadan orogeny, -isoclinal folding and -penetrative fabric ?	Post-D_1 Syn-metamorphic
Structures and Textures assigned to post-intrusion deformation	Subparallel, spaced, chloritic shear zone at intrusion contacts with mafic-ultramafic rocks		Post-ore faulting Stylolites across gold-bearing quartz veins
Mode of occurence	Swarm of narrow dikes with limited lateral extent (300-500 m)		
Comments	1. Protolith: hornblende-plagioclase porphyry dikes emplaced in deformed mafic-ultramafic volcanic rock sequence	Emplaced near the Late Jurassic "Melones" fault zone ("tectonic melange")	1. Emplaced in "Bralorne" diorite (270±5 Ma) bounded by "Ferguson" thrust fault and "Cadwallader" fault 2. Emplaced in folded mafic-ultramafic volcanic rock sequence
References	Perring et al. (1991) Witt (1992)	Knopf (1929) Landefeld (1988)	Leitch (1990)

those with more felsic compositions commonly show relic porphyritic textures. Most of the dikes, however, are generally characterized by an aplitic, granitoid texture. The main mineral constituent of the dikes is pure albite (An_{0-5}) although the occurrence of alkali-rich pyroxenes and/or amphiboles is occasionally reported (e.g. Mother Lode belt). The remaining albitite assemblage consists of lesser quartz, frequently observed as vermicular intergrowth with albite (myrmekite), and trace amounts of magnetite, apatite, sphene and epidote. All albitite dikes are pre-mineral intrusions closely related in space and time to main-stage gold mineralization (e.g. Kiena, Kerr-Addison-Chesterville). This relation is particularly substantiated by the presence of xenoliths of mineralized albitite dikes in younger intermineral and late-mineral albitite intrusions (e.g. Kerr-Addison-Chesterville).

In summary, Kiena's albitite dikes form a narrow dike swarm, probably emplaced along a bedding-parallel fault zone in a southerly-overturned mafic-ultramafic volcanic rock sequence. The dikes, which exhibit characteristics of both igneous and hydrothermal rocks, are pre-mineral and exert a strong control on the distribution of gold-ore. They share the overall characteristics of albitite dikes at other gold deposit localities; however, they have more in common with those of dioritic compositions found in the Kerr-Addison-Chesterville and Malartic Mines.

3.5.3 Intermineral intrusions

Two narrow porphyritic felsic intrusions cut across Kiena's orebody (**Figures 3.27** and **3.28**, section **12514.6 N** in back pocket). Both dikes are of calc-alkaline affinity (**Figure 3.29**) but have been subjected to alkalic metasomatism (**Figure 3.30**). The oldest porphyry predominantly occurs in the volcanic sequence *west of the S-50 zone* and has the composition of a sodium-rich granodiorite (tonalite), whereas the youngest dike, which cuts across the granodiorite dike, predominantly occurs in the volcanic sequence *east of the S-50 zone* and has the average composition of a sodium-rich quartz monzonite (section **12514.6 N**, back pocket; **Appendix C**). The granodiorite dike usually runs parallel to, or is in contact with,

Figure 3.27 - Photograph of the intermineral granodiorite dike cutting across the high-grade ore of the "S-50" zone at upper mine levels. The contact is sharp and the dike is cut by narrow carbonate-quartz-pyrite stockwork veins (at the center of the photo). As this rock face is sub-parallel to the deposit's main schistosity, the fabric is not readily visible on this outcrop (moderately-dipping to the right). However, deformation is clearly indicated by the presence of microfolded stockwork veins (see arrow). Zircons from this dike have been dated as 2686 ±2 Ma (see Chapter 7).

"D" zone, ore drift 3025, Kiena Mine level 30.

Photo du dike de granodiorite interminéralisation recoupant le minerai haute teneur de la zone "S-50" aux niveaux supérieures de la mine. Le contact est franc et net et le dyke est recoupé de fines veinules à carbonate-quartz-pyrite en stockwork (au centre de la photo). Cette section étant presque dans le plan de la schistosité principale du gisement, il est difficile d'observer les effets du clivage sur cet affleurement (fabrique ayant un pendage modéré vers la droite). Cependant, la déformation est clairement signalée par la présence de microplis affectant les veinules de carbonate (voir flèche). Des zircons provenant de ce dyke ont été daté à 2686 ±2 Ma (voir Chapitre 7).

Zone "D", galerie à minerai 3025, niveau 30 Mine Kiena.

Figure 3.28 - Photograph of the intermineral feldspar porphyry dike cross-cutting the tail end of the "B" zone at lower mine levels (see schematic plan map of level 57 in back pocket). The yellow painted lines indicate the contact between the feldspar porphyry and the ore. The dike is cut by a moderately north-northeast-dipping (to the left) schistosity. The apparent fabric at the top of the photo is caused by the intersection of the rock face with the main schistosity.

Hangingwall "B" zone, ore drift 5804, Kiena Mine level 58.

Photo du dyke de porphyre feldspathique interminéralisation recoupant l'extrémité inférieure de la zone "B" (se référer au plan schématique du niveau 57 situé en pochette). Les lignes jaune marquent le contact entre le porphyre feldspathique et le minerai. Le dike est affecté d'une schistosité à pendage modéré vers le nord-nord-est (vers la gauche). La fabrique planaire visible dans le haut de la photo est apparente et causée par l'intersection de la schistosité principale avec la face supérieure du chantier d'exploitation.

Zone "B" éponte supérieure, galerie à minerai 5804, niveau 58.

Figure 3.27

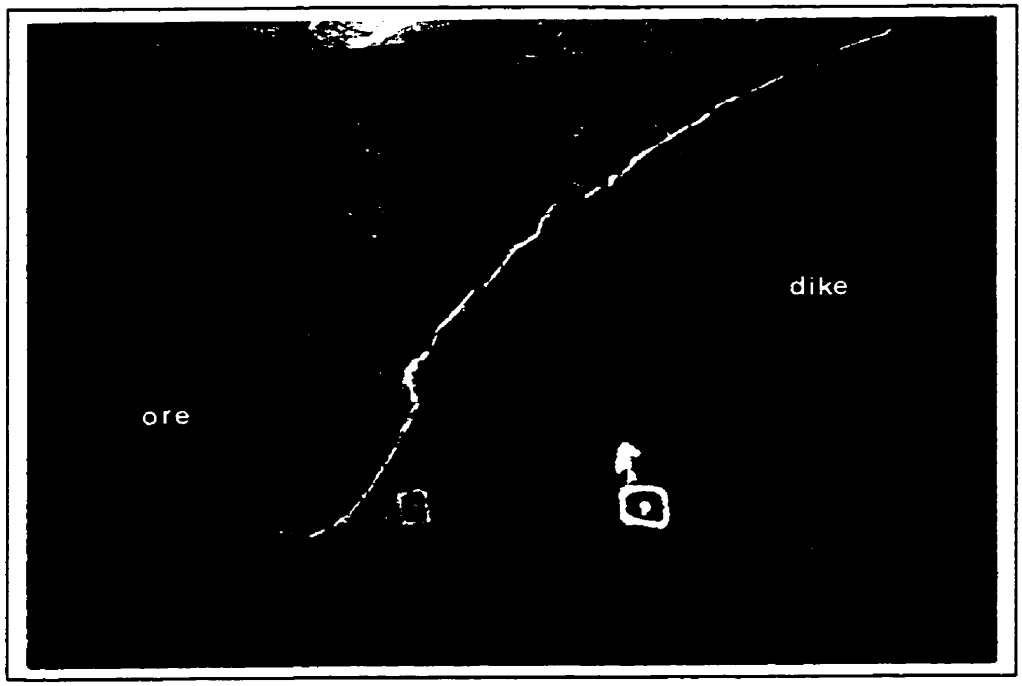

Figure 3..28

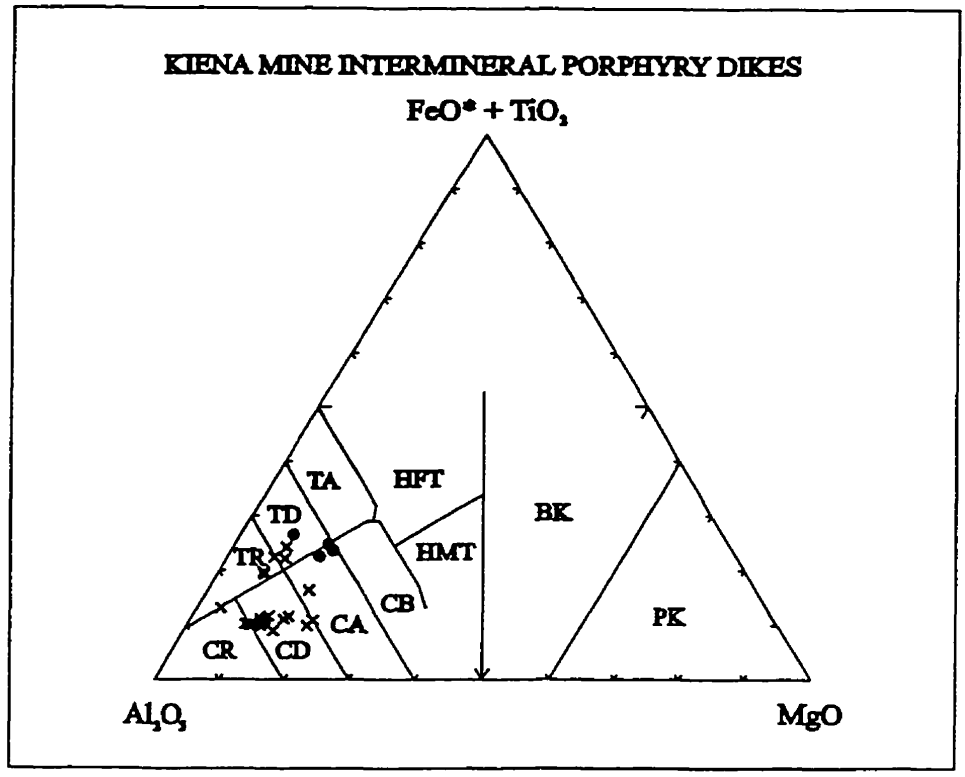

Figure 3.29 - Compositions of intermineral granodiorite and feldspar porphyry dikes reported on a Jensen (1976) cation plot. Total iron recalculated as FeO (Newpet, 1993). Most data points indicate that these rocks are of calc-alkaline affinity. Data points in the tholeiitic field may reflect the effects of biotite, magnetite and/or pyrite alteration. The compositions of granodiorite and feldspar porphyry dikes used in this plot are from Appendix C and Muir (1981).

Compositions de dykes de granodiorite et porphyre feldspathique interminéralisation reportées sur un diagramme cationique de Jensen (1976). Le fer total a été recalculé sous forme de FeO (Newpet, 1993). La plupart des points d'analyse indiquent que ces roches sont d'affinité calco-alkaline. Cependant, les points d'analyse situés dans le champ tholéitiique reflètent possiblement les effets de l'altération en biotite, magnétite et/ou pyrite. La composition des échantillons de granodiorite et porphyre feldspathique utilisés dans ce diagramme proviennent de l'Appendice C ainsi que de Muir (1981).

Abbreviations: *PK - peridotitic komatiite; BK - basaltic komatiite; HFT - high iron tholeiite; HMT - high magnesian tholeiite; TA - tholeiitic andesite; TD - tholeiitic dacite; TR - tholeiitic rhyolite; CB - calc-alkalic basalt; CA - calc-alkalic andesite; CD - calc-alkalic dacite; CR - calc-alkalic rhyolite.*

Samples: *x granodiorite dike • feldspar porphyry dike*

Abréviations: *PK - komatiite péridotitique; BK - komatiite basaltique; HFT - tholéiite hautement ferrifèrel; HMT - tholéiite hautement magnésienne; TA - andésite tholéiitique; TD - dacite tholéiitique; TR - rhyolite tholéiitique; CB - basalte calc-alkalin; CD - dacite calc-alkaline; CR - rhyolite calc-alkaline.*

Échantillons: *x dyke de granodiorite • dyke de porphyre feldspathique*

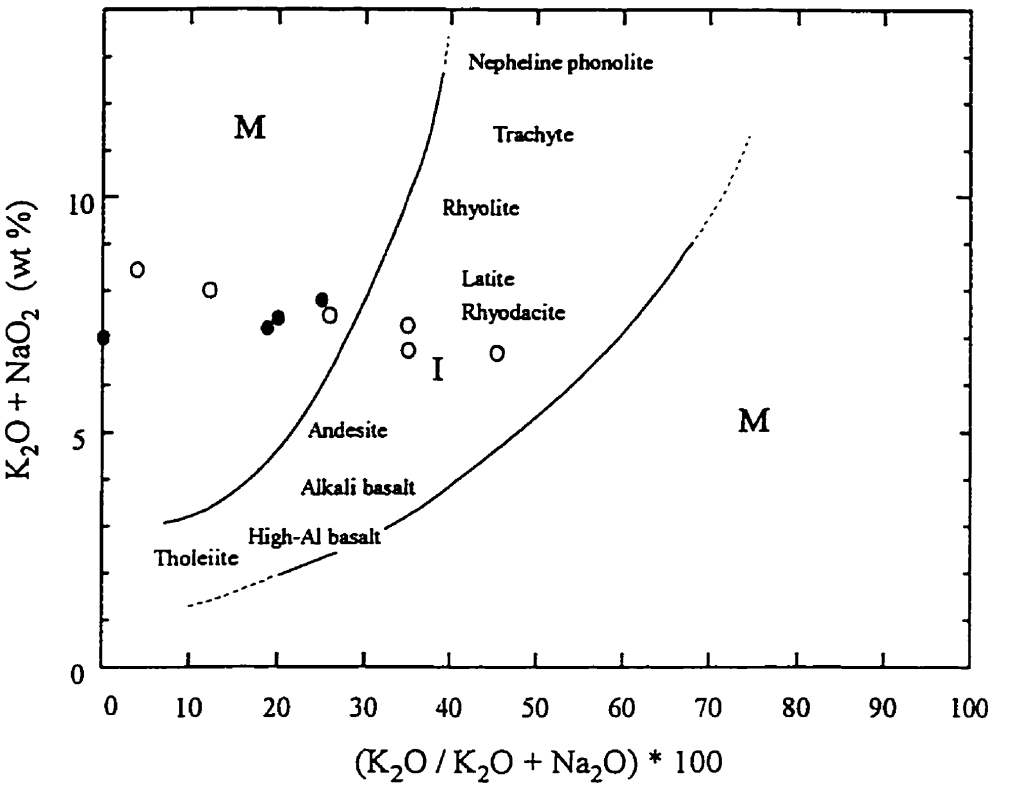

Figure 3.30 - Compositions of intermineral porphyry dikes reported on a Hughes (1973) diagram. Most data points lie outside the "igneous spectrum" suggesting that the initial rock compositions were variously modified by alkali-metasomatism. The scatter of data points for granodiorite porphyry dike samples is caused by the localized effects of alteration characterized by a strong depletion of K_2O (0.36-1.91 wt.%), coupled with anomalously high Na_2O contents (5.55-8.13 wt.%). See Appendix C for rock compositions. I= field of primary igneous rock compositions; M= field of igneous rock compositions modified by alkali-metasomatism.

o *granodiorite dike* • *feldspar porphry dike*

Compositions de dykes de porphyre interminéralisation reportées sur un diagramme de Hughes (1973). La plupart des points d'analyse se situent à l'extérieur du "spectre igné", ce qui suggère que la minéralogie originelle de ces roches a été modifiée par métasomatisme alkalin. La répartition des points d'analyse des échantillons de granodiorite s'explique par les effets localisés de l'altération qui se caractérisent par une forte déficience en K_2O (0.36-1.91 wt.%), de concert avec des quantités anormalement élevées en Na_2O (5.55-8.13 wt. %). Se référer à l'Appendice C pour obtenir la composition des échantillons. I= aire incluant la composition originelle d'une suite de roches ignées; M= aire reflétant la composition de roches ignées modifiée par métasomatisme alkalin.

o *dyke de granodiorite* • *dyke de porphyre feldspathique*

an albitite dike and is characterized by the presence of large xenoliths of country rocks, including xenoliths of gold ore, albitite dikes, and carbonate-talc-chlorite schist (e.g. section **12697.5 N** and **41 Level Map**, back pocket). Parts of the main orebody have been engulfed by the granodiorite dike and form the "hangingwall" "B" zone, "J", "K" and "L" ore zones (e.g. section **12636.5 N** and **33 Level Map**, back pocket). Although the granodiorite and feldspar porphyry dikes show distinct compositions, they are difficult to distinguish in the field because their primary igneous textures have often been obliterated by sericite and carbonate alteration, and by deformation (**Figures 3.31** and **3.32**).

Granodiorite textures range from granular to seriate porphyritic, through to coarse-grained porphyritic (**Figure 3.31**). The least-altered and least-deformed specimen of porphyry dikes are characterized by a "crowded" porphyritic texture[12] consisting of 35-45% euhedral albite phenocrysts (0.5-3.0 mm) in a groundmass predominantly composed of microcrystalline albite (An_{0-1}) (**Figures 3.33 A** and **B**). This albite texture is interpreted as the result of pervasive albite alteration of the granodiorite porphyry dike. Quartz phenocrysts are rare and only seen in thin sections. They are characterized by large embayments (**Figure 3.33 B**) suggesting they have been magmatically resorbed. The resorbed grains also show ragged boundaries with the albitic groundmass, suggesting that quartz phenocrysts may have been further resorbed during hydrothermal albite alteration.

Feldspar porphyry textures are similar to granodiorite textures and consist of 45-65% subhedral to rounded oligoclase phenocrysts (1-6 mm), with rare anhedral quartz phenocrysts, in a microcrystalline groundmass composed of albite (An_{0-1}). Away from the ore zone, plagioclase phenocrysts have been replaced by epidote, chlorite and minor calcite, and are surrounded by a clear rim of albite (**Figure 3.33 C**). As in the case of quartz phenocrysts in the granodiorite porphyry dike, the feldspar phenocrysts observed in this section of feldspar

---

[12] Phenocrysts rich phases (> 25 % phenocrysts) of differentiated intrusions, or porphyry dikes, commonly occurring in porphyry molybdenum and porphyry copper deposits (e.g. Henderson Mine, White et al., 1981).

porphyry dike show numerous microscopic embayments (**Figure 3.33 C**). This observation suggests that feldspar phenocrysts were partially resorbed during an early hydrothermal albite alteration of the porphyry.

Kiena's porphyry dikes have been weakly mineralized[13] by thin carbonate-quartz-pyrite-Au stockwork veins (**Figure 3.33 D**) and overprinted by sericite, biotite-magnetite stringer veins, later replaced by chlorite (**Figure 3.32 B**). Sericite stringer veins are confined to the porphyry dikes, whereas biotite-magnetite and chlorite stringer veins transgress porphyry dikes, gold ore and volcanic wall-rock contacts. As the phyllosilicate vein alteration appears to be restricted to the deposit's outer gold alteration halo, it is interpreted as the last hydrothermal event of the pro-grade alteration-mineralization sequence. Based on criteria set forth by Kirkham (1971), the porphyry dikes of the Kiena Mine are interpreted as intermineral[14] dikes because: 1) they host xenoliths of ore indicating that the dikes post-date the bulk of gold mineralization, and 2) they are also cut and weakly mineralized by minor auriferous carbonate-quartz pyrite veins, in turn overprinted by fracture-controlled phyllosilicate alteration. This suggests that hydrothermal activity associated with the emplacement of albitite dikes and gold mineralization, continued subsequent to the intrusion of the granodiorite and feldspar porphyry dikes.

---

[13] Samples of porphyry dikes assayed during this study (see **Appendix C**), show that gold values can range between 70-650 ppb, and that there is a one to one relationship between the stockwork vein alteration and these elevated gold concentrations. Regional background gold levels in barren mafic volcanic rocks range between 3-11 ppb Au (Muir, 1979; Bourget, 1986).

[14] Throughout this thesis, an "intermineral" dike refers to a type of intrusion frequently encountered in porphyry copper and molybdenum deposits, characteristically emplaced between distinct episodes of alteration and mineralization. Cross-cutting relationships between dikes and mineralized veins indicate that igneous and hydrothermal activity are linked to mineralization, and broadly contemporaneous. As specifically stated by R.V. Kirkham (1971, p. 1246): "Through-going veins that both pre-date and post-date the dike, or breccia, are the most convincing evidence that an intrusion is "intermineral". Vein fragments, alteration, and other features could also be of value in determining whether or not an intrusion is intermineral."

Weakly mineralized and phyllosilicate-altered porphyry dikes are penetratively deformed by a steeply, north-dipping schistosity. Their texures range from weakly foliated (**Figure 3.31 A**), to gneissic (**Figure 3.32 C**), to mylonitic (**Figure 3.32 B**) and schistose (**Figure 3.31 C**). The dikes are deformed, together with the ore, by an asymmetric z-shaped fold and related north-dipping schistosity (e.g. 43 Level Map, back pocket). The dikes, the ore, and the main schistosity were subsequently deformed by a north-northwest-plunging fold (e.g. section 12438.4 N, back pocket) and overprinted by a gently east-dipping crenulation cleavage (**Figure 3.32 B**). Although strain intensity increases with depth in the mine, the amount of strain recorded in these rocks is primarily a function of hydrothermal phyllosilicate alteration.

A section of porphyry dike cutting the ore at level 30 and originally mapped as intermineral granodiorite dike (**Figure 3.27**), has yielded a concordant U-Pb zircon age of 2686 ± 2 Ma (Morasse et al., 1993; Morasse et al., 1995, see also Chapter 6). The dike, however, could not be distinguished texturally from the feldspar porphyry dike (refer to sections 12438.4 N and 12514.6 N in back pocket). The age of 2686 ± 2 Ma is thus interpreted as the age of both intermineral granodiorite and feldspar porphyry dikes.

Figure 3.31 - Photographs of slabbed hand samples of intermineral granodiorite dike. Photographies d'échantillons de dyke de granodiorite interminéralisation.

A- Weakly foliated granodiorite dike showing a "crowded" porphyritic texture (35-40 % feldspar phenocrysts). Note the presence of a weakly developed chlorite-biotite stringer vein alteration (Chl), parallel to foliation. The present composition of feldspar phenocrysts is albite.
Sample K91-3025-106, "D" zone, ore drift 3025, Kiena Mine level 30.

B- Gneissic to mylonitic granodiorite porphyry (45-55 % feldspar phenocrysts) exhibiting discontinuous wisps of chlorite-biotite (Chl-Bo) wrapping around elongated, augen albite phenocrysts. Note also the presence of strained pyrite (Py) grains along the gneissosity.
Sample K90-3627-077, "J" zone, ore drift 3627, Kiena Mine level 36.

C- Highly schistose granodiorite porphyry. The primary porphyritic texture has been partly obliterated by hydrothermal sericite and minor carbonate alteration. The strong mineral lineation is defined by small aggregates of chlorite and biotite (Chl-Bo).
Sample K90-41092-038, "C" zone, ore drift 41092, Kiena Mine level 41.

D- Weakly schistose granodiorite porphyry exhibiting a "crowded" porphyritic texture composed of 45-50 % fine, euhedral feldspar phenocrysts. The fabric of the porphyry is cut by carbonate-quartz-pyrite (Py) veinlets. Note also the presence of wispy and irregular chlorite-biotite (Chl-Bo) stringer veins.
Sample K92-6446-222, "lower C" zone, ore drift 6446, Kiena Mine level 64.

A- Échantillon de dyke de granodiorite faiblement folié montrant une texture porphyritique à forte concentration de phénocristaux de feldspath (35-40 %). Notez la présence d'une altération en veinules de chlorite-biotite (Chl) parallèle à la foliation. La composition actuelle des phénocristaux de feldspath correspond à celle de l'albite.
Échantillon K91-3025-106, zone "D", galerie à minerai 3025, niveau 30 Mine Kiena.

B- Porphyre de granodiorite à forte concentration de phénocristaux de feldspath (45-55 %) dont la texture est gneissique à mylonitique. Notez la présence de segments discontinus de veinules de chlorite-biotite (Chl-Bo) enveloppant les "yeux" de feldspath, ainsi que les grains de pyrite (Py) finement disséminés le long de la gneissosité.
Échantillon K90-3627-077, zone "J", galerie à minerai 3627, niveau 36 Mine Kiena.

C- Porphyre de granodiorite fortement schistosé. La texture porphyrique a été partiellement oblitérée par l'altération en séricite et carbonate. La forte linéation minérale est constitué d'un alignement de petits aggrégats de chlorite et biotite (Chl-Bo).
Échantillon K90-41092-038, zone "C", galerie à minerai 41092, niveau 41 Mine Kiena.

D- Porphyre de granodiorite faiblement schistosé, montrant les reliques d'une texture porphyrique à forte concentration de feldspath composée de 45-50 % de phénocristaux automorphes et finement grenus de feldspath. La fabrique du porphyre est recoupée par des veinules de carbonate-quartz-pyrite (Py). Notez également la présence de veinules de chlorite-biotite (Chl-Bo) réticulées et irrégulières au sein de l'échantillon.
Échantillon K92-6446-222, zone "C". galerie à minerai 6446, niveau 64 Mine Kiena.

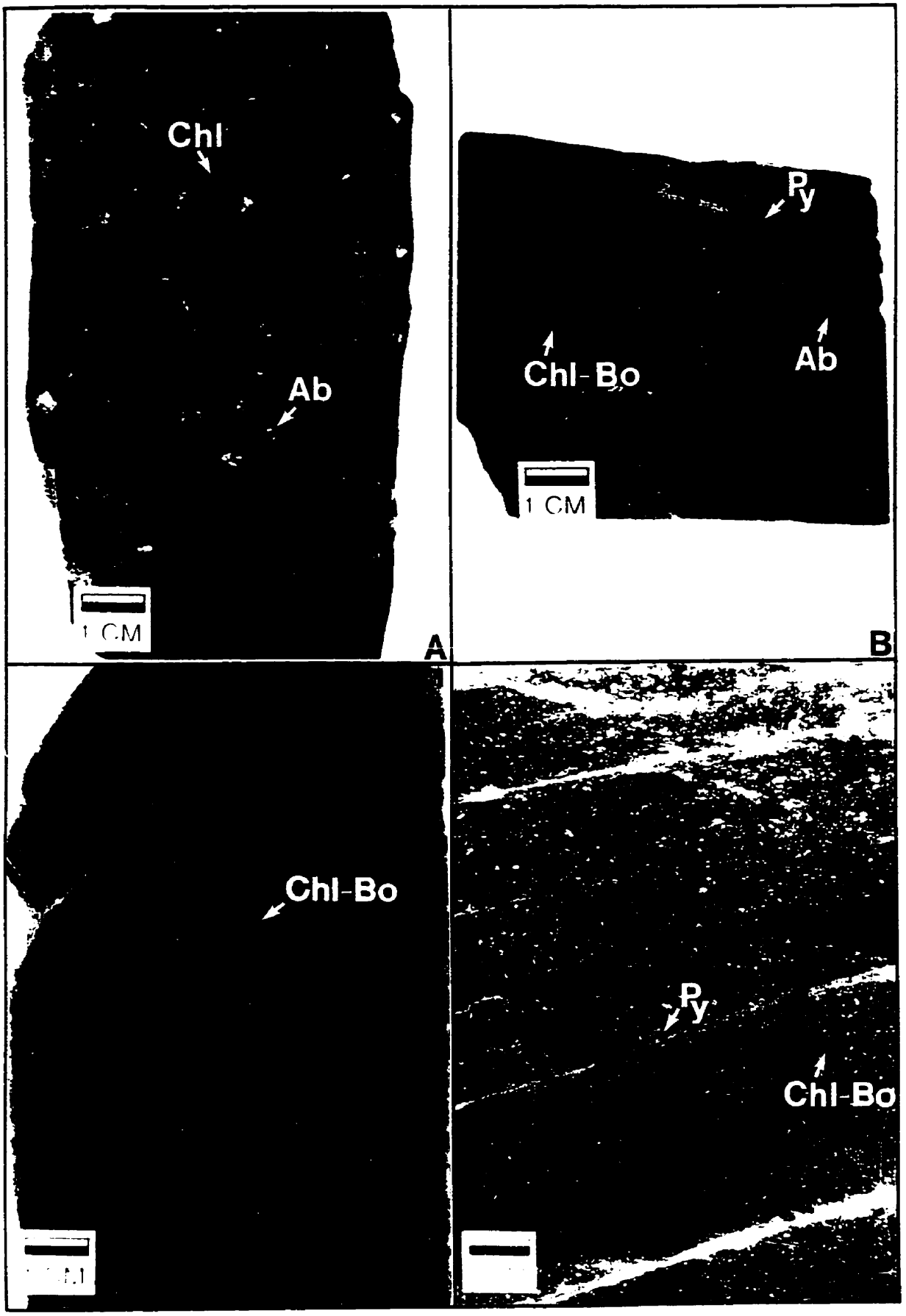

Figure 3.31

Figure 3.32 - Photographs of slabbed hand samples of intermineral porphyry dike.
Photographies de dykes de porphyre feldspathique interminéralisation.

A- Weakly foliated granodiorite porphyry showing a "crowded" porphyritic texture (lower half of the photograph) grading into a fine-grained equigranular rock (upper half of photograph). Note the presence of quartz-carbonate veins and the high incidence of fine disseminated pyrite (Py) grains in the fabric of the porphyry.
Sample K92-2752-207, "A" zone, ore drift 2752, Kiena Mine level 27.

B- Gneissic feldspar porphyry exhibiting a strong foliation and weak crenulation cleavage. Note the presence of a boudinaged carbonate-quartz veinlet (lower half of the sample) cross-cutting the fabric of the porphyry.
Sample K93-3813-268, "B" zone, ore drift 3813, Kiena Mine level 38.

C- Gneissic feldspar porphyry exhibiting a moderate to intense chlorite-biotite (Chl-Bo) stringer vein alteration and strong foliation. Phyllosilicate veins overprint carbonate-quartz-pyrite (Py) veinlets.
Sample K93-5804-264, "B" zone, ore drift 5804, Kiena Mine level 58.

D- Least-altered and least-deformed sample of feldspar porphyry. The low strain state of the porphyry is possibly attributed to the lack of hydrothermal phyllosilicate alteration.
Sample K92-6402-230, access drift 6402, east of the "lower C" zone, Kiena Mine level 64.

A- Porphyre de granodiorite faiblement folié montrant une texture porphyrique à forte concentration de phénocristaux de feldspath (moitié inférieure de la photo), devenant graduellement équigranulaire et finement grenue (moitié supérieure de la photo). Notez la présence de veinules de quartz-carbonate et la forte concentration de fine pyrite (Py) disséminée à travers la fabrique de l'échantillon.
Échantillon K92-2752-207, zone "A", galerie à minerai 2752, niveau 27 Mine Kiena.

B- Porphyre feldspathique à texture gneissique montrant une forte foliation ainsi qu'un faible clivage de crénulation. La veinule de carbonate-quartz recoupant la fabrique du porphyre (au bas de l'échantillon) a été boudinée.
Échantillon K93-3813-268, zone "B", galerie à minerai 3813, niveau 38 Mine Kiena.

C- Porphyre feldspathique à texture gneissique montrant une forte altération en veinules de chlorite-biotite (Chl-Bo) ainsi qu'une forte foliation. Les veinules de phyllosilicate recoupent les veinules de carbonate-quartz-pyrite (Py).
Échantillon K93-5804-264, zone "B", galerie à minerai 5804, niveau 58 Mine Kiena.

D- Échantillon le moins altéré et le moins déformé de porphyre feldspathique. La déformation restreinte du porphyre est possiblement attribuable à l'absence d'altérations hydrothermales en phyllosilicate.
Échantillon K92-6402-230, zone "C" inférieure, galerie d'accès 64-02, niveau 64 Mine Kiena.

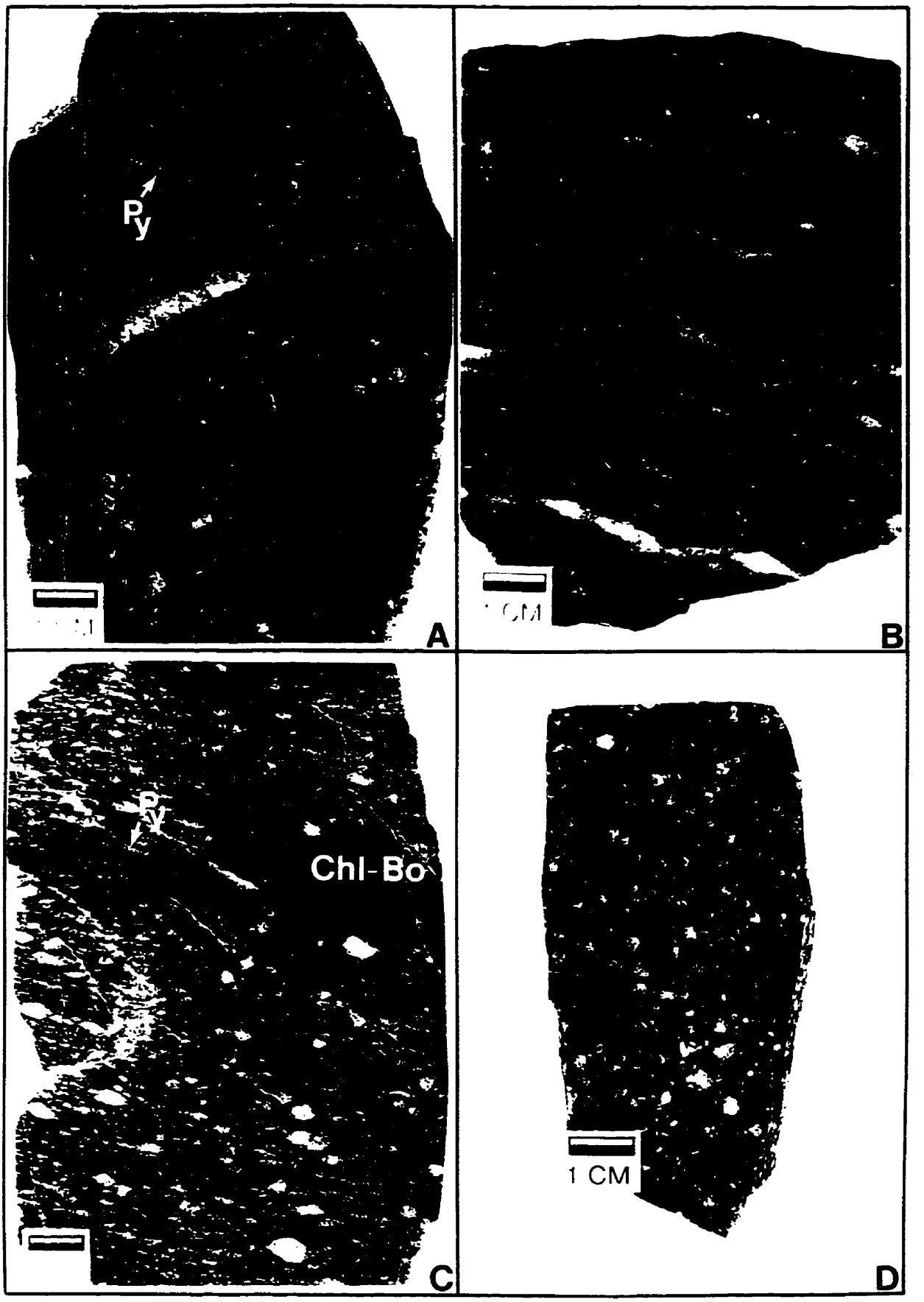

Figure 3.32

Figure 3.33 - Photomicrographs of intermineral granodiorite and feldspar porphyry dikes. Microphotographies de dykes de granodiorite et porphyre feldspathique interminéralisation.

A- Granodiorite porphyry showing a weakly foliated fabric consisting of subhedral albite phenocrysts in a groundmass composed of microcrystalline albite. Albite phenocrysts are replaced by sericite. The albitic groundmass is cut by chlorite-biotite (Chl-Bo) veinlets.
Sample K91-3025-106, crossed nicols. "D" zone, ore drift 3025, Kiena Mine level 30.

B- Granodiorite porphyry showing a magmatically resorbed quartz phenocryst in a microcrystalline albite groundmass. Sericite alteration is overprinted by aggregates of chlorite (Chl).
Sample K90-41092-038, crossed nicols. "C" zone, ore drift 41092, Kiena Mine level 41.

C- Feldspar porphyry showing euhedral oligoclase phenocrysts pseudomorphosed by epidote (Ep), chlorite and calcite. The feldspar phenocrysts are rimmed by clear albite. The groundmass is composed of an assemblage of microcrystalline albite (Ab).
Sample K92-6402-230, crossed nicols. Access drift 6402, Kiena Mine level 64.

D- Fabric of an albite-altered feldspar porphyry (microcrystalline albite) overprinted by sericite stringer vein alteration (Ser).
Sample K93-3813-268, crossed nicols. "B" zone, ore drift 3813, Kiena Mine level 38.

A- Dyke de granodiorite montrant une fabrique faiblement foliée, composée de phénocristaux hypidiomorphes d'albite dans une matrice d'albite microgrenue. Les phénocristaux d' albite sont altérés en séricite et la matrice est recoupée par des veinules de chlorite-biotite (Chl-Bo).
Échantillon K91-3025-106, microscope à lumière transmise, Nicols croisés. Zone "D", galerie à minerai 3025, niveau 30 Mine Kiena.

B- Dyke de granodiorite montrant un phénocryste de quartz résorbé par processus magmatique, au sein d'une matrice d'albite microgrenue. De petits aggrégats de chlorite (Chl) remplacent localement l'altération en séricite (Ser).
Échantillon K90-41092-038, microscope à lumière transmise, Nicols croisés. Zone "C", galerie à minerai 41092, niveau 41 Mine Kiena.

C- Porphyre feldspathique montrant des phénocristaux d'oligoclase pseudomorphisés par de l'épidote (Ep), de la chlorite, et de la calcite. Les phénocrystes d'oligoclase sont auréolés d'un liséré d'albite limpide. La matrice du porphyre est composée d'un assemblage d'albite microgrenue.
Échantillon K92-6402-230, microscope à lumière transmise, Nicols croisés. Galerie d'accès 6402, niveau 64 Mine Kiena.

D- Fabrique de porphyre feldspathique altéré en albite (albite microgrenue) recoupée par des veinules de séricite (Ser).
Échantillon K93-3813-268, microscope à lumière transmise, Nicols croisés. Zone "B", galerie à minerai 3813, niveau 38 Mine Kiena.

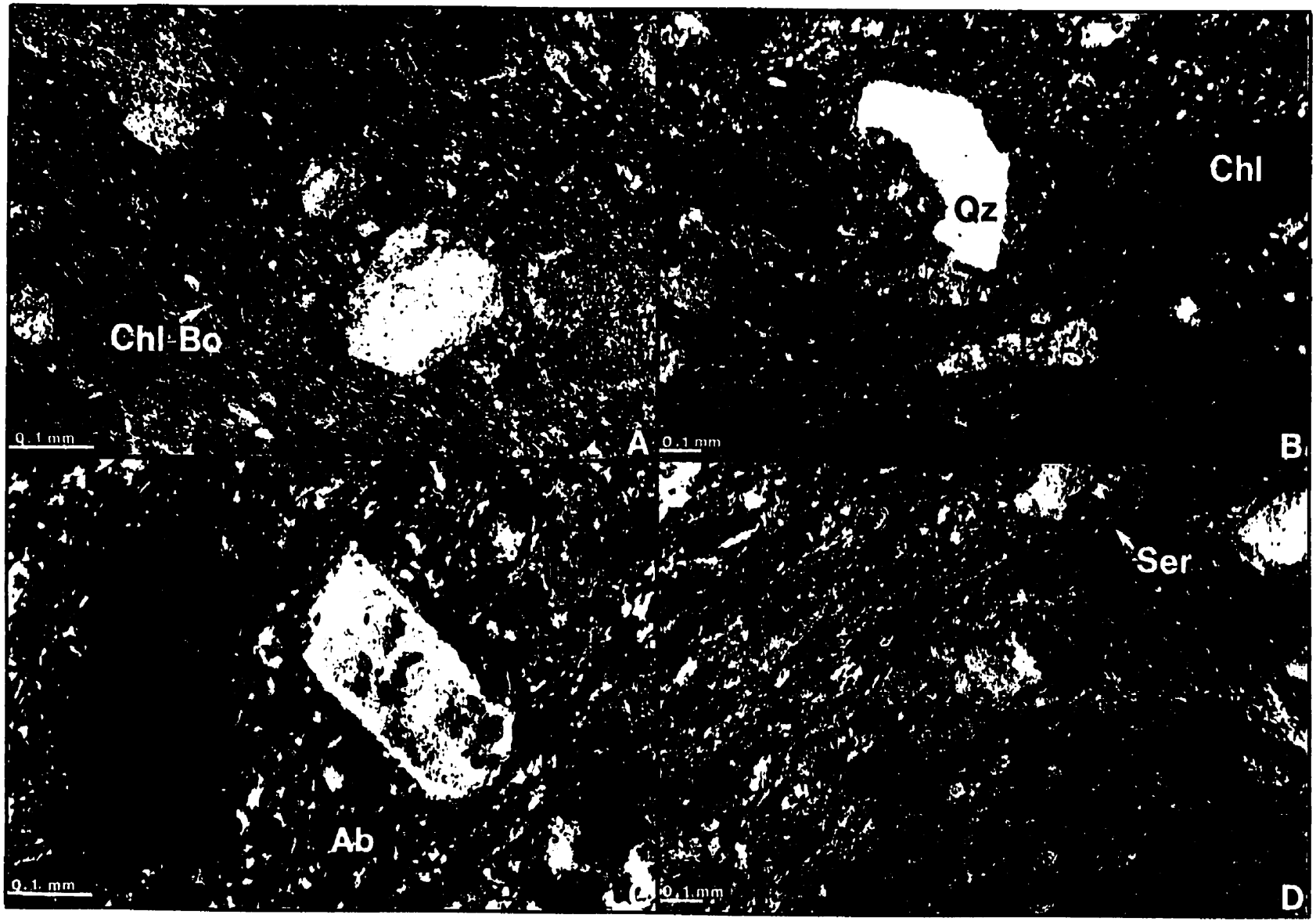

Figure 3.33

CHAPTER 4 KIENA MINE MAGMATIC-HYDROTHERMAL SYSTEM

4.1 INTRODUCTION

The Kiena orebody consists of a superposition of alteration assemblages centered on an upward-flaring albitite dike swarm. Eleven distinct alteration-mineralization facies can be recognized from overprinting relationships recorded in Kiena's altered rock sequence, which are subdivided into early, main-stage, intermediate, and late-stage alteration (**Table 4.1**). ***Early-stage alteration*** consists of alteration facies developed prior to the emplacement of gold mineralization. It consists of a pervasive albite alteration, thought to be related to the intrusion of albitite dikes, followed by a minor calcite stockwork vein alteration which defines a zone of crackle breccia around the main orebody. ***Main-stage alteration*** are those alteration facies associated with gold mineralization which overprint early alterations. It consists of four overprinting alteration stages comprised, from the oldest to the youngest, of a "Stwk Cb-Qz-Py(Po)±Ab-Au" vein ore type, a "Breccia 1" and "Breccia 2" ore type, and minor, subeconomic, quartz-calcite-biotite-albite vein alteration. Development of the first ore type is focused on the albitite dike swarm, but at upper mine levels, its areal distribution extends beyond the dikes to affect the enclosing mafic and ultramafic volcanic rocks of the Jacola Formation. "Stwk Cb-Qz-Py(Po)±Ab-Au" vein ore consists of a network of carbonate-quartz stockwork veins with discrete alteration halos composed of an assemblage of albite, disseminated pyrite and/or pyrrhotite and gold. By contrast, the second ore type or Breccia 1 ore, is restricted to the upper part of the intrusive centre and consists of ankerite-pyrite-gold replacement veins. The third ore type or Breccia 2 ore, overprints and is confined to the same area as, the Breccia 1 ore type. It consists of albite-cemented breccias and stockwork veins containing disseminated pyrite, chalcopyrite, scheelite and gold. Coarse-grained quartz-calcite-biotite-albite veins with minor tourmaline, disseminated pyrite and

chalcopyrite locally overprint, and are restricted to, the albite-cemented breccias. The deposit's highest gold concentrations occur in the upper and central part of the deposit where Breccia 2 ore is superimposed on Breccia 1 ore. ***Intermediate- and late-stage alterations*** refer to alteration facies which developed during, and shortly after, the emplacement of intermineral porphyry dikes into the deposit's alteration-mineralization sequence, but before the ore-dike complex was affected by penetrative deformation. Intermediate-stage alteration is confined to intermineral dikes and consists of a pervasive albite alteration followed by a minor calcite-quartz-pyrite stockwork vein alteration event, tentatively correlated with the introduction of gold in the porphyries. ***Late-stage alteration*** extends to the entire volume of mineralized rocks, including the intermineral dikes. It consists of a sequence of overprinting phyllosilicate vein alterations composed, from the oldest to the youngest, of sericite, biotite-magnetite, and chlorite.

The upward-flaring zonation pattern thus defined by Kiena's alteration-mineralization sequence consists of a high-grade core of feldspathized rocks mineralized by stockwork veins and breccias, grading outward into a lower-grade ore zone and gold alteration halo with the progressive decrease of stockwork vein alteration away from the mineralization centre. Ore sulfides also exhibit a clear upward and outward zonation pattern: pyrrhotite is the predominant sulfide at depth, in the "root zone" of the alteration-mineralization system whereas pyrite is the main sulfide throughout the apical part of the deposit. Zonation of ore sulfides and the distribution of gold concentrations are consistent with Kiena's albitite dike swarm acting as main ore fluid conduit for hot, hydrothermal fluids gradually cooling as they flow upward and away from the centre of the deposit. Kiena is envisaged as a porphyry-style, magmatic-hydrothermal ore system emplaced at relatively shallow depth based on the upward-flaring geometry of its albitite dike swarm and zoned alteration-mineralization fracture pattern, the intrusion of granodiorite and quartz monzonite porphyry dikes in the deposit's alteration sequence, and mineralization in stockwork veins and breccias.

4.2 KIENA DEPOSIT ALTERATION-MINERALIZATION SEQUENCE

4.2.1 Early-stage alteration facies

4.2.1.1 Pervasive albite alteration

Albitization is the first alteration stage of Kiena's alteration-mineralization sequence because all the subsequent fracture-controlled alteration types that we can recognized in the mine overprint this early albite alteration (**Table 4.1**). It consists of a deposit-wide alteration facies which predominantly occurs in pre-ore albitite intrusions but goes beyond the dikes to transform the enclosing komatiitic and tholeiitic wall-rocks into aplitic, albite-rich rocks. Albite alteration thus extends as far as the eastern and westernmost albitite dike occurrences in the mine which are located in and around the "L" and "J" ore zones, respectively (see 33 Level Map, back pocket).

Kiena's albitite dikes are monomineralic rocks essentially composed of and assemblage of pure albite (An_{0-1}) with no relics of feldspar and/or mafic mineral phenocrysts (see section **3.5.2**). By contrast, albite-altered mafic volcanic rocks in contact with the dikes show relics of primary feldspar phenocrysts (now with a pure albite composition) set in a matrix composed of a distinctive microcrystalline assemblage of amoeboidal-shaped, pure albite grains (**Figure 3.14**). Most of these albite crystals are free of albite twins, show highly serrated grain boundaries and undulatory extinction. To the untrained eye, this deformed hydrothermal albite assemblage can easily be mistaken for a granoblastic assemblage of partially recrystallized quartz. Microprobe analysis of a few grains at random may thus be necessary to positively identify the alkaline feldspars and obtain their An ($_{0-1}$) composition (**Appendix F**).

If the lack of albite-rich glass, as pointed out by Bowen (1928), suggests that all albite-rich rocks form by a replacement process (see section 3.5.2), it follows that primary igneous

Table 4.1 Major alteration stages and facies of the Kiena deposit

Stages	Facies	Areal distribution	Diagnostic features
1. Early	1.1 Albite	Overprints upward-flaring albitite dike swarm and contiguous mafic and ultramafic wall-rocks of the Jacola Formation Defines Kiena's mineralization centre	Pervasive albite alteration Microcrystalline assemblage of pure albite An_{0-1}, plumose to dentritic grains, micrographic to myrmekitic quartz-albite intergrowth
	1.2 Calcite stockwork veinlets	Upper mine levels Forms a zone of crackle breccia in periphery of the high-grade ore	Diamond-shaped fracture pattern Overprinted by, and in sharp contact with, Breccia ore
2. Main	2.1 Carbonate-quartz-pyrite-pyrrhotite±albite- Au stockwork veins (Stwk Cb-Qz-Py(Po)±Ab-Au vein ore type)	Upward-flaring fracture system developed over, and slightly beyond, the deposit's albitite dike swarm	Breccia veins characterized by crustiform and sharp-angular, mosaic breccia vein-infill textures Albite composition An_{0-1}
	2.2 Ankerite-pyrite-Au replacement veins (Breccia 1 ore type)	Upper mine levels Partially blankets early, stockwork vein mineralization	Distinct buff-beige color Sets of microfractures defined by strings of disseminated pyrite grains and carbonate veinlets
	2.3 Albite-pyrite±chalcopyrite-scheelite-Au stockwork veins and breccias (Breccia 2 ore type)	Upper mine levels Overprints Breccia 1 ore	Sharp-angular, mosaic to mottled breccia with stockwork veins emanating, and radiating, from the breccia Cockade breccia-infill texture Albite composition An_{0-1}
	2.4 Coarse-grained quartz-calcite-biotite-albite ±tourmaline-pyrite-chalcopyrite-Au veins	Occurs locally throughout the Breccia 2 ore type	Large booklets of biotite Rosettes of tourmaline needles
3. Intermediate	3.1 Intrusion of intermineral porphyry dikes Albite	Confined to porphyry dikes	Pervasive albite alteration: microcrystalline assemblage of pure albite An_{0-1} Pure albite overgrowth around more calcic feldspar phenocrysts
	3.2 Calcite-quartz-pyrite-(Au) stockwork veinlets	Confined to porphyry dikes	Cuts albite assemblage and is overprinted, in turn, by biotite-magnetite-chlorite stringer veins
4. Late	4.1 Sericite stringer veins	Restricted to porphyry dikes	
	4.2 Biotite-magnetite stringer veins	Upward-flaring fracture system overprinting the ore-dike complex and extending to the deposit's outer gold alteration halo	Phlogopitic biotite (11-13 wt.% MgO) Abundant relics of biotite and magnetite throughout the chlorite vein system Better preserved at upper mine levels
	4.3 Chlorite stockwork and stringer veins	Upward-flaring fracture system overprinting the ore-dike complex and extending to the deposit's outer gold alteration halo	Replaced by stilpnomelane at upper mine levels

textures of the deposit's albitite dikes were probably destroyed and replaced by hydrothermal albite. Thus, the preservation of primary igneous textures in albitized volcanic rocks adjacent to albitite dikes suggests that albitization is most intense in the dikes. This, in turn, may indicate that the deposit's early albite alteration emanated from, and accompanied the emplacement of the albitite dikes. Based on criteria set forth by Titley (1982 , p.99), Kiena's early albite alteration is interpreted as a pervasive type of alteration akin to K-feldspar alteration associated with main-stage Cu-Mo mineralization in porphyry ore systems[1].

Feldspathised rocks of the Kiena deposit are overprinted by a fracture-controlled, alteration-mineralization sequence which, in turn, is penetratively deformed by folds and related penetrative planar fabrics (see Chapter 5). As with other rock types in the deposit, the amount of deformation strain recorded in albite-altered rocks increases with depth, from an unfoliated assemblage of highly sutured (almost stylolitic) albite grains at upper mine levels (e.g. **Figure 3.25C**), to a weak foliation defined by the alignment of the long axis of albite phenocrysts at mid-mine levels (e.g. **Figure 3.13**), to a strongly schistose mineralized rock at lower mine levels (e.g. **Figure 4.4**).

4.2.1.2 Calcite stockwork vein alteration (crackle breccia)

A minor calcite stockwork vein system forms the second alteration stage of Kiena's alteration mineralization sequence because these veins overprint the strongly albitized, tholeiitic volcanic rocks east of the S-50 Zone, but are overprinted by stockwork veins and breccias of main-stage gold mineralization (**Table 4.1**). The narrow (1-2 cm) calcite-filled fractures dip steeply to the north-northwest and to the northeast to form a zone of crackle breccia characterized

---

[1] Pervasive K-feldspar alteration is a texturally destructive, non-selective alteration restricted to the centre of Cu/Mo mineralization. Rock types involved in orthoclase metasomatism are generally those with igneous rocks mineralogies.

by a diamond-shaped fracture pattern (see Index map 4313, back pocket). This early vein system, which intensifies near the contact with the ore, is abruptly cut by the massive breccia of the S-50 Zone. The presence of a similar zone of crackle breccia is thought to occur also in albitized komatiitic volcanic rocks west of the S-50 zone, but it was not mapped due to restricted access in this part of the mine.

4.2.2 Main-stage alteration facies

4.2.2.1 Carbonate-quartz-pyrite(pyrrhotite)±albite-Au stockwork vein alteration (Stwk Cb-Qz-Py(Po)±Ab-Au vein ore type)

The first, and most extensive gold alteration type encountered at Kiena consists of carbonate-quartz stockwork breccia veins accompanied by discrete alteration halos composed of albite, disseminated pyrite or pyrrhotite, and free gold (**Figures 4.1** to **4.6**). The veins overprint the zone of crackle breccia east of the S-50 zone (see Index map 4313, back pocket) and are overprinted, in turn, by the replacement veins and breccias of the "Breccia 1" and "Breccia 2" ore types (e.g. **Figure 4.7**). This alteration-mineralization type is referred to as the "Stwk Cb-Qz-Py(Po)-Ab-Au" vein ore type (**Table 4.1**).

The Kiena deposit carbonate-quartz stockwork vein system has an upward-flaring geometry (see **Figure 4.22**) and consists, from lower to upper mine levels, of gold-bearing stockwork veins essentially confined to albitite dikes and iron tholeiite between the dikes (e.g. **64 Level Map**, back pocket and **Figure 4.4**) grading upward and outward into stockwork veins cutting the tholeiitic and komatiitic wall-rocks enclosing the breccia body of the S-50 Zone (e.g. **41 Level Map**, back pocket and **Figure 4.1**). The auriferous stockwork vein system is zoned, from the centre outward, into a high-grade core, a lower-grade ore shell, and an outer gold alteration halo (**Figure 4.22**). The high-grade core of the stockwork vein system grades an average 5-10 g/t Au and occupies the lower mine levels (below level 62, **Figure 4.22**). It is characterized by a *high density* of carbonate-quartz veinlets and the occurrence of pyrrhotite

as the main disseminated sulfide in the alteration halos to the veins (**Figure 4.4**). By contrast, lower-grade "Stwk Cb-Qz-Py(Po)±Ab-Au" vein ore type yields an average 3-5 g/t Au and is restricted to upper mine levels where it surrounds the high-grade breccia body of the S-50 zone (**Figure 4.22**). It is characterized by a lower density of, and more widely-spaced, carbonate-quartz veinlets and the occurrence of pyrite, as opposed to pyrrhotite, as the main ore sulfide in the alteration halos to the veins (**Figure 3.1** and **4.1**). Lower-grade ore progressively leads, with increasing distance from the mineralization centre, to the deposit's gold alteration halo which consists of komatiitic and tholeiitic country rocks sporadically overprinted by carbonate-quartz-pyrite stockwork veins grading on average 0.34-1 g/t Au. The upward and outward pyrrhotite-pyrite zonation within the stockwork vein system suggests a decrease in ore fluid temperatures with decreasing depth and away from the main ore fluid conduits (e.g. White and Hedenquist (1995), Barton and Skinner (1979)).

A patchwork of zones of sharp-angular mosaic breccia, interconnected by crustiform textured veins, characterize the mineralized stockwork vein system (**Figure 4.1, 4.4** and **5.17**). The breccias have sharp contacts and consist of albite-altered tholeiitic wall-rock fragments (dark green to light grey) cemented by vein carbonate and disseminated sulfide (e.g. **Figure 5.1**). Crustiform veins are filled, from the selvage inward, by carbonate and quartz and are accompanied by alteration halos composed essentially of albite and disseminated sulfide (**Figures 4.2** and **4.6**). Hydrothermal vein albite have an $An_{(0-1)}$ composition (see **Appendix F**) and share the same cleavelandite-type crystal habit as albitite-forming albites (compare **Figures 4.3** and **3.25**). Vein pyrites are partly recrystallized and characterized by a medium to coarse-grained poikiloblastic texture (**Figure 4.2**), except at lower mine levels where they are strongly deformed (strung out) along schistosity planes, just as disseminated pyrrhotite grains (**Figure 4.5**).

Breccias and crustiform veins are thought to have formed coevally because the veins do not overprint, and share the same mineralogy as, the breccias. On the one hand, the absence of rock flour or gouge in the breccia veins suggests that rock attrition was not the result of fault

movement. The lack of rotation displayed by the angular rock fragments (e.g. **Figure 5.1**) and the gradational transition between breccia and veins (**Figure 4.1**) also preclude any explosive mechanism for brecciation. The fracture patterns in and around the breccias do suggest, however, that fracturing, hydrothermal fluid flow, and subsequent crystallization proceeded from the brecciated areas outward to the open-space fractures. Based on these observations, a brecciation mechanism possibly caused by retrograde boiling of mineralized fluids is thus proposed to explain the formation of the Kiena deposit carbonate-quartz stockwork vein system.. High fluid pressure possibly initiated fracturing and brecciation, followed by the replacement of rock fragments during continued hydrothermal fluid flow. Additionally, the overprint of the upward-flaring fracture pattern of the "Stwk Cb-Qz-Py(Po)±Ab-Au" vein ore type onto the albitite dike swarm suggests the following: 1) that the albitite dikes channelled ascending ore fluids and, 2) that the magma and gold-bearing hydrothermal fluids share the same igneous source at depth.

Kiena's "Stwk Cb-Qz-Py(Po)±Ab-Au" vein ore type is overprinted by breccia ores, cut by intermineral porphyry dikes and late-stage phyllosilicate vein alterations (**Table 4.1**). Present vein geometry (e.g. **Figures 4.1**, **4.4** and **4.6**) clearly shows that the mineralized carbonate-quartz stockwork vein system is penetratively deformed by post-ore, flattening-dominated strain (see Chapter 5). The main characteristics of Kiena's "Stwk Cb-Qz-Py(Po)±Ab-Au" vein ore type are summarized in **Table 4.1**.

4.2.2.2 Ankerite-pyrite-Au replacement vein alteration (Breccia 1 ore type)

The second mineralization stage recognized at Kiena is the "Breccia 1" ore type. It consists of ankerite-pyrite-Au replacement veins which overprint the earlier "Stwk Cb-Qz-Py(Po)±Ab-Au" vein ore type (**Figure 4.7**) and is overprinted in turn, by breccias and stockwork veins of the "Breccia 2" ore type (**Figure 4.10**). This alteration-mineralization is labelled as a *breccia* ore type because parts of the tholeiitic wall-rock previously mineralized by stockwork

Figure 4.1 - *Mosaic of photographs (view looking North) showing Kiena's "Stwk Cb-Qz-Py(Po)±Ab-Au" vein ore type. Carbonate-quartz stockwork veins are characterized by open-space vein-infill textures and discoloured alteration halos composed of albite and disseminated pyrite. The stockwork is cut by the intermineral feldspar porphyry dike (upper right) and overprinted by the deposit's main schistosity (S_n, dashed line). Veins at a low angle to cleavage are boudinaged whereas those at high angle to cleavage are folded. Small, carbonate-filled extension veins, perpendicular to cleavage, overprint the stockwork veins (arrows). The iron rod to the right measures approximately 30 centimetres in length.*

Access to ore drift 3838, "C" zone, Kiena Mine level 38.

Collage photographique avec regard vers le nord, montrant le minerai de type "Stwk Cb-Qz-Py(Po)±Ab-Au" à Kiena. Les veines de carbonate-quartz en stockwork sont charactérisées par des textures de remplissage en fractures ouvertes ainsi que par des épontes altérées renfermant de l'albite et de la pyrite disséminée. Le stockwork est recoupé par le dyke de porphyre feldspathique (coin droit) et il est déformé par la schistosité principale du gisement (S_n, ligne pointillée). Les veinules sub-parallèles au clivage sont boudinées tandis que celles qui sont sub-perpendiculaires au clivage sont plissées. De petites veinules d'extension à carbonate, perpendiculaires au clivage, se superposent localement aux veines du stockwork (flèche). La barre de fer située sur la droite mesure environ 30 centimètres.

Galerie d'accès du chantier 3838, zone "C", niveau 38 Mine Kiena.

Figure 4.1

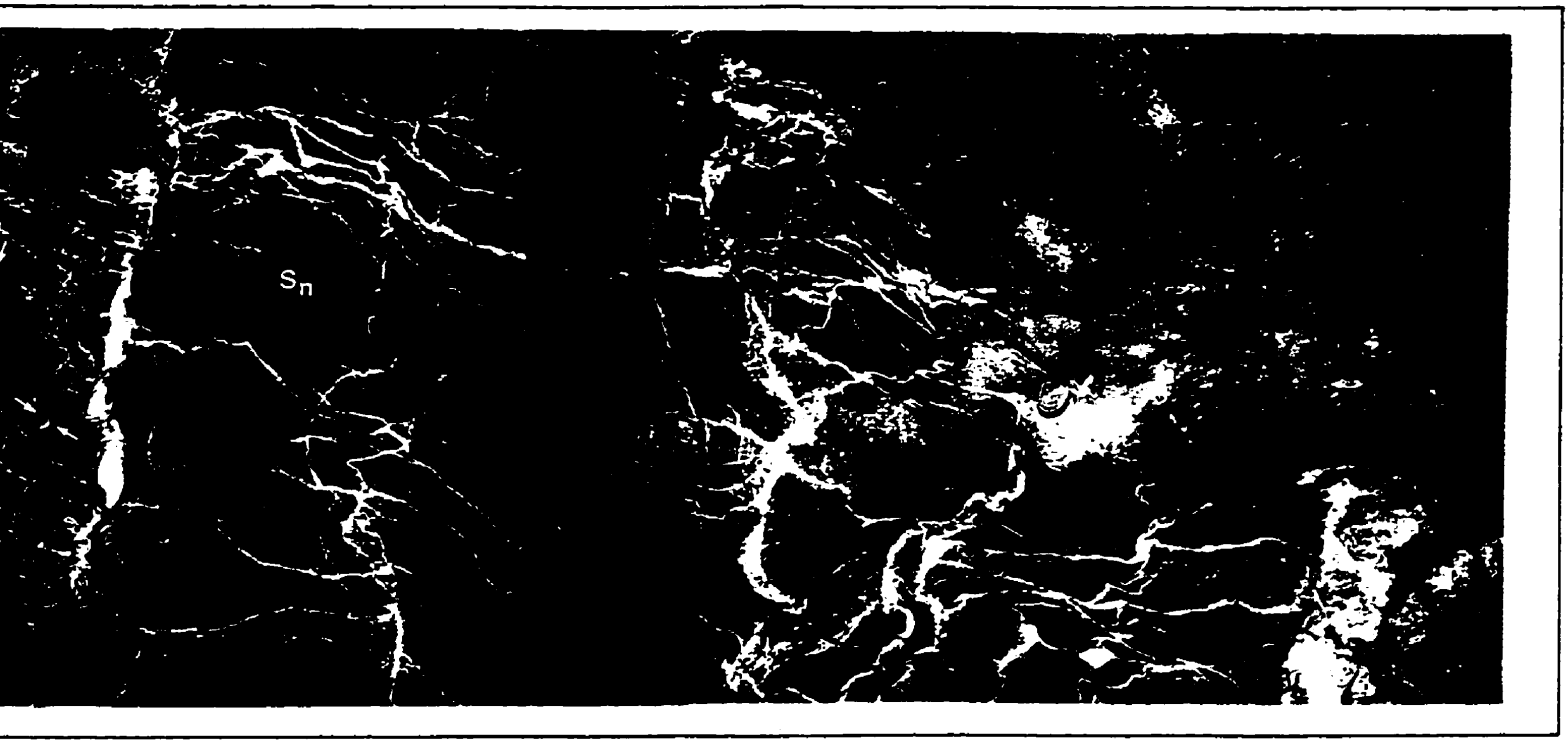

Figure 4.1

Figure 4.2 - Photograph of a polished rock slab of the "Stwk Cb-Qz-Py(Po)±Ab-Au" vein ore type shown on Figure 4.1. Carbonate is white (Cb), albite is opalescent white (Ab), and quartz is light grey (Qz). Note the presence of a sigmoidal carbonate extension vein overprinting the stockwork vein.

Sample K91-3838-079 , access to ore drift 3838, "C" zone, Kiena Mine level 38.

Photographie de la surface polie d'un échantillon de minerai de type "Stwk Cb-Qz-Py(Po)±Ab-Au" provenant de l'affleurement montré à la Figure 4.1. Le carbonate est blanc (Cb), l'albite est blanc opalescent, tandis que le quartz est gris clair (Qz). Notez la présence d'une veinule d'extension remplie de carbonate de forme sigmoide, recoupant la veine du stockwork.

Échantillon K91-3838-079, galerie d'accès du chantier 3838, zone "C", niveau 38 Mine Kiena.

Figure 4.3 - Photomicrograph of the selvage of the carbonate-quartz stockwork vein shown on Figure 4.2. Vein albite textures are characterized by an assemblage of platy to dendritic crystals of pure albite (An_{0-1}) composition (see Appendix F). Albite grain boundaries are highly sutured, almost stylolitic, indicating that this hydrothermal albite assemblage is deformed. Similar crystal habits and albite compositions also characterize albitite-forming albites (see Figure 3.25).

Sample K91-3838-079, transmitted light, crossed Nicols. Access to ore drift 3838, Kiena Mine level 38.

Microphotographie de l'éponte de la veinule de carbonate-quartz en stockwork montrée à la Figure 4.2. La texture de l'albite en veinule est formée par un assemblage de cristaux d'albite de composition (An_{0-1}) à caractère "dendritique" (voir Appendice F). La bordure fortement dentelée (suturée), presque stylolitique, des grains d'albite indique que cet assemblage d'albite hydrothermale est déformé. De semblabes arrangements de cristaux d'albite pure charactérisent les assemblages d'albite formant les albitites (Figure 3.25).

Échantillon K91-3838-079, microscope à lumière transmise, Nicols croisés. Galerie d'accès du chantier 3838, niveau 38 Mine Kiena.

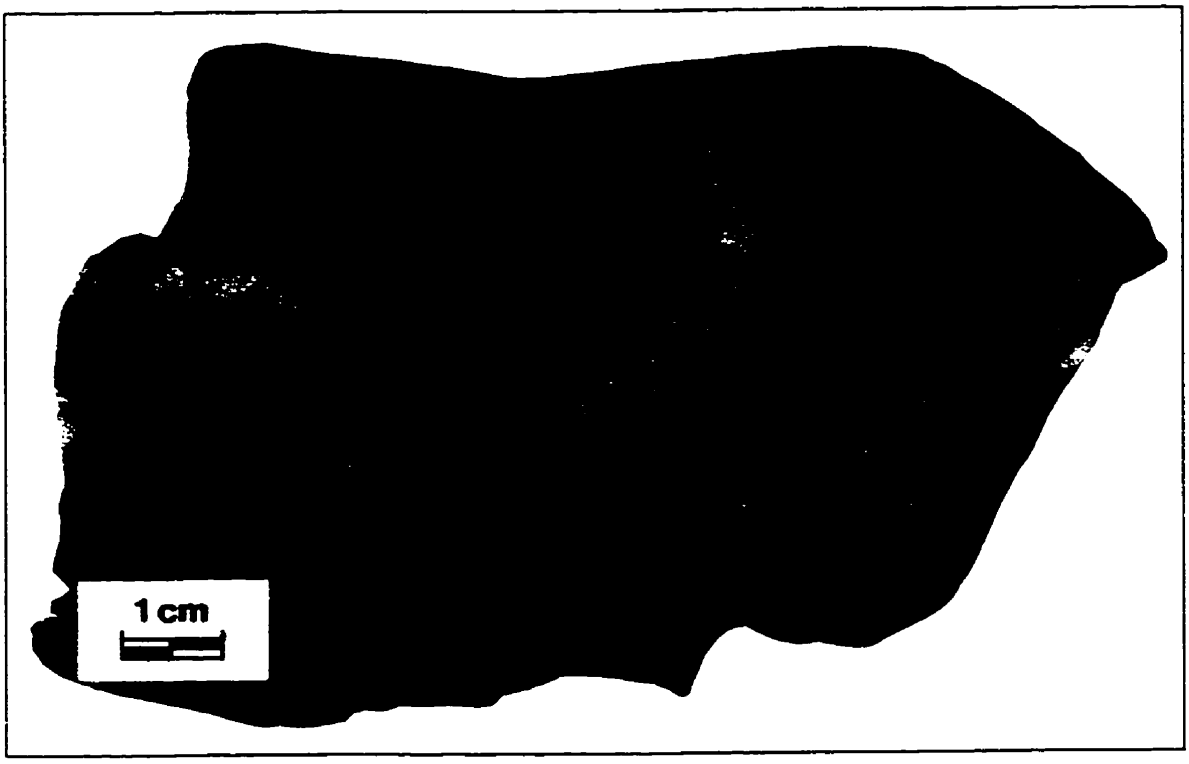

Figure 4.2

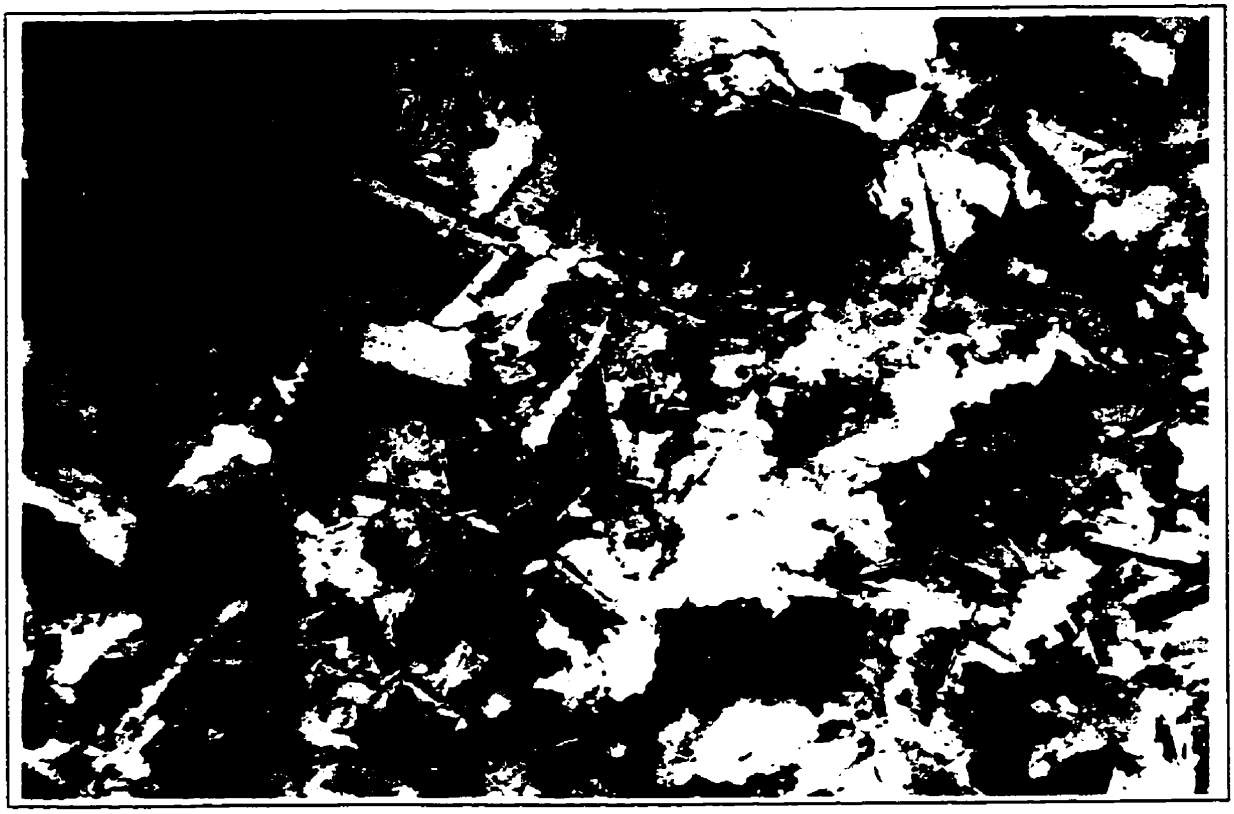

Figure 4.3

Figure 4.4 - Photograph of "Stwk Cb-Qz-Py(Po)±Ab-Au" vein ore type in albitite dikes at lower mine levels. Mineralization is overprinted by chlorite stockwork veins and penetratively deformed by a steeply, northeast-dipping schistosity (to the right). Note that in spite of the ductile deformation, the brittle character of the ore structures is well preserved (see details on Figure 4.5). Disseminated sulfides consist essentially of pyrrhotite with minor pyrite.

Ore drift 6446, lower "C" zone, Kiena Mine level 64.

Photographie du minerai de type "Stwk Cb-Qz-Po(Py)±Ab-Au" affectant les albitites des niveaux inférieurs de la mine. Les veines minéralisées sont recoupées par des veines de chlorite, puis déformées pénétrativement par une schistosité à pendage nord-est (vers la droite). Cependant, en dépit de cette déformation à caractère ductile, l'on peut aisément identifier plusieurs embranchements de veines minéralisées qui confèrent un caractère fragile à la minéralisation (voir la Figure 4.5). La pyrrhotine forme la majeure partie des sulfures disséminés, le reste étant de la pyrite.

Galerie à minerai, zone "C" inférieure, niveau 64 Mine Kiena.

Figure 4.5 - Photograph of a polished rock slab of "Stwk Cb-Qz-Py(Po)±Ab-Au" vein ore type from the outcrop shown on Figure 4.4, exhibiting well-preserved breccia-infill textures. Sharp-angular albitite dike fragments are set in a carbonate-quartz vein matrix and form a mosaic breccia. Note the "stringy" appearance of disseminated pyrrhotite (Po) and pyrite (Py), and the smaller stockwork vein at the bottom of the photograph deformed by a fold and quartz extension veinlets along strike.

Sample K92-6446-218, lower "C" zone, Kiena Mine level 64.

Photographie de la surface polie d'un échantillon de minerai de type "Stwk Cb-Qz-Py(Po)±Ab-Au" provenant de l'affleurement montré à la Figure 4.4, exhibant l'excellent degré de préservation de la texture de remplissage en fracture ouverte d'une veine minéralisée. La matrice filonienne de carbonate et quartz renferme des fragments très angulaires de dyke d'albitite formant une brèche de type "mosaique". Remarquez l'aspect "effiloché" des grains disséminés de pyrrhotine (Po) et de pyrite (Py), ainsi que le pli et les veinules d'extension de quartz (Qz) dont est affectée la veinule en stockwork apparaissant au bas de la photo.

Échantillon K92-6446-218, zone "C" inférieure, niveau 64 Mine Kiena.

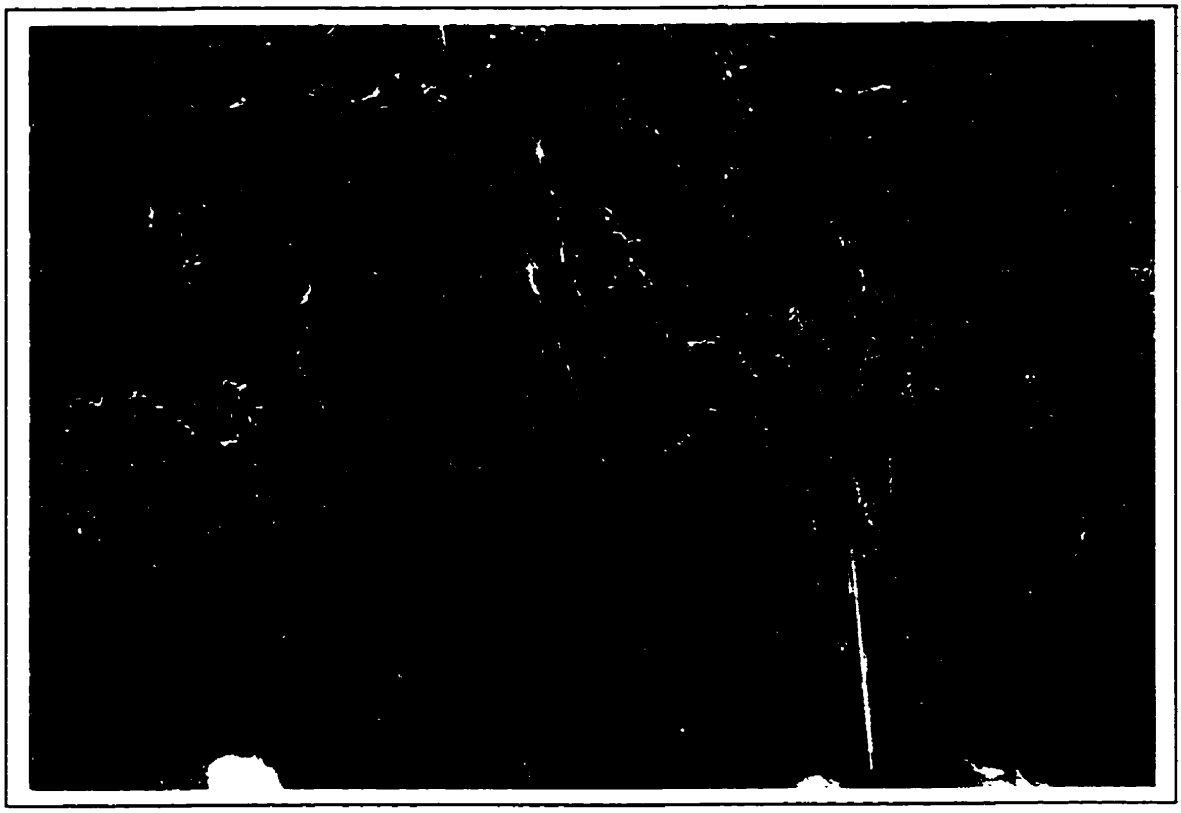

Figure 4.4

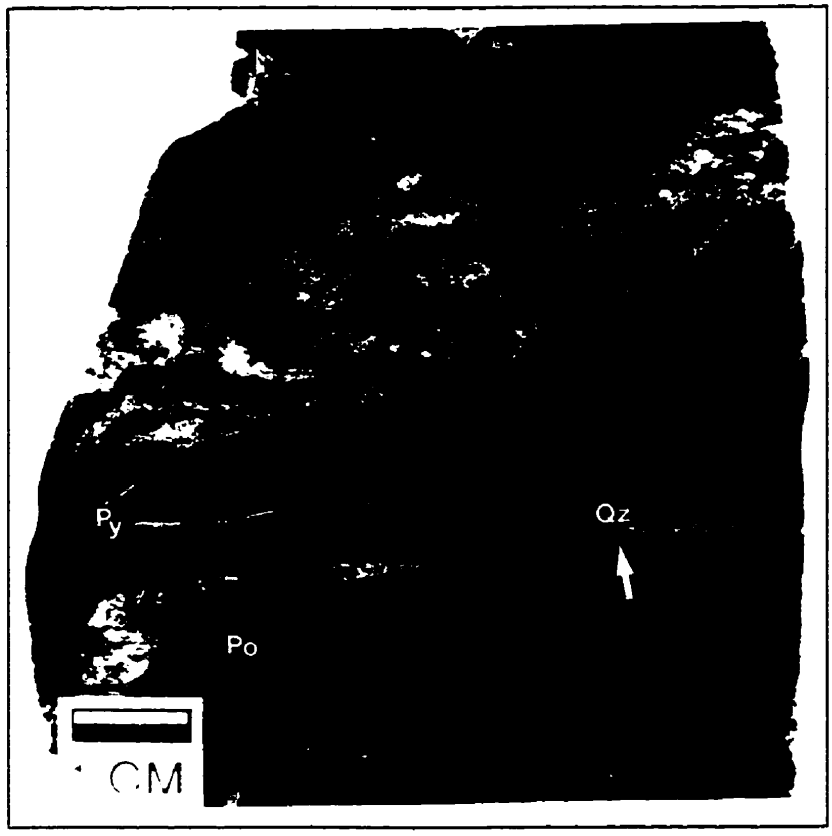

Figure 4.5

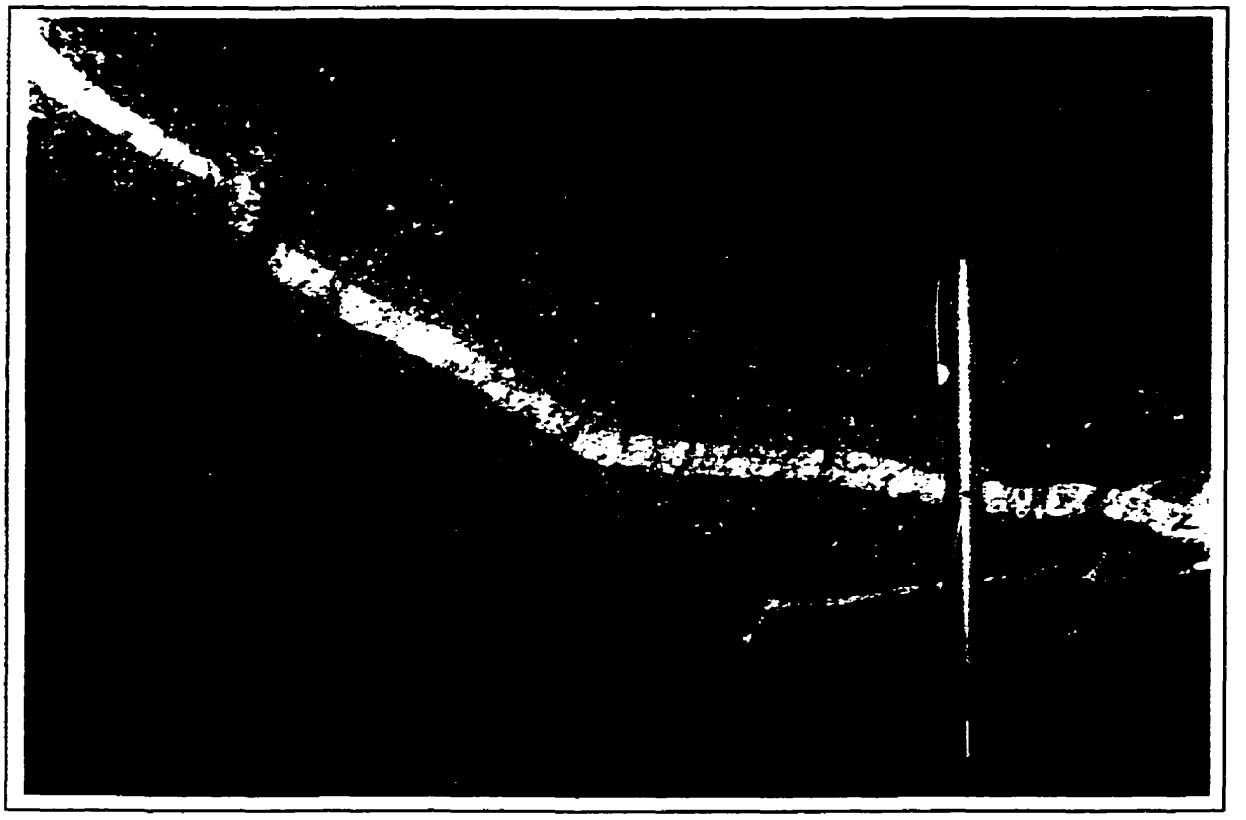

Figure 4.6 - Photograph of a carbonate-quartz stockwork vein from the outcrop of "Stwk Cb-Qz-Py(Po)±Ab-Au" vein ore type shown on **Figure 4.1.** *The vein is sub-parallel to the deposit's main schistosity (S_n). It is characterized by the overprint of quartz extension veinlets onto a pre-existing crustiform infill-vein texture (inner quartz, outer carbonate). The opening vector is in the same direction as the shortening vector, precluding the formation of the open-space stockwork vein during penetrative deformation (see also* **Figure 5.4**). *The arrow is pointing to a quartz extension veins.*

Access to ore drift 3838, "C" zone, Kiena Mine level 38.

Photographie d'une veine de carbonate-quartz en stockwork provenant de l'affleurement de minerai de type "Stwk Cb-Qz-Py(Po)±Ab-Au" montré à la Figure 4.1. La veine est sub-parallèle à la schistosité principale du gisement (S_n). Elle est charactérisée par la superposition d'une série de veinules d'extension à quartz sur une texture de remplissage pré-existante de type crustiforme (quartz au coeur, carbonate en bordure). Puisque le vecteur d'ouverture de la veine a la même orientation que le vecteur d'applatissement de la veine, cela suggère que la veine en stockwork à texture de remplissage en fracture ouverte ne peut s'être formée pendant la déformation (se référer également à la **Figure 5.4**). *La flèche pointe en direction d'une veinule d'extension.*

Galerie d'accès du chantier 3838, zone "C", niveau 38 Mine Kiena.

Table 4.2 Characterization of main-stage gold mineralization at the Kiena Mine

ORE TYPES	"STWK Cb-Qz-Py-(Po) ± Ab-Au"	"BRECCIA 1 "	" BRECCIA 2 "
RELATIVE TIME SEQUENCE	1 st mineralizing event	2 nd mineralizing event	3 rd mineralizing event
LOCATION AND DISTRIBUTION	Throughout the mine upper levels: "J", "K", "L", and "C" ore Zones lower levels: lower "C" ore Zone	Erraticaly distributed within, and at the margins of, the high-grade S-50 zone. Restricted to upper mine levels: "A", "D", and "B" Zones	Centered on, and most abundant within, the core of the S-50 Zone or "A" Zone Restricted to upper mine levels: "A", "D", and "B" Zones
VEIN TYPE	Stockwork breccia veins (0.2-2.0 cm)	Buff-beige replacement veins (0.5-5.0 m)	Stockwork breccia veins and massive breccia body (0.5-30 m)
INFILL-TEXTURE	Open-space filling 1. Crustiform veinlets: 1.1 outer zone of comb- textured carbonate 1.2 inner quartz 2. Monolithic, sharp-angular, mosaic breccia	"Pseudo-breccia" 1. Microfracture-controlled, metasomatic replacement front	Open-space filling 1. Monolithic, sharp-angular, mosaic to mottled breccias* 2. Cockade: breccia fragments rimmed by crustiform albite
MINERAL PARAGENESIS (In order of abundance)	Carbonate (ferroan dolomite) Albite Pyrite (Pyrrhotite) Quartz Native gold *Pyrite:* Abundant in upper mine levels (down to a depth of 500 m), 3-10 % small to medium-grained, disseminated along vein selvages, highly irregular crystal forms, partly recrystallized. *Pyrrhotite:* Abundant at lower mine levels, 5-10% at vein selvages, highly strained along S_2.	Ankerite Pyrite (Gold) *Pyrite:* Restricted to upper mine levels (down to a depth of 410 m), 10-15% very fine-grained, disseminated along vein selvages, highly irregular crystal forms, partly recrystallized, some carbonate-filled pressure shadows.	Albite Pyrite Chalcopyrite Scheelite Native gold Trace[1]: galena, pentlandite, sphalerite Rare[1]: tourmaline, cobaltite, asenopyrite *Pyrite:* Common down to a depth of 410 m but occurs down to 600 m, 2-8% coarse poikiloblastic crystals, idiomorphic to xenomorphic, commonly fractured, disseminated in albite vein matrix to breccia. Au : Ag = 85 : 15 [1] Muir (1981)
FRACTURE ORIENTATION	95% sub-parallel to cleavage N 240-260 30-50 NW 5% at high angle to cleavage N180-190 75-85W	N 275-290 35-40NE	Stockwork breccia veins: N 272 60N Breccia body: N180-190 30-45 NW (long axis)
HYDROTHERMAL VEIN ALTERATION OVERPRINT	← Upper Mine Levels: chlorite-biotite-magnetite-(stilpnomelane) stringer veins → ← Lower Mine Levels: → chlorite veins		
DEFORMATION STRAIN	**Post-ore** 1. Flattening of stockwork veins: folds, boudins 2. Overprinted by carbonate or quartz tension veins 3. Overprinted by deposit's main schistosity and crenulation cleavage 4. Cut by oblique-slip faults	**Post-ore** 1. Overprinted by deposit's main schistosity: gneissic to schistose 2. Carbonate-filled pressure shadows to pyrite 3. Cut by oblique-slip faults	**Post-ore** 1. NNW-plunging, Z-shaped fold 2. Overprinted by deposit's main schistosity: wavy, irregular spaced cleavage 3. Cut by oblique-slip faults
GOLD-GRADE	$0.34 \leq x \leq 5.0$ g/t	$5 \leq x \leq 12$ g/t	$5 \leq x \leq 25$ g/t

* *Descriptive terminology of breccias after Laznicka (1988)*

veins, which remained unaffected by the buff-colour replacement veins, were originally interpreted as breccia fragments by mine geologists (see **Figure 4.8**). Although, these are more appropriately designated as "pseudo-fragments" incorporated in carbonate-pyrite replacement veins, the term "Breccia 1" was retained to avoid confusion with the ore terminology previously introduced at Kiena.

This ore type is not as common or as widespread as the "Stwk Cb-Qz-Py(Po)±Ab-Au" vein ore type, but it is the most conspicuous type of mineralization to occur in the mine due to its pronounced buff-beige colour and its high pyrite content (up to 15 %). Because these replacement veins were mapped as breccias prior to this study and were not distinguished from the true albite-cemented breccias which overprint them, their distribution is not fully known. However, this mapping of the "Breccia 1" ore type reveals that ankerite-pyrite-Au replacement veins are restricted to the breccia body of the S-50 zone and confined to the upper part of the orebody (down to a depth of 410 m). They form irregular veins, with either sharp (**Figure 4.7**) or diffuse (**Figure 4.8**) contacts, blanketing the "Stwk Cb-Qz-Py(Po)±Ab-Au" vein ore type. The alteration is most intense in the core of the deposit (**Figure 4.10**) and more diffuse on the margins of the S-50 zone (**Figure 4.8**). Although this ore type has a massive appearance, the study of polished rock specimens and thin section reveals that it consists of numerous microfractures filled with ankerite and strings of pyrite grains (**Figures 4.9** and **4.11**). Gold grades in the Breccia 1 ore type range between 4.5 and 12 g/t Au. These grades are similar to those reported for the high-grade "Stwk Cb-Qz-Py(Po)±Ab-Au" vein ore type found at lower mine levels, but in sharp contrast with gold grades of 3-5 g/t Au for the lower-grade stockwork vein mineralization in contact with Breccia 1 ore. In thin section, ankerite-pyrite replacement veins are characterized by a granoblastic assemblage composed of microcrystalline albite, coarser albites with highly serrated grain boundaries, hypidiomorphic ankerite with sweeping undular extinction patterns, and partially recrystallized poikiloblastic pyrite.

Breccia 1 ore is overprinted by stockwork veins and breccias of the Breccia 2 ore type,

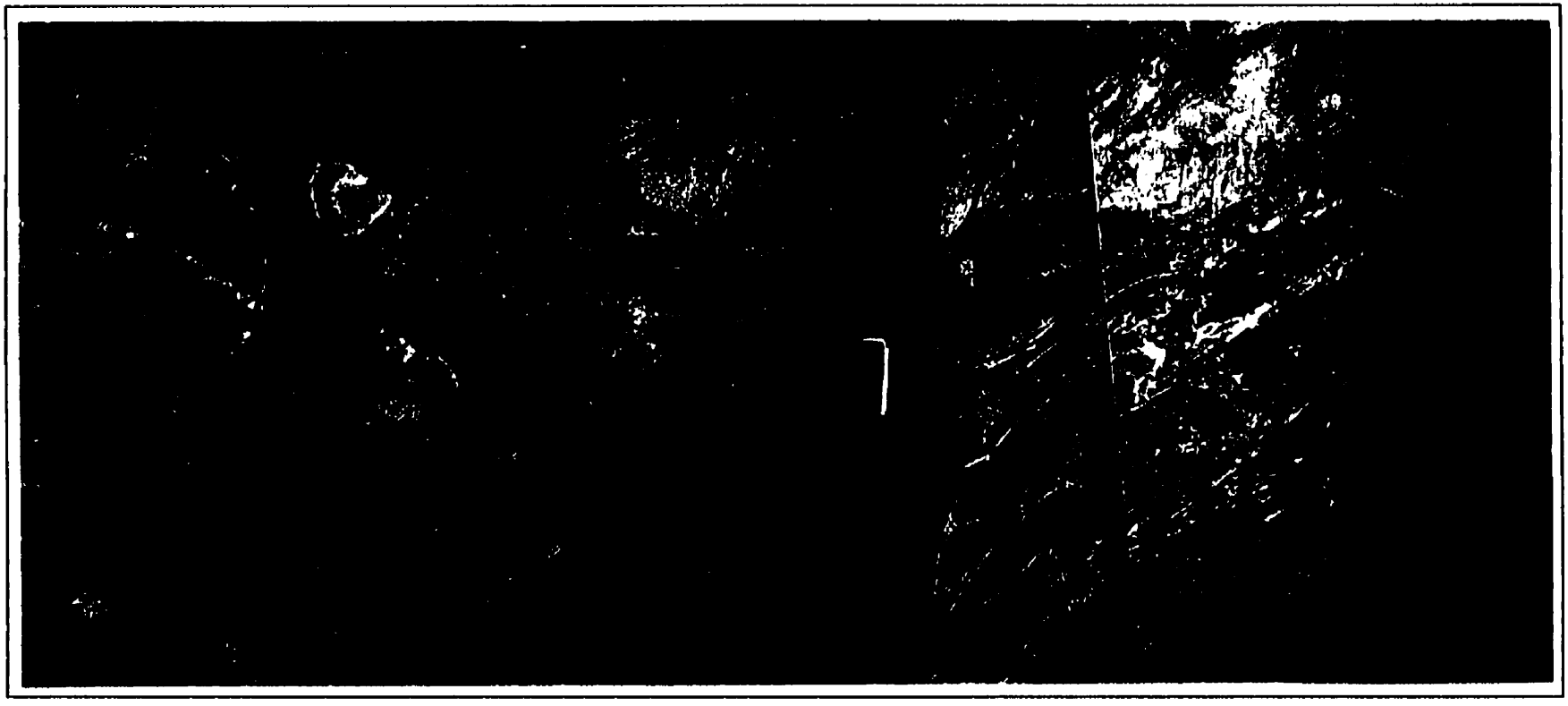

Figure 4.7 - *Mosaic of photographs showing the overprint of Breccia 1 ore type onto the Stwk Cb-Qz-Py(Po)±Ab-Au vein ore type. Mineralization is somewhat diffuse exhibiting a patchwork of buff-beige carbonate-pyrite-Au alteration of different intensities. Through-going schistosity (stippled line) post-dates both Stwk Cb-Qz-Py(Po)±Ab-Au and Breccia 1 ore types.*

Junction of "B" and "C" ore zones, ore drift 3838, Kiena Mine level 38.

Collage photographique illustrant l'empreinte du minerai de type "Breccia 1" sur le minerai de type "Stwk Cb-Qz-Py(Po)±Ab-Au". Le caractère de la minéralisation est diffus et l'affleurement montre des zones d'altération de couleur brun-beige d'intensité différentes. La schistosité (ligne pointillée) recoupe, et donc post-date, les minerais de type "Stwk Cb-Qz-PyP(o)±Ab-Au" et "Breccia 1".

Jonction des zones "B" et "C", galerie à minerai 3838, niveau 38 Mine Kiena.

Figure 4.8 - Mosaic of photographs showing the "pseudo-breccia" character of the Breccia 1 ore type. The "pseudo-fragment" highlighted by the hammer represents a zone of albite-rich rock mineralized by carbonate-pyrite-albite-Au stockwork veins that remains unaffected by the carbonate-pyrite hydrothermal alteration. Replacement veins are cut by pegmatitic veins (arrows). Mineralization and late-stage pegmatitic veins are penetratively deformed by the deposit's main schistosity (S_n, dashed line).

Ore drift 3838, "C" zone, Kiena Mine level 38.

Collage photographique montrant le caractère "pseudo-bréchique" du minerai de type "Breccia 1". Le large "pseudo-fragment" situé sous le marteau, représente une zone minéralisée par des veins de carbonate-quartz en stockwork, qui fut épargnée par le front d'altération hydrothermale à carbonate-pyrite. Les veines de remplacement sont recoupées localement par des veines pegmatitiques (flèches). La minéralisation ainsi que les veines pegmatitiques sont déformées par la schistosité principale du gisement (S_n, ligne pointillée).

Galerie à minerai 3838, zone "C", niveau 38 Mine Kiena.

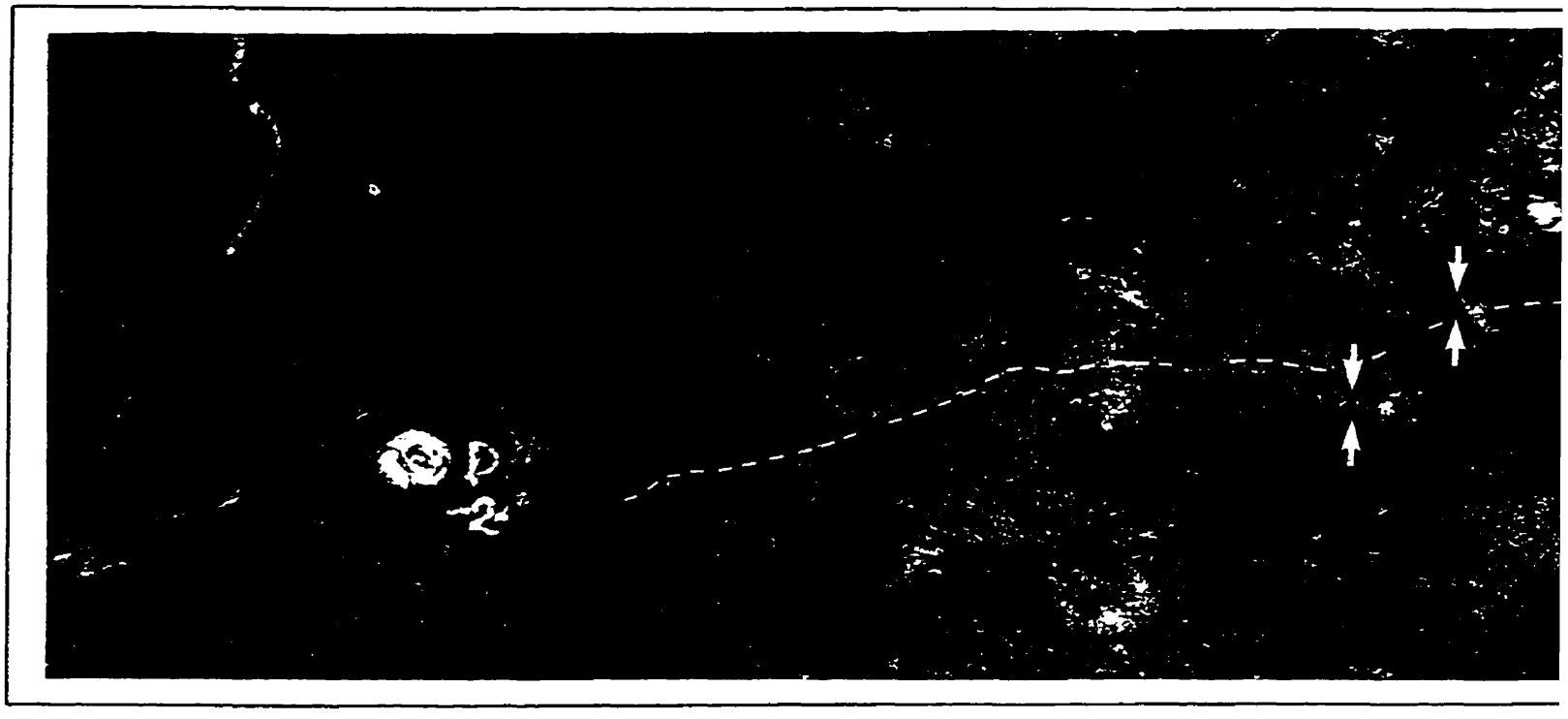

Figure 4.8

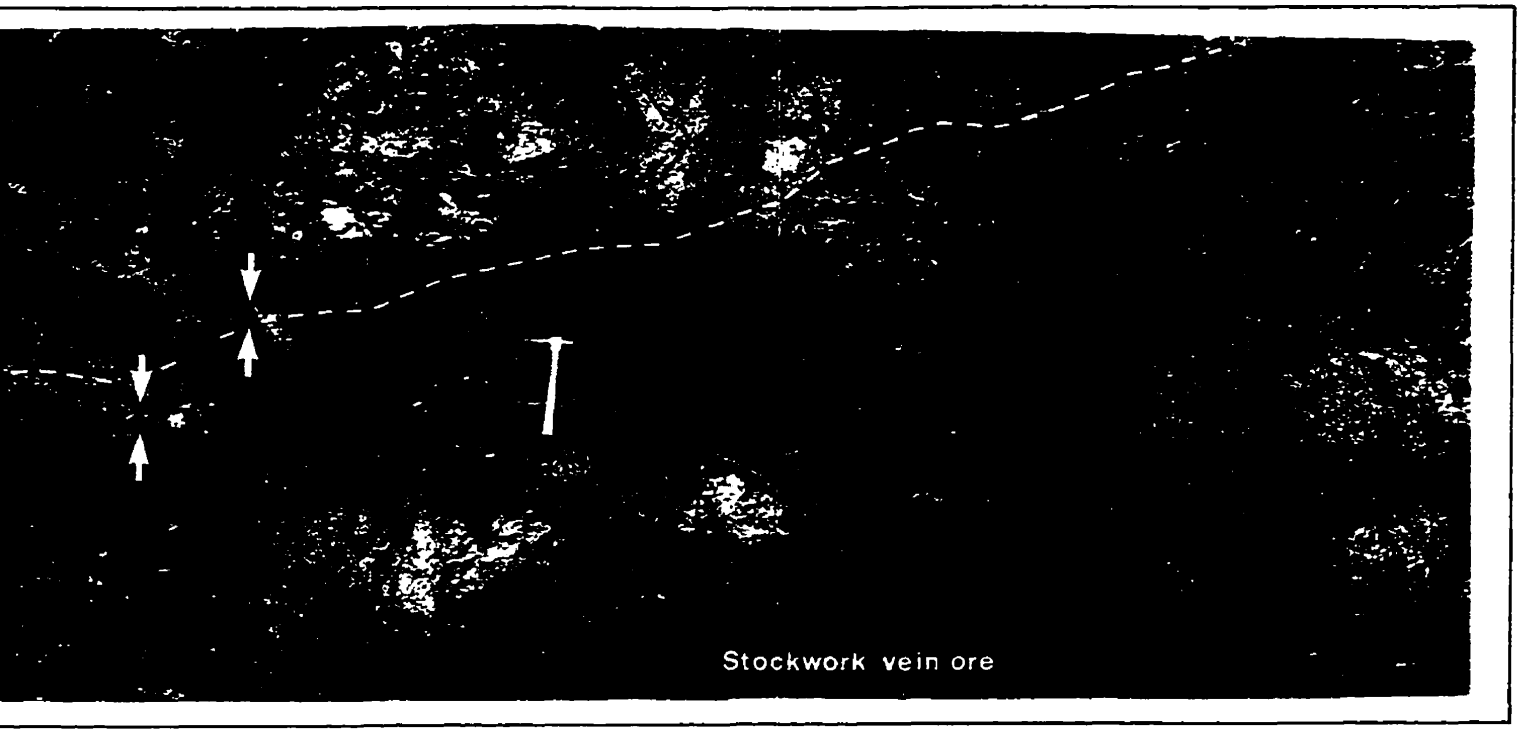

Figure 4.8

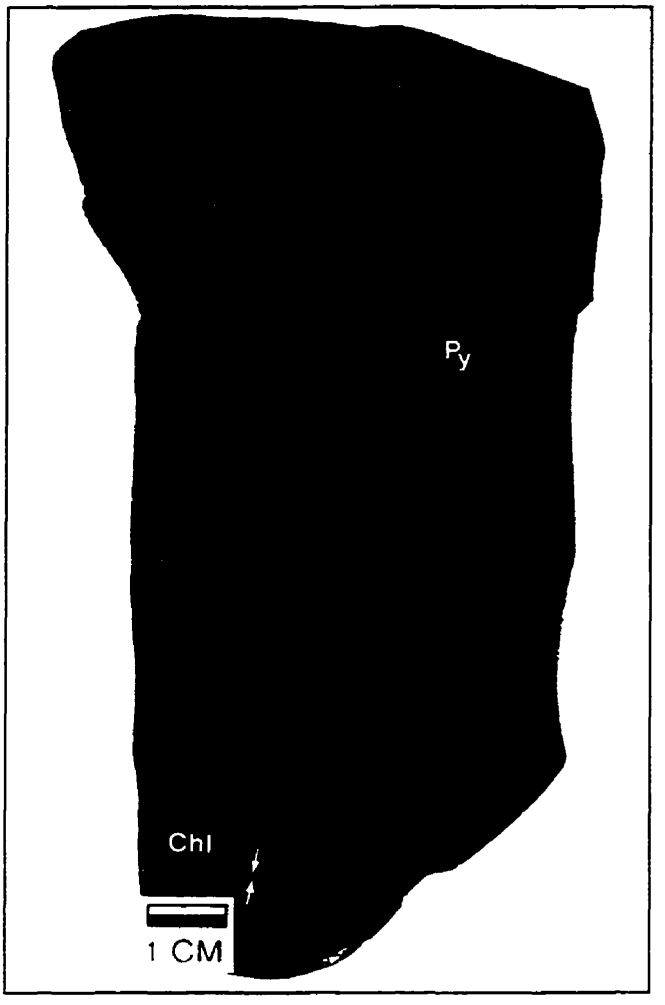

Figure 4.9 - Photograph of a polished hand specimen from the outcrop shown on ***Figure 4.7****. Microfracture-controlled carbonate-pyrite alteration of the "Breccia 1 ore type is defined by carbonate veins and linear arrays of fine-grained pyrite (Py). The ore is cut by chlorite stringer veins (Chl) and overprinted by the deposit's main schistosity (see* ***Figure 4.7****). In this exemple of "Breccia 1" ore type, post-ore deformation is illustrated by a moderate gneissosity defined by the alternation of elongated and partly recrystallized pyrite grains and carbonate veins.*

Sample K91-3838-094, Junction of "B" and "C" ore zones, Kiena Mine level 38.

Photo d'un échantillon de minerai de type "Breccia 1" provenant de l'affleurement montré à la ***Figure 4.7****. L'altération en carbonate-pyrite du dit minerai est contrôlé par un système de microfractures, lequel est illustré par la présence de veinules de carbonate ainsi que par la distribution "en chapelet" de petits grains de pyrite (Py). Le minerai est recoupé par des veinules réticulées de chlorite (Chl), puis découpé par la schistosité principale du gisement (voir* ***Figure 4.7****). Dans ce spécimen de minerai de type "Breccia 1" la déformation du minerai s'exprime par le développement d'une gneissosité, laquelle est marquée par une alternance entre "chapelets" de grains de pyrite déformés et partiellement recrystallisés et veinlules de carbonate.*

Échantillon K91-3838-094, Jonction des zones "B" et "C", niveau 38 Mine Kiena.

Figure 4.10 - Photograph of the Breccia 1 ore type cut by albite-pyrite stockwork veins of the Breccia 2 ore type. The fine black lines observed throughout the outcrop are biotite-chlorite stringer veins overprinting the ore (see details on Figure 4.19).

Ore drift 3025, "D" zone, Kiena Mine level 30.

Photographie du minerai de type "Breccia 1" recoupé par des veinules d'albite-pyrite du minerai de type "Breccia 2". Le réseau de fines lignes noires que l'on observe sur cet affleurement sont des veinules réticulées de biotite-chlorite recoupant le minerai(voir les détails à la Figure 4.19).

Galerie à minerai 3025, zone "D", niveau 30 Mine Kiena.

Figure 4.11 - Photomicrograph of the sample of Breccia 1 ore type represented on Figure 4.9 showing carbonate-pyrite veinlets clearly overprinting a pre-existing microcrystalline albite assemblage. Pyrite crystals are partly recrystallized and contain albite and carbonate inclusions.

Sample K91-3838-094, "C" zone, transmitted light, crossed polars. Kiena Mine level 38.

Microphotographie de l'échantillon de minerai de type "Breccia 1" représenté à la Figure 4.9, montrant des veinules à carbonate-pyrite recoupant un assemblage d'albite microgrenue. Les grains de pyrite sont partiellement recristallisés et renferment des inclusions de carbonate et pyrite.

Échantillon K91-3838-094, zone "C", lumière transmise, nicols croisés. Niveau 38 Mine Kiena.

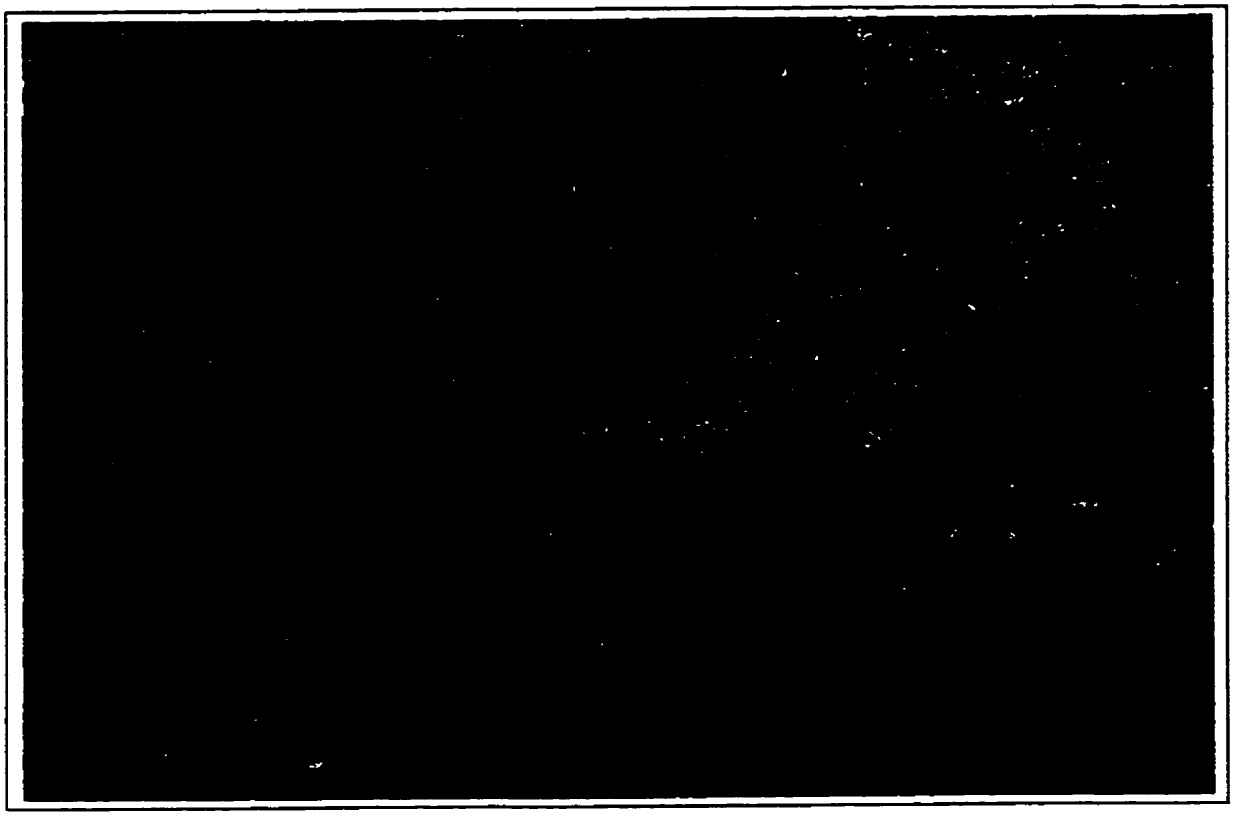

Figure 4.10

Figure 4.11

pegmatitic veins, and late-stage phyllosilicate vein alterations (**Figures 4.8** and **4.10, Table 4.1**)). As is the case for the first ore type, auriferous carbonate-pyrite replacement veins are penetratively deformed by the deposit's main schistosity (e.g. **Figure 4.7**). The main characteristics of Kiena's Breccia 1 ore type are summarized in **Table 4.2.**

4.2.2.3 Abite-pyrite±chalcopyrite-scheelite-Au stockwork veins and breccias alteration (Breccia 2 ore type)

Albite-cemented breccias and stockwork veins form the third mineralization stage in the mine's alteration sequence. They overprint the ankerite-pyrite-Au replacement veins of the "Breccia 1" ore type (**Figures 4.10** and **4.19**) and are overprinted, in turn, by gold-bearing pegmatitic veins (**Figure 4.17**). Albite veins and breccias containing disseminated pyrite, lesser chalcopyrite and scheelite, and traces of galena, pentlandite and sphalerite[2], are referred to as the "Breccia 2" ore type.

Breccia 2 ore occupies the core of the deposit and forms the bulk of the high-grade ore recovered from the S-50 zone between mine levels 17 and 62 (see **Figures 3.2** and **4.22**), with grades ranging between 5-25 g/t Au (see sections **12438.4 N** and **12514.6 N** in back pocket). It is predominantly hosted by albitite dikes and iron tholeiite adjacent to the dikes (e.g. 33 Level Map, back pocket) and, not surprisingly, Breccia 2 ore and albitite dikes have similar compositions (samples K92-3025-238 and K92-4313-253, Table C.13 and Tables C.5 and C.6, **Appendix C**). Mapping of the breccia body of the S-50 zone at levels 41 and 43 (see schematic plan maps in back pocket) reveals that it is zoned and consists of a massive zone of mottled breccia at the southwestern end of the "B" zone (**Figures 4.12**), grading to a zone of sharp-angular mosaic breccias associated with stockwork veins (**Figure 4.13**), through to a swarm of stockwork breccia veins at the northeastern end of the "B" zone

---

[2] The occurrence of scheelite in the ore was not reported prior to this study. As for galena, pentlandite and sphalerite they were reported by Muir (1979) in a petrographic study of drill core samples from the S-50 Zone .

(**Figure 3.7**). Accordingly, gold grades at the southern end of the "B" zone are higher that those recovered at the northern tip. The decrease in the intensity of hydrothermal alteration and fracturing, associated with the falling off of ore grades away from the mottled breccia, suggests the presence of a hydrothermal gradient along the strike-length of the "B" zone. Breccias and stockwork breccia veins contain pervasively albite-altered rock fragments (light grey, **Figures 4.12** and **4.13**) and carbonate-pyrite-altered rock fragments (buff-beige, **Figures 4.10** and **4.19**), cemented by albite, disseminated sulfides and minor scheelite. Mottled breccia rock fragments have diffuse margins and are not easily distinguished from the albite vein matrix (**Figure 4.15**). Albite breccia veins locally display cockade-infill textures, such as represented on **Figure 4.14**. In thin section, Breccia 2 ore is characterized by a crudely foliated assemblage of platy albite grains with serrated edges, with interstitial carbonate and coarse-grained pyrite (**Figure 4.16**). Pyrite textures range from elongated and irregular-shaped partially recrystallized grains with albite and carbonate inclusions (**Figures 4.15** and **4.16**), to almost equant poikiloblastic crystals (**Figure 4.14 B**). Most of the gold contained in Breccia 2 ore occurs as free-milling, disseminated grains in the albite vein matrix, and the remainder (10%) as micro-inclusions in the pyrite (Muir, 1981).

As in the case of the "Stwk Cb-Qz-Py(Po)±Ab-Au" vein ore type, the absence of rock flour or gouge in the matrix of the breccia, the lack of apparent movement between rock fragments, and the progressive change from true breccia to stockwork veins, rule out any fault movement or explosion mechanism as the cause of brecciation. Instead, open-space infill-vein textures and the decrease in fracturing away from the mottled breccias suggest that Kiena's Breccia 2 ore formed as a result of brecciation under conditions appropriate for ore fluid pressure to exceed lithostatic pressure and the tensile stress of the rocks (e.g. Phillips, (1972; 1973)).

Breccia 2 ore is cut by pegmatitic veins, intermineral dikes, and late-stage phyllosilicate veins (**Figures 4.18, 3.27, 3.28** and **4.19**; **Table 4.1**). Subsequently, the rigid body of Breccia 2 ore was penetratively deformed by the deposit's main schistosity (**Figure 4.17**, Chapter 5). A summary of the characteristics of Kiena's Breccia 2 ore type is presented in **Table 4.2**.

Figure 4.12 - Photograph of a "mottled" breccia of the Breccia 2 ore type showing mineralized fragments of albitite cemented by an albite vein matrix with disseminated pyrite. The margins of the fragments are diffuse and are not easily distinguished from the vein matrix.

Ore drift 4313, "B" zone, Kiena Mine level 43.

Photographie du minerai de type "Breccia 2" à caractère "nébuleux" (mottled) montrant des fragments d'albitite cimentés par de l'albite filonienne et de la pyrite disséminée. Le contour diffus des fragments les rend difficile à distinguer de la matrice d'albite.

Galerie à minerai 4313, zone "B", niveau 43 Mine Kiena.

Figure 4.13 - Photograph of a mosaic breccia of the Breccia 2 ore type showing an array of sharp-angular fragments of albitite cemented and replaced by an albite vein matrix with disseminated pyrite and chalcopyrite. The breccia is without rock flour or gouge and the fragments show no sign of rotation.

Ore drift 4117, "B" zone, Kiena Mine level 41.

Photographie du minerai de type "Breccia 2" montrant une brèche à texture de mosaique renfermant des fragments anguleux d'albitite à la fois cimentés et remplacés par de l'albite filonienne. Les fragments de la brèche ne semblent pas avoir subit de rotation; la brèche elle-même ne renferme aucune farine de roche et ses contacts ne montrent aucune boue de faille.

Galerie à minerai 4117, zone "B", niveau 41 Mine Kiena.

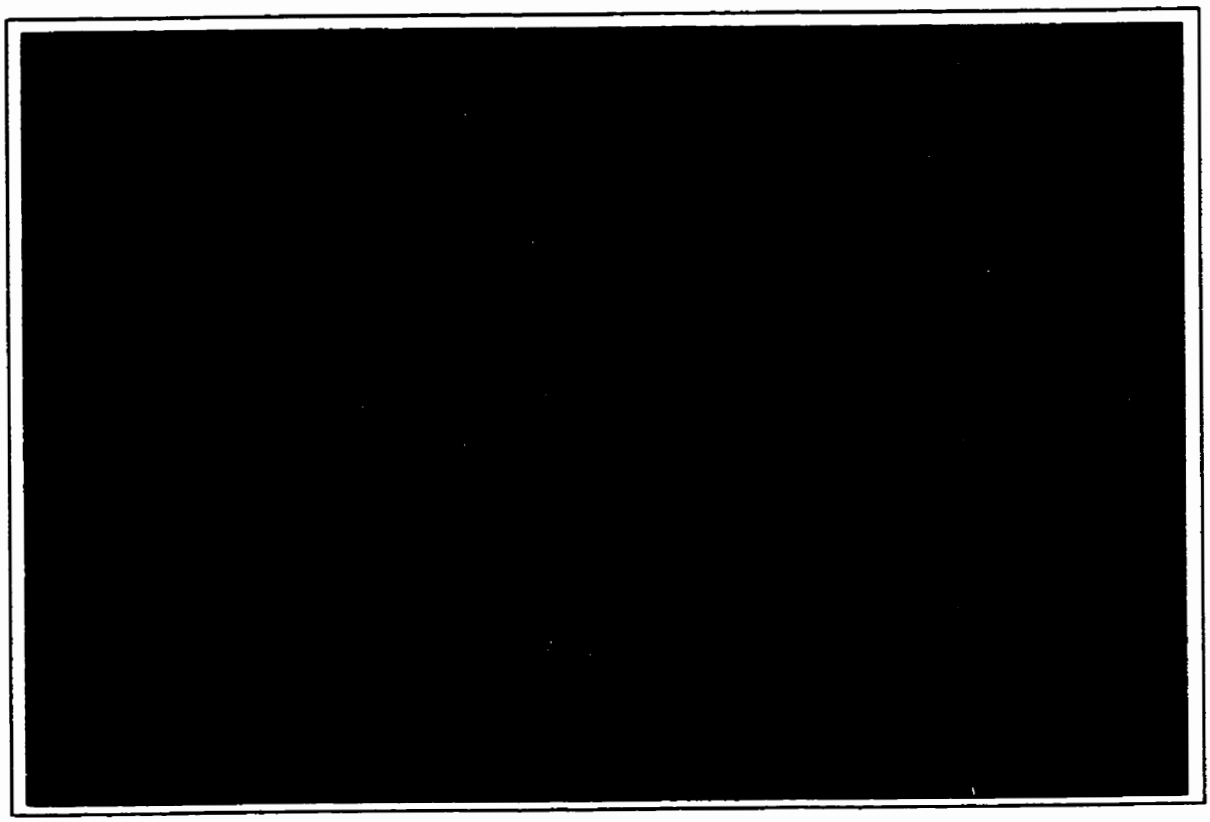

Figure 4.12

Figure 4.13

Figure 4.14 A - *Photograph of a polished hand specimen of Breccia 2 ore showing an exceptionally well preserved, cockake vein-infill texture. Mineralized, sharp-angular fragments are rimmed by crustiform albite crystals. Notice the mottled appearance of the wall-rock in contact with the vein caused by the selective replacement of the rock by stockwork vein albite.*

B - *Detail of Figure 4.14 A.*

Sample K90-4116-050, ore drift 4116, Kiena Mine level 41.

A - *Photographie de la surface polie d'un échantillon de minerai de type "Breccia 2" montrant une texture de remplissage en cocarde magnifiquement bien préservée. Les fragments minéralisés sont angulaires et sont décorés de cristaux d'albite crustiformes. Remarquez l'aspect bigarré de la roche située aux épontes de la veine, causé par le remplacement sélectif de l'albite filonienne.*

B - *Vue détaillée de la Figure 4.14 A.*

Échantillon K90-4116-050, galerie à minerai 4116, niveau 41 Mine Kiena.

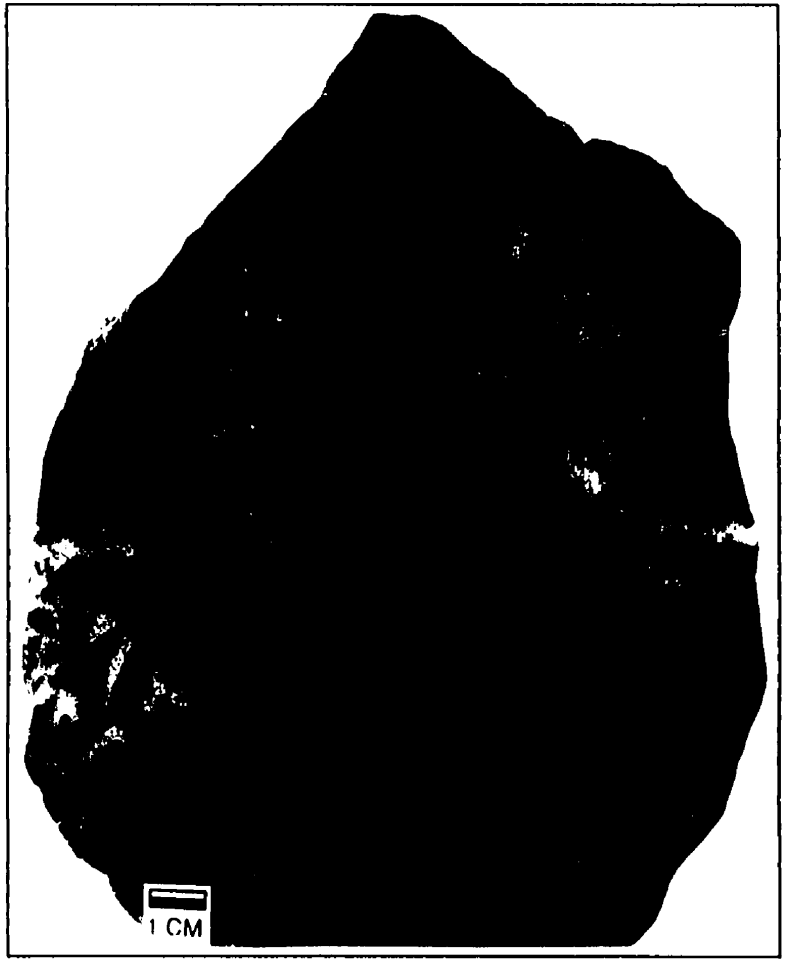

Figure 4.14 A

Figure 4.14 B

Figure 4.15 - *Photograph of a polished rock slab of mottled breccia of the Breccia 2 ore type showing a brecciated rock characterized by highly irregular and deformed rock fragments almost entirely replaced by hydrothermal vein albite (An_{0-1}). Deformed, fractured and partially recrystallized pyrite grains define a crude and irregular foliation.*

Sample K91-4313-149, ore drift 4313, "B" zone, Kiena Mine level 43.

Photographie de la surface polie d'un échantillon de brèche à caractère "nébuleux" (mottled) du minerai de type "Breccia 2", montrant une brèche charactérisée par des fragments déformés aux contours diffus et très irréguliers, presqu'entièrement remplacés par l'albite filonienne (An_{0-1}). Une faible et très irrégulière foliation se manifeste par l'alignement des grains de pyrite déformés, fracturés et partiellement recrystallisés.

Échantillon K91-4313-149, galerie à minerai 4313, zone "B", niveau 43 Mine Kiena.

Figure 4.16 - *Photomicrograph of the sample of mottled breccia of the Breccia 2 ore type shown on Figure 4.15. The hydrothermal albite (An_{0-1}) assemblage is characterized by poorly twinned, dendritic crystals with highly serrated (sutured) grain boundaries (see arrow). This texture is interpreted as deformation of the high-grade ore by mechanisms of pressure-solution. Partly recrystallized pyrite grains exhibit a poikiloblastic texture. The large grain in the photograph contains a few albite inclusions and has partially engulfed several other albite grains from the vein matrix.*

Sample K91-3413-149, transmitted light, crossed Nicols. Ore drift 4313, "B" zone, Kiena Mine level 43.

Microphotographie d'une section mince d'échantillon de brèche à caractère "nébuleux" (mottled) du minerai de type "Breccia 2" montrée à la Figure 4.15. Des cristaux d'albite de forme dendritique montrant des bordures fortement dentelées (suturées) caractérisent cet assemblage d'albite hydrothermale (An_{0-1}) (voir flèche). Cette texture suggère que le minerai haute teneur a été déformé par processus de pression-dissolution. Les grains de pyrite sont partiellement recristallisés et possèdent une texture poikiloblastique. Le large specimen apparaissant dans la photo renferme quelques inclusions d'albite et est en voie d'assimiler plusieurs autres grains d'albite filonienne.

Échantillon K91-4313-149, microscope à lumière transmise, Nicols croisés. Galerie à minerai 4313, zone "B", niveau 43 Mine Kiena.

Figure 4.15

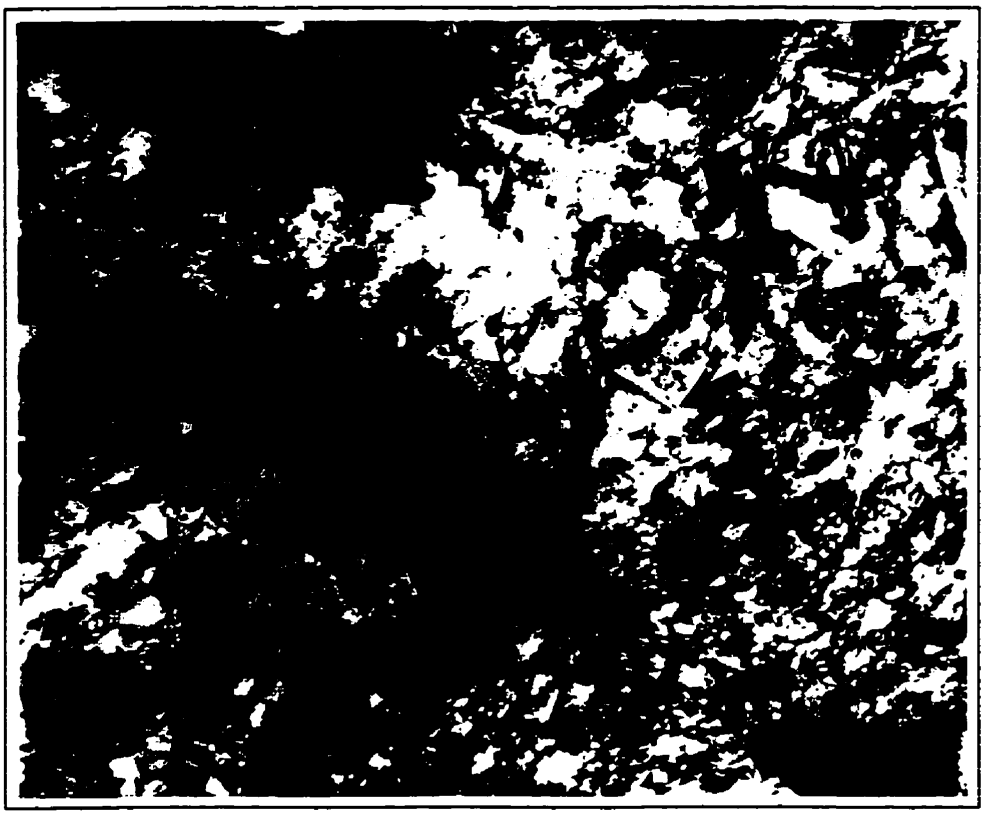

Figure 4.16

4.2.2.4 Coarse-grained quartz-calcite-biotite-albite±tourmaline-pyrite-chalcopyrite-Au vein alteration

Quartz-calcite-biotite-albite veins with lesser tourmaline and pyrite and traces of chalcopyrite and gold were not previously recognized as an alteration facies. They form the last stage of the deposit's main-stage alteration-mineralization sequence because they cut albite-cemented breccias of the Breccia 2 ore type and are overprinted, in turn, by late-stage phyllosilicate veins (**Table 4.1**). The veins are irregular to wavy, coarse-grained (**Figures 4.8, 4.17** and **4.18**) and characterized by open-space crystal growth, as indicated by infill-vein textures such as rosettes of tourmaline needles and large booklets of biotites (**Figure 4.19**). The veins are weakly mineralized, containing up to 3 g/t Au, but their exact time of emplacement is unclear because of the lack of cross-cutting relationships with the intermineral porphyry dikes. However, since the veins do not appear to overprint the dikes, they probably formed after the bulk of gold mineralization and just before the intrusion of the granodiorite and quartz monzonite porphyries.

Main-stage quartz-calcite-biotite-albite±tourmaline-pyrite-chalcopyrite-gold are deformed and overprinted by the deposit's main schistosity (see **Figure 4.8**).

4.2.3 Intermediate-stage alteration facies

4.2.3.1 Pervasive albite alteration of intermineral dikes

Kiena's alteration-mineralization sequence is interrupted by the intrusion of intermineral granodiorite and quartz monzonite porphyry dikes (see section 3.5.3). A pervasive albite alteration predominantly affects the groundmass of the porphyries. It is characterized by an

Figure 4.17 - *Photograph of a massive, mottled breccia of Breccia 2 ore cut by a coarse-grained calcite-biotite-quartz-pyrite vein (arrows). The ore and the vein are deformed by the deposit's main schistosity (S_n).*

Ore drift 2652, "A" zone, Kiena Mine level 27.

Photographie d'une brèche minéralisée de type "Breccia 2" à caractère "nébuleux" (mottled), recoupée par une veine de calcite-biotite-quartz-pyrite à texture grenue (flèches). Le minerai et la veine sont déformés par la schistosité principale du gisement (S_n).

Galerie à minerai 2752, zone "A", niveau 27 Mine Kiena.

Figure 4.18 - *Photograph of the coarse-grained and weakly mineralized vein cutting the carbonate-pyrite replacement vein shown on Figure 4.8. The vein clearly shows a delicate rosette of toumaline needles (arrow), suggesting open-space crystal growth. Both, the ore and the vein, are deformed by the deposit's main schistosity (see Figure 4.8).*

Ore drift 3838, "C" zone, Kiena Mine level 38.

Photo de la veine aurifère à texture grenue recoupant la veine de remplacement à carbonate-pyrite montrée à la Figure 4.8. La veine est charactérisée par une texture de remplissage en fracture ouverte tel que le suggère la présence d'une délicate rosette formée d'aiguilles de tourmaline (flèche). Le minerai, ainsi que la veine faiblement minéralisée, sont tous deux déformés par la schistosité principale du gisement (voir Figure 4.8).

Galerie à minerai 3838, zone "C", niveau 38 Mine Kiena.

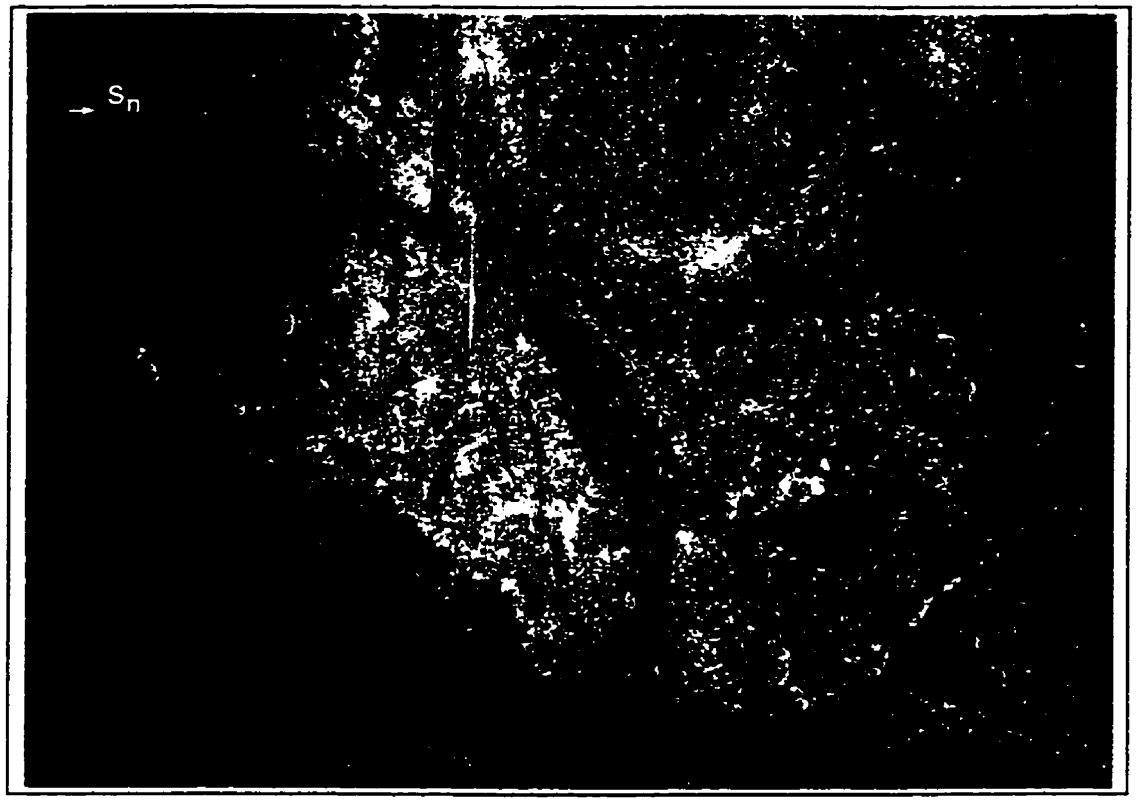

Figure 4.17

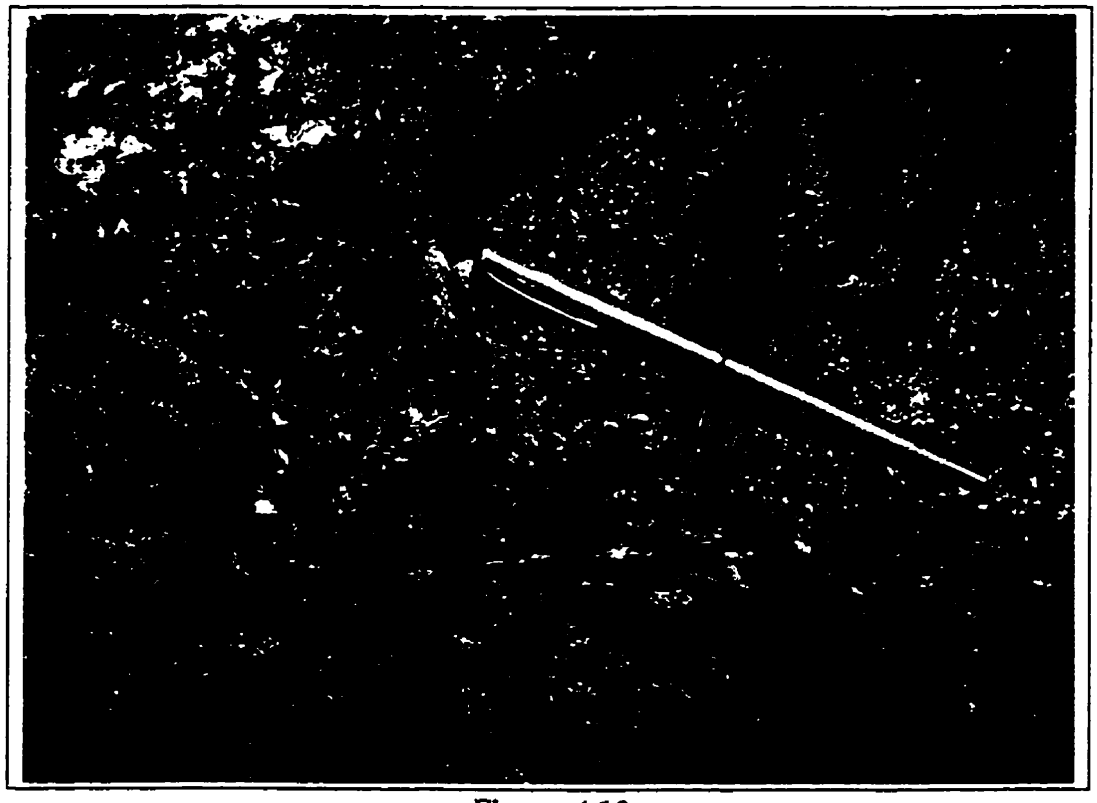

Figure 4.18

assemblage of poorly twinned, microcrystalline albite grains with an An (0-1) composition enclosing feldspar and rare quartz phenocrysts (**Figure 3.33**, A to D, **Appendix F**). Quartz phenocrysts display several large embayments, but both feldspar and quartz phenocrysts show highly corrugated grain margins (**Figures 3.33 B** and **C**) suggesting that hydrothermal albite alteration post-dates the magmatic resorption of the quartz phenocrysts. Based on the preservation of primary porphyritic textures, pervasive albite alteration of the deposit's intermineral dikes is considered less intense than that of albitite dikes (compare Figures 3.25, 3.14 and 3.33).

Albite-altered porphyries are overprinted by intermediate-stage calcite-quartz-pyrite-(Au) stockwork veins and late-stage phyllosilicate vein alteration (**Figures 3.31 D** and **3.32 A** ,**Table 4.1**), and subjected to penetrative deformation (see Chapter 5).

4.2.3.2 Calcite-quartz-pyrite-(Au) stockwork vein alteration

A minor calcite-quartz-pyrite-(Au) stockwork vein alteration forms the second intermediate alteration facies of the deposit's alteration mineralization sequence (**Table 4.1**). The veins are confined to the albitized porphyry dikes and overprinted in turn, by late-stage chlorite-biotite stringer veins (**Figures 3.31** and **3.32**). The veins typically display crustiform infill vein-textures consisting of inner quartz and outer calcite, accompanied by variable amounts of disseminated pyrite (**Figures 3.31 D** and **3.32 A**).

In a previous study, Muir (1981) concluded that Kiena's felsic igneous rocks were barren based on 21 samples of porphyries which contained an average of 9 ppb Au (see Tilling *et al.*, 1973). However, ten samples of porphyry dikes were similarly assayed during this study and returned an average 112 ppb Au per sample (see **Appendix C**). On the basis of these gold values, which are several times above background (70-650 ppb Au versus 3-11 ppb Au, Bourget (1986)), Kiena's intermineral dikes are interpreted as anomalously enriched in gold. The relatively high gold content of the porphyries could be caused by minor gold

remobilization during the emplacement of the felsic dikes across the orebody, however, this interpretation does not explain why samples of granodiorite dike collected away from gold-ore xenoliths or in the deposit's outer gold alteration halo, have returned the highest gold values (140 and 650 ppb Au). Alternatively, minor gold mineralization of the porphyry dikes may be related to intermediate-stage calcite-quartz-pyrite stockwork vein alteration, although gold was not directly observed in the veins.

Calcite-quartz stockwork veins are cut by chlorite-biotite veins and subsequently deformed by the deposit's main schistosity (**Figures 3.32B** and **C**, **Table 4.1**).

4.2.4 Late-stage alteration facies

4.2.4.1 Phyllosilicate vein alterations

Late-stage alteration facies of the Kiena deposit alteration-mineralization sequence consist of a succession of three fracture-controlled phyllosilicate alterations comprised, from the oldest to the youngest, of sericite, biotite-magnetite, and chlorite (**Table 4.1**). Sericite veinlets are confined to the porphyry dikes (**Figure 3.33 A** and **D**) but biotite-magnetite-chlorite veins overprint the entire ore-dike complex and extend to the deposit's outer gold alteration halo.

The biotite-magnetite-chlorite vein system is thus funnel-shaped as the stockwork vein-breccia ore (see **Figure 4.22**) and shows a clear upward and outward zonation that consists, from lower to upper mine levels, of a stockwork of large chlorite veins (1-4 cm wide) overprinting albitite dikes mineralized by the stockwork vein ore type (**Figure 4.4**), flaring upward into a broader network of smaller but more numerous chlorite-biotite-magnetite veins overprinting the breccia body of the S-50 zone and enclosing lower-grade ore shell and outer gold alteration halo (**Figure 4.19**, see also **Figures 3.13** and **6.4**). Accordingly, biotites are more abundant in the upper part of the deposit and gradually disappear with depth (below level 48). They occur as discontinuous arrays of whispy grains associated with clusters of

small disseminated magnetites, and are commonly replaced by chlorite along grain boundaries and cleavage planes (**Figure 4.20**). Late-stage vein biotites are magnesium-rich[3] and characterized by a light-brown to faint yellow pleochroism similar to that of phlogopite. Based on their mode of occurrence and relationship to chlorite, biotite and related magnetite are interpreted as relics of earlier veins later replaced by chlorite. A small amount of pyrite may occur in chlorite veins overprinting the ore (e.g. **Figures 4.4, 4.10** and **4.19**). However, the pyrite's affiliation to previous gold mineralization or chlorite vein alteration remains ambiguous.

The upward-flaring geometry of the chlorite-biotite-magnetite vein system in addition to the predominance of chlorite over biotite at depth, suggests the emplacement of the late chlorite vein alteration by ascending hydrothermal fluids. Chlorite vein alteration is interpreted as the last hydrothermal event in the deposit's alteration-mineralization sequence because it overprints post-porphyry biotite-magnetite vein alteration, and is restricted to the deposit's outer gold alteration halo.

At upper mine levels (down to a depth of 500 metres), chlorite veins are progressively replaced by yellowish-brown stilpnomelane (**Figure 4.22**). It occurs as rosettes of leafy to acicular grains often transgressing chlorite vein selvages into surrounding carbonate. Crystal habit and its confinement to upper mine levels, suggests that stipnomelane is of metamorphic origin.

Late-stage sericite, chlorite-biotite-magnetite veins are deformed by the deposit's main schistosity with various intensity (see Chapter 5).

---

[3] Late-stage vein biotites contain 11-13 wt. % MgO (Appendix F) as opposed to MgO contents of 4-8 wt.% reported for common biotite and 22 wt. % MgO for phlogopite (Deer et al., 1985, p.199).

Figure 4.19 A - Photograph of late-stage phyllosilicate vein alteration at upper mine levels. This polished hand specimen of Breccia 2 ore shows a mosaic breccia composed of sharp-angular fragments of Breccia 1 ore cemented by vein albite, cut by biotite-chlorite-pyrite±stilpnomelane stringer veins. Although the orebody is deformed by a z-shaped fold and its related north-dipping schistosity (S_n,see 27 Level Map in back pocket), the delicate weblike texture of the phyllosilicate veins is preserved by the highly competent Breccia 2 ore.

B - Detail of Figure 4.19 A.

Sample K92-2752-235, "A" zone, Kiena Mine level 27.

A - Photo illustrant l'altération à veines de phyllosilicates aux niveaux supérieurs de la mine. La surface polie de cet échantillon de minerai "Breccia 2" montre une brèche en mosaique composée de fragments angulaires de minerai de type "Breccia 1" cimentés par de l'albite filonienne , recoupée par des veinules réticulées à biotite-chlorite-pyrite±stipnomelane. La délicate texture des veines réticulées est bien préservée au sein de la très compétente brèche à ciment d'albite, en dépit du fait que le corps minéralisé soit déformé par un pli en "z" et sa schistosité de plan axial à pendage nord (S_n, voir le plan niveau 27 en pochette).

B - Vue détaillé de la Figure 4.19 A.

Échantillon K92-2752-235, zone "A", niveau 27 Mine Kiena.

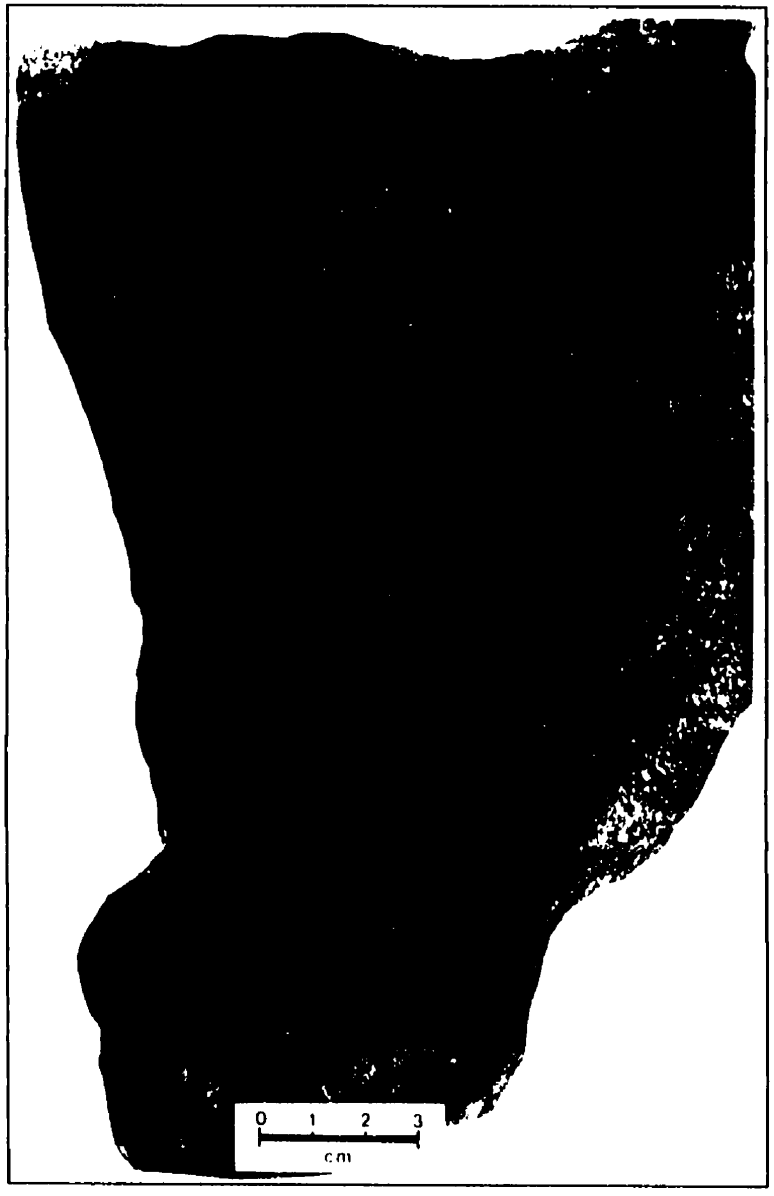

Figure 4.19 A

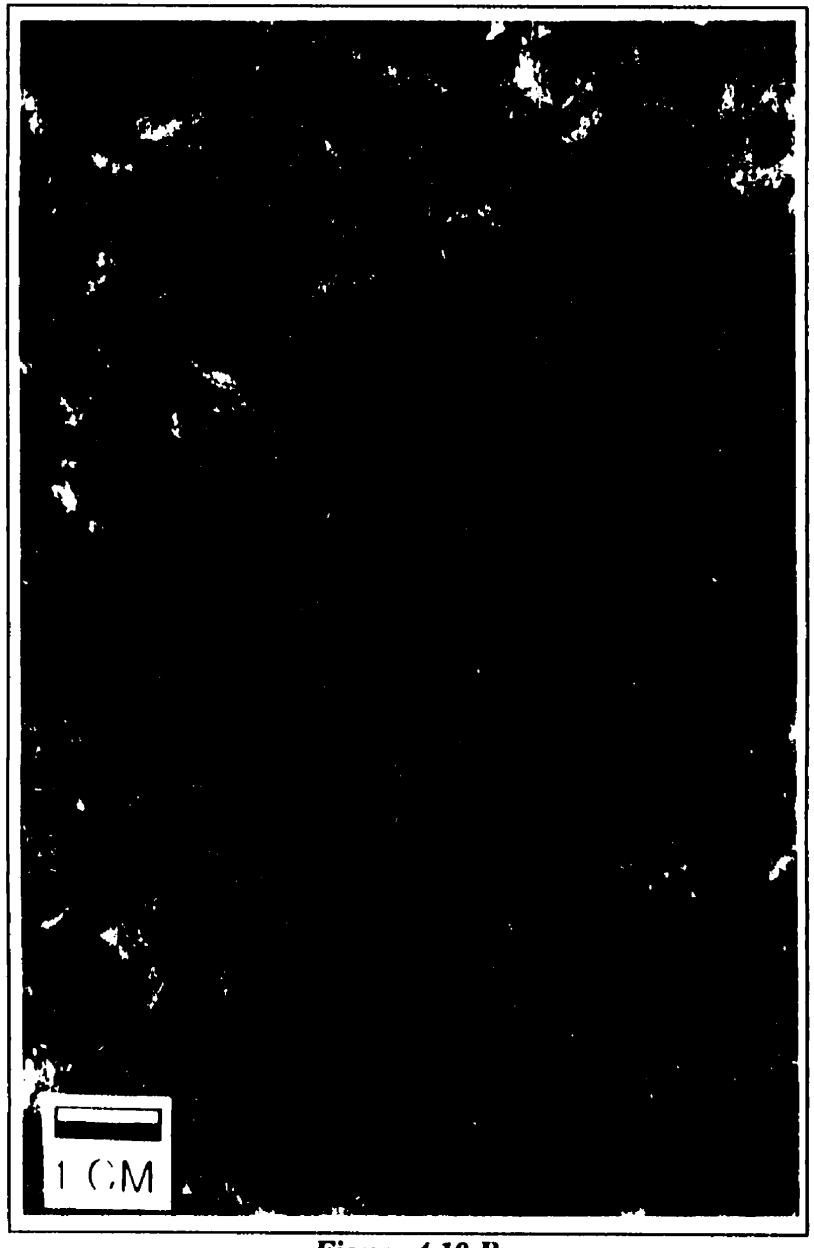

Figure 4.19 B

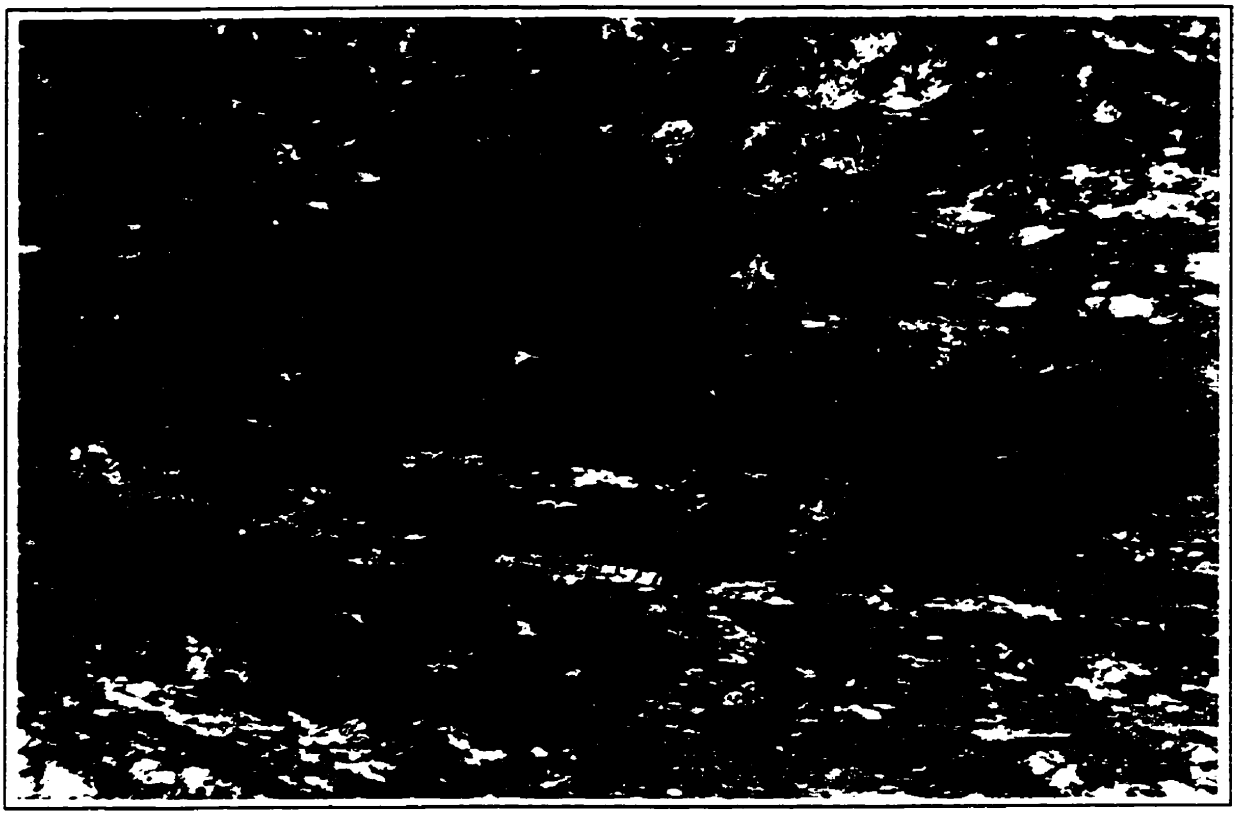

Figure 4.20 - *Photomicrograph of chlorite stringer vein alteration exhibiting relics of hydrothermal biotite and disseminated magnetite (opaques). These relics of biotites, which show a characteristic light-brown to yellow pleochroism similar to phlogopite, are magnesium-rich (see Appendix F for biotite compositions). High relief crystals are carbonate grains.*

Sample K90-41091-026, plane polarized light. Access drift to "C" zone, Kiena Mine level 41.

Microphotographie de l'altération à veinules de chlorite, montrant des reliques de biotite hydrothermale et magnétite disséminées (opaques). Cette variété de biotite est riche en magnésium et se charactérise par un pléochroisme allant du brun pâle à jaune, similaire à celui de la phlogopite (voir l'Appendice F afin de connaître la composition de la biotite). Les cristaux à fort relief sont des grains de carbonate.

Échantillon K90-41091-026, lumière naturelle. Galerie d'accès de la zone "C", niveau 41 Mine Kiena.

Figure 4.21 A - Photomicrograph of leafy to needlelike stilpnomelane replacing pre-existing carbonate and chlorite veins.

Sample K91-4117-159, plane-polarized transmitted light. Ore drift 4117, Kiena Mine level 41.

A - Microphotographie d'aiguilles de stipnomélane remplaçant des veinules pré-existantes de carbonate et chlorite.

Échantillon K91-4117-159, microscope à lumière transmise, lumière naturelle. Galerie à minerai 4117, niveau 41 Mine Kiena.

B - Idem (transmitted light, crossed Nicols).

B - Idem (Microscope à lumière transmise, Nicols croisés).

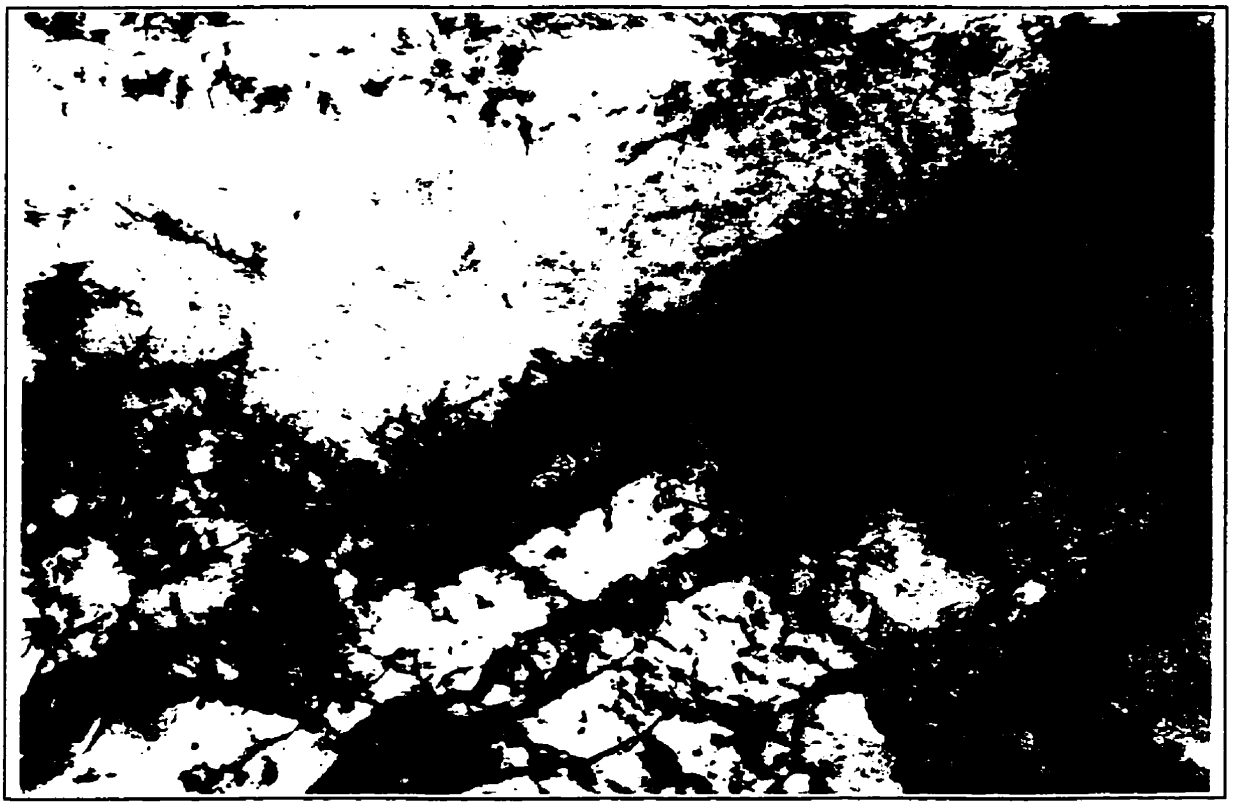

Figure 4.21 A

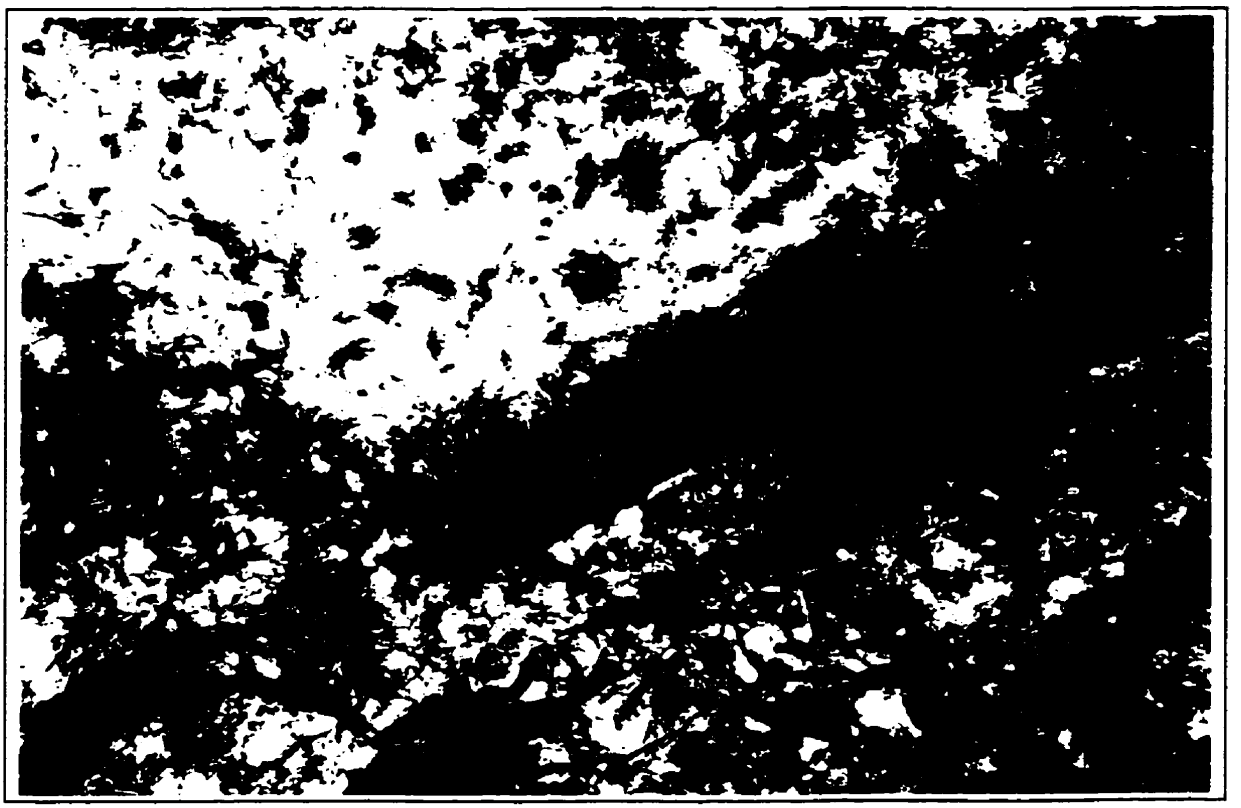

Figure 4.21 B

4.3 ZONATION OF GOLD CONCENTRATIONS AND STYLES OF MINERALIZATION

The successive overprint of carbonate-quartz-pyrite(pyrrhotite)±albite-Au stockwork vein mineralization, carbonate-pyrite-Au replacement veins and auriferous albite-cemented breccias and stockwork veins has resulted in a clear upward and outward zonation of gold concentrations and styles of mineralization across the Kiena deposit.

The vein-breccia system is funnel-shaped and can be subdivided into a *root zone*, composed of albitite dikes overprinted by the Stwk Cb-Qz-Py(Po)±Ab-Au vein ore type, flaring upward into an *apical zone* consisting of albitite dikes almost entirely obliterated by the Breccia 1 and Breccia 2 ore types changing to country rocks mineralized by the Stwk Cb-Qz-Py(Po)±Ab-Au vein ore type away from the central breccias (**Figure 4.22**). The breccia and replacement vein style of mineralization is thus confined to the upper part of the orebody (down to a depth of 600 m), and surrounded by the more extensive stockwork vein style of mineralization. The zonation of gold concentrations across the breccia-vein orebody has resulted in a central, sheet-like high-grade ore zone (5-25 g/t Au) grading outward into a lower-grade ore zone (3-5 g/t Au) and outer gold alteration halo with gold values below the mine's cut-off grade of 3 g/t Au (**Figure 4.22**). The style of mineralization and gold concentration zonation patterns are thus initiated by the early stockwork vein mineralization and subsequently emphasized by carbonate-pyrite and albite-cemented breccia mineralization. The areal distribution of mineralization decreases with each successive gold alteration event, but more gold appears to be introduced each time (dissolved and reconcentrated ?). This suggests that each successive pulse of hydrothermal fluids carried gold upward through the same ore fluid channels, possibly up-grading the early root zone stockwork vein mineralization.

Figure 4.22 - Schematic north-south longitudinal section of the Kiena deposit, looking east, showing an upward and outward zonation of gold concentrations in relation to style of mineralization and distribution of ore sulfides. The orebody consists of a high-grade core composed of albitite dikes overprinted by stockwork vein mineralization (Stwk Cb-Qz-Py(Po)±Ab-Au ore type) at lower mine levels and albitite dikes overprinted by carbonate-pyrite replacement veins (Breccia 1 ore type) and albite-cemented breccias (Breccia 2 ore type) at upper mine levels, grading outward into a lower-grade ore shell and outer gold alteration halo composed of mafic and ultramafic volcanic country rocks overprinted by stockwork vein mineralization. An upward hydrothermal fluid flow is suggested by the funnel-shaped geometry of the early stockwork vein mineralization, its overprint by Breccia 1 and Breccia 2 ore at upper mine levels, and the upward pyrrhotite-pyrite zonation.

Section longitudinale schématique du corps minéralisé de la mine Kiena, orientée nord-sud avec regard vers l'est, montrant la zonation verticale et latérale du contenu en or du gisement en fonction du style de minéralisation et de la distribution des sulfures associés. Le gisement est composé d'une zone de minerai à forte teneur formée de dykes d'albitite recoupés par la minéralisation en stockwork (minerai de type Stwk Cb-Qz-Py(Po)±Ab-Au) aux niveaux inférieurs de la mine et par des veines de remplacement à carbonate-pyrite (minerai de type Breccia 1) et des brèches à ciment d'albite (minerai de type Breccia 2) aux niveaux supérieurs de la mine, se changeant latéralement en une zone de minerai à plus faible teneur et en un halo d'altération constituées des roches mafiques et ultramaficques encaissantes recoupées par la minéralisation en stockwork. La forme en entonnoir du minerai de type Stwk Cb-Qz-Py(Po)±Ab-Au, sa superposition par les minerais de type Breccia 1 et Breccia 2 aux niveaux supérieurs de la mine, ainsi que le changement progressif de pyrrhotite à pyrite avec la diminution de la profondeur, suggèrent le mouvement ascendant des fluides hydrothermaux.

ORE ZONATION ACROSS THE KIENA MINE DEPOSIT

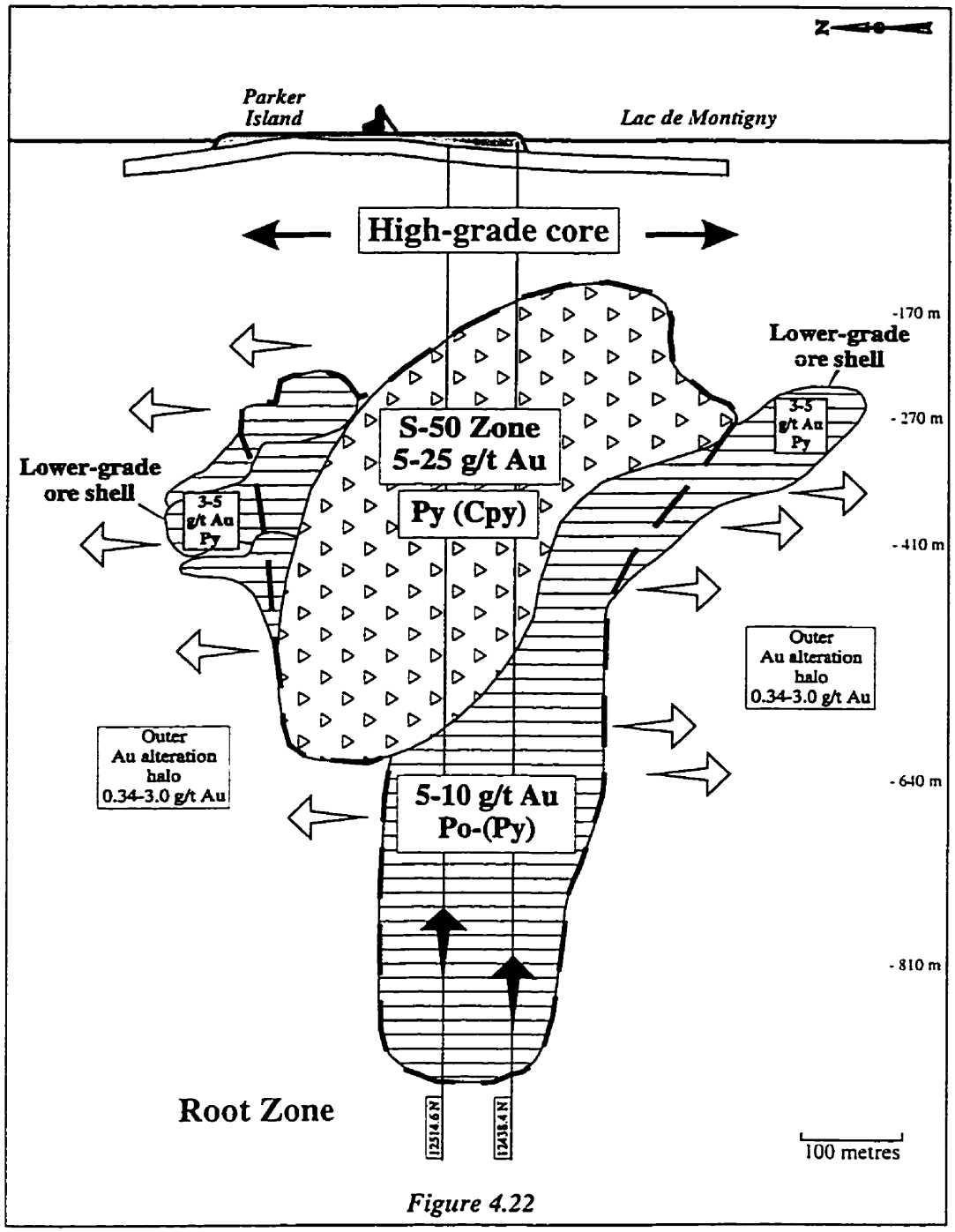

Figure 4.22

Breccia 1 and Breccia 2 ore

Stwk Cb-Qz-Py(Po)±Ab-Au ore

Contour of high-grade ore

Decrease in stockwork vein alteration away from main ore fluid conduits

Hydrothermal fluid flow suggested by ore zonation pattern

Stwk Cb-Qz-Py(Po)±Ab-Au ore: carbonate-quartz±albite stockwork veins with disseminated pyrite and/or pyrrhotite and native gold; Breccia 1 ore: carbonate-pyrite-gold replacement veins; Breccia 2 ore: albite stockwork veins with disseminated pyrite, ± chalcopyrite, ± scheelite and native gold.

Ab: albite; Au: gold; Cb: carbonate; Cpy: chalcopyrite; Po: pyrrhotite; Py: pyrite; Qz: quartz; Stwk: stockwork.

4.4 SUMMARY

Albitite dikes are an important host to mineralization at Kiena. The remainder of the ore is hosted by an overturned sequence of komatiitic and tholeiitic volcanic flows which were pervasively albite-altered presumably during the intrusion of the dikes. Pre-ore pervasive albite alteration occurs at, and determines the extent of, the centre of mineralization. The ore is fracture-controlled and the predominant styles of mineralization are stockwork veining and brecciation. Intense fracturing and alteration are restricted to the albitite dike environment and progressively decrease away from the dikes. The persistent funnel-shaped geometry of albitite intrusions and fracture-guided alterations indicate that the present configuration of the magmatic-hydrothermal system is upright, and that the flow of magma and hydrothermal fluids intermittently occurred through the same fracture zone. This in turn, may indicate that the source of magmatic and hydrothermal activity lies beyond the root of Kiena's alteration-mineralization system.

The presence of mineralized rock fragments in Breccia 1 and Breccia 2 ore indicates that main-stage Stwk Cb-Qz-Py(Po)±Ab-Au, Breccia 1 and Breccia 2 mineralization were separated in time. Successive alteration-mineralization overprints, breccia-infill textures devoid of rock flour or gouge, and the upward and outward pyrrhotite-pyrite zonation pattern suggest that mineralization is related to a sequence of autobrecciation events caused by the episodic up-surge of hot, high-pressure fluids. Differences in vein paragenesis are interpreted as changes in ore fluid composition with time, whereas differences in mineralization styles are interpreted as changes in ore fluid pressure-temperature conditions and as changes in the mechanical properties of the host rocks with time. Several observations are compatible with a high-level of emplacement for the ore at Kiena, including the upward-flaring geometry of the ore, fracture-controlled alteration-mineralization, the intrusion of porphyry dikes in the alteration-mineralization sequence, and the presence of open-space crystal growth in veins and breccias.

CHAPTER 5 STRUCTURE

5.1 INTRODUCTION

This section has three objectives: the first is to clarify the structural evolution of the Kiena deposit by establishing the hierarchy of pre-, syn-, and post-ore structures, the second is to identify the structural controls on gold mineralization, and the third is to determine the time relationship between mineralization and penetrative deformation.

Clearly recognizable pre-ore structures comprise: an upward-flaring swarm of albitite dikes and the Kiena Mine Fault Zone, a structure previously identified by Clark (1963)and here interpreted as a regional-scale fault which guided the emplacement of albitite dikes. Ore-related structures, on the other hand, are local structures controlling the development of the Kiena deposit magmatic-hydrothermal system. They are subdivided into early-stage calcite stockwork veins, main-stage stockwork veins and breccias, intermineral porphyry dikes, intermediate-stage calcite-pyrite stockwork veins, and late-stage phyllosilicate stockwork and stringer veins. By contrast, post-ore structures are unrelated to the ore-forming process, because they clearly overprint ore structures. They include an asymmetric z-shaped fold and related east-west axial planar schistosity dipping moderately to the north, a northwest-plunging open fold and related crenulation cleavage dipping gently to the northeast, and several late-stage north-dipping oblique-slip faults. Post-ore structures are interpreted as regional synmetamorphic deformation structures altering the original geometry of Kiena's ore-forming fracture system.

This division of the deposit's structures emphasizes that its structural evolution occurred in three main phases: a *regional* pre-ore faulting phase affiliated with the development of a fault lineament during the overturning of volcanic strata, which assisted the emplacement of dioritic and granodioritic, high-level intrusions (i.e. Val d'Or plutonic belt ca. 2694-2680 Ma), a *local* phase of mineralization controlled by fracture-induced permeability related to magmatic-

hydrothermal activity (i.e. stockwork veins and breccias, ca. 2694-2686 Ma), and a *regional* post-ore deformation phase (D_2, F_2, S_2, and S_3) modifying the shape and orientation of pre-existing ore structures (ca. 2677-2645 Ma). Kiena's main penetrative fabric is interpreted as post-ore and attributed to regional folding, rather than syn-ore and associated with the development of regional shear zones, as previously thought (Roy, 1983; Bourget, 1986; Quirion, 1988). Differences in strain intensity between the ore and schistose country rocks are attributed to strain partitioning between rock types showing competency contrasts as a result of hydrothermal alteration. A description of the structures controlling and later deforming the Kiena deposit, is presented below.

5.2 PRE-ORE STRUCTURES

5.2.1 Albitite dikes and the Kiena Mine Fault Zone

The albitite dikes and Kiena Mine Fault Zone formed prior to gold mineralization and assisted the emplacement of the magmatic-hydrothermal system (**Table 5.1**). The dikes consist of narrow dioritic intrusions characterized by thin blueish-grey chilled margins and a"sugary" aplitic texture, emplaced into folded strata (see section 3.5.2). The dike swarm has a funnel shape defined by a few closely-spaced intrusions at lower mine levels, flaring upward into several thinner dikes straddling the upper contact of a tholeiite with an overturned, west-dipping komatiite at upper mine levels. Schematic sections and plan maps prepared for this study (in back pocket) show that mineralized albitite dikes are deformed by a north-northwest-plunging, asymmetric z-shaped fold and overprinted by the deposit's main schistosity and northeast-dipping crenulation cleavage (see also section 5.4). Removing the effects of vertical shortening, which produced the crenulation cleavage, by unfolding the lower part of the orebody (see sections 12438.4 N and 12514.6 N, back pocket) restores the ore-dike complex to a steep, west-dipping fault. Based on this reconstruction, it appears that albitite dikes were emplaced along a bedding-parallel fault, but that the dikes predominantly developed in the komatiitic hangingwall of the fault at upper mine levels (see Level map 33

and 41, back pocket). This observation suggests that magma was guided by the fault at depth and progressively extended the main fault by splaying upward into the hangingwall as it reached higher levels in the crust (e.g. Phillips (1972)). The precursor fault zone inferred from the partially restored configuration of albitite dikes is referred to as the Kiena Mine Fault Zone. Clark (1963) initially proposed the existence of the Kiena Mine Fault Zone by noting the parallelism between mineralization and the deposit's felsic porphyry dikes.

The attitude of the Kiena Mine Fault Zone prior to deformation by the z-shaped fold is not known, but the predominant bedding-parallel attitude of other fault zones intruded by diorite and granodiorite dikes on the property (see **Figure 3.1**) suggests that it was initially a northwest-southeast high-angle fault. These bedding-parallel faults are interpreted to have formed either during, or shortly after, the tilting of volcanic strata during the first episode of regional deformation (D_1), and were intruded later by intermediate to felsic magma during a protracted episode of orogenic plutonism (see sections 2.2.3 and 2.2.4). Because of the lack of markers around albitite dikes and the subsequent deformation, the sense of movement of the Kiena Mine Fault Zone is unknown, but the preference of albitite dikes for the fault hangingwall at upper mine levels suggests that it is a normal fault (e.g. Phillips (1972)). The Kiena Mine Fault zone could not be dated directly because the albitite dikes did not yield any zircons or baddeleyite, but the age is bracketed between ca. 2694-2686 Ma. The upper age limit is defined by the Sigma-Lamaque Mines dioritic dikes which are the first dikes emplaced after the regional tilting of volcanic strata at ca. 2694 ± 2 Ma (Wong et al., 1991). The lower age limit of 2686 ± 2 Ma is provided by the intermineral granodiorite porphyry dike cross-cutting mineralized albitites at Kiena (see Chapter 6). This is consistent with the minimum age of 2692 ± 2 Ma obtained for mineralized "microdiorite" dikes cut by a tonalite dike (Pilote et al., 1993) at the neighbouring Norlartic Mine (see **Figure 2.2**), which according to descriptions of Sauvé (1993) and Couture *et al.* (1994) are very similar to Kiena's albitite dikes.

In summary, two types of pre-ore structures are the focus of gold mineralization at Kiena:

a regional-scale fault zone created during an early episode of regional deformation, and a local set of fractures associated with the emplacement of albitic magma during an episode of regional plutonism that followed the overturning of volcanic strata (**Table 5.1**). Whereas the first is unrelated to the mineralization process, the second set of structures is genetically related to the ore (see section 4.2.1).

5.3 ORE STRUCTURES

Ore structures cut pre-ore albitite dikes and are overprinted in turn, by post-ore penetrative fabrics. They control the deposit's pro-grade alteration-mineralization sequence and are subdivided, from the oldest to the youngest, into early-stage calcite stockwork veins, main-stage stockwork veins and breccias, intermineral porphyry dikes, intermediate calcite-pyrite stockwork veins and late-stage phyllosilicate stockwork and stringer veins (**Table 5.1**). Ore structures control the zoned patterns of alteration-mineralization and determine the extent of fracture damage around the orebody.

5.3.1 Early-stage calcite stockwork veins

This calcite stockwork vein system is the earliest recognized vein-controlled alteration in the deposit's alteration-mineralization sequence. The veins overprint albite-altered volcanic rocks and form a discrete zone of crackle breccia restricted to the immediate ore-wallrock contact (section 4.2.2). The stockwork is characterized by a diamond-shaped fracture pattern which intensifies near the contact with the ore, and is sharply truncated by the high-grade breccia body of the S-50 zone. Although these veinlets do not control the gold mineralization, they point toward the main orebody. This suggests that this early fracture system served as ground preparation control for mineralization by enhancing the permeability of albite-rich host rocks.

Table 5.1 Hierarchy of structures at the Kiena deposit

PRE-ORE STRUCTURES · *Guide the emplacement of "dioritic" magma*	***Regional fault lineament and high-level intrusions*** 1. Kiena Mine Fault Zone (steeply-dipping normal fault ?) 2. Albitite dikes or "ore zone andesite", "grey diorite", "diorite", "quartz diorite", "microdiorite" dikes
SYN-ORE STRUCTURES *Control the emplacementof Kiena's pro-grade alteration-mineralization sequence*	***Local, fracture-induced permeability linked to magmatic-hydrothermal activity*** 1. **Early-stage** Cc stockwork veins (crackle breccia) 2. **Main-stage** Cb-Qz-Py(Po)±Ab-Au stockwork veins " Cb-Py-Au replacement veins " Ab-Py-Cpy-Sch-Au stockwork veins and breccias " Qz-Cb-Bo-Ab-±Tl-Py-Cpy-Au veins 4. **Intermineral** granodiorite and feldspar porphyry dikes 5. **Intermediate-stage** Cc-Py-Au stockwork veins in porphyry dikes 6. **Late-stage** phyllosilicate stockwork and stringer veins (Ser, Bo-Mt, Chl)
POST-ORE STRUCTURES *Modify the shape and orientation of pre-existing ore structures*	***Regional dynamothermal deformation*** (D_2, F_2, S_2) 1. Asymmetric Z-shaped fold (F_2) (visible in plan view) Main schistosity ($S_n = S_2$) (moderately N-dipping to steeply NE-dipping) 2. NNW-plunging, broad open fold (F_3) (visible in section) Crenulation cleavage ($S_{n+1} = S_3$) (shallowly NE-dipping) 3. Late-stage, oblique-slip faults (steeply NW-dipping)

Key: Ab= albite; Au= gold; Bo= biotite; Cb= carbonate; Cc= calcite; Chl= chlorite; Cpy= chalcopyrite; Mt= magnetite; Py=

5.3.2 Main-stage stockwork veins and breccias

Main-stage stockwork veins and breccias are the most important ore structures in the deposit because they host all of the economic mineralization. They overprint the albitite dikes of the Kiena Mine Fault Zone and the crackle breccia zone which is centered on the dikes, and they are cut by the deposit's post-ore schistosity and crenulation cleavage.

They consist of four overprinting vein sets which are comprised, from the oldest to the youngest, of carbonate-quartz-pyrite(pyrrhotite)±albite-Au stockwork veins, carbonate-pyrite-Au replacement veins, albite-pyrite±chalcopyrite-scheelite-Au stockwork veins and breccias, and minor quartz-carbonate-biotite-albite±tourmaline-pyrite-chalcopyrite-Au pegmatitic veins (see section 4.2.3). Overall, the upward and outward zoned orebody consists of a sheet-like, high-grade core composed of carbonate-quartz-pyrrhotite stockwork veins at lower mine levels and albite-cemented breccias at upper mine levels, grading outward into a lower-grade ore shell and outer gold alteration halo composed of carbonate-quartz-pyrite stockwork veins (**Figure 4.22**). The fracture damage caused by carbonate-quartz-pyrite veining around the deposit extends approximately 20 metres in the tholeiitic footwal east of the S-50 zone and 120-140 metres in the komatiitic and tholeiitic hangingwall west of the S-50 zone at mid-levels in the mine.

Apart from carbonate-pyrite replacement veins, all veins and breccias show open-space crystal growth such as in crustiform - and cockade-textured carbonate-quartz stockwork veins and albite-cemented breccias (e.g. **Figures 3.15** and **4.14**). These textures are interpreted as evidence that fractures remained open during mineralization. The upward-flaring alteration pattern created by these ore structures and their open-space infill textures are characteristic of brittle fracturing at high levels in the crust (e.g. Phillips (1972)). Furthermore, the overprint of Kiena's albitite dike swarm by main-stage stockwork veins and breccias showing a decrease in the intensity of fracturing away from the intrusive centre, is reminiscent of the fracture-alteration pattern one would expect in a porphyry environment at relatively shallow

depth (e.g. Burnham, (1979) and Titley, (1982; 1993)).

5.3.3 Intermineral porphyry dikes and intermediate-stage calcite-quartz-pyrite stockwork veins

The dikes form narrow greyish-pink intrusions, either sub-parallel to, or in contact with, albitite dikes (see section 3.5.3). They cut and dismember the ore into smaller ore zones and contain xenoliths of ore, albitite dikes, and altered komatiitic wallrock (e.g. level map 33 in back pocket). The dikes are interpreted as high-level structures because they often branch out (see section 12514.6 N, back pocket), have a porphyritic texture (**Figures 3.31** to **3.33**), and coincide with the albitite dike swarm. They are albitized and subsequently fractured and weakly mineralized by a minor carbonate-quartz-pyrite vein alteration, prior to being overprinted by vein-controlled phyllosilicate alteration and later deformed by folds and related planar fabrics (e.g. **Figures 3.27** and **4.1**). The deposit's intermineral granodiorite and feldspar porphyry dikes are interpreted as ore structures because they cut main-stage alteration of the Kiena Mine Fault Zone but they were still affected by the mineralization process prior to being overprinted by the deposit's main schistosity and crenulation cleavage.

5.3.4 Late-stage phyllosilicate stockwork and stringer veins

This phyllosilicate vein system overprints, and has the same funnel-shaped configuration as the pre-existing carbonate-quartz-pyrite(pyrrhotite)±albite-Au stockwork vein system. It consists of chlorite stockwork veins confined to mineralized albitites at lower mine levels, flaring-upward into a widespread network of chlorite-biotite-magnetite stringer veins transgressing albitite dikes into surrounding country rocks at upper mine levels (see section 4.2.5). The blossoming of the phyllosilicate vein system with decreasing depth, suggests that it formed by brittle fracturing at relatively shallow depth. Kiena's phyllosilicate veins are interpreted as ore structures because they form the last alteration stages of the deposit's alteration-mineralization sequence and are penetratively deformed by the main schistosity and crenulation cleavage.

5.4 POST-ORE STRUCTURES

Post-ore structures have overprinted all pre-existing ore structures. From the oldest to the youngest, they are comprised of an asymmetric z-shaped fold and related north-dipping schistosity (S_n), a north-northwest-plunging open fold and related northeast-dipping crenulation cleavage (S_{n+1}), and several late-stage oblique-slip faults (**Table 5.1**). By contrast with ore structures, which are related to the ore-forming process and control alteration-mineralization patterns, post-ore structures deform the orebody by modifying its volume, shape and orientation. They are thus unrelated to mineralization but have had and influence on the geometry of the ore-dike complex.

5.4.1 Deposit-scale z-shaped fold and related north-dipping schistosity (S_n)

The first identifiable post-ore structure in the Kiena deposit is a schistosity striking approximately east-west and dipping moderately to the north, which disrupts pre-existing ore structures (**Figures 5.1 and 5.2**). The fabric, which is referred to as S_n, cuts the ore-dike complex at, or near, a right-angle and is subparallel to the axial plane of a deposit-scale, asymmetric z-shaped fold visible in plan map. The fold occurs approximately 250 metres below surface and extends to a depth of about 580 metres.. It is characterized by a long axis, trending approximately north-south, formed by the breccia body of the S-50 zone, albitite dikes and granodiorite porphyry and of northern and southern hinges coinciding with the tapering-off of the breccia body into main-stage stockwork vein mineralization of the "J"-"K"-"L" and "C" ore zones, respectively (e.g. 41 level plan map in back pocket).

In areas dominated by main-stage stockwork vein mineralization (e.g. **Figure 4.1**), the relationship between S_n and stockwork veins is as follows: veins subparallel to schistosity are cut by the schistosity (**Figure 5.3**) or deformed by boudins and quartz extension veinlets along strike (**Figure 5.4**, see also **Figure 4.6**), whereas veins set at high-angle to schistosity are folded and cut by the axial planar schistosity (**Figures 4.1** and **4.4**). Schistosity planes are

refracted into carbonate-pyrite replacement veins (**Figure 5.2**) and gradually become irregular, wavy spaced-cleavage planes in the high-grade albite breccia of the S-50 zone (**Figure 5.9**).

The deposit's main schistosity is associated with deformation and metamorphic recrystallization of hydrothermal minerals in ore structures. Pyrite and/or pyrrhotite disseminated along the selvages of carbonate-quartz stockwork veins are stretched parallel to schistosity, or in the case of pyrite, is partially recrystallized, fractured and reoriented parallel to schistosity and locally display carbonate-filled strain shadows (**Figures 5.5 to 5.7**). In replacement veins and albite breccia, trails of deformed and partially recrystallized pyrite grains define the main penetrative planar fabric (S_n, **Figures 4.9** and **4.15**). Relics of biotite in chlorite veins are coarsely recrystallized and reoriented parallel to schistosity (**Figure 5.8**), as does the chlorite in the veins (**Figure 3.20**). Strongly schistose rocks in areas of intense chloritic alteration show stylolitic dissolution cleavages developed across the schistosity (**Figure 3.10**), suggesting that these rocks were subjected to pressure-dissolution shortening mechanisms. Another important, but minor aspect of the main north-dipping schistosity at Kiena is the local occurrence of native gold slickenfibres displaying oblique, normal steps on wavy schistosity planes across the high-grade breccia ore of the S-50 zone (**Figures 5.9** and **5.10**). Such striations are interpreted as local remobilization of main-stage gold mineralization on schistosity planes during post-ore penetrative deformation and fault movement. This is not a common phenomenon in the mine as most of the gold recovered at Kiena occurs as free milling grains in stockwork veins and breccia (Muir, 1979).

Prior to this study, S_n was interpreted as a shear zone fabric related to the formation of the Kiena deposit during late- to post-metamorphic regional deformation (Roy, 1983; Bourget, 1986; Quirion, 1988)but, as clearly pointed out by Sauvé *et al.* (1993, p. 125), the formation of an east-west planar fabric is incompatible with that of a north-south shear zone. The deposit's z-shaped fold and main penetrative planar fabric (S_n) are herein interpreted as post-ore structures formed coevally during the shortening of the ore-dike complex in an

Figure 5.1 - Photograph of albitite laced with gold-bearing, albite-pyrite stockwork veins,and overprinted by the deposit's main schistosity (S_n).

Ore drift 4116, "B" zone, Kiena Mine level 41.

Photo de veines d" albite-pyrite recoupant une albitite, découpées par la schistosité principale du gisement (S_n).

Galerie à minerai 4116, zone "B", niveau 41 Mine Kiena.

Figure 5.2 - Detail from Figure 4.7. Photograph showing the deposit's main schistosity cutting across the Stwk Cb-Qz-Py(Po)±Ab-Au vein and Breccia 1 ore contact. Note how the schistosity planes are refracted into the more competent carbonate-pyrite replacement vein.

Ore drift 3838, junction of "B" and "C" zones, Kiena Mine level 38.

Détail de la Figure 4.7. Photo montrant la schistosité principale du gisement recoupant le contact entre les minerais de type Stwk Cb-Qz-Py(Po)±Ab-Au et Breccia 1. Les plans de schistosité sont réfractés vers la veine de remplacement à carbonate-pyrite de compétence plus élevé.

Galerie à minerai 3838, junction des zones "B" et "C", niveau 38 Mine Kiena.

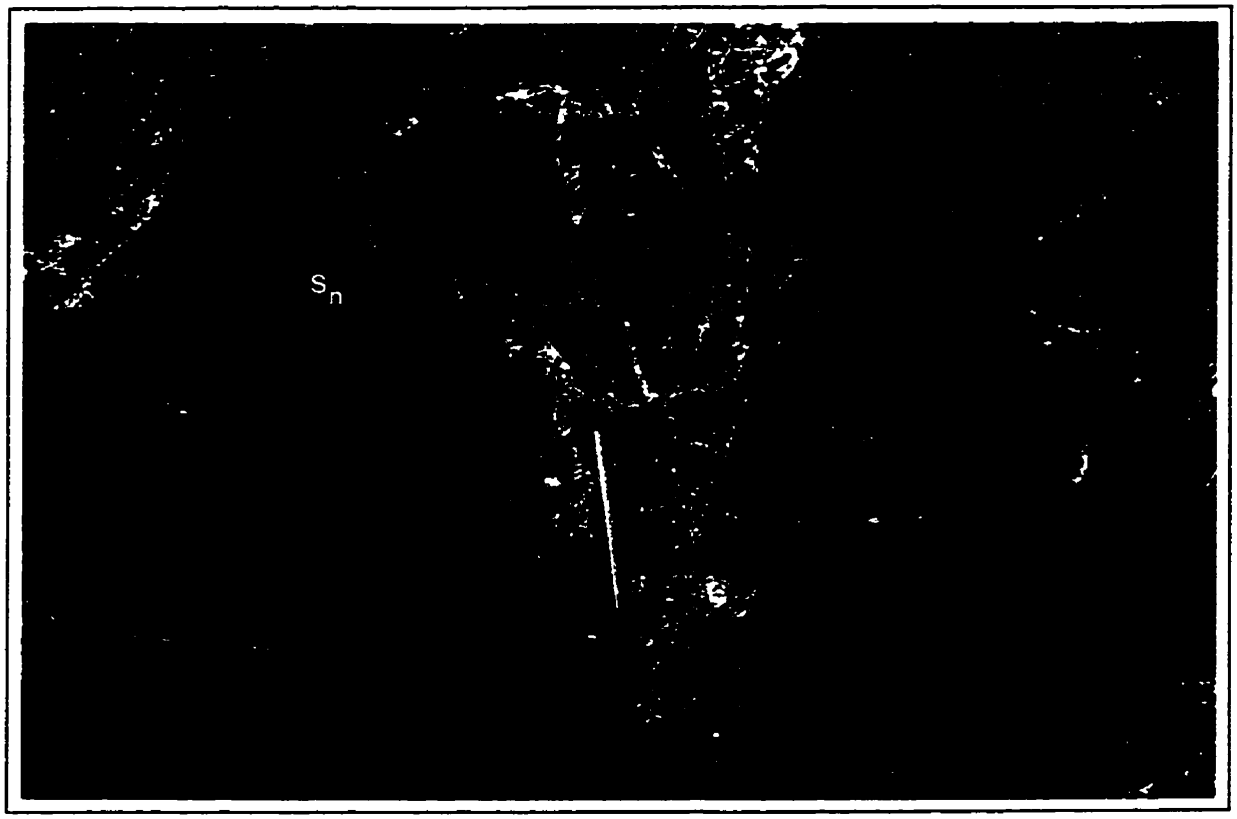

Figure 5.1

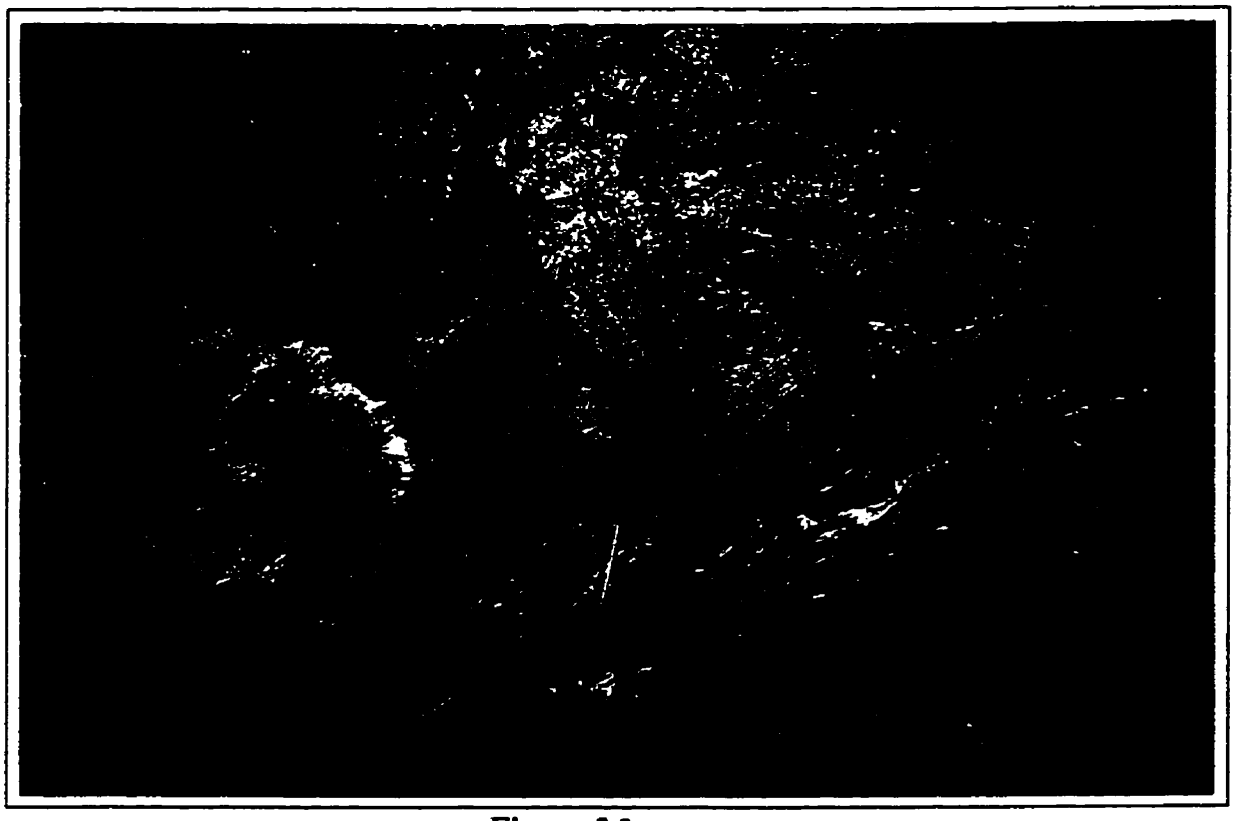

Figure 5.2

Figure 5.3 - Close-up view of a polished hand specimen of the Stwk Cb-Qz-Py(Po)±Ab-Au vein ore type shown on Figure 4.1, illustrating the effects of penetrative deformation on carbonate-quartz stockwork veins and associated pyrite grains. Veins which are sub-parallel to schistosity are boudinaged and overprinted by carbonate-filled extension veins (see arrow). Pyrite grains are deformed and stretched out along schistosity (see Figures 5.5 and 5.6). The relic crustiform texture preserved in one of the boudinaged veins further indicates that stockwork veins formed during extension and were subsequently deformed by shortening.

Sample K91-3838-098, access drift 3838, junction of "B" and "C" zones, Kiena Mine level 38.

Vue en plan rapproché de la surface polie d'un échantillon du minerai de type Stwk Cb-Qz-Py(Po)±Ab-Au montré à la Figure 4.1, illustrant les effets de la déformation sur des veines de carbonate-quartz-pyrite en stockwork. Les veines qui sont sub-parallèles à la schistosité, sont boudinées, et recoupées par de fines veinules d'extension remplies de carbonate (voir flèche). Les grains de pyrite sont déformés (voir Figures 5.5 et 5.6), et étirés dans le sens de la schistosité. La relique de texture crustiforme préservée au sein de l'une des veines en stockwork boudinée, indique de plus que celles-ci se sont formées lors d'une extension et furent subséquemment déformées par applatissement.

Échantillon K91-3838-098, galerie d'accès 3838, junction des zones "B" et "C", niveau 38 Mine Kiena.

Figure 5.4 - Photomicrograph of a carbonate stockwork vein with a relic comb texture. The vein is nearly parallel to S_n but is clearly cut by it. The relic open-space texture shows that the vein formed during extension, and was overprinted by the schistosity during deformation by shortening parallel to the former extension direction.

Sample K90-41092-040, transmitted light, crossed Nicols. Ore drift 41092, "C" zone, Kiena Mine level 41.

Microphotographie d'une veine de carbonate en stockwork exhibant la relique d'une texture "en peigne". La veine est presque parallèle, mais clairement recoupée, par la schistosité principale (S_n) du gisement. La texture relique de remplissage en fracture ouverte indique de plus que la veine s'est d'abord formée par extension, et fut subséquemment déformée lors d'un applatissement dans la même direction que l'extension qui l'a précédé.

Échantillon K91-41092-040, microscope à lumière transmise, Nicols croisés. Galerie à minerai 41092, zone "C" niveau 41 Mine Kiena.

Figure 5.3

Figure 5.4

Figure 5.5 - Photomicrograph of deformed pyrite (Py) grains associated with carbonate-quartz stockwork veins shown on Figure 5.3. The grains are stretched out and reoriented parallel to schistosity. Some pyrites are fringed by carbonate-filled pressure shadows (see arrow). The small disseminated opaque minerals in chlorite veins are magnetite (Mt) grains.

Sample K91-3838-098, transmitted plane-polarized light. Junction "B" and "C" zones, Kiena Mine level 38.

Microphotographie de grains de pyrite (Py) déformés qui sont associés aux veines de carbonate-quartz en stockwork montrés à la Figure 5.3. Les grains de pyrite sont étirés selon la schistosité et montrent des ombres de pression remplies de carbonate (flèche). Les petits grains d'opaques disséminés dans les veines de chlorite sont des grains de magnétite (Mt).

Échantillon K91-3838-098, microscope à lumière transmise, lumière naturelle. Junction des zones "B" et "C", niveau 38 Mine Kiena.

Figure 5.6 - Idem Figure 5.5. Fractured and streched out pyrite. Each grain fragment is linked to the other by carbonate-filled strain shadows.

Sample K91-3838-098, plane-polarized transmitted light. Junction of "B" and "C" zones, Kiena Mine level 38.

Idem Figure 5.5. Grain de pyrite fracturé et étiré suivant la schistosité. Chaque morceau de grain est lié au suivant par des ombres de pression remplies de carbonate.

Échantillon K91-3838-098, microscope à lumière transmise, lumière naturelle. Junction des zones "B" et "C", niveau 38 Mine Kiena.

Figure 5.5

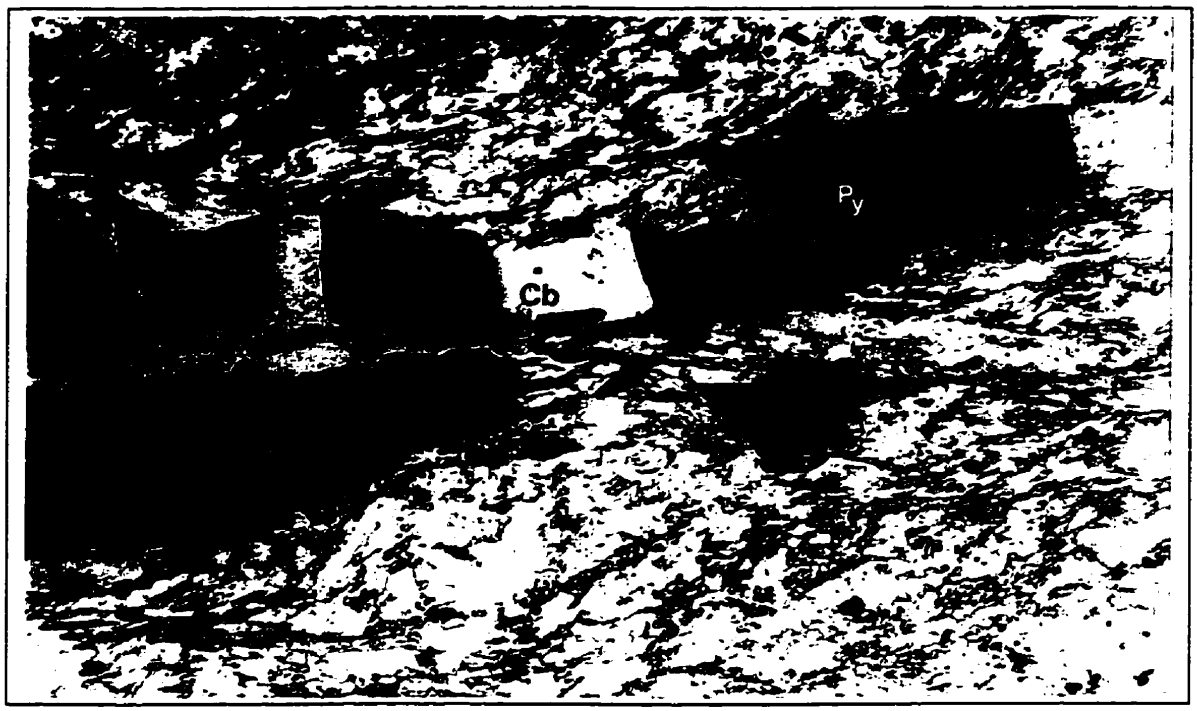

Figure 5.6

Figure 5.7 - Photomicrograph of mineralized albitite at lower mine levels showing partly recrystallized, disseminated pyrrrhotite grains re-oriented parallel to schistosity.

Sample K92-6446-218, transmitted light, crossed polars. Ore drift 6446, lower "C" zone, Kiena Mine level 64.

Microphotographie d'une albitite minéralisée située aux niveaux inférieurs de la mine, montrant des grains de pyrrhotite disséminés et partiellement recristallisés, réorientés selon la schistosité.

Échantillon K92-6446-218, microscope à lumière transmise, Nicols croisés. Galerie à minerai 6446, zone "C" inférieure, niveau 64 Mine Kiena.

Figure 5.8 - Photograph of a chlorite vein showing relics of hydrothermal vein biotite reoriented, with chlorites, along the schistosity.

Sample K90-41091-028A,transmitted , plane-polarized light. Ore drift 41091, "C" zone, Kiena Mine level 41.

Microphotographie d'une veine de chlorite montrant des porphyroblastes de reliques de biotite hydrothermale, de même que des grains de chlorite, réorientés dans le sens de la schistosité.

Échantillon K90-41091-028A, microscope à lumière transmise, lumière naturelle. Galerie à minerai 41091, zone "C", niveau 41 Mine Kiena.

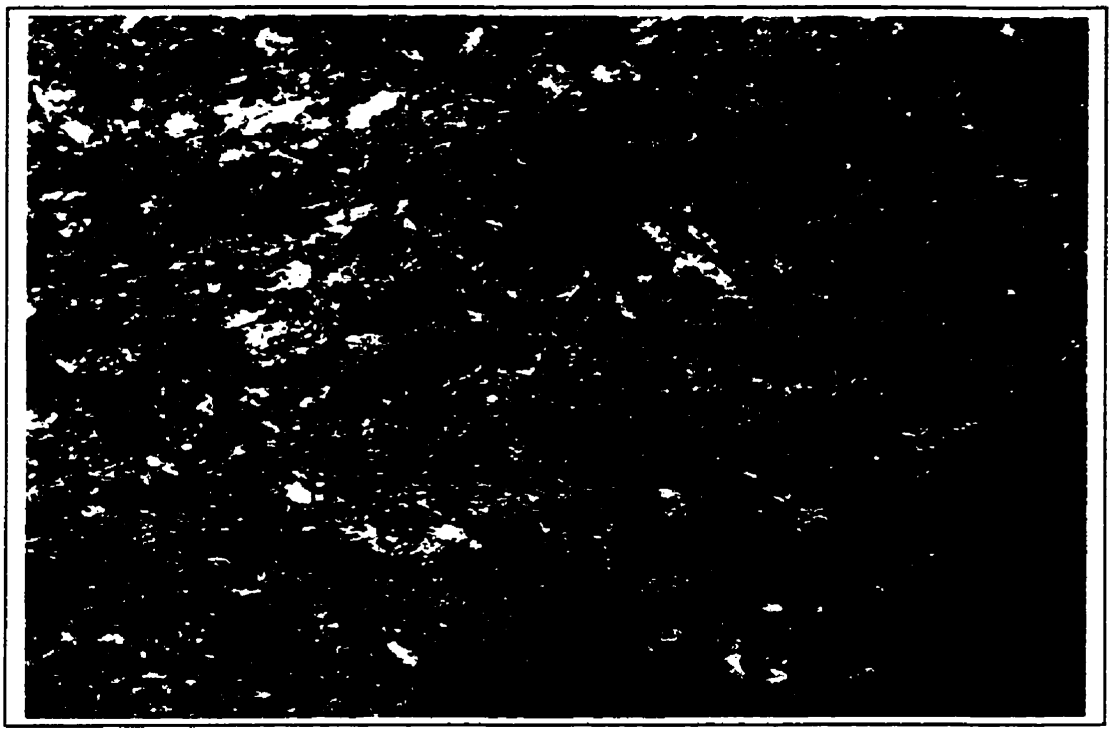

Figure 5.7

Figure 5.8

Figure 5.9 - Example of minor gold remobilization on wavy to irregular schistosity planes (S_n) cross-cutting the high-grade breccia ore of the S-50 zone..

Ore drift 4313, "B" zone, Kiena Mine level 43.

Exemple de remobilisation mineure d'or sur un plan de schistosité sinueux et irrégulier (Sn) recoupant la brèche à haute teneur de la zone S-50.

Ore drift 4313, zone "B", niveau 43 Mine Kiena.

Figure 5.10 - Ore sample from the breccia shown on Figure 5.9, exhibiting gold and pyrite slickenfibers on a schistosity plane. This type of gold occurrence is uncommon at Kiena, however, it clearly shows that some gold was remobilized in situ during, or shortly after, penetrative deformation.

Ore drift 4313, zone "B", Kiena Mine level 43.

Échantillon de brèche minéralisée illustrée à la Figure 5.9, montrant un plan de schistosité portant des stries formées d'or natif et de pyrite. L'or se présente rarement sous cette forme à Kiena, quoiqu'il indique sans équivoque la remobilisation in situ d'une infime quantité d'or pendant, ou peu de temps après, la déformation pénétrative.

Galerie à minerai 4313, zone "B", niveau 43 Mine Kiena.

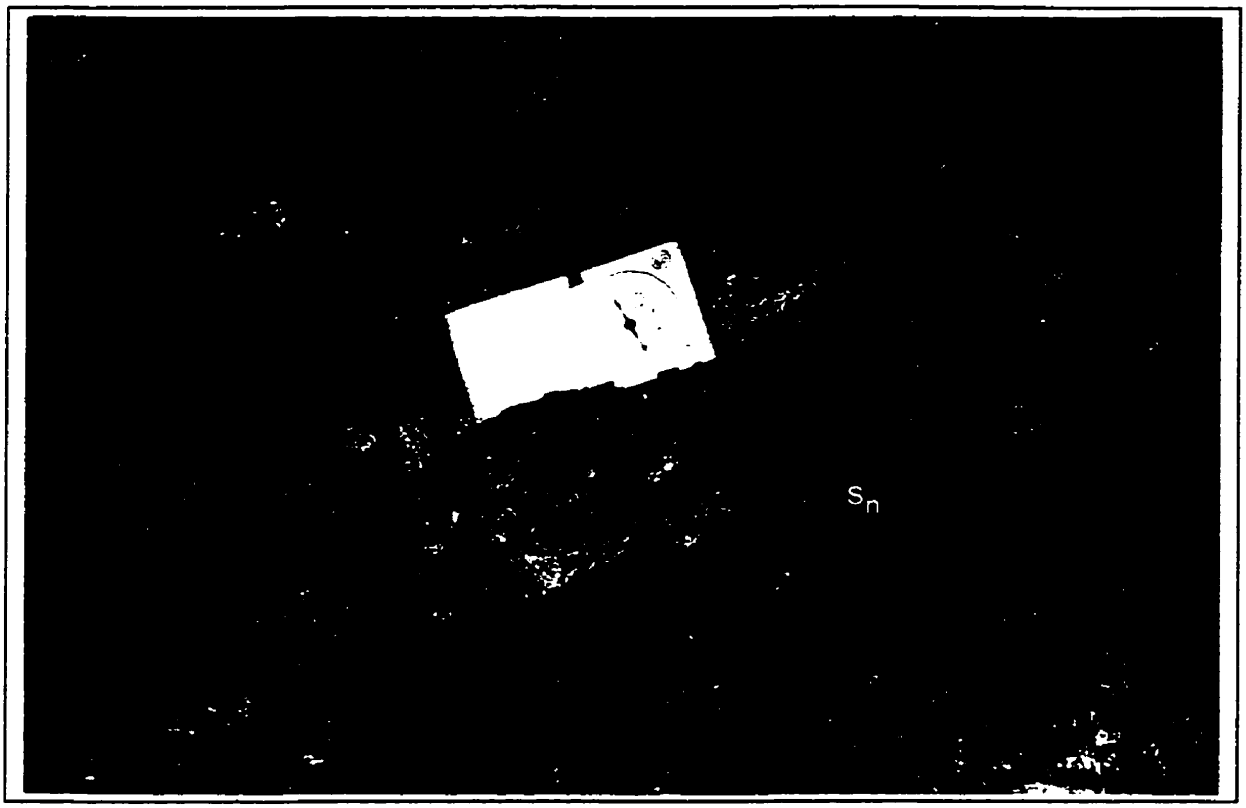

Figure 5.9

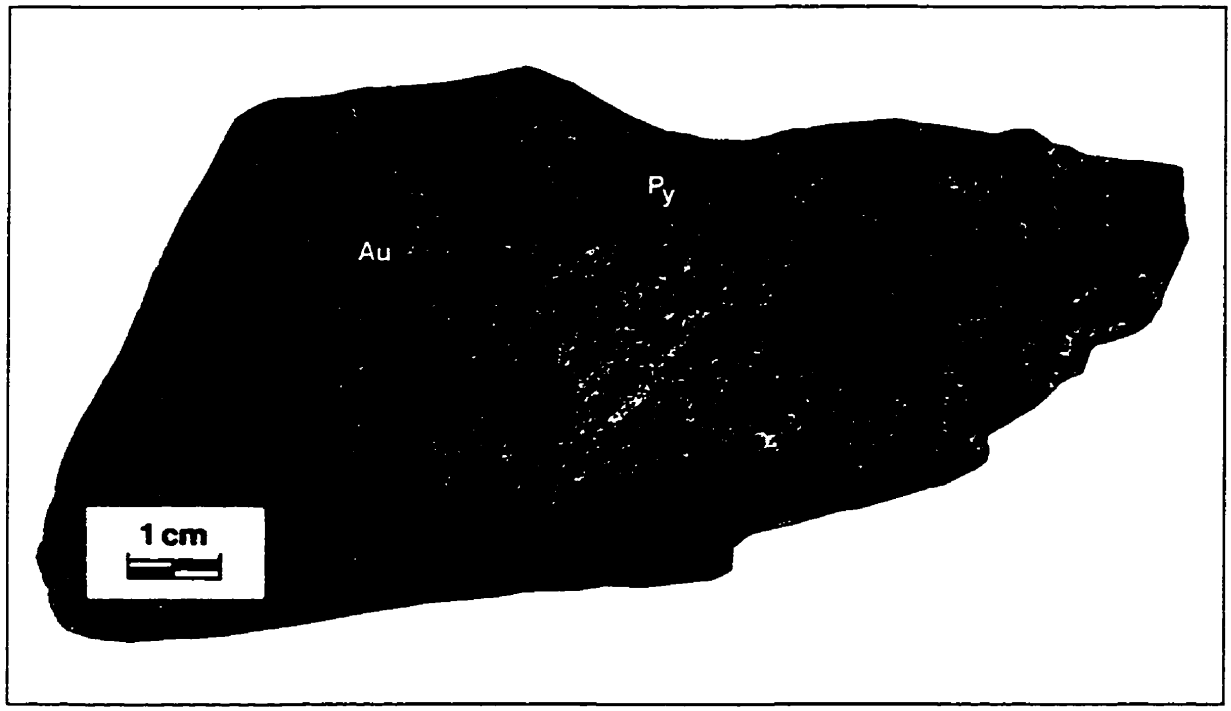

Figure 5.10

approximately north-south direction based on the following: both structures disturb pre-existing ore structures, the main schistosity is overprinted by north-south stylolitic dissolution cleavages, and it is axial planar to the asymmetric z-fold and main-stage stockwork veins deformed by folds. The Kiena deposit z-fold is remarkably similar to another z-fold structure occurring in the Val d'Or-Malartic area. The Camflo deposit z-fold, located 10 km west-northwest of Kiena, deforms southerly-overturned volcanic and sedimentary strata and is cut by a north-dipping axial-planar S_2 schistosity associated with the regional synmetamorphic D_2 deformation (see Chapter 2). By analogy, the Kiena deposit z-fold and related axial planar schistosity are herein interpreted also as a regional F_2 fold and S_2 schistosity for the following reasons: 1) they are post-ore structures superimposed on volcanic strata overturned during the early regional D_1 (F_1) deformation event, 2) the deposit's main schistosity is related to the deformation and metamorphic recrystallization of hydrothermal ore minerals and 3) S_n has the same east-west, north-dipping attitude as the regional S_2 fabric axial planar to the Camflo deposit z-fold.

5.4.2 Northwest-plunging open-fold and related crenulation-cleavage (S_{n+1})

The deposit's main schistosity is deformed, together with the ore, by a moderately northwest-plunging fold and a gently northeast-dipping crenulation cleavage (**Figures 5.11** to **5.14**). This fold, which is clearly visible on schematic cross-sections 12438.4 N and 12514.6 N (in back pocket), has a broad, open shape and encompasses the entire vertical extent of the Kiena orebody. The crenulation cleavage, termed S_{n+1}, overprints the ore and the main schistosity (**Figures 5.11** and **5.12**) and is nearly parallel to the fold axial surface. Similar stereographic projections for poles to main-stage stockwork veins of the Stwk Cb-Qz-Py(Po)±Ab-Au vein and Breccia 2 ore types (**Figure 5.13**) and poles to the main schistosity (**Figures 5.14a**), indicate that the vein-breccia system and post-ore schistosity are deformed by a north-northwest plunging fold. Poles to crenulation cleavage planes (**Figure 5.14 b**) are broadly coincident with the main schistosity great circle shown on **Figure 5.14a**, indicating that the attitude of S_{n+1} is compatible with the folding of S_n.

Geometric relations between the fold and crenulation cleavage depicted in schematic cross-sections and stereographic projections, suggest that these post-ore structures formed coevally as a result of near-vertical shortening. Accordingly, the fold and its related crenulation cleavage are interpreted as an F_3 fold and S_3 planar fabric because they overprint the z-fold and main schistosity interpreted as regional F_2 fold and S_2 schistosity.

Figure 5.11 - Example of highly-strained, main-stage stockwork vein mineralization at upper mine levels. Photograph of the Stwk Cb-Qz-Py(Po)±Ab-Au vein ore type deformed by the deposit's main schistosity (S_n) and crenulation cleavage (S_{n+1}).

Ore drift 3025, "D" zone, Kiena Mine level 30.

Exemple de minerai ayant subit une forte déformation aux niveaux supérieurs de la mine. Photo du minerai de type "Stwk Cb-Qz-Py(Po)±Ab-Au" déformé par la schistosité principale du gisement (S_n) et le clivage de crénulation (S_{n+1}).

Galerie à minerai 3025, zone "D", niveau 30 Mine Kiena.

Figure 5.12 - Example of highly-strained rocks at upper mine levels. Photograph of talc-chlorite-sericite±albite schist in contact with high-grade breccia ore of the S-50 zone. The schist is laced with carbonate-quartz stockwork vein deformed by the deposit's main schistosity (S_n) and crenulation cleavage (S_{n+1}).

Access drift 3814, "B" zone, Kiena Mine level 38.

Example de roche ayant subit une forte déformation aux niveaux supérieurs de la mine. Photo d'un schiste à talc-chlorite-séricite±albite en contact avec la brèche à forte teneur de la zone S-50. Le schiste est lacéré par des veines à carbonate-quartz en stockwork ayant été déformées par la schistosité principale (S_n) du gisement et le clivage de crénulation (S_{n+1}).

Galerie d'accès 3814, zone "B", niveau 38 Mine Kiena.

Figure 5.11

Figure 5.12

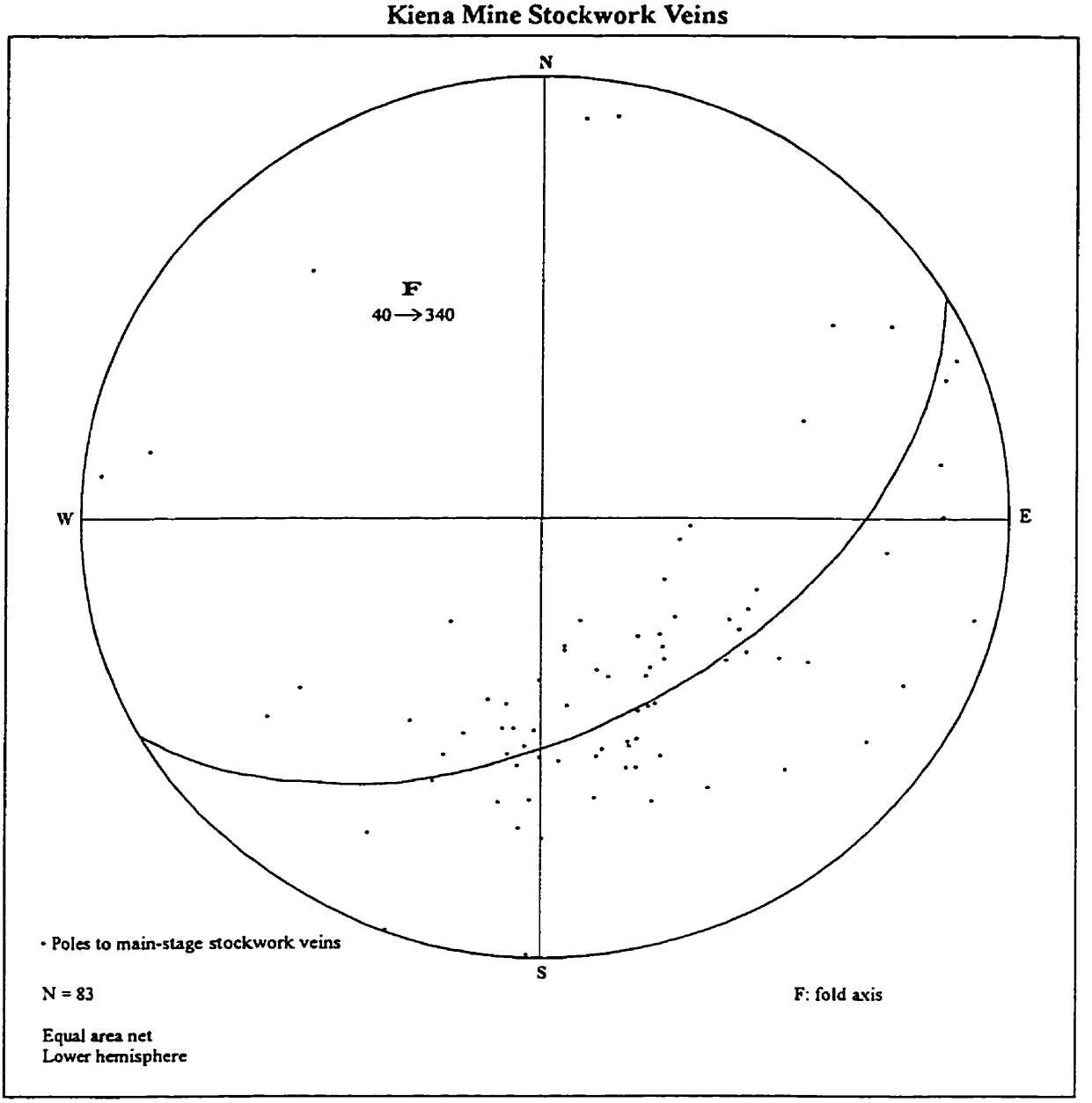

Figure 5.13 - Stereographic projection of poles to main-stage stockwork veins of the Stwk Cb-Qz-Py(Po)±Ab-Au vein and Breccia 2 ore types across the Kiena orebody. The scatter of poles near a great circle shows that the vein-breccia system is deformed by a north-northwest-plunging fold (see also sections 12438.4 N and 12514.6 N in back pocket). Data from Table D.5, Appendix D.

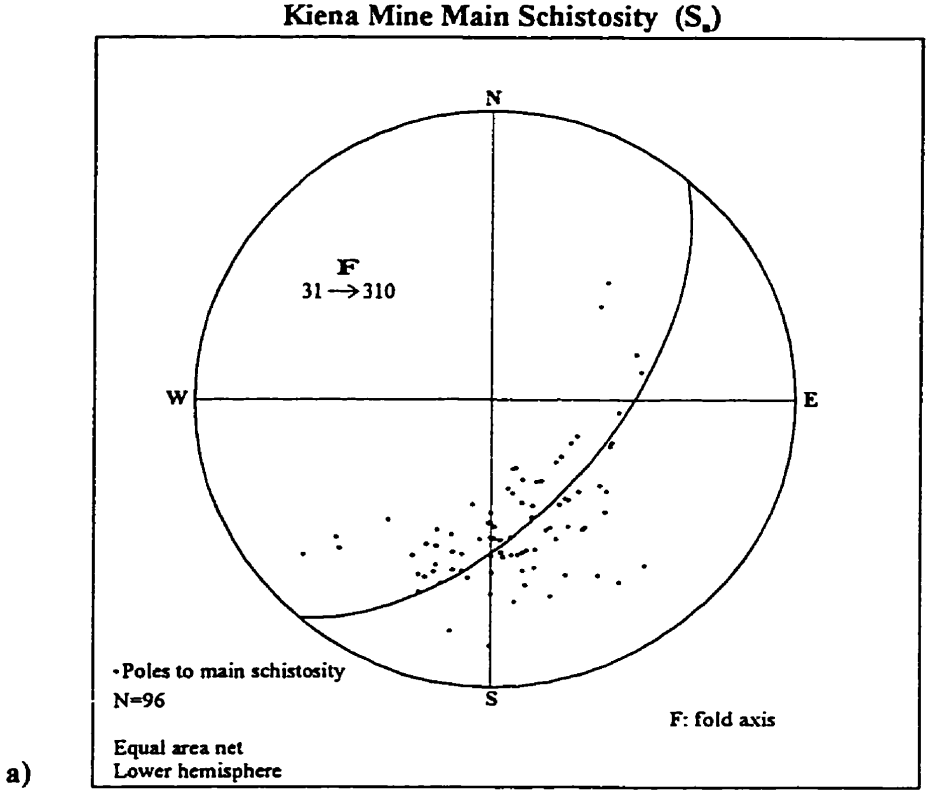

a)

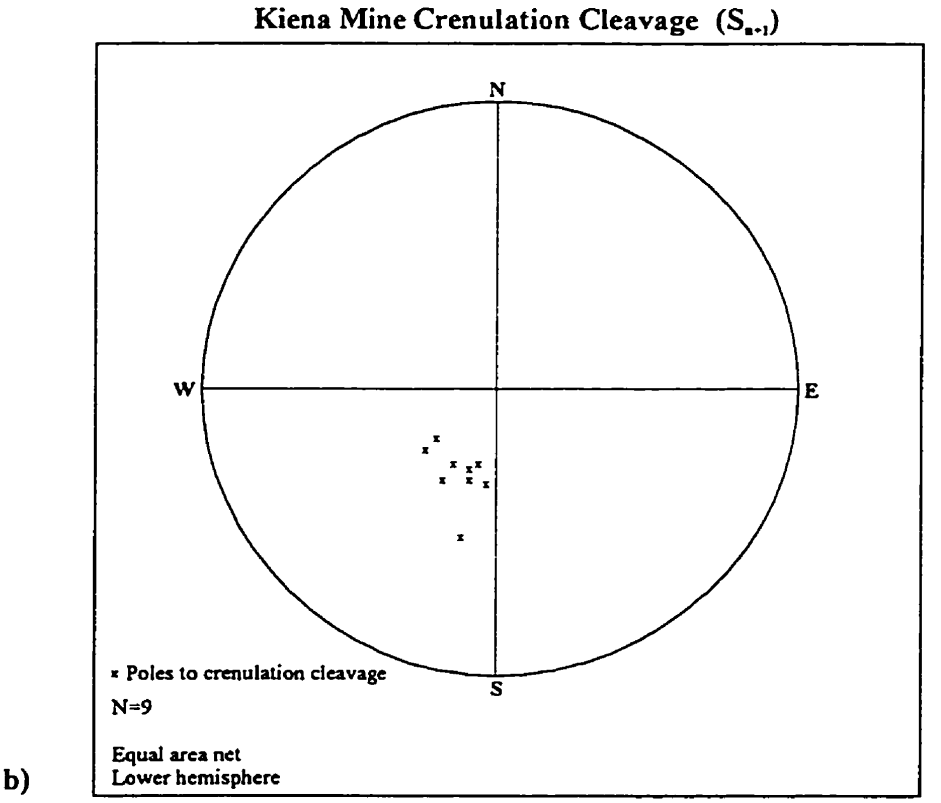

b)

Figure 5.14 - Stereographic projection of poles to main schistosity and crenulation cleavage planes across the Kiena deposit: a) scatter of poles to main schistosity near a great circle, similar to the stereographic projection obtained for mineralized stockwork veins shown on Figure 5.13, b) cluster of poles to crenulation cleavage partly overlapping with the main schistosity great circle shown on Figure 5.14a.

5.4.3 Late-stage oblique-slip faults

Two major oblique-slip faults cut the ore-dike complex of the Kiena deposit along the eastern and western ore-wallrock contacts. The faults, which strike northeast and dip steeply to the northwest, are mapped through the entire vertical extent of the orebody (see level maps 33 and 41 in back pocket). Striations on the surface of these brittle faults indicate that displacement is a combination of the northwest side moving to the left and down. In the absence of reliable markers around the fault planes, the magnitude of the displacement along these structures is unknown. These two oblique-slip faults were previously interpreted as early, shear zone faults controlling gold mineralization and post-ore deformation (Roy, 1983; Bourget, 1986; Quirion, 1988). However, they are clearly post-ore structures unrelated to mineralization or the bulk of deformation because they cut the deposit's main schistosity and the limbs of the z-fold (**Figure 5.15** and level map 33 in back pocket).

Another important post-ore structure, mapped at level 41 during this study, consists of a ductile fault zone cutting across the southern hinge of the deposit's z-fold and late-stage oblique slip faults (e.g. level map 41 in back pocket). It strikes northwest and dips steeply to the southwest. By contrast with the oblique-slip faults which present discrete fault surfaces, this fault consists of a mylonite zone composed of talc-chlorite-sericite±albite schist laced with carbonate-quartz stockwork veins (**Figure 3.18**, see also Index map 41-38 in back pocket). This mylonite zone is also characterized by the presence of large fragments of altered and weakly mineralized albitite dike (**Figures 3.17**). Striations on slip-planes at the margins of the mylonite zone indicate that the southwest block moved to the left and up relative to the footwall block. This structure probably extends to the upper and lower mine levels, but was not mapped because the corresponding areas on level 33 and 43 had been mined-out and closed-off.

Figure 5.15 - Example of post-ore oblique-slip fault located at the eastern margin of the Kiena orebody. This fault, which strikes N225 and dips 65° to the northwest (to the right), cuts the ore and the main post-ore schistosity (S_n). Striations on the slickensided fault surface indicate that the fault block composed of Breccia ore moved to the left and down relative to the footwall block (see also Level Map 43 located in back pocket).

Ore drift 4313, "B" Zone, Kiena Mine level 43.

Exemple de faille de décrochement postérieure à la minéralization, située en marge du corps minéralisé de la mine Kiena. Cette faille, qui est orientée N225 et pend 65° vers le nord-ouest (vers la droite), recoupe le minerai ainsi que la schistosité principale du gisement (S_n). Les stries gravées sur le plan de faille indiquent que le bloc faillé à minerai de type Brèche s'est déplacé vers la gauche et vers le bas par rapport au block formant le mur de la faille (voir également le plan niveau 43 situé en pochette).

Galerie à minerai 4313, zone "B", niveau 43 Mine Kiena

5.5 STRAIN PARTITIONING ACROSS THE ZONED OREBODY

The Kiena deposit is characterized by variations in strain intensity across the width and vertical extent of the orebody (**Figure 5.16**). Strain intensity was estimated on the basis of intensity of penetrative fabric development and the degree of preservation of relic primary igneous or hydrothermal textures (i.e. porphyritic, cockade textures etc.) observed in the deformed rocks. Rocks showing the least amount of deformation and the best preserved igneous/hydrothermal textures occur in the central part of the deposit (**Figure 5.16**) and coincide with high-grade, albite-cemented breccias and carbonate-pyrite replacement veins (e.g. **Figure 4.19**). The Stwk Cb-Qz-Py(Po)±Ab-Au vein ore type and albitite dikes show moderate strain at upper mine levels (**Figure 5.17**), but show high-strain at lower mine levels (**Figure 5.18**). Differences in strain intensities in the same ore type but at different mine levels, suggest that deformation increases with depth. This is compatible with the progressive disappearance of stilpnomelane and actinolite and the progressive appearance of hornblende in metamorphosed altered volcanic rocks around the orebody with increasing depth. However, the greater strain observed in the stockwork vein ore in albitite dikes at lower mine levels may be attributed also to more intense chlorite vein alteration in the root of the hydrothermal system prior to deformation (see **Figures 4.4** and **4.23**). The fact that different ore types show different strain intensities at the same depth, is interpreted as strain partitioning between rocks of different competency (see **Figure 4.7** and **Figures 4.10** and **5.11**). As Kiena's tholeiitic and komatiitic volcanic host rocks were subjected to successive overprinting alteration phases prior to deformation, this competency contrast is attributed to initial differences in rock compositions and/or hydrothermally-enhanced competency during the pro-grade alteration-mineralization process. Similarly, the discontinuous talc-chlorite schist zones surrounding the orebody (see level maps and sections in back pocket), are interpreted as deformed and metamorphosed, hydrothermally-altered basaltic komatiite. The deformational behaviour of rocks at the Kiena deposit is thus related to albite, carbonate, and phyllosilicate hydrothermal alterationprior to deformation. As a rule, albite and carbonate-altered rocks are more competent and the least-deformed, whereas albite-carbonate-poor and

Figure 5.16 - *Schematic north-south longitudinal section of the Kiena deposit, looking east, showing the partition of penetrative strain across the orebody (see text for details).*

Section longitudinale schématique de la minéralisation de la mine Kiena, orientée nord-sud avec regard vers l'est, montrant la répartition de la déformation pénétrative à travers le gisement (consulter le texte pour de plus amples détails).

STRAIN PARTITIONING ACROSS THE KIENA MINE DEPOSIT

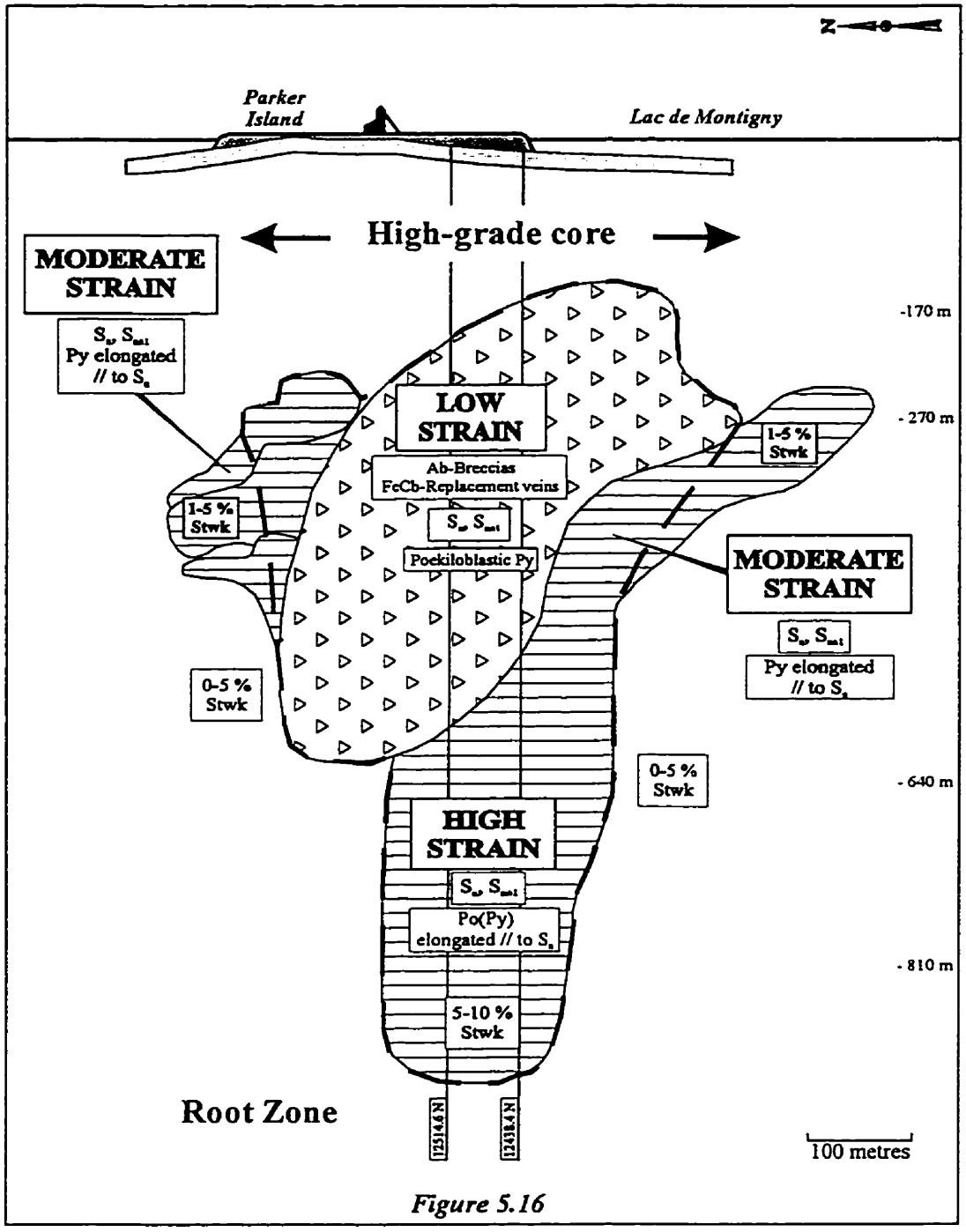

Figure 5.16

Breccia 1 and Breccia 2 ore

Stwk Cb-Qz-Py(Po)±Ab-Au ore

Contour of high-grade ore

S_o, S_{ss1} Main schistosity, crenulation cleavage

Stwk Cb-Qz-Py(Po)±Ab-Au ore: carbonate-quartz±albite stockwork veins with disseminated pyrite and/or pyrrhotite and native gold; Breccia 1 ore: carbonate-pyrite-gold replacement veins: Breccia 2 ore: albite stockwork veins with disseminated pyrite, ±chalcopyrite, ±scheelite and native gold.

Figure 5.17 - Example of moderately-strained "Stwk Cb-Qz-Py(Po)±Ab-Au" vein ore type at upper mine levels. Veins are boudinaged and deformed by folds, but relic vein-infill textures are preserved in some veins (breccia and crustiform texture)..

Sample K90-3627-076, ore drift 3627, "J" zone, Kiena Mine level 36.

Exemple de la déformation d'intensité moyenne affectant le minerai de type "Stwk Cb-Qz-Py(Po)±Ab-Au". Malgré que les veinules soient boudinées et déformées par des plis, elles ont préservé les reliques de leurs textures de remplissage (brèche, texture crustiforme).

Échantillon K90-3627-076, galerie à minerai 3627, niveau 36 Mine Kiena.

Figure 5.18 - Example of highly-strained Stwk Cb-Qz-Py(Po)±Ab-Au vein ore type at lower mine levels. The rock is strongly schistose and original vein-infill textures are almost entirely obliterated by strain. Veins, wall-rock fragments in the veins, and deformed pyrrhotite grains are all reoriented parallel to schistosity.

Sample K92-6446-220, ore drift 6446, lower "C" zone, Kiena Mine level 64.

Exemple de minerai de type "Stwk Cb-Qz-Py(Po)±Ab-Au" fortement déformé. Cette roche est très schistosée et la texture originale de remplissage des veines bréchiques est presqu'entièrement oblitérée par la déformation. Les veines, les fragments d'éponte dans les veines, ainsi que les grains disséminés de pyrrhotite déformée sont tous réorientés parallèlelement à la schistosité.

Échantillon K92-6446-220, galerie à minerai 6446, zone "C" inférieure, niveau 64 Mine Kiena.

Figure 5.17

Figure 5.18

Figure 5.19 - *Example of strain partitioning between an albite-altered rock and albite-iron carbonate vein. The albitite and the vein are cut by chlorite-stilpnomelane veins and overprinted in turn, by the deposit's main schistosity (S_n). In the hangingwall of the albite-carbonate vein, deformed chlorite-stilpnomelane veinlets are subparallel to schistosity, but the same veinlets are reticulated and appear undeformed as they cut across the more competent albite-carbonate vein.*

Ore drift 4117, "B" zone, Kiena Mine level 41.

Exemple de la répartition de la déformation entre une roche fortement albitisée et une veine à albite et carbonate de fer. L'albitite et la veine sont recoupées par des veinules de chlorite et stilpnomélane ainsi que par la schistosité principale du gisement (S_n). Les veinules de chlorite-stilpnomélane situées dans l'éponte supérieure de la veine d'albite-carbonate sont déformées et subparallèles à la schistosité, tandis que les même veinules sont réticulées et n'apparaissent pas déformées lorsqu'elles recoupent la veine d'albite-carbonate de plus forte compétence.

Galerie à minerai 4117, zone "B", niveau 41 Mine Kiena.

phyllosilicate-rich rocks are less competent and more deformed, particularly in the margins of the breccia body of the S-50 zone.

5.6 SUMMARY

The hierarchy of pre-, syn-, and post-ore structures shows that mineralization is localized in a brittle fracture system formed prior to penetrative fabric development (**Table 5.1**). Mineralization is confined to an upward-flaring, magmatic-hydrothermal fracture system developed in a regional, bedding-parallel fault named the Kiena Mine Fault Zone. The fracture pattern defined by ore structures is akin to that of porphyry ore systems emplaced at relatively high levels in the crust. The orebody is deformed by a z-fold and related east-west schistosity followed by the deformation of the ore-dike complex and the main schistosity by a moderately, north-northwest plunging fold and gently, east-dipping crenulation cleavage. The z-fold and its axial planar schistosity are inferred to have formed predominantly under flattening strain, whereas the broad, open fold and the axial planar crenulation cleavage are probably the result of near-vertical shortening. Based on criteria set forth by Dimroth *et al.* (1982, see Chapter 2) and a comparison with the z-fold structure occurring at the Camflo deposit, Kiena's main schistosity is interpreted as the regional synmetamorphic S_2 schistosity. Similar rock types show contrasting style of deformation at upper and lower mine levels, suggesting that the intensity of deformation increases with depth. Strain partitioning is invoked to explain differences in strain intensities between different rock types occurring at same depth in the mine, as a result of competency contrasts acquired during the development of a zoned alteration-mineralization sequence characterized by early, inner albitization. The presence of gold slickenfibres on schistosity planes suggests the local remobilization of a minor quantity of gold during post-ore deformation.

CHAPTER 6 GEOCHRONOLOGY

6.1 INTRODUCTION

Having established the relative timing of gold mineralization in the previous chapter as predating penetrative deformation and greenschist facies metamorphism, the focus of this chapter is on the precise U-Pb zircon dating of the Kiena deposit porphyry dikes and Snowshoe stock and $^{40}Ar/^{39}Ar$ dating of ore-related hydrothermal vein biotite. This is followed by a discussion of the absolute age of gold-ore formation at Kiena in relation to other isotopically dated geological events in the Val d'Or-Malartic area.

The concordant U-Pb zircon date of 2686 ± 2 Ma obtained for igneous zircons from the Kiena deposit intermineral granodiorite dike assigns a firm lower age constraint on gold mineralization, and by extension, a maximum age for the regional synmetamorphic S_2 schistosity. The concordant U-Pb zircon date of 2697 ± 2 Ma obtained for xenocrystic zircons from the intermineral feldspar porphyry dike, on the other hand, suggests a close time relationship between the intermineral dikes and the Snowshoe stock dated as 2693 ± 2 Ma. A much younger, $^{40}Ar/^{39}Ar$ plateau age of 2313 ± 14.9 Ma acquired for a magmatic-hydrothermal biotite, in addition to several disturbed age spectra for similar biotites, are interpreted as thermally reset ages of pre-metamorphic gold-related alteration. The crystallization age of 2686±2 Ma for the granodiorite porphyry cutting the ore and the overprint of the regional S_2 schistosity, suggest that gold mineralization at Kiena is coeval with a district-wide episode of orogenic calc-alkaline to alkaline plutonism at ca. 2694 to 2680 Ma, which closely followed the tilting of volcanic strata (D_1, ca. 2700-2694 Ma) but preceded regional synmetamorphic deformation and fabric development (i.e. D_2, ca. 2677-2645 Ma). The minimum age of 2692 ± 2 Ma obtained for gold mineralization cut by a granodiorite dike at the neighbouring Norlartic deposit, is compatible with that of 2686 ± 2 Ma acquired at Kiena, lending additional support to early gold mineralization in the Val d'Or plutonic belt. Gradually younging post-metamorphic isotopic dates from hydrothermal

minerals associated with gold-bearing veins at other deposits in the belt, have produced a drawn-out series of dates for gold mineralization from minerals with progressively lower blocking temperatures. This trend is tentatively interpreted as a cooling path following the peak of the Kenoran orogeny in the Val d'Or-Malartic area, punctuated by episodic hydrothermal events in faults zones across the district between ca. 2600 and 2300 Ma.

6.2 U/Pb ZIRCON AGE DATING OF INTERMINERAL PORPHYRY DIKES

Samples of the granodiorite dike, the feldspar porphyry dike, the host volcanic rocks of the Jacola Formation and altered breccias were collected in the mine and mineralogically separated using standard procedures of the Royal Ontario Museum (Krogh (1973; 1982a; 1982b); **Table 6.1**). Zircons were separated from the dike samples and from the Snowshoe stock, a small granodiorite intrusion located under Lac de Montigny approximately 4 kilometres north of Kiena (Sauve (1987); **Figure 2.2**). Other samples were devoid of useful uranium-bearing minerals other than small amount of tiny rutile crystals in one of the breccia samples. Sample preparation and isotopic geochemical analyses were performed by Dr. Hardolph Wasteneys at the Royal Ontario Museum. The zircons were dissolved in equilibrium with a mixed $^{205}Pb/^{235}Pb$ spike in Teflon capsules at 220°C and the U and Pb purified by HCl anion exchange procedures as developed by Krogh (1973; 1982a; 1982b). Isotopic ratios were measured with a Daly detector in a VG354 mass spectrometer in a dynamic peak hopping mode. Isotopic uncertainties were calculated by numerical propagation of measurement uncertainties and established uncertainty in the isotopic composition of common lead and spike.

Two granodiorite dike samples were collected on level 30 of the mine (see **Figure 3.27**) and euhedral, sharp-faceted prismatic zircons with 3:1 axial ratios were separated from both samples (**Figure 6.1**). The zircons are commonly pale brown and optically devoid of cores, but to test for inherited components, tips were broken off from larger prisms and analysed individually. The zircons were abraded to remove surficial lead loss domains apparent in one

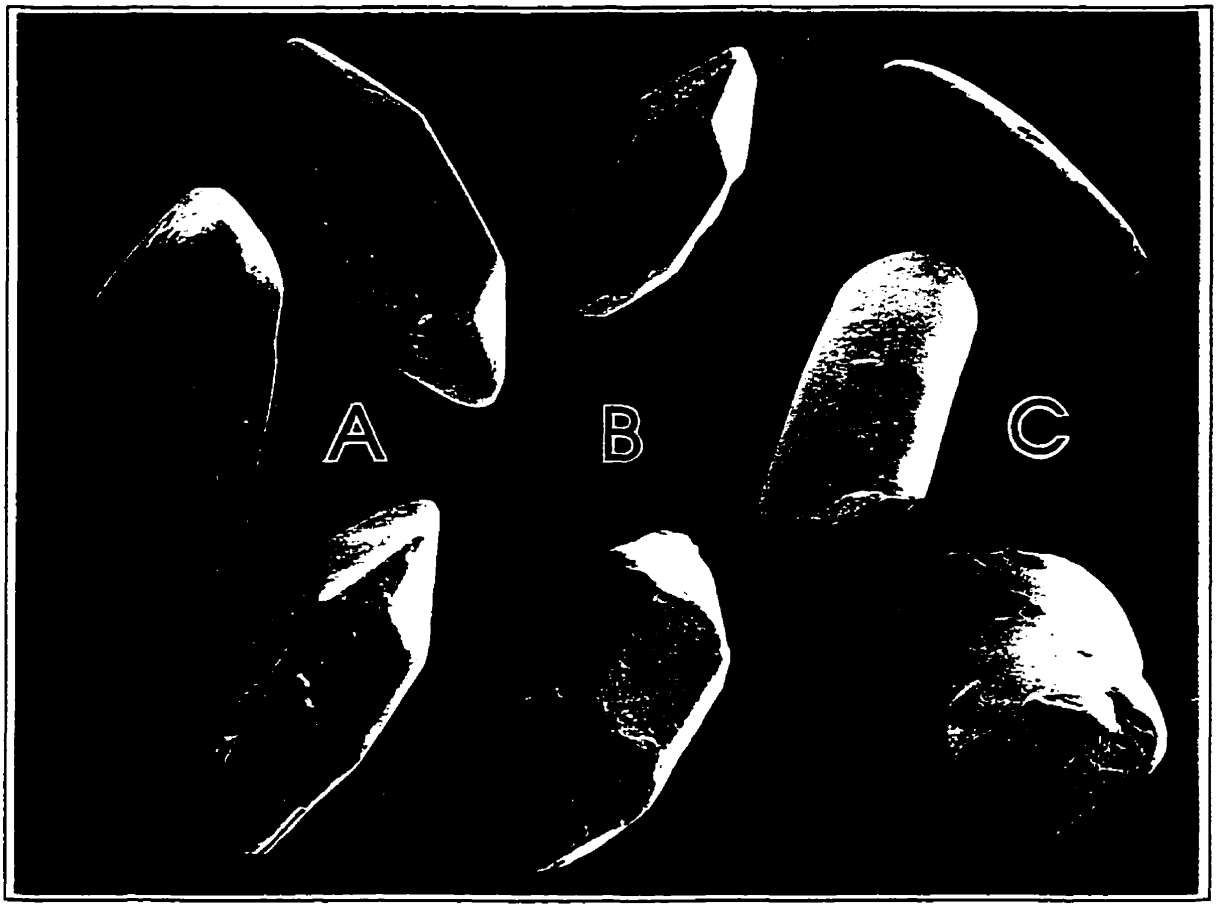

Figure 6.1 - *Composite scanning electron photomicrographs of zircons similar to those analyzed showing morphological contrast between euhedral crystals separated from the intermineral granodiorite dike (A, 3 grains to the left) and the Snowshoe stock (B, 2 central grains), and the resorbed grains typical of the intermineral feldspar porphyry dike (C, 3 grains to the right). The images are at various magnification. Average grain masses are 0.002 g for A, 0.002 g for B, and .015 g for C.*

Microphotographie composite de zircons similaires à ceux qui ont été analysé, prise à la microsonde à balayage, montrant la morphologie contrastante des zircons euhédraux provenant du dyke de granodiorite interminéralisation (A, 3 grains sur la gauche) et du stock de Snowshoe (B, 2 grains au centre), et des zircons résorbés qui sont caractéristiques du dyke deporphyry feldspatique interminéralisation (C, 3 grains sur la droite). Le plan de rapprochement varie d'une image à l'autre. La masse moyenne des grains est de 0.002 g pour A, 0.002 g pour B, et de .015 g pour C.

Table 6.1 Mass calculations of volumetric estimates of U and Pb isotopes measured from zircons of the Snowshoe stock and Kiena Mine porphyry dikes

Description	Weight (mg)	U (ppm)	Th / U	Common Pb (pg)	$^{206}Pb/^{204}Pb$	$^{206}Pb/^{238}U$	1σ %	$^{207}Pb/^{235}U$	1σ %	$^{207}Pb/^{206}Pb$	1σ Ma	Disc. %
KIENA MINE INTERMINERAL GRANODIORITE DIKE												
A1 Hw101, 1 prism	0.002	21	0.34	1.6	842	0.38906	0.28	9.7036	0.37	2661	5.1	23.87
A2 HW129, 5 prisms	0.013	48	0.48	2.2	9167	0.51224	0.20	12.9703	0.20	2686	1.5	0.90
A3 HW3, 4 prisms	0.002	55	0.62	1.5	1804	0.51306	0.28	12.9916	0.28	2686	3.5	0.75
A4 HW27, 1 tip	0.002	300	0.49	1.8	10673	0.51565	0.18	13.0476	0.18	2685	1.4	0.19
A5 HW28, 1 tip	0.001	175	0.49	21.8	278	0.51642	0.30	13.1011	0.85	2689	12.6	0.24
A6 HW102, 1 prism	0.002	27	0.55	3.3	548	0.51811	0.48	13.1417	0.58	2689	6.6	-0.10
SNOWSHOE GRANODIORITE STOCK												
B1 HW104, 12 prisms	0.003	203	0.46	2.0	9645	0.51689	0.16	13.1453	0.16	2693	1.5	0.33
B2 HW205, 15 prisms	0.004	26	0.52	2.1	1595	0.51867	0.26	13.1825	0.29	2692	2.9	-0.06
KIENA MINE INTERMINERAL FELDSPAR PORPHYRY DIKE												
C1 HW204, 1 resorbed	0.009	34	0.79	4.3	2288	0.51819	0.16	13.2161	0.18	2698	1.3	0.29
C2 HW103, 1 resorbed	0.020	35	0.88	4.9	4690	0.51933	0.17	13.2258	0.17	2696	1.7	-0.03

Morasse et al. (1995)

Comment: *$^{206}Pb/^{204}Pb$ ratio corrected for fractionation and spike only. $^{206}Pb/^{238}U$ and $^{207}Pb/^{235}U$ corrected for total common lead, spike and fractionation. Decay constant from Jaffey et al. (1971). Common lead assigned to laboratory blank composition ($^{206}Pb/^{204}Pb$ = 18.3, 7/6 = 0.85, and $^{208}Pb/^{206}Pb$ = 2.056 and 4% uncertainty). U and Pb fractionation 0.1% amu loaded on Si-gel. Th/U model calculated on basis of $^{208}Pb/^{206}Pb$ (radiogenic) and $^{207}Pb/^{206}Pb$ age assuming concordance.*

Figure 6.2 - *Composite U/Pb concordia diagram of abraded zircon analyses shown in Table 6.1, from the intermineral granodiorite dike (A2, A6), Snowshow stock (B1, B2), and intermineral feldspar porphyry dike (C1, C2). Ellipses represent 2σ uncertainty in U-Pb isotope ratios calculated by numerical propagation of measurement deviations and uncertainties in isotopic compositions of the spike and common lead. Large uncertainty shown by dotted ellipses for points A5 and A6 represent relatively high common lead levels of 22 and 3.3 pg and low measured $^{206}Pb/^{204}Pb$ ratio. However, in spite of the large uncertainty the points are significant. A4 and A5 are crystal tip samples to test for inheritance which might have biased the age of the dike.*

Diagramme concordia U/Pb composite construit à partir des résultats d'analyse de zircons érodés par abrasion, montrées au Tableau 6.1. Les zircons proviennent du dyke de granodiorite interminéralisation (A2, A6), du stock de Snowshoe (B1, B2) ainsi que du dyke de porphyre feldspathique interminéralisation (C1, C2). Les ellipses représentent le degré d'incertitude 2σ lié au rapport isotopique U-Pb calculé à partir de la propagation numérique de la déviation des mesures, du degré d'incertitude rattaché à la composition du "spike", et du taux de plomb ambiant. La forte incertitude représentée par les ellipses pointillées qui sont rattachées aux points A5 et A6, est attribuée au taux anormalement élevé de plomb ambiant de 22 et 3.3 pg ainsi qu'au faible rapport $^{206}Pb/^{204}Pb$ chez ces zircons. En dépit de cela, ces points d'analyse ont une valeur significative. Les points A4 et A5 proviennent de l'analyse de la pointe de zircons du dyke de granodiorite, ceci afin de tenter de détecter un possible héritage dans le taux de plomb isotopique, ce qui aurait pu biaiser l'âge du dyke.*

* *Quantité connue d'un isotope artificiel ajouté à un soluté isotopique lors d'une analyse par dilution.*

Kiena Mine Composite Concordia Diagram

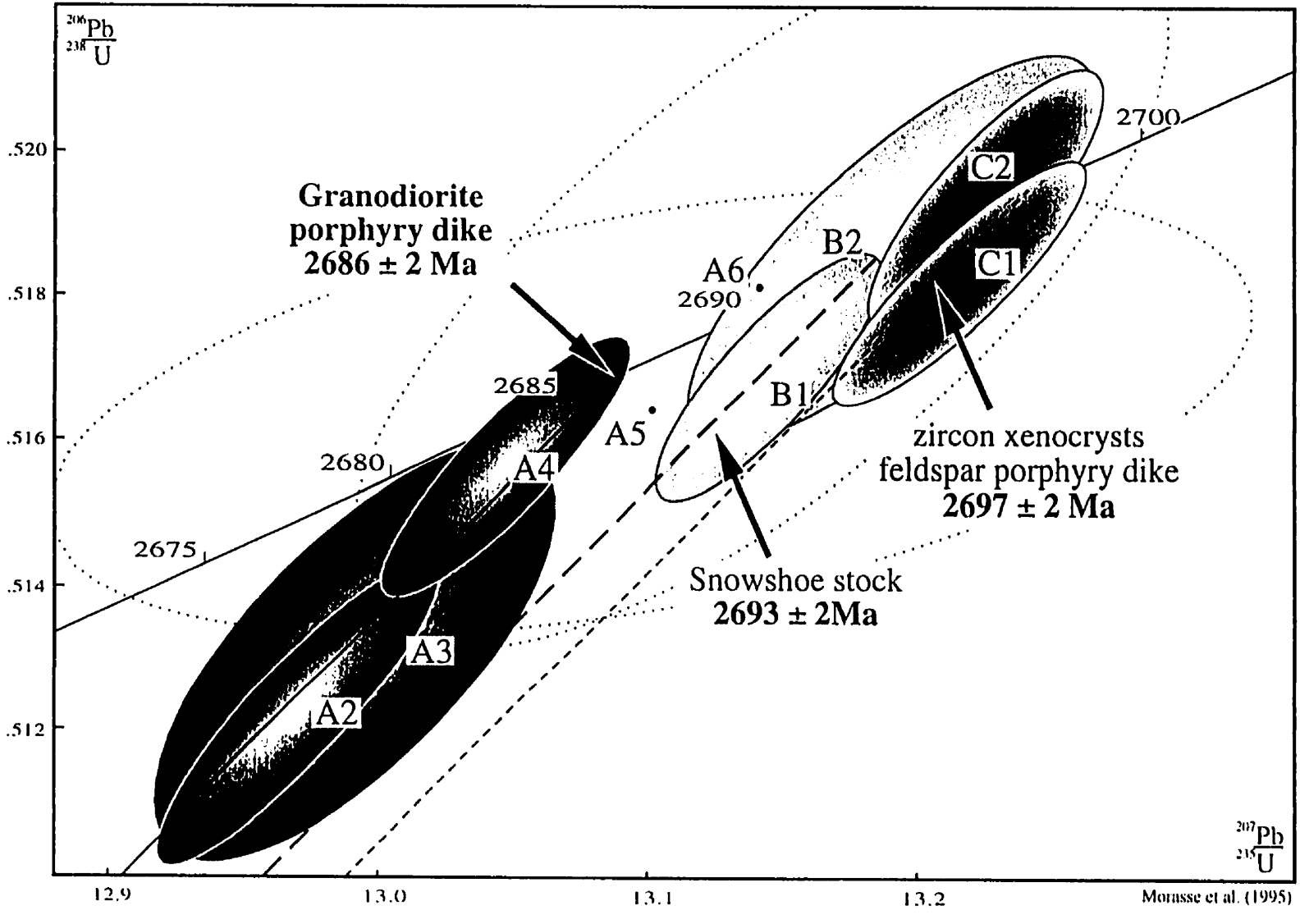

Figure 6.2

analysis (A1). Six single-grain or small fraction analyses of zircons from two samples of the dike define an unambiguous age of 2686 ± 2 Ma for crystallization of the dike (**Figure 6.2**). Two single prism ends (A4 and A5, **Figure 6.2**), analysed to bias measurements away from possible inherited components, yielded near-concordant U-Pb ages that are identical within uncertainty to two small multigrain fractions (A2 and A3, **Figure 6.2**) and a single prism (A6, **Figure 6.2**). A lower intercept of 500 Ma was established by discordant U-Pb ages for a single unabraded prism (A1). Although two of the analyses have low measured $^{206}Pb/^{204}$ Pb ratios caused by high common lead (A5 and A6, **Table 6.1**), the concordance of their U-Pb ages with those of the precise analyses is geologically significant in supporting the age of 2686 ± 2 Ma for the dike. The feldspar porphyry dike yielded a few zircons, all large (average grain masse of 0.015 mg) and distinctively resorbed into smooth irregular shapes (**Figure 6.1**), but was devoid of euhedral zircon crystals. Two resorbed grains that were analysed separately both yielded concordant U-Pb ages (C1 and C2, **Figure 6.2**) identical within 2σ uncertainty at an average age of 2697 ± 2 Ma. This age is significantly older than the age of the granodiorite dike, although geologic relations show coeval emplacement. The resorption textures are clearly compatible with an origin for the zircons as an inherited component of an older igneous body and, therefore, they are considered to be xenocrysts in the feldspar porphyry dike. The lack of unresorbed zircons in this dike suggests that undersaturation of the magma in zirconium caused resorption of the zircons assimilated from an older source. As part of the geochronology study at Kiena, small, sharp-faceted euhedral zircons separated from drill core samples of the Snowshoe stock (see **Figure 2.2** for location) were also analysed. Two zircon fractions (B1 and B2, **Figure 6.1**) yielded identical concordant U-Pb ages averaging 2693 ± 2 Ma (**Figure 6.2**). Proximity of the granodioritic Snowshoe stock to the Kiena deposit, in addition to similar ages for the Kiena feldspar porphyry dike inherited zircons (2697 ± 2 a) and the Snowshoe stock (2693 ± 2 Ma), suggest that the Snowshoe intrusion may share the same igneous source as that of the older zircon xenocrysts.

6.3 $^{40}Ar/^{39}Ar$ DATING OF HYDROTHERMAL VEIN BIOTITE

Samples of hydrothermal biotite were obtained from main-stage carbonate-albite-biotite-pyrite pegmatite vein (**Figure 6.3**) and late-stage biotite-magnetite-chlorite stringer veins (**Figure 6.4**), collected at various depths in the mine. The veins, which are deformed and schistose (see **Figures 4.8** and **6.4**), feature partially recrystallized biotite grains (see **Figures 4.20** and **5.8**). The pegmatitic biotite was picked by hand directly from the vein sample, whereas biotite concentrates from the stringer vein biotite were prepared from crushed and sieved samples. The preparation method is described in Appendix E. Isotopic geochemical analyses were performed by Dr. Sandra McBride at Queen's University.

Out of the four biotite separates analysed, only one yielded a significant plateau age of 2313 ± 15 Ma comprising approximately 84% of the ^{39}Ar released (**Figure 6.5**). This biotite is from one of the two samples of stringer vein biotite collected at mid-mine level. Based on the size fraction of the aliquot (80-100 mesh), it is doubtful that the age spectrum for this biotite displays a false plateau. Consequently, knowing that late-stage biotite stringer veins which are part of Kiena's alteration-mineralization sequence are metamorphosed and that 2686 ± 2 Ma is the minimum age for gold mineralization, this much lower age can only mean that the biotites have been thermally reset. The plateau age of ca. 2313 Ma probably represents the time at which the biotite last cooled through its closure temperature (approximately 300°C; Hanes, 1991). The date is thus interpreted as geologically significant but cannot be correlated with a known thermal event of this age. Medium-grade regional dynamothermal metamorphism in the Camflo Mine area approximately 10 km west of Kiena (< 450°C, Powell (1994)) is dated as ca. 2665 Ma (Powell, 1994; Powell et al., 1995a), whereas the S-type granite of the Lacorne batholith (410-450°C, Powell *et al.* (1995a)), approximately 12 km north of Kiena, is dated as ca. 2643 Ma (Feng and Kerrich, 1991). The only other significant regional thermal event occurring in the Kiena Mine area is the intrusion of the northeast-trending Preissac diabase dikes dated as ca. 2150 Ma (Hanes and York, 1979). As this event is younger than the ca. 2313 plateau age of the vein biotite and it is unlikely that

Figure 6.3 - Photograph of pegmatitic vein biotite similar to the aliquot of pegmatitic biotite analysed and represented on the $^{40}Ar/^{39}Ar$ age spectra shown in Appendix E.

Sample K91-3838-081, ore drift 3838, "B" and "C" zones, Kiena Mine level 38.

Photo de biotite pegmatitique similaire à celle composant la fraction de biotite analysée qui est représentée sur le spectre de détermination d'âge isotopique du système $^{40}Ar/^{39}Ar$ montré à l'Appendice E.

Échantillon K91-3838-081, galerie à minerai 3838, zones "B" et "C", niveau 38 Mine Kiena.

Figure 6.4 - Photograph of hydrothermal vein biotite similar to the aliquot of biotite analysed and represented on the $^{40}Ar/^{39}Ar$ age spectra shown on Figure 6.5.

Ore drift 4802, margins of "B" zone, Kiena Mine level 48.

Photo de biotite hydrothermale similaire à celle composant la fraction de biotite analysée qui est représentée sur le spectre de détermination d'âge isotopique du système $^{40}Ar/^{39}Ar$ montré à la Figure 6.5.

Galerie à minerai 4802, périphérie de la zone "B", niveau 48 Mine Kiena.

Figure 6.3

Figure 6.4

Age Spectra for Kiena Deposit Late-Stage Hydrothermal Vein Biotite

K91-3829-185 biotite

Run: SM146 90/103

Date: July 14/92

Mass: 15.5 mg

J Value: 0.02484

Aliquot: grinded and paper filter sieved 80-100 mesh fraction

Comment: trace of chlorite, pre-metamorphic

Total ^{39}Ar: 32.892 E-8 cm^3 NTP, Approx 12% K

Integrated Age: 2291.9 ± 15.6 Ma

Plateau Age: 2313.3 ± 14.9 Ma (84.5% of ^{39}Ar, steps marked by *)

Location: Vein biotite-magnetite-chlorite overprinting Cb-Qz-Py(Po)-±Ab-Au stockwork vein mineralization of lower-grade ore shell, 'L' ore zone, ore drift 38-29

Analyzed by: S. McBride, Queen's University

	Tem °C	40/39	36/39	37/39	Vol ^{39}A E-8 cm^3	Fraction ^{39}Ar	%^{40}Ar Rad	Age Ma	±	Error 2 sigma
	550	72.107	0.0080	0.002	1.429	0.043	96.67	1813.0	±	10.4
	600	102.758	0.0017	0.000	2.453	0.075	99.47	2280.3	±	24.7
*	675	105.320	0.0005	0.000	2.393	0.073	99.82	2316.8	±	13.9
*	750	105.050	0.0008	0.000	5.087	0.155	99.75	2312.5	±	23.0
*	830	104.698	0.0009	0.000	5.688	0.173	99.72	2307.8	±	7.4
*	890	104.279	0.0006	0.000	6.297	0.191	99.82	2303.8	±	12.8
*	940	105.109	0.0010	0.000	4.628	0.141	99.69	2312.5	±	12.0
*	1000	107.174	0.0010	0.000	3.684	0.112	99.69	2337.9	±	22.9
	1150	111.964	0.0032	0.013	1.233	0.037	99.14	2388.2	±	19.4

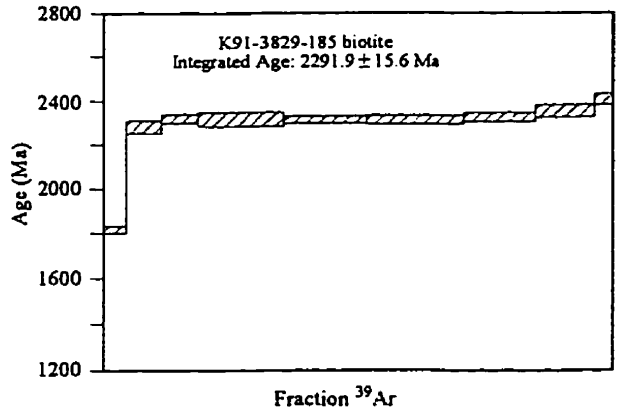

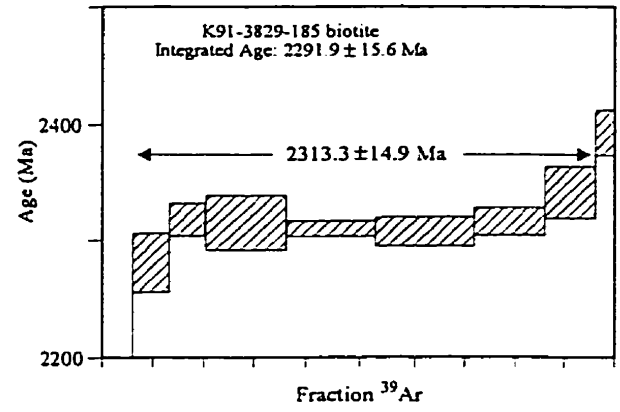

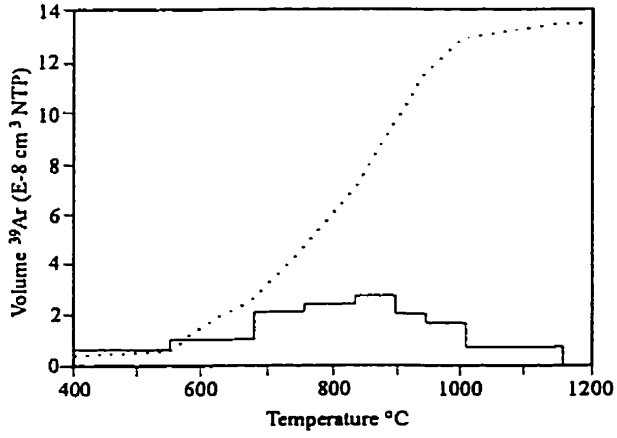

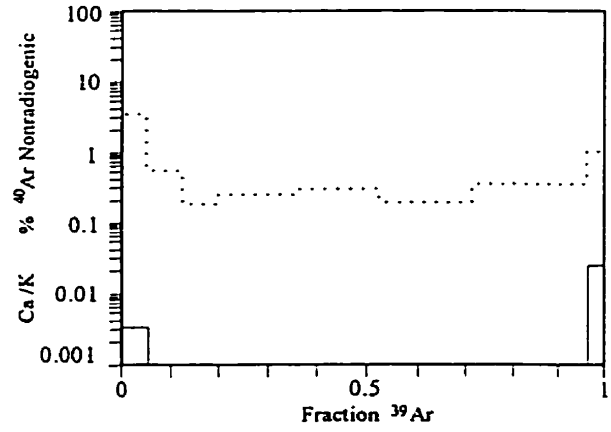

Figure 6.5

Kiena hydrothermal biotites took ca. 330 millions years to cool through their blocking temperature following the Lacorne batholith intrusion, the cause of the thermal resetting may be attributed to hydrothermal fluids permeating the Kiena deposit fault zone following post-orogenic magmatism (refer to Regional Sequence of Events diagram in back pocket).

The other age spectra, including the one obtained from the main-stage pegmatitic biotite, are disturbed (see **Appendix E**). These spectra are characterized by monotonically climbing (K91-U2417-124), saddle-shaped (K91-3838-140) or sagging (K91-3828-170) profiles. The thermal disturbances could be caused in part by the inhomogeneity of the separate (chloritization of the biotite) and, based on the geometry of the profiles, by the effects of variable argon loss (e.g. Hanes (1991)). The age spectrum of the pegmatitic biotite (K91-3838-140) is also characterized by a high apparent date in the initial gas step, which is generally interpreted as the effect of excess argon at grain boundary sites (Hanes, 1991). It is thus concluded that isotopic $^{40}Ar/^{39}Ar$ biotite dates cannot be used to interpret the age of the Kiena gold mineralization. The low blocking temperature of this mineral and its propensity to alteration appear to predominantly yield age spectra with individual gas steps that cannot be interpreted geologically. All age spectra, including that with the plateau age of ca. 2313 Ma, show that primary hydrothermal biotites of the Kiena deposit have been thermally reset.

6.4 GOLD MINERALIZATION AT KIENA IN RELATION TO OTHER GEOLOGICALEVENTS IN THE VAL D'OR-MALARTIC AREA

The timing of geological events marking the evolution of the Val d'Or-Malartic area has been constrained by age determinations derived from three main radiometric systems including U-Pb, K-Ar and Sm-Nd. These ages, with their corresponding references, are reported in Table **6.2** and they are represented in a regional time sequence diagram appearing in one of the pockets located in the back cover of this thesis.

Table 6.2 Summary of geochronological data for the Val d'Or-Malartic region

VOLCANISM AND ASSOCIATED SUB-VOLCANIC EVENTS	AGE (Ma)	ISOTOPIC SYSTEM	SOURCE
Ultramafic volcanism	2710±(5,4)	U-Pb / zircon altered xenoliths in Bourlamaque "batholith"	Taner and Trudel, 1989
Val d'Or Formation Colombière "rhyolite"	2704.7± 1.1	U-Pb / zircon	Wong et al., 1991
Sigma Mine porphyritic diorite ("C" porphyry)	2703.7± 2.5	U-Pb / zircon	Wong et al., 1991
Blake River Group	2701 ± 2	U-Pb / zircon	Corfu et al., 1989
rhyolite	2698 ± 1	U-Pb / zircon	Mortensen, 1987
Bourlamaque "batholith"	2711 ± 12	SHRIMP	Claoué-Long et al., 1990
(Val d'Or Formation)	2699.8 ± 1	U-Pb / zircon	Wong et al., 1991
PLUTONIC EVENTS	**ca. 2694-2680 Ma**		
Kiena Mine feldspar porphyry dike	2693 ± 3	U-Pb / inherited zircon	Morasse et al., 1993
Snowshoe granodiorite stock	2693 ± 2	U-Pb / zircon	Morasse et al., 1993
Sigma - Lamaque Mines feldspar porphyry dikes ("G" dikes)	2694 ± 2.2	U-Pb / zircon	Wong et al., 1991
Norlartic Mine tonalite dike	2692 ± 2	U-Pb / zircon	Pilote et al., 1993
Kiena Mine intermineral granodiorite dike	2686 ± 2	U-Pb / zircon	Morasse et al., 1993
Lamaque Mine diorite-tonalite stock	2685 ± 3	U-Pb / zircon	Jemielita et al.,1989
	2682 ± 2	U-Pb / titanite	
Camflo Mine quartz-monzonite stock	2685 ± 7,8	U-Pb / zircon	Zweng and Mortensen, 1985
	2683 ± 3	U-Pb / zircon	Jemielita et al., 1990
	2680 ± 6	U-Pb / titanite	Jemielita et al., 1989

Table 6.2 continued...

GOLD MINERALIZATION EVENTS	ca. 2694-2680 Ma: (2694-2686 Ma) (2680-2677 Ma)		
Bras d'Or Mine hydrothermal zircons in quartz-tourmaline vein	2693 ± 2 2688 ± 7	U-Pb / zircon	Kerrich and Kyser, 1994
Norlartic Mine post-ore tonalite dike	> 2692 ± 2	U-Pb / zircon	Pilote et al., 1993
Kiena Mine intermineral granodiorite dike	> 2686 ± 2	U-Pb / zircon	Morasse et al., 1993
Sigma - Lamaque Mines: pre-ore diorite-tonalite	< 2685 ± 3	U-Pb / zircon	Jemielita et al., 1989
"shear" vein hydrothermal zircons	2682 ± 8	SHRIMP	Claoué-Long et al., 1990; Claoué-Long et al., 1992; Kerrich and King, 1993
"shear" vein coarse-grained hydrothermal scheelite	2602 ± 20	Sm/Nd / scheelite	Anglin, 1990
"shear" vein hydrothermal rutile (alteration halo)	2599 ± 9	U-Pb / rutile	Wong et al., 1991
	2593 ± 7	U-Pb / rutile	Jemielita et al., 1989
"shear" vein, coarse-grained hydrothermal muscovite	2579 ± 3	$^{40}Ar/^{39}Ar$	Hanes et al., 1989
Bevcon Mine: hydrothermal zircons from Au-bearing vein	2681 ± 6	SHRIMP	Claoué-Long et al., 1990
Camflo Mine: pre-ore quartz-monzonite	< 2685 ± (7,8)	U-Pb / zircon	Zweng and Mortensen, 1985
gold-bearing vein (titanite from alteration halo)	2625 ± 7	U-Pb / titanite	Jemielita et al., 1989
Stage 3 gold-bearing veins (post-main-stage mineralization)* hydrothermal titanite and K-spar	2621 ± 4	U-Pb / titanite	Zweng et al., 1993 (* Spooner and Barrie (1993), p. 1317)
gold-scheelite-bearing vein (rutile)	2600 ± 3	U-Pb / rutile	Zweng, 1990 Jemielita et al., 1990

Table 6.2 continued...

REGIONAL THERMAL METAMORPHISM RELATED TO POST-D_1 PLUTONIC EVENTS (VAL D'OR PLUTONIC BELT)		**ca. 2694-2680 Ma**	
Core of amphibole Sigma Mine "C" porphyry	2693 ± 11	$^{40}Ar/^{39}Ar$ magnesio-hornblende	Hanes et al., 1989
Metamorphic rutile Val d'Or Formation Colombière "rhyolite"	2684 ± 7	U-Pb / rutile	Wong et al., 1991
Rim of amphibole Sigma Mine "C" porphyry	2171 ± 17	$^{40}Ar/^{39}Ar$ ferro-hornblende	Hanes et al., 1989
POST-D_1 LOCAL UPLIFT AND RELATED SEDIMENTATION EVENTS		**ca. 2695-2680 Ma and < 2680 Ma**	
ABITIBI SUBPROVINCE (north of CTZ)	**ca. 2695-2680**		
Lac Caste Formation greywackes	< 2695 ± 4	$^{207}Pb/^{206}Pb$ detrital zircons	Feng and Kerrich, 1991
Cadillac Group graywackes	< 2688 ± 3	U-Pb / detrital zircons	Davis, 1991
Kewagama Group graywackes (equivalent to "early Timiskaming phase" of Corfu (1993) at ca. 2687-2685 Ma)	ca. 2687-2683		
	< 2687 ± 3	U-Pb / detrital zircons	Davis, 1991
	> 2685 ± (7,8)	U-Pb / detrital zircons	Zweng and Mortensen, 1985
	> 2682 ± 3	U-Pb / detrital zircons	Mortensen, 1993
PONTIAC SUBPROVINCE (south of CTZ)	**< 2683**		
Pontiac Group graywackes	< 2683 ± 1	U-Pb / detrital zircons	Mortensen and Card, 1993

Table 6.2 continued...

REGIONAL DYNAMOTHERMAL EVENTS		**ca. 2677-2645 Ma**	
Penetrative planar fabrics and metamorphism:	**peak: ca. 2660**		
post-Timiskaming and pre-D_2 porphyry dike	2677 ± (3,2)	U-Pb / zircon	Corfu et al., 1991
Murdock Creek syenite overprinted by Larder Lake-Cadillac penetrative fabric	2673 ± 2	$^{207}Pb/^{206}Pb$ zircon, brown titanite	Wilkinson et al., 1993
	2665 ± 4	$^{207}Pb/^{206}Pb$ turbid yellow titanite	Wilkinson et al., 1993
Cléricy syenite Porcupine-Destor/Parfouru faults area	2682 ± 3	U-Pb / zircon	Mortensen, 1993
	2657 ± 3	$^{40}Ar/^{39}Ar$ biotite	Powell, 1994
PLUTONIC EVENTS ACCOMPANYING LATE- TO POST-REGIONAL SYN-METAMORPHIC DEFORMATION		**ca. 2685-2670 Ma and ca. 2663-2611 Ma**	
Lacorne batholith gabbroic to granodiorite	ca. 2685-2670		
	2671 ± 4	$^{207}Pb/^{206}Pb$ zircon	Feng and Kerrich, 1991
	2675 ± 25		
Abitibi Subprovince S-type granites	2655 ± 8	$^{207}Pb/^{206}Pb$ zircon	Feng and Kerrich, 1991
	2630 ± 20		
Lacorne pluton (musc-bo-gt)	2643 ± 4		
Pontiac Subprovince S-type granites	2632 ± 3	U-Pb / zircon	Machado et al., 1991

Table 6.2 continued...

CAMFLO MINE COOLING HISTORY	**ca. 2621-2450**		
	2621 ± 4	U-Pb / titanite quartz-Au-titanite vein post-dating "porphyry" ore	Zweng, 1993 Spooner and Barrie, 1993
Resetting of Ar isotopes by multiple post-metamorphic hydrothermal events (?) Powell et al. (1995 b)	2600 ± 3	U-Pb / rutile	Jemielita et al., 1990
	2553 ± 7	$^{40}Ar/^{39}Ar$	Zweng, 1991
	2546 ± 7	vein muscovite level 3475	Zweng et al., 1993
	2513 ± 7	$^{40}Ar/^{39}Ar$	
	2511 ± 7	wall-rock muscovite level 3475	
	2507 ± 8	$^{40}Ar/^{39}Ar$ biotite level 3475 (radius: 225µm)	
	2452 ± 7	$^{40}Ar/^{39}Ar$ wall-rock biotite (radius:125µm)	
KIENA MINE LATE-MINERAL HYDROTHERMAL VEIN BIOTITE (PRE-METAMORPHIC)	2313 ± 14.9	$^{40}Ar/^{39}Ar$ stringer vein biotite "L" ore zone level 38	This study
NE PREISSAC DIABASE DIKES	2150 ± 25	$^{40}Ar/^{39}Ar$ green-brown amphibole	Hanes and York, 1978

The *Regional Sequence of Events diagram*, which covers approximately 600 m.y. of the geological history of the Val d'Or-Malartic area, is subdivided into late-Archean pre-orogenic (> 2705-2700 Ma), orogenic (ca. 2700-2645 Ma) and post-orogenic (ca. 2645-2632 Ma) events, and into an early Proterozoic (ca. 2150 ± 25 Ma) event. Pre-orogenic events (pre-D_1, >2705-2700 Ma) include regional volcanism dated as ca. 2705 Ma (Wong et al., 1991) and the emplacement of the Bourlamaque sills at ca. 2700 Ma as synvolcanic intrusions (Campiglio and Darling, 1976). The Bourlamaque diorite-trondhjemite sills are inferred to have been overturned to the south (**Figure 2.2**) during the regional D_1 deformation event (Campiglio and Darling, 1976; Morasse et al., 1996b) and later folded during the subsequent regional D_2 deformation event (**Figure 2.2**, Morasse and Wasteneys (1994)). Ultramafic and mafic volcanic rocks of the Lower Malartic Group have not been dated by radiometric methods, but are regarded as older than the Val d'Or Formation calc-alkaline volcanic rocks by most authors (e.g. Dimroth *et al.*(1982)). Orogenic events consist of the early D_1 regional deformation event (ca. 2700-2694 Ma), post-D_1 plutonic events (ca. 2694-2680 Ma), post-D_1 gold mineralization events (ca. 2694-2677 Ma), thermal metamorphism possibly related to post-D_1 orogenic plutonism (ca. 2693-2671 Ma), post-D_1 uplift and sedimentation (ca. 2695-2683), and the regional dynamothermal D_2 deformation event (ca. 2677-2645 Ma). The regional D_1 deformation event is defined by Dimroth *et al.* (1983a) as a north-south compressional event characterized by the formation of northwest- to east-west-trending, southerly-facing recumbent F_1 folds with shallowly north-dipping axial planar S_1 schistosity, and the sets of bedding- and S_1-parallel faults hosting most of gold mineralization in the Malartic camp (Sansfaçon and Hubert, 1990). The upper age limit of the regional D_1 deformation event is defined by the Bourlamaque sills (Wong et al., 1991), whereas the lower age constraint is provided by the Sigma-Lamaque No. 2 feldspar porphyry dikes. These are the first dikes emplaced after the tilting of volcanic strata at ca. 2694 Ma (Daigneault et al., 1983; Robert and Brown, 1984; Wong et al., 1991). The Kiena Mine Fault Zone is postulated to have formed during or shortly after the D_1 deformation event because it is subparallel to bedding but locally cuts across the westerly-overturned iron tholeiite east of the S-50 zone (see schematic sections and plan maps in back pocket).

Regional overturning and faulting of volcanic strata (D_1) was followed by a protracted, district-wide plutonic event resulting in the formation of the synorogenic Val d'Or plutonic belt between ca.2694-2680 Ma (**Figure 2.2**). Successive plutons exhibit an evolutionary trend from an early granodiorite-tonalite to late monzonite-syenite (Burrows and Spooner, 1991; Feng and Kerrich, 1992). The oldest intrusions are the Sigma-Lamaque No. 2 feldspar porphyry dikes and the granodioritic Snowshoe stock dated as ca. 2694 Ma (Wong *et al.* (1991); this study), whereas the youngest intrusions are the Camflo deposit aplite dikes. According to Zweng(1993), numerous narrow aplite dikes overprint and are centered on the Camflo monzonite stock dated as ca. 2685-2683 Ma (Zweng and Mortensen, 1989; Jemielita et al., 1990). The dikes, which are similar to "grey" and "pink" porphyries found in the mines of the Malartic camp, predate hydrothermal alteration and mineralization and those located on the margins of the pluton are folded and boudinaged (Zweng, 1993, p. 17-19). The Camflo monzonite stock appears similarly affected by penetrative deformation as it exhibits several boudinaged, dike-like offshoots sub-parallel to the regional east-west S_2 schistosity, which is axial planar to the district-scale z-fold affecting the sedimentary rocks of the Kewagama Group (Sauvé and Makila, 1990, p. 247). Similar transposition of intrusive contacts in S_2 schistosity planes is frequently observed throughout the Malartic camp (e.g. **Figure 8.1**). The Camflo monzonite stock and aplite dikes are thus interpreted as post-D_1 intrusions emplaced prior to the regional D_2 penetrative deformation. Although Malartic camp intrusions (Malartic Goldfields, Barnat, etc...) have not been dated by radiometric methods, structural field relationships indicate that gold-bearing diorite, "grey" and "pink" porphyry dikes were emplaced in fractures parallel to the S_1 schistosity and later deformed by the regional S_2 schistosity ((Sansfaçon and Hubert, 1990); see also Chapter 8). Similarly, the Kiena deposit albitite dikes and the neighbouring Norlartic deposit "microdiorite" dikes have no upper age limit, however, structural relationships suggest that both sets of dikes were emplaced after the tilting of volcanic strata (this study; Couture *et al.* (1994)). The timing of the Lamaque deposit quartz-feldspar porphyry dikes is also postulated as post-D_1 and pre-D_2, because the dikes cut the diorite-tonalite Lamaque intrusion dated as 2685 ± 3 Ma (Jemielita et al., 1989) and are deformed by z-folds (Daigneault et al., 1983).

The post-D_1, but pre-D_2, gold mineralization time interval (ca. 2694-2677 Ma) includes gold mineralization events directly dated by U-Pb on zircons (i.e. vein hydrothermal or magmatic zircons in cross-cutting intrusions) and the relative timing of gold mineralization inferred from the hierarchy of pre- to post-ore structures prepared for this study (**Tables 2.4** to **2.6**, Chapter 8). The upper age limit of ca. 2694 Ma is defined by the mineralized feldspar porphyry dikes of the Sigma-Lamaque No.2 deposits which cut the overturned contact of pillowed, andesitic flows with the sub-volcanic "C" porphyry (Robert and Brown, 1986). The lower age limit is provided by a deformed and foliated quartz-feldspar porphyry dike, dated as 2677 ± 3 Ma, cutting a Timiskaming sandstone unit south of Larder Lake (Corfu et al., 1991). At present, this dike is the youngest, radiometrically dated, post-D_1 and pre-D_2 intrusion in the southern Abitibi belt (Powell et al., 1995a). Only two deposits of the Val d'Or-Malartic area have been directly dated by zircons in cross-cutting intrusions: the Kiena deposit dated as 2686 ± 2 Ma, and the Norlartic deposit dated as 2692 ± 2 Ma (**Figure 2.2**, Couture *et al.*, (1994); Morasse *et al.*, (1995)). These firm lower age limits for gold mineralization are consistent with post-ore penetrative deformation and metamorphism at Kiena (see Chapter 5) and support the deduction that gold deposits formed much earlier in the geological history of the southern Abitibi greenstone belt than previously thought (e.g. Hanes *et al.*, (1992)). Malartic camp deposits and the Orion Vein No.8, Goldex and Siscoe deposits were not dated by radiometric methods, however, the relative timing of gold mineralization suggested by structural relationships (Auger, 1947; Trudel, 1985; Sansfaçon and Hubert, 1990; Trudeau and Raymond, 1992; Still and Mason, 1995) is similar to Kiena (i.e. post-D_1, S_1 and pre-D_2S_2, see **Table 2.6** and Chapter 8). Dates of ca. 2625 to 2579 Ma obtained from radiogenic systems other than U-Pb on igneous zircons (e.g. Jemielita *et al.*, (1989) and Hanes *et al.*, (1989)) suggest that gold mineralization at the Camflo, Sigma-Lamaque No. 2 and main Lamaque deposits post-date the regional synmetamorphic D_2 deformation dated as ca. 2680-2660 Ma (Powell et al., 1995a). However, quartz-tourmaline lode gold veins of the Bras d'Or and Sigma deposits were directly dated by hydrothermal zircons as ca. 2693-2688 Ma and as 2682 ± 8 Ma, respectively (Claoué-Long et al., 1990; Kerrich and King, 1993; Kerrich and Kyser, 1994). These zircon dates have generated some controversy (Corfu and Davis,

1991; Claoué-Long et al., 1992; Kerrich and King, 1993), but they are compatible with a pre-metamorphic (ca. 2677-2645 Ma) origin for vein development as suggested by the overprint of penetrative deformation on all pre-existing ore structures documented in this study (Chapter 8, see also Morasse *et al.*, (1996a)). Post-ore deformation is also postulated at the Lamaque deposit based on the existence of Sigma-type quartz-tourmaline lode gold veins deformed by folds and cut by axial planar space cleavages subparallel to the regional S_2 schistosity (**Figure 8.27,** Karvinen (1985)). In the case of the Camflo deposit, a pre-metamorphic origin for gold mineralization is postulated and preferred to the post-metamorphic and discordant titanite age of 2621 ± 4 Ma (e.g. Zweng (1993)), because this date is inconsistent with the ubiquitous cataclastic deformation of the bulk of the ore (i.e. porphyry-style ore of Sauvé and Makila (1990) and Trudel and Sauvé (1992)), and main-stage gold-quartz veins of Zweng (1993) and the overprint and offset of main-stage gold-quartz veins by shear zones (Zweng, 1993, Figure 12b p. 85). According to former Camflo mine geologists J. Daigneault and D.M. Der. Charner (as quoted in Spooner and Barrie (1993)), the quartz-free gold-titanite vein dated by Zweng *et al.* (1993) post-dates the thin (~ 1-5 mm) gray, quartz-pyrite veinlets accompanied by pale pyrite-Au bearing alteration haloes which formed the bulk of gold mineralization or "porphyry ore" at Camflo. Hence, the U-Pb titanite age of 2621 ± 4 Ma may signify the remobilisation of "porphyry" gold into post-metamorphic veins. However, an identical U-Pb rutile age of 2626 Ma (Jemielita et al., 1989) obtained from rutiles in the alteration halo of main-stage gold quartz veins suggests that both, titanite and rutile ages, were thermally reset during the emplacement of the garnet-biotite monzogranite phase of the Lacorne batholith at ca. 2645 Ma (see discussion on the Camflo deposit in Chapter 8). In the absence of firm lower age constraints for gold-ore formation at Camflo, Sigma, and Lamaque, and in view of the consistent overprint of penetrative deformation on pre-existing ore structures, gold mineralization at these deposits is postulated to have occurred after the intrusion of the Camflo monzonite and Lamaque diorite-tonalite stocks dated as ca. 2685 Ma, but prior to the onset of the regional dynamothermal D_2 deformation event bracketed between ca. 2677 to 2645 Ma.

The north-south D_2 compressional event has resulted in the formation of easterly to northwesterly-trending and southerly-overturned F_2 folds accompanied by a synmetamorphic, easterly to northwesterly-striking regional S_2 schistosity, and the many shear zones coincident with gold deposits in the Val d'Or-Malartic area (Dimroth et al., 1983a; Dimroth et al., 1983b; Sauvé et al., 1993; Powell et al., 1994). The upper age limit of the D_2 deformation event is provided by the youngest, post-D_1 and pre-D_2 felsic dike in the southern Abitibi belt dated as 2677 ± 3 Ma (Corfu et al., 1991; Powell et al., 1995a). The lower age limit is provided, in turn, by the post-orogenic monzogranite of the nearby Lacorne batholith (**Figure 2.2**) dated as 2643 ± 4 Ma (Feng and Kerrich, 1992). At Kiena, regional D_2 deformation has resulted in the development of an asymmetric z-shaped fold accompanied by a moderately to steeply north-dipping S_2 schistosity, followed by the formation of a moderately north-northwesterly-plunging fold of S_2 and related east-dipping crenulation cleavage. Field and geochronological evidence in the Val d'Or area is consistent with four regional metamorphic events after D_1: a thermal metamorphism related to the intrusion of calc-alkaline to alkaline granitoid stocks and dikes along the Val d'Or plutonic belt (ca. 2694-2680 Ma) directly dated as ca. 2693-2671 Ma on amphiboles and rutiles (Hanes et al., 1989; Wong et al., 1991), a dynamothermal metamorphic event that produced a penetrative synmetamorphic foliation (S_2) thought to be related to the earlier stages of the collision between the Abitibi and Pontiac subprovinces between ca. 2677 to 2645 Ma (Powell et al., 1995a), a thermal event related to the emplacement of S-type granites between ca. 2645 to 2611 Ma (Feng and Kerrich, 1992) inferred to have occurred during the last stages of the greenstone-metasedimentary subprovinces accretionary process (e.g. Card (1990), Jackson and Fyon (1991)), and a shield-wide thermal event related to the intrusion of Proterozoic diabase dikes at ca. 2490 to 2450 Ma (Stockwell, 1964; Hanes and York, 1979; Heaman, 1988) thought to represent the initial break-up of the first supercontinent (Mason, 1995).

In contrast with models of late Archean gold mineralization advocating two distinct episodes of gold mineralization, an early pre-metamorphic gold mineralization event at ca. 2690 Ma and syn- to post-metamorphic gold mineralization events synchronous with shear

zone development (Couture et al., 1994; Robert, 1996), this regional time sequence suggests that ore-forming gold hydrothermal activity in the Val d'Or-Malartic area coincides with a ca. 20 m.y episode of orogenic calc-alkaline and alkaline magmatism accompanied by local uplift and sedimentation (ca. 2694-2677 Ma), but that it preceded peak synmetamorphic deformation (D_2, S_2, M_2, at ca. 2660 Ma) and post-orogenic peraluminous magmatism (ca. 2645-2632 Ma). Other compilations of radiometric dates encompassing this area of the southern Abitibi belt (e.g. Corfu (1993), Kerrich and Cassidy (1994), Goutier *et al.* (1994), Powell (1995b)), infer that gold mineralization is predominantly a syn- to post-metamorphic event. The drawn-out series of titanite, rutile, scheelite, and muscovite dates (ca. 2625 to 2579 Ma), however, is broadly coincident with post-orogenic magmatic activity between ca. 2645-2611 Ma, suggesting the gradual thermal resetting of U-Pb, Sm/Nd, and $^{40}Ar/^{39}Ar$ isotopes in minerals with closure temperatures lower than zircon (< 800°C, Heaman and Parrish (1991)) following peak regional dynamothermal activity. Isotopic disturbance may be attributed also to multiple, post-metamorphic hydrothermal events in permeable gold-bearing fault zones as postulated by Powell *et al.* (1995b).

CHAPTER 7 GEOLOGICAL SYNTHESIS OF THE KIENA DEPOSIT

7.1 INTRODUCTION

Geological and geochronological data on the Kiena deposit presented in this study support the emplacement of porphyry-style gold mineralization along a bedding-parallel fault zone at ca. 2694-2686 Ma. The geological evolution of Kiena is thus coincident with, and controlled by, the folding/thrusting and calc-alkalic/alkalic plutonic stages of the collisional orogeny characterizing the evolution of the southern Abitibi greenstone belt between 2700 and 2670 Ma (Card, 1990; Corfu, 1993). Regional and local geological controls on gold-ore formation specifically recognized at Kiena include: the early structural control exerted by the Kiena Mine fault zone (ca. 2700-2694), followed by pervasive albitization and fracture-induced magmatic-hydrothermal controls exerted during the development of a zoned alteration-mineralization sequence related to the emplacement of an albitite-porphyry dike complex (ca. 2694-2686 Ma). The overprint of all preexisting ore structures at Kiena by folds, the regional S_2 schistosity, and late-stage strike-slip faults signify that regional synmetamorphic penetrative deformation and shear zone development, which conclude the evolution of the Abitibi-Pontiac orogen at ca. 2660-2645 Ma, are post-ore geological events.

The late-Archean geodynamic setting and evolution of the Kiena deposit resembles that of Cenozoic porphyry-style gold deposits encountered in Circum-Pacific gold provinces. At the regional-scale, the Val d'Or plutonic belt, which parallels the faulted boundary of the Abitibi/Pontiac subprovinces and is coincident with many gold deposits in the Val d'Or-Malartic area, is comparable to the discrete belts of intrusion-related gold-rich and gold only deposits developed along Andean and western Pacific orogens. At the deposit-scale, the style of mineralization and gold-related alteration assemblages observed at Kiena more closely resemble those occurring at the lower levels of the Santo Thomas II Cu-Au deposit in the

Luzon Central Cordillera of the Phillipines.

7.2 GEOLOGIC HISTORY AND CONTROLS ON GOLD MINERALIZATION

The succession of geologic events leading to the formation and subsequent deformation of the Kiena orebody is summarized in **Figure 7.1** and **Table 7.1.** As shown on the regional time sequence (in back pocket) and as previously discussed in Chapter 6 (section 6.4), the deposit time sequence post-dates the sub-marine Malartic Group komatiitic, tholeiitic and calc-alkalic volcanism (> 2700Ma) and the early phase of folding and thrusting that quickly followed (D_1 ca. 2700-2694 Ma). The geologic history of Kiena begins with the development of a steeply-dipping bedding-parallel fault, the Kiena Mine fault zone, which probably formed during or shortly after the regional overturning of volcanic strata at ca. 2700-2694 Ma. Across the Val d'Or-Malartic district, regional folding and thrusting was followed by the progressive emplacement of epizonal calc-alkalic and alkalic intrusions now forming the Val d'Or plutonic belt (see Regional Sequence of Events diagram in back pocket). The alignment of these intrusions (see **Figure 2.2**) suggests that they are controlled by a regional-scale fault zone which parallels the tectonic break between the Abitibi and Pontiac Subprovinces to the south. At Kiena, faulting of the overturned sequence of mafic and ultramafic volcanic flows of the Jacola Formation was followed by the emplacement of an albitite dike swarm in the komatiitic hangingwall of the Kiena Mine fault zone at ca. 2694-2686 Ma. The upward-branching geometry of Kiena's albitite dikes and confinement to the fault hangingwall suggest that episodic fault movements must have focused the rise of albitic magma from deep levels to relatively high levels in the crust. Pervasive wall-rock albite alteration adjacent to the dikes, the low calcicity of albitite-forming albites, and the occurrence of micrographic to myrmekitic albite-quartz intergrowths, suggests that the intrusion of the Kiena deposit albitite dikes is also characterized by the release of an aqueous phase at the margins of the intrusions.

In the Kiena Mine fault zone, the loci of gold alteration-mineralization are the albitite dikes and albitization is the first event in the mines's alteration-mineralization sequence (**Figure 7.1,**

Figure 7.1 - Sequence of events at the Kiena deposit

SEQUENCE OF EVENTS AT THE KIENA DEPOSIT

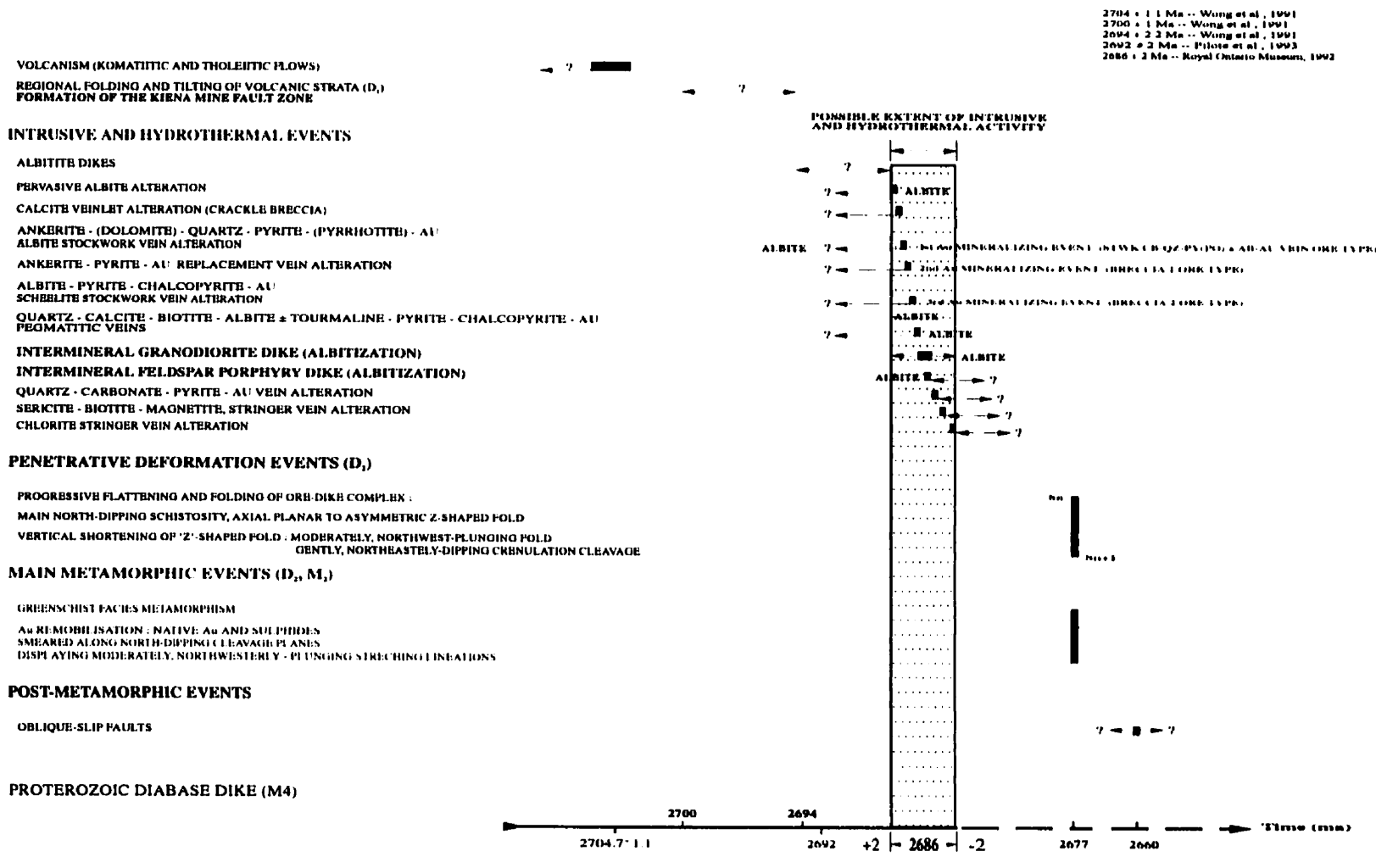

Figure 7.1

Table 7.1 Geologic history and controls on gold-ore formation at Kiena

Time (Ma) U-Pb zircon ages	Regional sequence of events	Sequence of events at Kiena
?	Komatiitic Tholeiitic Calc-alkaline Volcanism [1,2,3]	Jacola Fm (Malartic Group): Sub-marine komatiites and tholeiites
2705	Intrusion of Bourlamaque[3,4] diorite-trondhjemite sills	
2700	D_1: Tilting of volcanic strata, Bourlamaque sills[4,5] (F_1, S_1, L_1) Faulting across the Val d'Or plutonic belt	**REGIONAL FAULT CONTROL** Development of bedding-parallel fault zone
2694		
2694	Post -D_1 and pre-D_2 Thermal metamorphism (M_1) related to calc-alkalic orogenic plutonism in the Val d'Or-Malartic area[6]	**KIENA MINE FAULT ZONE CONTROL (ca. 2694 Ma)**
	Plutonic Events	Magmatic Hydrothermal Events
		Pre- 2686 Ma
	2694 ± 2 Ma Sigma-Lamaque Mines feldspar porphyry dikes ("G" dikes)	GROUND PREPARATION CONTROL: 1. Intrusion of albitite dike swarm broadly coeval with albitization of adjacent wall-rocks (An_{0-1})
	2693 ± 2 Ma Snowshoe granodiorite-tonalite stock[5]	2. Calcite stockwork veining and minor crackle brecciation
	2692 ± 2 Ma Norlartic Mine tonalite dike cross-cutting the main ore zone[7] Kiena Mine albitite dike swarm (?)	3. FeCb-Qz-Py(Po)-Au stockwork veining and minor brecciation
		4. FeCb-Au replacement veining
		5. Ab-Py-Cpy-Sch-Au stockwork veining and brecciation
2686	2686 ± 2 Ma Kiena Mine granodiorite and feldspar porphyry dikes[5]	2686 ± 2 Ma
		6. Intrusion of granodiorite porphyry dike (albitization)
		7. Intrusion of feldspar porphyry dike (xenocrystic zircons at 2697 ± 2 Ma)(albite)
		Post-2686 Ma
	2685 $\pm^{7}_{4}$ Ma Camflo Mine monzonite stock[9]	8. Cb-Qz-Py-Au stockwork veining
		9. K-phyllosilicate (sericite, biotite) stringer veining (potassic alteration)
	2685 ± 3 Ma Lamaque Mine granodiorite-tonalite stock[8]	10. Replacement of vein sericite and biotite by chlorite (propylitic alteration)
2680		
2677-2660	D_2: Regional dynamothermal metamorphism (M_2)[10,11,12] (F_2, S_2, L_2)	Z-shaped fold and EW, north-dipping regional S_2 schistosity; NNW-plunging fold of S_2 and NE-dipping S_3 crenulation cleavage
2645		

REGIONAL FAULT-LINEAMENT CONTROL (EARLY FAULT SYSTEM)

EPIZONAL INTRUSIONS OF THE VAL D'OR PLUTONIC BELT

FRACTURE - INDUCED MAGMATIC-HYDROTHERMAL CONTROL

modified from Morasse et al. (1995)

Key: 1. Imreh, 1984 2. Corfu, 1993 3. Wong et al., 1991 4. Campiglio and Darling, 1976 5. Morasse and Wasteneys, 1994 6. Hanes et al., 1989 7. Pilote et al., 1993 8. Jemielita et al., 1989 9. Zweng and Mortensen, 1985 10. Corfu et al., 1991 11. Feng and Kerrich, 1991 12. Powell (1995) ; FeCb=iron carbonate, Qz=quartz, Py=pyrite, Po=pyrrhotite, Au=gold, Cpy=chalcopyrite, Sch=scheelite

Table 7.1). Pervasive albite alteration synchronous with the emplacement of albitite dikes, is postulated to have served as ground preparation control in the mineralization process by enhancing the competency of the albitite intrusions and their metasomatised tholeiitic and komatiitic wall rocks. This hydrothermally induced competency contrast between albitite dikes and mafic/ultramafic volcanic wall rocks appears to have favoured the ensuing microfracturing and brecciation of these rocks. Albitization was followed by the development of calcite stockwork vein alteration, creating a zone of secondary permeability (i.e. crackle breccia) in the competent albitized rocks. A succession of overprinting main-stage gold alterations was then developed over the early crackle breccia zone, causing extensive fracture damage to the column of albitized rocks in and around the Kiena Mine fault zone. The pre-2686 Ma main-stage gold alteration-mineralization sequence is comprised, from the oldest to the youngest, of the following stages: 1) carbonate-quartz-albite-pyrite-(pyrrhotite)-Au stockwork veins (Stwk Cb-Qz-Py(Po)±Ab-Au vein ore type), 2) ankerite-pyrite-Au replacement veins (Breccia 1 ore type), 3) albite-pyrite-chalcopyrite-scheelite-Au stockwork veins and breccias (Breccia 2 ore type), and 4) minor quartz-carbonate-biotite-albite±tourmaline-pyrite-chalcopyrite-Au veins. The areal extent of vein-breccia mineralization decreases (maximum of 120 in the hangingwall and 20 metres in the footwall to the Kiena Mine fault zone) with each successive gold alteration stage, but new gold was introduced each time and resulted in the formation of a sheet-like, high-grade ore zone at the centre of the orebody. Kiena's alteration-mineralization sequence was interrupted at ca. 2686 Ma by the intrusion of intermineral granodiorite and quartz monzonite porphyry dikes (**Figure 7.1**, **Table 7.1**), which partly dismembered the orebody. Similarly to pre-ore albitite dikes, Kiena's felsic porphyry dikes were pervasively albite-altered during their emplacement, and subsequently fractured and weakly mineralized by carbonate-quartz-pyrite-Au stockwork veins before being overprinted, in turn, by late-stage vein sericite. The entire ore-dike complex was then overprinted by late-stage vein biotite-magnetite, later replaced by chlorite. The presence of high temperature hydrothermal minerals in the veins (i.e. albite, biotite), the upward and outward pyrite-pyrrhotite zonation (see Chapter 4), and the progressive change from breccia to stockwork veins away from the centre of mineralization,

suggest that Kiena's orebody was formed as a result of the decompression of hot, Au-rich brines episodically ascending through the Kiena Mine fault zone. The magmatic-hydrothermal origin of ore-fluids is suggested by intermineral dikes (i.e. temporal association of magmatic and gold hydrothermal activity) and the recurrence of pure albite (An_{0-1}) throughout the deposit's alteration-mineralization sequence (inferred genetic link between albitic magma and albite-rich gold solutions). The deposit's zoned alteration-mineralization pattern is thought to have formed as a result of the physico-chemical variations occurring during episodic hydrothermal fluid flow. Cooling of the Kiena deposit magmatic-hydrothermal system following gold-ore formation is indicated by the replacement of vein biotite by chlorite. This retrograde alteration probably occurred in response to the natural collapse of the underlying magmatic-hydrothermal regime, which in turn, put an end to gold mineralization.

As magmatic-hydrothermal activity tapered off at Kiena, other gold ore systems continued to form throughout the Val d'Or plutonic belt (see section 6.4 and Chapter 8). Then, during the final collision stage of the Abitibi/Pontiac orogen i.e. at the onset of the regional synmetamorphic D_2 deformation event at ca. 2677-2660 Ma, magmatic and gold hydrothermal activity across the Val d'Or-Malartic district ceased (see Regional Sequence of Events in back pocket). At Kiena, regional penetrative deformation resulted in the formation of an asymmetric z-shaped fold and the superimposition of a moderately to steeply north-dipping S_2 schistosity on the ore-dike complex , followed by the formation of a moderately north-northwesterly plunging fold of S_2, and a related north-easterly-dipping crenulation cleavage. Kiena's hydrothermally-altered rocks were subjected to peak, metamorphic greenschist facies conditions (~ 250°C and < 3.3 kbar, Powell *et al.* (1995)) at ca. 2660 Ma (Powell, 1994; Powell et al., 1995), and re-heated once more (≥410-450°C, Feng (1990), Powell (1995)) during the up-rise of the peraluminous granite phase of the Lacorne batholith at ca. 2643 ± 4 Ma (Feng and Kerrich, 1991). It is postulated that metamorphosed hydrothermal biotites were thermally reset during both these, and probably during several other post-metamorphic hydrothermal events, based on the $^{40}Ar/^{39}Ar$ age of ca. 2313 Ma obtained from such biotite. Volcanic rock units west of the orebody were subsequently cut

by a northeasterly-trending diabase dike (see Figure 3.1 and level map 33 at 1:5 000 in the back pocket). The dike has not been directly dated but is similar to the Proterozoic Preissac dikes dated as 2150 ± 25 Ma (Hanes and York, 1979).

7.3 KIENA IN RELATION TO PORPHYRY ORE SYSTEMS

Prior to this study, the Kiena deposit was interpreted as a post-metamorphic and shear zone-controlled orebody (Roy, 1983; Bourget, 1986; Quirion, 1988). However, as demonstrated by this study, the deposit is pre-metamorphic and related to orogenic magmatic-hydrothermal activity. As penetrative deformation and greenschist facies metamorphism are post-ore, a porphyry-style intrusion-related ore model is probably more plausible.

Kiena has two features that are diagnostic of intrusion-related ores: 1) mineralization consists essentially of vein-veinlet altered and brecciated intrusive rocks, and 2) hydrothermal activity giving rise to the densely-fractured orebody is temporally-related to magmatic activity by intermineral diking (Kirkham, 1971; Titley, 1982; Titley, 1993). The deposit also shows many of the attributes of porphyry ore systems world-wide (e.g. Sawkins (1990)) including the funnel-shaped geometry of the ore, the upward and outward zoned alteration patterns, early feldspathization, and sequential and fracture-controlled alteration-mineralization. This point is illustrated in a comparative table listing the ore morphology, host rocks, mineral paragenesis of alteration-mineralization sequences, and magmatic events related to ore formation at Kiena and selected porphyry deposits (**Table 7.2**). The geological setting of Kiena, however, more closely resembles that of the Cenozoic gold-rich end member of this class of deposits which occur throughout the Pacific rim regions. Similarities exist at both the deposit- and regional-scales, and are summarized in **Table 7.3**.

The essential features of gold-rich, or gold-only, porphyry deposits are as follows: 1) mineralization occurs in fault-guided, composite intrusions of low-potassium calc-alkalic composition, 2) zoned alteration patterns consist of a central potassium- and calc-silicate

Table 7.2 Hypogene magmatic-hydrothermal alteration sequence at Kiena and selected Cu-Mo, Cu-Au and Au-rich porphyry deposits

	KIENA ABITIBI BELT, VAL D'OR, QUÉBEC
CONFIGURATION OF ORE SHOOT	Funnel-shaped: upward and outward zonation of fracture-controlled alterations **Apical zone:** ~150 metres-wide: core of albitite dike swarm obliterated by breccia body, enclosed in stwk vein ore **Root zone:** ~50 metres-wide albitite dike swarm predominantly mineralized by stock-work breccia veins
PRE-ORE ALTERATION 1. Type, style, paragenesis 2. Host rocks 3. Location	**1. Pervasive albitization ($An_{<1}$):** "cleavelandite"-type albites associated with micrographic to myrmekitic Ab-Qz intergrowths; fluid inclusion-rich albites; mosaic of equigranular, anhedral albites 2. Restricted to aplitic albitite dikes and adjacent komatiitic and tholeiitic wall-rocks. 3. Centered over pre-ore albitite dikes in bedding parallel fault zone.
MAIN-STAGE ALTERATION-MINERALIZATION 1. Type, style, paragenesis 2. Host rocks 3. Location	1. Stockwork veins and breccias: 1.1 Cc stwk veins (crackle breccia) 1.2 Cb-Qz-Py(Po)± Ab-Au stwk veins (crustiform texture) 1.3 Ak-Py-Au replacement veins 1.4 Ab-Py-Cpy-Sch-Au stwk veins and breccias (cockade texture) 1.5 Qz-Cb-Bo-Ab±Tm-Py-Cpy-Au pegmatitic veins 2. Mostly albitite dikes and minor volume of adjacent komatiitic-tholeiitic wall-rocks. 3. Centered on pre-ore, bedding-parallel Kiena Mine fault zone
LATE-STAGE ALTERATION 1. Type, style, paragenesis 2. Host rocks 3. Location	1.1 Minor Cc-Qz-Py-Au stwk veins 1.2 Sericite; Phlogopitic vein biotite-magnetite (pyrite ?) 1.3 **Replacement of vein biotite by chlorite** 2. Porphyry dikes, the ore and komatiitic-tholeiitic wall-rocks 3. Widespread but restricted to outer stockwork vein alteration halo grading 0.34 - 3.0 Au/t.
MAGMATIC EVENTS TEMPORALY-RELATED TO HYDROTHERMAL ALTERATION-MINERALIZATION	Pre-mineral albitite dikes Intermineral granodiorite and feldspar porphyry dikes
AGE	Archean ca. 2694-2686 Ma (U-Pb, zircon)
TECTONIC AND CRUSTAL SETTING	Accreted island arc (?) - Synorogenic **Epizonal**: calc-alkaline intrusions estimated depth: 1-5 km
REFERENCES	Clark (1963); Morasse et al. (1995); this study.

Key: Ab=albite Act=actinolite Ak=ankerite Anh=anhydrite Au=gold Bar=barite Bo=biotite Cc=calcite Cb=carbonate Chl=chlorite Cpy=chalcopyrite Ep=epidote Mo=molybdenite Orth=orthoclase Phlo=phlogopite Po=pyrrhotite Py=pyrite Qz=quartz SCC=sericite-clay-chlorite Sch=scheelite Ser=sericite Stwk=stockwork Tm=tourmaline

Table 7.2 continued...

	SW US CU-MO PORPHYRY DEPOSIT: SIERRITA-ESPERANZA, ARIZONA*, **	CU-AU PORPHYRY DEPOSIT: BINGHAM, UTAH
CONFIGURATION OF ORE SHOOT	Downward-constricting funnel-shaped: **Apical, zoned mineralized breccia:** up to 760 m across at 3900' elevation **Root zone:** discontinuous bodies of variable sizes (50-/50 m) below 3750' elevation	Hollow dome or molar-shaped orebody: (inverted cone-shaped Bo-Cpy alteration) **Apical zone:** top of quartz monzonite porphyry **Root zone:** vertically extending, thinner quartz monzonite porphyry dikes
PRE-ORE ALTERATION 1. Type, style, paragenesis 2. Host rocks 3. Location	1. **Pervasive potassic alteration: groundmass biotite and vein biotite-magnetite** 2. Inner "Ruby Star" Qz-monzonite porphyry (57 m.y.) - peripheral "Harris Ranch" Qz-monzonite (200 ± 10 m.y.) - outer biotite Qz diorite (67 m.y.) 3. Widespread over "Sierrita" intrusion complex	**Calc-silicate and K-silicate alteration:** 1. **Actinolite** replaces magmatic augite and minor replacement of plagioclase by **orthoclase**; disseminated **magnetite?** 2. Quartz-monzonite porphyry (i.e. major porphyry phase of "Bingham" stock) characterized by an aplitic groundmass 3. Around the top of quartz-monzonite porphyry itself located at the intersection of left-lateral northeast-trending faults with the "Copperton" anticline, beneath the "Midas" thrust
MAIN-STAGE ALTERATION-MINERALIZATION 1. Type, style, paragenesis 2. Host rocks 3. Location	1. **Potassic alteration: orthoclase** 1.1 Vein/veinlet Qz-Orth-Cpy-Py-Mo--(Po) with accessory Chl-Ser-Ab-Cc-Anh 1.2 Orthoclase 'flood type' 1.3 Albite veins: Ab-Qz-Orth-Chl ± Py -Cc-Ep 2. Mostly Inner "Ruby Star" Qz monzonite porphyry (57 m.y.) and outer biotite quartz diorite (67 m.y.), centered on "Serrita" breccia pipe 3. NE-trending high density fracturing zone centered on the "Ruby Star" Qz monzonite porphyry which occupies a pre-ore north -northwest-trending regional fault	1. **Potassic alteration: orthoclase** Vein/veinlet Qz-Orth-Bo-Phlo-Mo-Cpy-Bar-Py: sulphides replace disseminated magnetite 2. Quartz monzonite porphyry, "Bingham" stock and minor "Last Chance" stock 3. Zone of high-density planar fractures centered over the quartz monzonite porphyry; fracturing is co-extensive with biotite alteration
OTHER HYDROTHERMAL ALTERATIONS 1. Type, style, paragenesis 2. Host rocks 3. Location	1.1 **Propylitic alteration**[1]:Ep veins (Py-Cc-Qz) 1.2 Vein/veinlet sericitization and phyllic alteration[2]: Qz-Ser-Py 2. Mostly restricted to Ruby Star Qz monzonite porphyry stock 3. In fringes of ore shell into margins of deposit and to depth: "Harris Ranch" Qz monzonite and biotite quartz diorite	1.1 **Propylitic alteration**[1]:Act-Chl-(Ep) 1.1.1 Disseminated and vein-controlled chlorite replacing actinolite-augite-biotite commonly accompanied by epidote 1.1.2 Vein-controlled sericite alteration[2]: Clay-Ser-Qz 2. Mostly "Bingham" stock 3. Outer fringes of potassic alteration zone 3 and ore shell
MAGMATIC EVENTS TEMPORALY-RELATED TO HYDROTHERMAL ALTERATION-MINERALIZATION	Pre-mineral biotite quartz diorite stock Pre-mineral "Ruby Star" granodiorite Pre-mineral "Ruby Star" quartz monzonite: aphanitic-phaneritic-aplitic-dacitic Pre-mineral "Sierrita" hydrothermal breccia pipe Late-mineral quartz latite porphyry dikes	Pre-mineral equigranular and quartz-poor "Last Chance" and "Bingham" monzonite stocks Pre-mineral quartz-monzonite porphyry dike Intermineral latite porphyry dikes Late-mineral quartz-latite porphyry dikes: one reported occurrence of Cpy-bearing vesicles in dike Post-mineral "Kilkinny" breccia pipe
AGE	Cenozoic: ca. 57 - 47 Ma	Cenozoic: ca. 38.9 - 38.8 Ma (K-Ar, biotite)
TECTONIC AND CRUSTAL SETTING	Continental margin; **Epizonal:** high-K calc-alkaline intrusions estimated depth: 0-6.4 km	Continental margin; **Epizonal:** high-K calc-alkaline intrusions estimated depth: 2.3 ± 0.3 km
REFERENCES	Cooper (1973) West and Aiken (1993)	Moore et al. (1973); Warmaars et al. (1978) Lanier et al. (1978); John (1978);

Key: Ab=albite Act=actinolite Ak=ankerite Anh=anhydrite Au=gold Bar=barite Bo=biotite Cb=carbonate Cc=calcite Cpy=chalcopyrite Ep=epidote Mo=molybdenite Orth=orthoclase Phlo=phlogopite Po=pyrrhotite Py=pyrite Qz=quartz SCC=sericite-clay-chlorite Sch=scheelite Ser=sericite Stwk=stockwork

* Argillic and/or supergene alteration sequences have been omitted ** No coeval volcanic rocks

1. Broadly synchroneous with the development of potassic alteration but in periphery of the center of mineralization

2. Late-stage and distal alteration

Table 7.2 continued...

	WESTERN PACIFIC RIM AU-RICH PORPHYRY DEPOSIT SANTO THOMAS II, LUZON CENTRAL CORDILLERA, PHILIPPINE**	ANDEAN AU-ONLY PORPHYRY DEPOSITS MARTE, MARICUNGA BELT, CHILE*
CONFIGURATION OF ORE SHOOT	Steep cylinder with barren core of poorly fractured and weakly mineralized intermineral diorite dikes	Steeply inclined and elongate orebody with a high-grade core grading > 2 g/t Au **Apical zone:** Top of composite intrusion between 4300-4100 m elevation, centered beneath "Volcán Pastillitos" **Root zone:** subore grade microdiorite intrusion breccia below 4100 m elevation
PRE-ORE ALTERATION 1. Type, style, paragenesis 2. Host rocks 3. Location	**1. Potassic alteration: biotite** 1.1 Pervasive biotitization (black biotite and brown Mg-rich biotite) of magmatic hornblende 1.2 Actinolite and magnetite veinlets 2. Pre-mineral hornblende diorite porphyry dike 3. Centered on pre-mineral diorite intrusion, along "Albian" fault zone at the margins of batholith - upper part of orebody	**1. Potassic alteration: albite + biotite** 1.1 Leafy biotite replacing biotite in diorite porphyry groundmass; biotite after hornblende phenocrysts; phenocryst and groundmass plagioclase replaced by albite 2. Mostly coarse- and find-grained diorite porphyry intrusion 3. Coincides with zone of intermediate argillic alteration affecting the apex of the composite dioritic intrusion
MAIN-STAGE ALTERATION-MINERALIZATION 1. Type, style, paragenesis 2. Host rocks 3. Location	1. Qz-Py-copper sulfide stockwork veins with anhydrite 2. Pre-mineral hornblende diorite porphyry dike 3. Centered on pre-mineral intrusion emplaced along NE-striking "Albian" fault zone localized at the margins of regional-scale batholith - upper part of orebody	1. Qz-Py-Au-(Cpy)-(Bar) stockwork veins 2. Mostly coarse- and fine-grained diorite porphyry intrusion 3. Coincides with zone of intermediate argillic alteration affecting the apex of the composite dioritic intrusion
OTHER HYDROTHERMAL ALTERATIONS 1. Type, style, paragenesis 2. Host rocks 3. Location	**1.1. Propylitic alteration[1]:** 1.1.1 Chl after mafics minerals & in veinlets 1.1.2 3 vol.% disseminated and veinlet magnetite 1.1.3 Traces of Cpy and biotite 1.1.4 Occasional Qz veinlets with chloritized biotite 2. Late-mineral biotite-hornblende quartz diorite 3. At depth - root of hydrothermal system below the orebody	**1.1 Propylitic alteration[1]** 1.2 Intermediate argillic alteration (SCC) 1.3 Pervasive chloritization (tourmaline) 2.1 Coeval andesitic volcanic host rocks 2.2 Coarse and fine-grained diorite porphyries and root zone of coeval andesitic volcanic rocks 2.3 Late-mineral microdiorite intrusion breccia
MAGMATIC EVENTS TEMPORALY-RELATED TO HYDROTHERMAL ALTERATION-MINERALIZATION	Pre-mineral hornblende diorite porphyry dike Intermineral biotite-hornblende quartz diorite, hornblende diorite and andesite porphyry dikes Intermineral hydrothermal breccia Late-mineral, phaneritic to porphyritic biotite; hornblende quartz diorite dike at depth Post-mineral diatreme	Pre-mineral composite intrusion: coarse-grained diorite porphyry, fine-grained diorite porphyry and microdiorite Intermineral microdiorite intrusion breccia Late-mineral microdiorite intrusion breccia Post-mineral linear bodies of hydrothermal breccia
AGE	Cenozoic: 1.4 Ma	Cenozoic: ca. 13-14 Ma (K-Ar, hornblende)
TECTONIC AND CRUSTAL SETTING	Island Arc - synorogenic **Epizonal:** calc-alkaline intrusions estimated depth: 1-3 km	Continental margin - synorogenic **Epizonal:** calc-alkaline intrusions estimated depth: 0.6-1.0 km
REFERENCES	Sillitoe and Gappe (1984) Sillitoe (1989) Sillitoe (1993)	Vila et al. (1991) Vila and Sillitoe (1991) Sillitoe (1993)

Key: Ab=albite Act=actinolite Ak=ankerite Anh=anhydrite Au=gold Bar=barite Bo=biotite Cb=carbonate Cc=calcite Chl=chlorite Cpy=chalcopyrite Ep=epidote Mo=molybdenite Orth=orthclase Phlo=phlogopite Po=pyrrhotite Py=pyrite Qz=quartz SCC=sericite-clay-chlorite Sch=scheelite Ser=sericite Stwk=stockwwork

* Argillic and/or supergene alteration sequences have been omitted ** No coeval volcanic rocks

1. Broadly coeval with the development of potassic alteration but at higher elevations

Table 7.3 Similarities between Kiena and Cenozoic, Circum-Pacific gold-rich porhyry copper deposits

CENOZOIC AU-RICH PORPHYRY COPPER DEPOSITS CIRCUM-PACIFIC OROGENS	ARCHEAN INTRUSION-RELATED KIENA DEPOSIT ABITIBI-PONTIAC OROGEN
REGIONAL- SCALE • Discrete belts at convergent plate margins (magmatic arc) • Fault-lineament control • Distribution of deposits: nesting geometry (closely-spaced and pairs of deposits) • Calc-alkaline to alkaline magmas • Intrusions cluster in restricted time intervals • Contrasting styles of gold mineralization within a mineral belt: epithermal, porphyry-style, skarn • Two populations of deposits: > 60 t Au (66-1400 t) < 60 t Au (18-57 t) **Examples:** Luzon Central Cordillera, Phillipines [1,2]	**REGIONAL- SCALE** • Val d'Or Plutonic Belt, sub-parallel to Abitibi-Pontiac terrane boundary (plutonic arc) • Fault-lineament control • Pairs and small clusters of deposits in the VPB ex.: Sigma-Lamaque, Callahan-Marban-Norlartic, Malartic deposits • Dioritic, granodioritic and monzonitic intrusions • Intrusions cluster between ca. 2694-2680 Ma • Differences in vein paragenesis, styles and patterns of alteration-mineralization between western and eastern deposits of the Val d'Or plutonic belt (Figure 8.28) • Three populations of deposits: < 3 t Au 3-30 t Au > 30 t Au (41-258 t)
DEPOSIT- SCALE • Hypogene mineralization hosted by dioritic intrusions and/or coeval volcanic rocks • Fault-guided, composite intrusions • Upward and outward zoned alteration patterns • Early potassic (phlogopite ± albite or orthoclase) and calc-silicate (actinolite, hornblende, ± magnetite) alterations [2,3] • Fracture-controlled alteration-mineralization • Episodic stockwork veining and brecciation • Gold predominantly occurs as native gold in association with pyrite, chalcopyrite and bornite • Gold grades range between 0.4 and 2 g/t Au • Molybdenum is deficient or occurs in the halos of gold orebodies • Propylitic alteration : veinlet biotite replaced by chlorite • Inter- and late-mineral diking • Depth range: 1-3 km **Examples:** Santo Thomas, Luzon, Philippines (1-3 km)[1]	**DEPOSIT- SCALE** • Mineralization mainly hosted by albitite dikes of dioritic composition, and mafic-ultramafic wall-rocks • Kiena Mine fault control: albitite dike swarm • Upward and outward zoned alteration-mineralization pattern • Early, pervasive albitization • Fracture-controlled alteration-mineralization • Episodic stockwork veining and brecciation • Gold occurs as free native grains in the gangue or occluded in pyrite • Gold grades range between 3 and 25 g/t Au • Molybdenum is deficient • Vein biotite(Mg-rich)-magnetite overprinted by chlorite • Granodiorite and quartz monzonite intermineral dikes • Estimated depth: 1-5 km [4]

1. Sillitoe and Gappe (1984) 2. Sillitoe (1993) 3. Arancibia and Clark (1996) 4. Burnham (1979)

alteration zone grading upward and outward into propylitic alteration, 3) mineralization is centred on the K- and calc-silicate alteration zone and is controlled by stockwork veins, 4) gold essentially occurs as native gold in association with pyrite, chalcopyrite and bornite, and 5) intermineral to late-mineral diking are an intrinsic part of the hydrothermal alteration sequence. Potassium and calc-silicate types of alterations consist of selectively pervasive or pervasive biotite-albite and actinolite alterations, respectively, with or without vein magnetite (e.g. Island copper, Arancibia and Clark (1996)). Arancibia and Clark (1996) have presented evidence supporting an early magnetite-rich alteration phase including actinolite, hornblende and albite preceding the universal biotite alteration of gold-rich porphyry deposits. Potassic and propylitic alterations, on the other hand, are generally interpreted as coeval (Titley, 1982; Sillitoe, 1993). The hydrothermal biotite present in these magmatic-hydrothermal systems is invariably phlogopitic (Mg-rich, e.g. Sillitoe and Gappe, (1984); see also Reyes (1990)). Gold-rich porphyry systems generally lack a phyllic alteration zone but commonly develop an intermediate argillic alteration zone (i.e. SCC or sericite-clay-chlorite of Vila and Sillitoe (1991)) in the upper part of the intrusive complex, as well as an advanced argillic alteration zone in the coeval volcanic rocks located above the mineralized intrusions (Sillitoe and Gappe, 1984). Kiena shows the following list of features in common with the above generalized model for gold-rich porphyry copper deposits: 1) the ore is hosted by albitite dikes[1], 2) the alteration zoning consists of a core of albitized and mineralized dikes overprinted by vein biotite-magnetite grading outward into vein chlorite, 3) the hydrothermal biotite is of a magnesium-rich variety, 4) mineralization is controlled by stockwork veins and breccias, 5) gold predominantly occurs as free native gold whereas the remainder is occluded by pyrite, and 6) the alteration-mineralization sequence is interrupted by intermineral dikes (**Figure 7.1**). Notable aspects that distinguish Kiena from gold-rich intrusion-related ores, on the other hand, are as follows: 1) dikes rather than small stocks form the composite

---

[1] Kiena's albitite dikes have a dioritic composition with a low K_2O:Na_2O ratio cause in part by Na-metasomatism (see Figure 3.26).

intrusions, 2) calc-silicate alteration is apparently lacking[2], 3) the early, barren alteration stage consists of pervasive albitization as opposed to biotite, 4) chalcopyrite is only found in trace amounts in main-stage stockwork and pegmatitic veins, 5) the biotite-magnetite alteration is late-stage rather than early or coeval with mineralization, 6) intermediate and advanced argillic alterations and post-ore diatremes are missing from the hydrothermal alteration sequence, and 7) coeval volcanic rocks are completely absent from the local geological setting. Another important contrasting feature between Kiena and gold-rich or gold-only porphyry ores is the grade and gold contents of the deposits. Almost half of the gold-rich porphyry deposits in western Pacific regions, for example, contain in excess of 60 tonnes of gold, and in a few cases, total gold contents reach giant proportions (e.g. 1400 tonnes of gold at Grasberg); however, the other half of the deposit's population averages around 35 tonnes of gold which compares with the minimum 52 tonnes of gold estimated at Kiena. The grades of gold-rich porphyry deposits vary between 0.4 and 2 g/t Au (Sillitoe, 1993), whereas Kiena's grades range between 3 and 25 g/t Au.

However, the differences between Kiena and Cenozoic gold-rich porphyry copper deposits do not imply that this more modern, intrusion-related ore deposit model is inconsistent with Kiena geology. They suggest instead, that Kiena's alteration-mineralization sequence is comparable to the deeper, hypogene type of alterations within these porphyry-style magmatic-hydrothermal systems. The absence of an advanced argillic alteration zone, post-ore diatreme, and coeval volcanic rocks at Kiena, may be explained in one of two ways: either Kiena developed these features in the upper part of a sub-volcanic porphyry system and they were subsequently removed by post-metamorphic uplift and erosion, or Kiena's ore system developed above a larger igneous body without connection to an overlying volcanic edifice (e.g. Mason, (1992)) and was subsequently depressed to mid-greenschist facies levels,

---

[2] Areas characterized by high actinolite concentrations in and around the orebody have previously been reported by mine geologists (Michel Cormier, personal communication) and by Quirion (1988), but relation of actinolite to the mine's alteration-mineralization sequence is unknown.

uplifted and eroded to its present exposure level. Departure from the generalized magmatic-hydrothermal alteration sequence observed in gold-rich porphyries could be caused by any number of variables playing a role in the ore-forming process, such as: differences in magma temperature, concentrations of gold in the source magma, fluid-phase composition, and overall mechanisms of magma emplacement. For example, an alkali fluid-rich phase accompanying the up-rise of Kiena's albitite dikes is suggested by the monomineralic composition of the dikes which consists of assemblages of pure albites (An_{0-1}, Bowen (1928)). The presence of high concentrations of chloride in the magma giving rise to albitite dikes is also suggested by the occurrence of micrographic to myrmekitic replacement textures in the albitites (e.g. White *et al.* (1981)). In addition, an extremely rapid emplacement for the albitic magma and related ore-fluids is suggested by the aplitic texture of the albitite dikes, the confinement of the ore to stockwork veins and breccias, and the limited extent of gold and propylitic alteration halos. This condition provides a mechanism that favours the retention of a fluid-rich phase in the magma until the latter has reached a high-level of emplacement in the crust, at which point hydrostatic decompression could trigger the release of Na-rich fluids causing albitization at the dikes margins (e.g. MacDonald and Arnold (1994; 1995)).

Several aspects of the regional geological setting of Cenozoic, intrusion-related gold deposits can be compared to that of Kiena. Gold-rich, porphyry copper deposits of the Andean and Western Pacific orogens, for example, occur in clusters of closely-spaced deposits (0.3 to 3 km) distributed along discrete linear belts in subduction-related plate margin environments (e.g. Luzon Central Cordillera; Sillitoe and Gappe (1984), Sillitoe (1989)). These trends of intrusion-related deposits are characterized by post-collision calc-alkaline magmatism, and define mineral belts of similar-age deposits parallel to plate margins. By analogy, Kiena is located in an Archean gold district where the majority of deposits are coincident with calc-alkaline and alkaline dike swarms and small plutons which define the Val d'Or plutonic belt (**Figure 2.2**). These intrusions were emplaced over a ca. 20 m.y. period, immediately following the regional overturning of volcanic strata (D_1), which is thought to have been initiated during the early stages of collision

between the Abitibi and Pontiac subprovinces (e.g. Card (1990) and Jackson (1994)). The resulting curvi-linear belt of gold deposits is subparallel to the district-wide Malartic-Cadillac "tectonic" zone defining the boundary between the predominantly meta-volcanic Abitibi terrane, to the north, and the predominantly meta-sedimentary Pontiac terrane, to the south (see Clowes (1996)). In addition, all the post-volcanic gold deposits occurring in the Val d'Or-Malartic area are inferred, in this study, to have formed in the 20 m.y. hiatus between the first (D_1) and second (D_2) collisional events of the Abitibi/Pontiac orogen (see **figure 8.28**). This is based on the absolute ages of deposits directly dated by cross-cutting igneous intrusions (i.e. Kiena $\geq 2686 \pm 2$ Ma and Norlartic $\geq 2692 \pm 2$ Ma), and the assessment of the period ranging between ca. 2694 and 2680 Ma as the relative time of mineralization at other deposits in the Val d'Or-Malartic gold district (see Chapter 6, section 6.4). The latter is based on the fact that virtually every deposit in the belt is hosted, at least in part, by intermediate to felsic intrusions intruded after the regional overturning of volcanic strata (D_1), and the fact that all the deposits visited during this study, or as previously reported by several authors, are ubiquitously overprinted by the regional S_2 schistosity and cut by shear zones (see Chapter 8). This means that post-D_1 and pre-D_2 calc-alkaline and alkaline intrusions are not only spatially associated with gold deposits, but are also temporally-related to mineralization. Several of these gold deposits show evidence for the contemporaneity of magmatic and gold hydrothermal activity based on intermineral diking and brecciation (e.g. Kiena, Orion, Siscoe, Sigma-LamaqueN0.2 deposits), whereas others display styles of alteration-mineralization (densely-fractured wall-rocks centred on the host intrusion, zoned alteration patterns) similar to porphyry ore systems (e.g. Camflo and Malartic Mines) (see Chapter 8). A genetic link between orogenic magmas and ore fluids is also suspected for the Val d'Or plutonic belt deposits based on the common occurrence of pervasive feldspathization (e.g. Kiena, Norlartic, Camflo, Callahan, Sigma-Lamaque N0.2) and the too commonly overlooked effects of selective biotitization of host intrusions and adjacent wall-rocks (e.g. Sigma-Lamaque N0.2).

Additional similarities between deposits of the Val d'Or-Malartic segment of the southern Abitibi belt and those of Cenozoic porphyry gold provinces are that deposits occur in pairs

of, or small clusters of, large deposits (e.g. Sigma-Lamaque N0.2/Lamaque and Malartic camp deposits, **Figure 2.2**), and that deposits are classified as two different ore types (Malartic-type carbonate-quartz stockwork vein deposits and Sigma-type lode gold vein deposits, see Chapter 8). The coexistence and proximity of diverse types of intrusion-related ore deposit is a hallmark of porphyry gold districts. For instance, at the Baguio and Marian deposits and the Paracale and Masara deposits located on Luzon and Mindanao Islands, respectively, epithermal-style mineralization controlled by a steeply-dipping fracture system occurs only 2-4 kilometres away from mineralized porphyry stocks (Sillitoe, 1989). The Ertsberg mining district of Irian Jaya, Indonesia (western half of the island of New Guinea), is another example of closely-spaced copper-gold, magmatic-hydrothermal deposits displaying the following contrasting mineralization types: 1) monzodiorite-hosted, porphyry-style and stockwork vein-controlled mineralization of the main Grasberg deposit, 2) skarn-type mineralization of the Ertsberg deposit diorite stock located 2 kilometres south of Grasberg, 3) vein-controlled mineralization of the Dalam diatreme hosted by volcanic rocks overlying the Grasberg igneous complex, and 4) porphyry-skarn mineralization of Lembah Tembaga stock located 2 kilometres west of Grasberg (MacDonald and Arnold, 1994; MacDonald and Arnold, 1995). The short distance separating deposits of the Ertsberg district, suggests that each of these deposits shares a link with the same underlying magma. By analogy, the similarly short distance separating the Sigma-Lamaque N0.2 and main Lamaque deposits, for example, may be an indication that these distinct deposits (see Chapter 8) are part of a single large magmatic-hydrothermal ore system rather than unrelated, individual deposits. The occurrence of different types of intrusion-related deposits in western Pacific gold belts, suggests also that gold deposits of the Val d'Or-Malartic area may exhibit contrasting styles of mineralization in response to diverse magmatic-hydrothermal connections created during the ca. 20 m.y. evolution of regional orogenic plutonism. Evidence supporting the concept of a district-wide magmatic-hydrothermal connection among the Val d'Or plutonic belt deposits is presented in Chapter 8. It is based on the unifying character of mineralization observed at many deposits (e.g. albitization, stockwork veining, etc.), and the presence of intermineral dikes and breccias tying hydrothermal gold alteration to magmatic activity.

deposits is presented in Chapter 8. It is based on the unifying character of mineralization observed at many deposits (e.g. albitization, stockwork veining, etc.), and the presence of intermineral dikes and breccias tying hydrothermal gold alteration to magmatic activity.

Hence, the regional geological setting of Cenozoic intrusion-related gold deposits occurring in discrete belts along circum-Pacific orogens (e.g. Luzon central Cordillera, Philippines) is remarkably similar to that of Val d'Or plutonic belt deposits and implies a tectonic control for pre-metamorphic gold mineralization at Kiena. The Val d'Or plutonic belt is regarded as a zone of weakness with connections to deep-seated calc-alkalic and alkalic magma seeking access to higher levels in the crust. It formed during the late Archean (ca. 2694-2680 Ma) along the southern margin of the Abitibi subprovince following the initial collision stage of the Abitibi/Pontiac orogen and is thus similar to present-day magmatic arcs developed at convergent plate margins. At the deposit-scale, Kiena more closely resembles the mineralization style and zoned alteration pattern exposed at the more deeply eroded sub-volcanic Santo Thomas II Cu-Au deposit, Luzon Central Cordillera, Philippines (**Table 7.2** and **7.3**). On the basis of deposit- and regional-scale similarities, Kiena is thus envisaged as a metamorphosed Archean analogue of Cenozoic gold-rich, and gold-only, porphyry deposits encountered in circum-Pacific gold provinces.

CHAPTER 8 KIENA IN RELATION TO OTHER DEPOSITS OF THE VAL D'OR-MALARTIC GOLD DISTRICT

8.1 INTRODUCTION

The results of this study are of considerable significance to the problem of timing of gold mineralization in the southern Abitibi belt, but they also have profound implications for the genesis of other gold deposits sharing important attributes with Kiena geology. At present, two types of gold deposits have been distinguished in the Val d'Or-Malartic district based on mineral assemblages and spatial distribution of auriferous veins, the radiometric age of mineralization, and the presence or absence of cross-cutting intrusions: deposits east of Kiena, which predominantly consist of hosted by quartz-tourmaline-carbonate lode gold veins, and deposits west of Kiena, which are predominantly hosted by networks of carbonate-quartz stockwork veins with auriferous sulfide (pyrite, pyrrhotite) disseminations (Couture et al., 1994; Robert, 1994). Quartz-tourmaline lode gold vein systems are predominantly exemplified by the Sigma, Lamaque and Siscoe deposits (Robert, 1994) and are referred to as "Sigma-type" mineralization, whereas auriferous stockwork vein systems dominated by carbonate and related sulphide disseminations are represented by deposits of the Malartic camp, as well as the Camflo deposit (Robert (1994), **Figure 2.2**), and are referred to as "Malartic-type" deposits. Malartic-type mineralization is cut by narrow dikes of intermediate to felsic compositions (e.g. Sansfaçon and Hubert (1990); Couture *et al.* (1994); this study), whereas Sigma-type mineralization has only been cut by ca. 2490-2150 Ma Proterozoic diabase dikes (Robert, 1994; Robert, 1996); **Figure 2.2**). Malartic-type deposits are considered part of an early gold mineralization event based on the 2692 ± 2 Ma tonalite intrusion cutting the Norlartic orebody (Couture et al., 1994), whereas Sigma-type deposits are considered part of a much younger gold mineralization event, unrelated to the Malartic gold event (Robert, 1994; Robert, 1996), based on the ca.2685 ± 3 Ma Lamaque intrusion (Jemielita et al., 1990) hosting quartz-tourmaline lode gold veins. The proposed age and genetic relationship between Malartic and Sigma-type deposits is consistent with the overprint

of the post-ore Norlartic tonalite by quartz-tourmaline-pyrite veins resembling Sigma-type mineralization (Couture et al., 1994). On the basis of vein geometry and deformation, Robert (1994) has further contrasted the Malartic-type deposits as deformed and folded and Sigma-type deposits as undeformed. However, according to a plan map of Wilson (1948, p. 885), the composite cross-section of Daigneault *et al.* (1983, p. 114), and a plan map of Karvinen (1985, p. 14), gold-bearing quartz-tourmaline veins of the Sigma and Lamaque deposits have been folded, thrusted, and deformed by the regional S_2 schistosity.

The demonstration in this study that gold mineralization at Kiena is linked to post-volcanic but pre-metamorphic igneous activity, opens the question as to whether a similar relationship exists at other gold deposits of the Val d'Or plutonic belt. However, before any deposits of the Val d'Or plutonic belt may be envisaged as an intrusion-related orebody, it must be shown that: mineralization occurred in the post-D_1 and pre-D_2 time interval, as at Kiena, and that mineralization has the diagnostic signs of high level magmatic-hydrothermal activity similar to Kiena. The purpose of this discussion is thus to compare the geology of Kiena to that of Malartic- and Sigma-type deposits to find out if other Val d'Or plutonic belt gold deposits share time and genetic affiliations with Kiena. The following Val d'Or plutonic belt deposits will be examined, from west to east and with reference to **Figure 2.2**: Canadian Malartic ("Sladen fault zone", "A" zone), Camflo ("porphyry ore", "fault ore"), Orion Vein No.8 (quartz breccia), Goldex (main ore zone), Siscoe ("Main Ore Zone" and "C" veins, "K" zone), Sigma-Lamaque No. 2 ("shear-extensional vein system" and "stringer veins"), and Main Lamaque (stockwork vein-breccia ore system, quartz-tourmaline lode gold veins). The geological overviews of these gold deposits are based on literature and on personal observations made during this study. The emphasis is on the hierarchy of structures, styles and patterns of alteration-mineralization, and on radiometric age dating of mineralization. The comparison shows that in spite of disparities in mineralization styles in the deposits, the timing of gold-ore formation appears to be everywhere post-volcanic and pre-metamorphic. As a genetic link between plutonism and gold hydrothermal activity is evident in both, Malartic and Sigma-type deposits, the concept of a district-wide magmatic-hydrothermal

connection is proposed. Mineralization in both types of deposits is thought to be coincident with the ca. 20 m.y. evolution of post-accretionary calc-alkaline and alkaline plutonism in this segment of the southern Abitibi greenstone belt following suggestions of Burrows and co-workers (e.g. Burrows and Spooner (1989), Burrows (1990)).

8.2 GEOLOGY OF SELECTED VAL D'OR PLUTONIC BELT AU DEPOSITS: ALTERATION-MINERALIZATION AND TIMING OF GOLD-ORE FORMATION

8.2.1 Canadian Malartic Deposit

The Canadian Malartic deposit is located in the section of the Malartic tectonic zone that overprints the Pontiac Group graywackes at the southwestern edge of the town of Malartic (Sansfaçon and Hubert, 1990, deposit No. 1 on Figure 2.2). The deposit has produced some 35 tonnes of gold over its 30 years of mine life from one of the lowest-grade orebodies encountered throughout the Val d'Or-Malartic region (i.e. 2.4 g/t Au with a range of 1 to 6.9 g/t Au; Sansfaçon and Hubert,(1990)). The main mineralized zone of the Canadian Malartic property is termed the "Sladen fault zone", a mineralized deformation zone described by Sansfaçon and Hubert (1990) as the southern boundary of the "Malartic Tectonic Zone". It occurs along the southern contact of an east-west monzonite intrusion which is chilled against the southwesterly-overturned beds of the Pontiac Group metasediments. The deposit consists of a zone of intensely feldspathized (albite-orthoclase-hematite) graywacke cut by a network of irregular, "cherty" quartz-pyrite-Au-telluride veinlets with pyrite-telluride disseminations locally marked by brecciation and overprinted by "pegmatitic" veins composed of "vitrous" quartz, albite, orthoclase, biotite and carbonate with lesser pyrite, chalcopyrite, gold and rare rutile, purple fluorite, tourmaline and garnet (O'Neil, 1934; Derry, 1939; Gunning and Ambrose, 1940; Eakins, 1962; Sansfaçon and Hubert, 1990; Trudel and Sauvé, 1992). According to Derry (1939) and Trudel and Sauvé (1992), a strong biotite alteration preceded the intense, fracture-controlled feldspathization and subsequent mineralization of the "Sladen fault zone". Hydrothermal biotites in alteration halos of gold quartz veins similar to those shown on **Figure 8.3**, are enriched in MgO (i.e. 12.8 to 14 wt. % MgO, Taner *et al.* (1986)),

resembling vein biotites from Kiena which contain 13 wt.% MgO (**Table 8.2**). Using the F/Cl-Mg variation diagram of Gilzean and Brimhall (1983), Taner *et al.* (1986) showed that the Canadian Malartic biotites straddle the compositional field of secondary biotites related to Cu-Mo porphyry mineralization at the Butte deposit in Montana.

Surface geology maps by Derry (1939) and Gunning and Ambrose (1940) show that the western end of the mineralized graywacke and adjacent monzonite porphyry, forming the "Sladen fault zone", is progressively deflected into a steeply, northeast-dipping shear zone. Cross-sections over the same area by Derry (1939) and Sansfaçon and Hubert (1990), show a folded "Sladen fault zone" which is cut by the steeply, north-dipping, axial planar S_2 schistosity. The emplacement of the monzonite porphyry in overturned strata and the imposition of the regional S_2 schistosity and deformation of the "Sladen fault" mineralization, suggest that the timing of gold mineralization at Canadian Malartic is post-D_1 and pre-D_2. Similar field relations between mineralization and deformation were observed also at the "A zone", another mineralized zone of the Canadian Malartic property, located some 300 metres due south of the "Sladen fault zone", i.e. south of the "Malartic Tectonic Zone" (see Figure 34 in Trudel and Sauvé (1992)). Mineralization at the "A zone" occurs as low-grade (1-3 g/t Au) "cherty" quartz-pyrite-Au veinlets accompanied by disseminated pyrite, biotite and tellurides cross-cutting monzonite dikes and the southwesterly-overturned Pontiac Group graywackes (**Figures 8.1** to **8.3**). Mineralized monzonite porphyry dikes are folded, cut and partially transposed by the regional, northwest-southeast S_2 schistosity (**Figures 8.1** and **8.2**), whereas mineralized veins in the graywacke are buckled and cut by S_2 (**Figure 8.3**), once again demonstrating the post-D_1 and pre-D_2 time relationship for mineralization at Canadian Malartic. Clearly, if the mineralized graywackes and monzonite porphyry of the "Sladen fault zone" are cut by faults of the "Malartic Tectonic Zone", and the mineralized "A zone" occurs outside the "Malartic Tectonic Zone", the latter does not control mineralization at Canadian Malartic. The same can be said of other deposits of the Malartic camp as well, as Sansfaçon and Hubert (1990) have shown that gold-quartz veins and felsic intrusions related to mineralization at East Malartic, Malartic Gold Field and Sladen-Barnat (see **Figure 2.2**) are

Figure 8.1 - *Outcrop from the "A" Zone" of the Canadian Malartic property, 300 metres south of the mineralized "Sladen fault zone" (see text for details), showing the southwesterly-overturned Pontiac Group graywackes cut by a monzonite porphyry dikel. The dike is folded, cut and partially transposed by the regional S_2 schistosity (N300 75NE).*

Stop No. 1, Figure 1 and Figure 2A of Sansfaçon and Hubert (1990) Malartic gold district field trip.

Affleurement situé dans la "Zone A" de la propriété de Canadian Malartic, se trouvant approximativement 300 mètres au sud de la zone minéralisée de "Sladen" (se référer au texte pour plus de détails), montrant les greywackes du Groupe de Pontiac déversés vers le sud-ouest et recoupés par un dyke de porphyre monzonitique. Le dyke est plissé, recoupé et partiellement transposé par la schistosité régionale S_2 (N300 75NE).

Arrêt No. 1, Figure 1 et Figure 2A de l'excursion géologique du district aurifère de Malartic de Sansfaçon et Hubert (1990).

Figure 8.2 - *Outcrop of Pontiac Group graywackes from the "A" Zone of the Canadian Malartic Mine, cut by a monzonite dike. The intrusion is cut by a low-grade auriferous quartz vein (pencil). Both the dike and the vein are overprinted by the regional S_2 planar fabric.*

Stop No. 1, Figure 1 and Figure 2A of Sansfaçon and Hubert (1990) Malartic gold district field trip.

Affleurement de grauwackes du Groupe de Pontiac situé dans la Zone A de la mine Canadian Malartic, recoupé par un dyke de monzonite. Celui-ci est recoupé par une veine de quartz aurifère à faible teneur (crayon). L'intrusif et la veine sont tous deux recoupés par la schistosité régionale S_2.

Arrêt No. 1, Figure 1 et Figure 2A de l'excursion géologique du district aurifère de Malartic de Sansfaçon et Hubert (1990).

Figure 8.3 - *Outcrop of Pontiac Group graywackes from the "A" Zone of the Canadian Malartic Mine, cut by a "cherty" gold-bearing quartz vein. The vein is buckled and cut by the regional S_2 fabric.*

Stop No. 2, Figure 3 of Sansfaçon and Hubert (1990) Malartic gold district field trip.

Affleurement de graywackes appartenant au Groupe de Pontiac situé dans la zone "A" de mine Canadian Malartic, recoupé par une veine de quartz aurifère ayant l'aspect de chert. La veine est plissée et recoupée par la fabrique pénétrative planaire régionale S_2.

Arrêt No. 2, Figure 3 de l'excursion géologique du district aurifère de Malartic de Sansfaçon et Hubert (1990).

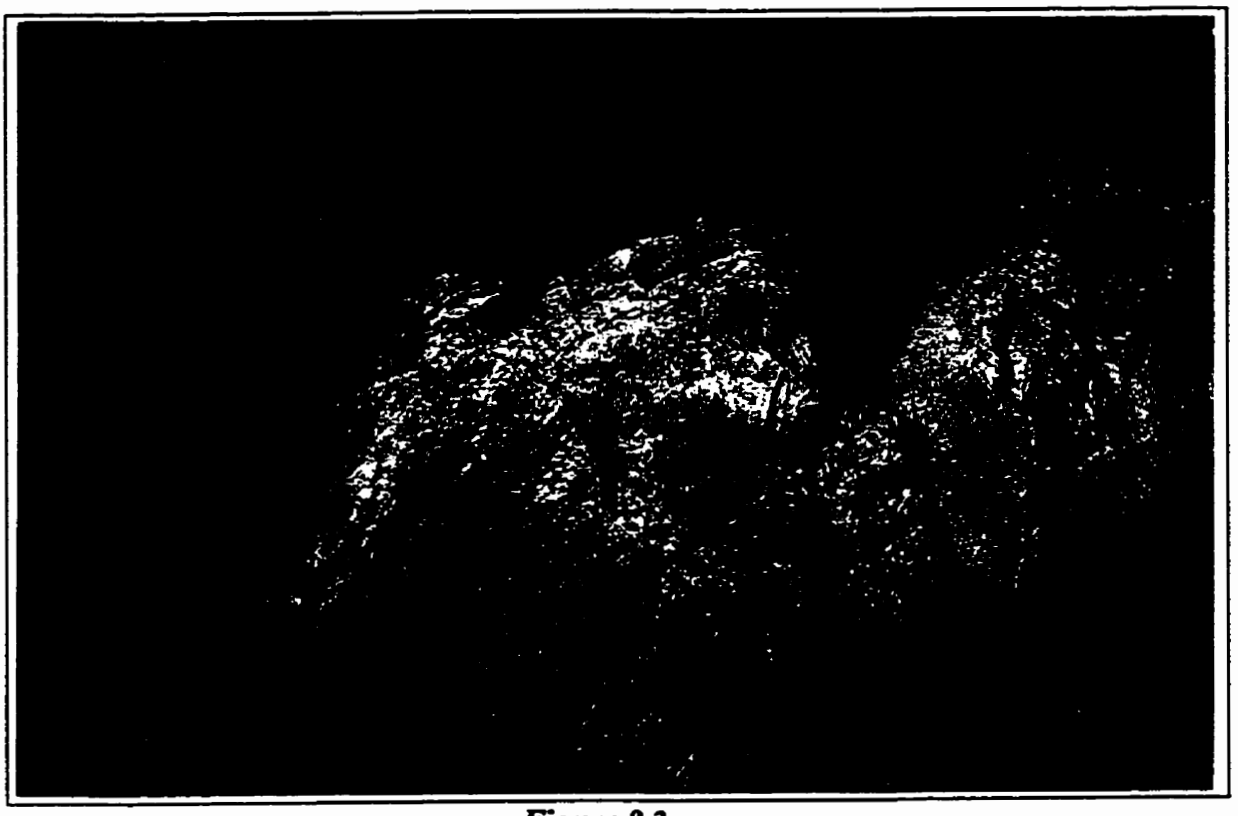

Figure 8.2

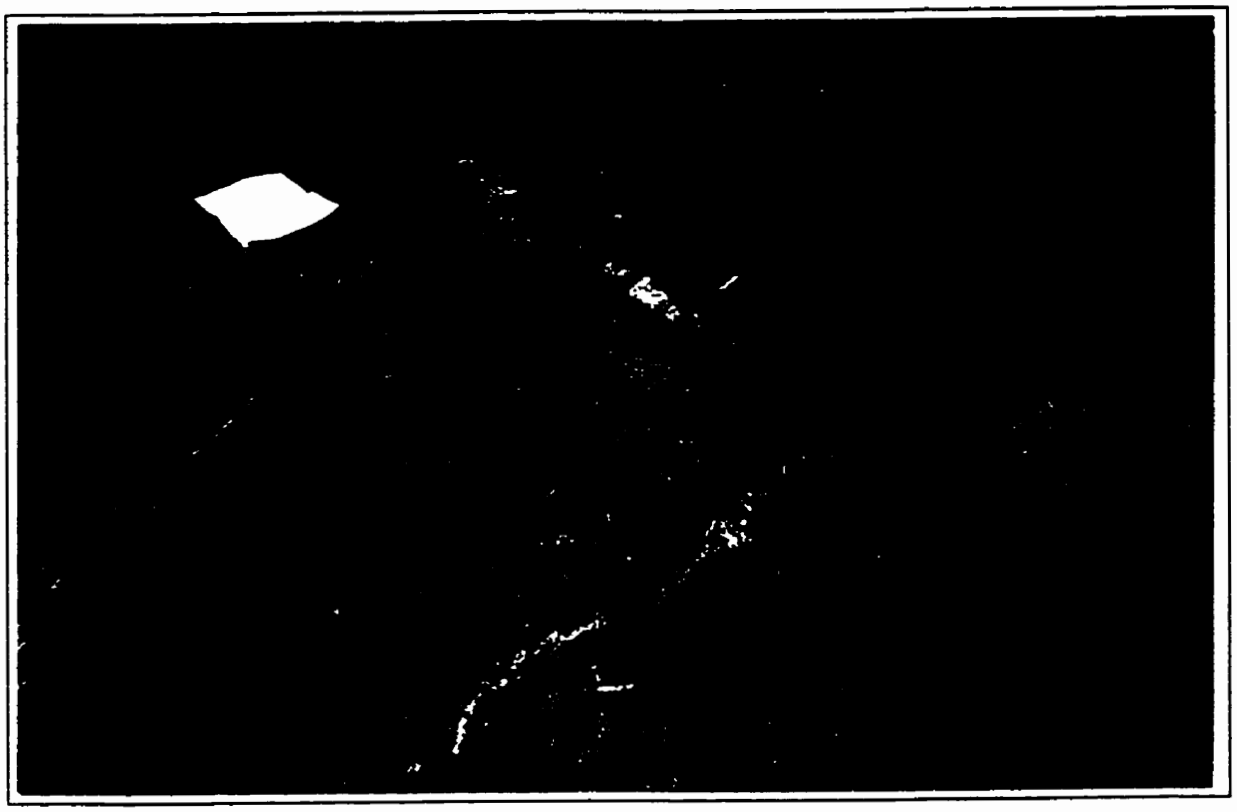

Figure 8.3

controlled by sets of fractures subparallel to the trace of an early S_1 schistosity (N315-340°) axial planar to early F_1 folds, which were subsequently refolded by upright F_2 folds and cut by the S_2 schistosity and faults of the Malartic tectonic zone.

The time sequence and field relations at Canadian Malartic may be summarized as follows: 1) regional volcanism and sedimentation, 2) overturning of volcanic and sedimentary strata during the first regional deformation event (D_1, S_1), 3) emplacement of monzonite dikes along fractures subparallel to the northwest-southeast S_1 schistosity preferentially developed in the Pontiac Group graywackes, 4) development of a succession of overprinting hydrothermal alterations comprised, from oldest to youngest, of the biotitization of the "Sladen" monzonite/graywacke contact zone, overprinted by an albite-orthoclase-hematite assemblage (commonly referred to as "silicification"), subsequently fractured and mineralized by "cherty" quartz-sulfide-telluride veinlets and overprinted again by pegmatitic quartz-albite-orthoclase-biotite-carbonate-sulfide veins, 5) folding of monzonite intrusions and gold quartz veins, imposition of the regional S_2 schistosity, and overprint by faults of the Malartic tectonic zone during the regional D_2 synmetamorphic deformation. This sequence of events suggests not only that Canadian Malartic shares the post-D_1 and pre-D_2 timing of gold mineralization at Kiena, but it also emphasizes ore controls similar to Kiena, namely, that of pre-ore fractures related to an early folding event as well as pre-ore feldspathization (albite, K-feldspar). In contrast with Kiena, where Mg-rich biotite alteration is a late-stage hydrothermal event related to gold mineralization, biotitization occurs prior to, and accompanies, main-stage gold mineralization at Canadian Malartic. The recurrence of biotite and K-feldspar throughout the Canadian Malartic alteration-mineralization sequence is akin to the recurrence of hydrothermal albite (An_{0-1}) in pre-ore albitite dikes, main-stage vein albite and albite-cemented breccias at Kiena (see Chapter 4). By analogy, hydrothermal biotite, albite and K-feldspar may indicate a temporal relationship between monzonitic magmatism and gold mineralization at Canadian Malartic, and further suggest a genetic link between the source of magma and ore fluids. The Canadian Malartic deposit is envisaged as an intrusion-related gold deposit analogous to Kiena in part because the post-D_1 and pre-D_2 timing of gold quartz veins

precludes their formation by "metamorphic-magmatic" fluids during or shortly after regional dynamothermal deformation (e.g. Sibson *et al.* (1988), Groves, (1993)), and in part because of the presence of Mg-rich biotite and alkali-feldspar alterations in the deposit's alteration-mineralization sequence. As gold-related biotitization and feldspathization as well as the pre-D_1 and pre-D_2 timing of vein mineralization is also recognized at the East Malartic, Malartic Gold Fields and Barnat-Sladen deposits (Derry, 1939; Taner et al., 1986; Sansfaçon and Hubert, 1990; Trudel and Sauvé, 1992), the latter are also envisaged as intrusion-related deposits (see Figure 8.25). The findings of Issigonis (1980), which established the presence of potassic (K-feldspar, biotite, quartz, pyrite, gold) and propylitic (chlorite, calcite, magnetite, pyrite, minor gold) alteration assemblages in porphyritic intrusions hosting mineralization at Barnat-Sladen, together with the confinement of the ore to the core of the potassic alteration zone, lends additional support to the proposed magmatic-hydrothermal origin for Malartic camp deposits.

8.2.2 Camflo Deposit

This important Malartic-type deposit occurs in the Val d'Or plutonic belt approximately 10 kilometres west of Kiena (deposit No. 4 on **Figure 2.2**) and is almost entirely hosted (i.e. 90 % of total gold production) by a monzonite-aplite dike complex dated as 2685 ± 10 Ma and as 2685 ± 3 Ma by Zweng and Mortensen (1989) and Jemielita *et al.* (1990), respectively. The monzonite porphyry is emplaced wholly within the southwesterly-overturned Kewagama Group sedimentary rocks along the northeast-plunging axis of a regional z-fold, developed at the contact between a pebble conglomerate of the Kewagama Group to the south, and a gabbroic sill of the Malartic Group Heva Formation to the north (Sauvé and Makila, 1990). The contact between the monzonite porphyry stock and Kewagama Group graywackes is characterized by several dike-like off-shoots striking parallel to the east-west regional S_2 schistosity, which is axial planar to the regional z-fold (Trudel and Sauvé, 1992), and by a contact metamorphic aureole extending to a maximum of 100 metres around the stock

(Zweng, 1993). An aplite dike swarm cuts the Camflo monzonite porphyry stock and predates hydrothermal alteration and mineralization (Zweng, 1993). The reddish-coloured aplite dikes (quartz-albite-K-feldspar-zircon-magnetite) occupy the northern part of the Camflo stock, with a few dikes occurring outside the intrusion margin (Zweng, 1993).

Two types of mineralization are recognized at Camflo: the main "porphyry ore" and subsidiary "fault ore" (Sauvé and Makila, 1990; Trudel and Sauvé, 1992). "Porphyry ore", referred to as "main-stage gold-quartz veins" by Zweng (1993), consists of auriferous quartz-pyrite-microcline stockwork veins overprinting the intensely altered and fractured monzonite-aplite igneous complex, whereas "fault ore", which is also referred to as "transitional stage mineralization" by Zweng (1993) (see below), consists of three main east-west quartz-pyrite-Au veins with sericitized margins. These faults cut the porphyry ore but concentrate the transitional stage mineralization outside the Camflo stock in parts of the faults which intersect thin beds of Kewagama Group iron formation and a magnetite-rich granophyre belonging to a differentiated gabbroic sill of the Héva Formation (Sauvé and Makila, 1990). Zweng (1993) has shown that the distribution of high-grade ore in the Camflo monzonite porphyry coincides with the distribution of aplite dikes cut by early, crustiform-textured, microcline-quartz-calcite-fluorite veins and overprinted, in turn, by ribboned quartz-pink calcite±barite±galena±pyrite veins. Main-stage gold alteration is preceded by an actinolite-epidote±chlorite±magnetite±anhydrite alteration of the stock (Zweng, 1993), as well as by the pervasive alteration of igneous mafic minerals (e.g. hornblende) by secondary carbonate-biotite-magnetite-pyrite (Trudel and Sauvé, 1992), but the relationship between these pre-ore alterations is unknown.

Gold mineralization at Camflo is associated with alkali-feldspar alteration (microcline, albite) (Sauvé and Makila, 1990; Zweng, 1993). It consists of quartz-microcline-calcite-pyrite-titanite-Au±telluride±scheelite stockwork veins accompanied by a cream-coloured alteration envelope composed essentially of pure microcline (Or_{96}) and lesser albite (An_{0-2}) grading into a grey-coloured outer alteration envelope composed of phlogopitic biotite (19 wt. % MgO)-

calcite±pyrite±magnetite±titanite±quartz and white mica (Zweng, 1993). According to Sauvé and Makila (1990) the occurrence of native gold is linked to the replacement of vein perthite by albite. Some stages of this hydrothermal alteration sequence are illustrated in Figures **8.4 to 8.7**. The photographs were taken on the 2400' level (approximately 1300 metres below surface) in a traverse from the southern margin of the Camflo porphyry toward the high-grade ore zone located in the northern part of the intrusion. **Figure 8.4** shows a network of hairline fractures filled with quartz and accompanied by K-feldspar alteration halos cutting across the pervasively biotite-calcite-magnetite-altered monzonite porphyry. The stockwork of quartz-microcline veins intensifies toward the high-grade ore zone and, as a result, coalescing alteration envelopes to the veins form a zone of pervasive K-feldspar alteration (**Figure 8.5**). High-grade mineralization (average of 6.9 g/t Au; Trudel and Sauvé (1992)) coincides with the greatest intensity of microfracture-controlled alteration and the discolouration of the pink-coloured porphyry stock in response to the replacement of secondary, perthitic K-feldspar by pure albite (**Figure 8.7**; Trudel and Sauvé (1992)). Barren quartz-microcline-fluorite±hematite "pegmatitic" veins which commonly overprint the high-grade ore zone, are illustrated in **Figures 8.6 and 8.7**. Main-stage gold mineralization of the Camflo porphyry is followed by "transitional" (i.e. fault-ore type of Trudel and Sauvé (1992)) and "late-stage" alteration-mineralization. "Transitional" mineralization is described by Zweng (1993) as "sericitic alteration", because the veins, which are mineralized outside the porphyry but barren within the porphyry, consist of quartz-pyrite-sericite±albite±calcite±rutile. Tourmaline-quartz-albite veins and quartz-pyrite-sericite veins cut main-stage gold-quartz veins and are overprinted, in turn, by late-stage chlorite-quartz-calcite-hematite-cemented "breccias". Zweng (1993) interpreted the latter as fault breccias related to deformation; however, the mosaic-texture, the lack of rock flour or gouge and the branching character of the interstitial chlorite are reminiscent of microfracturing by a network of chlorite stringer veins (see Zweng (1993) , p. 89).

Based on the age of the Camflo stock (2685 ± 10 Ma) and with reference to the time interval of 2700-2690 Ma, thought to represent the age of peak metamorphism in the southern Abitibi

Figure 8.4 - Photograph of the biotite-calcite-magnetite-altered Camflo monzonite (dark coloured) cut by hairline fractures filled with quartz (arrows) and accompanied by microcline-pyrite-Au alteration halos (distal gold-quartz vein facies of Zweng, 1993).

Southern margin of Camflo monzonite porphyry. Camflo deposit, 2400' level.

Photo du porphyre monzonitique de Camflo altéré par un assemblage de biotite-calcite-magnétite (couleur fonçée), recoupé par des filonnets de quartz (flèches) accompagnés d'un halo d'altération composé de microcline-pyrite-Au (faciès veines de quartz aurifères distales de Zweng, 1993).

Bordure méridionale du porphyre monzonitic de Camflo. Mine Camflo, niveau 2400'.

Figure 8.5 - Photograph of gold-quartz stockwork veins, northeast of the distal gold-quartz veins shown on Figure 8.4. As the density of gold-quartz veins increases near the southern contact with the high-grade ore zone, alteration envelopes coalesce to form a zone of pervasive K-feldspar alteration .

Southern part of the Camflo monzonite porphyry. Camflo deposit, 2400' level..

Photo de veinlules aurifères de quartz en stockwork, situées au nord-est des veinule de quartz-or montrées à la Figure 8.4. Près du contact avec le minerai forte teneur, la densité des veines de quartz-or augmente, créant une zone d'altération à feldspaths potassiques causée par la coalescence des enveloppes d'alterations.

Partie méridionale du porphyre monzonitique de Camflo. Mine Camflo, niveau 2400'.

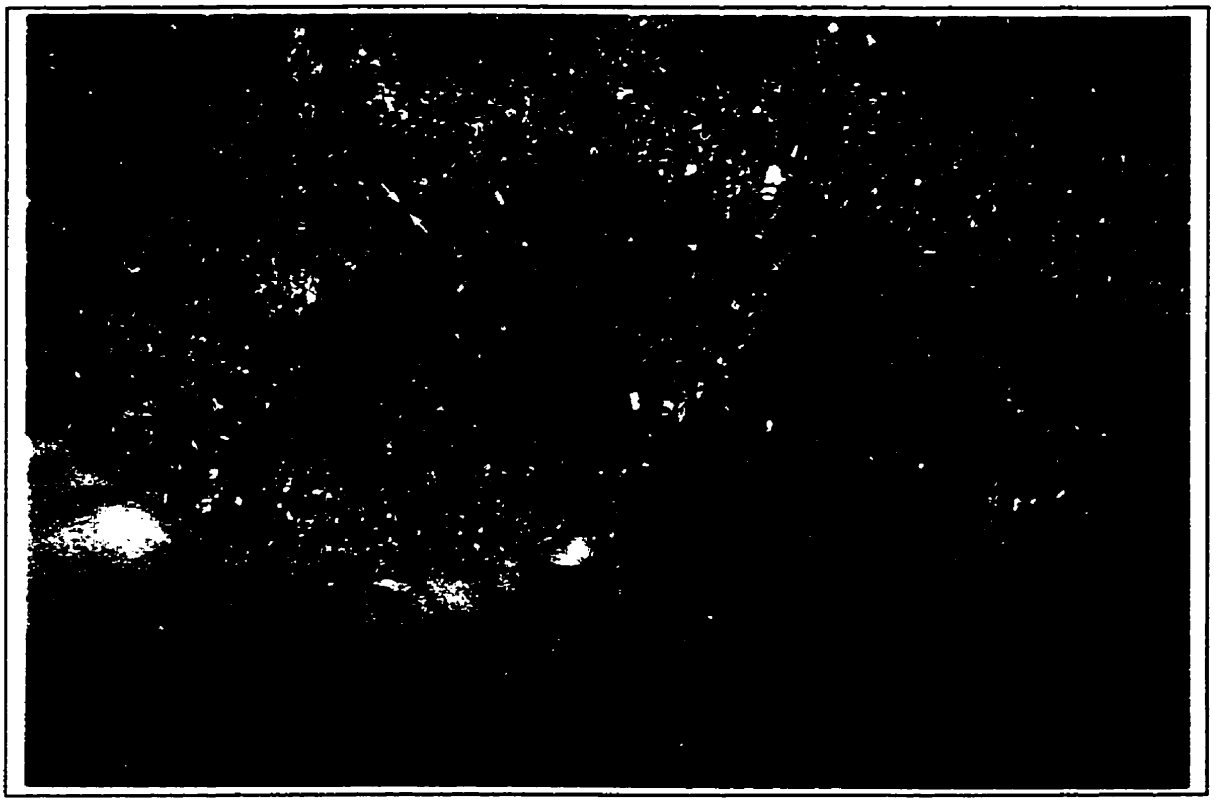

Figure 8.4

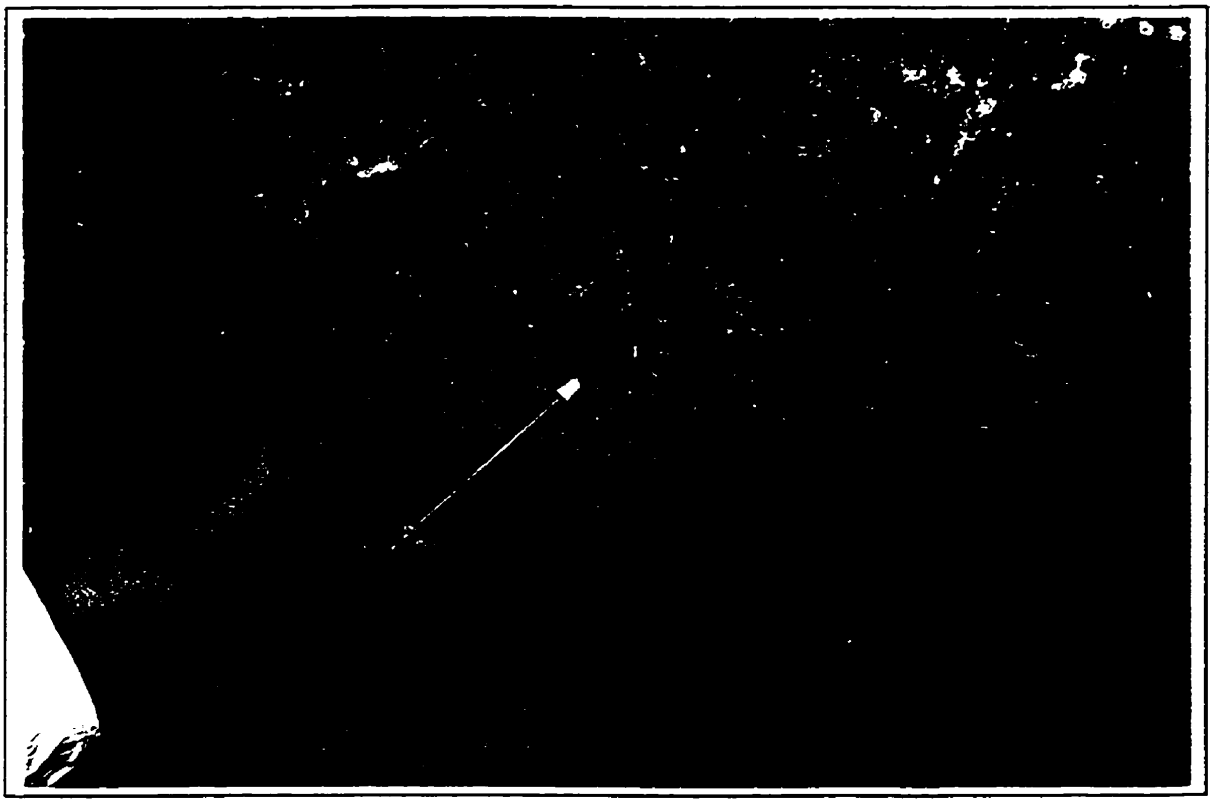

Figure 8.5

Figure 8.6 - *Progressive discolouration of altered monzonitic wall-rocks to gold-quartz veins at the contact with the Camflo high-grade ore zone, created by the replacement of secondary, perthitic K-feldspar by albite. Note the overprint of fracture-controlled gold alteration by barren quartz-microcline-fluorite±haematite veins.*

Central part and eastern margin of the Camflo monzonite porphyry. Camflo deposit, 2400' level.

Décoloration progressive de la monzonite altéré aux épontes des veines de quartz-or au contact du minerai haute teneur de Camflo, causé par le remplacement du feldspath potassique perthitique secondaire par de l'albite. Notez la superposition de veines stériles de quartz-microcline-fluorite±hématite sur le minerai à veinules de quartz.

Partie centrale et bordure orientale du porphyre monzonitique de Camflo. Mine Camflo, niveau 2400'.

Figure 8.7 - *High-grade (0.3 oz Au/t) mineralization or so-called "porphyry ore" of Sauvé and Makila (1990) in the Camflo monzonite porphyry. This ore type accounts for 90% of the total gold production. The densely fractured intrusion is no longer pink but grey, a change in colour attributed to quartz-albite vein alteration. The ore contains 2-3% finely disseminated pyrite which is associated with native gold and traces of chalcopyrite, galena and molybdenite. A barren quartz-microcline-fluorite±hematite vein overprints the high-grade ore (upper right corner).*

Northern part and eastern margin of the Camflo monzonite porphyry. Camflo deposit, 2400' level.

Minerai haute-teneur (0.3 oz Au/t)du porphyre monzonitique de Camflo, aussi appelé "minerai de type porphyre" par Sauvé et Makila (1990). Ce type de minerai constitue 90% de la production d'or de la mine. L'intrusif est intensément fracturé et de couleur grise au lieu de rose. Ce changement de couleur est attribué à l'altération en veinules de quartz-albite. Le minerai renferme 2-3% de pyrite disséminée, laquelle est intimement associée avec de l'or natif ainsi qu'une faible quantité de chalcopyrite, galène et molybdénite. Une veine stérile à quartz-microcline-fluorite±hématite recoupe le minerai (coin supéreur droit).

Partie septentrionale et bordure orientale du porphyre monzonitique de Camflo. Mine Camflo, niveau 2400'.

Figure 8.6

Figure 8.7

belt at the time of his study (e.g. Mortensen (1987); Card (1990); Corfu (1993)), Zweng (1993) concluded that the timing of gold-ore formation at Camflo was post-metamorphic. Accordingly, he estimated the depth of emplacement of the mineralized porphyry as ~ 15 kilometres, in agreement with the epidote-amphibolite facies metamorphism determined for nearby diorite dikes belonging to the Malartic Group. Zweng (1993) thus proposed that mineralization formed during deformation and was controlled by the development of shear zones; see also Zweng *et al.*(1993). He interpreted "porphyry ore" as microfractures formed during the down-plunge, uniaxial extension of the Camflo stock, overprinted shortly after by en-échelon dip-slip faults filled with quartz-pyrite-Au accompanied by foliated, sericite-rich alteration halos (i.e. fault-ore), during continued regional deformation by subhorizontal shortening. According to Zweng (1993), late-stage tourmaline-quartz-albite veins and chlorite seams post-date and are unrelated to regional compressional deformation. Zweng *et al.* (1993) consolidated this sequence of events at Camflo by producing a U-Pb age of 2621 ± 4 Ma for hydrothermal titanite occurring in a main-stage gold-quartz vein at the 1500' level. Based on the ca. 60 m.y. hiatus between the U-Pb zircon age of 2685 ± 10 Ma for magma emplacement and the 2621 ± 4 Ma U-Pb titanite age for gold mineralization, they ruled out the possibility of a genetic link between monzonitic magmatism and gold-ore formation. However, the significance of the discordant U-Pb titanite age of 2621 ± 4 Ma for a gold-quartz vein is not clear when compared to the 2626 Ma (no error given) U-Pb rutile age obtained for main-stage gold mineralization by Jemielita *et al.* (1990).

In view of the indistinguishable ages produced by the isotopically "strong" titanite U-Pb system (i.e. closure temperature of ~ 620-670°C; e.g. Mezger *et al.* (1991)) and isotopically "weaker" U-Pb rutile system (i.e. closure temperature of ~ 400°C, e.g. Mezger *et al.* (1989)), the best means by which to ascertain the age of mineralization at Camflo remains the documentation of field relations between mineralization and regional synmetamorphic deformation. For example, the following field relations are commonly referred to as evidence for the emplacement of the ore at Camflo during regional dynamothermal deformation (i.e. D_2): 1) the parallelism of the northeast-plunging (55° east) monzonite porphyry with the fold

axis of a regional z-fold at upper mine levels (at depth the axis of the fold shallows out to 45° whereas the stock axis steepens to 63°), 2) the folding or boudinage of aplite dikes emplaced outside the Camflo stock, 3) the widespread cataclasis of the feldspathised and mineralized monzonite, 4) the boudinage of dike-like off-shoots of the monzonite stock which are oriented subparallel to the S_2 schistosity, 5) the folding or boudinage of main-stage gold quartz veins located in the vicinity of the sericitic faults cutting across the mineralized Camflo stock (i.e. "fault ore"), 6) the reverse vertical sense of movement indicated by steeply-plunging striations on the sericite-chlorite-carbonate-pyrite coated walls of the "transitional" quartz-pyrite-sericite-albite veins and 7) the regional-scale z-folding of the "transitional" gold-bearing veins or "fault ore" (see Figures 48 and 52 in Trudel and Sauvé (1992)). However, the syndeformation interpretation proposed to explain these field relations is equivocal, as the observed geometric relations between monzonite stock, aplite dikes, gold quartz veins, folds, and penetrative planar and linear fabrics may have resulted, alternatively, from the mineralization of the Camflo monzonite-dike complex prior to regional synmetamorphic deformation and fabric development.

In fact, features of the Camflo deposit porphyry ore (i.e. bulk of mineralization) are reminiscent of the pre-metamorphic, intrusion-related character of mineralization at Kiena. For example, the overprint of the Camflo monzonite by a pre-ore aplite dike swarm and the occurrence of several large Kewagama Group xenoliths in the porphyry, suggest a high-level of emplacement for the mineralized igneous complex. The Camflo orebody is characterized also by a zoned alteration-mineralization sequence comprised of early actinolite-epidote-chlorite-magnetite-anhydrite and carbonate-biotite-magnetite-pyrite alterations, overprinted by main-stage quartz-microcline-albite-biotite-pyrite-telluride-Au stockwork vein alteration (porphyry ore) and quartz-microcline fluorite-hematite pegmatitic veins, subsequently cut by late-stage tourmaline-quartz-albite veins, auriferous quartz-pyrite sericite veins (fault ore), and chlorite stringer veins and breccias. High-grade ore is coincident with aplite dikes, increase fracturing, inner feldspathization of the host intrusions, and post-ore pegmatitic veins. As at Kiena, deformation in and around the Camflo orebody, from the cataclasis of the

feldspathized and mineralized monzonite porphyry to the folding, boudinage and imposition of the S_2 schistosity on aplite dikes and gold-bearing veins in the margin of the Camflo stock, can be explained by post-ore strain partitioning. Contrasting styles of deformation for mineralized stock and adjacent country rocks may be the result of enhanced competency differences acquired during the development of a zoned alteration pattern characterized by main-stage K-feldspar and albite alteration.

In summary, Camflo shares many characteristics of high-level, porphyry-style gold mineralization at Kiena, suggesting that a pre-metamorphic intrusion-related origin for the Camflo deposit cannot be dismissed as previously thought (e.g. Zweng, (1993)). In fact, now that the regional synmetamorphic D_2 deformation is bracketed between ca. 2677-2645 Ma (Corfu et al., 1991; Feng and Kerrich, 1991; Powell et al., 1995), a post-2685 Ma but pre-2677 Ma timing for gold mineralization at Camflo, as suggested by post-ore strain partitioning, is plausible. However, the U/Pb titanite age of 2621 ± 4 Ma (Zweng, 1993) appears to preclude the pre-metamorphic origin and genetic link of the monzonite-dike complex to gold alteration-mineralization at Camflo. Isotopic disturbance of the gold-related titanites during regional deformation and metamorphism, which could explain this post-metamorphic age for mineralization, has been ruled out (Zweng, 1993; Powell, 1994). According to Powell (1994), greenschist-amphibolite facies temperature conditions in the Camflo deposit area were approximately 150°C lower (< 450°C) than the thermal closure temperature of titanite for the diffusion of Pb (~ 600°C). In spite of this, it may be post-orogenic magmatism at ca. 2645 Ma, not the regional synmetamorphic D_2 deformation event, that is responsible for thermal peak and the young apparent age of ca. 2621 Ma for mineralization at Camflo (e.g. Kerrich and Feng (1992)). In the absence of single zircon age constraints for gold mineralization, and based on similarities with Kiena, a post-2685 but pre-2677 magmatic-hydrothermal origin is favoured for the Camflo deposit. A porphyry ore system related to the emplacement of the Camflo monzonite adequately explains the existence of a zoned alteration sequence replacing the garnet matrix of the skarnoid rocks in the contact aureole of the Camflo stock, the concentration of gold mineralization in a potassic alteration

zone (phlogopitic biotite, k-feldspar, albite), and the development of fluorite-bearing pegmatitic veins and chlorite stringer veins in the waning stages of magmatic-hydrothermal activity.

8.2.3 Orion Vein No. 8

A few kilometres to the northeast of Camflo lies the Orion Vein No. 8 deposit, hosted by southwesterly-overturned mafic and ultramafic volcanic follows assigned to the Jacola formation (deposit No. 4A on **Figure 2.2**), which is also intruded and mineralized by the Kiena deposit's albitite dikes further east (deposit No. 10 on **Figure 2.2**). The deposit is much smaller than Camflo or Kiena (< 1 t Au, Trudeau and Raymond (1992)), but the timing and style of mineralization are similar to Kiena. The Orion Vein No. 8 orebody lies along the southern margin of a high-strain deformation zone termed the "Marban-Norlartic deformation zone" (Trudeau and Raymond, 1992). The steeply northeast-dipping deformation zone is subparallel to bedding and located to the southeast of an asymmetric regional z-fold resembling the one described at Camflo (**Figure 2.2**). The nose of the z-fold is cut by the east-west regional S_2 schistosity, whereas the southern limb of the fold and the Marban-Norlartic deformation zone are both offset by north to northwest-dipping faults related to the S_2 schistosity (see Figures 2 and 3 of Trudeau and Raymond (1992)). Two of these faults, which have a reverse and left-lateral sense of movement, mark the eastern and western boundaries of the Orion Vein. The 160 metres-long and 2 to 15 metres-wide, pinching and swelling ore zone, is exposed at surface (**Figures 8.8 to 8.10**) and consists of a moderately to steeply north-dipping quartz breccia vein containing pyritized and auriferous basalt fragments (**Figure 8.8**) grading to the south into a zone of low-grade pyritized and albitized basalt. The latter, which is referred to as the "transition zone" by Trudeau and Raymond (1992), consists of an intricate network of quartz-carbonate stockwork veins accompanied by pyrite and minor pyrrhotite disseminations (**Figure 10A**). A cross-section of the Orion Vein No. 8 orebody shows that mineralization cross-cuts a grey-coloured, quartz diorite porphyry dike at approximately 200 metres below surface (**Figure 8.9**), whereas a

Figure 8.8 - *Photograph of the auriferous quartz breccia vein of the Orion No. 8 Vein deposit. The monolithic breccia is characterized by the presence of sharp-angular, altered mafic volcanic rock fragments with pyrite disseminations, cemented by a vein matrix composed of milky quartz, carbonate, and albite. The breccia exhibits a mosaic texture and grades into a network of stockwork veins (see Figure 8.10). View is to the northeast.*

Photo de la veine bréchique aurifère du gisement Orion Veine No. 8. La brèche est monolithique et se charactérise par la présence de fragments angulaires de roche volcanique mafique renfermant de la pyrite disséminée, cimentés par une matrice filonienne composée de quartz laiteux, carbonate et albite. La veine bréchique possède une texture en mosaique et se change progressivement en un stockwork en marge de l'encaissant (voir Figure 8.10). La photo est prise avec un regard vers le nord-est.

Figure 8.9 - *Plan view of the grey porphyry/mafic volcanic rock contact, situated immediately south of the Orion breccia vein. This intrusion is similar to the quartz diorite porphyry hosting the main ore zone at depth (Trudeau and Raymond, 1992). In this photograph, the grey porphyry and mafic volcanic rocks are both cut by the east-west, regional S_2 schistosity(left to right).*

Vue en plan du contact entre un porphyre gris et son encaissant de roche volcanique mafique, situé immédiatement au sud de la veine bréchique minéralisée Orion. Cet intrusif est similaire au porphyre de quartz diorite qui est recoupé par la zone minéralisée principale sous la surface (Trudeau and Raymond, 1992). Sur cette photo, le porphyre gris et son encaissant sont tous deux recoupés par la schistosité régionale S_2, orientée est-ouest (de gauche à droite).

Figure 8.8

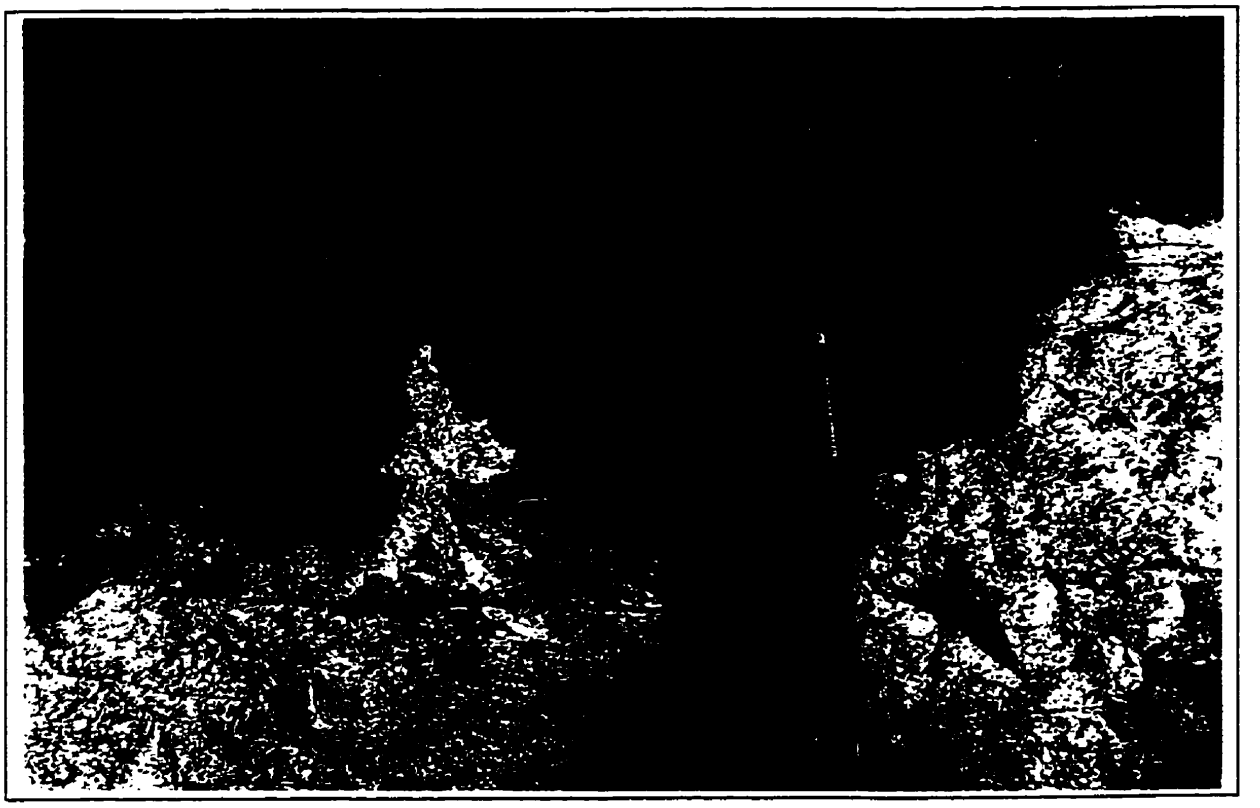

Figure 8.9

Figure 8.10 A - *Plan view of the stockwork vein ore zone grading into the Orion Vein No. 8 quartz breccia. Altered mafic volcanic rocks contain pyrite and minor pyrrhotite disseminations. The vein network is flattened as suggested by northwest-southeast elongated fragments, parallel to the Marban-Norlartic deformation zone (see text for detail). Intense albite-ankerite alteration imparts a buff colour to the host volcanic rocks.*

Vue en plan de la zone de minerai en stockwork en marge de la veine Orion No. 8. Les fragments renferment de la pyrite et un peu de pyrrhotite disséminées. Le réseau de veines en stockwork est déformé par aplatissement, tel que le suggère plusieurs fragments de forme allongée, orientés nord-ouest-sud-est, en parallèle avec la zone de déformation Marban-Norlartic (voir le texte pour de plus amples détails). L'intense albitization et ankéritization donnent localement une couleur brun rouille à l'encaissant.

Figure 8.10 B - *Plan view of the Orion No.8 Vein stockwork vein ore zone overprinted by a shear zone parallel to the regional S_2 schistosity.*

Vue en plan de la zone de minerai en stockwork de la Veine Orion No. 8 recoupée par une zone de cisaillement parallèle à la schistosité régionale S_2.

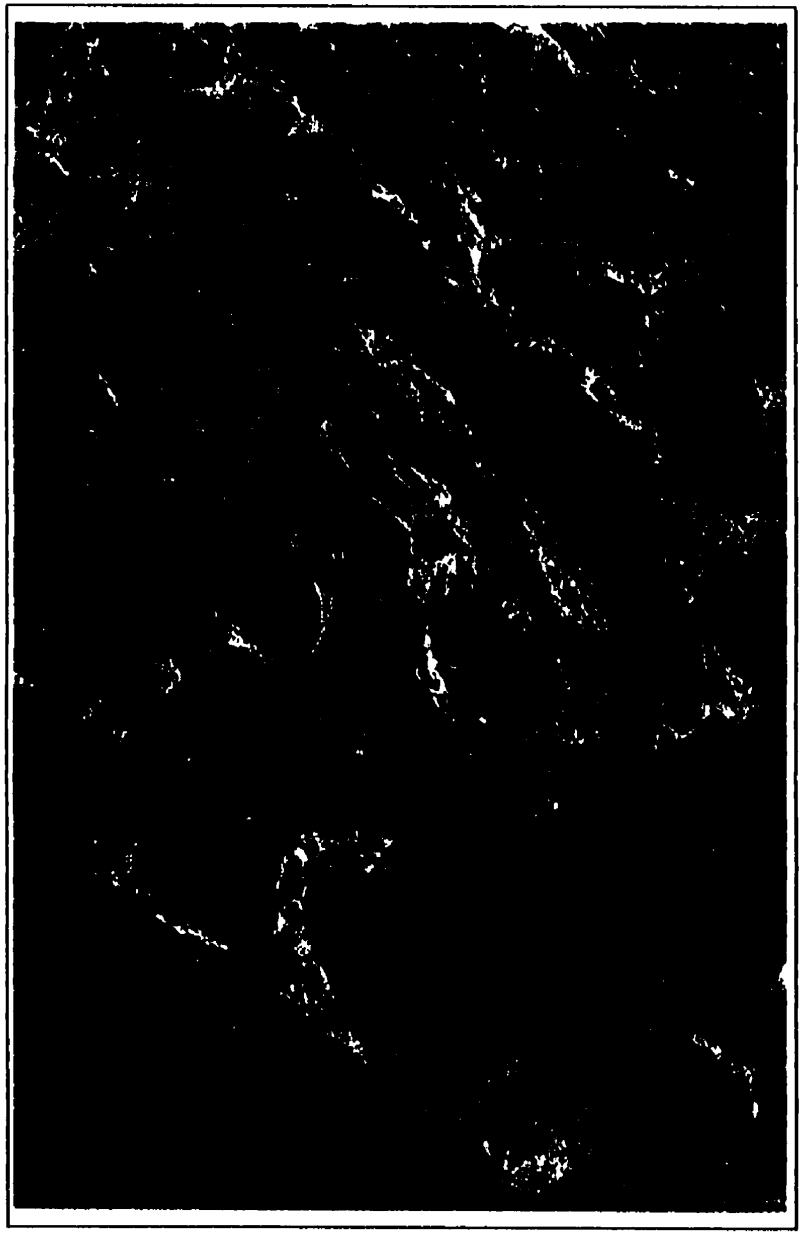

Figure 8.10 A

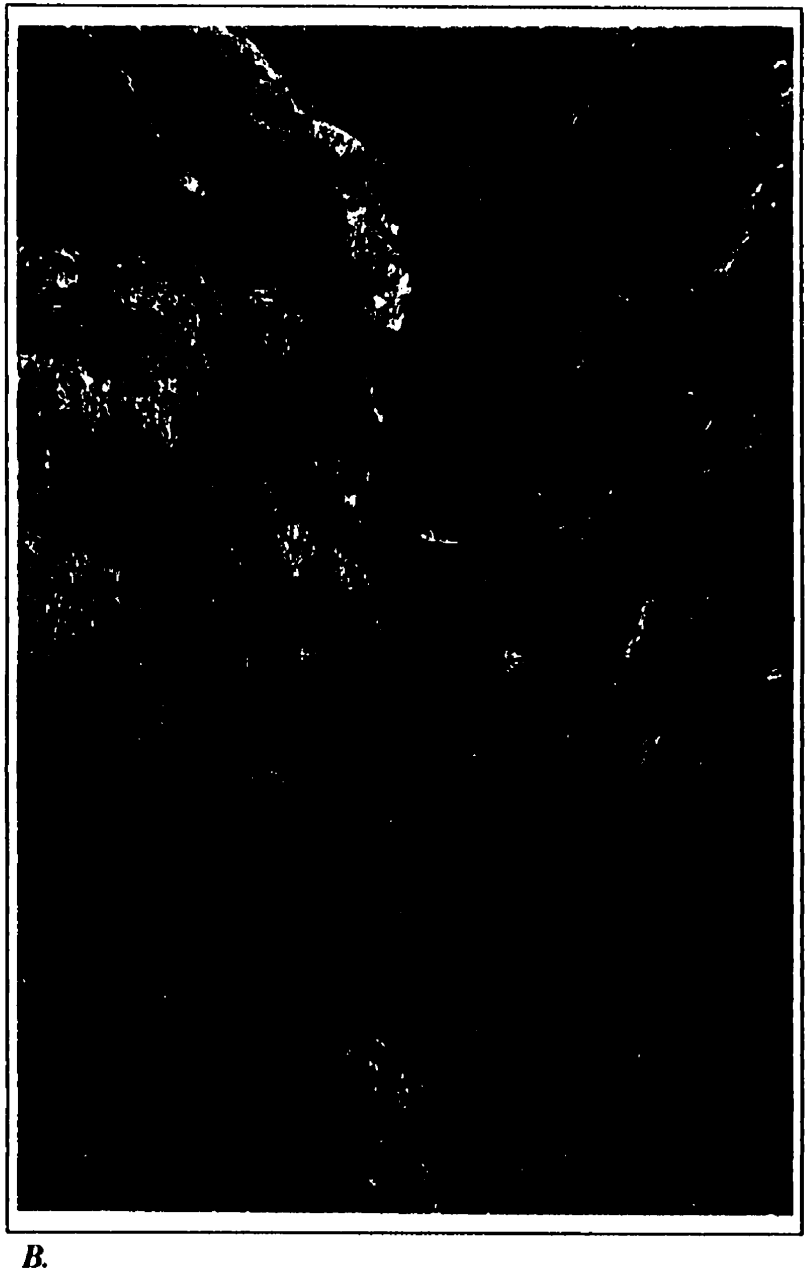

B.

photograph of an underground exposure shows another dark-grey to pink-coloured felsic dike cutting mineralization (Trudeau and Raymond, 1992). Both dikes, which contain disseminated sulfides and carry gold anomalies of up to 690 ppm Au, are perceived as temporally- and genetically-related to the ore- forming process at Orion by Trudeau and Raymond (1992). An upward pyrrhotite-pyrite sulfide zonation is observed in the orebody: pyrrhotite dominates over pyrite (1-10% versus 1-3%) at depth, whereas pyrite is most abundant at surface with minor pyrrhotite and traces of chalcopyrite, galena, sphalerite, molybdenite and gold tellurides (Sauvé, 1987). Episodic gold mineralization at Orion is suggested by the occurrence of pyrite-associated gold in rock fragments to the main breccia vein and by the presence of gold in the quartz matrix. Grades are systematically higher with a greater incidence of pyritized auriferous basalt fragments (Trudeau and Raymond, 1992). The breccia-dike system is cut by the regional S_2 schistosity and related shear zones (**Figure 8.10B**) and, as indicated by Trudeau and Raymond (1992), coarse-grained visible gold is locally remobilized along schistosity planes. Quartz-breccia vein mineralization partially hosted by a bedding-parallel quartz-diorite porphyry dike cutting overturned volcanic strata and subsequently overprinted by the regional S_2 schistosity and related shear zones, suggests a post-D_1 and pre-D_2 timing of gold-ore formation at the Orion Vein No. 8 deposit. Apart from the relative timing of gold mineralization in common with Kiena, intrusion-related features of the Orion deposit are: 1) the main ore zone cuts, and is overprinted by, felsic dikes, 2) alteration-mineralization is episodic and fracture-controlled, 3) stockwork veins progressively grade into the high-grade mosaic quartz breccia and suggest a high-level of emplacement for the ore, 4) the felsic porphyries show gold anomalies of several hundred ppm Au in relation to disseminated sulfides, and 5) mineralization is characterized by an upward pyrrhotite-pyrite zonation. Because of the Kiena-like magmatic-hydrothermal character of its mineralization (this study) and the contemporaneity of felsic magmatism and vein-breccia formation prior to regional synmetamorphic deformation (Trudeau and Raymond, 1992), the Orion Vein No. 8 deposit is envisaged, as Camflo and Malartic camp deposits, as a high-level intrusion-related deposit of the Val d'Or plutonic belt.

8.2.4 Goldex Deposit

Goldex is located approximately 5 kilometres southeast of Kiena (see deposit No. 15 on **Figure 2.2**). Based on criteria set forth by Robert (1994), it consists of Sigma-type tourmaline-quartz-pyrite lode gold veins cutting the "Goldex intrusion", a quartz-diorite sill emplaced into a southerly-overturned sequence of mafic-ultramafic volcanic rocks of the Jacola Formation (Still and Mason, 1995). The Goldex intrusion is also one of the intrusions of the Val d'Or plutonic belt. Several feldspar porphyries are intruded along the steeply north-dipping volcanic rock contacts near the Goldex orebody, but their relation to it and their composition are unknown. Still and Mason (1995), however, have reported that the porphyritic intrusions are not as altered as the mineralized quartz-diorite sill, which suggests they may be younger than the latter. Two types of ore occur at Goldex: the main tourmaline-quartz-pyrite lode gold veins which are centred on the quartz-diorite intrusion, and a minor and peripheral sulfide vein-ore type (pyrite-pyrrhotite-chalcopyrite±sphalerite±arsenopyrite) occurring in the enclosing carbonate- and phyllosilicate-altered mafic volcanic rocks (Still and Mason, 1995). According to Still and Mason (1995), main-stage mineralization at Goldex overprints pre-ore alterations comprised, from the oldest to the youngest, of a pervasive albite alteration accompanied by disseminated pyrite, followed by chlorite-sericite vein alteration of the quartz-diorite sill and biotite vein alteration at the margins of the sill, which extend outward into the host mafic volcanic rocks (see **Table 8.1**). Main-stage gold mineralization essentially consists of tourmaline-quartz-pyrite lode gold veins associated with a strong, buff-coloured alteration halo composed of albite, disseminated auriferous pyrite and minor scheelite. The majority of the veins strike northwest-southeast and dip steeply to the south, whereas the remaining veins which branch-off the main subvertical veins dip gently to the southeast. Locally, quartz is the main vein constituent, however, normally the veins show crustiform textures consisting, from the margins of the vein inward, of aggregates of acicular tourmaline with fine, disseminated euhedral pyrite, coarse-grained and equant pyrite crystals lining the tourmaline walls, and inner translucent to milky quartz with minor scheelite and rare anhydrite. Some tourmaline-quartz gold veins progressively grade outward into net-textured

Table 8.1 Preliminary time sequence at the Goldex deposit after Still and Mason (1995)

1. Regional mafic-ultamafic volcanism

2. Regional overturning of volcanic strata

3. Intrusion of **Goldex quartz-diorite sill** and feldspar porphyry dikes (?)

4. Hydrothermal alteration-mineralization of Goldex quartz-diorite

   4.1 Pervasive **albitization** ● disseminated pyrite

   4.2 Phyllosilicate vein alteration

      4.2.1 Chlorite-sericite stringer veins in quartz-diorite
      4.2.2 **Biotite** stringer veins at margins of quartz-diorite intrusion and outward into mafic volcanic wall-rocks

   4.3 Main-stage gold mineralization

      Essentially subvertical (N102 64S) and minor subhorizontal (N056 07SE) **tourmaline-quartz-pyrite-Au** veins with minor **scheelite** and traces of **anhydrite**, accompanied by **albite** and disseminated auriferous **pyrite** alteration halos

      Tourmaline-cemented breccias: angular and rounded fragments of carbonate-albite and quartz veins and clasts of albitized and sericite-chlorite altered wall-rocks
      3-5% disseminated pyrite

   4.4 Carbonate vein alteration
      (throughout the alteration-mineralization sequence)

5. Late-stage quartz, epidote and calcite veins

6. Regional greenschist facies metamorphism and deformation :

   S- and Z-folded auriferous veins
   NW-SE penetrative foliation overprint (N288-297 60-77 N)
   Goldex mylonite zone (N280-305 65-75N)
   Late-stage faults

7. Intrusion of northeast-trending Proterozoic diabase dikes

tourmaline veinlets with disseminated pyrite overprinting the pervasively albite-altered quartz-diorite, whereas locally, sections of the larger veins become tourmaline breccia veins and tourmaline-cemented breccias. They contain angular and rounded fragments of carbonate-albite and vein quartz as well as clasts of albitized and sericite-chlorite-altered wall-rocks. Crustiform textures and breccias suggest that ore-fluids circulated in open-fractures at relatively high-levels, whereas hydrothermally-altered wall-rock fragments and veins clasts in the matrix of the tourmaline breccias provide evidence for the episodicity of gold mineralization. Goldex tourmaline-quartz lode gold veins, tourmaline-pyrite stringer veins and breccias, and their host quartz-diorite intrusion are overprinted by a penetrative, north-dipping foliation parallel to the regional S_2 schistosity, deformed by s- and z-shaped folds, and cut by faults and shear zones (i.e. Goldex mylonite; see **Table 8.1**). Still and Mason (1995) have noted that the Goldex intrusion was overprinted by shear zones only in areas coincident with strong phyllosilicate alteration, suggesting strain partitioning across the altered and mineralized and unaltered quartz-diorite.

In summary, similarities in the timing of deformation between Kiena and Goldex include the following sequence: 1) emplacement of the Goldex quartz diorite sill in southerly-overturned mafic-ultramafic volcanic rocks of the Jacola Formation, 2) overprint of the sill by a fracture-controlled alteration-mineralization sequence, and 3) folding of the auriferous tourmaline-quartz veins and imposition of the regional S_2 schistosity and related shear zones. Mineralization at Goldex is thus, post-D_1 and pre-D_2, and coincident with regional calc-alkaline and alkaline plutonism at ca. 2694-2680 Ma. Many intrinsic features of the Goldex deposit suggest a Kiena-like magmatic-hydrothermal origin for the orebody, such as: vein-controlled alteration-mineralization localized about a calc-alkaline intrusive centre, pre-ore and gold-related feldspathization (albite), vein sericite, chlorite and biotite, episodic mineralization characterized by open-spaced ore structures (crustified veins and breccias), as well as the pre-shear zone development of the mineralized vein-breccia system. Although the Goldex deposit resembles Kiena, its tourmaline-quartz-pyrite lode gold vein-breccia style of mineralization is more akin to Sigma-type mineralization. As the timing of the Goldex gold

mineralization is also post-D_1 and pre-D_2 as at Sigma (see discussion below), a post-2685 Ma but pre-2677 Ma timing of gold-ore formation is envisaged for Goldex.

8.2.5 Siscoe Deposit

The Siscoe deposit, which produced approximately 27 tonnes of gold and 9 tonnes of silver (e.g. Sauvé *et al.* (1993), is located on an island of the same name situated in the northeast corner of Lac de Montigny, some 4 kilometres north of Kiena (see deposit No. 11 on **Figure 2.2**). Although not a very large deposit, Siscoe was noted for its elevated ore grade (average of 18 g/t Au for the first five years of production) and its spectacular amounts of visible gold (Sauvé et al., 1993).

Most of the Siscoe ore originated from an intensely albite-chlorite-carbonate-actinolite-altered portion of the Siscoe stock, a gabbroic intrusion similar in composition to the enclosing tholeiitic, mafic-ultramafic volcanic flows assigned to the Dubuisson Formation (Imreh, 1984; Tessier et al., 1990). The Siscoe stock and the Dubuisson Formation have been interpreted as co-magmatic on the basis of similar whole-rock compositions, Y/Zr ratios and REE profiles (Tessier et al., 1990), and it may be assumed that the stock was overturned to the south similar as the neighbouring Bourlamaque sills during the regional tilting of volcanic strata (D_1) at ca. 2700-2694 Ma (Regional Sequence of Events diagram in back pocket). This is supported by the steeply north-dipping and south-facing attitude of mafic pillow flows enclosing the gabbroic stock (Imreh, 1984). The main centre of hydrothermal alteration and vein mineralization coincides with a concentration of intermediate and felsic dikes composed, from the oldest to the youngest, of microdiorite, feldspar porphyry and albitite dikes followed by a second generation of diorite and microdiorite dikes (Sauvé et al., 1993).

Based on the amount of gold produced, Siscoe's mineralized veins are subdivided into three groups: 1) a main zone of gold-quartz veins hosted by the Siscoe stock, 2) a subsidiary zone of gold-quartz veins hosted by the "K" zone, a high-strain zone composed of talc-chlorite

Figure 8.11 - *Surface exposure of quartz-tourmaline veins hosted by the southerly-overturned mafic volcanic rocks of the Dubuisson Formation, south of the "K" shear zone on Siscoe Island (southwest of Siscoe Mine shaft at the end of golf course). Main, east-west quartz vein with northerly and southerly branching veins cut by a network of tourmaline veinlets predominantly oriented east-west. The veins are folded and penetratively deformed by the steeply north-dipping regional S_2 schistosity. Canadian dollar coin used for scale measures 2.5 cm across. See Figure 8.15 to compare quartz-tourmaline lode gold veins of the Siscoe and nearby Sigma deposits.*

Affleurement montrant des veines de quartz-tourmaline encaissées dans des roches volcaniques mafiques déversées vers le sud appartenant à la Formation de Dubuisson, situé au sud de la zone de cisaillement "K" sur l'île de Siscoe (au sud du chevalement de la mine Siscoe, au bout du terrain de golfe). La veine principale, qui est orientée est-ouest,se subdivise en petits embranchements allant en direction nord et en direction sud. La veine et ses embranchements sont recoupés par un réseau de veinules de tourmaline d'orientation est-ouest. La veine de quartz et les veinules de tourmaline sont déformées par des plis ainsi que par la schistosité régionale S2. La pièce de monnaie (dollar Canadien) utilisée comme échelle mesure 2.5 cm de diamètre. Se référer à la Figure 8.15 afin de comparer les veines aurifères de quartz-tourmaline de Siscoe avec celles du gisement avoisinnant de Sigma.

Figure 8.12 - *Close-up view of the main quartz-tourmaline vein of Figure 8.11, showing a stylolitic tourmaline veinlet with peaks oriented north-south.*

Vue détaillée de la veine de quartz-tourmaline de la Figure 8.11, montrant une veinule de tourmaline stylolitique dont les pointes sont orientées nord-sud.

Figure 8.11

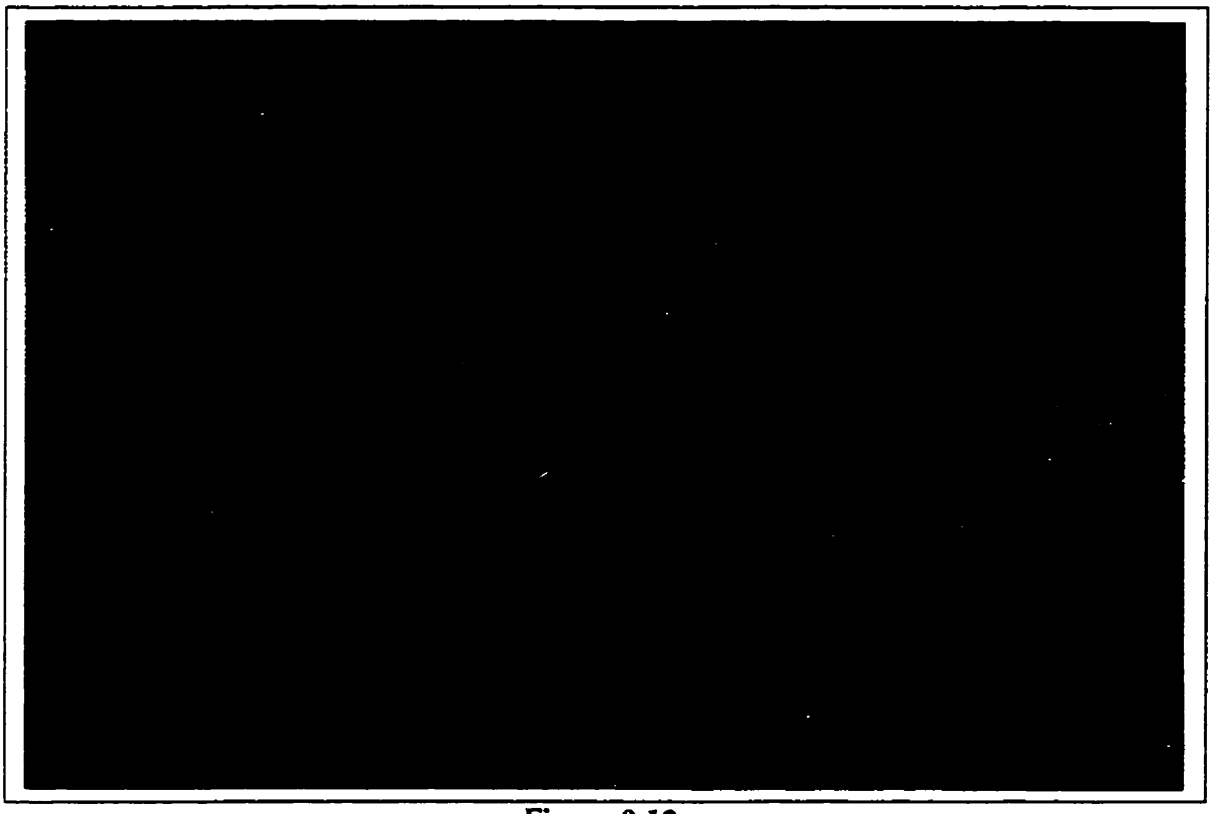

Figure 8.12

Figure 8.13 *- Detail of* ***Figure 8.11*** *showing a buckled branch off the main quartz-tourmaline vein, clearly cut by the east-west S_2 schistosity.*

Vue détaillée de la ***Figure 8.11*** *montrant une ramification de la veine de quartz-tourmaline principale. Cette veine est plissée et nettement recoupée par la schistosité régionale S_2 d'orientation est-ouest.*

schist truncating the southern margin of the Siscoe stock, and 3) a minor zone of gold-quartz veins located in the Dubuisson Formation mafic volcanic rocks south of the "K" zone (see Figure 27 in Sauvé *et al.* (1993); **Figures 8.11 to 8.13**). Within the altered and mineralized Siscoe stock three major lode-gold vein systems are recognized: the north-striking and east-dipping "Main Ore Zone" veins, the southerly-dipping "Siscoe" vein situated west of the "Main Ore Zone" veins, and the northwesterly-dipping "C" vein located east of the "Main Ore Zone" veins. All three sets of veins coincide with inner albite-Fe-chlorite±pyrite±chalcopyrite±magnetite±haematite±apatite±biotite and carbonate-chlorite (up to 60 %)-quartz ±epidote±pyrite±tourmaline±sericite alteration facies of the Siscoe stock outlined by Tessier *et al.* (1990), and are surrounded by a more widespread Mg-Fe-chlorite alteration facies, extending outward to an actinolite (up to 20%)-Mg-chlorite alteration facies at the southwestern margin of the stock. Two generations of lode gold-quartz veins are recognized among the Siscoe stock veins based on vein paragenesis and cross-cutting relationships. Older lode-gold veins composed essentially of milky quartz with lesser tourmaline and minor sulfides (pyrite±chalcopyrite±pyrrhotite±sphalerite±galena), are either cut or re-opened and sealed, by younger tourmaline veins with disseminated pyrite accompanied by translucent quartz, scheelite and rare magnetite and petzite ($AuAg_3Te_2$) (Hawley, 1932; Auger, 1947; Trudel, 1985; Sauvé et al., 1993). The older veins are typified by the "Main Ore Zone" and "Siscoe" veins, whereas the "C" vein is an example of the younger vein generation. The two generation of veins are further distinguished by the occurrence of deep yellow native gold in the older quartz veins and of pale yellow native gold, thought to reflect a lower Au:Ag ratio in the younger tourmaline-quartz-pyrite veins (Hawley, 1932; Auger, 1947; Trudel, 1985). Backman (1936) and Auger (1947) reported that the older generation of gold-quartz veins are cut by barren quartz-carbonate veinlets, whereas Trudel (1985), quoting Cooke (1923) and Hawley (1930), reports that the younger tourmaline-quartz-pyrite-gold veins are also cut by barren quartz-carbonate veins. The "C" vein is now mined out but was zoned and consisted, from the margins inward, of aggregates of tourmaline grading to radiating tourmaline needles in translucent quartz with native gold and scheelite (Auger, 1947). This is reminiscent of the tourmaline-pyrite-quartz-scheelite

infill-vein textures described earlier from the Goldex deposit (see previous section).

Level plan maps of Moss (1939) and Auger (1947) as well as a section of Backman (1936) across the mineralized veins show the early "Siscoe"and "Main Ore Zone" veins cutting an albitite dike, and the "Main Ore Zone" veins cut, in turn, by another albitite dike. The plan maps and sections also show an "andesite" dike (chlorite altered diorite or microdiorite dike?) off-setting the albitite dike which cuts the "Main Ore Zone" veins, cut by the younger tourmaline-quartz-pyrite "C" vein. Mutual cross-cutting relationships between the older gold-quartz veins, albitite dikes, and younger tourmaline-quartz-pyrite veins suggest that albitite dikes are intermineral (Kirkham, 1971; Trudel, 1985). Pointing to the gradational contacts between albitite dikes and the enclosing gabbroic rocks of the Siscoe stock, Auger (1947) concluded that albitization (An_{0-1}) of the host intrusion was coeval with the emplacement of the albitite dikes, and that secondary albites were replaced by quartz and chlorite. Gold-quartz veins in the "K" zone and those located in the mafic volcanic rocks south of it (see **Figures 8.11 to 8.13**) are similar to the older lode-gold veins of the Siscoe stock, because they are composed essentially of quartz with little tourmaline (Auger, 1947). They are nonetheless distinguished from the Siscoe veins by the occurrence of sulfide (pyrite-chalcopyrite-pyrrhotite) and chlorite veinlets overprinting the quartz veins (Backman, 1936; Auger, 1947).

According to early sketches of J.E. Gill in Moss (1939) and Asbury (1941) and to descriptions and maps of Auger (1947), north-south albitite dikes and related gold-quartz veins in the Siscoe stock were progressively deflected (e.g. horse tail zone of the "Main Ore Zone" vein system) into the east-west "K" zone with depth. The 300' level plan map of Auger (1947) also shows gold-quartz veins in the "K" zone deformed by folds, as well as a boudinaged albitite dike extended parallel to the strike-length of the deformation zone. Figures **8.11** to **8.13** are examples of gold-quartz veins in the mafic volcanic rocks south of the "K" shear zone, similarly deformed by folds and overprinted by an axial planar, regional S_2 schistosity.

Although a number of authors recognized a temporal relation between intermediate and felsic diking and gold mineralization at Siscoe, most did not consider the possibility of a genetic relationship between calc-alkaline magmatism and hydrothermal gold activity but favoured a shear zone-controlled ore model contemporaneous with regional deformation (Hawley, 1932; Backman, 1936; Trudel, 1985; Robert, 1994). However, the geologic relations presented above resemble those described at Kiena in the following aspects: 1) the emplacement of intermediate and felsic dikes in a southerly-overturned gabbroic stock and related mafic volcanic rock sequence, 2) alteration-mineralization of the dikes by a succession of gold-quartz veins, quartz-carbonate veins and tourmaline-quartz-pyrite veins, and 3) folding of the vein-dike complex and imposition of the regional S_2 schistosity and related shear zones (i.e. "K" zone). Moreover, a Kiena-like magmatic-hydrothermal origin for the Siscoe deposit is strongly suggested by the presence of intermineral albitite dikes, early albite alteration (An_{0-1}), episodic vein-controlled mineralization and crustiform infill-vein textures, in addition to the pre-shear zone development of the mineralized vein system.

8.2.6 Sigma-Lamaque No. 2 Deposits

The vein-dike system of the Sigma-Lamaque No. 2 deposits is situated at the eastern entrance to the city of Val d'Or, less than 1 kilometre north of the main Lamaque deposit(**Figure 8.14**) and approximately 12 kilometres east of Kiena (**Figure 2.2**). Sigma-type gold mineralization has been considered as a classic example of a metamorphogenic, shear zone-controlled Archean gold deposit (Robert and Brown, 1986a; Robert and Brown, 1986b; Sibson et al., 1988; Robert, 1990; Robert et al., 1994) that apparently has nothing in common with porphyry-style gold mineralization at Kiena (Robert, 1996). However, the lower part of the Sigma orebody, which is different from the upper part traditionally described and modelled by Robert and coworkers, resembles Kiena.

Robert and Brown (1986a) have shown that the upper part of the Sigma deposit consists of steeply south-dipping, funnel-shaped quartz-tourmaline veins accompanied by sericitized and

Figure 8.14 - *Simplified geological compilation map of the area encompassing the Sigma-Lamaque No. 2 vein-dike system and the main Lamaque deposit.*

Carte géologique simplifiée du secteur des mines Sigma-Lamaque No. 2 et de la mine Lamaque

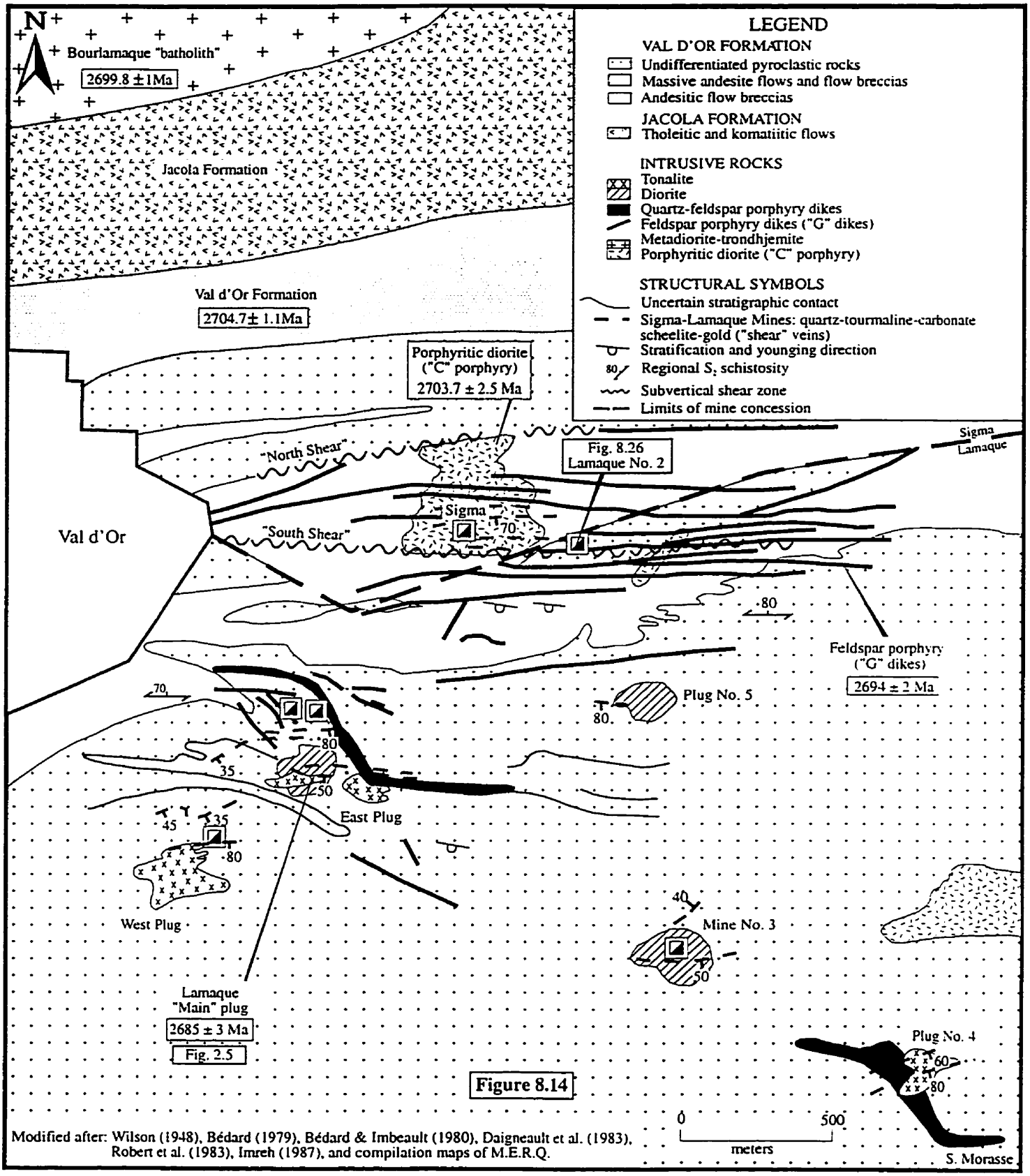

Figure 8.14

Modified after: Wilson (1948), Bédard (1979), Bédard & Imbeault (1980), Daigneault et al. (1983), Robert et al. (1983), Imreh (1987), and compilation maps of M.E.R.Q.

*See Table 6.2 for age dating authorship.

pyritized wall rocks (**Figures 8.15** to **8.18**) which coincide with a similarly funnel-shaped feldspar porphyry dike swarm dated as 2694 ± 2 Ma (Wong et al., 1991), intruding the southerly overturned volcanic strata of the Val d'Or Formation dated as 2705 ± 1 Ma (Wong et al., 1991). In the literature, Sigma veins are either referred to as "lode" gold veins because of the thickness (0.2-3 m), considerable lateral and vertical dimensions (in excess of 100 m), and high-grade gold contents (average 25-50 g/t Au in subhorizontal veins) of single veins (e.g. Robert *et al.* (1994), Kerrich and Cassidy (1994)) or, more commonly as "subvertical" and "flat" veins (e.g. Robert and Brown (1986a)). They have also been referred to as "shear" and "extensional" veins (e.g. Boullier and Robert (1992), because steeply south-dipping veins and north-south, gently west-dipping veins are interpreted to have formed together within an east-west shear zone during regional compressional deformation (Robert, 1990; Robert, 1994; Robert, 1996). The post-D_1 porphyry dikes have a tonalitic composition (Sauvé et al., 1993) and are referred to as G dikes by Sigma mine geologists.

In contrast with the upper part, the lower part of the Sigma orebody is characterized by fewer dikes and the presence of pyritic, tourmaline-cemented breccias (Robert et al., 1983) associated with auriferous quartz veins and tourmaline stockwork veins (**Figures 8.19** to **8.24**). The breccias and veins are predominantly hosted by the C porphyry, a dioritic intrusion dated as ca. 2703.7 ± 2.5 Ma and interpreted as subvolcanic to the Val d'Or Formation (Grant, 1986; Robert and Brown, 1986a; Wong et al., 1991). The tourmaline-cemented breccias have several notable features suggesting they may represent the root zone of the Sigma lode gold vein-breccia-dike complex. For example, at level 38 (approximately 1.6 km below surface), pyritic, tourmaline-cemented breccias which contain angular and rounded fragments of the host C porphyry as well as clasts of quartz veins, are cut by quartz lode gold veins. At the margin of the tourmaline breccia, clasts of diorite porphyry are pervasively albite altered and criss-crossed by quartz-carbonate veinlets restricted to the wall rock fragments as well as by through-going tourmaline veinlets (**Figure 8.20**), whereas in the centre of the breccia quartz vein fragments are shattered into small, angular pieces by a network of tourmaline stringer veins (**Figure 8.23**). The breccias grade outwardly through

a zone of mosaic breccia composed of large, sharp-angular, albitized diorite fragments cemented by tourmaline veinlets (**Figure 8.19**), into unalbitized but biotite-rich diorite porphyry (**Figure 8.25**). As seen in thin section, the porphyry shows a well preserved primary igneous texture with pale brown biotites similar to the phlogopitic vein biotite (11.8 to 13.2 wt. % MgO) encountered at Kiena, replacing hornblende phenocrysts and the quartzo-feldspathic groundmass, which is also cut by carbonate veinlets. Taner *et al.* (1986) analysed four biotites from "unaltered" wall rocks and two vein biotites from Sigma and obtained similar compositions (8.8 to 10.1 wt. % MgO) for all six biotites. On the F/Cl, Mg variation diagram of Gilzean and Bimhall (1983), the Sigma biotites lie in the compositional field of secondary biotites occurring at the Santa Rita porphyry Cu deposit, New Mexico (Taner et al., 1986). The mode of occurrence, composition, and the resulting rock texture enhancement (see **Figure 8.25**) are indeed reminiscent of early, selectively pervasive biotite alteration near the thermal centre of porphyry Cu and Cu-Au ore systems (e.g. Moore and Czamanske (1973); Sillitoe and Gappe (1984) and Reyes (1990)).

The granoblastic texture of the diorite porphyry, characterized by idioblastic quartz and poikiloblastic biotites, indicates that the igneous rock is deformed and partially recrystallized. The lode gold veins, tourmaline veins, and breccias which overprint the albitized diorite porphyry are penetratively deformed by folds and a through-going, steeply north-dipping schistosity (**Figures 8.21** to **8.24**). The albitized diorite porphyry at the margin of the tourmaline-cemented breccia appears undeformed because it is not schistose; however, it exhibits tear-shaped fragments (**Figure 8.19**) elongated in the same direction as the schistosity in the central part of the tourmaline breccia. This suggests that the albitized diorite porphyry wall rocks are also deformed. Hence, field relationships reveal that, in the deeper part of the Sigma orebody, quartz and tourmaline veins formation are separate hydrothermal events of a zoned alteration-mineralization sequence, and that penetrative deformation affects all the preexisting ore structures. Pre-ore pervasive albite alteration, quartz-carbonate vein alteration, and possibly the biotitization of the C porphyry may be part of the early gold alteration sequence. Mutual cross-cutting relationships between gold quartz veins and

tourmaline breccia also suggest that the tourmaline hydrothermal event is intermineral (see Kirkham (1971)).

Although crustified veins indicate that quartz and tourmaline have coprecipitated in some lode gold veins located in the upper part of the deposit (Robert and Brown, 1986a; Boullier and Robert, 1992), several other banded veins, for example at level 14, consist of quartz veins accompanied by zoned alteration halos subsequently cut by tourmaline stringer veins (**Figures 8.17** and **8.18**). In Figure 8.17, parts of the network of tourmaline veinlets confined to the quartz vein are stylolitic, whereas the sericitized, pyrite- and tourmaline vein-altered wall rocks are schistose. This suggests that the quartz vein, the altered wall rocks, and the younger tourmaline veinlets, were deformed together by pressure-solution. Similarly, Figure 8.18 shows a buckled, subhorizontal quartz-tourmaline vein cut by a through-going and steeply north-dipping schistosity. At surface, the Sigma deposit quartz-tourmaline lode gold veins clearly form a stockwork vein system which trend parallel to the regional east-west S_2 schistosity (**Figure 8.15**). Northerly-branching veins off the main quartz-tourmaline vein are buckled and cut by the S_2 schistosity (**Figure 8.16**). These relationships are consistent with observations at lower mine levels and strongly suggest that the Sigma deposit was deformed during regional penetrative fabric development, following vein breccia formation.

Timing of vein development in relation to penetrative deformation

Across the boundary of the Sigma property, similar relationships to those observed between the quartz-tourmaline vein system and penetrative deformation at Sigma, are documented at the Lamaque N0. 2 deposit (**Figure 8.14**, Daigneault *et al.* (1983)) and at the main Lamaque deposit (**Figure 8.14**, Karvinen (1985)). At the Lamaque N0. 2 deposit, the synoptic cross-section of Daigneault *et al.* (1983) shows thrusted and imbricated segments of subhorizontal quartz-tourmaline veins and sigmoidal z-shaped dragfolds in tourmaline bands (**Figure 8.26**). At the main Lamaque deposit, Sigma-type quartz-tourmaline veins cut across the altered and mineralized Lamaque diorite-tonalite intrusion (**Figure 8.27**) dated as 2685 ± 3 Ma (Jemielita

Figure 8.15 - *Overview of the Sigma Mine discovery outcrop showing auriferous quartz-tourmaline stockwork veins similar to those occurring on Siscoe Island (see* ***Figure 8.11****). The steeply south-dipping veins, which trend parallel to the east-west regional S_2 schistosity, are hosted by the southerly-overturned mafic volcanic rocks of the Val d'Or Formation. View is to the east.*

Vue d'ensemble de l'affleurement signifiant la découverte de la mine Sigma, montrant des veines de quartz-tourmaline aurifères en stockwork similaires à celles observées sur l'île de Siscoe (voir ***Figure 8.11****). Les veines, qui pendent fortement vers le sud, sont parallèles à la schistosité régionale S_2 d'orientation est-ouest. Elles sont encaissées par les roches volcaniques mafiques déversées vers le sud de la Formation de Val d'Or. Le regard de la photo est vers l'est.*

Figure 8.16 - *Detail of Figure 8.14, showing a north-south veinlet branching off the main east-west quartz-tourmaline vein. That veinlet is buckled and overprinted by the regional east-west S_2 schistosity.*

Vue détaillée de la Figure 8.14, montrant une veinlule à direction nord-sud se détachant de la veine de quartz-tourmaline principale qui est orientée est-west. La veine est plissotée et recoupée par la schistosité régionale S_2 d'orientation est-ouest.

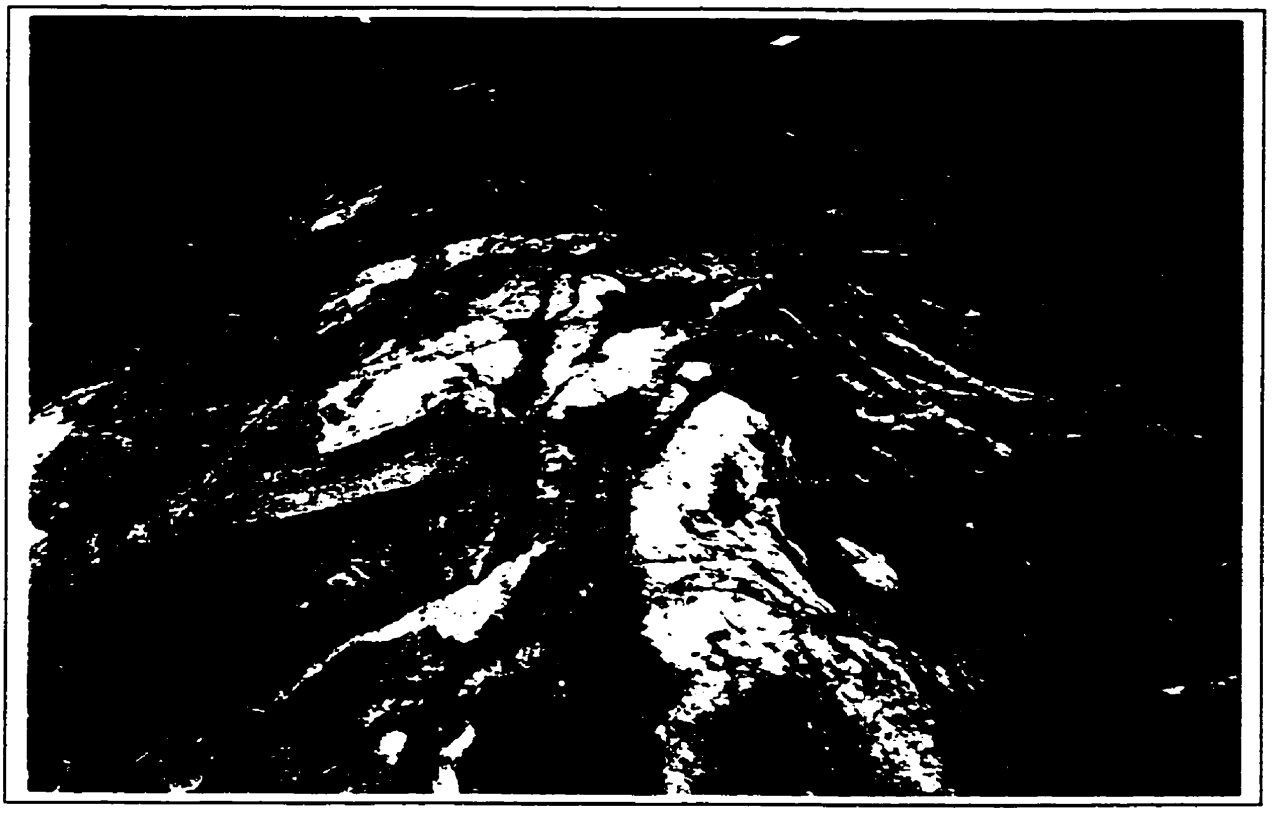

Figure 8.15

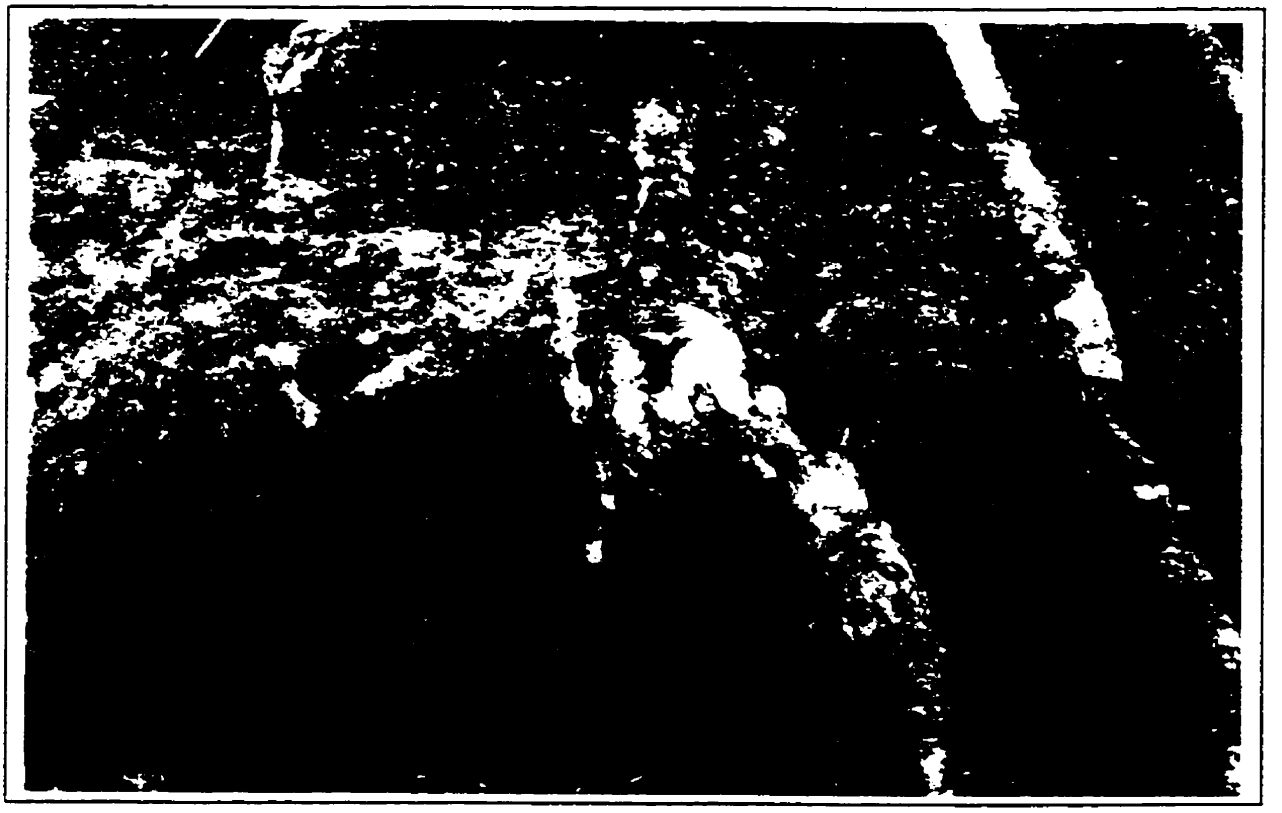

Figure 8.16

Figure 8.17 - *Sectional view, looking up, of a Sigma Mine subhorizontal quartz lode gold vein associated with sericitized and pyritized wall rocks cut by a network of tourmaline veinlets. The tourmaline veins are stylolitic indicating that they, and the enclosing quartz lode gold vein, are deformed. Stylolitic cleavages perpendicular to the deposit's main schistosity suggest that altered wall rocks and quartz-tourmaline veins were deformed coevally by pressure-solution. Strain partitioning is invoked to explain the different deformation styles exhibited by the main quartz vein and altered wall rocks.*

Stope 1405, Sigma Mine level 14.

Vue en section, avec regard vers le haut, d'une veine de quartz aurifère sub-horizontale aux épontes séricitsées et pyritisées de la Mine Sigma, recoupées par un réseau de veinules de tourmaline. La tourmaline stylolitique indique que les veines de tourmaline ainsi que la veine de quartz encaissante sont toutes deux déformées. Le fait que les clivages stylolitiques soient perpendiculaires à la schistosité principale du gisement suggère que la roche encaissante séricitisée et pyritisée et la veine de quartz-tourmaline ont été déformés simultanément par pression-dissolution. Le contraste entres les styles de déformation de la veine de quartz et de l'encaissant peut s'expliquer par une répartition de la déformation pénétrative (strain partitioning).

Chantier 1405, niveau 14 Mine Sigma.

Figure 8.18 - *Sigma Mine sub-horizontal quartz-tourmaline-Au vein hosted by a sericite-altered feldspar porphyry dike at upper mine levels. The vein is buckled (arrows) and clearly cut by the through-going east-west regional S_2 schistosity. View is to the east.*

Stope 1405, Sigma Mine level 14.

Veine sub-horizontale à quartz-tourmaline-Au de la mine Sigma encaissé par un dyke de porphyre feldspathique séricitisé, située aux niveaux supérieurs de la mine. La veine est déformée par des plis ondulés (flèches) et elle est nettement recoupée de part et d'autre par la schistosité régionale S_2 d'orientation est-ouest. Le regard de la photo est vers l'est.

Chantier 1405, niveau 14 Mine Sigma.

Figure 8.17

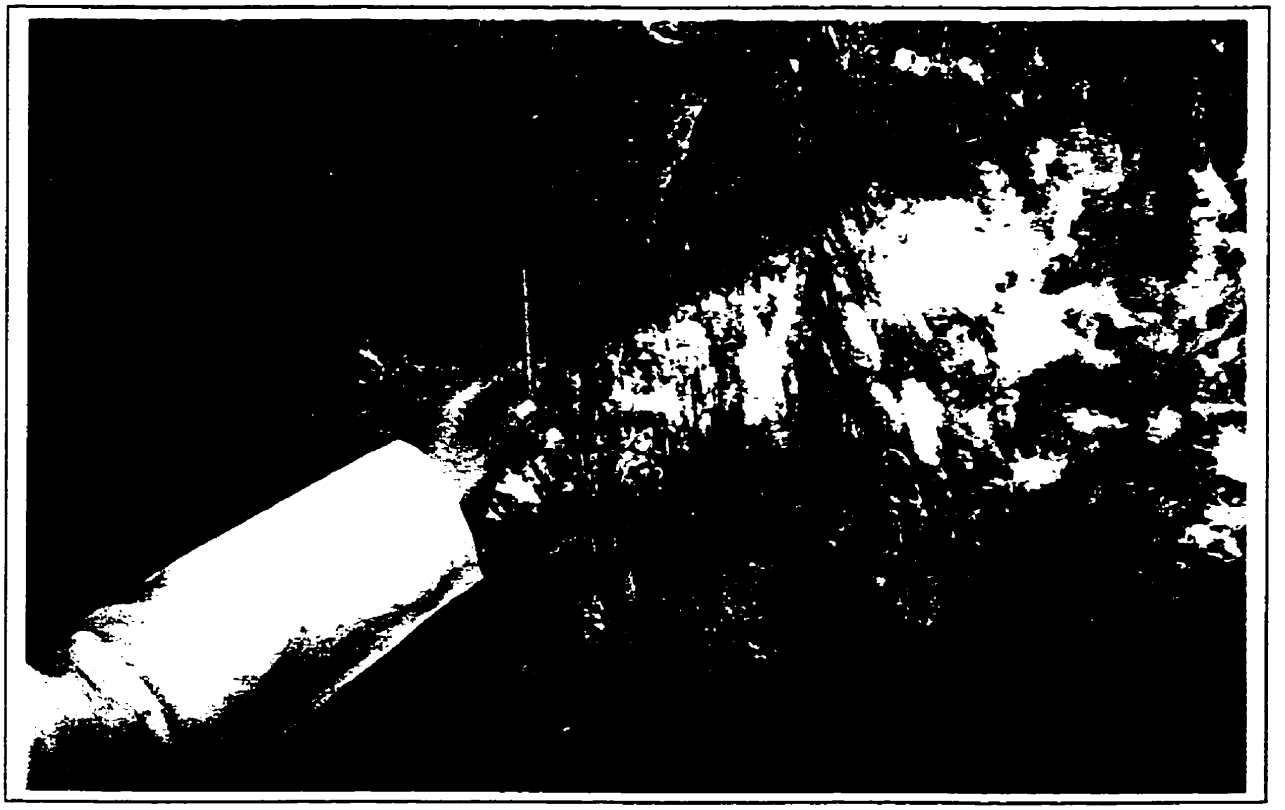

Figure 8.18

Figure 8.19 - *Contact zone of the Sigma deposit tourmaline-cemented breccia with the host porphyritic diorite ("C" porphyry) at mine level 38. Mosaic-textured breccia characterized by tear-shaped albitized wall rock fragments cemented by tourmaline and minor pyrite. The contact with unbrecciated porphyry is gradational. Back face of underground workings, looking east.*

Stope 38-16, Sigma Mine level 38.

Contact entre la brèche à ciment de tourmaline de la mine Sigma et son encaissant de porphyre dioritique (C" porphyry) au niveau 38. Brèche à texture de mosaique charactérisée par la présence de fragments de porphyre dioritique albitisé de forme allongée cimentés par de la tourmaline et de la pyrite disséminée. Le contact entre la brèche et l'intrusif dioritique non bréchifié est graduel. Vue sur le toît du chantier souterrain, avec regard vers l'est.

Chantier 38-16, niveau 38 Mine Sigma.

Figure 8.20 - *Margin of the pyritic, tourmaline-cemented breccia at level 38 of the Sigma deposit. Photograph of rounded to angular clasts of pervasively albite-altered diorite porphyry locally showing quartz-carbonate veinlets which are restricted to the albitized wall-rock fragments (arrow). The rock face is parallel to the main east-west schistosity(S_2).*

Stope 38-16, sigma Mine level 38.

Photo prise en marge de la brèche pyritique à ciment de tourmaline au niveau 38 de la mine Sigma. Fragments arrondis à anguleux de porphyre dioritique albitisé renfermant des veinules de quartz-carbonate (flèche). La face du chantier est parallèle à la schistosité principale du gisement (S_2).

Chantier 3816, niveau 38 Mine Sigma.

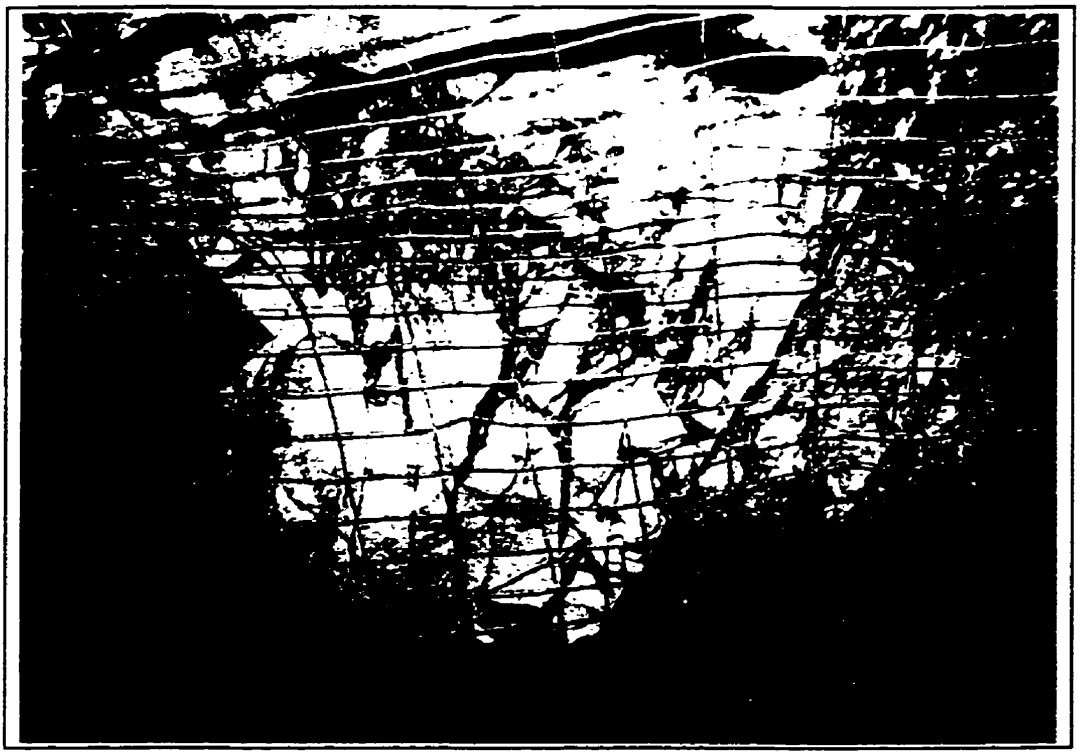

Figure 8.19

Figure 8.20

Figure 8.21 - *Centre of the tourmaline breccia at level 38 of the Sigma deposit. Photograph of albitized (light grey) diorite porphyry hosting a network of subhorizontal and subvertical quartz veins associated with biotite-chlorite-pyrite wall-rock alteration, cut by a network of tourmaline veinlets overprinted, in turn, by a moderately, north-dipping schistosity (to the right). The quartz-scheelite vein set at a high-angle to schistosity is buckled (see yellow pen magnet), and pyrite is streched along schistosity planes (upper part of the photograph).*

Stope 38-16, Sigma Mine level 38.

Photo prise au centre de la bréche à ciment de tourmaline au niveau 38 de la mine Sigma. Photo du porphyre dioritique albitisé recoupé par des veines sub-horizontales et sub-verticales de quartz associées à l'assemblage d'altération biotite-chlorite-pyrite, elles-même recoupées par un réseau de veinules de tourmaline, puis déformé par une forte schistosité à pendage modéré vers le nord. La veine de quartz-scheelite qui est à fort angle avec la schistosité (voir le crayon-aimant de couleur jaune) est déformée par des plis ondulés et la pyrite est étirée le long des plans de schistosité (haut de la photo).

Chantier 38-16, niveau 38 Mine Sigma.

Figure 8.22 - *Centre of the tourmaline breccia at level 38 of the Sigma deposit. Photograph of buckled tourmaline stringer veins across the albitized porphyritic diorite. Note also the tightly folded quartz veinlet at the bottom of the photograph (arrows).*

Stope 38-16, Sigma Mine level 38.

Photo prise au centre de la bréche à ciment de tourmaline au niveau 38 de la mine Sigma. Photo d'une veinule de tourmaline recoupant la diorite porphyrique albitisée, déformée par un pli ondulé. Prendre note également de la veinule de quartz déformée par un pli très serré, située au bas de la photo (flèches).

Chantier 38-16, niveau 38 Mine Sigma.

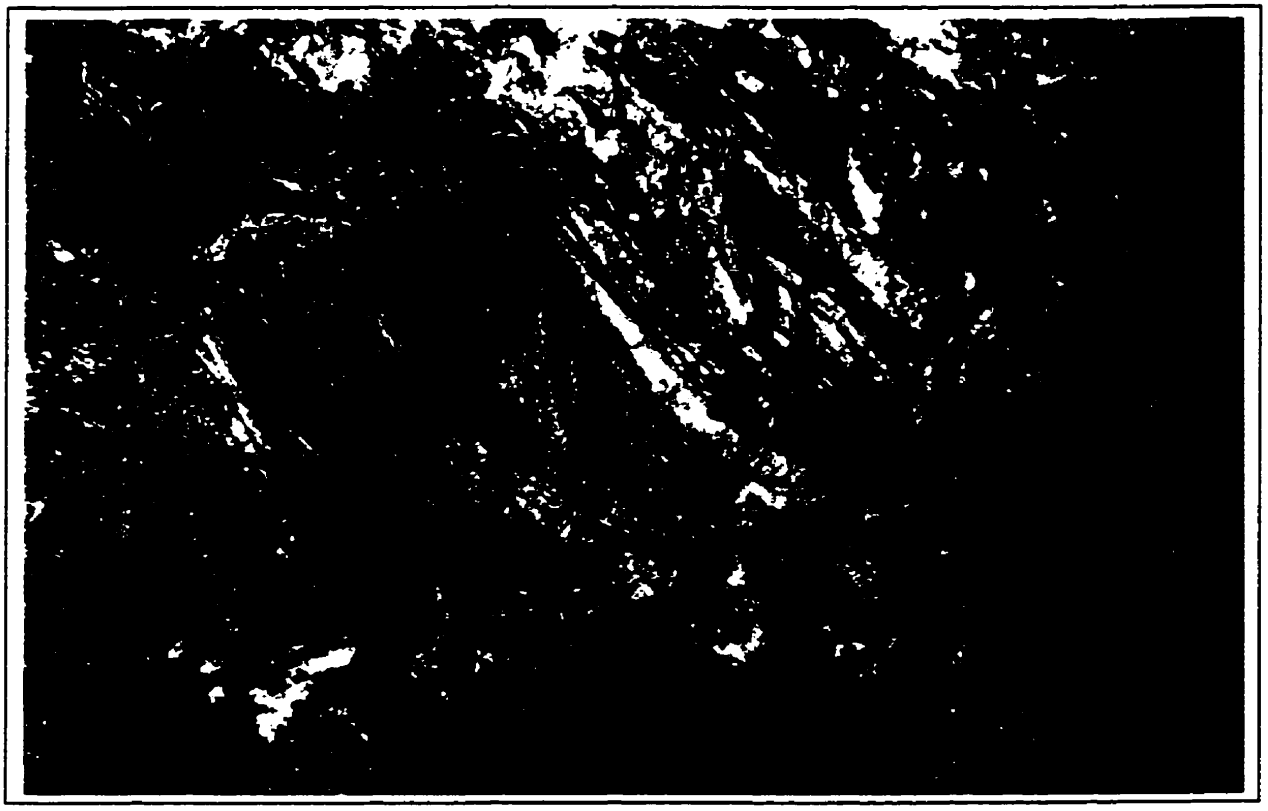

Figure 8.21

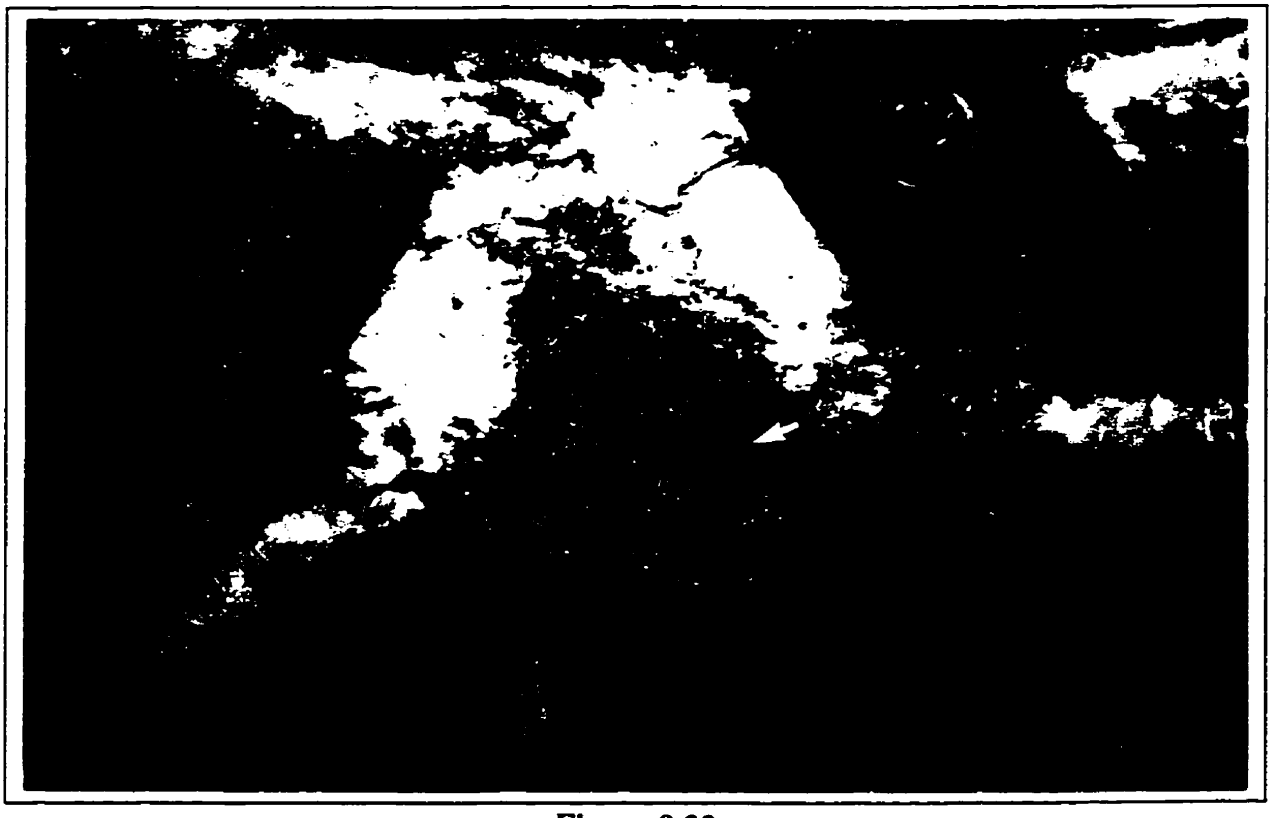

Figure 8.22

Figure 8.23 - *Centre of the Sigma deposit pyritic, tourmaline-cemented breccia at level 38. Photograph of a polished hand specimen of the tourmaline breccia showing angular to rounded quartz vein fragments dissected by a network of tourmaline veinlets. Note the effects of strain partitioning across the breccia sample: the main tourmaline vein is folded but quartz vein fragments appear undeformed, whereas disseminated pyrite grains are partially recrystallized and show signs of deformation in the tightly folded portion of the tourmaline vein.*

Stope 38-16, Sigma Mine level 38.

Centre de la brèche pyritique à ciment de tourmaline de la mine Sigma au niveau 38. Échantillon à surface polie de la brèche à ciment de tourmaline montrant des fragments arrondis et anguleux de veines de quartz, dissectés par un réseau de veinules de tourmaline. Remarquez les effets de la répartition de la déformation sur cet échantillon de la brèche: la veine de tourmaline principale est plissée alors que les fragments de veine de quartz n'apparaissent pas déformés; les grains de pyrite disséminés, quant à eux, sont partiellement recrystallisés et montrent des signes de déformation dans la région située en marge d'un pli serré affectant la veine de tourmaline.

Chantier 38-16, niveau 38 Mine Sigma.

Figure 8.24 - *Centre of the Sigma deposit pyritic, tourmaline-cemented breccia at level 38. Photograph of a large, subhorizontal quartz lode gold vein postdating the network of tourmaline veinlets cutting earlier quartz veins, overprinted by the through-going, north-dipping S_2 schistosity (to the right). Note the bulge in the vein (arrows) and the modified vein-wall rock contact, which are attributed to shortening of the vein and development of the penetrative planar fabric.*

Stope 38-16, Sigma Mine level 38.

Centre de la brèche pyritique à ciment de tourmaline de la mine Sigma au niveau 38. Photo d'une grosse veine de quartz subhorizontale recoupant le réseau de veinlules de tourmaline qui, recoupe lui-même une précedente génération de veines de quartz. Remarquez le renflement de la veine (flèches), ainsi que la déformation du contact entre la veine et l'encaissant, lesquels sont attribués au racourcissement de la veine et à l'imposition de la fabrique pénétrative planaire (schistosité S_2) pendant abruptement vers le nord (vers la droite) .

Chantier 38-16, niveau 38 Mine Sigma.

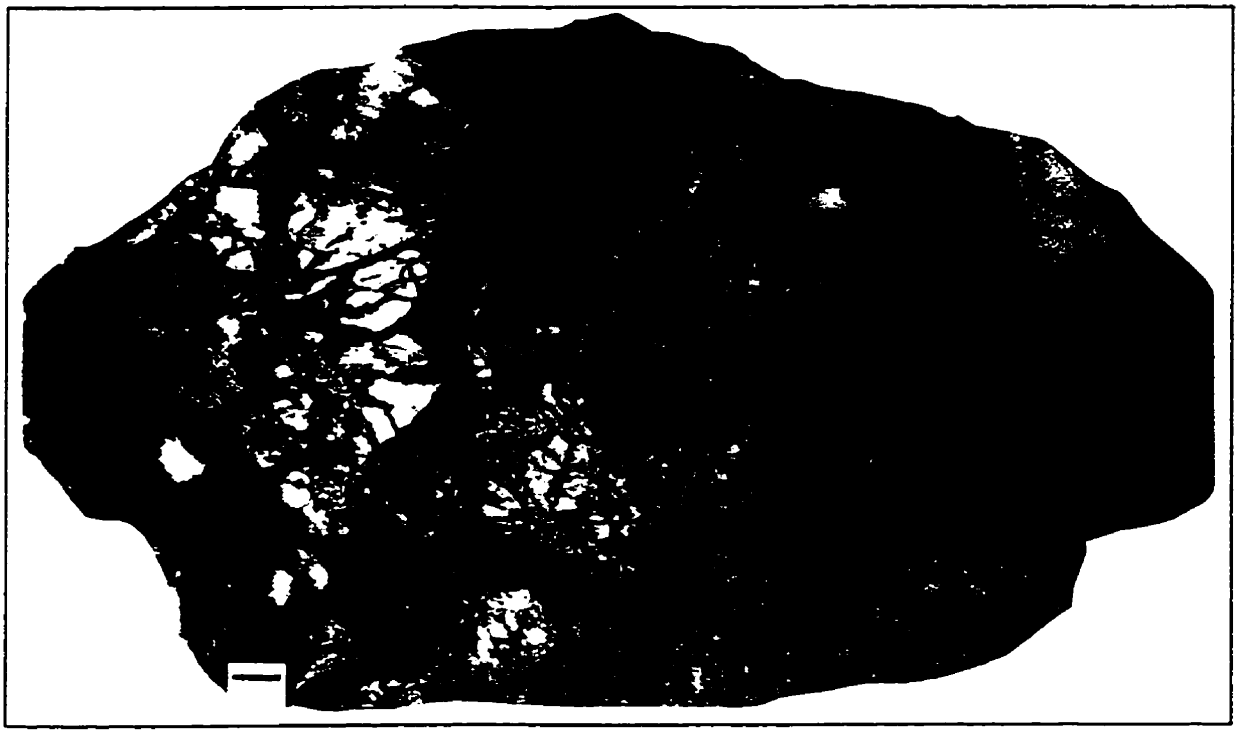

Figure 8.23

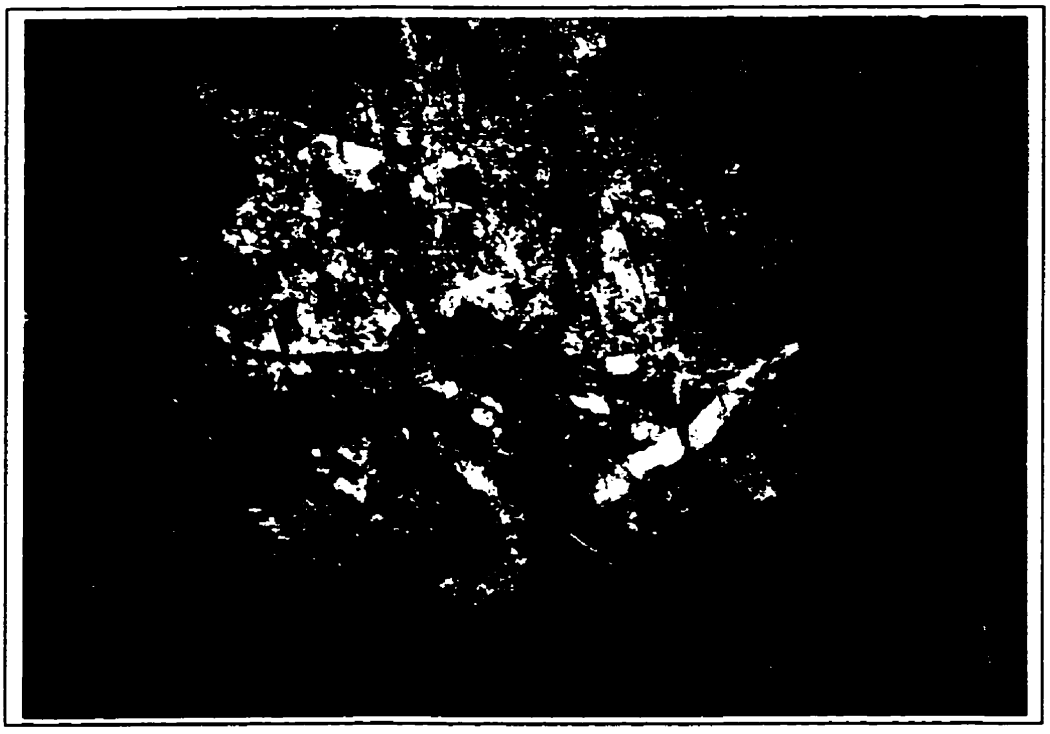

Figure 8.24

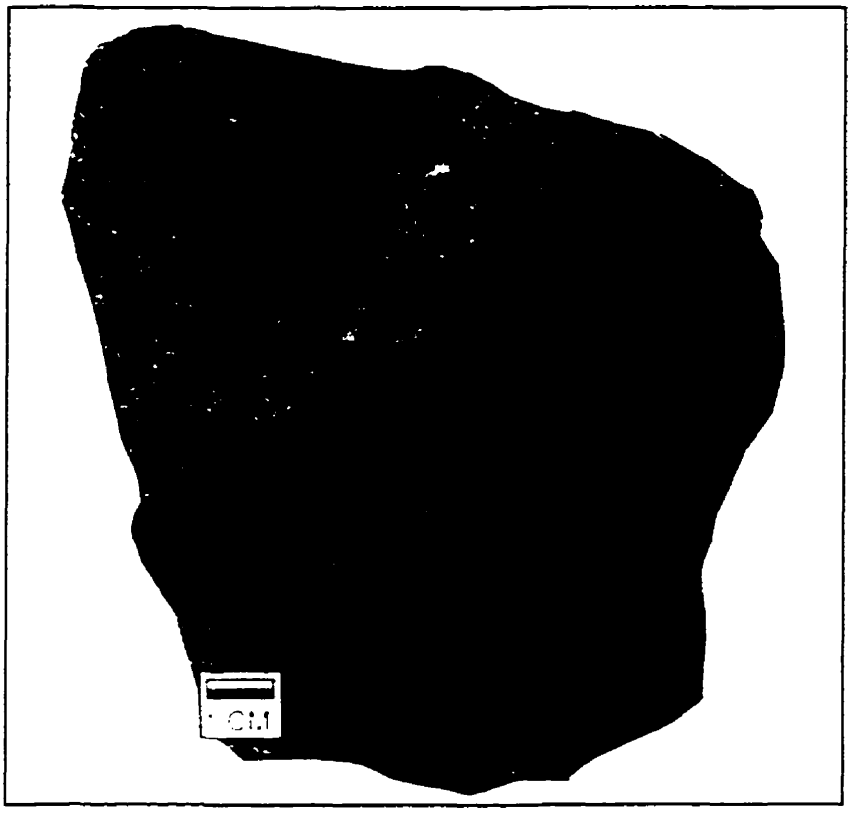

Figure 8.25 - *Polished rock slab from a sample of the Sigma deposit porphyritic diorite, or "C" porphyry, collected at the entrance of stope 38-16 some 15-20 metres away from main-stage gold quartz veins and tourmaline breccia. The primary igneous texture of the dioritic intrusion is conspicuously enhanced by the presence of clots of biotite pseudomorphosing hornblende phenocrysts. The biotite is characterized by a pale brown color under the microscope and by an elevated MgO content (8.8 to 10.6 wt.%, Taner et al., 1986). Color, composition, mode of occurrence and resulting enhancement of primary igneous rock texture, are reminescent of the selectively pervasive biotite alteration observed in Cu and Cu-Au porphyry deposits (e.g. Titley, 1982; Sillitoe and Gappe, 1984).*

Stope 38-16, Sigma Mine level 38.

Échantillon à surface polie de la diorite porphyrique, ou "C" porphyry, de la mine Sigma provenant de la galerie d'accès menant au chantier 38-16, à quelques 15-20 mètres de la minéralisation à veines de quartz et brèches de tourmaline. La texture originelle de l'intrusion dioritique semble rehaussée par la pseudomorphose des phénocristaux de hornblende par des aggrégats de biotite. Celle-ci se charactérise par sa couleur brun pâle sous le microscope, ainsi que par son contenu élevé en MgO (8.8 à 10.6 pds %, Taner et al. 1986). Sa couleur, composition, mode d'occurrence ainsi que le changement qu'elle apporte à la texture primaire ignée, rappellent l'altération sélectivement pénétrative de la biotite secondaire rencontrée dans les gisements Cu et Cu-Au de type porphyre (e.g. Titley, 1982; Sillitoe and Gappe, 1984).

Chantier 38-16, niveau 38 Mine Sigma.

et al., 1989). Quartz-tourmaline lode gold veins, which are thus younger than the bulk of the ore at Lamaque, are deformed by folds and cut by a steeply north-dipping axial planar spaced cleavage parallel to the regional S_2 schistosity (**Figure 8.27**)[1]. Robert (1994; 1996) recognizes some degree of deformation by shortening across the Sigma-Lamaque vein system, however, he advocates that quartz-tourmaline vein formation accompanies the development of shear zones after greenschist-grade metamorphism and attributes vein deformation to the reactivation of the host shear zones.

At the thin section scale, quartz, carbonate and scheelite show evidence of plastic deformation and recrystallization (undular extinction, deformation lamellae, stylolitic fluid inclusion trains, polygonal grains), tourmaline fibres are folded or kinked, and rosettes of tourmaline needles are deformed (e.g. Boullier and Robert (1992)). Gold occurs as inclusions in disseminated pyrite in the G dikes and in albite grains forming the bleached alteration halo around the quartz-tourmaline veins. Disseminated auriferous pyrite crystals in the host feldspar porphyry dikes are coarse porphyroblastic and exhibit pressure shadows filled with carbonate, quartz and gold (Robert and Brown, 1984), suggesting minor remobilization of primary gold occluded in pyrite during deformation. The bulk of gold mineralization, however, occurs in microfractures post-dating quartz-tourmaline-carbonate-scheelite veins. Photomicrographs of these gold-filled fractures show that they are deformed by microfolds (fig. 4E of Robert and Brown (1986b)) or that they conform to polygonal boundaries of recrystallized quartz grains (fig. 1G and 4D of Robert and Brown (1986b)). Gold-filled hairline fractures also outline the sutured mutual grain boundaries between gold, petzite ($AuAg_3Te_2$) and carbonate (fig. 4F in Robert and Brown (1986b)), suggesting that even the late-stage carbonate-gold-telluride veinlets are deformed. To explain this fact, Boullier and Robert (1992) proposed that the Sigma vein system formed during repeated vein-growth-deformation cycles contemporaneously with north-south shortening during the regional D_2 deformation. These

---

[1] As specifically stated by Karvinen (1985, p.15): "In the large shear veins, particularly near the noses of folds, a penetrative foliation cuts the enclosing tuffaceous material and a fracture cleavage is evident in the quartz-tourmaline material."

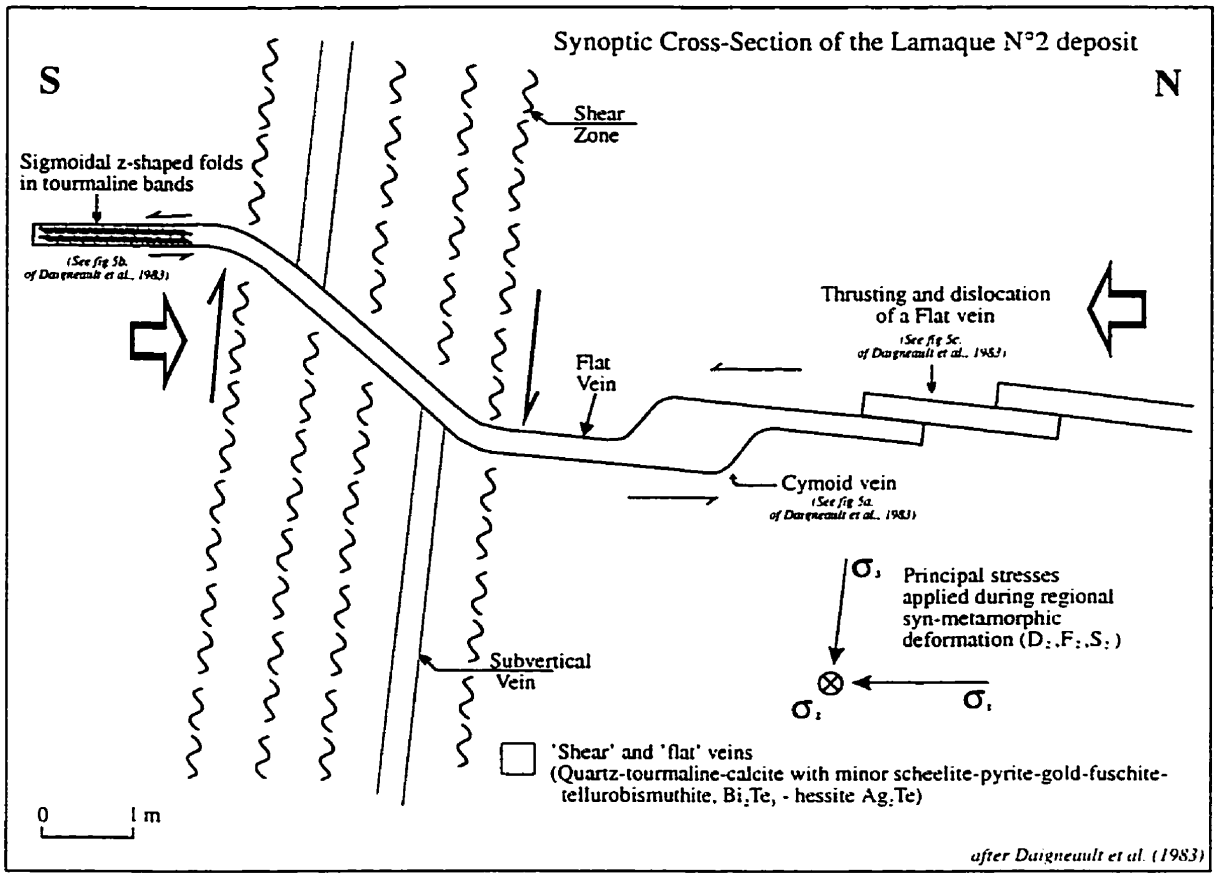

Figure 8.26 *Synoptic cross-section of Lamaque N° 2 deposit (see* **Figure 8.14** *for location) showing various deformation features observed along a "flat" lode-gold vein. Deformational strain has been ascribed to north-south compressive stresses.*

Diagramme synoptique d'une section verticale du gisement de la mine Lamaque N0. 2, montrant plusieurs types de structures résultant de la déformation d'un filon aurifère sub-horizontale (consulter la **Figure 8.14** *pour la localisation). Les effets de la déformation ont été attribués à des contraintes en compression orientées nord-sud.*

cycles are described as episodes of fracturing and healing by hydrothermal fluids, alternating with episodes of seismic, reverse-slip motion on subvertical quartz-tourmaline veins accompanied by deformation. The fracture episodes are evidenced by crustiform infill-vein textures whereas the slip episodes are inferred from sigmoidal foliation and dragfolds, and the presence of quartz-tourmaline slickenfibres on slip planes in shear zones (e.g. Boulllier and Robert (1992)).

Other evidence presented by Robert (1996) to support synchronous lode gold vein and shear zone development following regional metamorphism at Sigma include the following: 1) the presence of unfoliated, subhorizontal quartz-tourmaline veins hosted by sericitized and schistose wall rocks and showing no incipient buckling, 2) the replacement of "metamorphic" wall rock chlorite and biotite by hydrothermal sericite and carbonate in the alteration halo of gold-bearing quartz-tourmaline veins, and 3) the overgrowth of trails of rutile parallel to (and defining) the wall rock foliation by gold-related tourmaline porphyroblasts adjacent to subvertical veins. With regards to his first argument, differences in penetrative strain between the quartz-tourmaline veins and altered wall rock, as well as the contrasting styles of deformation exhibited by alteration-mineralization in the upper and lower parts of the deposit, are explicable by post-ore strain partitioning (e.g. **Figures 8.17, 8.19**, and **8.22**). At Kiena, hydrothermal vein biotite replaced by chlorite late in the deposits alteration-mineralization sequence was preserved during synmetamorphic deformation. Since chlorite, sericite, biotite, and carbonate are minerals compatible with greenschist facies metamorphism P-T conditions, such preservation of hydrothermal biotite and chlorite may also have occurred at Sigma. In the upper part of the Kiena orebody, post-ore spaced cleavages display native gold slickenfibres defining oblique normal steps which are interpreted as minor gold remobilization along these slip surfaces during post-ore fault movement. Quartz-tourmaline slickenfibres on slip surfaces such as illustrated at the Lucien Béliveau deposit by Robert (1996, fig. 3), may also be an example of post-ore remobilization suggesting a second generation of metamorphic tourmaline which may overgrow cleavage planes (Robert, 1996, fig. 1).

At present, it appears that the timing of gold ore formation in relation to the development of shear zones at Sigma cannot be resolved unequivocally on the basis of structural and textural overprinting relationships. However, it has been claimed that the Sigma vein system has been directly dated as 2682 ± 8 Ma by a hydrothermal zircon from a quartz-tourmaline vein (Claoué-Long et al., 1990). The results of this geochronological study have generated some controversy (e.g. Corfu and Davis (1991); Claoué-Long *et al.* (1992); Kerrich and King (1993)), but they are compatible with a pre-shear zone origin for vein development. As a result, a pre-metamorphic ca. 2685-2677Ma intrusion-related origin is herein postulated for gold mineralization at the Sigma-Lamaque No.2 vein deposits based on the overprint of the ca. 2685 Ma Lamaque intrusion by quartz-tourmaline veins, the ca. 2682 Ma zircon date, and similarities with Kiena which include: the upward-flaring geometry of the vein-breccia system, early albitization (and possibly biotitization) of the C porphyry, the zoned alteration pattern developed around the orebody, the recurrence of albite in the alteration-mineralization sequence including the paragenesis of gold with vein albite, an intermineral event (tourmaline breccia), and the post-ore timing of penetrative deformation in the deeper parts of the orebody.

Commentary

In spite of interpreting the timing of Lamaque N0.2's gold mineralization as syndeformation, Daigneault *et al.* (1983) made an analogy between Archean ore fluids at the Sigma-Lamaque N0. 2 deposits and fluids circulating through modern geothermal systems by comparing the ore-gangue mineralogy of the lode gold veins to the fluid compositions of selected active geothermal systems (e.g. White (1981)). The latter are characterized by elevated CO_2, S, and Cl contents and the occurrence of rare chemical elements such as B, Hg, Te, Bi, W, Ag, As, and Au, whereas similar fluid compositions for the mineralizing solutions at Sigma-Lamaque No.2 are shown by the occurrence of scheelite (W), tourmaline (B), tellurobismuthite (Te, Bi), abundant pyrite with lesser pyrrhotite and chalcopyrite (S), and high concentrations of gold (Au) and silver (Ag) in the veins. A fluid inclusion study by Robert and Kelly (1987), later confirmed the existence of a CO_2-rich ore fluid at Sigma, whereas Grant (1986) has

shown that Au and As concentrations in quartz-tourmaline veins are 1000-5000 times and 10 times higher, respectively, than in the surrounding country rocks. If, as White (1981) and others have suggested, epithermal precious metal (Au, Ag) ore deposits such as those occurring throughout the Great Basin of the western United States and Mexico are the fossil equivalent of present-day geothermal systems, the similarity of Sigma's ore-gangue-alteration mineralogy with the fluid geochemistry of active geothermal systems is an indication there may be a resemblance between the Sigma-Lamaque quartz-tourmaline vein system and Tertiary epithermal vein-type deposits. Indeed, Sigma-Lamaque No.2's lode gold vein system shares a number of the characteristic features of epithermal bonanza veins (e.g. Sawkins (1990); Romberger (1992); Sillitoe (1993)), including: 1) their occurrence in convergent plate boundary environments (Abitibi-Pontiac subprovinces boundary), 2) comparable vein dimensions (2mx100mx500m), ore grades (10-50 g/t Au at Sigma compared to 7-60 g/t Au in selected epithermal deposits of southwestern North and South America), and tonnages (~140 t Au and 22 t Ag at Sigma compared to 56-258 t Au in selected epithermal deposits of southwestern North and South America), 3) similar upward-flaring vein geometry and vein patterns (braided vein system (Robert et al., 1983, fig. 4) and cymoid veins (Daigneault et al., 1983, fig. 5a)), 4) episodic ore deposition in open-space fractures (banded and crustified veins) associated with stockwork veins and breccias, 5) the occurrence of quartz as the predominant gangue mineral and up to 10% disseminated pyrite, and 6) the co-existence of a nearby lower-grade but large disseminated deposit (e.g. Main Lamaque deposit[2], see description in the following section).

8.2.7 Main Lamaque Deposit

The Lamaque mine is located approximately 500 metres south-southwest of Sigma (**Figure**

---

[2] Of the 140 tonnes of gold produced at Lamaque , approximately 6 tonnes of gold originated from Sigma-type quartz-tourmaline lode gold veins situated in the uppermost part of the deposit, whereas the remaining 134 tonnes of gold were produced from disseminated ore at mid- and lower mine levels (Karvinen, 1985).

8.14). Lamaque's orebody is now mined out, but it remains the single largest gold producing deposit of the entire district (~ 140 tonnes of gold, (Karvinen, 1985)). Two types of mineralization are recognized at the main Lamaque deposit: Sigma-type quartz-tourmaline lode gold veins (**Figure 8.27**) and quartz-carbonate stockwork vein-tourmaline breccia ore also referred to as "stringer veins" or "zone ore" (Karvinen, 1985; Burrows, 1990). The stockwork vein-breccia type mineralization is contained within a diorite-tonalite intrusive body named the "Main" plug and within a smaller tonalitic intrusion named the "East" plug (**Figure 8.14**). Sigma-type quartz-tourmaline veins (mostly subvertical and moderately south-dipping veins) overprint the Main and East plugs stockwork vein-breccia ore but are mostly hosted by an overturned sequence of andesitic flows and pyroclastic rocks of the Val d'Or Formation (Imreh, 1984), near the contact and away form the plug (Karvinen, 1985).

At Lamaque, stockwork vein-breccia ore is centred on the tonalitic core of the Main plug, as is illustrated in a series of geological level plan maps in Wilson (1948). The zoned intrusive body is elliptical, with its long axis oriented east-west (i.e. parallel to the regional S_2 schistosity, **Figure 8.27**). On the basis of crudely outlined intrusive contacts and whole-rock and rare earth compositions, Burrows and Spooner (1989) proposed that a separate, dike-like tonalite intruded an earlier, co-magmatic diorite intrusion. However, because the tonalitic centre of the Main Lamaque plug coincides with irregular pipe-like zones of intense albite-carbonate alteration, stockwork veining and tourmaline breccias surrounding gold quartz veins, Karvinen (1985) considered the intrusive-looking rocks of tonalitic composition as the end product of progressive "granitization" of the former dioritic intrusion by albite-rich hydrothermal fluids related to gold mineralization. This interpretation is in part supported by the fact that the bulk of mineralization at Lamaque originated from zones of stockwork veins and breccias confined to the inner tonalite at mid-mine levels (350-750 metres below surface, e.g. Karvinen (1985) and Burrows (1990)), and in part by the progressive decrease in K_2O and increase in Na_2O with increasing silica recorded from the marginal zone of diorite to the inner zone of tonalite (Burrows and Spooner, 1989). The following sequence of vein-forming events have been recognized at the Lamaque deposit: 1) small, translucent blue quartz

Figure 8.27 - *Simplified plan map of the 950 level (~ 300 metres below surface) of the Lamaque mine, showing geologic relationships between Sigma-type quartz-tourmaline lode gold vein, "Main" diorite-tonalite intrusion, and penetrative planar fabric. The steeply-dipping vein has been folded and cut by an axial-planar fracture cleavage. Note the broad prallelism between the vein fold axis and the long axis of the intrusion. Flattening planar fabric and the ellipsoid shape of the intrusion are compatible with the orientation of principal stress axes deduced for regional synmetamorphic deformation at the Lamaque N0.2 deposit (see Figures 8.14 and 8.26). From Karvinen (1985).*

Plan de mine simplifié du niveau 950 (~ 300 mètres sous la surface) de la mine Lamaque, montrant les relations géologiques entre le filon aurifére de quartz-tourmaline de type Sigma, l'intrusion de diorite-tonalite, et la fabrique pénétrative planaire. La veine à fort pendage a été plissée et recoupée par un clivage d'espacement de plan axial. Notez le parallelisme entre le plan axial du pli et l'axe long de l'intrusion. La fabrique planaire ainsi que la forme ellipsoide de l'intrusion sont compatibles avec l'orientation des axes de contraintes principales de la déformation synmétamorphique régionale déduite au gisement Lamaque N0.2 (voir les Figures 8.14 et 8.26). D'après Karvinen (1985).

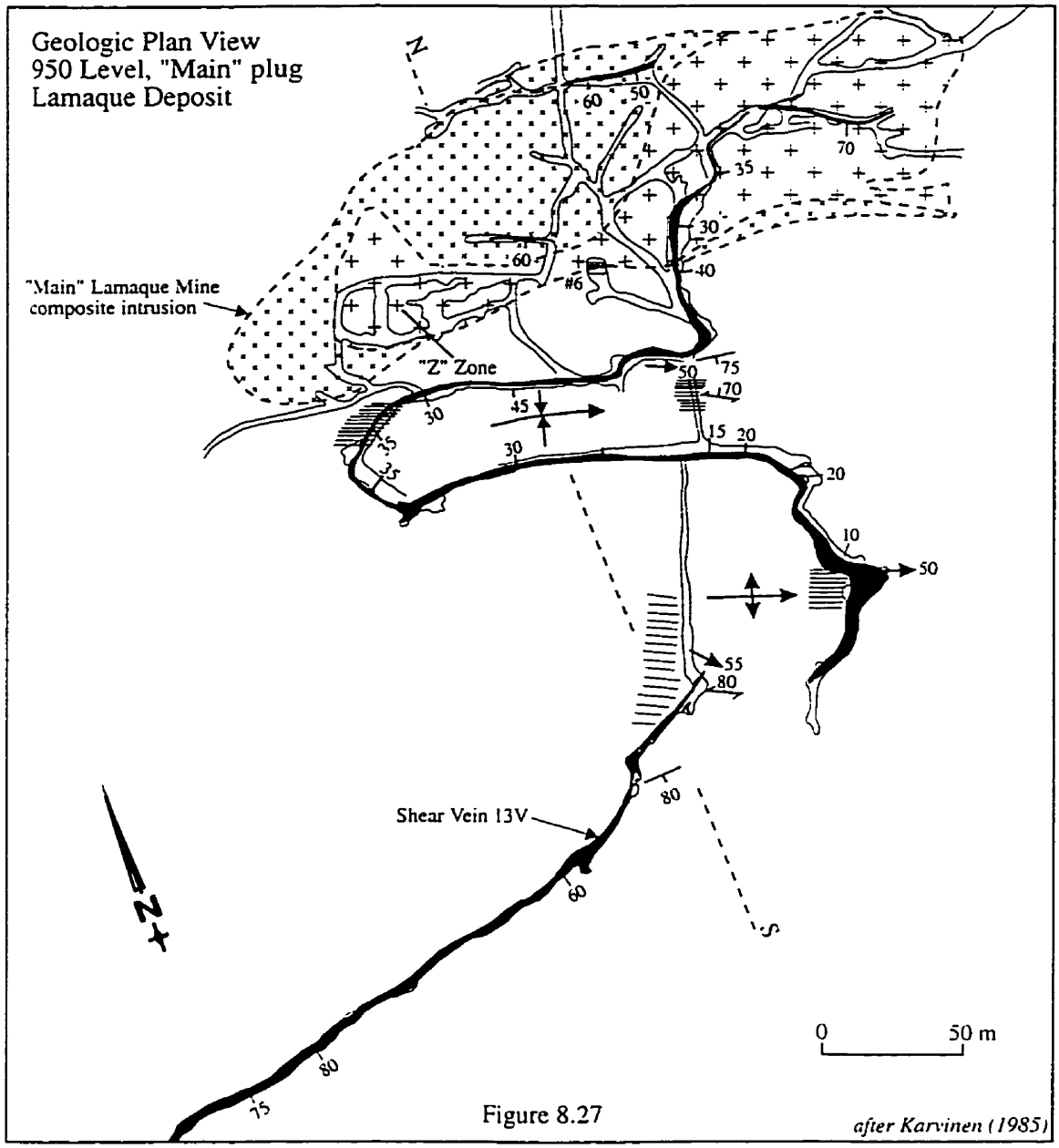

Figure 8.27

after Karvinen (1985)

(also reported by Wilson (1948) p.885-886)

Carbonate-tourmaline-quartz veins (Sigma-Lamaque "shear" veins)

Tonalite

Diorite

Mafic volcanic flows

Trace of synoptic cross-section Lamaque N°2 deposit shown on Figure 8.26

Zones of strong axial plane foliation (penetrative schistosity in mafic volcanic rocks and fracture cleavage in quartz-tourmaline vein)

Anticlinal fold axis

Synclinal fold axis

Presumed contact

Plunge of fold axis

Strike and dip

stringers veins occurring throughout the deposit, 2) quartz-carbonate-Au stringer veins and related pyritic tourmaline breccias and stockwork veins, 3) moderately to steeply south-dipping and minor subhorizontal milky quartz- tourmaline-Au veins, 4) barren quartz-tourmaline and quartz-carbonate-purple fluorite veins, 5) quartz-filled tension gashes (Wilson, 1936; Wilson, 1948; Burrows, 1990). Burrows (1990) reported the presence of early quartz-carbonate-anhydrite-chlorite±pyrite veins overprinted by biotite-quartz veins at depth (~ 1000 metres below surface), but their relationship to either quartz stringer veins or quartz-tourmaline veins is not known. Lamaque's quartz-tourmaline lode gold veins occupy high-angle, reverse faults which offset the contacts of the Lamaque Main plug and those of nearby quartz-feldspar and felspar porphyry dikes (Wilson, 1948; Karvinen, 1985). They are composed of quartz, tourmaline and carbonate with minor pyrite and scheelite, and traces of gold, chalcopyrite, pyrrhotite and tellurides (calaverite, krennite, sylvanite, altaite, e.g. Burrows, 1990). Steeply, south-dipping quartz-tourmaline veins are characterized by slickensided surfaces at their hanging wall and show, from the margin inward, wall-rock laminations and a banded texture consisting of alternating bands of quartz and tourmaline (e.g. Karvinen (1985)), whereas subhorizontal veins display crustiform textures which according to Wilson (1948) sometimes contain drusy, quartz-filled cavities. As at Sigma, these textures suggest multiple vein re-openings by a crack-seal mechanism and imply, at least for the subhorizontal veins, that fractures formed at relatively high levels in the crust and remained open during ore-fluid circulation. Gold is commonly intergrown with tellurides and chalcopyrite and, as at Sigma, pyrites contain gold blebs and/or exhibit gold-filled fractures (Burrows, 1990).

Karvinen (1985) has shown that the Lamaque orebody (Main plug) is characterized by a downward ore zonation. From the discovery outcrop down to a depth of approximately 600 metres below surface, mineralization consisted mainly of Sigma-type quartz-tourmaline lode gold veins located outside the Main plug, whereas quartz-carbonate stringer veins and pyritic tourmaline breccia in the Main plug was the predominant type of mineralization at mid-mine levels (i.e. 350-750 metres below surface). Mineralization progressively declined with

increasing depth and disappeared beyond the 3400 level (~ 1 km below surface). In contrast, a zonation of hydrothermal alteration minerals is not readily apparent; however, based on descriptions of Karvinen (1985), Burrows and Spooner (1989) and Burrows (1990) sericite in alteration halos to quartz-tourmaline veins is common at upper mine levels and decreases with increasing depth. Igneous hornblende and biotite are altered to secondary biotite preferentially at intermediate mine levels coinciding with the predominant stringer vein mineralization, and the occurrence of pyritic tourmaline breccia is more frequently reported from mid-mine levels downward (~ 1000 metres below surface). This crude zonation of gold-related hydrothermal alterations mimics that described earlier at the Sigma deposit.

Evidence of post-ore penetrative deformation abounds. Several of the steeply, south-dipping vein-thrust faults (e.g. veins No. 1, 13, 35, 39 and 56) are folded and cut by an east-west striking axial planar spaced cleavage corresponding to the regional S_2 schistosity (**Figure 8.27**; Wilson (1948); Karvinen (1985); Burrows (1990)). Stylolites are commonly observed in banded quartz-tourmaline veins (Karvinen, 1985) and, the compositionally zoned Lamaque "Main" plug is schistose and elongated parallel to the regional S_2 schistosity (Wilson, 1948; Karvinen, 1985). Vein quartz and tourmaline are plastically deformed and recrystallized (Burrows, 1990), and subvertical quartz-tourmaline veins are offset by slip-planes oriented parallel to the main east-west penetrative planar fabric.

Based on the following analogies with Kiena, a high-level, intrusion-related[3] and pre-metamorphic origin is postulated for the Lamaque deposit: 1) alteration-mineralization is fracture-controlled and centred on the albitized core of a dioritic intrusion, 2) stockwork veining and brecciation is the predominant style of mineralization, 3) gold is episodic, 4) vein biotite is confined to the gold-ore system, 5) the orebody exhibits an upward zonation in mineralization style and hydrothermal mineral assemblages, and 6) the mineralized intrusion

---

3 The magmatic derivation of the fluid associated with main-stage Au mineralization at the Lamaqe deposit has been suggested previously by Burrows and co-workers (e.g. Burrows and Spooner (1989) and Burrows (1990)).

and individual quartz-tourmaline lode gold veins are deformed by the regional S_2 schistosity. Mineralization at Kiena is, however, older than mineralization at Lamaque, as gold-bearing quartz veins and tourmaline breccias overprint the tonalitic "Main" plug dated as 2685 ± 3 Ma (Jemielita *et al.* (1989); see **Figure 8.28**).

8.3 TEMPORAL-GENETIC MODEL FOR AU MINERALIZATION IN THE VAL D'OR-MALARTIC AREA: A DISTRICT-WIDE MAGMATIC-HYDROTHERMAL CONNECTION

Viewed on its own, Kiena may appear as an oddity as the intrusion-related character of the deposit is incompatible with the still firmly entrenched "metamorphogenic/magmatic" and "shear zone-controlled" ore deposit model (e.g. Sibson *et al.* (1988), Groves (1993), Hodgson (1993)). However, the geological overview of selected Malartic and Sigma-type deposits in the previous section serves to show that in spite of disparities in local geological settings, mineralization styles and vein parageneses, many of the Val d'Or-Malartic area deposits exhibit common traits with Kiena, both at the regional and deposit-scale. At the regional-scale, gold-ore hydrothermal systems at Canadian Malartic, Camflo, Orion Vein No. 8, Goldex, Siscoe, Sigma-Lamaque No. 2 and the main Lamaque deposits resemble Kiena in being associated with swarms of aplitic dikes and porphyritic stocks and dikes which together define the Val d'Or plutonic belt, a fault lineament focusing calc-alkaline and alkaline magmatism along discrete fault zones preferentially developed along southerly-overturned stratigraphic contacts. At the deposit-scale, the following anatomical features are common to all deposits: 1) mineralization is the product of multiple hydrothermal events resulting in upward and outwardly zoned alteration-mineralization sequences, 2) economic gold mineralization is invariably centred on dike swarms or combinations of small porphyry stocks and dikes, 3) alkali feldspar and biotite (enriched in MgO) are common denominators in the alteration sequence, the mineralization coinciding with zones of pervasive albite and/or K-feldspar alteration, 4) at some stage in the evolution of the alteration-mineralization sequence (i.e. early in the case of Kiena and late in the case of Camflo) gold is concentrated in stockwork veins and/or breccias, 5) some deposits (e.g. Siscoe, Sigma) show more specific

time and apparent genetic relations between fracture-controlled gold alteration and magmatism, such as intermineral diking and tourmaline brecciation events, and 6) the funnel-shaped morphology of the vein-dike systems, in addition to brecciation, banding, crustifications, and voids filled by drusy quartz in veins, are all consistent with a high-level of emplacement for the ore. One of the most important aspects, however, is the fact that ore structures at all deposits are compatible with a post-D_1 (F_1) and pre-D_2 (S_2) timing for hydrothermal alteration and gold mineralization.

Temporal-genetic model for gold mineralization in the Val d'Or-Malartic area

A synopsis of the relationships between Kiena and other Val d'Or plutonic belt gold deposits is presented in a temporal-genetic model for gold mineralization in relation to the Abitibi-Pontiac orogen (**Figure 8.28**). The model assumes that the succession of geological events recorded in the Val d'Or-Malartic region is linked to a tectonic event involving the collision of the Abitibi and Pontiac subprovinces (e.g. Jackson and Fyon (1991), Calvert *et al.* (1995)). The model is subdivided into pre- and post-accretion phases. The pre-accretion phase (ca. 2705-2700 Ma) is characterized by calc-alkaline volcanism and the formation of syngenetic massive sulfide deposits, whereas the post-accretion phase is characterized by episodes of intermediate and felsic plutonism associated with gold-ore formation across the Val d'Or plutonic belt (ca. 2694-2677 Ma), followed by penetrative deformation, greenschist facies metamorphism , and shear zone development during the terminal stages of the Abitibi-Pontiac collision (ca. 2677-2660 Ma).

By contrast with the Rouyn-Noranda mining camp where significant amounts of Archean gold were recovered from volcanogenic massive sulfide deposits (e.g. Horne and Quémont deposits, Chartrand and Cattalani (1990)) and related subvolcanic calc-alkaline intrusions (e.g. Don Rouyn deposit, Goldie *et al.* (1979) and Couture and Verpaelst (1994)), most of the gold extracted in the Val d'Or-Malartic mining camps originated from orebodies formed during post-accretionary plutonism. At present, syngenetic gold is known only from the

Figure 8.28 - Temporal-genetic model for gold mineralization in the Val d'Or-Malartic area in relation to the Abitibi-Pontiac orogen

Figure 8.28 Temporal-genetic model for gold mineralization in the Val d'Or-Malartic

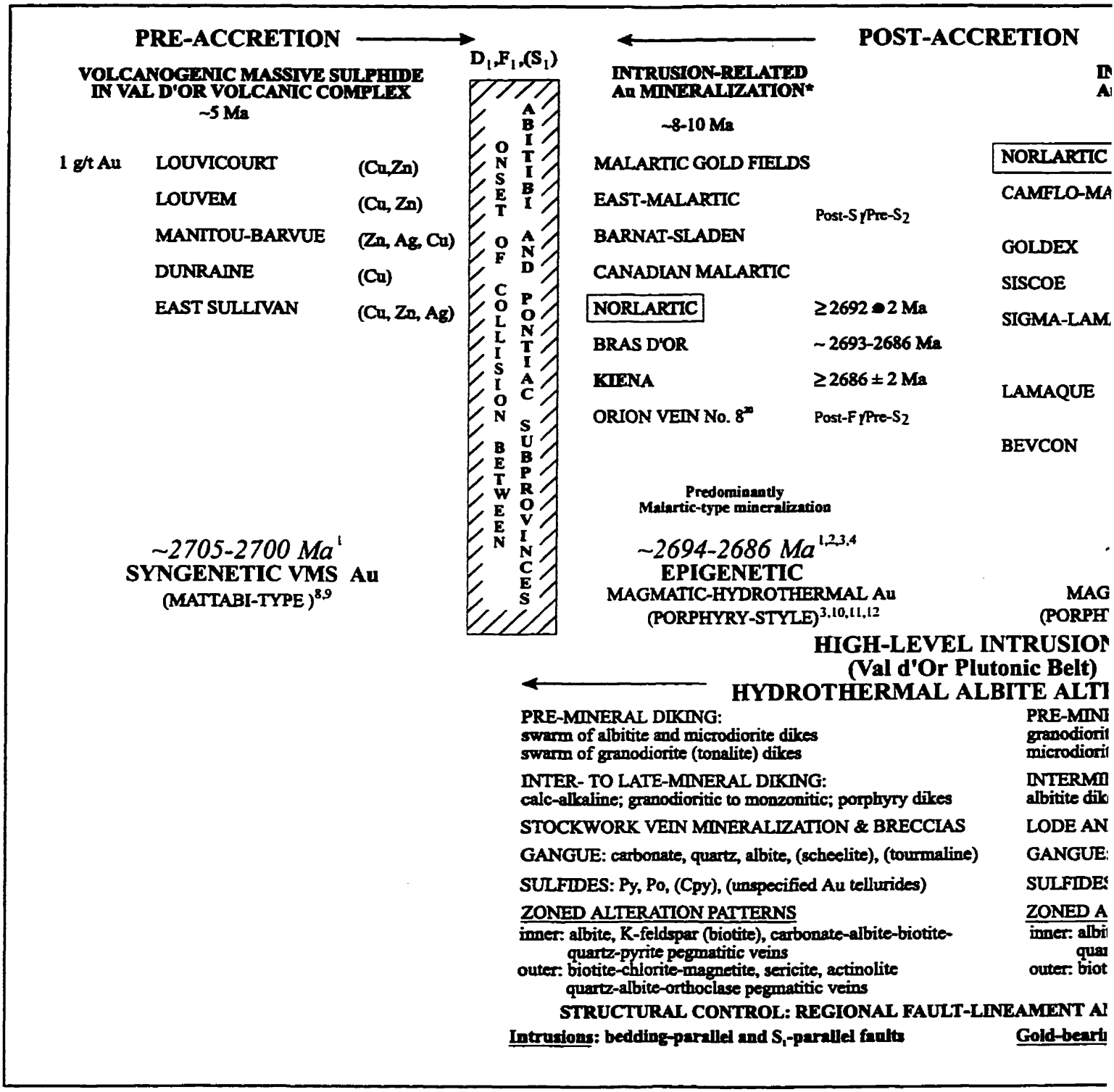

* *Broadly coeval with turbidite-dominated sedimentation of Lac Caste Fm (≤2695 Ma), Kewagama Group (ca. 2687-2683) and Cadillac Group (*

** *Broadly coeval with alluvial-fluvial sedimentation and spatially-associated alkalic volcanism in Kirkland Lake area, southwestern Abitibi greenstone belt: early and ma*

Reference: 1.Wong et al. (1991) 2.Couture et al. (1994) 3.Morasse et al. (1995) 4.Kerrich and Kyser (1994) 5.Zweng and Mortensen (1985) 6.Jemielita et al. (1989) 11.Sillitoe and Gappe (1984) 12.Sansfaçon and Hubert (1990) 13.Burrows and Spooner (1991) 14.Trudel and Sauvé (1992) 15.Spooner (1993) 16.Sillitoe Raymond (1992)

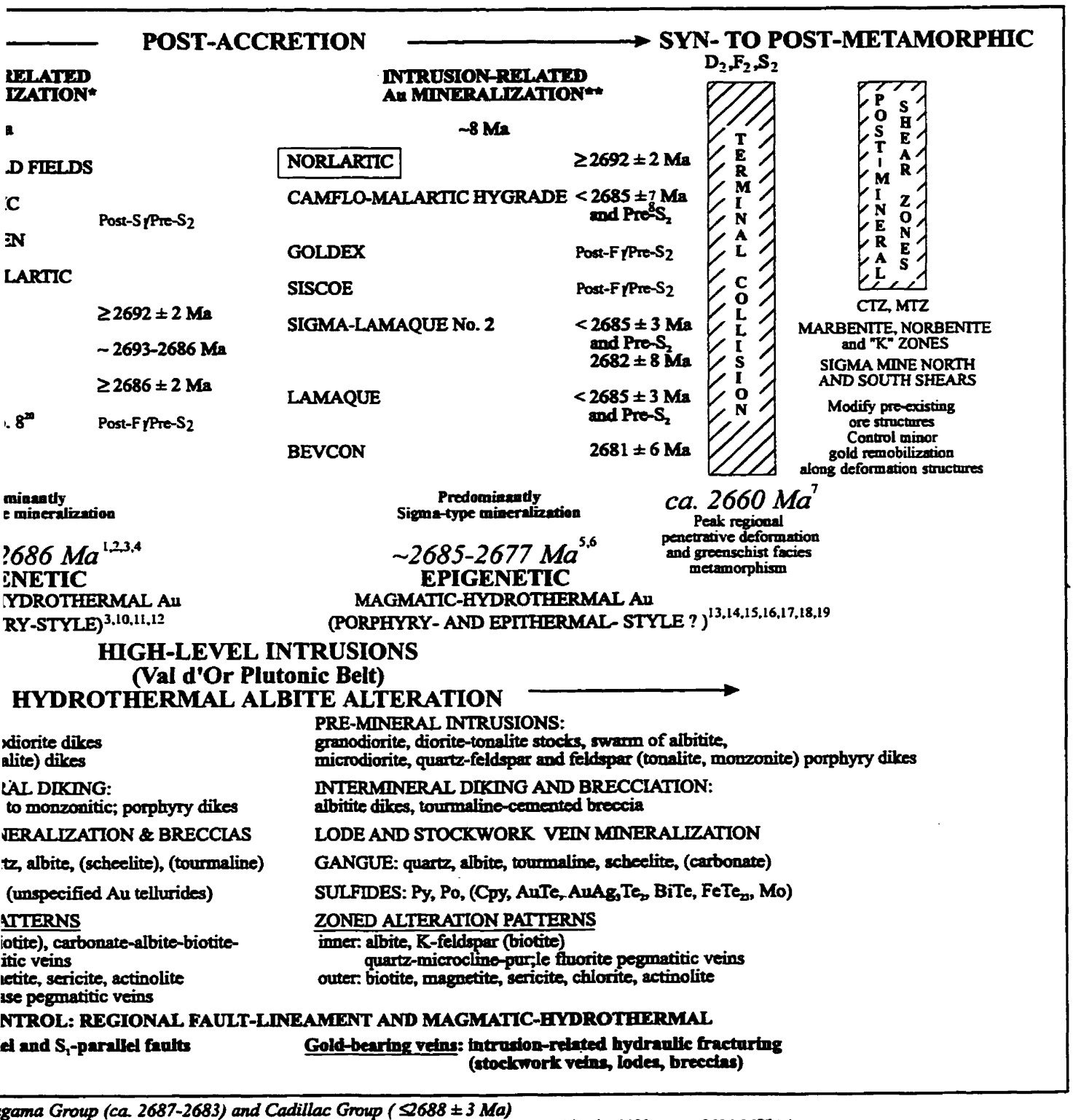

gama Group (ca. 2687-2683) and Cadillac Group (≤2688 ± 3 Ma)
ake area, southwestern Abitibi greenstone belt: early and main Timiskaming phases of Corfu (1993) at ca. 2686-2677 Ma
94) 5.Zweng and Mortensen (1985) 6.Jemielita et al. (1989) 7.Powell (1995a) 8.Chartrand and Cattalani (1990) 9.Morton and Franklin (1987) 10.Titley (1982)
) 14.Trudel and Sauvé (1992) 15.Spooner (1993) 16.Sillitoe (1994) 17.Tessier et al.(1990) 18. Claoué-Long et al. (1990). (1992) 19. Still (1995) 20. Trudeau and

Louvicourt Cu/Zn deposit (deposit No. 28 on **Figure 2.2**, 0.85-1.0 g/t Au, Chartrand andCattalani (1990); Econ. Geol., V.88 No. 6, frontispiece) which is hosted by felsic pyroclastic rocks and cherty tuffaceous exhalites ascribed to the Val d'Or Formation of Imreh (1984) (i.e. Central Pyroclastic Belt of Sharpe (1968)). As with other VMS deposits in the area (Louvem, Manitou Barvue, Dunraine, East Sullivan, **Figure 2.2**), the gold-bearing base metal sulfide concentration at Louvicourt formed near or at the end of the pre-accretionary calc-alkalic volcanic cycle at ca. 2705-2700 Ma (**Figure 8.28**) and has undergone penetrative deformation and recrystallization to greenschist facies assemblages during the regional D_2 (S_2) deformation event at ca. 2677-2660 Ma. (Chartrand, 1991; Wong et al., 1991; Powell et al., 1995).

The waning of tholeiitic and calc-alkalic volcanism in the Val d'Or-Malartic area was quickly followed by a first episode of regional folding and faulting (D_1). The D_1 deformation event, which is thought to occur at the onset of the Abitibi/Pontiac collision in the Val d'Or-Malartic region, is characterized by southwest overturned F_1 folds locally accompanied by a gently to moderately north-dipping S_1 schistosity and by the development of cleavage and bedding-parallel faults (e.g. **Table 2.3**, Sansfaçon and Hubert (1990)). It coincides with similar deformation events reported by Hodgson *et al.* (1990) in the western part of the southern Abitibi belt, bracketed between 2700-2688 Ma by Corfu (1993). In the Val d'Or area, the age of this early phase of folding and faulting is bracketed between ca. 2700 Ma, the age of the Val d'Or Formation (Wong et al., 1991), and ca. 2694 Ma, the age of Sigma-Lamaque No.2 feldspar porphyry dikes (Wong et al., 1991), the first to be emplaced after the tilting of volcanic strata (Robert and Brown, 1986a, see Regional sequence of events diagram in back pocket). Kiena and other gold deposits of intrusion-related character, which based on this study include Malartic, Camflo, Orion Vein No. 8, Goldex, Siscoe, Sigma-Lamaque No. 2 and Lamaque, formed during a protracted episode of regional diorite-granodiorite-tonalite-monzonite plutonism following the short compressional D_1 deformation event (**Figure 8.28**). Post-collisional plutonism, which marks the transition from a compressional to an extensional regime, is constrained between ca. 2694 Ma, the age of Sigma-Lamaque's post-D_1 feldspar

porphyry dikes (Wong et al., 1991), and ca. 2677-2660 Ma, the time interval estimated for the development of the regional S_2 schistosity across the southern Abitibi belt (Corfu et al., 1991; Wilkinson et al., 1993; Powell et al., 1995). Intrusions of dioritic, granodioritic, and tonalitic compositions were common in the early phases of orogenic plutonism (e.g. Snowshoe, ca. 2693 Ma; Norlartic, ca. 2692 Ma; Kiena, ca. 2686 Ma), whereas monzonitic intrusions prevailed during the last stages of pre- regional metamorphic magmatism (e.g. Camflo, ca. 2685 Ma).

Malartic and Sigma-type deposits are subdivided into two age groups: deposits which formed shortly after the regional tilting of volcanic strata but prior to 2686 Ma, and deposits which formed after ca. 2685 Ma but prior to regional synmetamorphic deformation at ca. 2677-2660 Ma (**Figure 8.28**). This subdivision is based in part, on absolute U-Pb zircon ages of gold mineralization provided by deposits directly dated by cross-cutting intrusions (i.e. Kiena, Norlartic), and in part on the relative ages of mineralization provided by post-D_1 (S_1) and pre-D_2 (S_2) field relationships, U-Pb zircon ages of host intrusions, overprinting mineralization styles, and the age of the post-ore S_2 schistosity. The older 2694-2686 Ma group of intrusion-related deposits is clustered in the western segment of the Val d'Or plutonic belt and includes Malartic camp deposits, Kiena, Norlartic, and Orion Vein No. 8 deposits (**Figure 2.2** and **8.28**). Mineralization at these deposits is porphyry-style and consists predominantly of upward-flaring carbonate-quartz-albite or quartz-carbonate and minor tourmaline stockwork veins and breccias with mainly pyrite, pyrrhotite and lesser chalcopyrite, telluride disseminations. By contrast, the younger 2685-2677 Ma Camflo, Goldex, Siscoe, Sigma-Lamaque No.2 and main Lamaque deposits, predominantly display an epithermal precious metal vein style of mineralization with upward-branching lode gold-quartz veins associated with tourmaline stockwork veins and breccias, and gold occurring with disseminated pyrite in zoned alteration halos to quartz-tourmaline veins or with tellurides in late-stage veins (see discussion on Sigma-Lamaque No. 2 in the previous section). The Norlartic deposit is featured in both groups of deposits (**Figure 8.28**) because minor, gold-bearing quartz-tourmaline veins resembling Sigma-Lamaque No. 2 lode gold veins overprint the ca. 2692 Ma

tonalite dike cross-cutting the main carbonate-quartz-pyrite stockwork vein mineralization. Camflo, however, is porphyry-style, because gold deposition is coeval with an intense quartz-K-feldspar-Au stockwork veining event overprinting a pervasively biotite-altered area of the host monzonite stock. Similarly, the main Lamaque deposit is also envisaged as porphyry-style gold mineralization, as the bulk of the ore forms an intense quartz stockwork broadly coeval with pervasive albitization of the host dioritic intrusion. Regardless of age or mineralization style, Kiena and all the mentioned Val d'Or plutonic belt deposits are associated with high-level intrusions and characterized by zoned alteration patterns grading from inner albite and/or K-feldspar alteration zones, coinciding with main-stage vein mineralization and brecciation, into outer biotite, sericite-chlorite, and actinolite-magnetite alteration zones away from the main ore fluid conduits. The early 2694-2686 Ma gold mineralization event is broadly synchronous with the deposition of clastic and turbiditic sediments of the Lac Caste ($\leq$2695 Ma, Feng and Kerrich (1991)), Kewagama Group (ca. 2687-2683 Ma, Davis (Jemielita et al., 1990; 1991)), and Cadillac Group ($\leq$ 2688 $\pm$ 3 Ma, Davis (1991)), whereas the younger 2685-2677 Ma gold mineralization event is broadly coeval with alluvial-fluvial type sedimentation spatially associated with alkalic volcanism in the Kirkland Lake area of the southwestern Abitibi greenstone belt (Corfu, 1993). Orogenic plutonic-gold hydrothermal activity and related uplift and sedimentation in and around the Val d'Or plutonic belt broadly coincide with mafic volcanism and sedimentation further south in the Pontiac Subprovince (Baby and Belleterre volcanic zones ca. 2689-2682 Ma, Pontiac Group sediments $\leq$ 2686-2683 Ma, Mortensen and Card (1993)). Val d'Or plutonic belt deposits of both age groups are penetratively deformed by the regional S_2 schistosity and related asymmetric z-shaped folds, and overprinted by shear zones and steeply-dipping strike-slip faults (**Table 2.6**, **Figure 8.25**). Overprinting by S_2 suggests that, following gold alteration-mineralization, Kiena, Malartic and Sigma-type orebodies were buried and deformed under P-T conditions corresponding to those of regional greenschist-amphibolite facies metamorphism.

The district-wide, intrusion-related model for gold mineralization in an evolving late Archean

geodynamic setting as presented herein, appears to explain the combined geological, structural, and geochronological data gathered at the discussed Val d'Or plutonic belt gold deposits. Individually and collectively, gold deposits of the Val d'Or-Malartic area bear many resemblances to recent gold deposits associated with epithermal and porphyry-style hydrothermal systems in tectonically active regions of the western Pacific (e.g. Sillitoe and Gappe (1984) and MacDonald and Arnold (1995); see section 7.4). By analogy with these and modern geothermal systems (e.g. White, 1981; Reyes (1990)), magmatic-hydrothermal ore-forming processes active throughout the Val d'Or-Malartic region during pre-metamorphic orogenic plutonism are inferred to adequately account for: 1) the age relationships between deposits of contrasting mineralization style by sporadic "thermal activity shifts" or migration" of the heat source causing magmatism and related gold hydrothermal activity along a fault lineament (i.e. Val d'Or plutonic belt) paralleling the Abitibi/Pontiac terrane boundary, 2) the age relationships between sets of gold-bearing veins and breccias within a single deposit as a progressive sequence of overprinting fracturing and microfracturing events, 3) the occurrence of phlogopitic biotites, pure albite (An_{0-1}, this study) and microcline (Or_{96}, Zweng (1993)) assemblages at mineralization centres, 4) structural complexities as a sequence of pre-ore and ore structures subsequently flattened during regional penetrative deformation, allowing for minor gold remobilization along S_2 schistosity planes, syn-metamorphic quartz veins, and late fault planes (e.g. Kiena, this study; Camflo, Sauvé and Makila (1990); Orion Vein No.8, Trudeau and Raymond (1992)), 5) the sympathetic variations in gold hydrothermal and metamorphic mineral assemblages with increasing depth (e.g. Sigma-Lamaque No. 2, Sauvé *et al.* (1993)) as the result of a metamorphic overprint over vertically zoned alteration-mineralization systems.

The drawn-out series of isotopic dates (see Regional Sequence of Events diagram in back pocket) previously interpreted to reflect the timing of gold mineralization approximately during and after regional metamorphism, is seen now as the result of thermal resettings of U-Pb titanite/rutile, Ar^{40}/Ar^{39} muscovite/biotite, and Sm-Nd scheelite isotopic systems following gold-ore formation. Isotopic disturbances may have been caused by one, or a combination

of several thermal pulses associated with the following geological events: 1) peak greenschist facies metamorphism in the upper crust (coeval with granulite facies metamorphism in the lower crust) at ca. 2660 Ma (Krogh, 1993; Moser, 1993; Powell et al., 1995), 2) the up-rise of the monzogranite phase of the Lacorne batholith at ca. 2643 ± 4 Ma (Feng and Kerrich, 1991), and 3) the emplacement of Proterozoic diabase dikes which are commonly found in and around gold deposits (i.e. similar to the Preissac diabase dikes dated as ca. 2150 ± 25 Ma).

The here proposed temporal-genetic model may also accommodate other Val d'Or-Malartic area deposits sharing similarities with Kiena that are not mentioned in the present discussion (e.g. Akasaba (Lebel, 1987), Callahan (Jenkins et al., 1989), Shawkey (Sauvé et al., 1993), East Sullivan (Taner, 1996)), however, diagnostic features of pre-metamorphic, intrusion-related alteration-mineralization sequences in these deposits have not been ascertained to date. Precise U-Pb zircon dating of gold orebodies with cross-cutting igneous rocks is still limited in spite of the reported presence of such post-ore intrusions (e.g. Orion Vein No.8, Siscoe, Shawkey, Greene-Stabell, Louvicourt Gold Field; Trudel and Sauvé (1992), Sauvé *et al.* (Sauvé et al., 1993). SHRIMP Pb/Pb isotopic ages of hydrothermal zircons in gold-bearing veins usually produce dates with errors that are too large to be confined to the ca. 2694-2677 Ma time interval for gold mineralization proposed in the model of **Figure 8.28** (with the exception of Sigma and Bevcon veins dated as 2682 ± 8 Ma and 2681 ± 6 Ma, respectively; Claoué-Long *et al.* (1990)). Using more precise U-Pb zircon dating techniques, Kerrich and Kyser (1994) have dated vein zircons at Bras d'Or (deposit No. 20 on **Figure 2.2**) as 2693 ± 2 Ma and 2688 ± 8 Ma, suggesting that some Sigma-type quartz-tourmaline vein mineralization is coeval, within analytical error, with carbonate-quartz-albite-pyrite stockwork vein mineralization at Norlartic and Kiena. Their data are compatible with the time interval allowed for gold mineralization in the here presented model but implies the occurrence of simultaneously active, but compositionally distinct, magmatic-hydrothermal gold-ore centres at both ends of the district. However, many current and past geological descriptions of Val d'Or plutonic belt deposits (e.g. Ferderber, Perron, Bras d'Or), are still

focused on the structural aspect of mineralization and, as a result, the deposits continue to be envisaged as "shear zone-controlled" by some authors (e.g. Vu (1990); Tessier (1990)). A renewed interest in the mapping of zoned alteration sequences emphasizing the distribution of albite (or K-feldspar) and biotite alterations and the identification of intermineral events (e.g. diking, brecciation) in other deposits, more dates of cross-cutting intrusions, and consideration of strain partitioning resulting from competence differences introduced by different alteration types, may help to test the premetamorphic, magmatic-hydrothermal model of gold mineralization advanced in this study for Kiena and reward renewed mineral exploration efforts in the Val d'Or-Malartic region.

CHAPTER 9 LISTING OF ORIGINAL CONTRIBUTIONS

The study of the Kiena deposit vein-breccia-dike system is of considerable significance to the problem of timing of gold mineralization in the southern Abitibi greenstone belt and provides important insights into the geology and metallogenesis of the Val d'Or-Malartic area. The recognition of a pre-metamorphic, magmatic-hydrothermal origin for gold mineralization at Kiena came from detailed underground mapping, geochronological, structural and petrographic studies of mineralized and unmineralized volcanic and igneous rocks. Refinements to the local geological history, i.e. the determination of the timing of orogenic plutonism and gold mineralization in relation to regional penetrative deformation and metamorphism, are the result of a compilation of structural relations and isotopic age dates at selected gold deposit localities across the Val d'Or-Malartic district, based on the literature and personal observations.

The absolute minimum age of 2686 ± 2 Ma for the Kiena orebody, obtained by dating mineralization with a cross-cutting igneous intrusion, the controls exerted by albitite dikes and related pervasive albititization on mineralization, in addition to the overprint of penetrative deformation on all pre-existing ore structures, revises the ductile shear zone-controlled, syn- to post-metamorphic models postulated for the origin of this Archean gold orebody. The preservation of high-level, porphyry-style gold mineralization at Kiena suggests that other deposits of the Val d'Or plutonic belt may share a Kiena-like intrusion-related origin. A proposed temporal-genetic model for mineralization in the Val d'Or-Malartic area, based on a comparison between Kiena and other gold deposits, suggests a district-wide magmatic-hydrothermal connection among deposits of the Val d'Or plutonic belt during a ca. 20 m.y. episode of orogenic plutonism. Based on remarkable similarities at the regional- and deposit-scale, Kiena is envisaged as a metamorphosed Archean analogue of Cenozoic gold-rich porphyry-style deposit occurring in discrete belts along Circum-Pacific orogens.

Specific contributions of this study of the Kiena deposit are as follow:

1. This is *the first study* of the Kiena mine where geological information was gathered from all ore zones at upper, middle and the deepest levels of the deposit. Detailed mapping (1:250 scale), combined with whole-rock geochemical and petrographic studies carried out on samples collected during field work, resulted in the production of 14 plan maps of underground workings. This was followed by the preparation of a set of 10 schematic compilation plan maps and sections (1:500 scale) to ascertain cross-cutting relationships at critical sections and depths (sections 12438.4N and 12514.6N are the first sections to depict the orebody through its entire vertical extent ever produced at the mine). The set of 14 geological plan maps, reporting sample and figure locations (Index maps in back pocket), are keyed into the set of schematic plan maps and sections (also in back pocket). Index maps were digitized and drafted using the Corel Draw™ software whereas the schematic maps and sections were digitized and drafted using the AutoCad™ software.

2. Careful study of the schematic cross-sections and plan maps enabled, for the first time, the characterization of the Kiena deposit internal geometry across its entire width and vertical extent. Contributions to the understanding of Kiena geology are as follows:

   2.1 The idea that the Kiena deposit consists of two distinct orebodies, an upper breccia orebody and a lower shear zone orebody, was revised. Sections 12438N and 12514N show that the Kiena deposit consists of a single, continuous orebody with a clear upward and outward zonation. Changes in deformation styles with depth (seemingly unfoliated breccia ore at upper levels and strongly schistose, albitite-hosted, stockwork vein mineralization at lower levels) are explicable by post-ore strain partitioning. The competency contrast of Kiena's mineralized rocks responsible for the strain partitioning was in part acquired during the development of a zoned alteration-mineralization pattern characterized by early, inner albitization followed by subsequent episodes of hydrothermal carbonate (ankerite) and albite alteration

restricted to the upper part of the orebody.

2.2 Igneous intrusions formerly named "ore zone andesite", "grey diorite", "quartz diorite" or "microdiorite" dikes were reinterpreted as albitite dikes. Chilled margins and granitoid textures suggest that albitite dikes are of igneous origin. However, the extremely low calcium content (An_{0-1}) and high density of fluid inclusions in the rock-forming albites, replacement-type textures such as myrmekitic intergrowths, and the occurrence of similar mineralogical characteristics in vein- and breccia-forming albites, suggest that these rocks may be affected by strong hydrothermal alteration. I propose that this rock type is the main ore host at Kiena because gold mineralization occurs within the confines of several albitite dikes (as at the lower mine levels), or the dikes are intimately related to the ore (either as xenolith in the granodiorite dike cutting the ore or as a cluster of weakly mineralized dikes in contact with the ore, at intermediate and upper mine levels). I suggest that the albitite protolith of Kiena's high-grade breccia ore is obscured by the most intense hydrothermal alteration observed in the deposit. A search for albitite dike occurrences showed that they occur as pre-ore intrusions in other Archean, as well as late Jurassic and Cretaceous gold deposits. The dikes are emplaced in deformed mafic-ultramafic volcanic rock sequences near regional-scale faults.

2.3 A zoned alteration-mineralization sequence was recognized that was caused by hydrothermal events, including the intrusion of albitite dikes and related pre-ore pervasive albitization, a sequence of overprinting vein-breccia alteration stages, the emplacement of intermineral porphyry dikes, and a late-stage sequence of overprinting vein phyllosilicate alterations. Albitite dikes, Stwk Cb-Qz-Py(Po)±Ab±Au ore, biotite-magnetite and chlorite vein alterations have a previously unrecognized upward-flaring shape. Careful study of polished rock slabs shows the presence of open-space infill vein and breccia ore textures (crustiform and cockade textures) previously unnoticed.

2.4 Qualitative electron microprobe analysis in the EDS mode has yielded significant new information on the composition of gold-related hydrothermal alteration minerals. Albitite-forming albites and hydrothermal vein albites share an An ($_{0-1}$) composition, whereas late-stage vein biotites are magnesium-rich (11-13 wt.% MgO).

2.5 Granodiorite and feldspar porphyry dikes were identified as intermineral dikes. The presence of large xenoliths of ore in the granodiorite and the occurrence of minor auriferous carbonate-quartz-pyrite stockwork veins overprinted, in turn, by phyllosilicate stringer vein alteration affecting the entire ore-dike system, signifies that Kiena's porphyries are temporally related to the ore-forming process. The Kiena deposit granodiorite and quartz monzonite porphyries are among the two dozen or so deposits occurring in the Val d'Or-Malartic gold belt. However, mutual cross-cutting relationships between igneous intrusions and gold-bearing veins are described at the nearby Siscoe deposit (e.g. Trudel 1985). This suggests that intermineral dikes may be a more common occurrence in the area but were not recognized as such in the past.

2.6 The deposit's hierarchy of structures was clarified and shows that deformation of the ore-dike complex is post-ore. All pre-existing ore structures, including intermineral porphyry dikes, are overprinted by the deposit's main schistosity (S_n). This east-west, north-dipping schistosity is axial planar to a z-fold which is subsequently deformed, together with the ore-dike complex, by a north-northwest-plunging fold and related crenulation cleavage (S_{n+1}). I suggest that the deposit's main schistosity, S_n, correlates with the regional S_2 schistosity of Dimroth et al. (1982, 1983a,b). This implies that the Kiena orebody is not controlled, but overprinted, by regional synmetamorphic deformation. Deposit-scale structures and microstructures described in this study suggest that the deposit was deformed by flattening.

2.7 Pre- and syn-ore controls were identified as both structural and magmatic-

hydrothermal. Pre-ore regional-scale structural control is exerted by the Kiena Mine Fault Zone, whereas the deposit's albitite dike swarm exerts, in turn, pre-ore magmatic-hydrothermal control. I suggest that pervasive albite alteration is broadly coeval with the emplacement of the dikes, because all subsequent fracture-controlled alteration types recognized in the mine overprint this early albite alteration occurring in or at the dike contacts. It is inferred that pre-ore pervasive albitization may have acted as ground preparation control by enhancing the original competency contrast between albitite dike and adjacent mafic-ultramafic volcanic rocks. Syn-ore controls are local and refer to fracture-induced permeability created during main-stage hydrothermal activity broadly contemporaneous with the emplacement of porphyry dikes in the Kiena Mine Fault Zone.

3. By producing the absolute minimum U-Pb zircon age of 2686 ± 2 Ma for the formation of gold-ore at Kiena, it was established that gold mineralization occurred early in the evolution of the southern Abitibi greenstone belt. The U-Pb zircon age of the nearby Snowshoe stock is determined as 2693 ± 2 Ma, signifying that the sub-circular intrusion is syn-tectonic as opposed to late-tectonic as previously thought (e.g. Sauvé et al. (1993)). As part of the geochronological study, $^{40}Ar/^{39}Ar$ dating of gold-related vein biotite yielded several disturbed spectra and only one plateau age of 2313 ± 15 Ma. This biotite age is not compatible with alteration-mineralization firmly dated as ≥2686 ± 2 Ma, suggesting that pre-metamorphic vein biotites are thermally reset. It is emphasized that although the author sampled the geologic units that required dating, sample preparation and U-Pb zircon dating were carried out at the Royal Ontario Museum by Dr. H. A. Wasteneys. Biotite samples requiring irradiation for $^{40}Ar/^{39}Ar$ dating were prepared by the author and were subsequently analyzed in the geochronological laboratory of Dr. E. Farrar by Dr. Sandra McBride at Queen's University. Results of the U-Pb zircon geochronological study are reported in Economic Geology (V. 90 No. 5).

4. A genetic ore model for the formation of the Kiena orebody is proposed. Mineralization

localized about an intrusive centre (i.e. albitite dike swarm), the upward-flaring geometry of the zoned alteration-mineralization pattern characterized by early pervasive feldspathization, episodic stockwork veining and mineralization, the presence of intermineral dikes dated as 2686 ± 2 Ma crosscutting the orebody and containing xenoliths of ore, open-space crystal growth in veins and cockade breccia-infill textures, and the overprint of penetrative deformation on all pre-existing ore structures, are consistent with a porphyry-style mineralization system emplaced at a relatively shallow depth prior to peak regional synmetamorphic deformation dated as ca. 2660 Ma (Powell, 1995a). This pre-metamorphic intrusion-related ore model for Kiena is in agreement with earlier findings of Clark (1963) who suggested a possible temporal and genetic link between "grey diorite" and felsic porphyry dikes, albitization and mineralization. The proposed magmatic-hydrothermal model postulates the episodic but rapid emplacement of an upward-flow of high-pressured hydrothermal fluids through a fault zone occupied by a swarm of albitite dikes acting as main ore-fluid conduits.

5. The Kiena deposit was also viewed in a broader, more regional context. This was achieved, in part, by producing the first geological-geochronological compilation map of the Val d'Or-Malartic area (1: 250 000), by comparing Kiena to other gold deposits in the Val d'Or-Malartic area and, in part, by constructing a regional time sequence encompassing the ca. 50 m.y. Kenoran orogeny. These contributions to Val d'Or-Malartic geology are detailed below:

   5.1 The geological-geochronological compilation map of the Val d'Or-Malartic area (Figure 2.2) shows for the first time a curvi-linear array of gold-related orogenic intrusions dated as ca. 2694-2680 Ma, which is designated as the "Val d'Or plutonic belt". I suggest that this belt of calc-alkaline and alkaline intrusions represents the surface expression of a deep-seated regional-scale structure not previously recognized. A regional tectonic control for pre-metamorphic porphyry gold mineralization at Kiena is inferred based on the parallelism between the Val d'Or

plutonic belt and the Abitibi-Pontiac subprovince boundary (i.e. Malartic and Cadillac tectonic zones). As the findings of Campiglio (1974) are in agreement with the regional sequence of events proposed in this study, the southerly-overturned Bourlamaque sills shown in this compilation map have replaced the Bourlamaque 'batholith'. The central portion of the map was published in Economic Geology (V.90 No.5).

5.2 A comparison between Kiena and other gold deposits of the Val d'Or-Malartic gold belt demonstrates that Kiena resembles Malartic-type carbonate-quartz stockwork vein mineralization. The comparison also shows that Sigma-type quartz-tourmaline lode gold mineralization shares many diagnostic features of high-level emplacement recognized at Kiena including the overall upward-flaring geometry of the vein-dike system, infill-vein and breccia textures, intermineral diking and brecciation, and zoned alteration-mineralization patterns characterized by early albite alteration. The hierarchy of pre- to post-ore structures at Malartic and Sigma-type deposits, as inferred from the ordering of structural relations gathered from the literature and personal observations (Table 2.6 and Chapter 8), reveals a systematic overprint of pre-existing ore structures by regional penetrative structures at all the deposits examined. This implies early, pre-metamorphic gold mineralization across the Val d'Or plutonic belt in accord with conclusions reached by Sansfaçon and Hubert (1990), Trudeau and Raymond (1992) and Still and Mason (1995) for deposits of the Malartic camp, Orion Vein No. 8 and Goldex, but different from the syn- to post-metamorphic timing of gold mineralization proposed by Robert (1996) at Sigma. A part of these findings was published in Economic Geology (V. 90 No.5 and V. 91 No. 4).

5.3 The new Val d'Or-Malartic time sequence proposed in this study is distinguished from other compilations of radiometric dates (e.g. Corfu (1993), Kerrich (1994), Gouthier et al. (1994) and Powell (1995)) based on the following: 1) it includes the age of gold

mineralization directly dated by U-Pb on zircons (vein hydrothermal or primary magmatic in cross-cutting intrusions), 2) it incorporates the relative timing of gold mineralization inferred from the hierarchy of pre- to post-ore structures prepared for this study, and *3)* it shows the timing of gold mineralization in relation to both, an early regional D_1 deformation event (ca. 2700-2694 Ma) and a subprovince-wide D_2 dynamothermal event (ca. 2677-2665 Ma). As a result, gold-ore formation across the Val d'Or plutonic belt is confined to ca. 2694-2680 Ma and coincides with the ca. 20 m.y. evolutionary trend of regional calc-alkaline and alkaline plutonism previously recognized by Burrows and Spooner (1991) . In contrast, the drawn-out series of dates obtained from titanite, rutile, scheelite, and muscovite in gold-bearing fault zones, is broadly coincident with post-orogenic magmatic activity (ca. 2645-2611 Ma) and suggest the gradual thermal resetting of U-Pb, Sm/Nd, and $^{40}Ar/^{39}Ar$ isotopes in minerals with closure temperatures lower than zircon following peak regional dynamothermal activity.

6. Synthesis of the data collected and analysed for this study resulted in the formulation of a temporal-genetic model for gold mineralization in the Val d'Or-Malartic area in relation to the Abitibi-Pontiac orogen. The model implies that the succession of events recorded in the Val d'Or-Malartic region is linked to a tectonic event involving the collision of the Abitibi and Pontiac subprovinces (e.g. Jackson and Fyon, 1991). The model is subdivided into pre- and post-accretion phases. The pre-accretion phase is characterized by calc-alkaline volcanism and related base metal mineralization, whereas the post-accretion phase is characterized by the emplacement of epizonal felsic intrusions and gold mineralization. Malartic-type gold mineralization (including Kiena) is coeval with calc-alkaline magmatic activity at ca. 2694-2680 Ma, and Sigma-type mineralization is coincident with calc-alkaline and alkaline magmatism at ca. 2685-2677 Ma. The temporal-genetic model also suggests that Malartic-type deposits represent porphyry-style mineralization, whereas younger Sigma-type deposits may represent epithermal-style mineralization. Penetrative deformation, metamorphism and ductile shear zone development are post-ore and associated with the terminal stages of the Abitibi-Pontiac orogen.

7. The pre-metamorphic tectonic-controlled emplacement of intrusion-related gold-ore at destructive plate margins as suggested by the temporal-genetic model proposed in this study, is reminiscent of the regional-scale geological setting of Cenozoic Circum-Pacific gold belts. At the deposit-scale, the zoned alteration-mineralization sequence of the porphyry-style mineralization uncovered at Kiena is comparable to those occurring at deeper levels within similar deposits of the Luzon Central Cordillera in the Philippines. It is thus proposed to envisage Kiena as a metamorphosed Archean analogue of Tertiary gold-rich and gold-only deposits encountered in Circum-Pacific orogens.

REFERENCES

Anglin, C. D., 1990, Preliminary Sm-Nd isotopic analyses of scheelites from Val D'Or gold deposits, Quebec: Canada Geological Survey, Paper 90-1C, p. 255-259.

Arancibia, O. N., and Clark, A. H., 1996, Early magnetite-amphibole-plagioclase alteration-mineralization in the Island Copper porphyry copper-gold-molybdenum deposit, British Columbia: Economic Geology, v. 91, p. 402-438.

Asbury, W. N., 1941, Faulting and ore deposition in the Rouyn-Bell River region: Unpub. M.Sc. thesis, Montréal , Québec, McGill University.

Auger, P. E., 1947, Région de la mine Siscoe, Cantons de Dubuisson et de Vassan, Comté d'Abitibi-Est, Ministère des Mines, Province de Québec, Rapport géologique 17, 45 p.

Babineau, J., 1983, Carte géologique et structurale de la région du Lac Malartic- Carte annotée, Ministère de l'Énergie et des Ressources du Québec, DP-83-30.

Babineau, J., 1984, Géologie de la région de La Motte, Abitibi, Québec, Ministère de l'Énergie et des Ressources du Québec, ET 84-03, 17 p.

Backman, O. L., 1936, Geology of Siscoe gold mine: Canadian Mining Journal, v. 57, p. 467-475.

Barton, P., and Skinner, B. J., 1979, Sulfide mineral stabilities, *in* Barnes, H. B., ed., Geochemistry of hydrothermal ore deposits, Second Edition: New York, John Wiley & Sons, p. 278-403.

Bass, M. N., 1961, Regional tectonics of part of the southern Canadian Shield: Journal of Geology, v. 69, p. 669-702.

Bédard, L. P., and Ludden, J. N., 1997, Nd-isotope evolution of Archaean plutonic rocks in southeastern Superior Province: Canadian Journal of Earth Sciences, v. 34, p. 286-298.

Belkabir, A., 1990, Géologie du gisement filonien d'or Dumont et géochimie de ces épontes altérées: Unpub. M.Sc. thesis, Montréal, Québec, École Polytechnique.

Belkabir, A., Hubert, C., Ji, S., and Hoy, L. D., 1994, Role of metasomatic reactions on the contrasted deformation styles of a multiphase granitic pluton: Geological Association of Canada Program with Abstracts, v. 19, p. A9.

Belkabir, A., Robert, F., Vu, L., and Hubert, C., 1993, The influence of dykes on auriferous shear zone development within granitoid intrusions: the Bourlamaque pluton, Val d'Or district, Abitibi greenstone belt: Canadian Journal of Earth Sciences, v. 30, p. 1924-1933.

Bell, L. V., and Bell, A. M., 1932, Terrains miniers de la région de Pascalis-Louvicourt, Service des Mines du Québec, Rapport annuel 1932, Partie B, p. 3-69.

Benn, K., Sawyer, E. W., and Bouchez, J. L., 1992, Orogen parallel and transverse shearing in the Opatica belt, Quebec: implications for the structure of the Abitibi Subprovince: Canadian Journal of Earth Sciences, v. 29, p. 2429-2444.

Boily, M., Pilote, P., and Williams-Jones, A. E., 1989, Geochemical evolution of the Li-, Ta-, Be-bearing pegmatites and associated monzogranites of the Preissac-Lacorne

plutonic complex, Abitibi, Canada, Special Paper No. 8, Finland Geological Survey, p. 17.

Boily, M., William-Jones, A. E., Mulja, T., and Pilote, P., 1990, Rare element granitic pegmatites in the Abitibi greenstone belt: a case study of the Preissac-Lacorne batholith, *in* Rive, M., Verpaelst, P., Gagnon, Y., Lulin, J.-M., Riverin, G., and Simard, A., eds., The Northwestern Quebec Polymetallic Belt: A summary of 60 years of mining exploration: Rouyn-Noranda, Canadian Institute of Mining and Metallurgy Special Volume 43, p. 299-311.

Bouchard, M. F., 1980, Région de Cadillac-Malartic, Ministère de l'Énergie et des Ressources du Québec, DPV-683, 10 p.

Boullier, A. M., and Robert, F., 1992, Paleoseismic events recorded in Archean gold-quartz vein networks, Val d'Or, Abitibi, Quebec, Canada: Journal of Structural Geology, v. 14, p. 161-179.

Bourget, A., 1986, Pétrographie et distribution de l'or autour du gîte S-50 à la mine d'or Kiena, Val d'Or, Québec: Unpub. M.Sc. thesis, Montréal, Québec, École Polytechnique de Montréal, 119 p.

Bowen, N. L., 1928, The evolution of the igneous rocks: New York, Dovers Publications, 332 p.

Boyle, R. W., 1987, Gold: history and genesis of deposits: New York, Van nostrand Reinhold Company Inc., 678 p.

Burnham, C. W., 1979, Magmas and hydrothermal fluids, *in* Barnes, H. L., ed., Geochemistry of Hydrothermal Ore Deposits, Second Edition: New York, John Wiley & Sons, p. 71-136.

Burrows, D. R., 1990, Relationships between Archean lode gold quartz vein deposits and igneous intrusions in the Timmins and Val d'Or areas, Abitibi Subprovince, Canada: Unpub. Ph.D. thesis, Toronto, Ontario, University of Toronto, 198 p.

Burrows, D. R., and Spooner, E. T. C., 1986, The McIntyre Cu-Au deposit, Timmings, Ontario, Canada, *in* Macdonald, A. J., ed., Proceedings of Gold 86, an International Symposium on the Geology of Gold: Toronto, Konsult International Inc., p. 23-29.

Burrows, D. R., and Spooner, E. T. C., 1989, Relationships between Archean gold quartz vein-shear zone mineralization and igneous intrusions in the Val d'Or and Timmins areas, Abitibi Subprovince, Canada, *in* Keays, R. R., Ramsay, W. R. H., and Groves, D. I., eds., The geology of gold deposits: the perspective in 1988, Monograph 6, Economic Geology, p. 424-444.

Burrows, D. R., and Spooner, E. T. C., 1991, The Lamaque Archean stockwork Au system, Val d'Or, Quebec; relationship to a ~ 20 Ma, calc-alkaline, intrusive sequence: Geological Association of Canada Program with Abstracts, v. 16, p. A17.

Burrows, D. R., Spooner, E. T. C., Wood, P. C., and Jemielita, A., 1993, Structural controls on formation of the Hollinger-McIntyre Au quartz vein system in the Hollinger Shear Zone, Timmins, southern Abitibi greenstone belt, Ontario: Economic Geology, v. 88, p. 1643-1663.

Calvert, A., Sawyer, E. W., Davis, W. J., and Ludden, J. N., 1995, Archean subduction inferred from seismic images of a mantle suture in the Superior Province: Nature, v.

375, p. 670-674.
Campiglio, C., 1974, Étude géochimique et pétrologique du batholite de Bourlamaque, Abitibi, Québec: Unpub. Ph.D. thesis, Montréal, Québec, École Polytechnique de Montréal, 294 p.
Campiglio, C., 1977, Batholite de Bourlamaque, ES-26, Ministère des Richesses Naturelles du Québec, p. 211 p.
Campiglio, C., and Darling, R., 1976, The geochemistry of the Archean Bourlamaque batholith, Abitibi, Quebec: Canadian Journal of Earth Sciences, v. 13, p. 972-986.
Card, K. D., 1990, A review of the Superior Province of the Canadian Shield, a product of Archean accretion: Precambrian Research, v. 48, p. 99-156.
Card, K. D., and Ciesielski, A., 1986, DNAG No. 1 Subdivisions of the Superior Province of the Canadian Shield: Geoscience Canada, v. 13, p. 5-13.
Card, K. D., Percival, J. A., Lafleur, J., and Hogarth, D. D., 1981, Progress report on regional synthesis, central Superior Province: Geological Survey of Canada, Paper 81-1A, p. 77-93.
Chartrand, F., 1991, Geological setting of volcanogenic massive sulfide deposits in the central pyroclastic belt of Val d'Or, *in* Chartrand, F., ed., Geology and gold, rare element, and base metal mineralization of the Val d'Or area, Quebec, Guidebook Series V. 9, Society of Economic Geologists, p. 75-89.
Chartrand, F., and Cattalani, S., 1990, Massive sulphide deposits in Northwestern Quebec, *in* Rive, M., Verpaelst, P., Gagnon, Y., Lulin, J.-M., Riverin, G., and Simard, A., eds., The Northwestern Quebec Polymetallic Belt: A summary of 60 years of mining exploration: Rouyn-Noranda, Canadian Institute of Mining and Metallurgy Special Volume 43, p. 77-89.
Chown, E. H., Daigneault, R., Mueller, W., and Mortensen, J., 1992, Tectonic evolution of the Northern Volcanic Zone of the Abitibi belt: Canadian Journal of Earth Sciences, v. 29, p. 2211-2225.
Claoué-Long, J. C., King, R. W., and Kerrich, R., 1990, Archean hydrothermal zircon in the Abitibi greenstone belt: constraints on the timing of gold mineralization: Earth and Planetary Science Letters, v. 98, p. 109-128.
Claoué-Long, J. C., King, R. W., and Kerrich, R., 1992, Reply to comment by F. Corfu and D.W. Davis on "Archean hydrothermal zircon in the Abitibi greenstone belt: constraints on the timing of gold mineralization: Earth and Planetary Science Letters, v. 109, p. 601-609.
Clark, L.A., 1963, Geological Report, Kiena Gold Mines Ltd., 27 p.
Cloutier, J. P., 1979, Geological compilation maps, scale 1: 5000, Falconbridge Ltd.
Clowes, R. M., 1993, Variations in continental crustal structure in Canada from LITHOPROBE seismic reflexion and other data: Tectonophysics, v. 219, p. 1-27.
Clowes, R. M., 1996, Lithoprobe Phase IV: Multidisciplinary studies of the evolution of a continent - Progress report: Geoscience Canada, v. 23, p. 109-123.
Colvine, A. C., Fyon, J. A., Heather, K. B., Marmont, S., Smith, P. M., and Troop, D. G., 1988, Archean lode gold deposits in Ontario, Part I. A depositional model Part II. A genetic model, Ontario Geological Survey, Miscellaneous Paper 139, p. 136 p.

Cooke, D. L., and Moorhouse, W. W., 1969, Timiskaming volcanism in the Kirkland Lake area, Ontario, Canada: Canadian Journal of Earth Sciences, v. 6, p. 117-132.

Cooke, H. C., 1923, Quelques gisements d'or de l'ouest du Québec, Commission Géologique du Canada, Rapport Annuel, Partie C, p. 92-95.

Corfu, F., 1991, Evolution of the southern Abitibi greenstone belt: a summary of U-Pb and Lu-Hf isotopic investigations: Geological Association of Canada Program with Abstracts, v. 16, p. A25.

Corfu, F., 1993, The evolution of the southern Abitibi greenstone belt in light of precise U-Pb geochronology: Economic Geology, v. 88, p. 1323-1340.

Corfu, F., and Davis, D. W., 1991, Comment on "Archean hydrothermal zircon in the Abitibi greenstone belt: constraints on the timing of gold mineralization" by J.C. Claoué-Long, R.W. King and R. Kerrich: Earth Planetary Science Letters, v. 104, p. 545-552.

Corfu, F., Jackson, S. L., and Sutcliffe, R. H., 1991, U-Pb ages and tectonic significance of late Archean alkalic magmatism and nonmarine sedimentation: Timiskaming Group, southern Abitibi belt, Ontario: Canadian Journal of Earth Sciences, v. 28, p. 489-503.

Corfu, F., Krogh, T. E., Kwok, Y. Y., and Jensen, L. S., 1989, U-Pb zircon geochronology in the southernwestern Abitibi greenstone belt, Superior Province: Canadian Journal of Earth Sciences, v. 26, p. 1747-1763.

Cormier, M., 1986a, Geology of the S-50 orebody, Les Mines d'Or Kiena Ltée., 33 p.

Cormier, M., 1986b, The Kiena gold mine, *in* Pirie, J., and Downes, M. J., eds., Abitibi Belt Rouyn to Val d'Or - Excursion Guidebook, Gold'86 An International Symposium on the Geology of Gold, Abitibi belt - Rouyn to Val d'Or, Konsult International Inc., p. 75-78.

Couture, J.-F., 1991, Carte géologique des gîtes métallifères des districts de Rouyn-Noranda et de Val d'Or, partie sud des feuillets SNRC 32 C et 32 D ouest -Carte - Carte annotée, Ministère de l'Énergie et des Ressources du Québec, DV 90-11.

Couture, J.-F., Pilote, P., Machado, N., and Desrochers, J.-P., 1994, Timing of gold mineralization in the Val d'Or district, southern Abitibi belt: evidence for two distinct mineralizing events: Economic Geology, v. 89, p. 1542-1552.

Couture, J.-F., and Verpaelst, P., 1994, Mineralization styles in the Rouyn-Noranda district: Constraints on the tectonic evolution of the area: Geological Association of Canada Program with Abstracts, v. 19, p. A24.

Daigneault, R., and Labbé, J.-Y., 1992, Problématique des zones de déformation de la Sous-province de l'Abitibi, DV 92-03, Ministère de l'Énergie et des Ressources du Québec, DV 92-03, p. pp. 45-49.

Daigneault, R., Mueller, W., and Chown, E. H., 1994, Accretion of the northern and the southern volcanic zones along the Manneville fault zone, Abitibi Subprovince, Quebec: Geological Association of Canada Program with Abstracts, v. 19, p. p. A25.

Daigneault, R., Perrault, G., and Bédard, P., 1983, Géologie et géochimie de la mine Lamaque, Val d'Or, Québec: Canadian Mining and Metallurgical Bulletin, v. 86, p. 111-127.

Davis, D. W., 1991, Age constraints on deposition and provenance of Archean sediments in

the southern Abitibi and Pontiac Subprovinces from U-Pb analyses of detrital zircons: Geological Association of Canada Program with Abstracts, v. 16, p. A29.

Davis, W. J., Machado, N., Gariepy, C., Sawyer, E. W., and Benn, K., 1995, U-Pb geochronology of the Opatica tonalite-gneiss belt and its relationship to the Abitibi greenstone belt, Superior Province, Quebec: Canadian Journal of Earth Sciences, v. 32, p. 113-127.

Dawson, K. R., 1966, A comprehensive study of the Preissac-Lacorne batholith, Abitibi County, Quebec, Geological Survey of Canada, Bulletin 142, 74 p.

de Rosen-Spence, A. F., 1976, Stratigraphy, development and petrogenesis of the central Noranda volcanic pile, Noranda, Quebec: Unpub. Ph.D. thesis, Toronto, Ontario, University of Toronto, 166 p.

Derry, D. R., 1939, The geology of the Canadian Malartic gold mine, Northern Quebec: Economic Geology, v. 34, p. 495-523.

Desrochers, J.-P., and Hubert, C., 1994, Structural evolution of an Archean accretionary zone: the Malartic composite block, southern Abitibi greenstone belt, Quebec: Geological Association of Canada Program with Abstracts, v. 19, p. A27.

Desrochers, J.-P., and Hubert, C., 1996, Structural evolution and early accretion of the Archean Malartic Composite Block, southern Abitibi greenstone belt, Quebec, Canada: Canadian Journal of Earth Sciences, v. 33, p. 1556-1569.

Desrochers, J.-P., Hubert, C., Ludden, J. N., and Pilote, P., 1992, Géologie du "Bloc composite de Malartic" - Région de Val d'Or, DV 92-03, Ministère de l'Énergie et des Ressources du Québec, p. 57-61.

Desrochers, J.-P., Hubert, C., Ludden, J. N., and Pilote, P., 1993a, Accretion of Archean oceanic plateau fragments in the Abitibi greenstone belt, Canada: Geology, v. 21, p. 451-454.

Desrochers, J.-P., Hubert, C., and Pilote, P., 1993b, Géologie du secteur de Lac de Montigny (phase 3) - Région de Val d'Or, Ministère de l'Énergie et des Ressources du Québec, MB 93-15, 17 p.

Desrochers, J.-P., Robert, F., and Hubert, C., 1994, Archean metallogenesis in a rifted accretionnary environment: the Malartic composite block of the southern Abitibi belt, Quebec: Geological Association of Canada Program with Abstracts, v. 19, p. A27.

Dimroth, E., Imreh, L., Cousineau, P., Leduc, M., and Sanschagrin, Y., 1985, Paleogeographic analysis of submarine flows and its use in the exploration for massive sulphide deposits, Geological Association of Canada, Special Paper 28, p. 203-222.

Dimroth, E., Imreh, L., Goulet, N., and Rocheleau, M., 1983a, Evolution of the south-central segment of the Archean Abitibi belt, Quebec. Part II: Tectonic evolution and geomechanical model: Canadian Journal of Earth Sciences, v. 20, p. 1355-1373.

Dimroth, E., Imreh, L., Goulet, N., and Rocheleau, M., 1983b, Evolution of the south-central segment of the Archean Abitibi belt, Quebec. Part III: Plutonic and metamorphic evolution and geotectonic model: Canadian Journal of Earth Sciences, v. 20, p. 1374-1388.

Dimroth, E., Imreh, L., Rocheleau, M., and Goulet, N., 1982, Evolution of the south-central

part of the Archean Abitibi belt, Quebec. Part I: Stratigraphy and paleogeographic model: Canadian Journal of Earth Sciences, v. 19, p. 1729-1758.

Douglas, R. J. W., 1973, Geological Provinces: Ottawa, Surveys and Mapping Branch Department of Energy Mines and Resources.

Eakins, P. R., 1962, Caractères géologiques des gisements aurifères du district de Malartic, Comté d'Abitibi-Est, Ministère des Richesses Naturelles du Québec, Rapport géologique 99, 143 p.

Faure, S., Jébrak, M., and Bouillon, J.-J., 1990, Géologie et minéralisation en Zn-Cu-Ag-Au des Mines Selbaie, *in* Rive, M., Verpaelst, P., Gagnon, Y., Lulin, J.-M., Riverin, G., and Simard, A., eds., The Northwestern Quebec Polymetallic Belt: A summary of 60 of mining exploration, 43: Rouyn-Noranda, Canadian Institute of Mining and Metallurgy Special Volume 43, p. 363-372.

Feng, R., and Kerrich, R., 1990, Geobarometry, differential block movements, and crustal structure of the southwestern Abitibi greenstone belt, Canada: Geology, v. 18, p. 870-873.

Feng, R., and Kerrich, R., 1991a, ~2645 Ma S-type collisional granites: their influence on gold mineralization in the Abitibi southern volcanic zone: Geological Association of Canada Program with Abstracts, v. 16, p. A36.

Feng, R., and Kerrich, R., 1991b, A high-grade tectonic window in the Abitibi southern volcanic zone: an Archean subduction complex: Geological Association of Canada Program with Abstracts, v. 16, p. A36.

Feng, R., and Kerrich, R., 1991c, Single zircon age constraints on the tectonic juxtaposition of the Archean Abitibi greenstone belt and Pontiac Subprovince, Quebec, Canada: Geochimica et Cosmochimica Acta, v. 55, p. 3437-3441.

Feng, R., and Kerrich, R., 1992, Geodynamic evolution of the southern Abitibi and Pontiac terranes: evidence from geochemistry of granitoid magma series (2700-2630 Ma): Canadian Journal of Earth Sciences, v. 29, p. 2266-2286.

Franklin, J. M., Sangster, D. F., and Lydon, J. W., 1981, Volcanic-associated massive sulphide deposits: Economic Geology (75th Anniversary Volume), v. 75, p. 485-627.

Fraser, R. J., 1993, The Lac Troilus gold-copper deposit, northwestern Quebec: a possible Archean porphyry system: Economic Geology, v. 88, p. 1685-1699.

Fyon, J. A., Breaks, F. W., Heather, K. B., Jackson, S. L., Muir, T. L., Stott, G. M., and Thurston, P. C., 1992, Metallogeny of metallic mineral deposits in the Superior Province of Ontario, *in* Thurston, P. C., ed., Geology of Ontario, 4, Geological Survey of Ontario, Special Volume 4, p. 1091-1177.

Gagnon, G., 1987, Campagne d'exploration de surface, Hiver 1987: Sondages S-195 à S-209, Les Mines d'Or Kiena Ltée, 30 p.

Gardiner, J., 1988, 1988 Summer diamond drilling report, Project 82 - Wesdome Val d'Or, Quebec, NTS 32 C/4, Les Mines Sigma Ltée., Placer Dome Inc., 44 p.

Gariepy, C., Allègre, C. J., and Lajoie, J., 1984, U-Pb systematics in single zircons from the Pontiac sediments, Abitibi greenstone belt: Canadian Journal of Earth Sciences, v. 21, p. 1296-1304.

Gaudreau, R., Lacoste, P., and Rocheleau, M., 1986, Géologie et gîtologie du secteur de

Louvicourt-Vauquelin, Abitibi, Ministère de l'Énergie et des Ressources du Québec, MB 86-67, 124 p.

Gélinas, L., and Ludden, J. N., 1984, Rhyolitic volcanism and geochemical evolution of an Archean central ring complex: The Blake River Group Volcanics in southern Abitibi belt, Superior Province: Physics of the Earth and Planetary Interiors, v. 35, p. 77-88.

Germain, M., 1971, Géologie du quart nord-ouest du canton de Denain Comté d'Abitibi-est, Ministère des Richesses Naturelles du Québec, DP-105, 20 p.

Germain, M., 1972a, Géologie de la demie-ouest du canton de Pershing, comté d'Abitibi-est, Québec, Ministère des Richesses Naturelles du Québec, DP-109, 12 p.

Germain, M., 1972b, Géologie du canton de Vauquelin, comté d'Abitibi-est, Ministère des Richesses Naturelles du Québec, DP-108, 56 p.

Germain, M., 1973, Géologie du quart nord-est du canton de Pershing, comté d'Abitibi-est, Québec, Ministère des Richesses Naturelles du Québec, DP-198, 22 p.

Germain, M., 1974, Géologie du quart sud-est du canton de Pershing, Comté d'Abitibi-est, Québec, Ministère des Richesses Naturelles du Québec, DP-266, 18 p.

Gibson, H. L., and Watkinson, D. H., 1990, Volcanogenic massive sulphide deposits of the Noranda cauldron and shield volcano, Quebec, *in* Rive, M., Verpaelst, P., Gagnon, Y., Lulin, J.-M., Riverin, G., and Simard, A., eds., The Northwestern Quebec Polymetallic Belt: A summary of 60 years of mining exploration, 43: Rouyn-Noranda, Canadian Institute of Mining and Metallurgy Special Volume 43, p. 119-132.

Gilzean, M. N., and Brimhall, G. H., 1983, Alteration biotite chemistry and nature of hydrothermal system, Silverton district, Colorado: Geological Society of America Abstracs with Programs, v. 15, p. 581.

Goldie, R., 1978, Metamorphism of the Flavrian and Powell plutons, Noranda area, Quebec: Journal of Petrology, v. 20, p. 227-238.

Goldie, R., 1979, Consanguineous Archean intrusive and extrusive rocks, Noranda area, Quebec: Precambrian Research, v. 9, p. 275-287.

Goldie, R., B., K., and Seward, D., 1979, The Don Rouyn Mine: an Archean porphyry copper deposit near Noranda, Quebec: Economic Geology, v. 74, p. 1680-1684.

Goodwin, A. M., and Ridler, R., 1970, The Abitibi orogenic belt, *in* Baer, A. J., ed., Basins and Geosynclines of the Canadian Shield, Geological Survey of Canada, Paper 70-40, p. 1-265.

Goulet, N., 1978, Stratigraphy and structural relationships across the Cadillac-Larder Lake fault, Rouyn-Beauchastel area, Quebec, Ministère de l'Énergie et des Ressources du Québec, DPV-602.

Goutier, J., Mélancon, M., Dion, C., Verpaelst, P., and Rive, M., 1994, Compilation des datations isotopiques des sous-Provinces de l'Abitibi et de quelques unités adjacentes (Québec et Ontario), Ministère Énergie Ressources du Québec, MB 94-55, 5 p.

Grant, M., 1986, Étude du métamorphisme et de la distribution verticale des teneurs en Au, As et Sb à la Mine Sigma, Val d'Or, Québec: Unpub. M.Sc. thesis, Montréal, Québec, École Polytechnique, 116 p.

Green, A. G., Milkereit, B., Mayrand, L. J., Ludden, J. N., Hubert, C., Jackson, S. L., Sutcliffe, R. H., West, G. F., Verpaelst, P., and Simard, A., 1990, Deep structure of

an Archean greenstone terrane: Nature, v. 344, p. 327-330.
Groves, D. I., 1993, The crustal continuum model for late-Archean lode-gold deposits of the Yilgarn Block, Western Australia: Mineralium Deposita, v. 28, p. 366-374.
Gunning, H. C., 1937, Région de Cadillac, Québec, Commission Géologique du Canada, Mémoire 206, 89 p.
Gunning, H. C., and Ambrose, J. W., 1940, Région de Malartic, Québec, Commission Géologique du Canada, Mémoire 222, 162 p.
Hanes, J., Archibald, D. A., Hodgson, C. J., and Robert, F., 1992, Dating of Archean auriferous quartz-vein deposits in the Abitibi Greenstone Belt, Canada: $^{40}Ar/^{39}Ar$ evidence for a 70-100 Ma time gap between plutonism/metamorphism and mineralization: Economic Geology, v. 87, p. 1849-1861.
Hanes, J. A., 1991, K-Ar and $^{40}Ar/^{39}Ar$ geochronology: methods and applications, *in* Heaman, L., and Ludden, J. N., eds., Applications of radiogenic isotope systems to problems in geology, Short Course Handbook, Volume 19, Mineralogical Association of Canada, p. 27-57.
Hanes, J. A., Archibald, D. A., Hodgson, J. C., and Robert, F., 1989, Preliminary $^{40}Ar/^{39}Ar$ geochronology and timing of Archean gold mineralization at the Sigma mine, Val d'Or, Quebec, Geological Survey of Canada, Paper 89-1C, 135-142 p.
Hanes, J. A., and York, D., 1979, A detailed $^{40}Ar/^{39}Ar$ age study of an Abitibi dike from the Canadian Superior Province: Canadian Journal of Earth Sciences, v. 16, p. 1060-1070.
Hannington, M. D., 1993, Shallow submarine hydrothermal systems in modern island arc settings: Geological Association of Canada, Mineral Deposits Division Newsletter The Gangue, v. 43, p. 6-9.
Hawley, J. E., 1930, Gisements d'or et de cuivre des cantons de Dubuisson et de Bourlamaque, Comté d'Abitibi, Services des Mines du Québec, Rapport Annuel, Partie C, p. 43-58.
Hawley, J. E., 1932, The Siscoe gold deposit: Transactions of the Institution of Mining and Metallurgy, v. 35, p. 368-386.
Heaman, L., and Parrish, R., 1991, U-Pb geochronology of accessory minerals, *in* Heaman, L., and Ludden, J. N., eds., Short Course Handbook on Applications of Radiogenic Isotope Systems to Problems in Geology, 19: Toronto, Mineralogical Association of Canada, p. 59-102.
Heaman, L. M., 1988, A precise U-Pb zircon for a Hearst dyke: Geological Association of Canada Program with Abstracts, v. 13, p. A53.
Hodgson, C. J., 1986, Place of gold ore formation in the geological development of the Abitibi greenstone belt, Ontario, Canada: Transactions of the Institution of Mining and Metallurgy, v. 95, p. 179-182.
Hodgson, C. J., 1993, Mesothermal lode-gold deposits, *in* Kirkham, R. V., Sinclair, W. D., Thorpe, R. I., and Duke, J. M., eds., Mineral Deposit Modelling, Special Paper 40, Geological Association of Canada, p. 635-678.
Hodgson, C. J., D.A., L., and J.V., H., 1993, Giant mesothermal gold deposits: descriptive characteristics, genetic model and exploration area selection, *in* Whiting, B. H.,

Hodgson, C. J., and Mason, R., eds., Giant Ore Deposits: Kingston, Ontario, SEG Special Publication Number 2, p. 157-212.

Hodgson, C. J., and Hamilton, J. V., 1989, Gold mineralization in the Abitibi greenstone belt: end-stage result of Archean collisional tectonics ?: Economic Geology, Monograph, v. 6, p. 86-101.

Hodgson, C. J., Hamilton, J. V., and Piroscho, D. W., 1990, Structural setting of gold deposits and the tectonic evolution of the Timmins-Kirkland Lake area, Southwestern Abitibi greenstone belt, *in* Ho, S. E., Robert, F., and Groves, D. I., eds., Gold and base-metal mineralization in the Abitibi Subprovince, Canada, with special emphasis on the Quebec segment, Publication No. 24: Perth, Australia, The University of Western Australia Publication No. 24, p. 101-120.

Hodgson, C. J., and MacGeehan, P. J., 1982, Geological characteristics of gold deposits in the Superior Province of the Canadian Shield, *in* Hodder, R. W., and Petruk, W., eds., Geology of Canadian Gold Deposits: Val d'Or, Quebec (September 1980), Canadian Institute of Mining and Metallurgy Special Volume 24, p. 211-232.

Hoffman, P. F., 1988, United Plates of America, the birth of a craton: Early Proterozoic assembly and growth of Laurentia: Earth and Planetary Science Letters, v. Annual Review, p. 543-603.

Hoy, L. D., Belkabir, A., and Hubert, C., 1994, Oxygen isotopic evidence for the nature and origin of the Au mineralization at the Mouska deposit, Bousquet district, Quebec: Geological Association of Canada Program with Abstracts, v. 19, p. A52.

Hubert, C., and Ludden, J., 1994, Tectonic evolution of the Abitibi-greenstone belt based on interpretations of LITHOPROBE seismic reflection data: Geological Association of Canada Program with Abstracts, v. 19, p. A52.

Hubert, C., Trudel, P., and Gélinas, L., 1984, Archean wrench fault tectonics and structural evolution of the Blake River Group, Abitibi belt, Quebec: Canadian Journal of Earth Sciences, v. 21, p. 1024-1032.

Hutchinson, R. W., 1993, A multi-stage, multi-process genetic hypothesis for greenstone-hosted gold lodes: Ore Geology Reviews, v. 8, p. 349-382.

Hyde, R. S., 1980, Sedimentary facies in the Archean Timiskaming Group and their tectonic implications, Abitibi greenstone belt, northeastern Ontario, Canada: Precambrian Research, v. 12, p. 161-195.

Imreh, L., 1974a, Le sillon serpentinitique de La Motte, comté d'Abitibi-Est, Ministère de l'Énergie et des Ressources du Québec, DP 215.

Imreh, L., 1974b, L'esquisse géologique du sillon serpentinitique archéen de La Motte-Vassan, Ministère de l'Énergie et des Ressources du Québec, DP 232.

Imreh, L., 1974c, L'utilisation des coulées ultrabasiques dans la recherche minière: esquisse structurale et lithostratigraphique de La Motte-Vassan, Abitibi-Est, Québec, Canada, Ministère de l'Énergie et des Ressources du Québec, 38-2, 291-314. p.

Imreh, L., 1976a, Nouvelle lithostratigraphie à l'ouest de Val d'Or - Appendix to DP 349 (v) - CIM Excursion Val d'Or area Guidebook, Ministère de l'Énergie et des Ressources du Québec, DP 361 (v), 83 p.

Imreh, L., 1976b, Nouvelle lithostratigraphie à l'ouest de Val d'Or et son incidence

gîtologique, Ministère de l'Énergie et des Ressources du Québec, DP 349 (v), 73 p.
Imreh, L., 1984, Sillon de La Motte-Vassan et son avant-pays mériodional: Synthèse volcanogénique, lithostratigraphique et gîtologique, Ministère de l'Énergie et des Ressources du Québec, MM 82-04, 72 p.
Issigonis, M. J., 1980, Occurrence of disseminated gold deposits in porphyries in Archean Abitibi belt, Northern Quebec, Canada: Canadian Institute of Mining and Metallurgy Transactions, Applied Earth Sciences, v. 89, Section B, p. 157-158.
Jackson, S. L., Cruden, A. R., White, D., and Milkereit, B., 1995, A seismic-reflection-based regional cross section of the southern Abitibi greenstone belt: Canadian Journal of Earth Sciences, v. 32, p. 135-148.
Jackson, S. L., Fyon, A. J., and Corfu, F., 1994, Review of Archean supracrustal assemblages of the southern Abitibi greenstone belt in Ontario, Canada: products of microplate interaction within a large-scale plate-tectonic setting: Precambrian Research, v. 65, p. 183-205.
Jackson, S. L., and Fyon, J. A., 1991, The western Abitibi Subprovince in Ontario, *in* Thurston, P. C., Williams, H. R., Sutcliffe, R. H., and Stott, G. M., eds., Geology of Ontario, Geology of Ontario, Ontario Geological Survey, Special Volume 4, Part 1, p. 405-485.
Jeansonne, P., 1992, Compilation géologique d'exploration, Les Mines d'Or Kiena Ltée. - Carte annotée, Échelle 1: 5000.
Jébrak, M., LeQuentrec, M. F., Mareschal, J.-C., and Blais, D., 1991, A gravity survey across the Bourlamaque massif, southeastern Abitibi greenstone belt, Quebec, Canada: the relationship between the geometry of tonalite plutons and gold mineralization: Precambrian Research, v. 50, p. 261-268.
Jemielita, R. A., Davis, D. W., and Krogh, T. E., 1990, U-Pb evidence for Abitibi gold mineralization postdating greenstone magmatism and metamorphism: Nature, v. 346, p. 831-834.
Jemielita, R. A., Davis, D. W., Krogh, T. E., and Jack, S., 1989, Chronological constraints on the origin of Archean lode gold deposits in the southern Superior Province from U-Pb isotopic analyses of hydrothermal rutile and titanite: Geological Society of America Abstracs with Programs, v. 21, p. A351.
Jenkins, C., Trudel, P., and Perrault, G., 1989, Progressive hydrothermal alteration associated with gold mineralization of the Zone 1 intrusion of the Callahan property, Val d'Or region, Quebec: Canadian Journal of Earth Sciences, v. 26, p. 2495-2506.
Jolly, W. T., 1978, Metamorphic history of the Archean Abitibi belt, *in* Fraser, J. A., and Heywood, W. W., eds., Metamorphism in the Canadian Shield, Geological Survey of Canada, Paper 78-10, p. 63-78.
Kalliokoski, J., 1987, The Pontiac problem, Quebec-Ontario, in light of gravity data: Canadian Journal of Earth Sciences, v. 24, p. 1916-1919.
Karvinen, W. O., 1985, Geology of the Lamaque Mine property, Val d'Or, Quebec, Institut de Recherche en Exploration Minérale, P-83-21, 35 p.
Kerrich, R., and Cassidy, K. F., 1994, Temporal relationships of lode gold mineralization to accretion, magmatism, metamorphism and deformation - Archean to present: A

review: Ore Geology Reviews, v. 9, p. 263-310.
Kerrich, R., and Feng, R., 1992, Archean geodynamics and the Abitibi-Pontiac collision: implications for advection of fluids at transpressive collisional boundaries and the origin of giant quartz vein systems: Earth-Science Reviews, v. 32, p. 33-60.
Kerrich, R., and King, R., 1993, Hydrothermal zircon and baddeleyite in Val d'Or Archean mesothermal gold deposits: characteristics, compositions, and fluid-inclusions properties, with implications for timing of primary gold mineralization: Canadian Journal of Earth Sciences, v. 30, p. 2334-2351.
Kerrich, R., and Kyser, T. K., 1994, 100 Ma timing paradox of Archean gold, Abitibi greenstone belt (Canada): new evidence from U-Pb and Pb-Pb evaporation ages of hydrothermal zircons: Geology, v. 22, p. 1131-1134.
Kirkham, R. V., 1971, Intermineral intrusions and their bearing on the origin of porphyry copper and molybdenum deposits: Economic Geology, v. 73, p. 618-627.
Kirkham, R. V., Pilote, P., Sinclair, W. D., Robert, F., and Daigneault, R., 1995, Clark Lake porphyry Cu-Mo(-Au) deposit, Chibougamau, Quebec, Canada - Preserved Island Arc Sequence: Precambrian'95, an International Conference on Tectonics and Metallogeny of Early/Mid-Precambrian Orogenic Belts, Program with Abstracts, Université du Québec à Montréal, Aug. 28 to Sept. 1, 1995, p. 50.
Krogh, T. E., 1973, A low contamination method for the hydrothermal decomposition of zircon and extration of U and Pb for isotopic age determinations: Geochimica et Cosmochimica Acta, v. 37, p. 485-494.
Krogh, T. E., 1982a, Improved accuracy of U-Pb zircon ages by the creation of more concordant systems using an air abrasion technique: Geochimica et Cosmochimica Acta, v. 46, p. 637-649.
Krogh, T. E., 1982b, Improved accuracy of U-Pb zircon dating by selection of more concordant fractions using a high gradinet magnetic separation technique: Geochimica et Cosmochimica Acta, v. 46, p. 631-635.
Krogh, T. E., 1993, High precision U-Pb ages for granulite metamorphism and deformation in the Archean Kapuskasing structural zone, Ontario: implications for structure and development of the lower crust: Earth Planetary Science Letters, v. 119, p. 1-18.
Lacroix, S., and Sawyer, E. W., 1995, An Archean fold-thrustbelt in the northwestern Abitibi greenstone belt: structural and seismic evidence: Canadian Journal of Earth Sciences, v. 32, p. 97-112.
Larocque, A. C. L., Hodgson, C. J., and Lafleur, P. J., 1993, Gold distribution in the Mobrun volcanic-associated massive sulphide deposit, Noranda, Quebec: a preliminary evaluation of the role of metamorphic remobilization: Economic Geology, v. 88, p. 1443-1459.
Larson, J. E., and Hutchinson, R. W., 1993, The Selbaie Zn-Cu-Ag deposits, Quebec, Canada: an example of evolution from subaqueous to subarerial volcanism and mineralization in an Archean caldera environment: Economic Geology, v. 88, p. 1460-1482.
Latulippe, M., 1966, The relationship of mineralization to Precambrian stratigraphy in the Matagami Lake and Val d'Or districts of Quebec, Geological Survey of Canada,

Special Paper 3, p. 21-42.
Latulippe, M., 1976, Val d'Or-Malartic, Excursion géologique, Ministère de l'Énergie et des Ressources du Québec, DP 367 (v), 124 p.
Laznicka, P., 1983, Giant Ore Deposits: a quantitative approach: Global Tectonics and Metallogeny, v. 2, p. 41-63.
Laznicka, P., 1993, Precambrian lithologic associations and metallic ores: Amsterdam, Elsevier, 1247 p.
Lebel, J., 1987a, Campagne de forage, automne 1987. Sondages S-219, S-222 et S-226, Les Mines d'Or Kiena Ltée., 24 p.
Lebel, J., 1987b, Description du gîte d'or Akasaba, Abitibi, Québec: Unpub. M.Sc. thesis, Montréal, Québec, École Polytechnique, 217 p.
Lebel, J., 1988a, Campagne de forage, bloc mine, année 1989. Sondages S-245 à S-250, Les Mines d'Or Kiena Ltée., 23 p.
Lebel, J., 1988b, Campagne de forage, bloc mine, secteur ouest, Hiver 1988. Sondages s-227 à S-244, Les Mines d'Or Kiena Ltée., 39 p.
Lebel, J., 1989, Campagne de forage, bloc mine, année 1989. Sondages S-251 à S-289, Les Mines d'Or Kiena Ltée., 58 p.
Lebel, J., 1990, Campagne de forage, bloc mine, année 1990. sondages S-290 à S-310, Les Mines d'Or Kiena Ltée., 40 p.
Lebel, J., 1991, Campagne de forage, bloc mine, Hiver 1991. Sondages S-319 à S-342, S-361 et S-362, Les Mines d'Or Kiena Ltée., 67 p.
Lebel, J., 1992, Campagne de forage bloc mine, Hiver 1992. Sondages S-365 à S-382, Les Mines d'Or Kiena Ltée., 83 p.
Leggatt, H., 1989, Prospector:: Quaterly magazine of Placer Dome Group Companies, v. 1, p. 1.
Ludden, J., and Hubert, C., 1986, Geologic evolution of the late Archean Abitibi greenstone belt of Canada: Geology, v. 14, p. 707-711.
Ludden, J., Hubert, C., and Gariepy, C., 1986, The tectonic evolution of the Abitibi greenstone belt of Canada: Geological Magazine, v. 123, p. 153-166.
MacDonald, G., and Arnold, L. C., 1995, Factors responsible for the extreme concentration of Cu and Au in the Grasberg deposit: a comparative look at the porphyry copper systems of the Ertsberg District, Indonesia, *in* Clark, A. H., ed., Giant Ore Deposits II - Controls on the scale of orogenic magmatic-hydrothermal mineralization: Queen's University, Queen's University, Kingston, Ontario, p. 1-19.
MacDonald, G. D., and Arnold, L. C., 1994, Geological and geochemical zoning of the Grasberg igneous complex, Irian Jaya, Indonesia: Journal of Geochemical Exploration, v. 50, p. 143-178.
Machado, N., M., R., Gariepiy, C., and Simard, A., 1991, U-Pb geochronology of granitoids from the Pontiac Subprovince: Preliminary results: Geological Association of Canada Program with Abstracts, v. 16, p. A78.
Magnan, M., 1993, Synchronisme et mise en place de la minéralisation aurifère du gisement du Lac Troilus, Ministère de l'Énergie et des Ressources du Québec, DV 93-03, p. 73-36.

Marquis, P., and Hubert, C., 1989, The Dumagami structural zone: its evolution and features for the Doyon, Bousquet No. 1 and 2, and Donald J. La Ronde gold mines of southwestern Abitibi, Quebec, *in* Bursnall, J. T., ed., Mineralization and Shear Zones, Geological Association of Canada Short Course Notes, Volume 6, p. 226-238.

Marquis, P., Hubert, C., Brown, A., Scherkus, E., Trudel, P., and Hoy, L. D., 1992, Géologie de la mine Donald J. La Ronde (Abitibi), Ministère de l'Énergie et des Ressources du Québec, ET 89-06, 106 p.

Marquis, R., 1983, Étude tectono-stratigraphique à l'est de Val d'Or: essai de corrélation structurale entre les roches métasédimentaires des Groupes de Trivio et de Garden Island et application à l'exploration aurifère: Unpub. M.Sc. thesis, Montréal, Québec, Université du Québec à Montréal, 173 p.

Mason, R., 1992, Felsic magmatism and hydrothermal gold deposits: a tectonic perspective, *in* Bartholomew, M. J., Hyndman, D. W., Mogk, D. W., and Mason, R., eds., Basement Tectonics 8: Characterization and comparison of Ancien and Mesozoic continental margins: Butte, Montana, Kluwer Academic Publishers, Dordrecht, The Netherlands, p. 679-687.

Mason, R., 1995, The Kenoran orogeny and the first supercontinent: Precambrian'95, an International Conference on Tectonics and Metallogeny of Early/Mid-Precambrian Orogenic Belts, Program with Abstracts, Université du Québec à Montréal, Aug. 28 to Sept. 1, 1995, p. 37.

Mason, R., and Melnik, N., 1988, The anatomy of an Archean gold system - The McIntyre-Hollinger complex at Timmins, Ontario, Canada, *in* MacDonald, A. J., ed., Gold 86: An International Ssymposium on the Geology of Gold: Toronto, Canada, Konsult International, p. 40-55.

MERQ-OGS, 1983, Lithostratigraphic map of the Abitibi Sub-Province, Map 2484, Échelle 1:500 000, Ministère de l'Énergie et des Ressources du Québec, DV 83-16.

Mezger, K., Hanson, G. N., and Bohlen, S. R., 1989, High-precision U-Pb ages of metamorphic rutile: application to the cooling history of high-grade terranes: Earth and Planetary Science Letters, v. 96, p. 106-118.

Mezger, K., Rawnley, C. M., Bohlen, S. R., and Hanson, G. N., 1991, U-Pb garnet, sphene, monazite and rutile ages: implications for the duration of high-grade metamorphism and cooling histories, Adirondak Mts., New York: Journal of Geology, v. 99, p. 415-428.

Moore, W. J., and Czamanske, G. K., 1973, Compositions of biotites from unaltered and altered monzonitic rocks in the Bingham mining district, Utah: Economic Geology, v. 68, p. 269-280.

Morasse, S., Helmstaedt, H., Mason, R., and Cormier, M., 1995a, High-level intrusion-related gold mineralization at the Kiena Mine, Val d'Or, Québec, southern Abitibi Subprovince: Precambrian'95, an International Conference on Tectonics and Metallogeny of Early/Mid-Precambrian Orogenic Belts, Program with Abstracts, Université du Québec à Montréal, Aug. 28 to Sept. 1, 1995a, p. 49.

Morasse, S., and Wasteneys, H. A., 1994, The chronology of deformation at the Kiena Mine and its implications on the timing of an early deformation event (D_1) in the Val d'Or

area: Geological Association of Canada Program with Abstracts, v. 19, p. A79.
Morasse, S., Wasteneys, H. A., Cormier, M., Helmstaedt, H., and Mason, R., 1993, La mine d'or Kiena: minéralisation magmatique hydrothermale kénoréenne précoce dans la ceinture minérale de Val d'Or, sud-est de l'Abitibi, Ministère de l'Énergie et des Ressources du Québec, DV 93-03, p. 67-71.
Morasse, S., Wasteneys, H. A., Cormier, M., Helmstaedt, H., and Mason, R., 1995b, A pre-2686 Ma intrusion-related gold deposit at the Kiena Mine, Val d'Or, Québec, southern Abitibi Subprovince: Economic Geology, v. 90, p. 1310-1321.
Morasse, S., Wasteneys, H. A., Cormier, M., Helmstaedt, H., and Mason, R., 1996a, A pre-2686 Ma intrusion-related gold deposit at the Kiena mine, Val d'Or, Québec, southern Abitibi Subprovince - A reply: Economic Geology, v. 91, p. 801-803.
Morasse, S., Wasteneys, H. A., Cormier, M., Helmstaedt, H., and Mason, R., 1996b, A pre-2686 Ma intrusion-related gold deposit at the Kiena mine, Val d'Or, Québec, southern Abitibi Subprovince - A reply: Economic Geology, v. 91, p. 807-811.
Mortensen, J. K., 1987a, Preliminary U-Pb zircon ages for volcanic and plutonic rocks of the Noranda-Lac Abitibi area, Abitibi Subprovince, Quebec, Paper 87-1A, Geological Survey of Canada, Paper 87-1A, p. pp. 581-590.
Mortensen, J. K., 1987b, U-Pb chronostratigraphy of the Abitibi greenstone belt: Geological Association of Canada Program with Abstracts, v. 12, p. 75.
Mortensen, J. K., 1993, U-Pb geochronology of the eastern Abitibi Subprovince. Part 2: Noranda-Kirkland Lake area: Canadian Journal of Earth Sciences, v. 30, p. 29-41.
Mortensen, J. K., and Card, K. D., 1993, U-Pb age constraints for the magmatic and tectonic evolution of the Pontiac Subprovince, Québec: Canadian Journal of Earth Sciences, v. 30, p. 1970-1980.
Morton, R. L., and Franklin, J. M., 1987, Two-fold classification of Archean volcanic-associated massive sulphide deposits: Economic Geology, v. 82, p. 1057-1063.
Moser, D. E., 1993, A geological structural and geochronological study of the central Wawa Gneiss Domain: implications for the development of different crustal levels of the Archean Abitibi-Wawa orogen of the southern Superior Province, Canadian Shield: Unpub. Ph. D. thesis, Kingston, Ontario, Queen's University, Kingston.
Moss, A. E., 1939, The geology of the Siscoe gold mine, province of Quebec: Unpub. Ph.D. thesis, Montreal, Quebec, McGill University, 159 p.
Mueller, W., and Donaldson, J. A., 1992, Development of sedimentary basins in the Archean Abitibi belt, Canada: an overview: Canadian Journal of Earth Sciences, v. 29, p. 2249-2265.
Muir, J. E., 1979, Petrology, petrochemistry and ore genesis at the Kiena gold mine Quebec, Thornhill, Ontario, Falconbridge Metallurgical Laboratories, Report MR1107, 28 p.
Muir, J. E., 1981, The Kiena gold deposit: lithogeochemistry and petrography with special emphasis on the S-50 ore zone, Thornhill, Ontario, Falconbridge Metallurgical Laboratories, Report FRL 613, p. 78.
Norman, G. W. H., 1941, Région de la carte de Vassan-Dubuisson, Comté d'Abitibi, Québec - Carte à l'échelle 1:24 000, Commission Géologique du Canada, Brochure 41-6.

Norman, G. W. H., 1942, La partie est du canton de Dubuisson, comté d'Abitibi, Québec - Carte à l'échelle 1:6 000, Commission Géologique du Canada, Brochure 42-9.

Norman, G. W. H., 1943, Bourlamaque, Abitibi County, Quebec - 2 maps at 1:12 000, Geological Survey of Canada, Paper 43-2.

Norman, G. W. H., 1946, Preliminary maps of NW, NE, SW, SE Bourlamaque, Abitibi County, Quebec - Maps at 1:12 000, Geological Survey of Canada, Paper 46-15, 46-17, and 46-18.

Norman, G. W. H., 1947a, Dubuisson-Bourlamaque-Louvicourt, Abitibi County, Quebec - Map at 1:63 360, Geological Survey of Canada, Paper 47-20.

Norman, G. W. H., 1947b, Northeast Dubuisson, Abitibi County, Quebec - Map at 1:12 000, Geological Survey of Canada, Paper 46-21.

O'Neil, J. J., 1934, La mine d'or Canadian Malartic, Comté d'Abitibi, Services des Mines du Québec, Rapport Annuel, Partie B, p. 69-95.

Péloquin, A. S., Potvin, R., Paradis, S., Laflèche, M. R., Verpaelst, P., and Gibson, H. L., 1990, The Blake River Group, Rouyn-Noranda area, Québec: a stratigraphic overview, *in* Rive, M., Verpaelst, P., Gagnon, Y., Lulin, J.-M., Riverin, G., and Simard, A., eds., The Northwestern Quebec Polymetallic Belt: A summary of 60 years of mining exploration, 43: Rouyn-Noranda, Canadian Institute of Mining and Metallurgy Special Volume 43, p. 107-118.

Péloquin, A. S., Verpaelst, P., and Ludden, J. N., 1996, Spherulitic rhyolites of the Archean Blake River Group, Canada: implications for stratigraphic correlation and volcanogenic massive sulfide exploration: Economic Geology, v. 91, p. 343-352.

Péloquin, S., Ludden, J. N., and Verpaelst, P., 1995, The Blake River Group in Quebec: a 2.7 Ga in situ propagating volcanic basin hosting volcanogenic massive sulphide deposits: Precambrian'95, an International Coference on Tectonics and Metallogeny of Early/Mid-Precambrian Orogenic Belts, Program with Abstracts, Université du Québec à Montréal, Aug. 28 to Sept. 1, 1995, p. 271.

Percival, J. A., and Card, K. D., 1983, Archean crust as revealed in the Kapuskasing uplift, Superior Province, Canada: Geology, v. 11, p. 323-326.

Phillips, W. J., 1972, Hydraulic fracturing and mineralization: Journal of Geological Society of London, v. 128, p. 337-360.

Phillips, W. J., 1973, Mechanical effects of retrograde boiling and its probable importance in the formation of some porphyry ore deposits: Institute of Mining and Metallurgy Bulletin, v. 82, p. B90-B98.

Picard, C., and Piboule, M., 1986, Pétrologie des roches volcaniques du sillon de roches vertes archéennes de Matagami-Chibougamau à l'ouest de Chapais, Abitibi-est, Québec: Le Groupe hautement potassique d'Opémiska: Canadian Journal of Earth Sciences, v. 23, p. 1169-1189.

Piché, M., 1984, The Hauy Formation: Subaerial volcanism in a braided stream environment, *in* Guha, J., and Chown, E. H., eds., Chibougamau - Stratigraphy and Mineralization, Special Volume 34: Chibougamau, Québec, Canadian Institute of Mining and Metallurgy Special Volume 34, p. 153-163.

Pilote, P., Couture, J.-F., Desrochers, J.-P., Machado, N., and Pelz, P., 1993,

Minéralizations aurifères multiphasées dans la région de Val d'Or: l'exemple de la mine Norlartic, Ministère de l'Énergie et des Ressources du Québec, DV 93-03, p. 61-66.

Polk, G. K., 1960, Geology of Parker Island and Lac de Montigny islands, Kiena Gold Mines Ltd., 21 p.

Polk, G. K., 1961, Interim geological report on Kiena Gold Mines Ltd. with maps at 1"=200', Ventures, Kiena Gold Mines Ltd., 21 p.

Poulsen, K. H., Card, K. D., and Franklin, J. M., 1992, Archean tectonic and metallogenic evolution of the Superior Province of the Canadian Shield: Precambrian Research, v. 58, p. 25-54.

Powell, W. G., 1994, A petrological and geochronological study of the metamorphic history of the Rouyn-Noranda area, Quebec: Unpub. Ph.D. thesis, Kingston, Ontario,Queen's University, 102 p.

Powell, W. G., Carmichael, D. M., and Hodgson, C. J., 1993, Conditions and relative timing of metamorphism during the evolution fo the southern Abitibi greenstone belt: Geological Association of Canada Program with Abstracts, v. 19, p. A90.

Powell, W. G., Carmichael, D. M., and Hodgson, C. J., 1994, Conditions and relative timing of metamorphism during the evolution of the southern Abitibi greenstone belt: Geological Association of Canada Program with Abstracts, v. 19, p. A90.

Powell, W. G., Carmicheal, D. M., and Hodgson, C. J., 1995a, Conditions and timing of metamorphism in the southern Abitibi greenstone belt, Quebec: Canadian Journal of Earth Sciences, v. 32, p. 787-805.

Powell, W. G., Hodgson, C. J., Hanes, J. A., Carmichael, D. M., McBride, S., and Farrar, E., 1995b, $^{40}Ar/^{39}Ar$ geochronological evidence for multiple postmetamorphic hydrothermal events focused along faults in the southern Abitibi greenstone belt: Canadian Journal of Earth Sciences, v. 32, p. 768-786.

Quirion, D., 1988, Étude structurale et pétrographique du gisement S-50 de la mine Kiena, Val d'Or, Québec: Unpub. M.Sc. thesis, Montréal, Québec, Université de Montréal, 124 p.

Reyes, A. G., 1990, Petrology of Philippine geothermal systems and the application of alteration mineralogy to their assessment: Journal of Volcanology and Geothermal Research, v. 43, p. 279-309.

Rive, M., Pintson, H., and Ludden, J., 1990, Characteristics of late Archean plutonic rocks from the Abitibi and Pontiac Subprovinces, Superior Province, Canada, *in* Rive, M., Verpaelst, P., Gagnon, Y., Lulin, J.-M., Riverin, G., and Simard, A., eds., The Northwestern Quebec Polymetallic Belt: A summary of 60 years of mining exploration: Rouyn-Noranda, Quebec, Canadian Institute of Mining and Metallurgy Special Volume 43, p. 65-76.

Robert, F., 1989, Internal structure of the Cadillac tectonic zone southeast of Val d'Or, Abitibi belt, Québec: Canadian Journal of Earth Sciences, v. 26, p. 2661-2690.

Robert, F., 1990, Structural setting and control of gold-quartz veins of the Val d'Or area, southeastern Abitibi Subprovince, *in* Ho, S. E., Robert, F., and Groves, D. I., eds., Gold and base-metal mineralization in the Abitibi Subprovince, Canada, with emphasis

on the Quebec segment, No. 24: Perth, Australia, The University of Western Australia Volume No. 24, p. 167-211.

Robert, F., 1994, Vein fields in gold districts: the example of Val d'Or, southeastern Abitibi, Quebec, Current Research 1994-C, Geological Survey of Canada, Paper 1994-C, p. 295-302.

Robert, F., 1996, A pre-2686 Ma intrusion-related gold deposit at the Kiena mine, Val d'Or, Québec, southern Abitibi Subprovince - A discussion: Economic Geology, v. 91, p. 803-807.

Robert, F., and Brown, A., 1984, Progressive alteration asociated with gold-quartz-tourmaline veins at the Sigma Mine, Abitibi greenstone belt, Quebec: Economic Geology, v. 79, p. 393-399.

Robert, F., Brown, A., and Audet, A., 1983, Structural control of gold mineralization at the Sigma Mine, Val d'Or, Quebec: Canadian Institute of Mining and Metallurgy Bulletin, v. 76, p. 72-80.

Robert, F., and Brown, A. C., 1986a, Archean gold-bearing quartz veins at the Sigma Mine, Abitibi greenstone belt, Quebec: Part I. Geologic relations and formation of the vein system: Economic Geology, v. 81, p. 578-592.

Robert, F., and Brown, A. C., 1986b, Archean gold-bearing quartz veins at the Sigma mine, Abitibi greenstone belt, Quebec: Part II. Vein paragenesis and hydrothermal alteration: Economic Geology, v. 81, p. 593-613.

Robert, F., and Kelly, W. C., 1987, Ore-forming fluids in Archean gold-bearing quartz veins at the Sigma Mine, Abitibi greenstone belt, Quebec, Canada: Economic Geology, v. 82, p. 1464-1482.

Robert, F., Poulsen, K. H., and Dubé, B., 1994, Structural analysis of lode gold deposits in deformed terranes, Geological Survey of Canada, Open File 2850, 140 p.

Robert, F., Poulsen, K. H., and Dubé, B., 1995, Diverse gold mineralization styles in Precambrian greenstone terranes in Canada: Precambrian'95, an International Conference on Tectonics and Metallogeny of Early/Mid-Precambrian Orogenic Belts, Program with Abstracts, Université du Québec à Montréal, Aug. 28 to Sept. 1, 1995, p. 126.

Roberts, R. G., 1988, Archean lode gold deposits, *in* Roberts, R. G., and Sheahan, P. A., eds., Ore Deposits Models # 11, Reprint Series 3, Geoscience Canada, Volume 14, p. 1-20.

Robinson, W. G., 1961a, Kiena Gold Mines Limited, Proposed exploration program, Kiena Gold Mines Ltd., 4 p.

Robinson, W. G., 1961b, Proposed drilling on Kiena-Wisik, Kiena Gold Mines Ltd., 4 p.

Robinson, W. G., 1962, Review of mineral deposits, Kiena Gold Mines Ltd., 10 p.

Rocheleau, M., Hébert, M., St-Julien, R., Racine, P., Gaudreau, R., and Lacoste, P., 1990, La ceinture de l'Abitibi à l'est de Val d'Or: un secteur économiquement méconnu, affecté par la tectonique et le métamorphisme Grenvillien, *in* Rive, M., Verpaelst, P., Gagnon, Y., Lulin, J.-M., Riverin, G., and Simard, A., eds., The Northwestern Quebec Polymetallic Belt: A summary of 60 years of mining exploration: Rouyn-Noranda, Canadian Institute of Mining and Metallurgy Special Volume 43, p.

269-284.

Romberger, S. B., 1992, A model for bonanza gold deposits, Ore Deposit Models, Geoscience Canada, Volume 19, Geological Association of Canada, p. 63-72.

Roy, C., 1983, Géologie de la mine d'or Kiena: Unpub. M.Sc. thesis, Montréal, Québec, École Polytechnique, 200 p.

Salt, D. J., 1960, Magnetometer Survey Kiena Gold Mines Ltd., Dubuisson Twp., P.Q., Falconbridge Nickel Mines Ltd.

Sansfaçon, R., and Hubert, C., 1990, The Malartic gold district, Abitibi greenstone belt, Quebec: Geological setting, structure and timing of gold emplacement at Malartic Gold Fields, Barnat, East-Malartic, Canadian Malartic and Sladen Mines, *in* Rive, M., Verpaelst, P., Gagnon, Y., Lulin, J.-M., Riverin, G., and Simard, A., eds., The Northwestern Quebec Polymetallic Belt: A summary of 60 years of mining exploration: Rouyn-Noranda, Canadian Institute of Mining and Metallurgy Special Volume 43, p. 221-236.

Sauvé, P., 1987a, Géologie des propriétés de Malartic Hygrade et de Black Cliff, Région de Malartic, Ministère de l'Énergie et des Ressources du Québec, MB 87-50, 50 p.

Sauvé, P., 1987b, Gisement Wesdome ou Western Quebec, Placer Dome Inc., 23 p.

Sauvé, P., 1988, Étude de lames minces et de leur contexte, Propriété Kiena: Projet Kiena Bloc Mine 1707-1 / 921-6100, Placer Dome Inc., 14 p.

Sauvé, P., Imreh, L., and Trudel, P., 1993, Description des gîtes d'or de la région de Val d'Or, Ministère de l'Énergie et des Ressources du Québec, MM 91-03, 178 p.

Sauvé, P., and Makila, A., 1987, Géologie de la mine Camflo, Région de Malartic, Ministère de l'Énergie et des Ressources du Québec, MB 87-40, 64 p.

Sauvé, P., and Makila, A., 1990, Geology of the Camflo mine, Malartic, Québec, *in* Rive, M., Verpaelst, P., Gagnon, Y., Lulin, J.-M., Riverin, G., and Simard, A., eds., The Northwestern Quebec Polymetallic Belt: A summary of 60 years of mining exploration: Rouyn-Noranda, Québec, Canadian Institute of Mining and Metallurgy Special Volume 43, p. 245-254.

Savoie, A., Trudel, P., Sauvé, P., Hoy, L., and Lao, K., 1991, Géologie de la mine Doyon (région de Cadillac), Ministère de l'Énergie et des Ressources du Québec, ET 90-05, 80 p.

Sawkins, F. J., 1990, Metal deposits in relation to plate tectonics: New York, Springer-Verlag, 461 p.

Sharpe, J. I., 1968, Canton de Louvicourt, comté d'Abitibi-est, Ministère des Richesses Naturelles du Québec, RG 135, 59 p.

Sibson, R. H., Robert, F., and Poulsen, K. H., 1988, High-angle reverse faults, fluid-pressure cycling, and mesothermal gold-quartz deposits: Geology, v. 16, p. 551-555.

Sillitoe, R. H., 1989, Gold deposits in Western Pacific island arcs: the magmatic connection: Economic Geology, Monograph, v. 6, p. 274-291.

Sillitoe, R. H., 1993, Gold-rich porphyry copper deposits: geological model and exploration implications, *in* Kirkham, R. V., Sinclair, W. D., Thorpe, R. I., and Duke, J. M., eds., Mineral Deposit Modelling: St. John's, Newfoundland, Geological Association of Canada, Special Paper 40, p. 465-478.

Sillitoe, R. H., and Gappe, I. M. J., 1984, Phillipine porphyry copper deposits: geologic setting and characteristics, United Nations ESCAP, CCOP Technical Publication 14, 89 p.

Sims, P. K., Card, K. D., Morey, G. B., and Peterman, G. E., 1980, The Great Lake Tectonic Zone - A major crustal structure in Central North America: Geological Society of America Bulletin, v. 91, p. 690-698.

Spooner, E. T. C., and Barrie, C. T., 1993, A special issue devoted to Abitibi ore deposits in a modern context - Preface: Economic Geology, v. 88, p. 1307-1322.

Still, A., and Mason, R., 1995, Interim report on hydrothermal alteration and gold mineralization at the Goldex mine, Val d'Or, Quebec, Department of Geological Sciencies, Queen's University, Kingston, Ontario, 64 p.

Stockwell, C. H., 1964, Age determinations and geological studies, Part II Geological studies: Fourth report on structural provinces, orogenies, and time-classification of rocks of the Canadian Precambrian Shield, Geological Association of Canada, Special Paper 64-17, p. 1-21.

Stockwell, C. H., 1982, Proposals for time classification and correlation of Precambrian rocks and events in Canada and adjacent areas of the Canadian Shield, Part I: A time classification of Precambrian rocks and events, Geological Survey of Canada, Paper 80-19, 135 p.

Stott, G. M., and Corfu, F., 1992, Uchi Subprovince, *in* Thurston, P. C., Williams, H. R., Sutcliffe, R. H., and Stott, G. M., eds., Geology of Ontario, Special Volume 4, Geology of Ontario, Ontario Geological Survey, Special Paper 4, Part 1, p. 145-238.

Sutcliffe, R. H., Barrie, C. T., Burrows, D. R., and Beakhouse, G. P., 1993, Plutonism in the southern Abitibi Subprovince: a tectonic and petrogenetic framework: Economic Geology, v. 88, p. 1359-1375.

Talbot, J. C., and Sokoutis, D., 1992, The importance of incompetence: Geology, v. 20, p. 951-953.

Taner, M. F., 1993, Gold abundance and an alumino-silicate-rich alteration zone in the Val d'Or mining district, Abitibi, Quebec: exemples of fossil geothermal fields: Ore Geology Reviews, v. 8, p. 451-475.

Taner, M. F., 1996a, The East Sullivan stock and its gold-copper potential, Val d'Or, Quebec, Canada: Exploration and Mining Geology, v. 5, p. 45-60.

Taner, M. F., 1996b, A pre-2686 Ma intrusion-related gold deposit at the Kiena mine, Val d'Or, Québec, southern Abitibi Subprovince - A discussion: Economic Geology, v. 91, p. 709-801.

Taner, M. F., and Trudel, P., 1989, Bourlamaque batholith and its gold potential, Val d'Or, Quebec: Canadian Mining and Metallurgical Bulletin, v. 82, p. 33-42.

Taner, M. F., and Trudel, P., 1991, Gold distribution in the Val d'Or Formation and a model for the formation of the Lamaque-Sigma Mines, Val d'Or, Quebec: Canadian Journal of Earth Sciences, v. 28, p. 706-720.

Taner, M. F., Trudel, P., and Perrault, G., 1986, Géochimie de la biotite associée à certains gisements d'Or de Val d'Or, Malartic et Chibougamau, Québec: Canadian Mineralogist, v. 24, p. 761-774.

Tessier, A., 1990, Structural evolution and host rock dilation during emplacement of gold quartz vein at the Perron Deposit, Val d'Or, Quebec: Unpub. M.Sc. thesis, Kingston, Ontario, Queen's University, 242 p.

Tessier, A., Trudel, P., and Imreh, L., 1990, Petrology and alteration of the Siscoe stock at the Siscoe gold mine, Val d'Or, Quebec, *in* Rive, M., Verpaelst, P., Gagnon, Y., Lulin, J.-M., Riverin, G., and Simard, A., eds., The Northwestern Quebec Polymetallic Belt: a summary of 60 years of mining exploration: Rouyn-Noranda, Canadian Institute of Mining and Metallurgy Special Volume 43, p. 285-298.

Thurston, P. C., 1990, The Superior Province - Emphasizing greenstone belts, *in* Ho, S. E., Robert, F., and Groves, D. I., eds., Gold and base metal mineralization in the Abitibi Subprovince, with special emphasis on the Quebec segment, Publication No. 24: Perth, Australia, The University of Western Australia, Publication No. 24, p. 1-53.

Thurston, P. C., and Chivers, K. M., 1990, Secular variation in greenstone sequence development emphasizing Superior Province, Canada: Precambrian Research, v. 46, p. 21-58.

Titley, S. R., 1982, The style and progress of mineralization and alteration in porphyry copper systems, *in* Titley, S. R., ed., Advances in geology of the porphyry copper deposits Southwestern North America: Tucson, Arizona, The University of Arizona Press, p. 93-116.

Titley, S. R., 1993, Characteristics of porphyry copper occurrence in the American Southwest, *in* Kirkham, R. V., Sinclair, W. D., Thorpe, R. I., and Duke, J. M., eds., Mineral Deposit Modelling, 40: St. John's, Newfoundland, Geological Association of Canada, Special Paper 40, p. 433-464.

Tourigny, G., Doucet, D., and Bourget, A., 1993, Geology of the Bousquet 2 Mine: an example of a deformed, gold-bearing, polymetalic sulfide deposit: Economic Geology, v. 88, p. 1578-1597.

Tourigny, G., and Hubert, C., 1986, The Bousquet Property, *in* Hubert, C., and Robert, F., eds., Structure and gold Rouyn to Val d'Or, Geological Association of Canada Guidebook Field Trip 14, p. 12-27.

Tourigny, G., Hubert, C., Brown, A., Crépeau, R., Trudel, P., Hoy, L., and Lao, K., 1992, Géologie de la mine Bousquet, Ministère de l'Énergie et des Ressources du Québec, ET 89-09, 92 p.

Trudeau, Y., and Raymond, D., 1992, Geology and structure, Orion Mine (No. 8 Zone), Val d'Or district, Quebec: Exploration and Mining Geology, v. 1, p. 223-230.

Trudel, P., 1985a, Géologie de la mine d'or Shawkey, Val d'Or, Québec, Ministère de l'Énergie et des Ressources du Québec, MB 85-17, 28 p.

Trudel, P., 1985b, Géologie de la mine Siscoe, Val d'Or, Québec, Ministère de l'Énergie et des Ressources du Québec, MB 85-18, 38 p.

Trudel, P., 1985c, Géologie de la mine Sullivan, Val d'Or, Québec, Ministère de l'Énergie et des Ressources du Québec, MB 85-16, 33 p.

Trudel, P., 1990, Géologie régionale du secteur de Cadillac, The Northwestern Quebec Polymetallic Belt: A summary of 60 years of mining exploration - Field guide: Rouyn-Noranda, Canadian Institute of Mining and Metallurgy, p. 64-89.

Trudel, P., and Sauvé, P., 1991, Métallogénie de l'or dans le secteur de Malartic: État de nos connaissances, Ministère de l'Énergie et des Ressources du Québec, MB 89-10, 359 p.

Trudel, P., and Sauvé, P., 1992, Synthèse des caractéristiques géologiques des gisements d'or du district de Malartic, Ministère de l'Énergie et des Ressources du Québec, MM 89-04, 113 p.

Trudel, P., Sauvé, P., Tourigny, G., Hubert, C., and Roy, L., 1992, Synthèse des caractéristiques géologiques des gisements de la région de Cadillac (Abitibi), Ministère de l'Énergie et des Ressources du Québec, MM 91-01, 106 p.

Verpaelst, P., Péloquin, A. S., Adam, E., Barnes, A. E., Ludden, J. N., Dion, D.-J., Hubert, C., Milkereit, B., and Labrie, M., 1995, Seismic reflection profiles across the "Mines Series" in the Noranda camp of the Abitibi belt, eastern Canada: Canadian Journal of Earth Sciences, v. 32, p. 167-176.

Vila, T., and Sillitoe, R. H., 1991, Gold-rich porphyry systems in the Maricunga belt, northern Chile: Economic Geology, v. 86, p. 1238-1260.

Vogel, D. E., 1972, Geology of Villebon Township, Abitibi-East county, and the north part of Freville Township, Pontiac county, Ministère des Richesses Naturelles du Québec, DP-80, 90 p.

Vu, L., 1990, Geology of the Ferderber gold deposit and gold potential of the Bourlamaque batholith, Belmoral Mines Ltd., Val d'Or, Quebec, *in* Rive, M., Verpaelst, P., Gagnon, Y., Lulin, J.-M., Riverin, G., and Simard, A., eds., The Northwestern Quebec Polymetallic Belt: A summary of 60 years of mining and exploration: Rouyn-Noranda, Quebec, The Canadian Institute of Mining and Metallurgy, Special Volume 43, p. 237-244.

White, D., 1981, Active geothermal systems and hydrothermal ore deposits: Economic Geology, 75th Anniversary Volume, p. 392-423.

White, N. C., and Hedenquist, J. W., 1995, Epithermal gold deposits: styles, characteristics and exploration: Society of Economic Geologists Newsletter, October 1995, v. 23, p. 9-13.

White, W. H., Bookstrom, A. A., Kamili, R. J., Ganster, M. W., Smith, R. P., Ranta, D. E., and Steininger, R. C., 1981, Character and origin of Climax-type molybdenum deposits: Economic Geology, 75th Anniversary Volume, p. 270-317.

Wilkinson, L., Cruden, A., and Krogh, T., 1993, Structure and timing of post-Timiskaming ductile deformation along Larder Lake-Cadillac deformation zone in the Kirkland Lake area: Geological Society of America Abstracts with Programs, p. A-236.

Wilson, H. S., 1936, Geology of Lamaque Mine: Canadian Mining Journal, v. 57, p. 511-516.

Wilson, H. S., 1948, Lamaque Mine: Structural Geology of Canadian Ore Deposits, Montreal, 1948, p. 882-891.

Wilson, M. E., 1910, Larder Lake and eastward, Geological Survey of Canada, Report 1909 A, p. 173-180.

Wong, L., Davis, D. W., Krogh, T. E., and Robert, F., 1991, U-Pb zircon and rutile chronology of Archean greenstone formation and gold mineralization in the Val d'Or region, Quebec: Earth Planetary Science Letters, v. 104, p. 325-336.

Wood, P. C., Burrows, D. R., Thomas, A. V., and Spooner, E. T. C., 1986, The Holinger-McIntyre Au-quartz vein system, Timmings, Ontario, Canada: geologic characteristics, fluid properties and light stable isotope geochemistry, *in* Macdonald, A. J., ed., Proceedings of Gold'86: an International Symposium on the Geology of Gold: Toronto, Konsult International, p. 56-80.

Zweng, P. L., 1991, Gold formation in the late Archean of the southern Superior Province; evidence from thermochronology of the Camflo Deposit, Malartic, Quebec: Geological Association of Canada Program with Abstracts, v. 16, p. A138.

Zweng, P. L., 1993, Formation of gold-quartz veins at Camflo, Malartic Quebec, in light of the tectonic and thermal evolution of the southern Abitibi Subprovince: Unpub. Ph.D. thesis, Palo Alto, California, Stanford University, 224 p.

Zweng, P. L., Mortensen, J., and Dalrymple, G., 1993, Thermochronology of the Camflo gold deposit, Malartic, Québec: implications for magmatic underplating and the formation of gold-bearing quartz veins: Economic Geology, v. 88, p. 1700-1721.

Zweng, P. L., and Mortensen, J. K., 1989, U-Pb age constraints on Archean magmatism and gold mineralization at the Camflo mine, Malartic, Quebec: Geological Society of America Abstracs with Programs, p. A351.

APPENDIX A - SUMMARY OF PREVIOUS WORK

Appendix A contains a comparative table listing the main contributions to Kiena geology made by previous workers between 1960 and 1988. The highlight is on the contribution of L.A. Clark (1963) to show the similarity between his findings and the conclusions reached in this study.

Table A.1 Detailed summary of previous work

	POLK, G.K. (1961)	CLARK, L.A. (1963)	MUIR, J.E. (1979-81)	ROY, C. (1983)	BOURGET, A. (1986)	QUIRION, D. (1988)
VOLCANIC ROCKS	Keewatin-type lavas Peridotite Gabbros/coarse flows	Andesite pillow flows Amygdaloidal basalt Andesitic fragmental rock Gabbro/coarse flows Peridotite	Ultramafic komatiite Basaltic komatiite Fe-tholeiite Mg-tholeiiite Fragmental Mg-tholeiite	Ultramafic flows Basalt	Ultramafic flows Mafic flows (Mylonite zone)	Komatiite Basalt (Mylonitic equivalents)
INTRUSIVE ROCKS	"Ore zone andesite" Syenite porphyry Feldspar porphyry	"Green diorite" (feeder dikes) "Grey diorite" (pre-ore dike) Monzonite porphyry (post-ore dike) Syenite porphyry (post-ore dike)	Granodiotite dike Feldspar porphyry dike	Granodiorite dike Feldspar porphyry dike "Diorite" dike	"Quartz diorite" dike Dike of intermediate composition Feldspar porphyry	"Diorite" or microdiorite dike Granodiorite dike Feldspar porphyry
ALTERATION	Albite Quartz Serpentinization of ultramafic rocks	Albite metasomatism over ore zone Quartz-carbonate-pyrite-Au over ore zone Magnetite (mostly in basalt) Muscovite in monzonite and syenite porphyries Suspects K-feldspar in mineralized basalt Serpentinization of peridotite	Pervasive carbonate alteration Albite metasomatism K-metasomatism (biotite-muscovite) Dolomite: komatiite, Mg-tholeiite Ankerite: Fe-tholeiite Carbonate-sericite-chlorite-biotite-pyrite-chalcopyrite alteration of granodiorite dike.	Albite metasomatism (beige coloration of ore breccia fragments) Biotite alteration of chlorite veinlets Carbonate-chlorite-sericite alteration of feldspar porphyry and granodiorite dikes	Quartz-albite-carbonate-pyrite-sericite alteration over the ore zone. Biotite alteration of "S-50" Zone and wallrocks. Upper mine levels: 20 m into footwall 100 m into hangingwall Au alteration: inner halo= 197 ppb outer halo = 27.2 ppb	Carbonate-chlorite-talc alteration of komatiite
VEINING	Quartz-albite-pyrite stringers	Quartz-carbonate veinlets in carbonate-chlorite-talc schists	Quartz-carbonate veinlets Chlorite veinlets	Quartz-albite veins Chlorite veinlets	Quartz veins	Quartz-albite veins Quartz-carbonate tension veins (4 sets)

Table A.1 continued...

MINERALIZED ROCK TYPES	"Ore zone andesite" dike	Andesite Basalt Peridotite "Grey diorite" dike	Na_2O-enriched Fe-tholeiite	"Diorite" dikes Basalt	Ultramafic flows Basalt "Quartz diorite" dike	Microdiorite dike ("B", "J", "K", "L" zones) Basalt ("C" zone)
SULPHIDE MINERALS	Pyrite, Pyrrhotite Chalcopyrite Galena, Sphalerite	Pyrite, Pyrrhotite, Chalcopyrite, Galena (?)	Pyrite-Pyrrhotite-Chalcopyrite-Galena-Pentlandite-Sphalerite-Cobaltite-Arsenopyrite	Cf. Muir (1979-81)	Cf. Muir (1979-81)	Cf. Muir (1979-81)
METAMORPHISM	Greenschist facies: actinolite, epidote, chlorite, albite	Greenschist facies Biotite Zone: actinolite, epidote, chlorite, albite, quartz, (hornblende)		Greenschist facies: actinolite-epidote-albite-quartz	Greenschist facies: actinolite-epidote-chlorite-quartz-albite	Greenschist facies: actionlite-epidote-chlorite-albite-quartz
MAIN STRUCTURES	Large drag fold "Strike shears"	North-trending ore zone dipping 30-40° westward. System of parallel fractures or fault zone: "grey diorite" and monzonite porphyry dikes. West-Northwest-trending deformation zone, steeply -dipping northeast, thought of as Marbenor break (?)	Strong penetrative fabric /schistosity Fault breccia (?)	North-trending ore zone dipping 30° westward. Northeast and Northwest conjugate shear fractures. Fractures and foliation development in granodiorite, feldspar porphyry, and "diorite" dikes.	Mylonite zone over Kiena gold ore coincident with biotite alteration halo. Upper mine levels: 20 m into footwall 130 m into hangingwall Faulted contacts between basalt, ultramafic flows and ore zone. Folding of ore zone, felsic intrusive rocks, and "quartz diorite" dike.	North-trending mylonite zone. C_1 S_1 shear zone fabrics (S_1 moderatly-dipping NNW) C_2 S_2 shear zone fabrics (S_2 steeply-dipping NNW and NE) Sub-horizontal, NE-dipping S_3. Kink-bands in carbonate-chlorite-talc schists. Banding: carbonate-rich and chlorite-rich bands in carbonate-chlorite-talc schists. Faulted contacts between ore zone and enclosing rocks. Ore breccia: jigsaw puzzle type breccia

Table A.1 continued...

DEFORMATION		Penetrative fabric in carbonate-chlorite-talc schist. Intense folding of quartz -carbonate veinlets in carbonate-chlorite-talc schists.		Pervasive fabric moderatly-dipping to the Northwest. Local crenulation fabric steeply dipping to the Northeast.	Cf. Roy (1983)	Boudinage of ore zone breccia. Intense folding of up above mentioned tension veins.
ORE GENESIS	Large concentration of veinlets in fold flexures. Multiple generation of veins.	Seismic pumping in an active thrust fault zone causes episodic brecciation and mineralization	Episodic waves of Au-mineralizing solutions (32 ppb, 32-560 ppb, >560 ppb) in a pyroclastic or fault breccia zone. Epigenetic origin Stratabound setting	1. Regional deformation 2. Albite alteration of mafic rocks 3. Development of conjugate shear fractures 4. Mineralization of fracture sets by gold-bearing fluids. 5. Brecciation of gold ore during development of assymetric drag fold.	1. Spilitization of oceanic basalts 2. Regional metamorphism 3. Deformation initiates mylonitization process 4. Au-pyrite-chalcopyrite-albite-CO_2-K-SiO_2 alteration/ mineralization	1. Regional deformation 2. Seismic pumping in active normal fault zones 3. Hydraulic fracturing and mineralization 4. Development of mylonite and carbonate alteration of ore zone wall rocks 5. Continued folding resulting in the boudinage of "S-50" ore zone Syn-tectonic and epigenetic setting.

Table A.1 continued...

CONCLUSIONS AND RECOMMENDATIONS	Kiena's ore akin to those of Norlartic, Shawkey, and Marban gold mines. Favors zones of intense alteration and deformation in vicinity of drag folds, and spatially associated with granodiorite dikes.	Chances of ore zone/thrust fault repetition at depth. Suspects presence of parent intrusion to felsic dikes at depth. Log drill core magnetically to better ascertain magnetic anomalies. To learn to distinguish between effects of albite and carbonate-quartz alteration, petrographically. Feldspathized rocks may signal the proximity of mineralization. Possible use of carbonate-chlorite-talc schist laced with quartz-carbonate veinlets as a "marker". Suggests genetic link between "grey diorite" monzonite porphyry, syenite porphyry dikes, and albite metasomatism.	S (pyrite), CO_2 (carbonate), and Na_2O (albite) signal the proximity to ore zone. Granodiorite dike akin to Malartic "porphyry". Geochemical similarities between "S-50" Zone and "diorite ores" of Malartic Camp. Favors spatial association with granodiorite dikes (Timmins Camp). Recommends mapping of alteration zones.		Does not confirm stratabound setting of Kiena gold ore due to faulted contacts between enclosing rocks and ore. Jacola Fm background = 3.3 ppb Au Outer ore zone halo = 13-60 ppb Au Inner ore zone halo = 197 ppb Au Gold ore = 5400 ppb Au Jacola Fm background = 2.3 ppm As Outer ore zone anomaly = 7.5 ppm As Has demonstrated the coincidence between biotite alteration, gold alteration halo, and "mylonite" zone.	

APPENDIX B - LIST OF SAMPLES

The following table contains the sample numbers, location and a brief description of the samples used in this thesis. Sample locations appear on the 1:250 scale geological plan maps located in back pockets (i.e. Index Maps) or on the 1:2500 scale schematic plan maps also located in back pocket.

TABLE B-1 Sample Location and Description

Sample No.	Location	Description
K90-41091-026	IM 4138, 'C' ore zone	Weakly mineralized and schistose footwall iron tholeiite - Chl veins with relic Bo and Mt - Fig. 4.20
K90-41091-028a	IM 4138, 'C' ore zone	Deformed and partly recrystallized Cb-Py-Au replacement vein (Breccia 1 ore type) - Bo porphyroblasts - Fig. 5.8
K90-41091-030	IM 4138, 'C' ore zone	Deformed Stwk Cb-Qz-Py(Po)±Ab-Au vein ore type - Chl stringer veins
K90-41091-031	IM 4138, 'C' ore zone	Cb-Chl-Tc-Ser schist - S_n and S_{n+1} - Fig. 3.18 - Post-ore fault zone (1:2500 scale 41 Level Plan Map)
K90-41091-032	IM 4138, 'C' ore zone	Schistose and partly recrystallized Stwk Cb-Qz-Py(Po)±Ab-Au vein ore type - ~30% Chl veins
K90-41092-034	IM4139, ' C' ore zone	Weakly mineralized and schistose footwall iron tholeiite - Chl stringer veins with diss. martite
K90-41092-035	IM 4139, 'C' ore zone	Schistose Stwk Cb-Qz-Py(Po)±Ab-Au vein ore type - ~ 15% Chl veins, traces of Bo and diss. Martite
K90-41092-036	IM 4139, 'C' ore zone	Highly stained and partly recrystallized Stwk Cb-Qz-Py(Po)±Ab-Au vein ore type - 10 % Chl stringer veins
K90-41092-037	IM 4139, 'C' ore zone	Highly stained and partly recrystallized Stwk Cb-Qz-Py(Po)±Ab-Au vein ore type - 10 % Chl-Bo stringer veins (± martites)
K90-41092-038	IM 4139, 'C' ore zone	Ab-Ser-Cb-Chl-Bo-altered and schistose intermineral granodiorite dike, Fig. 3.31C - Resorbed Qz phenocrysts, Fig. 3.33 B - Whole-rock geochemistry
K90-41092-040	IM 4139, 'C' ore zone	Chl-Cb-Ser schist zone around intermineral granodiorite dike - Deformed Cb-Qz stwk vein, relic crustiform texture, Fig. 3.15 and 5.4 - Deformed Chl stringers, Fig. 3.16
K90-4105-042	AD 4105	Ab-altered footwall iron tholeiite - Minor Cb-Qz stwk veining - Partly recrystallized - Fig. 3.5
K90-4116-047	IM 4116, 'B' ore zone	Albite-cemented breccia - coarse, recrystallized Py and scheelite
K90-4116-049	IM 4116, 'B' ore zone	Schistose Cb-Py-Au replacement vein (Breccia 1 ore type)
K90-4116-050	IM 4116, 'B' ore zone	Mixed ore - Cb-Py-Au replacement veins cut by albite breccia vein, relic cockade texture, Fig 4.14A and B
K90-4116-052	IM 4116, 'B' ore zone	Weakly mineralized and schistose footwall iron tholeiite - Cb-Qz±Py stwk veins - 25 % Chl-Bo-Mt (martite) stringer veins - Poeciloblastic Bo
K90-4317-053	IM 4317, 'B' ore zone	Weakly mineralized and schistose footwall iron tholeiite - 25 % Chl stringer veins with tr. Bo, 1% Martite - Deformed and partly recrystallized Py

K90-4317-056	IM 4317, 'B' ore zone	Stwk Cb-Qz-Py(Po)±Ab-Au vein ore type, Chl-Bo-Mt(martite) stringer veins
K90-4317-057	IM 4317, 'B' ore zone	Stwk Cb-Qz-Py(Po)±Ab-Au vein ore type, Chl-Bo-Mt(martite) stringer veins
K90-4317-058	IM 4317, 'B' ore zone	Stwk Cb-Qz-Py(Po)±Ab-Au vein ore type, ~ 25 % Cb-Qz-Py stwk veins, coarse recrystallized Py
K90-4313-060	IM 4313, 'B' ore zone	Ab-Cb-Ser-Chl-Bo-altered and schistose intermineral granodiorite dike - Whole-rock geochemistry
K90-4313-061	IM 4313, 'B' ore zone	Stwk Cb-Qz-Py(Po)±Ab-Au vein ore type, Chl-Bo-Mt (martite) stringer veins
K90-4313-062	IM 4313, 'B' ore zone	Stwk Cb-Qz-Py(Po)±Ab-Au vein ore type - Weakly foliated - Deformed Cb-Qz stwk veins, Fig. 3.13 - Pervasively Ab-altered groundmass, Fig.3.14
K90-4110-067	IM 4110, 'B' ore zone	Schistose and weakly mineralized footwall iron tholeiite - Cb veins, ~30 % Chl-Mt stringer veins, deformed and recrystallized Py
K90-4110-071	IM 4110, 'B' ore zone	Deformed albitite dike - Whole-rock geochemistry
K90-4110-073	IM 4110, 'B' ore zone	Stwk Cb-Qz-Py(Po)±Ab-Au vein ore type - ~20% Cb-Qz-Py stwk veins, 3-5% Chl veins, coarse recrystallized Py
K90-3627-074	IM 3627, 'J' ore zone	Idem K90-3627-074
K90-3627-076	IM 3627, 'J' ore zone	Moderately deformed mineralized albitite dike (Stwk Cb-Qz-Py(Po)±Ab-Au vein ore type), relic open-space infill-vein textures, Deformed and recrystallized Py, Fig. 5.17 - Whole-rock geochemistry
K90-3627-077	IM 3627, 'J' ore zone	Strongly schistose Cb-Py and Chl-Bo-altered intermineral granodiorite dike - Gneissic - Fig. 3.31 B - Whole-rock geochemistry
K91-3838-079	IM 3838, 'C' ore zone	Stwk Cb-Qz-Py(Po)±Ab-Au vein ore type, Fig. 4.1 and 4.2 - Partly recrystallized hydrothermal Ab, Fig. 4.3
K91-3838-080	IM 3838, 'C' ore zone	Schistose intermineral feldspar porphyry dike, Fig. 4.1
K91-3838-081	IM 3838, 'C' ore zone	Qz-Cb-Bo±Ab-Tm-Py-Cpy-Au pegmatite vein, rosettes of coarse-grained biotite, $^{40}Ar/^{39}Ar$ age dating, Fig. 6.3
K91-3838-094	IM 3838, 'C' ore zone	Schistose replacement vein (Breccia 1 ore), Fig. 4.9 and 5.2 - Deformed and partly recrystallized Py, Fig. 4.11
K91-3838-095	IM 3838, 'C' ore zone	Schistose Stwk Cb-Qz-Py(Po)±Ab-Au vein ore type, Fig. 4.7
K91-3838-098	IM 3838, 'C' ore zone	Highly strained Stwk Cb-Qz-Py(Po)±Ab-Au vein ore type, boudinaged Cb-Qz stwk veins, relic crustiform texture, deformed and recrystallized Py, Fig. 5.3 - Deformed Py with carbonate-filled strained shadows, Fig. 5.5 and 5.6
K91-4105-100	AC 4105, footwall	Schistose basaltic flow top breccia - Relic glomero-porphyritic texture - Calcite, Chl and Ser veinlets - Fig. 3.3
K91-4105-101	IM 4105, footwall	Idem K91-4105-100 - Duplicate for whole-rock geochemistry
K91-3025-105	IM 3025, 'D' ore zone	Intermineral granodiorite dike - zircon age dating, Fig. 3.27 and Fig. 6.1
K91-3025-106	IM 3025, 'D' ore zone	Ab-, Cb-, Ser-,Chl-Bo-altered intermineral granodiorite dike, Fig. 3.27, 3.31A and 3.33 A
K91-3025-112	IM 3025, 'D' ore zone	Cb-Chl-Tc- (Ab) schist with boudinage inclusions of albitite dike - Strain partitioning, S_n, S_{n+1}, Fig. 3.20
K91-3025-113	IM 3025, ' D' ore zone	Stwk Cb-Qz-Py(Po)±Ab-Au vein ore type: 30-35% stwk veins, presence of Chl-Bo-Mt stringer veins, strongly schistose

K91-3025-114	IM 3025, 'D' ore zone	Highly strained albitite dike - Chl veins - Whole-rock geochemistry
K91-3810-116	IM 3810, 'B' ore zone	Schistose intermineral feldspar porphyry dike - Whole-rock geochemistry
K91-3810-118	IM 3810, 'B' ore zone	Albitite dike - Fine-grained granoblastic, weakly foliated - Cb-Qz-Py stringer veins - Chl-Bo-Mt stringer veins - Whole-rock geochemistry
K91-3810-119	IM 3810, 'B' ore zone	Stwk Cb-Qz-Py(Po)±Ab-Au vein ore type
K91-3810-120	IM 3810, 'B' ore zone	Schistose and weakly mineralized footwall iron tholeiite, Fig. 3.6 - Deformed Cb-Qz-Ab-Py stwk veins, Chl-Mt veins
K91-3838-136	IM 3838, 'C' ore zone	Schistose intermineral feldspar porphyry dike, Fig. 4.1
K91-3838-140	IM 3838, 'C' ore zone	Deformed Qz-Cb-Bo±Ab-Tm-Py-Cpy-Au pegmatitic vein, Fig. 4.8 and 4.18
K91-4313-149	IM 4313, 'B' ore zone	Ab-cemented breccia (Breccia 2 ore), Fig. 4.15 - Deformed and recrystallized hydrothermal Ab and Py, Fig. 4.16
K91-4117-159	IM 4117, 'B' ore zone	Schistose Stwk Cb-Qz-Py(Po)±Ab-Au vein ore type, Stilpnomelane replacing Cb and Chl, Fig. 4.21A and B
K91-4117-160	IM 4117, 'B' ore zone	Ab-cemented breccia - Breccia 2 ore type - Partly mottled mosaic breccia, coarsely recrystallized Py, Fig. 3.23
K91-4117-163	IM 4117, 'B' ore zone	Schistose and weakly mineralized footwall iron tholeiite - 30-35% Chl-(Bo)-Mt stringer veins - Moderate strain: recrystallized Bo and Py
K91-4117-164	IM 4117, 'B' ore zone	Schistose and weakly mineralized footwall iron tholeiite -20 Cb-Qz-Ab-Py stwk veins - Recrystallized Py, Bo - 3-5% Mt
K91-3828-168	IM 3828, 'K' ore zone	Boudinaged albitite dike - Recrystallized Ab assemblage, Fig. 3.25A - Micrographic Ab-Qz intergrowths, Fig. 3.25C - Fluid inclusion-rich Ab grains, Fig 3.25D - Whole-rock geochemistry
K91-3838-170	IM 3838, 'C' ore zone	Stwk Cb-Qz-Py(Po)±Ab-Au vein ore type cut by Chl-Bo-Mt stringer veins and overprinted by S_n
K91-4105-173	IM 4105, footwall	Schistose footwall magnesian tholeiite, Cb stwk veins, Chl stringer veins - Whole-rock geochemistry
K91-3829-182	IM 3829, 'L' ore zone	Highly strained Stwk Cb-Qz-Py(Po)±Ab-Au vein ore type - 20-25% Chl-Bo-Mt stringer veins
K91-3829-183	IM 3829, 'L' ore zone	Deformed, weakly mineralized albitite dike - Whole-rock geochemistry
K91-3829-185	IM 3829, 'L' ore zone	Stwk Cb-Qz-Py(Po)±Ab-Au vein ore type cut by Chl-Bo-Mt stringer veins and overprinted by S_n
K91-4613-191	IM 4613, 'B' ore zone	Schistose Stwk Cb-Qz-Py(Po)±Ab-Au vein ore type - 20% Cb-Qz-Ab-Po stwk veins - 10% Chl-(Bo)-Mt(martite) veins
K92-4613-193	IM 4613, 'B' ore zone	Cb-Chl-Tc-Ab schist - Deformed Cb-Qz±Py stwk veins, Fig. 3.9 - Stylolitic dissolution cleavage, Fig. 3.10
K91-4613-194	IM 4613, 'B' ore zone	Schistose and weakly mineralized footwall iron tholeiite - 15-20% Chl-(Bo)-Mt stringer veins
K92-2752-200	IM 2752, 'A' ore zone	Boudinaged, weakly mineralized albitite dike, Fig. 3.22 - Assemblage of plumose to dendritic albite (cleavelandite), Fig. 3.25B - Whole-rock geochemistry
K92-2752-201	IM 2752, 'A' ore zone	Cb-Chl-Tc-Ab schist - Fig 3.19
K92-2752-207	IM 2752, 'A' ore zone	Weakly mineralized intermineral feldspar porphyry dike, Fig 3.32 A

K92-6446-213	IM 6446, 'C' ore zone	Albite-altered basaltic komatiite - Hydrothermal hornblende (?) - Fig. 3.12
K92-6446-214	IM 6446, 'C' ore zone	Highly strained Stwk Cb-Qz-Py(Po)±Ab-Au vein ore type - Mostly Po, lesser Py, large Chl veins, Fig. 3.24
K92-6446-218	IM 6446, 'C' ore zone	Highly strained Stwk Cb-Qz-Py(Po)±Ab-Au vein ore type (albitite dike), Chl veins, Fig. 4.4 - Relic breccia-infill texture, deformed Py, Po, Fig. 4.5 - Deformed Po, Fig. 5.7
K92-6446-220	IM 6446, 'C' ore zone	Highly strained Stwk Cb-Qz-Py(Po)±Ab-Au vein ore type, boudinaged Cb-Qz stwk breccia veins, Chl veins, Deformed Po, Fig. 5.18
K92-6446-222	IM 6446, 'C' ore zone	Highly schistose intermineral granodiorite dik, Cb-Qz-Py stwk veins, Chl-Bo-altered, Fig. 3.31 D
K92-6446-224	IM 6446, 'C' ore zone	Fragment of highly strained, weakly mineralized albitite dike in Cb-Chl-Tc-Ab schist - Whole-rock geochemistry
K92-6402-230	IM 6446, footwall	Ab-altered feldspar porphyry dike, Fig. 3.32 D and 3.33C - Whole-rock geochemistry
K92-6446-234	IM 6446, 'C' ore zone	Intermineral feldspar porphyry dike - Zircon age dating - Fig. 6.1
K92-2752-235	IM 2752, 'A' ore zone	Albite-cemented breccia (Breccia 2 ore type, relic Chl stringer vein network, Fig. 4.19 A - Recrystallized Py, Fig. 4.19B
K92-3025-236	IM 3025, 'D' ore zone	Idem K91-3025-105 and K91-3025-106
K92-3002-237	AD Stope 3025	Footwall iron tholeiite - Whole-rock geochemistry
K92-3025-238	IM 3025, 'D' ore zone	Mixed ores at 100 m - Whole-rock geochemistry
K92-3025-239	IM 3025, 'D' ore zone	Idem K91-3025-113 - Duplicate for whole-rock geochemistry
K92-3025-240	IM 3025, 'D' ore zone	Weakly mineralized intermineral granodiorite dike, Fig. 3.27 - Idem K91-3025-106 (Fig. 3.31A) - Duplicate for whole-rock geochemistry
K92-6446-242	IM 6446, 'C' ore zone	Idem K92-6446-226 - Duplicate for whole-rock geochemistry
K92-6446-243	IM 6446, 'C' ore zone	Idem K92-6446-214 - Duplicate for whole-rock geochemistry
K92-6446-244	IM 6446, 'C' ore zone	Idem K92-6446-229 - Duplicate for whole-rock geochemistry
K92-6401-245	1:2500 scale LPM 64	Footwall iron tholeiite - Whole-rock geochemistry
K92-6467-246	Ramp Level 64 to 67	Footwall basaltic komatiite? - Relic spinifex texture - Actinolite - Fig. 3.11 - Whole-rock geochemistry
K92-3033-247	Ramp 30-33	Footwall basaltic komatiite (Cb-Tc-Chl±Qz-Ab schist) - Relic spinifex texture - Fig. 3.8
K92-3629-248	S 3629, 'L' ore zone	Idem K91-3829-185 - duplicate fro whole-rock geochemistry
K92-3838-249	IM 3838, 'C' ore zone	Idem K91-3838-080 - Duplicate for whole-rock geochemistry
K92-3838-250	IM 3838, 'C' ore zone	Idem K91-3838-079 - Duplicate for whole-rock geochemistry
K92-3838-251	IM 3838, 'C' ore zone	Idem K91-3838-094 - Duplicate for whole-rock geochemistry
K92-3841-252	Ramp level 38 to 41	Footwall iron tholeiite - Whole-rock geochemistry
K92-4313-253	IM 4313, 'B' ore zone	Idem K91-4313-149 - Duplicate for whole-rock geochemistry
K92-4346-254	Ramp level 43 to 46	Footwall iron tholeiite - Whole-rock geochemistry
K92-8202-261	DDH 82-02, 583'	Snowshoe granodiorite - Zircon age dating - Fig. 6.1
K93-5804-264	S 5804, 'B' ore zone	Schistose intermineral feldspar porphyry dike, Chl-Bo stringer veins, Fig. 3.28 and 3.32C
K93-3829-267	IM 3829, 'L' ore zone	Deformed albitite dike - Whole-rock geochemistry
K93-3813-268	S 3813, 'B' ore zone	Highly strained and weakly mineralized feldspar porphyry dike, S_n and S_{n+1}, Fig 3.32B - Ser-Chl-Bo stringer veins, Fig. 3.33D
K93-5804-269	S 5804, 'B' ore zone	Idem K93-5804-264 - Duplicate for whole-rock geochemistry
K93-5808-270	S 5808, 'B' ore zone	Highly strained intermineral granodiorite dike cutting lower ' B' ore zone - Whole-rock geochemistry

K94-5904-274	S 5904, 'C' ore zone	Mineralized albitite dike - Whole-rock geochemistry
S93-3816-275	S 38-16 west B, Sigma	Center of Sigma deposit pyritic, tourmaline-cemented breccia, folded tm veins, deformed and recrystallized Py - Fig. 8. 23
S93-3816-276	S 38-16 west B, Sigma	Biotite-altered "C' porphyry - Cb veinlets - Near contact with main-stage tourmaline-cemented breccia - Fig. 825

Abbreviations: **Ab**= Albite; **AD**= Access Drift; **Au**=gold; **Bo**= Biotite; **Cb**=Carbonate; **Chl**=chlorite; **Cpy**= Chalcopyrite; **DDH**= Diamond drill hole; **diss.**= disseminated; **IM**=Index Maps; **LPM**= Level Plan Map; **Mt**= Magnetite; **Py**= Pyrite; **Po**= Pyrrhotite; **Qz**= Quartz; **S**= Stope; S_m= deposit's main schistosity; S_{m+1}= crenulation cleavage; **Ser**= Sericite; **Stwk**= Stockwork; **Tc**=Talc; **Tm**=tourmaline

APPENDIX C - WHOLE-ROCK GEOCHEMISTRY

Appendix C contains tables of major, minor and trace element analyses of volcanic rocks, albitite dikes, intermineral dikes, and the three ore types encountered at Kiena during this study. Chemical analyses were performed by Abilab Inc. and Lakefield Laboratories.

TABLE C.1 Major and minor element analyses (wt %) of the basaltic pillow flow breccia, east of the S-50 Zone

	K91-4105-101	*K91-4105-173*
SiO_2	45.2	45.4
Al_2O_3	19.1	18.7
Fe_2O_3	9.24	8.27
FeO	7.08	7.01
MgO	8.27	8.50
CaO	6.61	7.36
Na_2O	3.74	3.20
K_2O	0.02	0.27
TiO_2	0.36	0.33
P_2O_5	0.02	0.02
MnO	0.17	0.17
Cr_2O_3	0.01	0.01
LOI	7.26	7.63
$\sum$	107.08	106.87
Mineral assemblage	Ab-Cc-Qz-Chl < Mv, Py	Ab-Qz-Cc-Chl < Mv, Py

* *Chemical analyses by Abilab Inc.; See Appendix B for sample description and Index geological maps in the back pocket for sample location.*

Key:Ab=albite; Cc=calcite; Chl=chlorite; Mv=muscovite; Py=pyrite; Qz=quartz.

K91-4105-101 = year, stope, sample number

TABLE C.2 Trace element analyses of the basaltic pillow flow breccia, east of the S-50 Zone

	K91-4105-101	*K92-4105-173*
Au (ppb)	30	10
S (%)	0.23	0.17
As (ppm)	N.d.	N.d.
Cu (ppm)	119	89
Mo (ppm)	N.d.	N.d.
Ag (g/t)	N.d.	N.d.
Sb (ppm)	N.d.	N.d.
Bi (ppm)	N.d.	N.d.
Hg (ppb)	13	N.d.
Te (g/t)	N.d.	N.d.
Ni (ppm)	94	91
W (ppm)	N.d.	N.d.
Zn (ppm)	71	68
Mineral assemblage	Ab-Cc-Qz-Chl < Mv, Py	Ab-Qz-Cc-Chl < Mv, Py

* *Chemical analyses by Abilab Inc.; See Appendix B for sample description and Index geological plan maps in the back pocket for sample location.*

Key: Ab=albite; Cc=calcite; Chl=chlorite; Mv=muscovite; N.d.=non detected; Py pyrite; Qz=quartz
K91-4105-101 = year, stope, sample number

TABLE C.3 Major and minor element analyses (wt %) of least-altered facies of wall-rock iron tholeiite, east of the S-50 Zone

	K92-3002-237	K92-3033-247	K92-3841-252	K92-4346-254	K92-6401-245	K92-6467-246
SiO_2	46.4	43.9	48.1	47.3	49.5	47.1
Al_2O_3	12.8	11.6	12.0	12.5	13.6	12.8
Fe_2O_3	13.5	12.5	13.4	14.7	15.1	17.8
FeO	8.69	5.97	5.30	7.68	3.15	4.67
MgO	5.48	7.91	4.30	4.84	5.29	6.98
CaO	7.07	6.63	8.73	6.49	8.67	7.40
Na_2O	2.58	1.49	2.49	3.32	2.06	2.11
K_2O	0.68	0.94	0.04	0.24	0.10	0.09
TiO_2	0.86	0.80	0.78	0.84	0.80	0.87
P_2O_5	0.08	0.08	0.08	0.11	0.07	0.07
MnO	0.22	0.22	0.23	0.20	0.25	0.31
Cr_2O_3	0.02	0.02	N.d.	0.01	0.01	0.08
LOI	8.41	11.7	8.06	6.86	2.61	2.48
$\sum$	106.79	103.76	103.51	105.09	101.21	102.76
Mineral assemblage	Chl-Ab-Qz-Cb < Bo-Il-Mt	Chl-Cb-Ab-Qz < Tc-Il-Mt-Py	Chl-Ab-Qz-Cb < Ep-Mt	Chl-Ab-Qz < Cb-Mt-Py	Ab-Act-Qz < Ep-Cb-Il-Mt	Act < < Chl-Ep-Qz-Cb
Metamorphic facies	Greenschist	Greenschist	Greenschist	Greenschist	Upper Greenschist	Upper Greenschist

* *Chemical analyses by Abilab Inc.; See Appendix B for sample description and Index geological maps in the back pocket for sample location.*
Key:Ab=albite; Act=actinolite; Bo=biotite; Cb=carbonate; Chl=chlorite; Ep=epidote; Il=ilmemite; Mt=magnetite; Py=pyrite; Qz=quartz; Tc=talc
K92-3002-237 = year, stope, sample number

TABLE C.4 Trace element analyses of least-altered facies of wall-rock iron tholeiite, east of the S-50 Zone

	K92-3002-237	*K92-3033-247*	*K92-3841-252*	*K92-4346-254*	*K92-6401-245*	*K92-6467-246*
Au (ppb)	50.0	120	40.0	1490	50.0	20.0
S (%)	0.13	0.51	0.23	0.71	0.03	0.31
As (ppm)	N.d.	N.d.	N.d.	N.d.	N.d.	N.d.
Cu (ppm)	118	304	140	106	245	184
Mo (ppm)	N.d.	N.d.	N.d.	N.d.	N.d.	N.d.
Ag (g/t)	N.d.	1	N.d.	N.d.	N.d.	N.d.
Sb (ppm)	N.d.	N.d.	N.d.	N.d.	N.d.	N.d.
Bi (ppm)	N.d.	N.d.	N.d.	N.d.	N.d.	N.d.
Hg (ppb)	28	154	N.d.	13	13	150
Te (g/t)	2	1	4	2	2	1
Ni (ppm)	16	147	63	54	92	312
W (ppm)	N.d.	6	16	N.d.	N.d.	N.d.
Zn (ppm)	88	21	21	65	90	124
Mineral assemblage	Chl-Ab-Qz-Cb < Bo-Il-Mt	Chl-Cb-Ab-Qz < Tc-Il-Mt-Py	Chl-Ab-Qz-Cb < Ep-Mt	Chl-Ab-Cb-Qz < Cb-Mt-Py	Ab-Act-Qz < Ep-Cb-Il-Mt	Act < < Chl-Ep-Qz -Cb
Metamorphic facies	Greenschist	Greenschist	Greenschist	Greenschist	Upper Greenschist	Upper Greenschist

* *Chemical analyses by Lakefield Laboratories; See Appendix B for sample description and Index geological maps in the back pocket for sample location.*
Key: Ab=albite; Act=actinolite; Bo=biotite; Cb=carbonate; Chl=chlorite; Ep=epidote; Il=ilmenite; Mt=magnetite; Py=pyrite; Qz=quartz; Tc=talc
K92-3002-237 = year, stope, sample number

TABLE C.5 Major and minor element analyses (wt %) of albitite dikes

	K90-4110-071	*K90-3627-076*	*K91-3025-114*	*K91-3810-118*	*K91-3828-168*
SiO_2	48.2	53.1	47.7	51.4	53.0
Al_2O_3	16.9	12.9	16.0	16.7	16.9
Fe_2O_3	2.66	13.90	8.50	7.83	7.14
FeO	6.91	9.46	6.98	5.71	5.67
MgO	4.68	4.66	9.14	4.13	3.57
CaO	4.96	0.76	5.45	4.14	4.67
Na_2O	6.87	5.00	4.24	7.66	7.71
K_2O	0.38	0.12	0.30	0.16	0.20
TiO_2	0.99	0.79	0.33	0.22	0.73
P_2O_5	0.38	0.01	<0.01	0.38	0.35
MnO	0.13	0.14	0.01	0.13	0.11
Cr_2O_3	<0.01	<0.01	0.02	<0.01	<0.01
LOI	7.37	4.91	8.15	4.63	5.13
$\sum$	100.44	105.76	106.82	103.09	105.18
Mineral assemblage	Ab-Cb-Chl-Qz < Py, Mt	Ab-Cb-Chl-Qz < Py, Mt << Bo	Ab-Cb-Chl-Qz < Bo << Mt	Ab < Chl-Cb-Qz-Py << Mt	Ab < Chl-Cb-Qz-Py-Mt << Bo

* *Chemical analyses by Abilab Inc.; See Appendix B for samples description and Index geological maps in the back pocket for sample location.*
Key: Ab=albite; Bo=biotite; Cb=carbonate; Chl=chlorite; Mt=magnetite; N.d.=non detected; Py=pyrite; Qz=quartz
K90-4110-071 = year, stope, sample number

TABLE C.5 continued...

	K91-3829-183	*K91-2752-200*	*K93-6446-224*	*K93-3629-267*	*K94-5904-274*
SiO_2	50.00	53.50	48.30	56.40	45.60
Al_2O_3	16.90	16.50	12.80	17.40	12.30
Fe_2O_3	8.28	7.98	12.10	7.53	13.20
FeO	7.07	6.37	7.99	5.72	10.60
MgO	3.71	4.32	7.44	6.43	4.97
CaO	6.18	3.18	5.12	0.92	6.94
Na_2O	7.21	7.25	4.93	6.33	5.34
K_2O	0.09	1.46	0.02	0.08	0.01
TiO_2	0.87	0.94	1.05	0.86	0.67
P_2O_5	0.39	0.31	0.101	0.41	0.10
MnO	0.13	0.10	0.17	0.04	0.25
Cr_2O_3	<0.01	<0.01	0.04	<0.01	0.01
LOI	6.24	4.43	7.76	3.59	9.19
$\sum$	107.07	106.34	107.82	105.71	109.17
Mineral assemblage	Ab-Chl < Cb, Mt << Py, Bo	Ab-Bo-Chl-Qz < Mt << Cb, Py	Ab-Cb-Mt-Qt << Py	Ab-Cb-Chl-Mt < Py << Bo	Ab-Cb-Chl-Mt < Py, Po << Bo

* *Chemical analyses by Abilab Inc.; See Appendix B for sample description and Index geological maps in the back pocket for sample location.*
Key: Ab=albite; Bo=biotite= Cb=carbonate; Chl=chlorite; Mt=magnetite; N.d.=non detected; Po=phyrrotite; Py=pyrite; Qz=quartz
K91-3829-183 = year, stope, sample number

TABLE C.6 Trace element analyses of albitite dikes

	K90-4110-071	*K90-3627-076*	*K90-3025-114*	*K92-3810-118*	*K91-3828-168*
Au (ppb)	160	8900	47	740	63
S (%)	0.42	2.94	0.06	1.48	0.47
As (ppm)	N.d.	N.d.	N.d.	N.d.	N.d.
Cu (ppm)	52	213	98	55	37
Mo (ppm)	N.d.	N.d.	N.d.	N.d.	N.d.
Ag (g/t)	N.d.	N.d.	N.d.	N.d.	N.d.
Sb (ppm)	N.d.	N.d.	N.d.	N.d.	N.d.
Bi (ppm)	N.d.	9	5	N.d.	N.d.
Hg (ppb)	N.d.	N.d.	N.d.	N.d.	N.d.
Te (g/t)	N.d.	N.d.	N.d.	N.d.	N.d.
Ni (ppm)	28	56	113	19	42
W (ppm)	N.d.	N.d.	N.d.	n	N.d.
Zn (ppm)	83	75	65	56	57
Mineral assemblage	Ab-Cb-Chl-Qz < Py, Mt	Ab-Cb-Chl-Qz < Py, Mt << Bo	Ab-Cb-Chl-Qz < Bo << Mt	Ab < Chl-Cb-Qz-Py << Mt	Ab < Chl-Cb-Qz-Py-Mt << Bo

* *Chemical analyses by Lakefield Laboratories; See Appendix B for sample description and Index geological maps in the back pocket for sample location.*
Key: Ab=albite; Bo=biotite; Cb=carbonate; Chl=chlorite; Mt=magnetite; N.d.=non detected; Py=pyrite; Qz=quartz
K90-4110-071 = year, stope, sample number

TABLE C.6 continued...

	K91-3829-183	*K91-2752-200*	*K93-6446-224*	*K93-3629-267*	*K94-5904-274*
Au (ppb)	1140	17	160	77	3410
S (%)	0.20	0.27	0.49	0.54	1.08
As (ppm)	N.d.	N.d.	N.d.	N.d.	13
Cu (ppm)	60	50	206	21	109
Mo (ppm)	N.d.	N.d.	N.d.	N.d.	N.d.
Ag (g/t)	N.d.	N.d.	N.d.	N.d.	N.d.
Sb (ppm)	N.d.	N.d.	N.d.	N.d.	N.d.
Bi (ppm)	N.d.	N.d.	N.d.	N.d.	N.d.
Hg (ppb)	N.d.	N.d.	N.d.	N.d.	N.d.
Te (g/t)	N.d.	N.d.	N.d.	N.d.	N.d.
Ni (ppm)	22	45	104	26	68
W (ppm)	N.d.	N.d.	N.d.	N.d.	N.d.
Zn (ppm)	96	90	66	76	77
Mineral assemblage	Ab-Chl < Cb, Mt << Py, Bo	Ab-Bo-Chl-Qz < Mt << Cb, Py	Ab-Cb-Mt-Qz << Py	Ab-Cb-Chl-Mt < Py << Bo	

* *Chemical analyses by Lakefield Laboratories; See Appendix B for sample description and Index geological maps in the back pocket for sample location.*
Key: Ab=albite; Bo=biotite; Cb=carbonate; Chl=chlorite; Mt=magnetite; N.d.=non detected; Py=pyrite; Qz=quartz
K91-3829-183 = year, stope, sample number

TABLE C.7 Major and minor element analyses (wt %) of intermineral granodiorite dike

	K90-41092-038	*K90-4313-060*	*K90-3627-077*	*K92-3025-240*	*K92-6446-242*	*K92-5808-270*
SiO_2	64.9	61.5	65.6	54.6	64.0	65.5
Al_2O_3	16.2	17.3	17.3	16.4	16.2	16.1
Fe_2O_3	3.53	4.82	4.37	4.56	3.88	4.06
FeO	2.58	4.11	3.53	1.19	2.54	3.34
MgO	1.29	1.66	1.76	3.00	1.22	1.30
CaO	3.44	2.66	0.97	5.10	2.39	3.33
Na_2O	3.70	7.01	5.55	4.74	8.13	4.44
K_2O	2.98	0.99	1.91	2.53	0.36	2.35
TiO_2	0.30	0.44	0.43	0.35	0.33	0.32
P_2O_5	0.09	0.13	0.13	0.16	0.10	0.09
MnO	0.04	0.06	0.03	0.09	0.04	0.06
Cr_2O_3	<0.01	<0.01	<0.01	0.01	0.01	<0.01
LOI	3.78	3.01	1.98	5.60	4.37	2.98
$\sum$	102.83	103.69	103.56	98.33	103.57	103.87
Mineral assemblage	Qz-Ab-Ser-Chl < Bo, Cb, Mt	Qz-Ab-Ser < Chl, Cb, Bo, Mt	Qz-Ab-Ser-Mt < Chl << Cb	Qz-Ab-Ser-Cb < Chl-Mt << Py	Qz-Ab < Chl-Bo-Cb-Mt	Qz-Ab-Ser-Bo < Chl, Mt, Cb

* *Chemical analyses by Abilab Inc.; See Appendix B for sample description and Index geological maps in the back pocket for sample location.*

Key: Ab=albite; Bo=biotite; Cb=carbonate; Chl=chlorite; Mt=magnetite; N.d.=non detected; Py=pyrite; Qz=quartz; Ser=sericite

K90-41092-038 = year, stope, sample number

TABLE C.8 Trace element analyses of intermineral granodiorite dike

	K90-41092-038	*K90-4313-060*	*K90-3627-077*	*K92-3025-240*	*K92-6446-242*	*K93-5808-270*
Au (ppb)	10	100	67	630	70	5
S (%)	0.11	0.35	0.07	0.53	0.04	0.03
As (ppm)	N.d.	N.d.	N.d.	N.d.	N.d.	N.d.
Cu (ppm)	31	80	54	38	57	36
Mo (ppm)	N.d.	N.d.	N.d.	N.d.	N.d.	N.d.
Ag (g/t)	N.d.	N.d.	N.d.	N.d.	N.d.	N.d.
Sb (ppm)	N.d.	N.d.	N.d.	N.d.	N.d.	N.d.
Bi (ppm)	N.d.	N.d.	N.d.	N.d.	N.d.	N.d.
Hg (ppb)	N.d.	N.d.	N.d.	10	120	N.d.
Te (g/t)	N.d.	N.d.	N.d.	N.d.	N.d.	N.d.
Ni (ppm)	13	17	15	50	25	17
W (ppm)	N.d.	N.d.	N.d.	N.d.	N.d.	N.d.
Zn (ppm)	47	56	77	36	41	51
Mineral assemblage	Qz-Ab-Ser-Chl < Bo, Cb, Mt	Qz-Ab-Ser < Chl, Cb, Bo, Mt	Qz-Ab-Ser-Mt < Chl << Cb	Qz-Ab-Ser-Cb < Chl, Mt << Py	Qz-Ab < Chl, Bo, Cb, Mt	Qz-Ab-Ser-Bo < Chl, Mt, Cb

* *Chemical analyses by Lakefield Laboratories; See Appendix B for sample description and Index geological maps in the back pocket for sample location.*
Key: Ab=albite; Bo=biotite; Cb=carbonate; Chl=chlorite; Mt=magnetite; N.d.=non detected; Py=pyrite; Qz=quartz; Ser=sericite
K90-41092-038 = year, stope, sample number

TABLE C.9 Major and minor element analyses (wt %) of the intermineral feldspar porphyry dike

	K91-3810-116	*K92-6402-230*	*K92-3838-249*	*K93-5804-269*
SiO_2	58.0	64.1	56.8	58.8
Al_2O_3	16.5	17.2	15.3	15.7
Fe_2O_3	5.00	5.43	5.93	5.29
FeO	3.53	4.60	2.83	4.08
MgO	2.93	1.69	3.12	2.96
CaO	5.33	3.56	4.55	5.29
Na_2O	5.86	6.86	5.87	5.84
K_2O	1.35	0.02	1.50	1.94
TiO_2	0.32	0.46	0.38	0.33
P_2O_5	0.15	0.13	0.14	0.15
MnO	0.09	0.07	0.09	0.09
Cr_2O_3	0.02	<0.01	0.01	0.02
LOI	5.31	1.15	4.37	3.15
$\sum$	104.39	105.27	100.89	103.69
Mineral assemblage	Qz-Fp(Ab)-Cb Ser-Chl-Mt << Bo	Qz-Fp(Ab) < Ep, Chl, Cc	Qz-Fp(Ab-Chl-Bo < Cc, Py, Ser << Zr(Bo)	Qz-Fp(Ab)-Bo-Chl < Cb, Py, Cc << Ser, Zr(Bo) Ap

* *Chemical analyses by Abilab Inc.; See Appendix B for sample description and Index geological maps in the back pocket for sample location.*

Key: Ab=albite; Ap=apatite; Bo=biotite; Cb=carbonate; Cc=calcite; Chl=chlorite; Ep=epidote; Fp(Ab)=albitized plagioclase; Mt=magnetite; N.d.=non detected; Py=pyrite; Qz=quartz; Ser=sericite; Zr(Bo)=zircon inclusions in biotite

K91-3810-116 = year, stope, sample number

TABLE C.10 Trace element analyses (wt %) of the intermineral feldspar porphyry dike

	K91-3810-116	*K92-6402-230*	*K92-3838-249*	*K93-5804-269*
Au (ppb)	67	17	140	17
S (%)	0.25	0.11	0.29	0.25
As (ppm)	N.d.	N.d.	N.d.	N.d.
Cu (ppm)	46	71	43	52
Mo (ppm)	N.d.	N.d.	N.d.	N.d.
Ag (g/t)	N.d.	N.d.	N.d.	N.d.
Sb (ppm)	N.d.	N.d.	N.d.	N.d.
Bi (ppm)	N.d.	N.d.	N.d.	N.d.
Hg (ppb)	N.d.	N.d.	150	N.d.
Te (g/t)	N.d.	N.d.	N.d.	N.d.
Ni (ppm)	34	24	52	37
W (ppm)	N.d.	N.d.	N.d.	N.d.
Zn (ppm)	53	58	52	83
Mineral assemblage	Qz-Fp(Ab)-Cb Ser-Chl-Mt < Bo	Qz-Fp(Ab) < Ep, Chl, Cc	Qz-Fp(Ab)-Chl-Bo < Cc, Py, Ser << Zr(Bo)	Qz-Fp(Ab)-Bo-Chl < Cb, Py, Cc, Ap << Ser, Zr(Bo)

* *Chemical analyses by Abilab Inc.; See Appendix B for sample description and Index geological maps in the back pocket for sample location.*

Key: Ab=albite; Ap=apatite; Bo=biotite; Cb=carbonate; Cc=calcite; Chl=chlorite; Ep=epidote; Fp(Ab)=albitized plagioclase; Mt=magnetite; N.d.=non detected; Py=pyrite; Qz=quartz; Ser=sericite; Zr(Bo)=zircon inclusions in biotite

K91-3810-116 = year, stope, sample number

TABLE C.11 Major and minor element analyses (wt. %) of gold ores

	K92-3025-239	*K92-3629-248*	*K92-3838-250*	*K92-6446-243*	*K92-6446-244*	*K92-3838-251*	*K92-3025-238*	*K92-4313-253*
SiO_2	35.2	46.3	41.3	44.8	38.7	39.5	41.0	41.3
Al_2O_3	11.9	11.2	12.4	12.9	14.1	9.41	11.8	11.7
Fe_2O_3	11.0	11.9	12.2	13.9	9.02	13.4	12.0	10.6
FeO	8.10	6.30	5.70	3.16	3.17	3.35	2.90	4.79
MgO	8.88	4.43	6.32	4.55	13.0	4.81	3.91	4.59
CaO	11.3	9.63	7.47	5.77	5.90	9.50	7.96	9.07
Na_2O	3.08	3.25	4.86	5.80	3.51	5.29	5.68	6.29
K_2O	1.34	0.26	0.06	0.06	0.02	0.11	0.96	0.03
TiO_2	0.35	0.67	0.60	0.78	0.33	0.63	0.70	0.51
P_2O_5	0.01	0.05	0.02	0.06	0.02	0.01	0.01	0.01
MnO	0.21	0.20	0.23	0.19	0.16	0.21	0.17	0.22
Cr_2O_3	0.09	N.d.	0.01	0.01	0.12	0.01	N.d.	N.d.
LOI	12.5	9.29	10.9	7.19	13.3	8.22	9.14	9.70
$\sum$	103.95	103.48	102.07	99.17	101.35	94.44	96.23	98.81
Ore Type	"Stwk Cb-Qz-Py(Po)-±Ab-Au"	"Stwk Cb-Qz-Py(Po)-±Ab-Au"	"Stwk Cb-Qz-Py(Po)-±Ab-Au"	"Stwk Cb-Qz-Py(Po)-±Ab-Au"	"Stwk Cb-Qz-Py(Po)-±Ab-Au"	Cb-Py replacement veins ("Breccia 1")	Fragments of "Breccia 1" ore cemented by Ab-Py-Cpy Sch-Au stwk veins of "Breccia 2"	Mottled . Ab-Py-Cpy-Sch-Au breccia of "Breccia 2"

- *Chemical analyses by Lakefield Laboratories; See Appendix B for sample descriptions and Index geological maps in the back pocket for sample location.*
  Key: Ab=albite; Au=gold; Cb=carbonate; Cpy= chalcopyrite; N.d.= non detected; Po= pyrrhotite; Py= pyrite; Qz= quartz; Sch= scheelite; Stwk=stockwork
  K92-3025-239 = year, stope, sample number

TABLE C.12 Trace element analyses (wt. %) of gold ores

	K92-3025-239	*K92-3629-248*	*K92-3838-250*	*K92-6446-243*	*K92-6446-244*	*K92-3838-251*	*K92-3025-238*	*K92-4313-253*
Au (ppb)	1850	6690	1470	2360	40	9180	600	3350
S (%)	1.79	0.97	1.27	1.78	0.03	7.60	6.91	3.33
As (ppm)	6	N.d.	N.d.	N.d.	N.d.	9	6	7
Cu (ppm)	118	140	117	125	14	123	78	236
Mo (ppm)	85	N.d.	N.d.	33	N.d.	19	8	12
Ag (g/t)	0.90	1.60	0.7	0.60	N.d.	2.1	0.80	1.10
Sb (ppm)	N.d.	N.d.	N.d.	N.d.	N.d.	N.d.	N.d.	N.d.
Bi (ppm)	N.d.	N.d.	N.d.	N.d.	N.d.	N.d.	N.d.	N.d.
Hg (ppb)	13	118	20	63	N.d.	N.d.	10	10
Te (g/t)	2	3	3	1	2	4	2	3
Ni (ppm)	318	52	81	72	68	65	42	34
W (ppm)	N.d.	N.d.	7	5	N.d.	16	20	11
Zn (ppm)	64	60	72	81	67	21	18	28
Ore Type	"Stwk Cb-Qz-Py(Po)-±Ab-Au"	"Stwk Cb-Qz-Py(Po)-±Ab-Au"	"Stwk Cb-Qz-Py(Po)-±Ab-Au"	"Stwk Cb-Qz-Py(Po)-±Ab-Au"	"Stwk Cb-Qz-Py(Po)-±Ab-Au"	Cb-Py replacement veins ("Breccia 1")	Fragments of "Breccia 1" ore cemented by Ab-Py-Cpy Sch-Au stwk veins of "Breccia 2"	Mottled Ab-Py-Cpy-Sch-Au breccia of "Breccia 2"

- *Chemical analyses by Lakefield Laboratories; See Appendix B for sample descriptions and INdex geological maps in the back pocket for sample location.*

Key: Ab=albite; Au=gold; Cb=carbonate; Cpy= chalcopyrite; N.d.= non detected; Po= pyrrhotite; Py= pyrite; Qz= quartz; Sch=scheelite; Stwk=stockwork
K92-3025-239 = year, stope, sample number

APPENDIX D - STRUCTURAL DATA

Table D.1 Compilation of penetrative fabric (S_n, S_{n+1}) orientations across the Kiena deposit

Mine level - stope -	Ore zones	Type of penetrative fabric	Dip/dip azimuth	Rock type
27-52	"A"	S_n	25 ⟶ 294	Cb-Chl-Tc-Ab schist
"	"	"	27 ⟶ 348	Stwk Cb-Qz-Py(Po)±Ab-Au (iron tholeiite)
"	"	"	45 ⟶ 350	Stwk Cb-Qz-Py(Po)±Ab-Au (Breccia 1/2)
30-25	"D"	S_n	47 ⟶ 224	Breccia 1/2
"	"	"	40 ⟶ 228	Breccia 1/2
"	"	"	42 ⟶ 252	(iron tholeiite)
"	"	"	42 ⟶ 259	Stwk Cb-Qz-Py(Po)±Ab-Au (iron tholeiite)
"	"	"	35 ⟶ 276	Cb-Chl-Tc schist
"	"	"	35 ⟶ 292	Cb-Chl-Tc schist
"	"	"	40 ⟶ 310	Breccia 1/2
"	"	"	24 ⟶ 338	Stwk Cb-Qz-Py(Po)±Ab-Au (iron tholeiite)
"	"D"	S_{n+1}	42 ⟶ 014	Stwk Cb-Qz-Py(Po)±Ab-Au (Breccia 1/2)
"	"	"	20 ⟶ 015	Stwk Cb-Qz-Py(Po)±Ab-Au (Breccia 1/2)
"	"	"	24 ⟶ 018	Stwk Cb-Qz-Py(Po)±Ab-Au (Breccia 1/2)
"	"	"	22 ⟶ 020	Stwk Cb-Qz-Py(Po)±Ab-Au (Breccia 1/2)
"	"	"	20 ⟶ 056	Breccia 1/2
30-33	Wall-rock east of "D"	S_n	35 ⟶ 318	Stwk Cb-Qz-Py(Po)±Ab-Au (iron tholeiite)
33-01	Wall-rock east of "A"	S_n	25 ⟶ 314	Stwk Cb-Qz-Py(Po)±Ab-Au (iron tholeiite)
33-12	Wall-rock east of "B"	S_n	25 ⟶ 300	Cb-Chl-Tc schist
"	"	"	20 ⟶ 340	Iron tholeiite
"	"	"	20 ⟶ 344	Iron tholeiite

Table D.1 continued...

Mine level - stope -	Ore zones	Type of penetrative fabric	Dip/dip azimuth	Rock type
36-27	"J"	S_n	66 ⟶ 318	Albitite
"	"	"	32 ⟶ 340	Albitite
"	"	"	44 ⟶ 356	Breccia 1
"	"	"	40 ⟶ 360	Intermineral granodiorite dike
36-29	"L"	S_n	25 ⟶ 310	Stwk Cb-Qz-Py(Po)±Ab-Au (iron tholeiite)
38-10	"B"	S_n	35 ⟶ 324	Intermineral feldspar porphyry dike
"	"	"	45 ⟶ 326	Stwk Cb-Qz-Py(Po)±Ab-Au (iron tholeiite)
"	"	"	26 ⟶ 333	Stwk Cb-Qz-Py(Po)±Ab-Au (iron tholeiite)
"	"	"	60 ⟶ 344	Stwk Cb-Qz-Py(Po)±Ab-Au (iron tholeiite)
"	"	"	30 ⟶ 345	Breccia 1/2 Stwk Cb-Qz-Py(Po)±Ab-Au (iron tholeiite)
"	"	"	35 ⟶ 360	Breccia 1/2 Stwk Cb-Qz-Py(Po)±Ab-Au (iron tholeiite)
"	"	"	50 ⟶ 013	Breccia 1/2 Stwk Cb-Qz-Py(Po)±Ab-Au (iron tholeiite)
38-28	"B"	S_n	35 ⟶ 342	Stwk Cb-Qz-Py(Po)±Ab-Au (iron tholeiite)
"	"	"	45 ⟶ 353	Stwk Cb-Qz-Py(Po)±Ab-Au (iron tholeiite)
"	"	"	36 ⟶ 358	Albitite
"	"	"	40 ⟶ 358	Intermineral granodiorite dike
"	"	"	45 ⟶ 010	Stwk Cb-Qz-Py(Po)±Ab-Au (iron tholeiite)
"	"	"	40 ⟶ 022	Stwk Cb-Qz-Py(Po)±Ab-Au (iron tholeiite)
38-29	"L"	S_n	45 ⟶ 344	Stwk Cb-Qz-Py(Po)±Ab-Au (iron tholeiite)
"	"	"	40 ⟶ 347	Stwk Cb-Qz-Py(Po)±Ab-Au (iron tholeiite)
"	"	"	40 ⟶ 357	Stwk Cb-Qz-Py(Po)±Ab-Au (iron tholeiite)

Table D.1 continued...

Mine level - stope -	Ore zones	Type of penetrative fabric	Dip/dip azimuth	Rock type
38-38	"C"	S_n	65 ⟶ 326	Stwk Cb-Qz-Py(Po)±Ab-Au (iron tholeiite)
"	"	"	42 ⟶ 330	Breccia 1 Stwk Cb-Qz-Py(Po)±Ab-Au (iron tholeiite)
"	"	"	55 ⟶ 338	Intermineral feldspar porphyry dike
"	"	"	50 ⟶ 346	Stwk Cb-Qz-Py(Po)±Ab-Au (iron tholeiite)
36-29	"L"	S_n	55 ⟶ 350	Stwk Cb-Qz-Py(Po)±Ab-Au (iron tholeiite)
"	"	"	45 ⟶ 360	Breccia 1 Stwk Cb-Qz-Py(Po)±Ab-Au (iron tholeiite)
"	"	"	50 ⟶ 360	Stwk Cb-Qz-Py(Po)±Ab-Au (iron tholeiite)
"	"	"	35 ⟶ 002	Stwk Cb-Qz-Py(Po)±Ab-Au (iron tholeiite)
"	"	"	40 ⟶ 005	Breccia 1 Stwk Cb-Qz-Py(Po)±Ab-Au (iron tholeiite)
"	"	"	50 ⟶ 018	Stwk Cb-Qz-Py(Po)±Ab-Au (iron tholeiite)
"	"	"	45 ⟶ 024	Breccia 1/2
"	"	"	50 ⟶ 026	Stwk Cb-Qz-Py(Po)±Ab-Au (iron tholeiite)
41-05	Wall-rock east of "C"	S_n	35 ⟶ 325	Breccia 1 Iron tholeiite
"	"	"	40 ⟶ 338	Basaltic pillow flow breccia
41-10	"B"	S_n	60 ⟶ 330	Albitite (?)
"	"	"	70 ⟶ 010	Breccia 1/2
41-16	"B"	S_n	50 ⟶ 350	Albitite
"	"	"	57 ⟶ 360	Albitite
41-17	"B"	S_n	35 ⟶ 328	Stwk Cb-Qz-Py(Po)±Ab-Au (iron tholeiite)
"	"	"	45 ⟶ 348	Stwk Cb-Qz-Py(Po)±Ab-Au (iron tholeiite)
"	"	"	50 ⟶ 350	Stwk Cb-Qz-Py(Po)±Ab-Au (iron tholeiite)

Table D.1 continued...

Mine level - stope -	Ore zones	Type of penetrative fabric	Dip/dip azimuth	Rock type
41-17	"B"	S_n	60 ⟶ 354	Stwk Cb-Qz-Py(Po)±Ab-Au (iron tholeiite)
"	"	"	45 ⟶ 360	Stwk Cb-Qz-Py(Po)±Ab-Au (iron tholeiite)
"	"	"	52 ⟶ 008	Breccia 1/2 Stwk Cb-Qz-Py(Po)±Ab-Au
"	"	"	55 ⟶ 020	Breccia 1/2
41-17	"B"	S_{n+1}	20 ⟶ 015	Breccia 1/2
41-38	"C"	S_n	35 ⟶ 290	Breccia 1/2 Stwk Cb-Qz-Py(Po)±Ab-Au (iron tholeiite)
"	"	"	38 ⟶ 310	Stwk Cb-Qz-Py(Po)±Ab-Au (iron tholeiite)
"	"	"	45 ⟶ 316	Stwk Cb-Qz-Py(Po)±Ab-Au (iron tholeiite)
"	"	"	26 ⟶ 330	Breccia 1/2
"	"	"	40 ⟶ 336	Intermineral granodiorite dike
"	"	"	44 ⟶ 336	Stwk Cb-Qz-Py(Po)±Ab-Au (iron tholeiite)
"	"	"	25 ⟶ 350	Cb-Chl-Tc schist
"	"	"	45 ⟶ 351	Cb-Chl-Tc schist
"	"	"	32 ⟶ 360	Breccia 1
"	"	"	45 ⟶ 360	Stwk Cb-Qz-Py(Po)±Ab-Au (iron tholeiite)
"	"	"	50 ⟶ 010	Cb-Chl-Tc schist
41-38	"C"	S_{n+1}	25 ⟶ 006	Cb-Chl-Tc schist
43-13	"B"	S_n	45 ⟶ 014	Breccia 2 Stwk Cb-Qz-Py(Po)±Ab-Au (iron tholeiite)
"	"	"	52 ⟶ 018	Breccia 2
"	"	"	55 ⟶ 022	Breccia 2
"	"	"	45 ⟶ 040	Breccia 2

Table D.1 continued...

Mine level - stope -	Ore zones	Type of penetrative fabric	Dip/dip azimuth	Rock type
43-17	"B"	S_n	45 ⟶ 325	Stwk Cb-Qz-Py(Po)±Ab-Au (iron tholeiite)
"	"	"	74 ⟶ 360	Stwk Cb-Qz-Py(Po)±Ab-Au (iron tholeiite)
"	"	"	55 ⟶ 015	Breccia 2
"	"	"	52 ⟶ 018	Breccia 2
46-13	"B"	S_n	50 ⟶ 346	Stwk Cb-Qz-Py(Po)±Ab-Au (iron tholeiite)
"	"	"	40 ⟶ 352	Cb-Chl-Tc schist
"	"	"	30 ⟶ 010	Breccia 1/2
64-46	Lower "C"	S_n	62 ⟶ 045	Stwk Cb-Qz-Py(Po)±Ab-Au (albitite)
"	"	"	60 ⟶ 048	Stwk Cb-Qz-Py(Po)±Ab-Au (albitite)
64-46	Lower "C"	S_{n+1}	28 ⟶ 032	Albitite
"	"	"	25 ⟶ 052	Intermineral granodiorite dike

Key: S_n= deposit's main schistosity; S_{n+1}= crenulation cleavage; Cb=carbonate; Chl=chlorite; Tc=talc; Stwk Cb-Qz-Py(Po)±Ab-Au vein ore type = carbonate-quartz-pyrite(pyrrhotite)±albite-Au stockwork veins; Breccia1 ore type=carbonate-pyrite-Au replacement veins; Breccia2 ore type=albite-pyrite-chalcopyrite-scheelite stockwork veins and breccias; Breccia1/2 = hybrid rock type composed of Breccia1 and Breccia 2 ores.

Table D.2 Changes in the orientation of the Kiena orebody

Mine level	Ore zones	Strike	Dip	Dip/dip azimuth
27	"A"	N 213 N 125	30 NW 30 SW	30 → 303 30 → 215
33	"B" "J", "K", "L" "C"	N 208 N 133	35 NW 25 SW	35 → 298 25 → 223
41	"J", "K" "B" "C"	N 180 N 210 N 140	55 W 45 NW 90	55 → 270 45 → 300 90 → 230
43	"J","K" "B" "C"	N 180 N 210 N 140	90 50 NW 75 NE	90 → 090 50 → 300 75 → 060
57	"B" "C"	N 015 N 325	90 75 NE	90 → 105 75 → 055
64	"C"	N 322	65 NE	65 → 052

* See schematic cross-sections and plan maps in back pocket

Table D.3 Changes in the orientation of the Kiena deposit intermineral dikes

Mine level	Dike	Strike	Dip	Dip/dip azimuth
27	Feldspar porphyry	N 180	24 W	24⟶ 270
33	North granodiorite	N 205	45 NW	45⟶ 295
	South granodiorite	N 135	35 SW	35⟶ 225
41	North granodiorite	N 205	65 NW	65⟶ 295
	South granodiorite	N 138	58 SW	58⟶ 228
	Feldspar porphyry	N 165	80 W	80⟶ 255
43	North granodiorite	N 220	70 NW	70⟶ 310
	South granodiorite	N 342	45 NE	45⟶ 072
57	North granodiorite	N 042	90	90⟶ 132
	South granodiorite	N 325	50 NE	50⟶ 055
	Feldspar porphyry	N 310	65 NE	65⟶ 040
64	North granodiorite	N 180	90	90⟶ 270
	South granodiorite	N 330	85 NE	85⟶ 060
	Feldspar porphyry	N 315	65 NE	65⟶ 045

* See schematic cross-sections and plan maps in back pocket

Table D.4 Changes in the orientation of the Kiena deposit albitite dikes

Mine level	Dike	Strike	Dip	Dip/dip azimuth
27	North albitite dikes	N 212	15 NW	15 ⟶ 302
	South albitite dikes	N 225	25 NW	25 ⟶ 315
33	North albitite dikes	N 208	30 NW	30 ⟶ 298
	South albitite dikes	N 135	40 SW	40 ⟶ 225
41	North albitite dikes	N 198	45 NW	45 ⟶ 288
	South albitite dikes	N 145	90	90 ⟶ 235
43	Main albitite dike	N 212	90	90 ⟶ 302
57	Albitite swarm	N 315	66 NE	66 ⟶ 045
64	Albitite swarm	N 327	75 NE	75 ⟶ 057

* See schematic cross-sections and plan maps in back pocket

Table D.5 Attitude of the Kiena deposit main-stage stockwork veins, late-stage phyllosilicate stringer veins and post-ore extension veins

Mine level - stope -	Host rock	Vein type (angle to schistosity)	Mineralogy	Dip/dip azimuth
27-52	Cb-Chl-Tc schist	zoned stwk vein (low)	Cb-Qz-Py-Ab-Au	26 ⟶ 274
"	"	zoned stwk veins (high)	"	75 ⟶ 296 44 ⟶ 305
"	Stwk vein-altered iron tholeiite	extension veins	Cb-Qz-Tl	16 ⟶ 144 38 ⟶ 109
"	Iron tholeiite	zoned stwk veins (low)	Cb-Qz-Py-Ab-Au	47 ⟶ 005 40 ⟶ 010 43 ⟶ 019
"	"Breccia 2"	hairline stringer veins	Chl-Stilp	85 ⟶ 068
"	Cb-Chl schist	zoned stwk veins (low)	Cb-Qz-Py-Ab-Au	24 ⟶ 280 24 ⟶ 298
"	"	zoned stwk veins (high)	"	64 ⟶ 053 55 ⟶ 285
30-25	Cb-Chl-Tc schist	crenulated extension vein	Cb	80 ⟶ 158
"	"Breccia 1/2"	extension veins	Qz-Tl-Sch	40 ⟶ 116 25 ⟶ 112
36-27	Albitite/ iron tholeiite	zoned stwk veins (low)	Cb-Qz-Py-Ab-Au	66 ⟶ 318 45 ⟶ 340 45 ⟶ 346 42 ⟶ 310
"	"	breccia vein (low)	Ab-Py-Au	50 ⟶ 340
38-10	"	hairline stringer vein	Chl-Bo-Stilp	30 ⟶ 345
"	Albitite/ iron tholeiite	zoned stwk veins (low)	Cb-Qz-Py-Ab-Au	34 ⟶ 326 24 ⟶ 350 20 ⟶ 340 62 ⟶ 360
"	Iron tholeiite	zoned stwk veins (folded) stwk breccia vein	"	32 ⟶ 338 55 ⟶ 356 64 ⟶ 276
38-28	Iron tholeiite	zoned stwk veins (low)	Cb-Qz-Py(Po)-Ab-Au	34 ⟶ 331 46 ⟶ 340 55 ⟶ 008 43 ⟶ 004
"	"	zoned stwk vein (high)	"	70 ⟶ 028

Table D.5 continued...

Mine level - stope -	Host rock	Vein type (angle to schistosity)	Mineralogy	Dip/dip azimuth
38-29	Albitite	extension Vein (perpendicular)	Qz-Tl	40 ⟶ 184
"	Albitite/iron tholeiite	zoned stwk veins (low)	Cb-Qz-Py(Po)-Ab-Au	40 ⟶ 007 30 ⟶ 360
"	"	pegmatite vein	Qz-Cb-Bo-Py-Au	30 ⟶ 005
38-38	Iron tholeiite	zoned stwk veins (low)	Cb-Qz-Py-Ab-Au	54 ⟶ 022 45 ⟶ 008 35 ⟶ 016
"	"Breccia 1"	hairline stringer vein	Chl-Bo-Mt	35 ⟶ 354
"	Iron tholeiite	pegmatite vein (high)	Cb-Qz-Py-Bo-Tl-Cpy-Au	75 ⟶ 262
"	Intermineral feldspar porphyry	hairline stringer vein	Chl-Ser-Bo	55 ⟶ 338
"	"	stockwork veins	Cb-Qz-Py	75 ⟶ 240 89 ⟶ 020 25 ⟶ 302
"	Iron tholeiite	zoned stwk veins (low)	Cb-Qz-Py-Ab-Au	25 ⟶ 350 45 ⟶ 322 40 ⟶ 330 54 ⟶ 350 46 ⟶ 356 50 ⟶ 335 45 ⟶ 360
"	"	zoned stwk veins (high)	"	80 ⟶ 186 89 ⟶ 002
"	Albitite/iron tholeiite	extension vein	Qz-Cb-Chl	88 ⟶ 058
"	Cb-Chl-Tc schist	stringer veinlets (low)	Bo-Chl-Mt	25 ⟶ 020 25 ⟶ 030
"	"Breccia 1"	pegmatite veins (low)	Qz-Cb-Bo-Ab-Tl-Py	45 ⟶ 157 65 ⟶ 326
"	Iron tholeiite	extension veins across zoned stwk veins (perpendicular)	Qz	25 ⟶ 220 50 ⟶ 220 45 ⟶ 230 65 ⟶ 254
41-38	Iron tholeiite	zoned stwk veins (low)	Cb-Qz-Py-Ab-Au	40 ⟶ 002
"	"	extension vein across zoned stwk vein (perpendicular)	Qz	80 ⟶ 210

Table D.5 continued...

Mine level - stope -	Host rock	Vein type (angle to schistosity)	Mineralogy	Dip/dip azimuth
41-38	Cb-Chl-Tc-Ser schist (fault zone)	Qz-Cb-Chl extension Vein (perpendicular)		45 ⟶ 146
"	"	fibers in veins (schistosity)		69 ⟶ 282 (36 ⟶ 030)
"	Albitite/iron tholeiite	zoned stwk veins breccia veins (low)	Cb-Qz-Py-Ab-Au	40 ⟶ 332 30 ⟶ 316 35 ⟶ 010 25 ⟶ 040
"	Iron tholeiite	zoned stwk veins (high)	"	50 ⟶ 248 82 ⟶ 190 81 ⟶ 250 65 ⟶ 235
"	Albitite/iron tholeiite	zoned stwk vein (low)	Cb-Qz-Py-Ab-Au	28 ⟶ 322 40 ⟶ 290 40 ⟶ 301 38 ⟶ 300
41-10	Iron tholeiite	zoned stwk vein (low)	Cb-Qz-Py-Ab-Au	55 ⟶ 300 58 ⟶ 340 35 ⟶ 328 45 ⟶ 338
"	"	extension veins across zoned stwk vein (perpendicular)	Cb	35 ⟶ 078 45 ⟶ 188 50 ⟶ 198
"	Albitite dikes	ladder vein	Cb	60 ⟶ 224
41-16	Albitite/iron tholeiite	stringer veinlets (low)	Chl-Bo-Mt	50 ⟶ 350
"	"	stwk breccia vein (low)	Ab-Py-(Cpy)-Sch-Au	50 ⟶ 302
"	"	stwk breccia vein (high)	"	75 ⟶ 270 65 ⟶ 295
41-17	Iron tholeiite	zoned stwk veins (low)	Cb-Qz-Py-Ab-Au	50 ⟶ 342 45 ⟶ 360 32 ⟶ 318 40 ⟶ 334
"	"	zoned stwk veins (high)	"	65 ⟶ 138 75 ⟶ 100
"	"	extension vein across zoned stwk vein	Qz	80 ⟶ 312

Table D.5 continued...

Mine level - stope -	Host rock	Vein type (angle to schistosity)	Mineralogy	Dip/dip azimuth
41-17	Albitite/iron tholeiite	stwk breccia veins (low)	Ab-Py-Cpy-Sch-Au	30 ⟶ 340 46 ⟶ 348 30 ⟶ 308 48 ⟶ 022 45 ⟶ 032
"	"	stwk breccia veins (high)	"	85 ⟶ 248 75 ⟶ 306 85 ⟶ 284 80 ⟶ 274 55 ⟶ 054 85 ⟶ 096 60 ⟶ 004 60 ⟶ 330
"	"Breccia 2" stwk veins	stringer veinlets	Chl-Stilp-(Bo)	82 ⟶ 036 70 ⟶ 062
43-13	"Breccia 2"	stringer veinlet	Chl-Bo	55 ⟶ 022
"	Iron tholeiite	stwk breccia vein (low)	Cb-Qz-Py(Po)-Ab-Au	40 ⟶ 335
43-17	"Breccia 2"	stringer veinlet	Chl-Bo	55 ⟶ 014
"	"Breccia 1"	stwk breccia vein (high)	Ab-Py-(Cpy)-Sch-Au	40 ⟶ 295
46-13	Albitite/tholeiite	stwk breccia veins (low)	Ab-Py-(Cpy)-Au	54 ⟶ 002 75 ⟶ 350 35 ⟶ 352
"	"Breccia 2"	stringer veinlets	Chl	74 ⟶ 114 70 ⟶ 135 72 ⟶ 168 80 ⟶ 128

Key: Ab= albite; Au= gold; Bo= biotite; Breccia1= carbonate-pyrite-Au replacement vein; Breccia2= albite-pyrite-chalcopyrite-scheelite stockwork veins and breccia; Cb=carbonate; Chl=chlorite; Cpy=chalcopyrite; Mt= magnetite; Py= Pyrite; Po= Pyrrhotite; Qz= quartz; Sch=scheelite; Ser=sericite; Stil= stilpnomelane; Stwk=stockwork; StwkCb-Qz-Py(Po)±Ab-Au= carbonate-quartz-pyrite(pyrrhotite)-albite-Au stockwork veins; Tc= talc; Tl=tourmaline;

Table D.6 Attitude of post-ore strike-slip and oblique-slip faults cross-cutting the Kiena deposit main schistosity (S_n)

Mine level - stope -	Location	Dip/dip azimuth	Rake of fault striations	Trend/plunge	Vertical and/or horizontal component of movement
27-52	Orebody/Cb-Chl-Tc schist contact, east of S-50 Zone	26 ⟶ 314	60-65 N	286/23	Normal
"	Orebody Cb-Chl-Tc schist contact, west of S-50 zone	37 ⟶ 130			(?)
"	Across orebody	70 ⟶ 018			Normal
30-25	Orebody/Cb-Chl-Tc schist contact, west of the S-50 zone	40 ⟶ 232	85 SE	225/39	Reverse
"	Across orebody	40 ⟶ 116	45 NE	063/27	Reverse
33	Orebody/iron tholeiite contact, east of S-50 zone	60 ⟶ 297			Normal, dextral
"	Orebody/Cb-Chl-Tc schist contact, west of the S-50 zone	60 ⟶ 291			Normal, dextral
38-10	Orebody/iron tholeiite contact, east of S-50 Zone	55 ⟶ 325	65 SW	285/48	Normal, dextral
38-29	Across orebody	72 ⟶ 164	50 NE	094/46	Senestral
38-38	Orebody/iron tholeiite contact, east of the S-50 zone	56 ⟶ 075	45 NE	014/35	Normal, dextral
"	Across orebody	78 ⟶ 030	50 NW	313/48	Normal, dextral
41-10	Orebody/iron tholeiite contact, east of S-50 zone	52 ⟶ 318	84 N	308/52	Normal, dextral
"	Orebody/Cb-Chl-Tc schist contact, west of the S-50 zone	85 ⟶ 274	18 S	185/18	Normal, dextral
41-16	Orebody/iron tholeiite contact, east of S-50 zone	65 ⟶ 274	63 S	223/54	Normal, dextral
41-17	Orebody/iron tholeiite contact, east of the S-50 zone	60 ⟶ 276			(?)

Table D.6 continued...

Mine level - stope -	Location	Dip/dip azimuth	Rake of fault striations	Trend/plunge	Vertical and/or horizontal component of movement
41-38	Orebody/iron tholeiite contact, east of "C" Zone	55 ⟶ 030 65 ⟶ 040	25 NE	315/20	(?)
43-13	Orebody /iron tholeiite contact, east of S-50 zone	55 ⟶ 332			Dextral
43-17	Orebody/iron thloleiite contact, east of the S-50 zone	60 ⟶ 275	55 W	220/45	Normal, dextral
46-13	Orebody/Cb-Chl-Tc schist/feldspar porphyry contact, east of the S-50 zone	64 ⟶ 300			(?)
64-46	Orebody/basaltic komatiite contact, east of "C" Zone	75 ⟶ 135			(?)

Key: Cb= carbonate; Chl= chlorite; Tc= talc

APPENDIX E - ISOTOPIC AGE DATING

Sample preparation

The concentrates were placed in an ultrasonic vibrator and ground by hand with a mortar and pestle to try and dislodge attached pieces of carbonate and feldspar in order to increase the purity of the separates. The samples were then washed and further purified on a Frantz Isodynamic Magnetic separator. The biotite separates were shaken on a piece of filter paper to cause the angular carbonate and feldspar fragments to roll-off the paper, and the platy biotite flakes to remain on the paper. The latter procedure was repeated several times, until the desired purity of concentrate was achieved. Since biotite separates consists of composite biotite-chlorite grains, they were then examined under a binocular and chlorite-free biotites were hand-picked until there was enough of the concentrate to analyze (6.5 to 15.5 mg). The final biotite separates and neutron flux monitor (Hb3gr: hornblende age 1972 Ma) were individually wraped in a piece of aluminum foil and re-wrapped in a second piece of foil to prevent leakage. The samples were labelled and stacked into an aluminum irradiation cannister . The standards were evenly spaced along the length of the cannister and the position of both samples and standards, was recorded on a log sheet. This procedure allows the determination of unknown J-values for the samples based on known J-values provided by the standards. As J-values varied systematically along the length of the can, the J-value of the biotite separates was interpolated for each sample based on its position in the can.

Sample irradiation and age dating

The samples of biotite concentrate and neutron flux monitors were irradiated in the water-moderated, enriched-uranium reactor at McMaster University in can No. 90 for 10.3 days. The samples were returned and placed in a lead-lined box for a suitable "cooling" period, allowing further time for the decay of short-lived radionucleides. The samples and monitors were removed from the irradiation can, unwrapped and placed in individual niobium crucibles. The biotite separates were step-heated in a quartz furnace-tube using a Lindberg resistance furnace, and the gas was analyzed using an ultra-high vacuum, stainless steel argon extraction system, on line with a modified A.E.I. MS-10 mass spectrometer run in static mode. All the samples were analyzed by Dr. Sandra McBride in the K-Ar geochronology laboratory of Dr. Ed Farrar at Queen's University. Measured mass-spectrometric ratios were extrapolated to "zero time", corrected for neutron induced ^{40}Ar emitted by potassium and for ^{39}Ar and ^{36}Ar emitted by calcium. Dates and error were calculated using constants recommended by Steiger and Jager (1977) and formulae given by Dalrymple *et al.* (1981). The resulting data is presented on a "degassing curve" or "age spectrum". The abcissa represents the fraction of ^{39}Ar released and the ordinate is the apparent age. The width of the bars for each heating step represents the 2σ error. In this study, a "plateau age" refers to four or more consecutive heating steps whose ages overlap in 2σ errors and comprise more than 50% of the ^{39}Ar released.

Age Spectra for Kiena Deposit Late-Stage Hydrothermal Vein Biotite

K91-U2417-124 biotite

Run: SM147 90/102

Date: July 15/92

Mass: 6.5 mg

J Value: 0.02479

Aliquot: grinded and sieved 60-80 mesh fraction

Comment: pre-metamorphic

Total ^{39}Ar: 6.347 E-8 cm^3 NTP, Approx 5.6% K

Integrated Age: 2071.7 ± 23.8 Ma

Plateau Age: Nil

Location: Vein biotite-pyrite-magnetite overprinting high-grade ore zone, 'B' ore zone, level 58, section 12621.3N

Analyzed by: S. McBride, Queen's University

Tem °C	40/39	36/39	37/39	Vol ^{39}A E-8 cm^3	Fraction ^{39}Ar	%^{40}Ar Rad	Age Ma	±	Error 2 sigma
550	23.303	0.0085	0.073	0.497	0.078	89.12	749.4	±	11.9
600	79.764	0.0114	0.409	0.215	0.034	95.74	1917.2	±	93.2
675	93.938	0.0129	0.005	0.217	0.034	95.93	2117.4	±	19.8
750	94.790	0.0026	0.000	1.392	0.219	99.16	2170.3	±	13.7
830	94.568	0.0022	0.026	1.504	0.237	99.27	2168.8	±	32.6
890	98.283	0.0038	0.000	1.064	0.168	98.83	2211.9	±	22.6
940	98.627	0.0037	0/000	0.682	0.108	98.87	2216.9	±	25.0
1000	101.876	0.0082	0/000	0.505	0.080	97.61	2242.0	±	9.0
1150	109.969	0.0185	0/003	0.271	0.043	95.00	2305.8	±	26.4

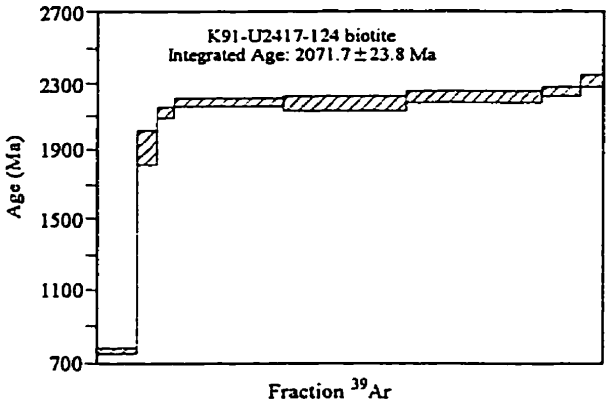

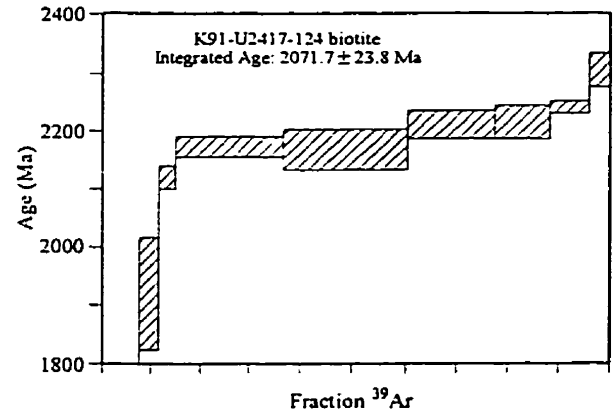

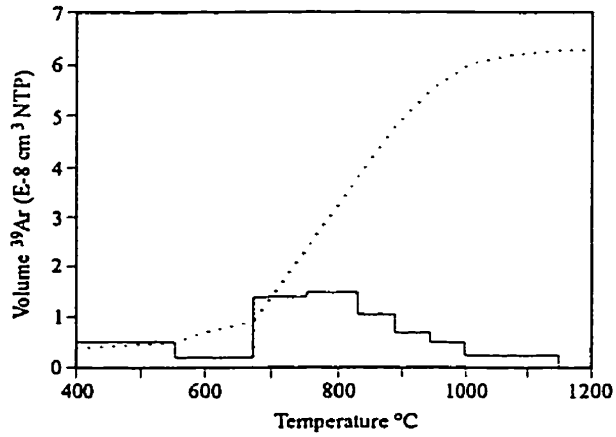

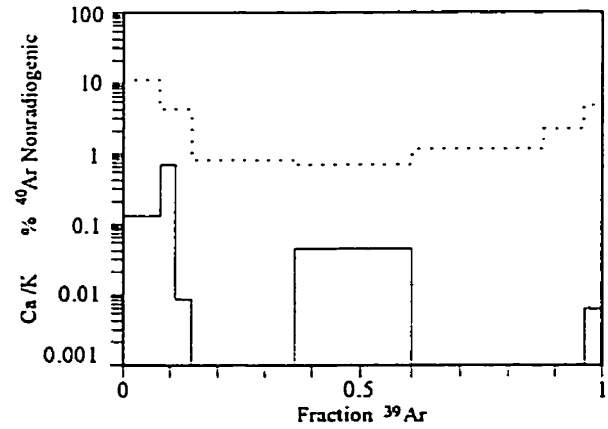

Age Spectra for Kiena Deposit Main-Stage Hydrothermal Pegmatitic Biotite

K91-3838-140 biotite

Run: SM145 90/105

Date: July 14/92

Mass: 12.5 mg

J Value: 0.02459

Aliquot: hand picked

Comment: pre-metamorphic

Total ^{39}Ar: 17.403 E-8 cm^3 NTP, Approx 8.0% K

Integrated Age: 2446.5 ± 16.1 Ma

Plateau Age: Nil

Location: Qz-Cc-Bo-Py-Cpy-Au vein overprinting high-grade ore zone; southern hinge of Z-shaped fold at junction of 'B' and 'C' ore zones; ore drift 38-38

Analyzed by: S. McBride, Queen's University

Tem °C	40/39	36/39	37/39	Vol ^{39}A E-8 cm^3	Fraction ^{39}Ar	%^{40}Ar Rad	Age Ma	±	Error 2 sigma
550	198.485	0.0150	0.098	0.639	0.037	97.75	3162.4	±	12.4
600	118.861	0.0018	0.200	1.620	0.093	99.54	2459.9	±	21.0
675	115.971	0.0009	0.065	3.408	0.196	99.76	2429.7	±	16.4
750	113.743	0.0011	0.000	2.890	0.166	99.70	2402.9	±	10.3
830	114.429	0.0006	0.000	3.259	0.187	99.83	2421.7	±	12.6
890	113.729	0.0009	0.000	3.279	0.188	99.75	2403.5	±	23.8
940	116.389	0.0028	0.000	1.291	0.074	99.26	2427.7	±	8.7
1000	124.033	0.0305	0.029	0.681	0.039	92.71	2421.5	±	17.4
1150	120.723	0.0146	0.005	0.335	0.019	96.41	2437.6	±	29.6

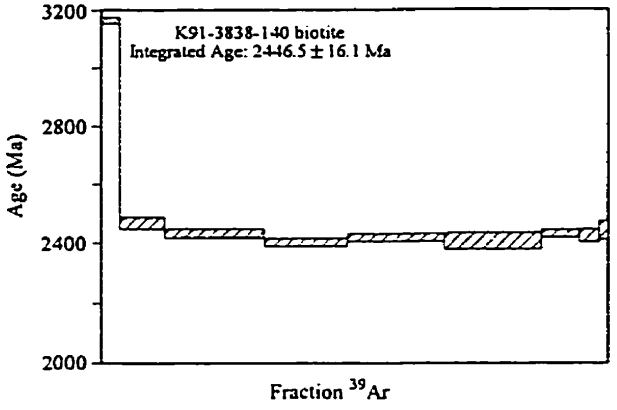

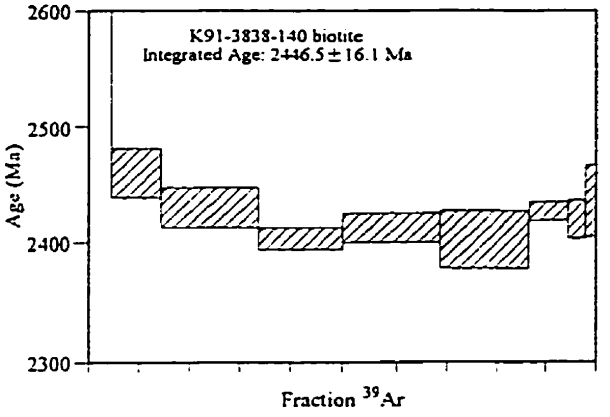

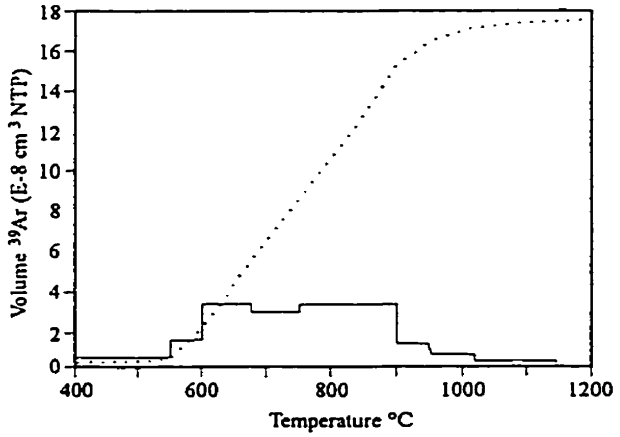

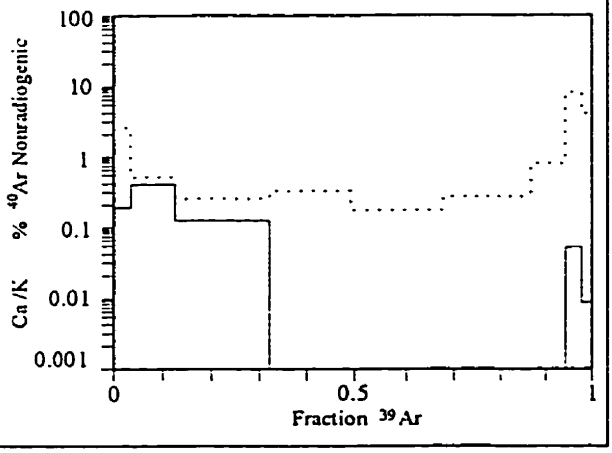

Age Spectra for Kiena Deposit Late-Stage Hydrothermal Vein Biotite

K91-3828-170 biotite

Run: SM144 90/104

Date: July 13/92

Mass: 10.0 mg

J Value: 0.02464

Aliquot: grinded and paper filter sieved 80-100 mesh fraction

Comment: weakly chloritized, pre-metamorphic

Total ^{39}Ar: 12.401 E-8 cm^3 NTP, Approx 7.1% K

Integrated Age: 2346.0 ± 18.6 Ma

Plateau Age: Nil

Location: Vein biotite overprinting Cb-Qz-Py(Po)±Ab-Au stockwork vein mineralization of lower-grade ore shell, 'K' ore zone, ore drift 38-28

Analyzed by: S. McBride, Queen's University

Tem °C	40/39	36/39	37/39	Vol ^{39}A E-8 cm^3	Fraction ^{39}Ar	%^{40}Ar Rad	Age Ma	±	Error 2 sigma
550	117.129	0.0102	0.151	0.503	0.041	97.41	2414.0	±	24.2
600	117.446	0.0026	0.002	1.089	0.088	99.33	2443.4	±	11.1
675	104.206	0.0018	0.000	1.406	0.113	99.47	2287.6	±	14.5
750	106.920	0.0009	0.000	1.593	0.128	99.72	2324.4	±	23.1
830	105.830	0.0013	0.000	1.706	0.138	99.61	2309.6	±	20.3
890	107.544	0.0016	0.032	2.453	0.198	99.53	2329.6	±	19.1
940	108.969	0.0019	0.000	1.531	0.123	99.46	2345.8	±	26.6
1000	110.678	0.0036	0.021	0.999	0.081	99.02	2360.5	±	13.1
1150	114.399	0.0038	0.000	1.121	0.090	99.00	2403.8	±	12.1

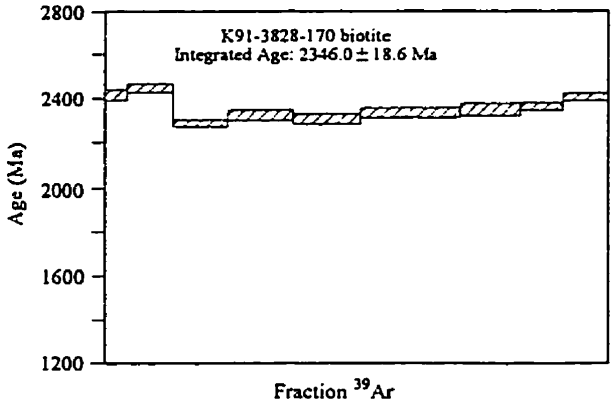

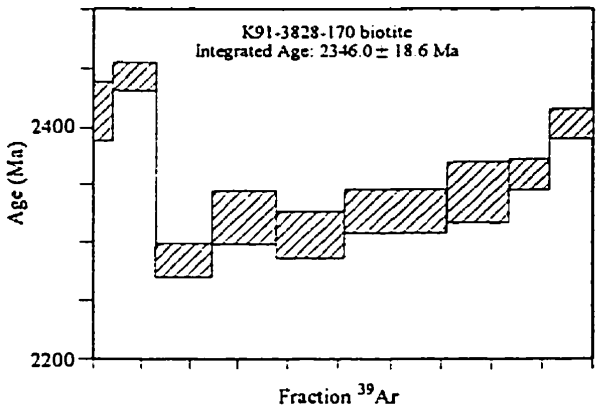

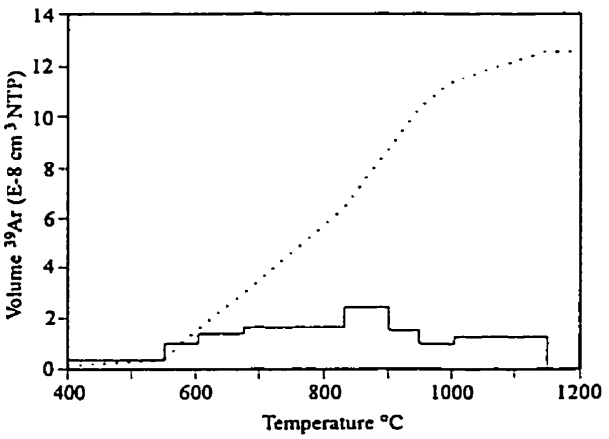

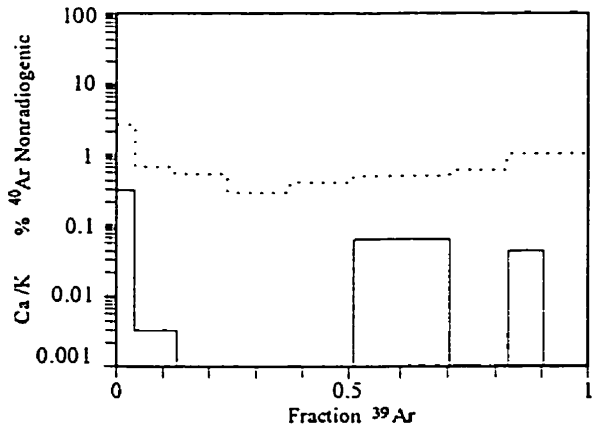

APPENDIX F - MICROPROBE ANALYSES

All minerals were analysed at Queen's University with an **ARL-SEMQ** electron microprobe using an energy dispersive spectrometer and an accelerating voltage of 15 KV. Kaersutite (Smithsonian Institute USNM 143965) was used as a primary standard. Each mineral composition represents a point analysis (200 s count time) within a grain. Structural formulae were computed using the **APL - MINERAL** software developed by Dr. Dugald Carmichael at the Department of Geological Sciences, Queen's University.

Table F.1 Electron microprobe analyses of albites in albitite dikes and albite vein

	K92-6446-218 twinned	K92-6446-218 dendritic	K92-6446-218 untwinned	K92-6446-218 untwinned	K90-3627-076 dendritic	K90-3627-076 untwinned	K90-3627-076 dendritic	K90-3627-076 untwinned
SiO_2	68.70	68.79	68.98	68.94	68.66	68.96	68.77	67.32
Al_2O_3	19.20	19.25	19.40	19.14	19.06	19.16	19.12	19.50
CaO	0.06	0.00	0.00	0.05	0.08	0.07	0.03	0.07
Na_2O	11.46	11.56	11.35	11.46	11.51	11.57	11.57	11.29
K_2O	0.00	0.00	0.00	0.00	0.00	0.05	0.03	0.11
Total	99.42	99.60	99.73	99.59	99.31	99.81	99.52	98.29
Si	3.003	3.006	3.003	3.012	3.009	3.008	3.008	2.982
Al (IV)	0.989	0.991	0.995	0.986	0.985	0.985	0.986	1.018
Al (VI)	0.000	0.000	0.000	0.000	0.000	0.000	0.000	0.000
Ca	0.003	0.000	0.000	0.002	0.004	0.003	0.001	0.003
Na	0.971	0.979	0.958	0.971	0.978	0.979	0.981	0.970
K	0.000	0.000	0.000	0.000	0.000	0.003	0.002	0.006
O	8.000	8.000	8.000	8.000	8.000	8.000	8.000	8.000
% An	0.3	0	0	0.2	0.4	0.3	0.1	0.3

Table F.1 continued...

	K90-3627-076 untwinned	K90-3627-076 untwinned	K91-3828-168 twinned	K91-3828-168 twinned	K91-3828-168 myrmekitic intergrowth	K91-3828-168 myrmekitic intergrowth	K91-3838-079 vein albite	K91-3838-079 vein albite
SiO_2	68.07	68.17	68.74	69.51	69.58	77.76	69.25	69.61
Al_2O_3	19.36	19.52	18.81	19.28	19.90	15.30	19.48	19.15
CaO	0.07	0.19	0.16	0.06	0.20	0.13	0.17	0.07
Na_2O	11.41	11.53	11.49	11.60	11.70	9.25	11.72	11.76
K_2O	0.04	0.00	0.00	0.05	0.00	0.03	0.05	0.00
Total	98.95	99.41	100.20	100.50	101.38	102.47	100.67	102.59
Si	2.996	2.987	3.028	3.011	2.988	3.240	3.002	3.015
Al (IV)	1.004	1.008	0.963	0.984	1.007	0.751	0.995	0.977
Al (VI)	0.000	0.000	0.000	0.000	0.000	0.000	0.000	0.000
Ca	0.003	0.009	0.007	0.003	0.009	0.006	0.008	0.003
Na	0.974	0.979	0.967	0.974	0.974	0.747	0.985	0.988
K	0.002	0.000	0.000	0.003	0.000	0.002	0.003	0.000
O	8.000	8.000	8.000	8.000	8.000	8.000	8.000	8.000
% An	0.3	0.9	0.7	0.3	0.9	0.8	0.8	0.3

Table F.2 Electron microprobe analyses of zoned plagioclase phenocrysts in granodiorite and quartz monzonite intermineral dikes

	K90-4317-055 granodiorite grain 1- core	K90-4317-055 granodiorite grain 1 - rim	K90-4317-055 grainodiorite grain 2 - core	K90-4317-055 granodiorite grain 2 - rim	K90-4317-055 granodiorite grain 3 - core	K90-4317-055 granodiorite grain 3 - rim	K90-4317-055 groundmass albite (2 analyses)
SiO_2	65.68	66.73	66.60	66.72	67.14	66.60	66.81
Al_2O_3	21.59	20.24	19.77	19.84	19.79	19.60	19.90
CaO	1.70	0.36	0.26	0.54	0.29	0.27	0.36
Na_2O	10.11	11.09	11.06	11.40	11.17	11.14	11.29
K_2O	0.52	0.38	0.25	0.04	0.04	0.18	0.18
Total	99.60	99.10	97.94	98.54	98.43	97.79	98.54
Si	2.895	2.950	2.967	2.955	2.971	2.969	2.957
Al (IV)	1.105	1.050	1.033	1.036	1.029	1.030	1.038
Al (VI)	0.016	0.004	0.006	0.000	0.003	0.000	0.000
Ca	0.080	0.017	0.012	0.026	0.014	0.013	0.017
Na	0.864	0.950	0.955	0.979	0.958	0.963	0.969
K	0.029	0.021	0.014	0.002	0.002	0.010	0.010
O	8.000	8.000	8.000	8.000	8.000	8.000	8.000
% An	8.2	1.7	1.2	2.6	1.4	1.3	1.7

Table F.2 continued...

	K92-5804-264 quartz monzonite grain 1 - core	K92-5804-264 quartz monzonite grain 1 - rim	K92-5804-264 quartz monzonite grain 2 - core	K92-5804-264 quartz monzonite grain 2 - rim
SiO_2	62.98	66.84	63.62	60.40
Al_2O_3	22.52	20.05	21.81	24.54
CaO	3.65	0.53	3.02	5.87
Na_2O	9.25	11.01	9.69	7.98
K_2O	0.08	0.19	0.12	0.11
Total	98.48	98.62	98.26	98.90
Si	2.815	2.956	2.846	2.703
Al (IV)	1.185-	1.044	1.150	1.294
Al (VI)	0.001	0.001	0.000	0.000
Ca	0.175	0.025	0.145	0.281
Na	0.802	0.944	0.841	0.692
K	0.005	0.011	0.007	0.006
O	8.000	8.000	8.000	8.000
% An	17.8	2.55	14.6	28.70

Table F.3 Electron microprobe analyses of late-stage vein biotite

	K91-3828-168	K91-3025-102	K91-3025-102	K91-3025-102	K91-3025-102
SiO_2	37.69	35.89	35.79	35.40	35.35
Al_2O_3	15.78	15.40	16.60	16.44	15.69
TiO_2	2.20	1.97	1.71	1.56	1.95
Fe_2O_3	21.28	19.45	17.95	18.21	19.58
FeO	0.00	0.00	0.00	0.00	0.00
MgO	11.82	12.59	13.25	13.12	13.18
MnO	0.00	0.00	0.11	0.09	0.10
CaO	0.05	0.11	0.07	0.13	0.00
Na_2O	0.00	0.30	0.25	0.33	0.25
K_2O	8.91	10.00	9.96	9.77	9.49
H_2O	4.19	4.07	4.09	4.06	4.08
Total	101.92	99.78	99.78	99.11	99.67
Si	3.180	2.641	2.620	2.612	2.599
Al (IV)	0.820	1.336	1.380	1.388	1.359
Al (VI)	0.762	0.000	0.052	0.041	0.000
Ti	0.141	0.109	0.094	0.087	0.108
Fe^{3+}	0.000	1.077	0.989	1.011	1.083
Fe^{2+}	0.000	0.000	0.000	0.000	0.000
Mg	1.498	1.381	1.446	1.443	1.444
Mn	0.000	0.000	0.007	0.006	0.006
Ca	0.005	0.009	0.005	0.010	0.000
Na	0.000	0.043	0.035	0.047	0.036
K	0.967	0.939	0.930	0.920	0.890
O	10.000	10.000	10.000	10.000	10.000
OH	2.000	2.000	2.000	2.000	2.000

Table F.4 Electron microprobe analyses of amphiboles in sample Ki92-6446-245

	Hornblende grain 1	Hornblende grain 1	Hornblende grain 1	Hornblende grain 2	Hornblende grain 2	Hornblende grain 2
SiO_2	41.48	41.48	41.48	43.31	43.31	43.31
Al_2O_3	15.98	15.98	15.98	13.86	13.86	13.86
TiO_2	0.16	0.16	0.16	0.25	0.25	0.25
Fe_2O_3	0.56	2.95	1.76	1.46	3.22	2.34
FeO	20.56	18.40	19.48	19.17	17.58	18.38
MgO	5.42	5.42	5.42	6.73	6.73	6.73
MnO	0.29	0.29	0.29	0.30	0.30	0.30
CaO	11.60	11.60	11.60	11.85	11.85	11.85
Na_2O	1.27	1.27	1.27	0.86	0.86	0.86
K_2O	0.37	0.37	0.37	0.40	0.40	0.40
H_2O	1.97	1.99	1.98	2.00	2.00	2.00
Total	99.66	99.91	99.79	100.19	100.36	100.28
Si	6.293	6.256	6.274	6.500	6.472	6.486
Al (IV)	1.707	1.744	1.726	1.500	1.528	1.514
Al (VI)	1.150	1.096	1.123	0.952	0.913	0.933
Ti	0.018	0.018	0.018	0.028	0.028	0.028
Fe^{3+}	0.064	0.335	0.200	0.165	0.362	0.264
Fe^{2+}	2.608	2.231	2.464	2.406	2.197	2.301
Mg	1.226	1.218	1.222	1.506	1.499	1.502
Mn	0.037	0.037	0.037	0.038	0.038	0.038
Ca	1.886	1.874	1.880	1.906	1.897	1.901
Na	0.374	0.371	0.372	0.250	0.249	0.250
K	0.072	0.071	0.071	0.077	0.076	0.076
O	22.000	22.000	22.000	22.000	22.000	22.000
OH	2.000	2.000	2.000	2.000	2.000	2.000

CURRICULUM VITAE

SUZANNE MARIE-ROSE IRMA MORASSE

Date of birth: November 4, 1957

EDUCATION

Ph D. Geology 1998
Queen's University, Kingston, Ontario
Thesis title: Geology, Structure and Timing of Gold Mineralization at the Kiena Deposit, Val d'Or, Québec

M.Sc. Geology 1988
Queen's University, Kingston, Ontario
Thesis title: Geological Setting and Evolution of the Lac Shortt Gold Deposit Waswanipi, Québec, Canada

B.Sc. Engineering Geology 1983
Université du Québec à Chicoutimi (U.Q.A.C.)
École Nationale Supérieure de Géologie et de Prospection Minière de Nancy, France (E.N.S.G.)
Thesis title: Pétrographie des Inclusions Fluides Liées au Filon de Quartz-Chalcopyrite du Canton de Scott, Chibougamau, Québec

AWARDS AND SCHOLARSHIPS

1994 Les Mines d'Or Kiena Limitée
1987 Reinhardt scholarship, Queen's University.
1985 Fonds pour la Formation de Chercheurs et l'Aide à la Recherche (F.C.A.R.).
1985 Falconbridge Copper/Minnova Inc., Lac Shortt Mine Division.
1982 Ministère de l'Éducation, Gouvernement de France.
1981 Canadian Society of Petroleum Geologists (C.S.P.G.)

EMPLOYMENT HISTORY

1990-1994	Placer Dome Canada Limited Research geologist
1988-1990	Homestake Mineral Development Company Exploration geologist
1985-1988	Department of Geological Sciences Queen's University Teaching assistant

1985-1986	Falconbridge Co. / Minnova Inc. Research geologist
1983-1985	Département des Sciences de La Terre, Université du Québec à Chicoutimi Research assistant
1980-1982	Ministère de l'Énergie et des Ressources du Québec Geologist
1978-1979	Société de Développement de la Baie James (S.D.B. J.) Geologist

PUBLICATIONS

Morasse, S., Wasteneys, H.A., Cormier, M., Helmstaedt, H., Mason, R., 1996, A pre-2686 Ma, intrusion-related gold deposit at the Kiena Mine, Val d'Or, Quebec, southern Abitibi Province - A reply: Economic Geology, v. 91, p. 807-812.

Morasse, S., Wasteneys, H.A., Cormier, M., Helmstaedt, H., Mason, R., 1996, A pre-2686 Ma, intrusion-related gold deposit at the Kiena Mine, Val d'Or, Quebec, southern Abitibi Province - A reply: Economic Geology, v. 91, p.801-803.

Morasse, S., Wasteneys, H.A., Cormier, M., Helmstaedt, H., Mason, R., 1995, A pre-2686 Ma, intrusion-related gold deposit at the Kiena Mine, Val d'Or, Quebec, southern Abitibi Province: Economic Geology, v.. 90, p.1310-1321.

Morasse S., Helmstaedt, H., and Mason, R., 1995, High-level intrusion-related gold mineralization at the Kiena Mine, Val d'Or, Quebec, southern Abitibi Subprovince: in "Precambrian 95", an International conference on Tectonic and Metallogeny of Early/Mid-Precambrian Orogenic Belts, Montreal, August 1995, Extended Abstract, p. 49

Morasse, S., Mason, R., Helmstaedt, H., and M. Cormier, 1995, Fracture-controlled alteration-mineralization at the Kiena Mine, Val d'Or, Quebec - Evidence for pre-2686 Ma epizonal Archean vein-gold: Geological Association of Canada Program with Abstracts, v. 20, p. A73.

Morasse, S., and Wasteneys, W., 1994, The chronology of deformation at the Kiena Mine and its implications on the timing of an early deformation event (D_1) in the Val D'Or area: Geological Association of Canada Program with Abstracts, v. 19, A 79.

Morasse, S., Wasteneys, H.A., Cormier, M., Helmstaedt, H., and R. Mason, 1993, La mine d'or Kiena: Minéralisation magmatique hydrothermale kénoréenne précoce dans la ceinture minérale de Val d'Or, sud-est de l'Abititi, Québec: In Séminaire Géoscientifique du Ministère de l'Énergie et des Ressources du Québec, DV 93-03,

p.56-60.

Morasse, S., Hodgson, C.J., Guha, J., and A. Coulombe, 1988, Oxidative, alkali-amphibole-bearing alteration and its relation to gold in the syenite-associated Lac Shortt deposit, Abitibi greenstone belt Quebec, Canada: In Bicentennial Gold'88 Extended Abstracts Poster Programme Volume I, Geological Society of Australia Abstract Series No.23, Melbourne 1988, p.92-94.

Morasse, S., Hodgson, C.J., Guha, J., and Coulombe A., 1986, Preliminary Report on the Geology of the Lac Shortt gold deposit, Desmaraisville Area, Quebec, Canada: In A.J. Macdonald ed., "Proceedings of Gold 86", an International Symposium on the Geology of Gold, Toronto 1986, p. 191-197.

Morasse, S., 1984, L'Étendue des applications des inclusions fluides en métallogénie: le procès du pour et du contre: Abstract Annales de l'A.C.F.A.S., v. 51, p. 311.

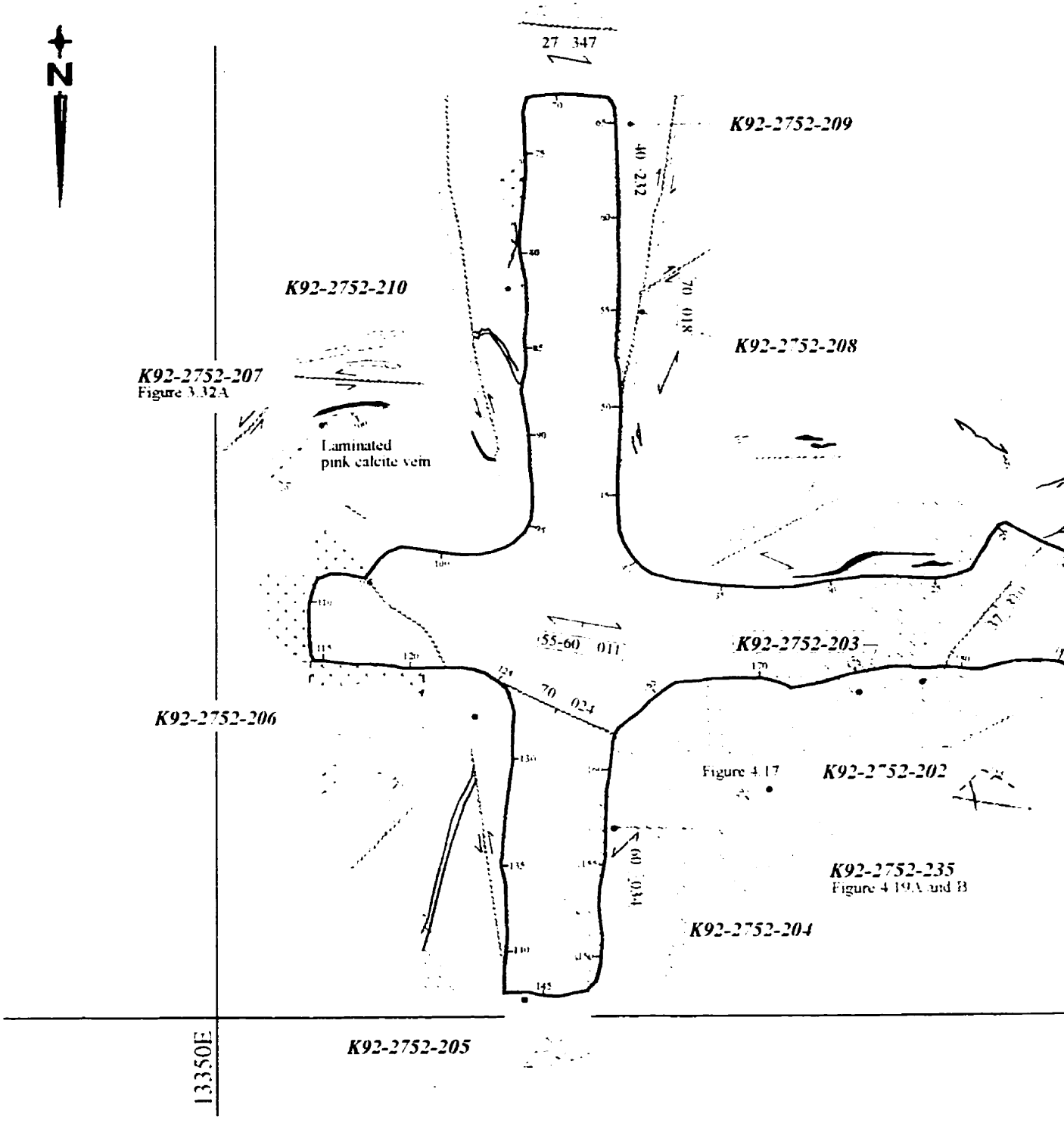
N
27 347
K92-2752-209
40 232
K92-2752-210
70 018
K92-2752-208
K92-2752-207
Figure 3.32A
Laminated
pink calcite vein
55-60 011
K92-2752-203
70 024
K92-2752-206
Figure 4.17
K92-2752-202
60 034
K92-2752-235
Figure 4.19A and B
K92-2752-204
K92-2752-205
13350E

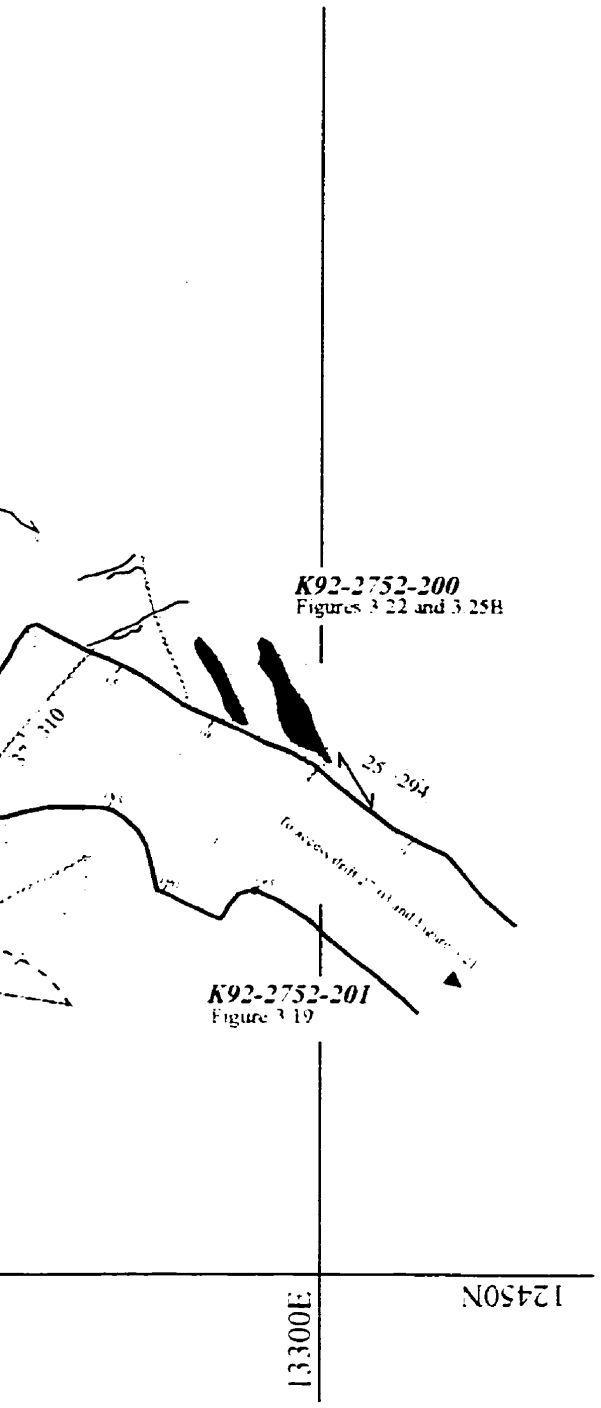

LEGEND

MAIN ORE ZONES (PART ALBITITE DIKES)

- Breccia 2
- Breccia 1
- Stwk Cb-Qz-Py(Po)±Ab-Au

INTRUSIVE ROCKS

- Albitite dike
- Intermineral granodiorite dike
- Intermineral feldspar porphyry dike

VOLCANIC ROCKS

- Schistose magnesian tholeiite (West)
- Schistose iron tholeiite (East)
- Pillowed magnesian tholeiite and flow top breccia
- Cb-Chl-Tc-(Ab) schist± boudinaged albitite dike inclusions (Dm-Qz stockwork vein-altered) - probable metakomatiite

STRUCTURAL SYMBOLS

- Carbonate-quartz ± albite extension veins
- 45 Main schistosity: S_n
- 28 Crenulation cleavage: S_{n+1}
- 65 Brittle-ductile, oblique slip fault
- Horizontal (or vertical) component of movement
- 40 Bedding and dip
- Stratigraphic younging direction
- 40 292 Dip - dip azimuth
- Fault gauge
- K92-2752-202 Sample number (see Appendix B)
- 215 Distance in metres along back face of ore drift

Horizontal display of vertical drift wall

LES MINES D'OR KENA LTEE.

INDEX MAP - PILLAR 2752

"A" ZONE

Mapped by S. Morasse

Date 08/1993

0m 2.5m 5m

S. Morasse 1997

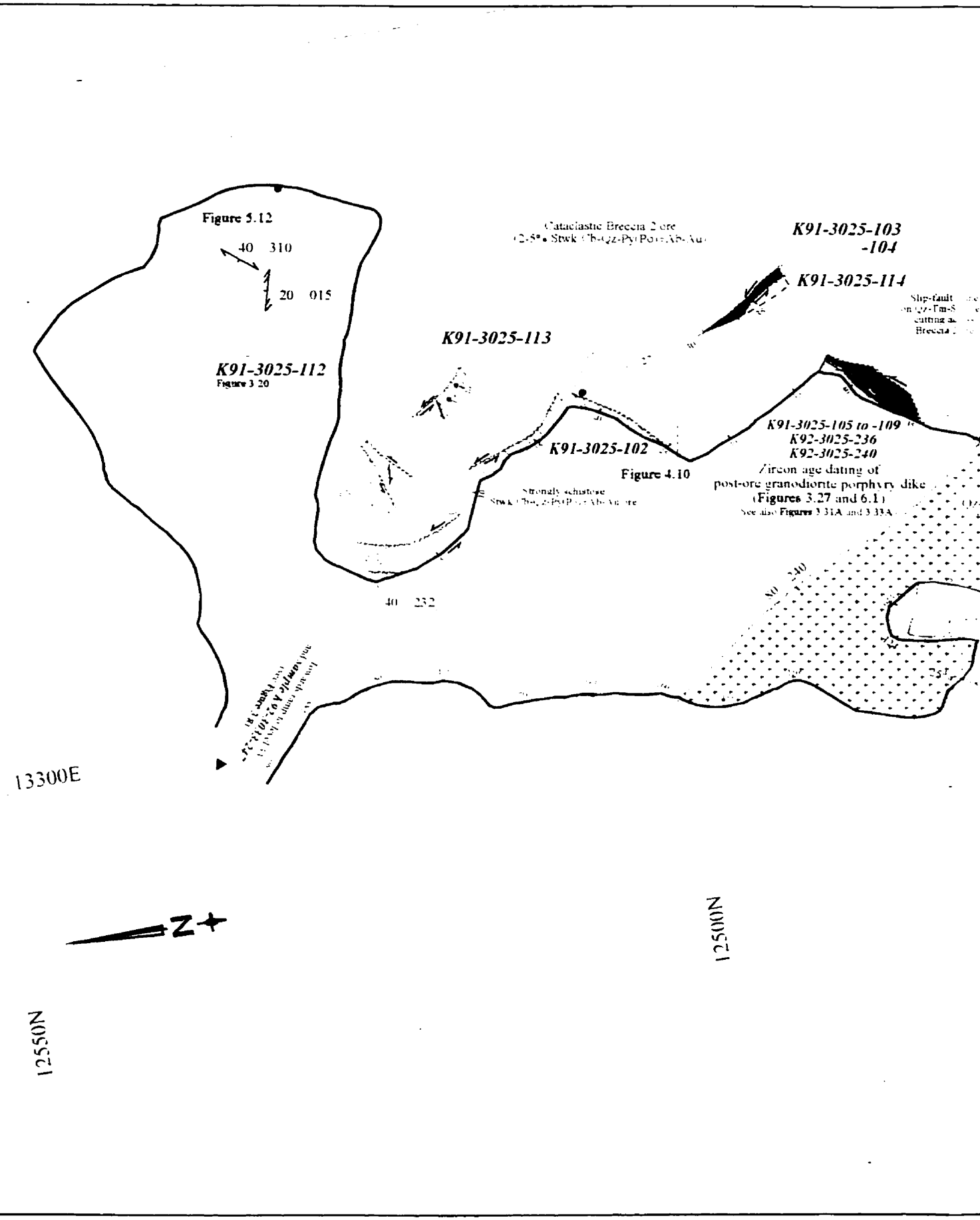

Geology, Structure and Gold Mineralization at the Kiena Deposit - Back pocket

12450N

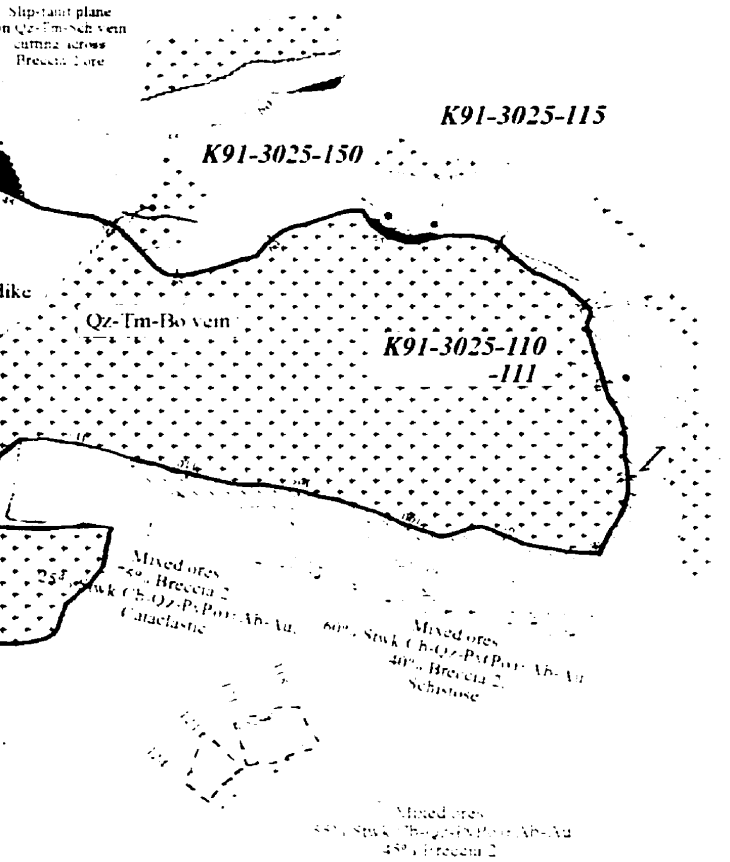

LEGEND

MAIN ORE ZONES (PART ALBITITE DIKES)

- Breccia 2
- Breccia 1
- Stwk Cb-Qz-Py(Po)±Ab-Au

INTRUSIVE ROCKS

- Albitite dike
- Intermineral granodiorite dike
- Intermineral feldspar porphyry dike

VOLCANIC ROCKS

- Schistose magnesian tholeiite (West)
- Schistose iron tholeiite (East)
- Pillowed magnesian tholeiite and flow top breccia
- Cb-Chl-Tc-(Ab) schist± boudinaged albitite dike inclusions (Dm-Qz stockwork vein-altered) - probable metakomatiite

STRUCTURAL SYMBOLS

- Carbonate-quartz ± albite extension veins
- 45 Main schistosity: S_1
- 28 Crenulation cleavage: S_{n+1}
- 65 Brittle-ductile, oblique slip fault
- Horizontal (or vertical) component of movement
- 40 Bedding and dip
- Stratigraphic younging direction
- 41 232 Dip - dip azimuth
- Fault gauge
- K92-2752-202 Sample number (see Appendix B)
- 15 Distance in metres along back face of ore drift
- Horizontal display of vertical drift wall

LES MINES D'OR KENA LTEE.

INDEX MAP - STOPE 3025

"A" ZONE

Mapped by S. Morasse

Date 07/1991

0m 2.5m 5m

S. Morasse 1997

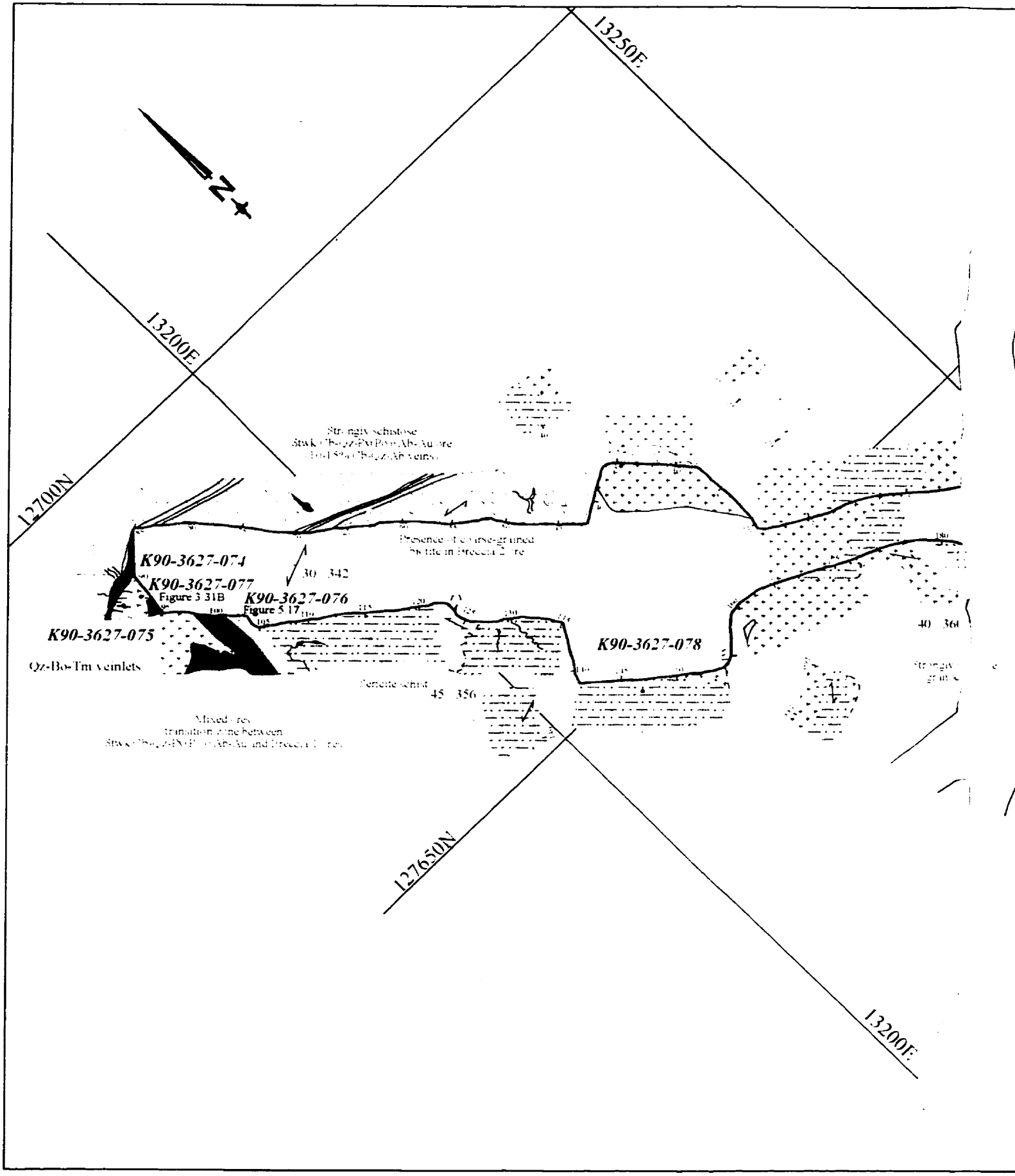

Geology, Structure and Gold Mineralization at the Kiena Deposit - Back pocket

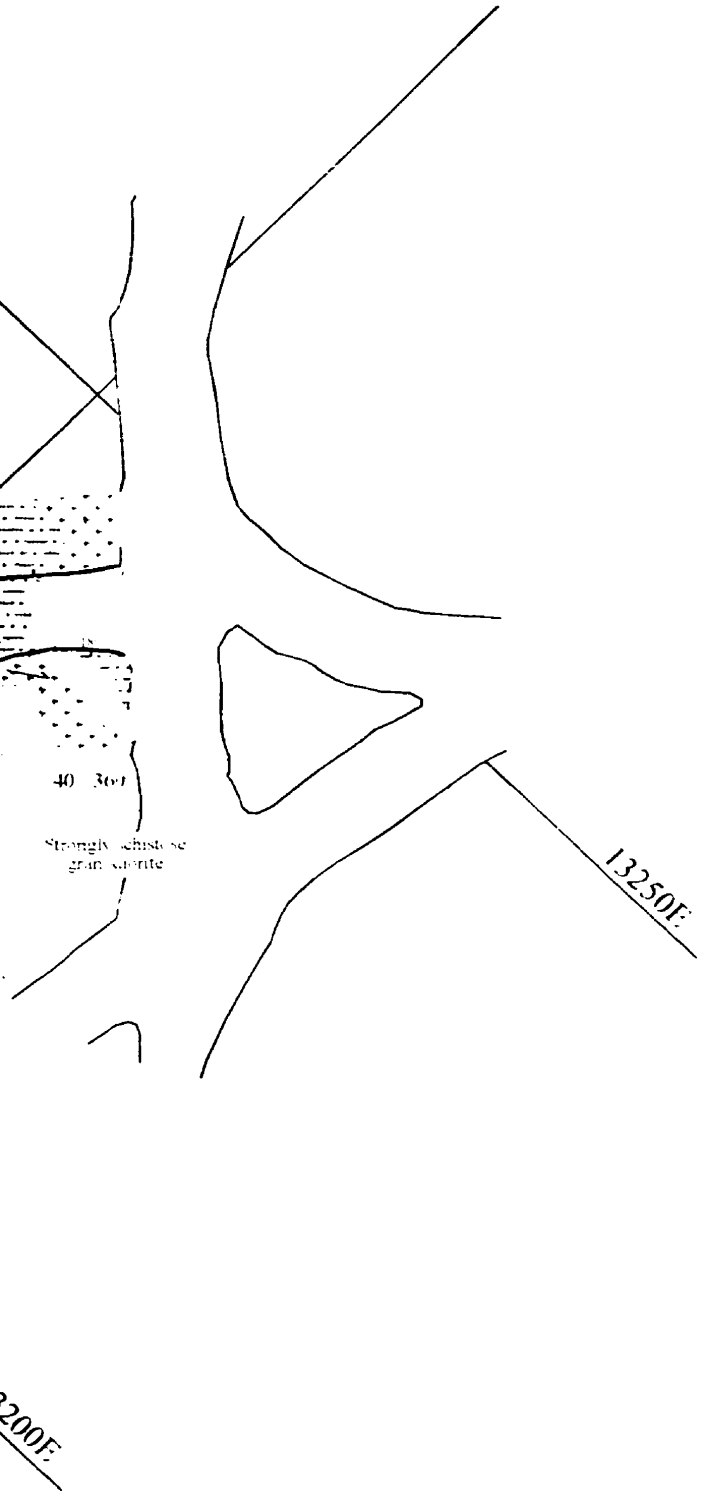

LEGEND

MAIN ORE ZONES (PART ALBITITE DIKES)

- Breccia 2
- Breccia 1
- Stwk Cb-Qz-Py(Po)±Ab-Au

INTRUSIVE ROCKS

- Albitite dike
- Intermineral granodiorite dike
- Intermineral feldspar porphyry dike

VOLCANIC ROCKS

- Schistose magnesian tholeiite (West)
- Schistose iron tholeiite (East)
- Pillowed magnesian tholeiite and flow top breccia
- Cb-Chl-Tc-(Ab) schist± boudinaged albitite dike inclusions (Dm-Qz stockwork vein-altered) - probable metakomatiite

STRUCTURAL SYMBOLS

- Carbonate-quartz = albite extension veins
- 45 Main schistosity: S_n
- 28 Crenulation cleavage: S_{n+1}
- 65 Brittle-ductile, oblique slip fault
- Horizontal (or vertical) component of movement
- 40 Bedding and dip
- Stratigraphic younging direction
- Dip - dip azimuth
- Fault gauge
- K92-2752-202 Sample number (see Appendix B)
- Distance in metres along back face of ore drift

Horizontal display of vertical drift wall

LES MINES D'OR KENA LTEE.

INDEX MAP - STOPE 3627

"J" ZONE

Mapped by S. Morasse

Date 02/1990

0m 2.5m 5m

S. Morasse 1997

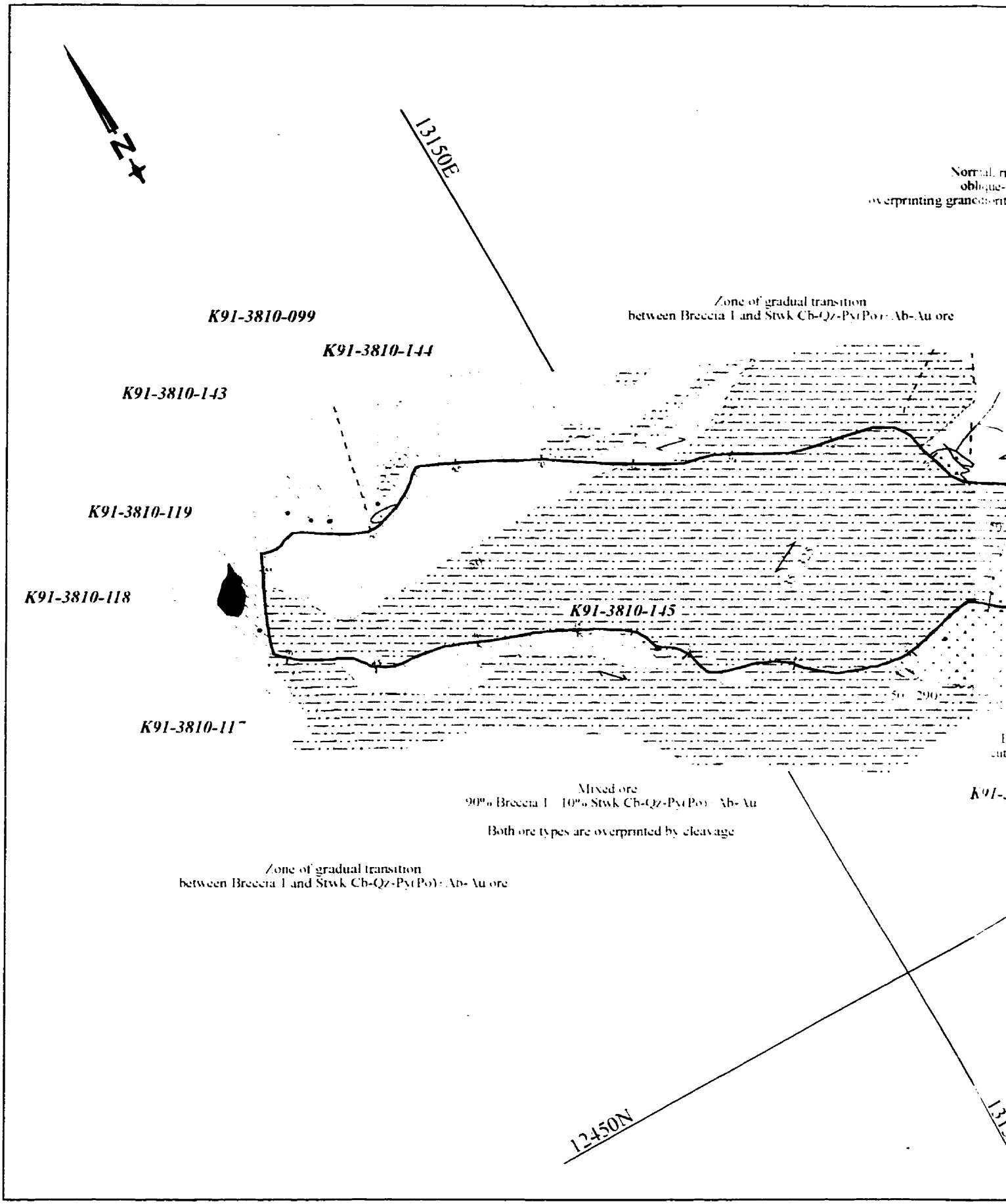

Geology, Structure and Gold Mineralization at the Kiena Deposit - Back pocket

Normal, right-lateral
oblique-slip fault
granodiorite dike Breccia 1 contact

Mineralised carbonate-quartz-albite-pyrite
stockwork veins part or the deposit's
alteration halo of 0.34-3 g t Au

Deposit's main cleavage
is axial planar to
folded cb-qz-ab stwk veins (see Figure 3.6)

ore

K91-3810-142

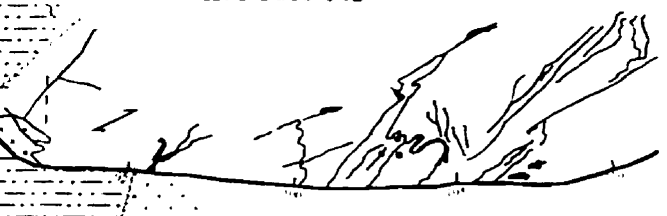

K91-3810-120

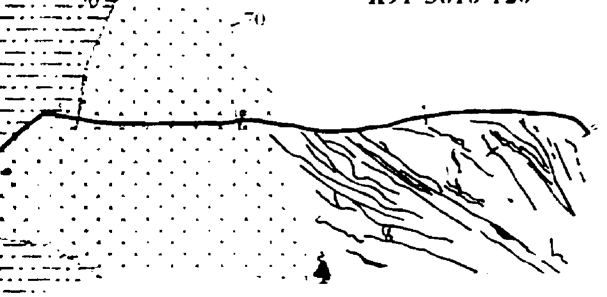

Highly strained granodiorite dike
cut by deposit's main schistosity (Sn)

K91-3810-116

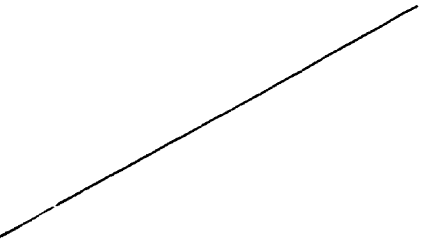

Cb-qz-ab-py stwk veins
overprinted by stockwork of
chlorite-biotite-magnetite-(stilpnomelane) veinlets

13150E

LEGEND

MAIN ORE ZONES (PART ALBITITE DIKES)

- Breccia 2
- Breccia 1
- Stwk Cb-Qz-Py(Po)±Ab-Au

INTRUSIVE ROCKS

- Albitite dike
- Intermineral granodiorite dike
- Intermineral feldspar porphyry dike

VOLCANIC ROCKS

- Schistose magnesian tholeiite (West)
- Schistose iron tholeiite (East)
- Pillowed magnesian tholeiite and flow top breccia
- Cb-Chl-Tc-(Ab) schist± boudinaged albitite dike inclusions (Dm-Qz stockwork vein-altered) - probable metakomatiite

STRUCTURAL SYMBOLS

- Carbonate-quartz ± albite extension veins
- 45 Main schistosity: S_n
- 28 Crenulation cleavage: S_{n+1}
- 65 Brittle-ductile, oblique slip fault
- Horizontal (or vertical) component of movement
- 40 Bedding and dip
- Stratigraphic younging direction
- 41 232 Dip - dip azimuth
- Fault gauge
- K92-2752-202 Sample number (see Appendix B)
- 15 Distance in metres along back face of ore drift
- Horizontal display of vertical drift wall

LES MINES D'OR KENA LTEE.

INDEX MAP - STOPE 3810

"B" ZONE

Mapped by S. Morasse

Date 07 1991

0m 2.5m 5m

S. Morasse 199

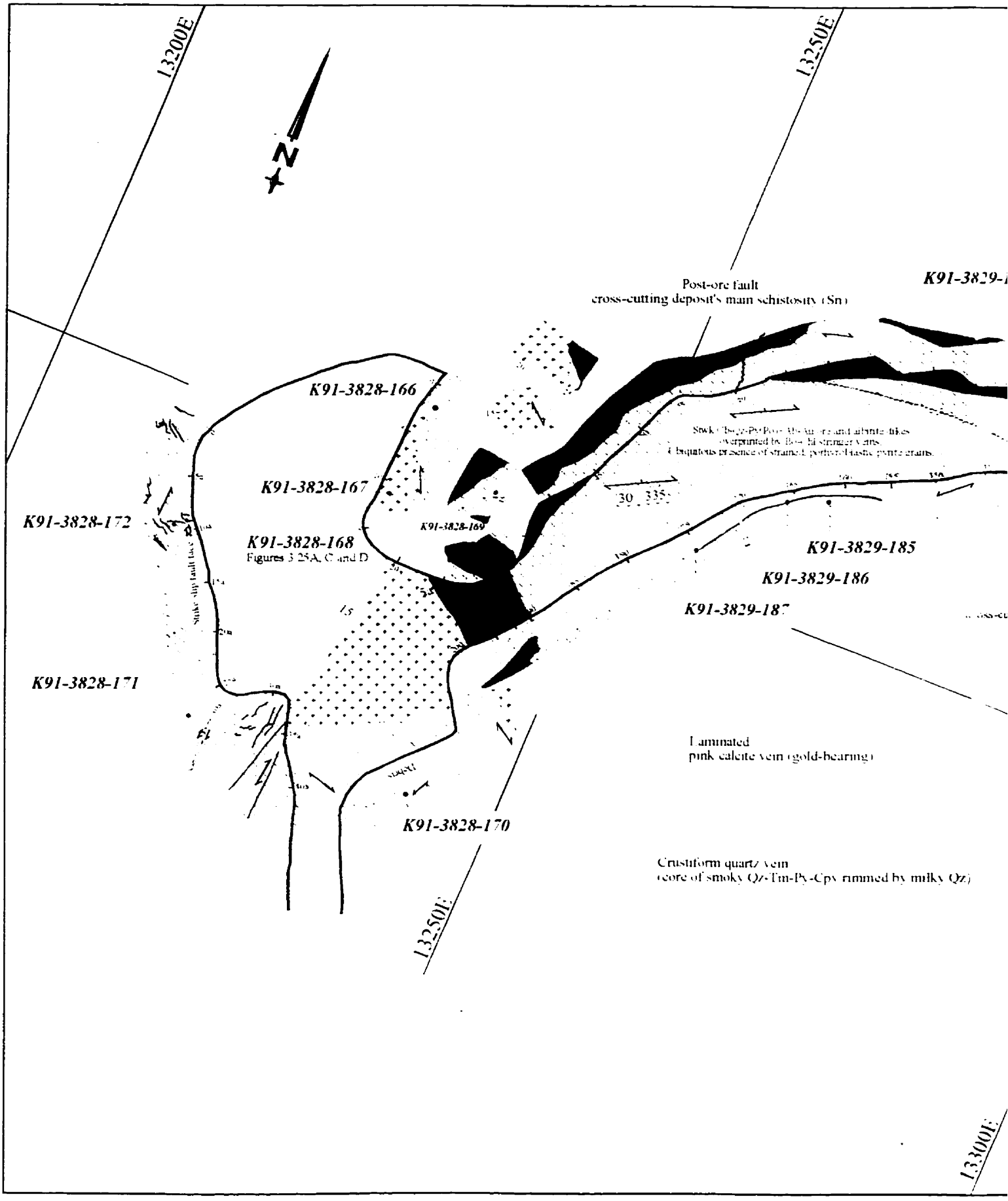

Geology, Structure and Gold Mineralization at the Kiena Deposit - Back pocket

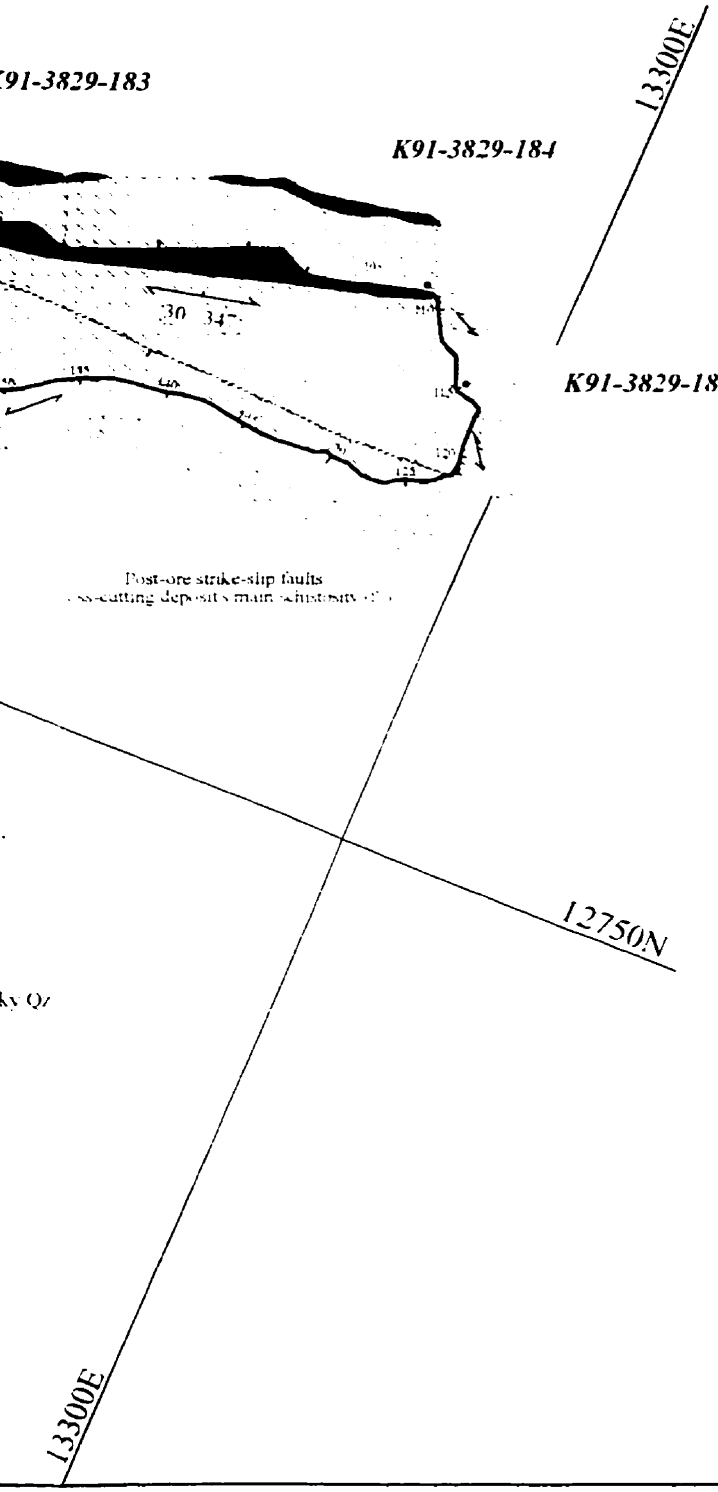

LEGEND

MAIN ORE ZONES (PART ALBITITE DIKES)

- Breccia 2
- Breccia 1
- Stwk Cb-Qz-Py(Po)±Ab-Au

INTRUSIVE ROCKS

- Albitite dike
- Intermineral granodiorite dike
- Intermineral feldspar porphyry dike

VOLCANIC ROCKS

- Schistose magnesian tholeiite (West)
- Schistose iron tholeiite (East)
- Pillowed magnesian tholeiite and flow top breccia
- Cb-Chl-Tc-(Ab) schist± boudinaged albitite dike inclusions (Dm-Qz stockwork vein-altered) - probable metakomatiite

STRUCTURAL SYMBOLS

- Carbonate-quartz ± albite extension veins
- 45 Main schistosity: S_n
- 28 Crenulation cleavage: S_{n+1}
- 65 Brittle-ductile, oblique slip fault
- Horizontal (or vertical) component of movement
- 40 Bedding and dip
- Stratigraphic younging direction
- Dip - dip azimuth
- Fault gauge
- K92-2752-202 Sample number (see Appendix B)
- Distance in metres along back face of ore drift

Horizontal display of vertical drift wall

LES MINES D'OR KENA LTEE.

INDEX MAP - STOPES 3828 & 3829

"K" and "L" ZONES

Mapped by: S. Morasse

Date: OCT 1991

0m 2.5m 5m

S. Morasse 1997

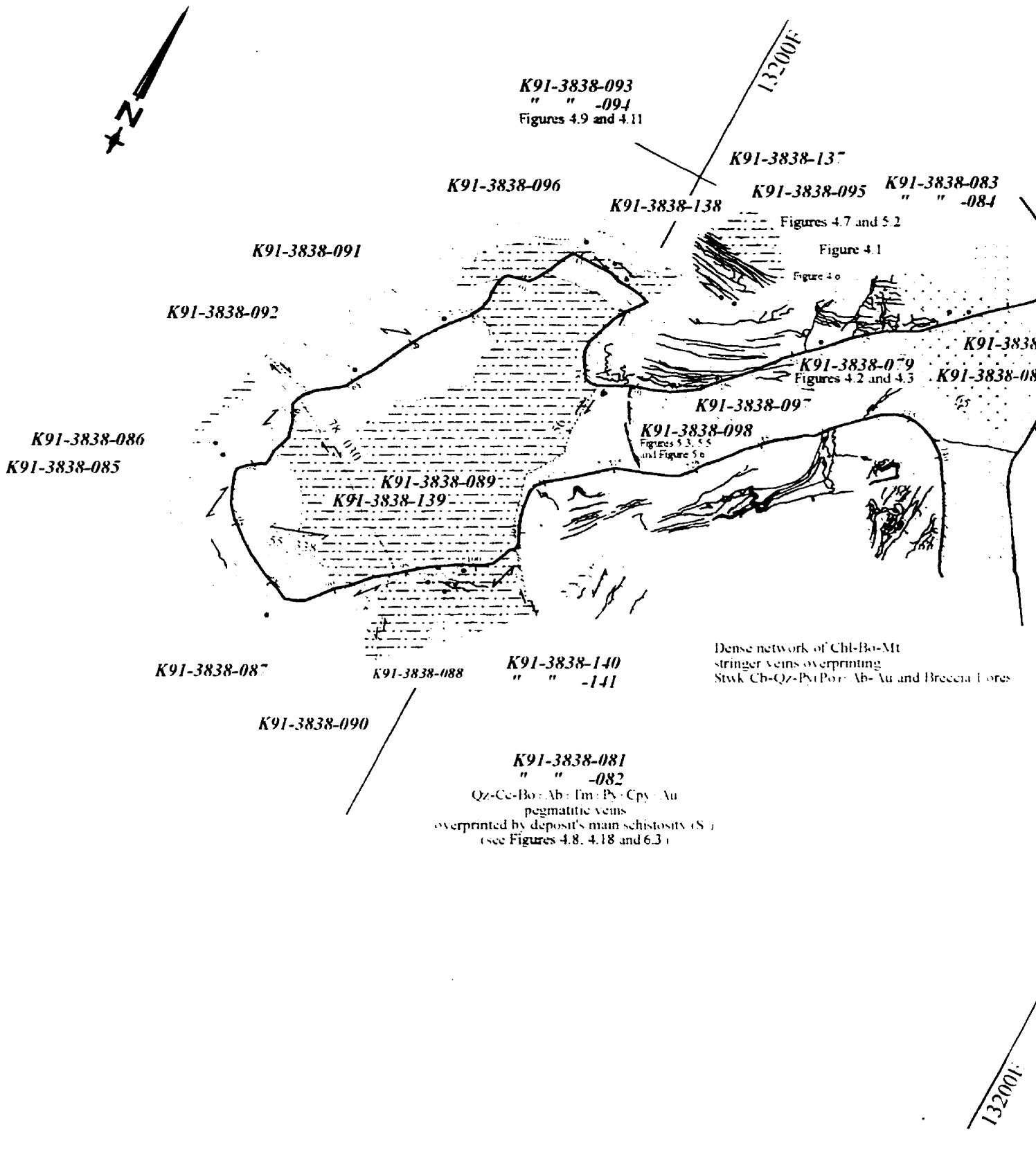
K91-3838-093
" " -094
Figures 4.9 and 4.11
13200E
K91-3838-137
K91-3838-096
K91-3838-095
K91-3838-083
" " -084
K91-3838-138
Figures 4.7 and 5.2
Figure 4.1
K91-3838-091
K91-3838-092
K91-3838-079
Figures 4.2 and 4.3
K91-3838-097
K91-3838-098
Figures 5.3, 5.5
and Figure 5.6
K91-3838-086
K91-3838-085
K91-3838-089
K91-3838-139
K91-3838-087
K91-3838-088
K91-3838-140
" " -141
Dense network of Chl-Bo-Mt
stringer veins overprinting
Stwk Ch-Qz-Py±Po±Ab-Au and Breccia Lores
K91-3838-090
K91-3838-081
" " -082
Qz-Ce-Bo±Ab±Tm±Py±Cpy±Au
pegmatitic veins
overprinted by deposit's main schistosity (S1)
(see Figures 4.8, 4.18 and 6.3)
13200E

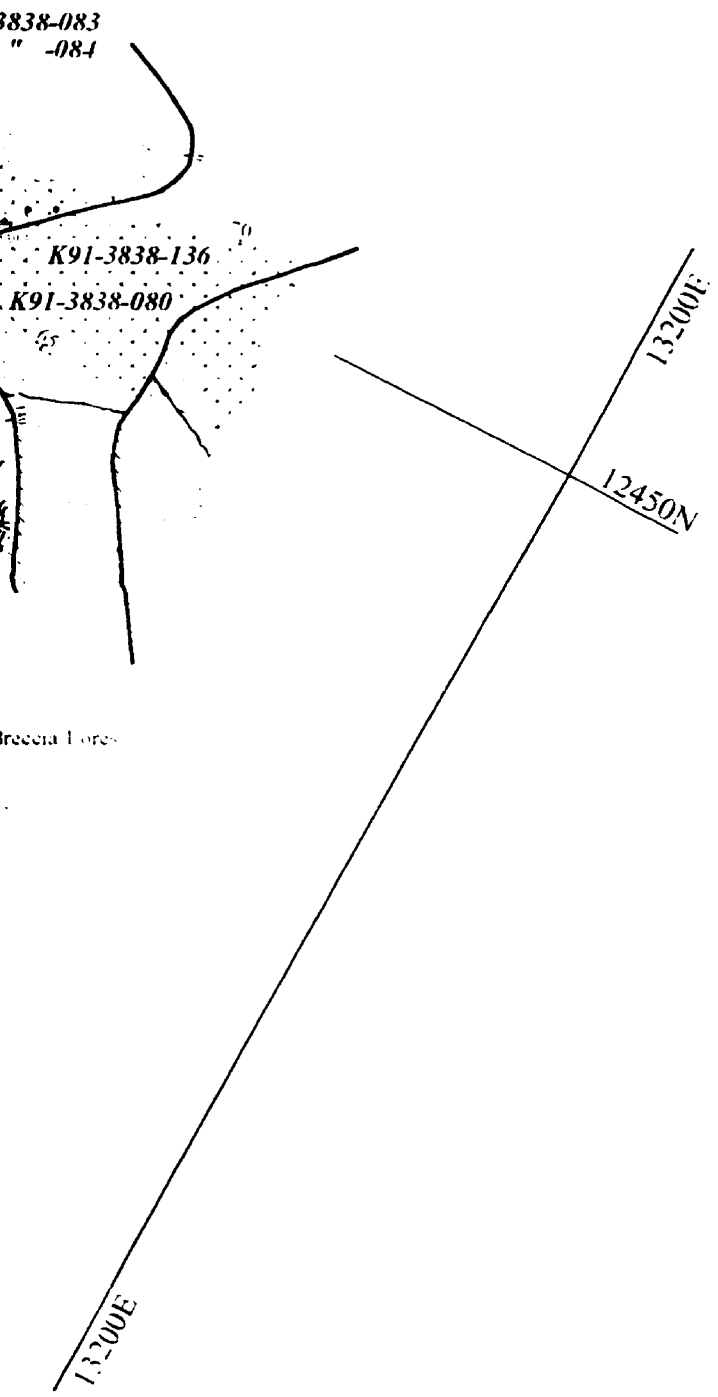

LEGEND

MAIN ORE ZONES (PART ALBITITE DIKES)

- Breccia 2
- Breccia 1
- Stwk Cb-Qz-Py(Po)±Ab-Au

INTRUSIVE ROCKS

- Albitite dike
- Intermineral granodiorite dike
- Intermineral feldspar porphyry dike

VOLCANIC ROCKS

- Schistose magnesian tholeiite (West)
- Schistose iron tholeiite (East)
- Pillowed magnesian tholeiite and flow top breccia
- Cb-Chl-Tc-(Ab) schist± boudinaged albitite dike inclusions (Dm-Qz stockwork vein-altered) - probable metakomatiite

STRUCTURAL SYMBOLS

- Carbonate-quartz ± albite extension veins
- 45 Main schistosity: S_n
- 28 Crenulation cleavage: S_{n+1}
- 65 Brittle-ductile, oblique slip fault
- Horizontal (or vertical) component of movement
- 40 Bedding and dip
- Stratigraphic younging direction
- Dip - dip azimuth
- Fault gauge
- K92-3752-202 Sample number (see Appendix B)
- Distance in metres along back face of ore drift

Horizontal display of vertical drift wall

LES MINES D'OR KENA LTEE.

INDEX MAP - STOPE 3838

Junction of "B" and "C" ZONES

Mapped by S. Morasse

Date Oct 1996

0m 2.5m 5m

S. Morasse 1997

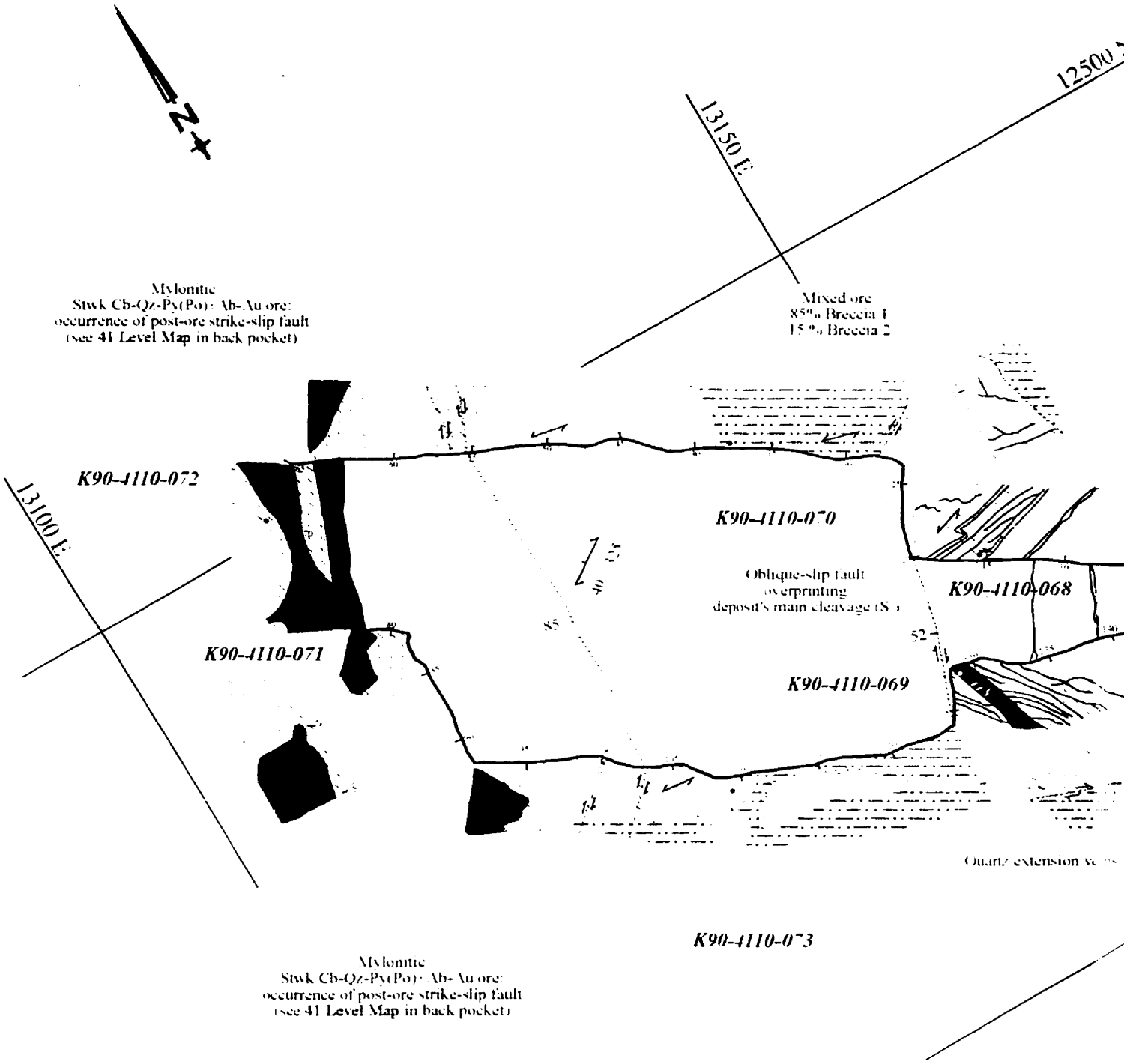

Geology, Structure and Gold Mineralization at the Kiena Deposit - Back pocket

LEGEND

MAIN ORE ZONES (PART ALBITITE DIKES)

- Breccia 2
- Breccia 1
- Stwk Cb-Qz-Py(Po)=Ab-Au

INTRUSIVE ROCKS

- Albitite dike
- Intermineral granodiorite dike
- Intermineral feldspar porphyry dike

VOLCANIC ROCKS

- Schistose magnesian tholeiite (West)
- Schistose iron tholeiite (East)
- Pillowed magnesian tholeiite and flow top breccia
- Cb-Chl-Tc-(Ab) schist± boudinaged albitite dike inclusions (Dm-Qz stockwork vein-altered) - probable metakomatiite

STRUCTURAL SYMBOLS

- Carbonate-quartz = albite extension veins
- 45 Main schistosity : S_n
- 29 Crenulation cleavage S_{n+1}
- 65 Brittle-ductile, oblique slip fault
- Horizontal (or vertical) component of movement
- 40 Bedding and dip
- Stratigraphic younging direction
- Dip - dip azimuth
- Fault gauge
- K92-2752-202 Sample number (see Appendix B)
- Distance in metres along back face of ore drift

Horizontal display of vertical drift wall

LES MINES D'OR KENA LTEE.

INDEX MAP -STOPE 4110

"B" ZONE

Mapped by S. Morasse

Date OCT 1996

0m 2.5m 5m

S. Morasse 1997

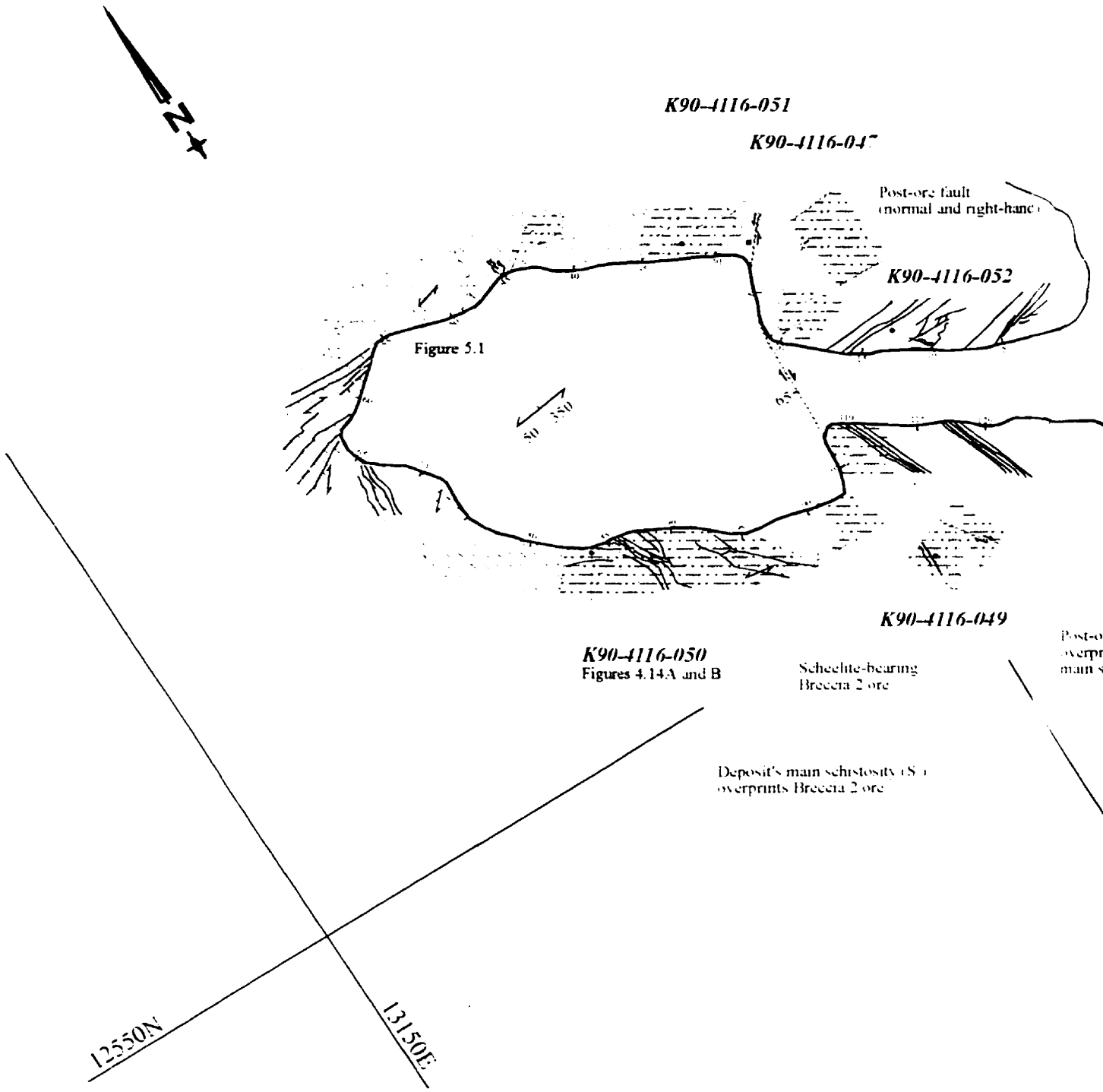
N
K90-4116-051
K90-4116-047
Post-ore fault
(normal and right-hand
K90-4116-052
Figure 5.1
K90-4116-049
K90-4116-050
Figures 4.14A and B
Scheelite-bearing
Breccia 2 ore
Deposit's main schistosity (S
overprints Breccia 2 ore
12550N
13150E

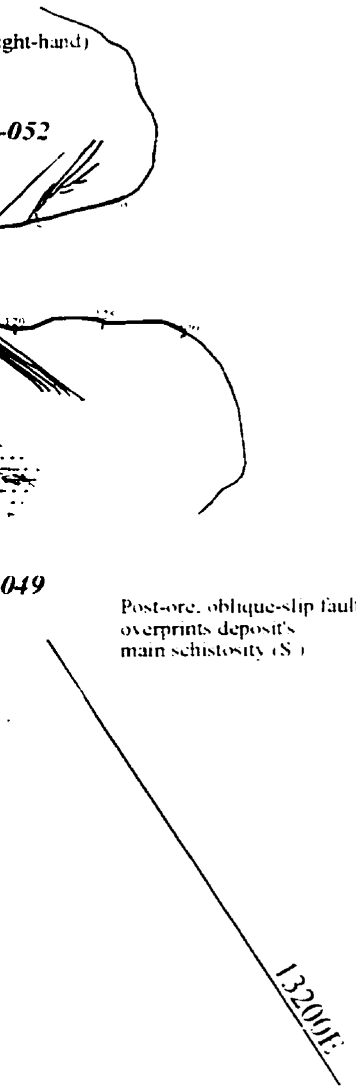

LEGEND

MAIN ORE ZONES (PART ALBITITE DIKES)

- Breccia 2
- Breccia 1
- Stwk Cb-Qz-Py(Po)±Ab-Au

INTRUSIVE ROCKS

- Albitite dike
- Intermineral granodiorite dike
- Intermineral feldspar porphyry dike

VOLCANIC ROCKS

- Schistose magnesian tholeiite (West)
- Schistose iron tholeiite (East)
- Pillowed magnesian tholeiite and flow top breccia
- Cb-Chl-Tc-(Ab) schist± boudinaged albitite dike inclusions (Dm-Qz stockwork vein-altered) - probable metakomatiite

STRUCTURAL SYMBOLS

- Carbonate-quartz ± albite extension veins
- Breccia 2 veins
- 45 Main schistosity: S_n
- 28 Crenulation cleavage: S_{n+1}
- 66 Brittle-ductile, oblique slip fault
- Horizontal (or vertical) component of movement
- 40 Bedding and dip
- Stratigraphic younging direction
- 232 Dip - dip azimuth
- Fault gauge
- K92-2752-202 Sample number (see Appendix B)
- 15 Distance in metres along back face of ore drift
- Horizontal display of vertical drift wall

LES MINES D'OR KIENA LTEE.

INDEX MAP - STOPE 4116

"B" ZONE

Mapped by S. Morasse

Date OCT 1990

0m 2.5m 5m

S. Morasse 1997

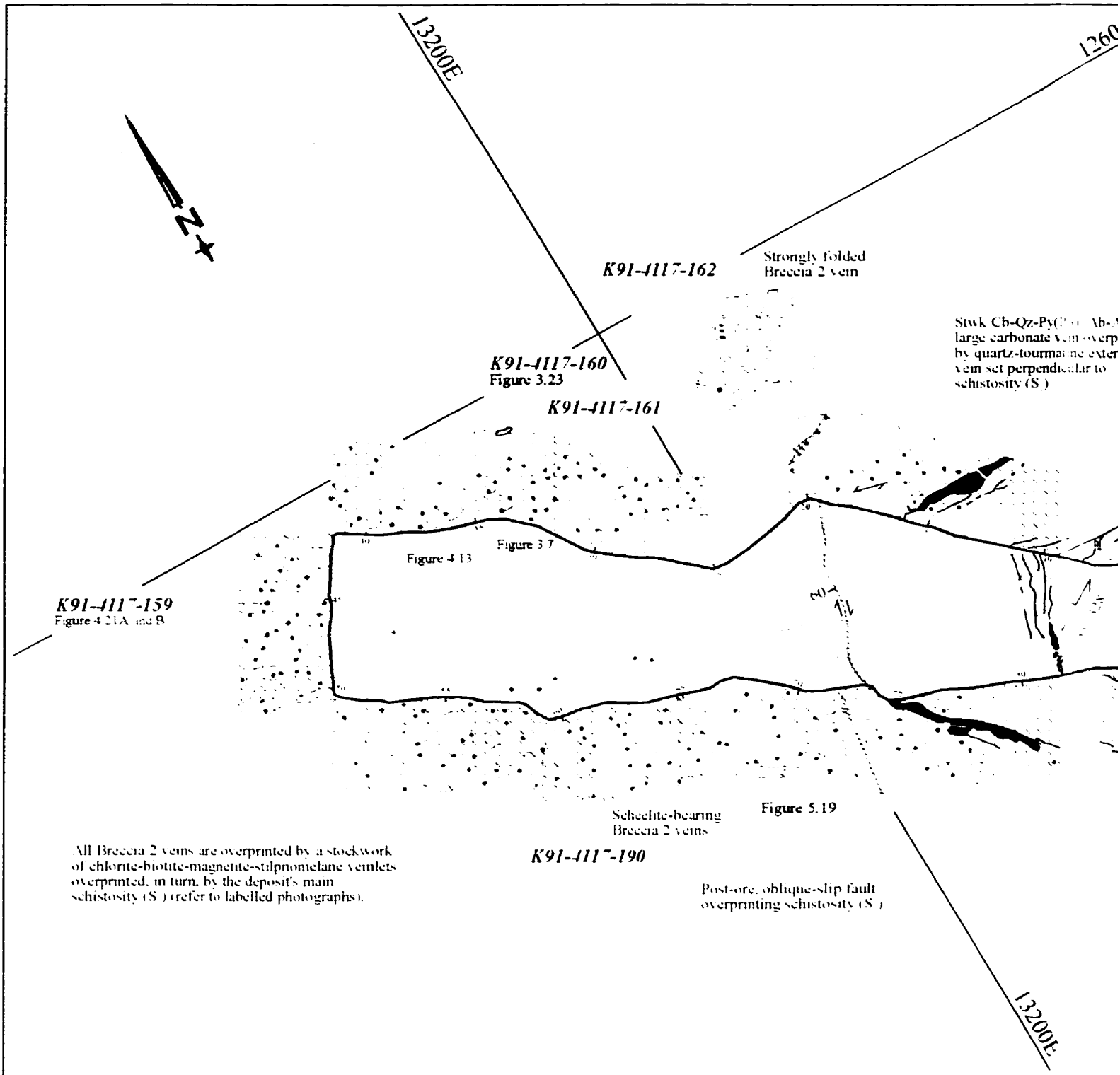
13200E
1260
N-Z
K91-4117-162
Strongly folded
Breccia 2 vein
Stwk Cb-Qz-Py(
large carbonate
by quartz-tourmaline
vein set perpendicular to
schistosity (S)
K91-4117-160
Figure 3.23
K91-4117-161
Figure 3 7
Figure 4 13
K91-4117-159
Figure 4 21A and B
Figure 5.19
Scheelite-bearing
Breccia 2 veins
All Breccia 2 veins are overprinted by a stockwork
of chlorite-biotite-magnetite-stilpnomelane veinlets
overprinted, in turn, by the deposit's main
schistosity (S) (refer to labelled photographs).
K91-4117-190
Post-ore, oblique-slip fault
overprinting schistosity (S)
13200E

12600N

wk Cb-Qz-Py(Po)±Ab-Au ore:
ge carbonate vein overprinted
quartz-tourmaline extension
in set perpendicular to
histosity (S

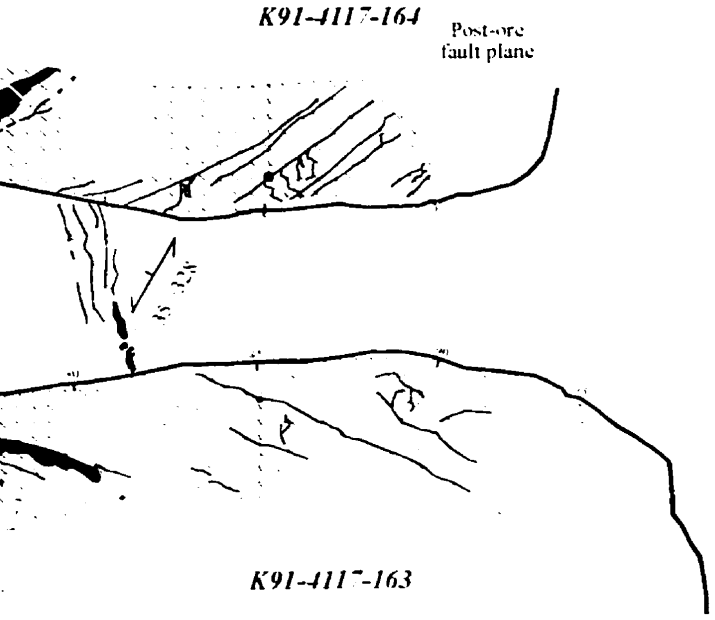

13200E

LEGEND

MAIN ORE ZONES (PART ALBITITE DIKES)

- Breccia 2
- Breccia 1
- Stwk Cb-Qz-Py(Po)±Ab-Au

INTRUSIVE ROCKS

- Albitite dike
- Intermineral granodiorite dike
- Intermineral feldspar porphyry dike

VOLCANIC ROCKS

- Schistose magnesian tholeiite (West)
- Schistose iron tholeiite (East)
- Pillowed magnesian tholeiite and flow top breccia
- Cb-Chl-Tc-(Ab) schist= boudinaged albitite dike inclusions (Dm-Qz stockwork vein-altered) - probable metakomatiite

STRUCTURAL SYMBOLS

- Carbonate-quartz = albite extension veins
- Breccia 2 veins with related disseminated pyrite
- 45 Main schistosity: S_1
- 28 Crenulation cleavage: S_{n+1}
- 65 Brittle-ductile, oblique slip fault
- Horizontal (or vertical) component of movement
- 40 Bedding and dip
- Stratigraphic younging direction
- Dip - dip azimuth
- Fault gauge
- K92-2752-202 Sample number (see Appendix B)
- Distance in metres along back face of ore drift
- Horizontal display of vertical drift wall

LES MINES D'OR KENA LTEE.

INDEX MAP - PILLAR 4117

"B" ZONE

Mapped by S. Morasse

Date Oct 1994

0m 2.5m 5m

S. Morasse 1997

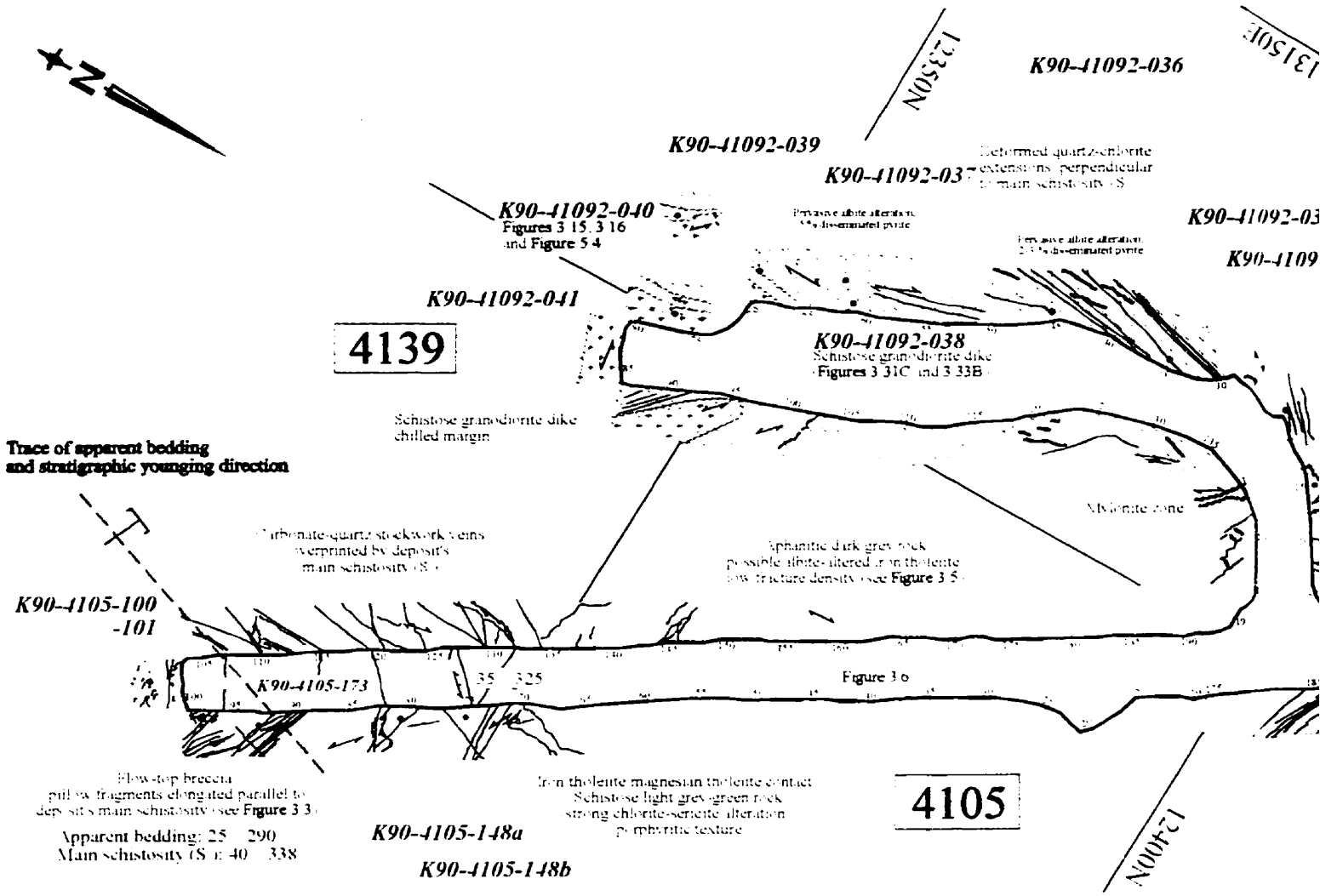

LEGEND

MAIN ORE ZONES (PART ALBITITE DIKES)

- Breccia 2
- Breccia 1
- Stwk Cb-Qz-Py(Po)±Ab-Au

INTRUSIVE ROCKS

- Albitite dike
- Intermineral granodiorite dike
- Intermineral feldspar porphyry dike

VOLCANIC ROCKS

- Schistose magnesian tholeiite (West)
- Schistose iron tholeiite (East)
- Pillowed magnesian tholeiite and flow top breccia
- Cb-Chl-Tc-(Ab) schist± boudinaged albitite dike inclusions (Dm-Qz stockwork vein-altered) - probable metakomatiite

STRUCTURAL SYMBOLS

- Carbonate-quartz ± albite extension veins
- 45 Main schistosity: S_1
- 28 Crenulation cleavage: S_2
- 65 Brittle-ductile, oblique slip fault
- Horizontal (or vertical) component of movement
- 40 Bedding and dip
- Stratigraphic younging direction
- 40 232 Dip - dip azimuth
- Fault gauge

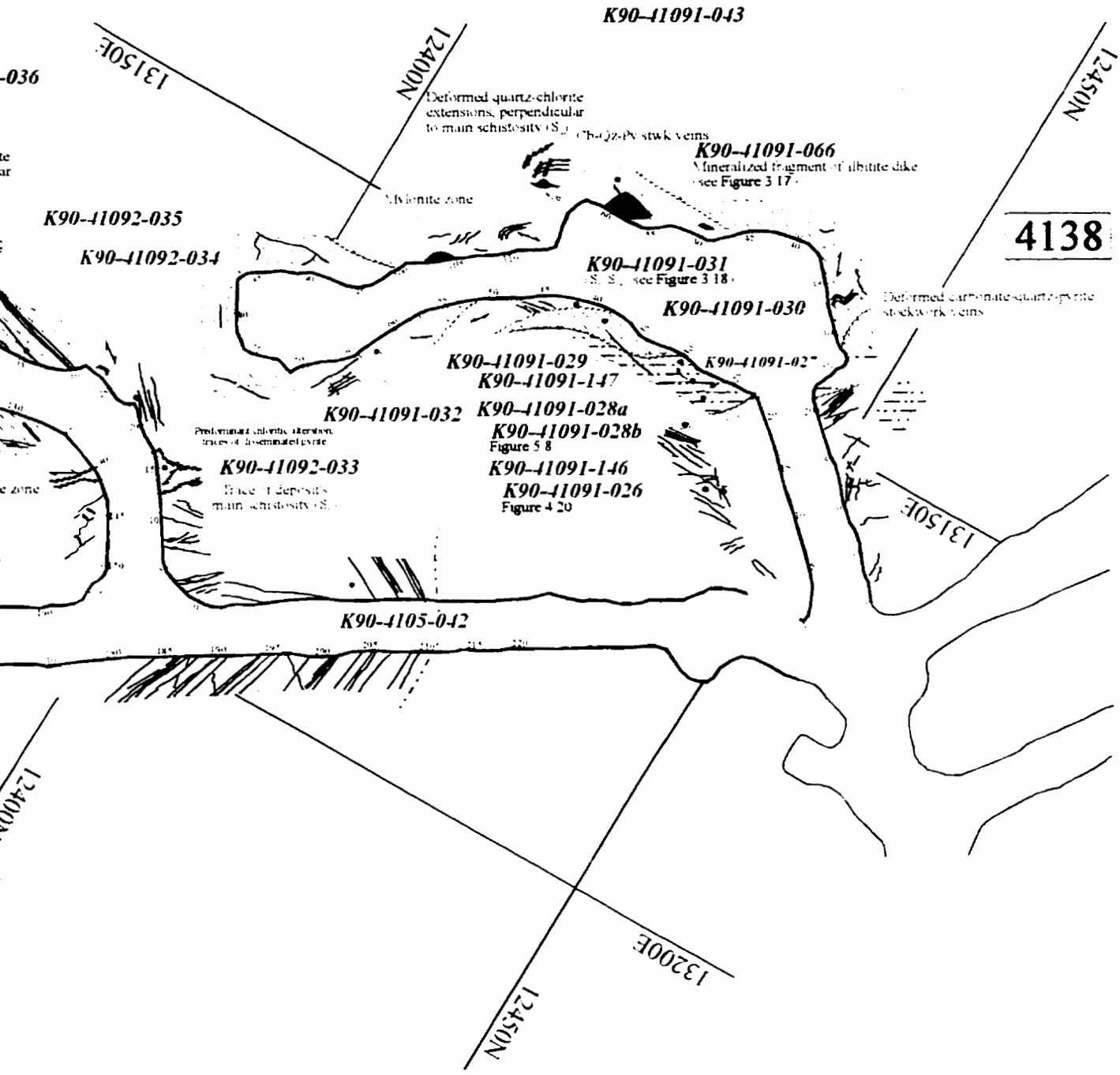

veins

of movement

Moderately strained pillow fragments

K92-2752-202 Sample number (see Appendix B)

15 Distance in metres along back face of ore drift

Horizontal display of vertical drift wall

LES MINES D'OR KENA LTEE.

INDEX MAP - STOPES 4138-39 & ACCESS DRIFT 4105

ZONE

Mapped by: S. Morasse

Date:

0m 2.5m 5m

S. Morasse 1997

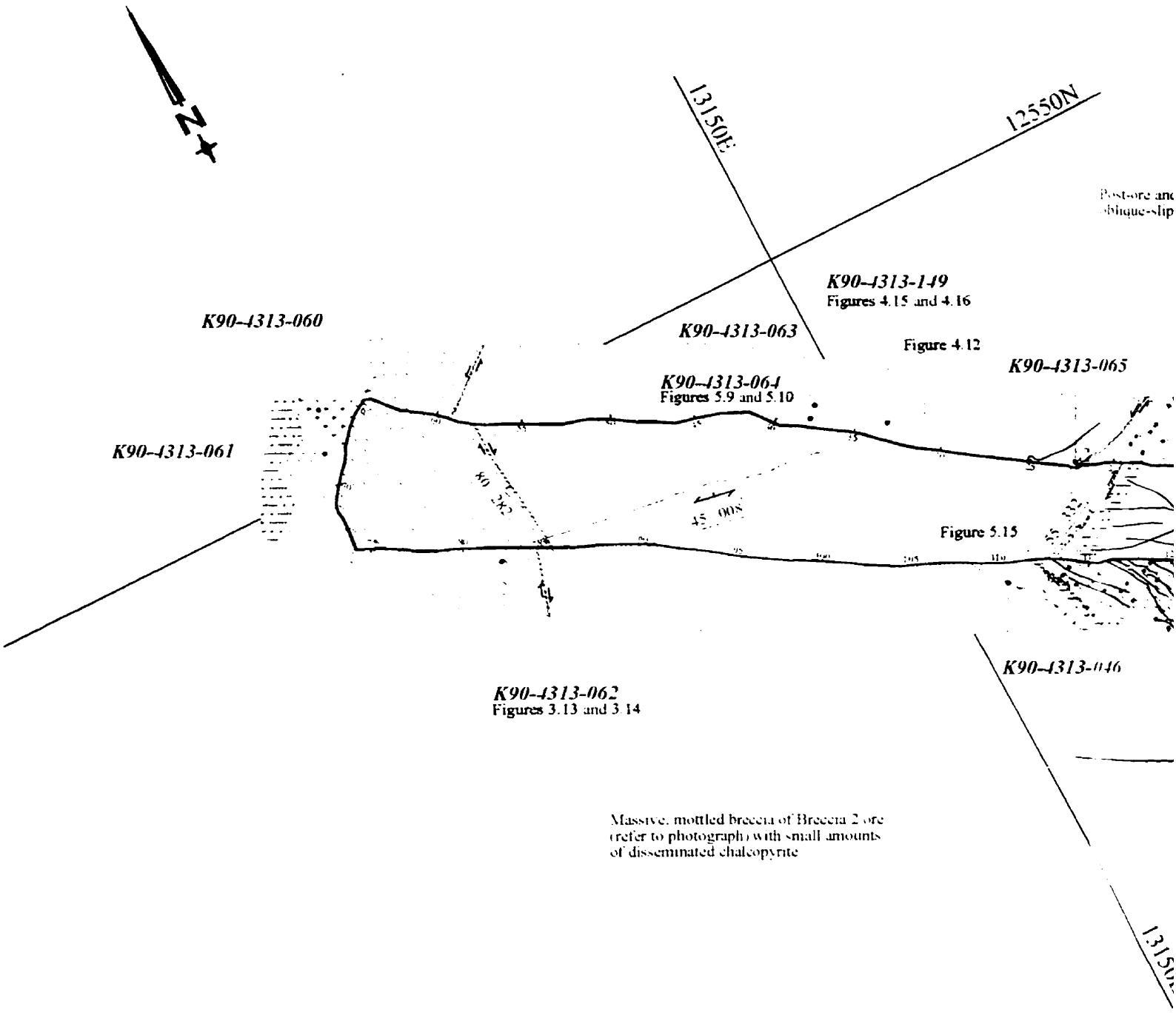
N
13150E
12550N
K90–4313-149
Figures 4.15 and 4.16
K90–4313-060
K90–4313-063
Figure 4.12
K90–4313-065
K90–4313-064
Figures 5.9 and 5.10
K90–4313-061
45° 008
Figure 5.15
K90–4313-046
K90–4313-062
Figures 3.13 and 3.14
Massive, mottled breccia of Breccia 2 ore (refer to photograph) with small amounts of disseminated chalcopyrite

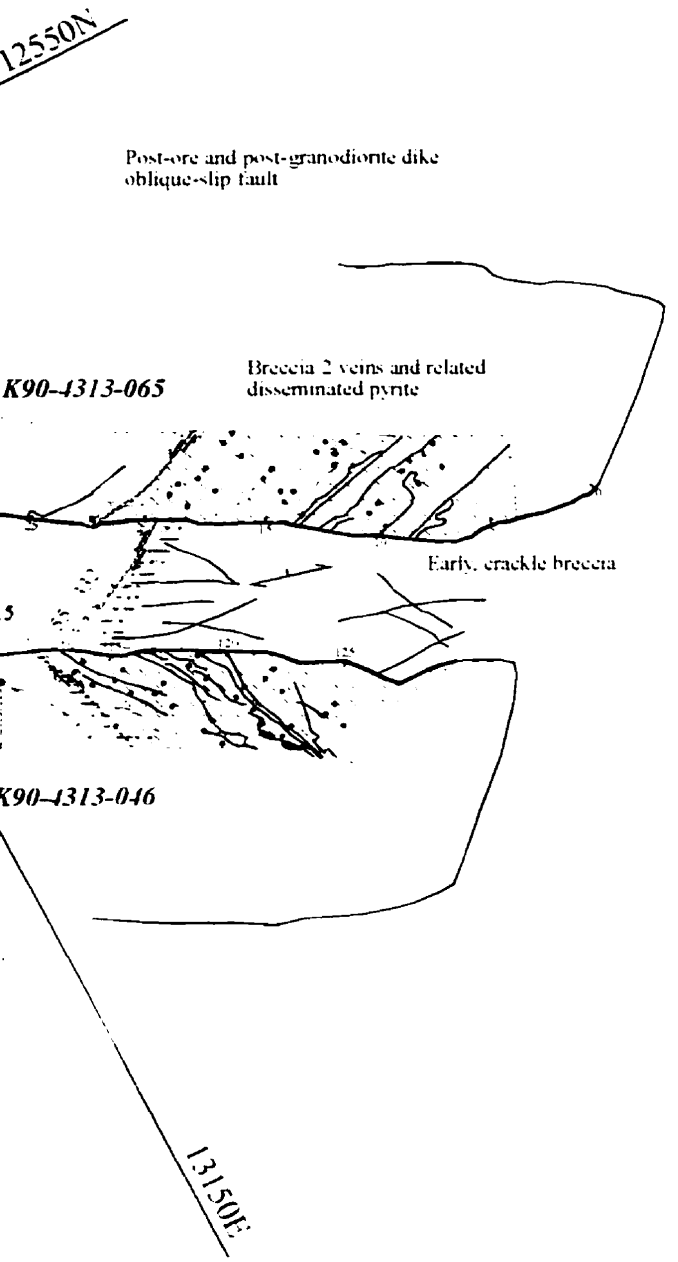

LEGEND

MAIN ORE ZONES (PART ALBITITE DIKES)

- Breccia 2
- Breccia 1
- Stwk Cb-Qz-Py(Po)±Ab-Au

INTRUSIVE ROCKS

- Albitite dike
- Intermineral granodiorite dike
- Intermineral feldspar porphyry dike

VOLCANIC ROCKS

- Schistose magnesian tholeiite (West)
- Schistose iron tholeiite (East)
- Pillowed magnesian tholeiite and flow top breccia
- Cb-Chl-Tc-(Ab) schist± boudinaged albitite dike inclusions (Dm-Qz stockwork vein-altered) - probable metakomatiite

STRUCTURAL SYMBOLS

- Carbonate-quartz ± albite extension veins
- Breccia 2 veins with related disseminated pyrite
- 46 Main schistosity : S_1
- 28 Crenulation cleavage: S_{1+2}
- 65 Brittle-ductile, oblique slip fault
- Horizontal (or vertical) component of movement
- 40 Bedding and dip
- Stratigraphic younging direction
- Dip - dip azimuth
- Fault gauge
- K92-2752-202 Sample number (see Appendix B)
- Distance in metres along back face of ore drift

Horizontal display of vertical drift wall

LES MINES D'OR KENA LTEE.

INDEX MAP - PILLAR 4313

"B" ZONE

Mapped by S. Morasse

Date Oct 1990

0m 2.5m 5m

S. Morasse 1997

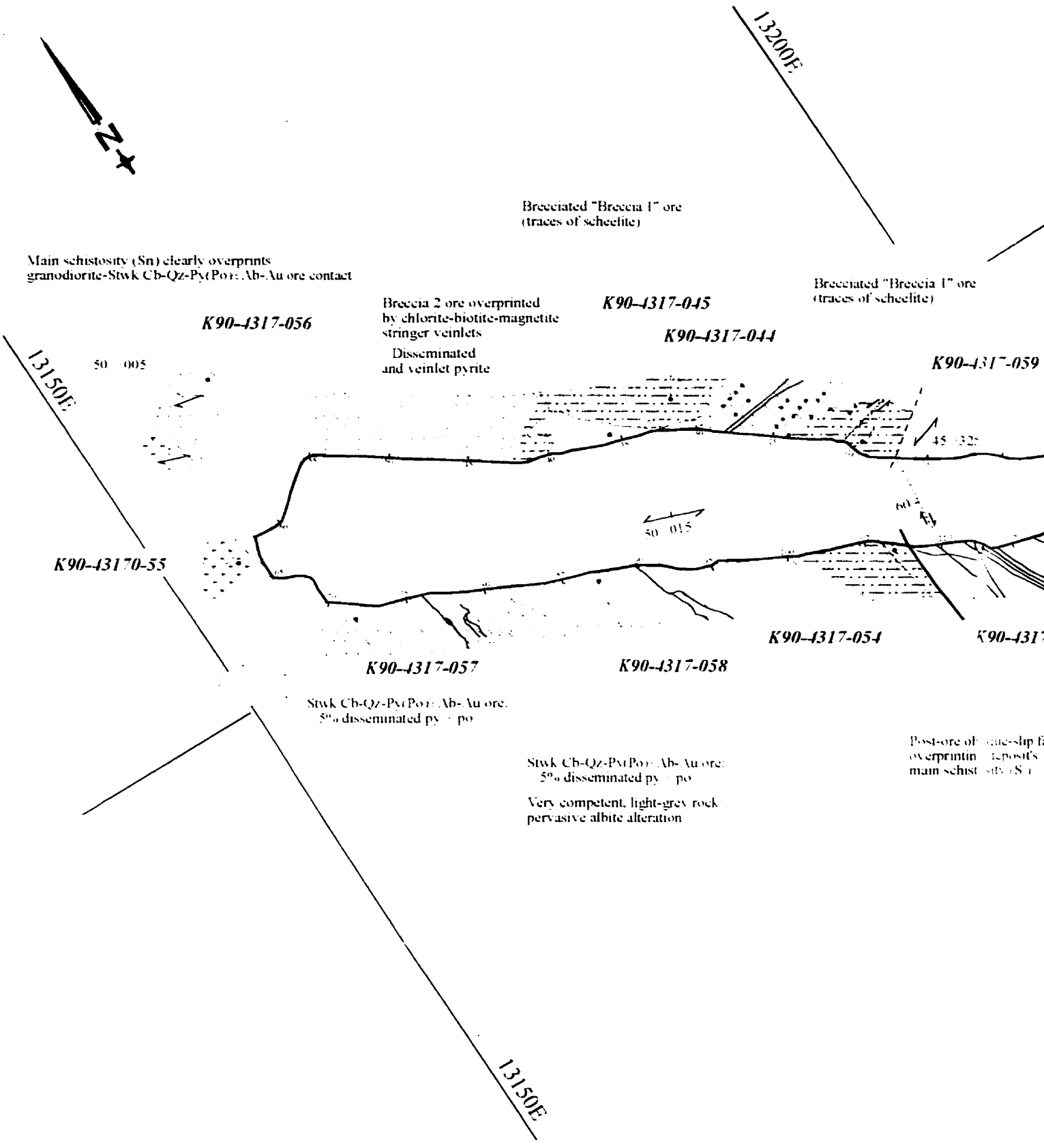

Geology, Structure and Gold Mineralization at the Kiena Deposit - Back pocket

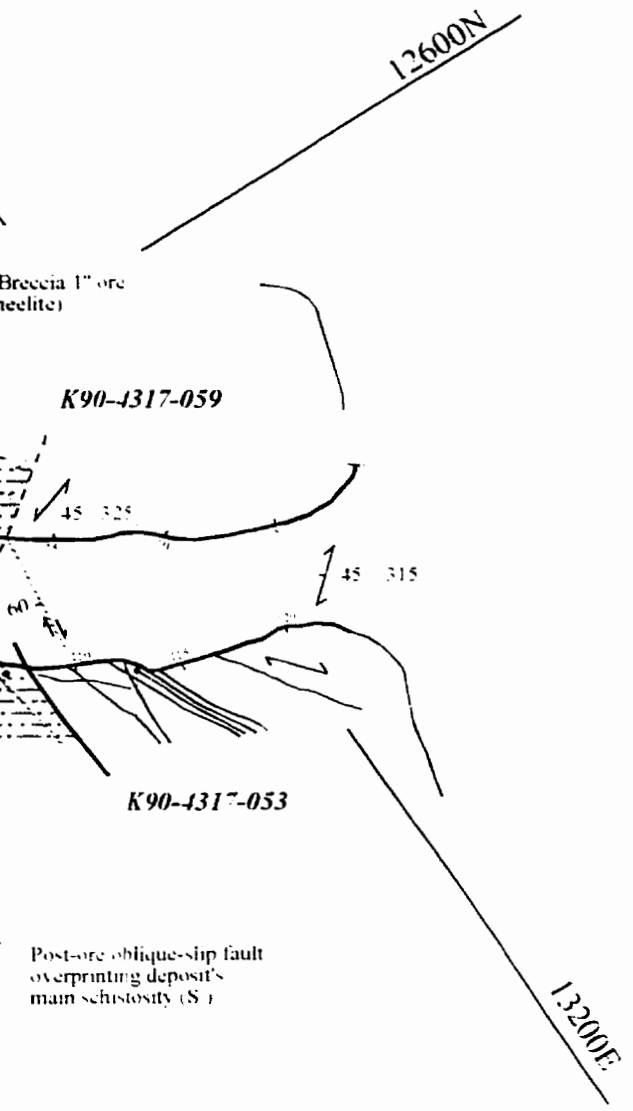

LEGEND

MAIN ORE ZONES (PART ALBITITE DIKES)

- Breccia 2
- Breccia 1
- Stwk Cb-Qz-Py(Po)±Ab-Au

INTRUSIVE ROCKS

- Albitite dike
- Intermineral granodiorite dike
- Intermineral feldspar porphyry dike

VOLCANIC ROCKS

- Schistose magnesian tholeiite (West)
- Schistose iron tholeiite (East)
- Pillowed magnesian tholeiite and flow top breccia
- Cb-Chl-Tc-(Ab) schist± boudinaged albitite dike inclusions (Dm-Qz stockwork vein-altered) - probable metakomatiite

STRUCTURAL SYMBOLS

- Carbonate-quartz ± albite extension veins
- Breccia 2 veins with related disseminated pyrite
- 45 Main schistosity : S_1
- 28 Crenulation cleavage: S_{n+1}
- 65 Brittle-ductile, oblique slip fault
- Horizontal (or vertical) component of movement
- 40 Bedding and dip
- Stratigraphic younging direction
- Dip - dip azimuth
- Fault gauge
- K92-2752-202 Sample number (see Appendix B)
- Distance in metres along back face of ore drift
- Horizontal display of vertical drift wall

LES MINES D'OR KENA LTEE.

INDEX MAP - PILLAR 4317

"B" ZONE

Mapped by S. Morasse

Date OCT 1996

0m 2.5m 5m

S. Morasse 1997

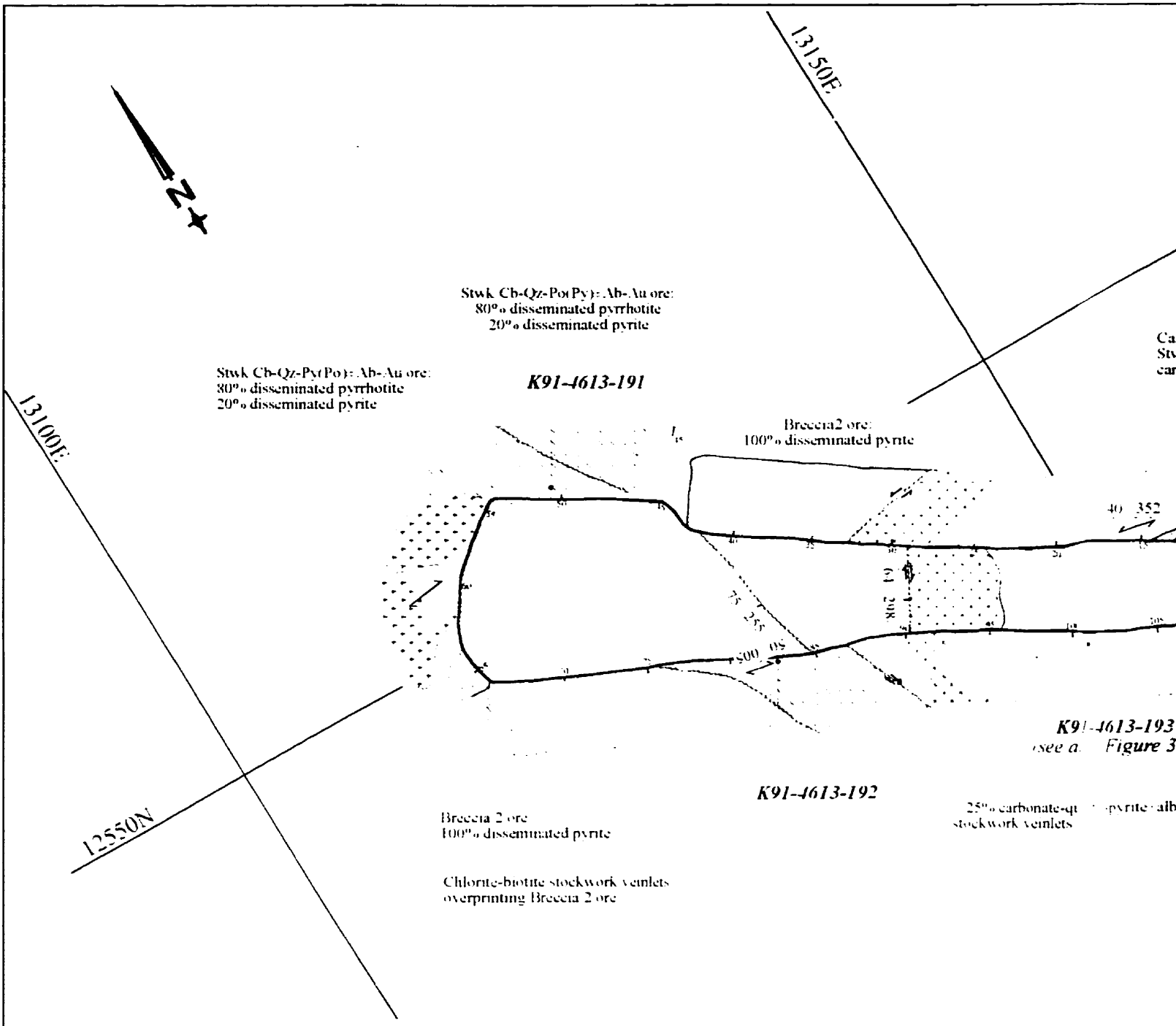

Geology, Structure and Gold Mineralization at the Kiena Deposit - Back pocket

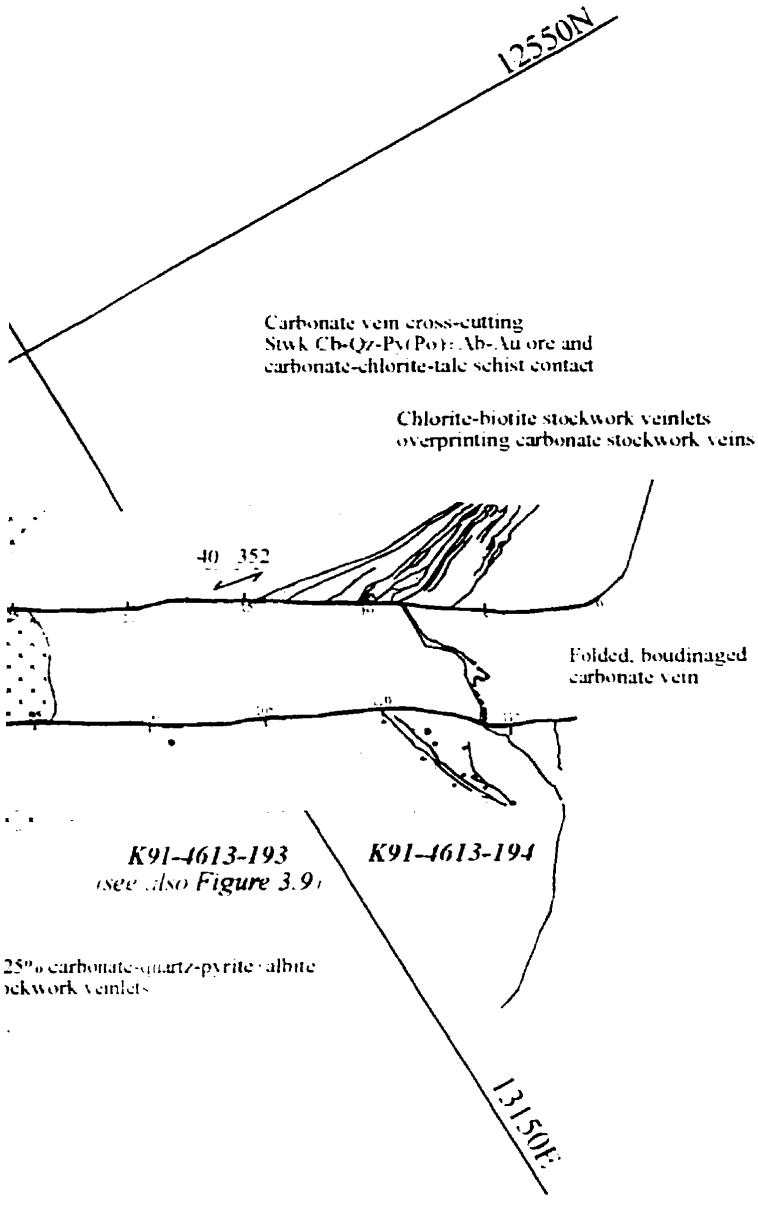

LEGEND

MAIN ORE ZONES (PART ALBITITE DIKES)

- Breccia 2
- Breccia 1
- Stwk Cb-Qz-Po(Py)±Ab-Au

INTRUSIVE ROCKS

- Albitite dike
- Intermineral granodiorite dike
- Intermineral feldspar porphyry dike

VOLCANIC ROCKS

- Schistose magnesian tholeiite (West)
- Schistose iron tholeiite (East)
- Pillowed magnesian tholeiite and flow top breccia
- Cb-Chl-Tc-(Ab) schist= boudinaged albitite dike inclusions (Dm-Qz stockwork vein-altered) - probable metakomatiite

STRUCTURAL SYMBOLS

- Carbonate-quartz ± albite extension veins
- Breccia 2 veins
- 45 Main schistosity : S_n
- 28 Crenulation cleavage: S_{n+1}
- 65 Brittle-ductile, oblique slip fault
- Horizontal (or vertical) component of movement
- 40 Bedding and dip
- Stratigraphic younging direction
- Dip - dip azimuth
- Fault gauge
- K92-2752-202 Sample number (see Appendix B)
- Distance in metres along back face of ore drift

Horizontal display of vertical drift wall

LES MINES D'OR KENA LTEE.

INDEX MAP - PILLAR 4613

"B" ZONE

Mapped by: S. Morasse

Date: 02 1991

0m 2.5m 5m

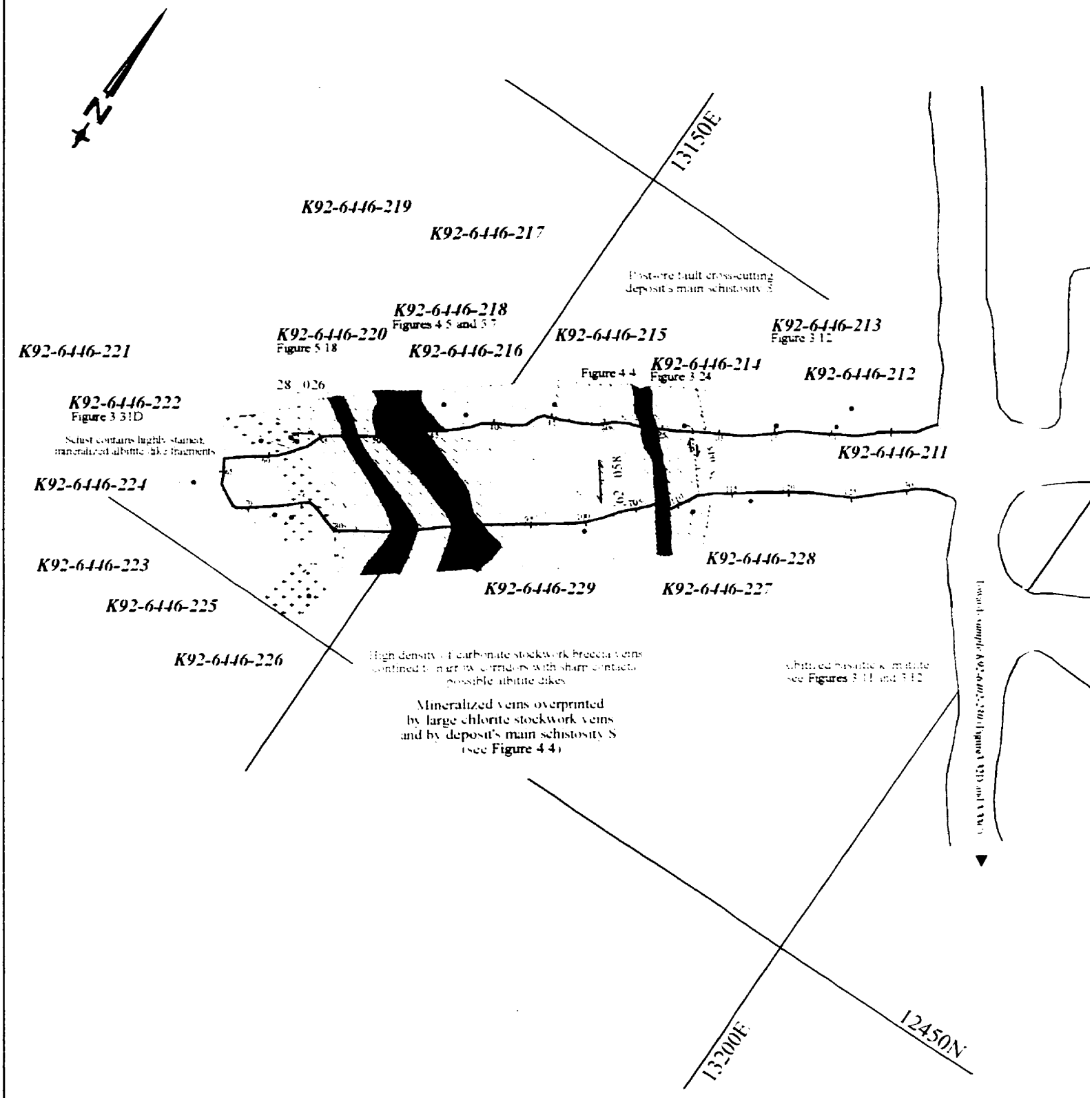

Geology, Structure and Gold Mineralization at the Kiena Deposit - Back pocket

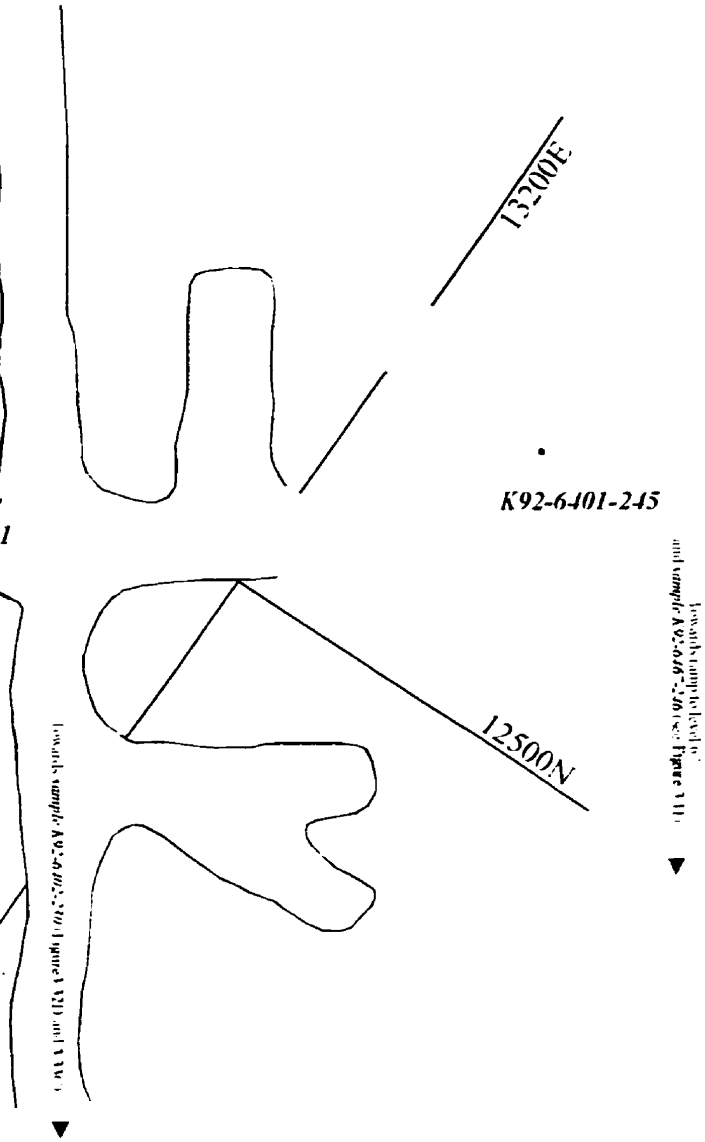

LEGEND

MAIN ORE ZONES (PART ALBITITE DIKES)

- Breccia 2
- Breccia 1
- Stwk Cb-Qz-Po(Py)±Ab-Au

INTRUSIVE ROCKS

- Possible albitite dikes
- Intermineral granodiorite dike
- Intermineral feldspar porphyry dike

VOLCANIC ROCKS

- Schistose magnesian tholeiite (West)
- Schistose iron tholeiite (East)
- Pillowed magnesian tholeiite and flow top breccia
- Cb-Chl-Tc-(Ab) schist± boudinaged albitite dike inclusions (Dm-Qz stockwork vein-altered) - probable metakomatiite

STRUCTURAL SYMBOLS

- Carbonate-quartz ± albite extension veins
- 45 Main schistosity: S_n
- 28 Crenulation cleavage: S_{n+1}
- 65 Brittle-ductile, oblique slip fault
- Horizontal (or vertical) component of movement
- 40 Bedding and dip
- Stratigraphic younging direction
- 40 232 Dip - dip azimuth
- Fault gauge
- K92-6752-202 Sample number (see Appendix B)
- 15 Distance in metres along back face of ore drift

Horizontal display of vertical drift wall

LES MINES D'OR KIENA LTEE.

INDEX MAP - STOPE 6446

"C" ZONE

Mapped by S. Morasse

Date 05/1997

0m 2.5m 5m

S. Morasse 1997

KIENA MINE - SECTION 12438.4 N

Schematic east-west vertical cross-section 12438.4 N, looking north, across the high-grade core of Kiena's orebody (see ***Figure 3.2****), showing the orebody and its relationships to country rocks, pre-mineral albitite dikes, intermineral dikes, and the deposit's outer gold alteration halo. Ore zone composition is given in relative percentages of the three ore types encountered at Kiena. The ore-dike complex and main schistosity are deformed by a large open fold plunging 30°-40° to the north-northwest and overprinted by a gently east-dipping crenulation cleavage. Traces of the intersection between the main schistosity and crenulation cleavage with the section appear west and east of the orebody, respectively.*

Représentation schématique de la section verticale 12438.4 N, orientée est-ouest avec regard vers le nord, à travers le coeur haute teneur du corps minéralisé de la Mine Kiena (voir ***Figure 3.2****), montrant la relation spatiale entre le corps minéralisé, les roches encaissantes, les dykes d'albitite pré-minéralisation, le dyke de granodiorite interminéralisation, et le halo d'altération aurifère autour du gisement. La composition de chacune des zones minéralisées est donnée en fonction du pourcentage relatif des trois types de minerai rencontrés à Kiena. Le minerai, les dykes et la schistosité principale sont déformés par un large pli ouvert plongeant 30-40° vers le nord-nord-ouest et recoupés par un clivage de crénulation pendant faiblement vers l'est. La trace de l'intersection entre la schistosité principale et la section, ainsi qu'entre le clivage de crénulation et la section, apparaissent à l'ouest et à l'est, respectivement, du corps minéralisé.*

Abbreviations: ***"Stwk Cb-Qz-Py(Po)±Ab-Au"*** *= carbonate-quartz stockwork veins with albite-pyrite (pyrrhotite)-Au in vein alteration halos (1st ore type);* ***"Breccia 1"*** *= ankerite-pyrite-Au replacement veins (2nd ore type);* ***"Breccia 2"*** *= albite-pyrite-chalcopyrite-scheelite-Au stockwork veins (3rd ore type);* ***Ak*** *= ankerite;* ***Dm*** *= dolomite;* ***Qz*** *= quartz;* ***Au*** *= gold;* ***Cb*** *= carbonate;* ***Chl*** *= chlorite;* ***Tc*** *= talc;* ***Ab*** *= albite;* ***g/t*** *= gram per tonne.*

Abréviations: ***"Stwk Cb-Qz-Py(Po)-±Ab-Au"*** *= stockwork de veines à carbonate et quartz avec halos d'altération à albite- pyrite (pyrrhotine)-Au (1er type de minéralisation);* ***"Breccia 1"*** *= veine de remplacement à ankérite-pyrite-Au (2ième type de minéralisation);* ***"Breccia 2"*** *= stockwork de veines à albite-pyrite-chalcopyrite-scheelite-Au (3ième type de minéralisation);* ***Ak*** *= ankérite;* ***Dm*** *= dolomie;* ***Qz*** *= quartz;* ***Au*** *= gold;* ***Cb*** *= carbonate;* ***Chl*** *= chlorite;* ***Tc*** *= talc;* ***Ab*** *= albite,* ***g/t*** *= gramme la tonne.*

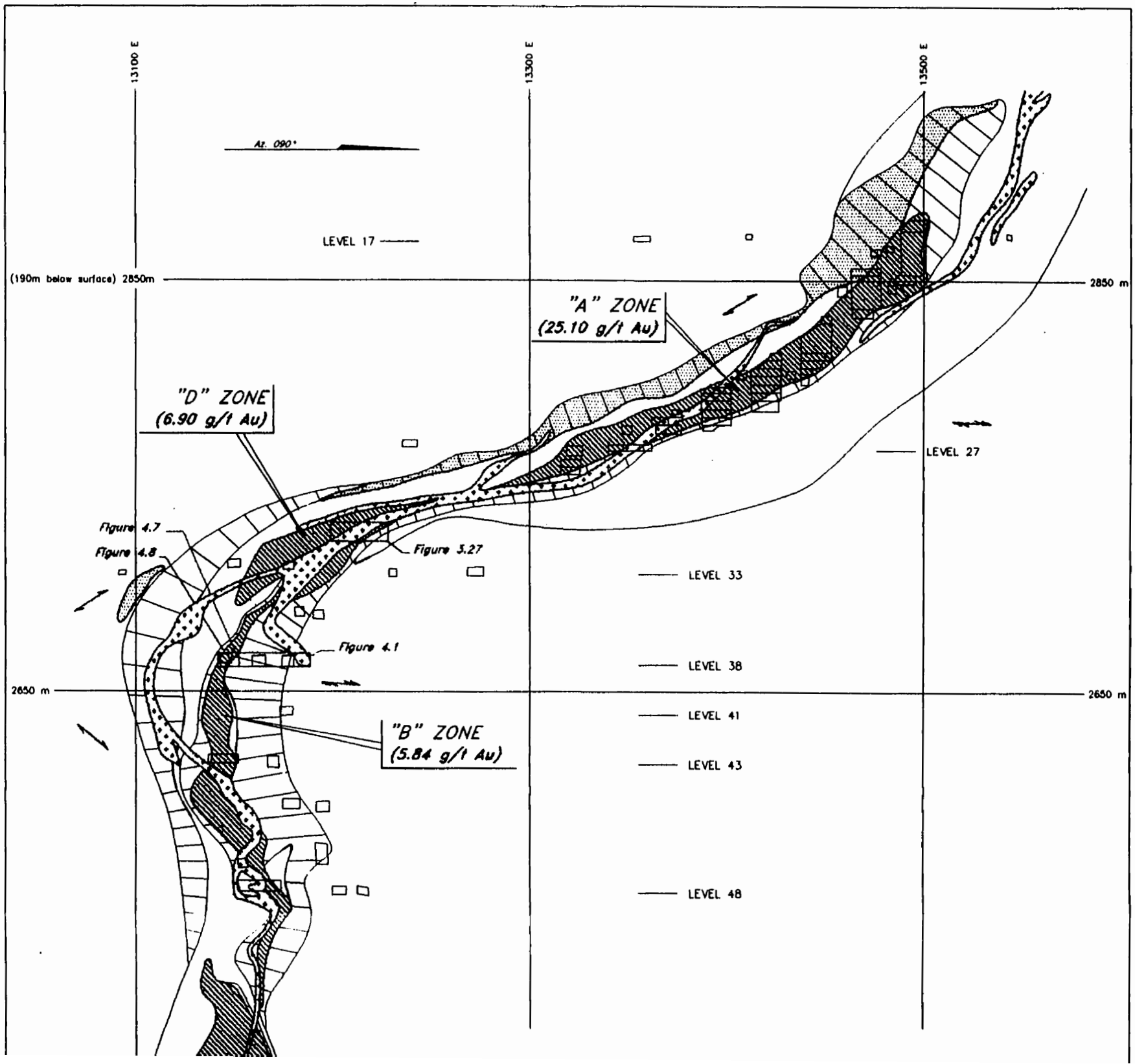
13100 E
13300 E
13500 E
Az. 090°
LEVEL 17
(190m below surface) 2850m
2850 m
"A" ZONE
(25.10 g/t Au)
"D" ZONE
(6.90 g/t Au)
LEVEL 27
Figure 4.7
Figure 4.8
Figure 3.27
LEVEL 33
Figure 4.1
LEVEL 38
2650 m
2650 m
LEVEL 41
"B" ZONE
(5.84 g/t Au)
LEVEL 43
LEVEL 48

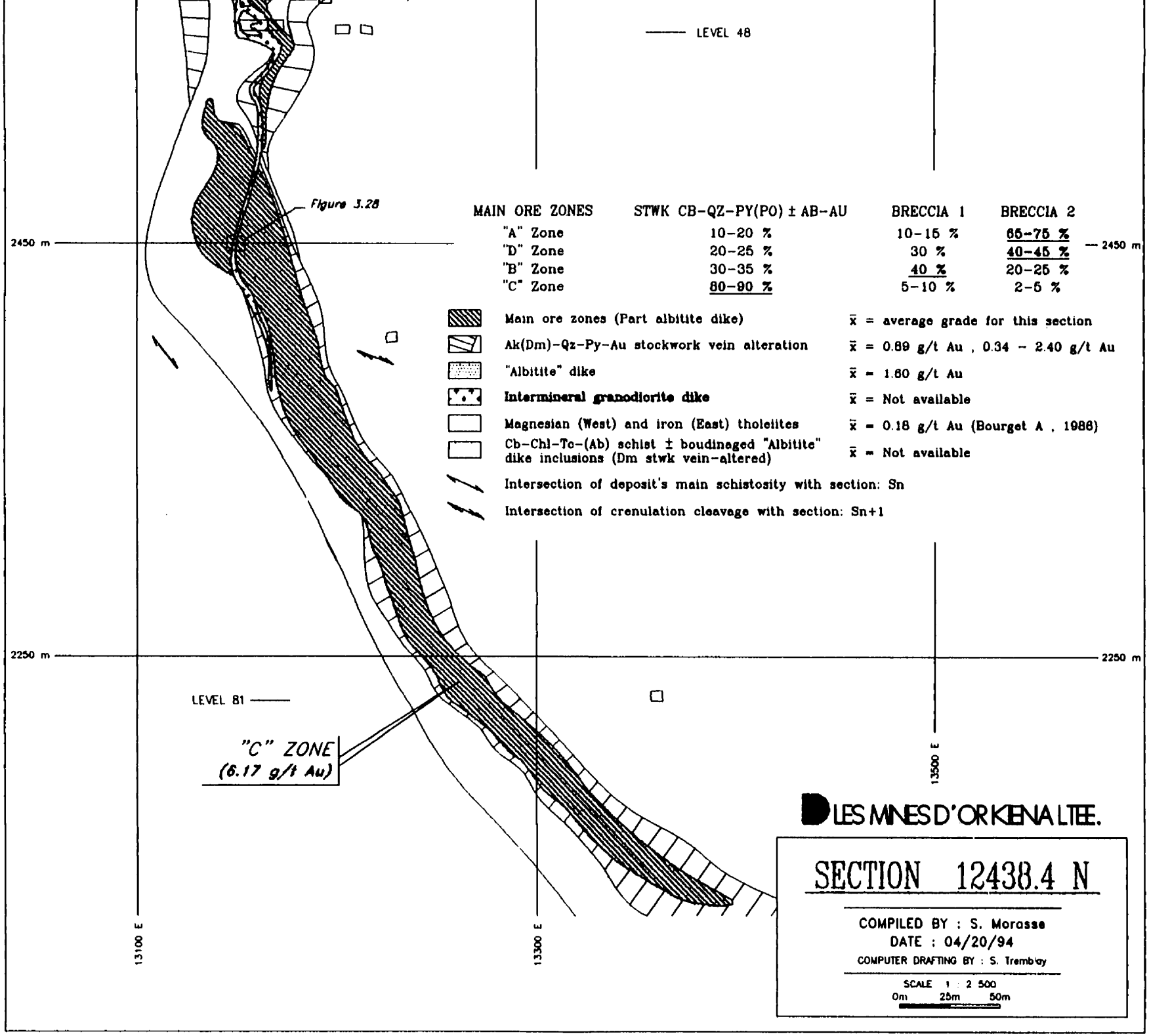
LEVEL 48
Figure 3.28
2450 m
2250 m
LEVEL 81
"C" ZONE
(6.17 g/t Au)
13100 E
13300 E
13500 E
MAIN ORE ZONES
STWK CB-QZ-PY(PO) ± AB-AU
BRECCIA 1
BRECCIA 2
"A" Zone 10-20 % 10-15 % 65-75 %
"D" Zone 20-25 % 30 % 40-45 %
"B" Zone 30-35 % 40 % 20-25 %
"C" Zone 80-90 % 5-10 % 2-5 %
Main ore zones (Part albitite dike)
Ak(Dm)-Qz-Py-Au stockwork vein alteration
"Albitite" dike
Intermineral granodiorite dike
Magnesian (West) and iron (East) tholeiites
Cb-Chl-Tc-(Ab) schist ± boudinaged "Albitite" dike inclusions (Dm stwk vein-altered)
Intersection of deposit's main schistosity with section: Sn
Intersection of crenulation cleavage with section: Sn+1
x̄ = average grade for this section
x̄ = 0.89 g/t Au , 0.34 - 2.40 g/t Au
x̄ = 1.60 g/t Au
x̄ = Not available
x̄ = 0.18 g/t Au (Bourget A , 1988)
x̄ = Not available
LES MINES D'OR KIENA LTEE.
SECTION 12438.4 N
COMPILED BY : S. Morasse
DATE : 04/20/94
COMPUTER DRAFTING BY : S. Tremblay
SCALE 1 : 2 500
0m 25m 50m

KIENA MINE - SECTION 124514.6 N

Schematic east-west vertical cross-section 12514.6 N, looking north, across the high-grade core of Kiena's orebody (see **Figure 3.2**), *showing the orebody and its relationships to country rocks, pre-mineral albitite dikes, intermineral granodiorite and feldspar porphyry dikes, and the deposit's outer gold alteration halo. Ore zone composition is given in relative percentages of the three ore types encountered at Kiena. The albitite dikes and the ore are cut by the granodiorite and feldspar porphyry dikes. The cross-cutting relationship between the latter two porphyries is not known form this section, however, it can be observed on section 12636.5 N and the 5" Level Map and indicates that the feldspar porphyry dike is the youngest. The ore-dike complex and the main schistosity are deformed by a gently (30-40 °) north-northwest-plunging fold and overprinted by a gently east-dipping crenulation cleavage. Traces of the intersection between the main schistosity and crenulation cleavage with the section appear west and east of the orebody, respectively.*

Représentation schématique de la section verticale 12438.4 N, orientée est-ouest avec regard vers le nord, à travers le coeur haute teneur du corps minéralisé de la Mine Kiena (voir **Figure 3.2**), *montrant la relation spatiale entre le corps minéralisé, les roches encaissantes, les dykes d'albitite pré-minéralisation, les dykes de granodiorite et de porphyre feldspathique interminéralisation, et le halo d'altération aurifère autour du gisement. La composition de chacune des zones minéralisées est donnée en fonction du pourcentage relatif des trois types de minerai rencontrés à Kiena. Les dykes d'albitite et le minerai sont recoupés par les dykes de granodiorite et de porphyre feldspathique. Il n'est pas possible d'établir la relation de recoupement entre les deux dykes de porphyres sur cette section. Cependant celle-ci peut être observée à la section 12636.5 N ainsi que sur le plan niveau 57, où elle indique que le dyke de porphyre feldspathique est le plus jeune. Le minerai, les dykes ainsi que la schistosité principale sont déformés par un pli plongeant 30-40 ° vers le nord-nord-ouest et recoupés par un clivage de crénulation pendant faiblement vers l'est. La trace de l'intersection entre la schistosité principale et la section, ainsi qu'entre le clivage de crénulation et la section, apparaissent à l'ouest et à l'est, respectivement, du corps minéralisé.*

Abbreviations: ***Stwk Cb-Qz-Py(Po)±Ab-Au*** *= carbonate-quartz stockwork veins with albite-pyrite (pyrrhotite)-Au in vein alteration halos (1st ore type);* ***Breccia 1*** *= ankerite-pyrite-Au replacement veins (2nd ore type);* ***Breccia 2*** *= albite-pyrite-chalcopyrite-scheelite-Au stockwork veins (3rd ore type);* ***Ak*** *= ankerite;* ***Dm*** *= dolomite;* ***Qz*** *= quartz;* ***Au*** *= gold;* ***Cb*** *= carbonate,* ***Chl*** *= chlorite;* ***Tc*** *= talc;* ***Ab*** *= albite;* ***g/t*** *= gram per tonne.*

Abréviations: ***Stwk Cb-Qz-Py(Po)-±Ab-Au*** *= stockwork de veines à carbonate et quartz avec halos d'altération à albite-pyrite (pyrrhotine)-Au (1er type de minéralisation);* ***Breccia 2*** *= veine de remplacement à ankérite-pyrite-Au (2ième type de minéralisation);* ***Breccia 2*** *= stockwork de veines à albite-pyrite-chalcopyrite-scheelite-Au (3ième type de minéralisation);* ***Ak*** *= ankérite;* ***Dm*** *= dolomie;* ***Qz*** *= quartz;* ***Au*** *= gold;* ***Cb*** *= carbonate;* ***Chl*** *= chlorite;* ***Tc*** *= talc;* ***Ab*** *= albite,* ***g/t*** *= gramme la tonne.*

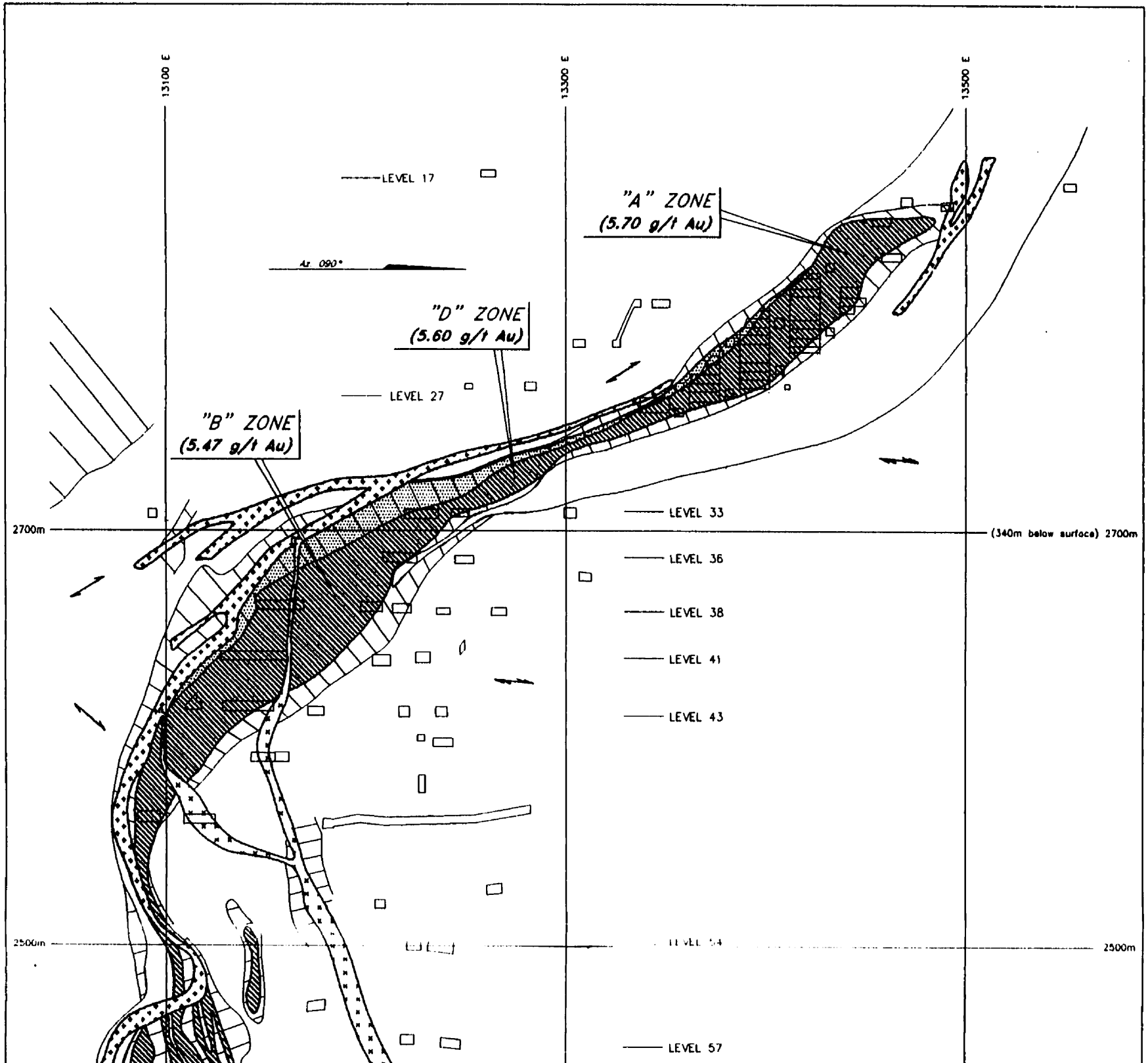
13100 E
13300 E
13500 E
LEVEL 17
"A" ZONE
(5.70 g/t Au)
Az. 090°
"D" ZONE
(5.60 g/t Au)
LEVEL 27
"B" ZONE
(5.47 g/t Au)
2700m
LEVEL 33
(340m below surface) 2700m
LEVEL 36
LEVEL 38
LEVEL 41
LEVEL 43
2500m
2500m
LEVEL 57

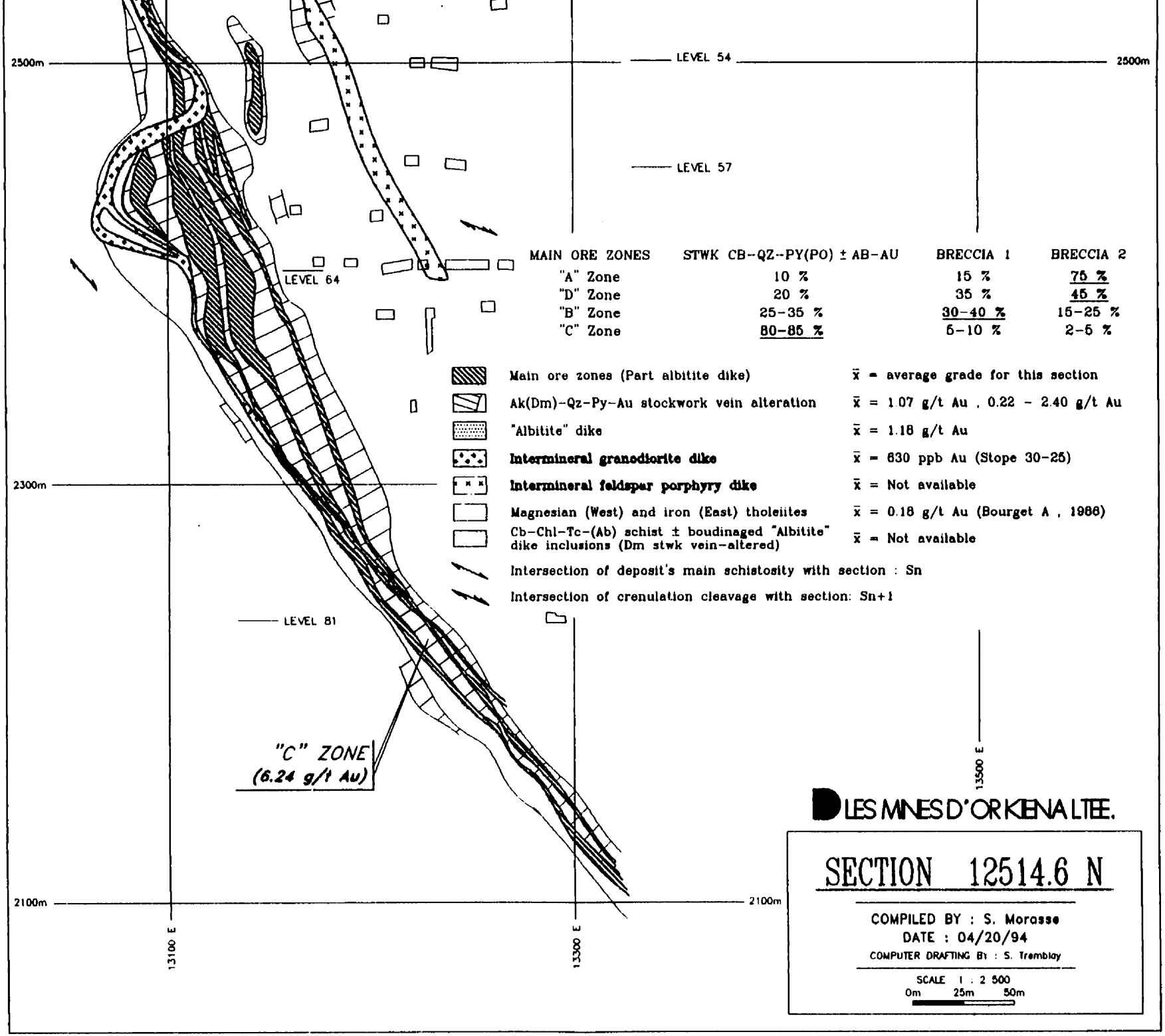

MAIN ORE ZONES	STWK CB-QZ-PY(PO) ± AB-AU	BRECCIA 1	BRECCIA 2
"A" Zone	10 %	15 %	75 %
"D" Zone	20 %	35 %	45 %
"B" Zone	25-35 %	30-40 %	15-25 %
"C" Zone	80-85 %	5-10 %	2-5 %

	Main ore zones (Part albitite dike)	$\bar{x}$ = average grade for this section
	Ak(Dm)-Qz-Py-Au stockwork vein alteration	$\bar{x}$ = 1.07 g/t Au , 0.22 - 2.40 g/t Au
	"Albitite" dike	$\bar{x}$ = 1.18 g/t Au
	Intermineral granodiorite dike	$\bar{x}$ = 630 ppb Au (Stope 30-25)
	Intermineral feldspar porphyry dike	$\bar{x}$ = Not available
	Magnesian (West) and iron (East) tholeiites	$\bar{x}$ = 0.18 g/t Au (Bourget A , 1986)
	Cb-Chl-Tc-(Ab) schist ± boudinaged "Albitite" dike inclusions (Dm stwk vein-altered)	$\bar{x}$ = Not available
	Intersection of deposit's main schistosity with section : Sn	
	Intersection of crenulation cleavage with section: Sn+1	

LES MINES D'OR KIENA LTEE.

SECTION 12514.6 N

COMPILED BY : S. Morasse
DATE : 04/20/94
COMPUTER DRAFTING BY : S. Tremblay

SCALE 1 : 2 500
0m 25m 50m

KIENA MINE - SECTION 12636.5 N

Schematic east-west vertical cross-section 12636.5N, looking north, across the lower-grade ore shell of Kiena's orebody (see ***Figure 3.2****), showing the orebody and its relationships to country rocks, intermineral granodiorite and feldspar porphyry dikes, and the deposit's outer gold alteration halo. Ore zone composition is given in relative percentages of the three ore types encountered at Kiena. Note how the main orebody is dismembered into smaller ore zones ("B", "J", and "K" ore zones) by the intermineral granodiorite dike. The ore-dike complex and the main schistosity are folded and overprinted by a gently east-dipping crenulation cleavage. Traces of the intersection between the main schistosity and crenulation cleavage with the section, appear west and east of the orebody, respectively.*

Représentation schématique de la section verticale 12636.5N, orientée est-ouest avec regard vers le nord, à travers le minerai à basse teneur du corps minéralisé de la Mine Kiena (voir ***Figure 3.2****), montrant la relation spatiale entre le corps minéralisé, les roches encaissantes, les dykes de granodiorite et de porphyre feldspathique interminéralisation, et le halo d'altération aurifère autour du gisement. La composition de chacune des zones minéralisées est donnée en fonction du pourcentage relatif des trois types de minerai rencontrés à Kiena. Le corps minéralisé principal est découpé en plusieurs petites zones minéralisées (zones "B", "J" et "K") par le dyke de granodiorite interminéralisation. Le minerai, les dykes et la schistosité principale sont déformés par un pli et recoupés par un clivage de crénulation pendant faiblement vers l'est. La trace de l'intersection entre la schistosité principale et la section, ainsi qu'entre le clivage de crénulation et la section, apparaissent à l'ouest et à l'est, respectivement, du corps minéralisé.*

Abbreviations: ***Stwk Cb-Qz-Py(Po)±Ab-Au*** *= carbonate-quartz stockwork veins with albite-pyrite (pyrrhotite)-Au in vein alteration halos (1st ore type).* ***Breccia 1*** *= ankerite-pyrite-Au replacement veins (2nd ore type);* ***Breccia 2*** *= albite-pyrite-chalcopyrite-scheelite-Au stockwork veins (3rd ore type);* ***Ak*** *= ankerite;* ***Dm*** *= dolomite;* ***Qz*** *= quartz;* ***Au*** *= gold;* ***Cb*** *= carbonate;* ***Chl*** *= chlorite;* ***Tc*** *= talc;* ***Ab*** *= albite;* ***g/t*** *= gram per tonne.*

Abréviations: ***Stwk Cb-Qz-Py(Po)-±Ab-Au*** *= stockwork de veines à carbonate et quartz avec halos d'altération à albite-pyrite (pyrrhotine)-Au (1er type de minéralisation);* ***Breccia 2*** *= veine de remplacement à ankérite-pyrite-Au (2ième type de minéralisation);* ***Breccia 2*** *= stockwork de veines à albite-pyrite-chalcopyrite-scheelite-Au (3ième type de minéralisation);* ***Ak*** *= ankérite;* ***Dm*** *= dolomie;* ***Qz*** *= quartz;* ***Au*** *= gold;* ***Cb*** *= carbonate;* ***Chl*** *= chlorite;* ***Tc*** *= talc;* ***Ab*** *= albite;* ***g/t*** *= gramme la tonne.*

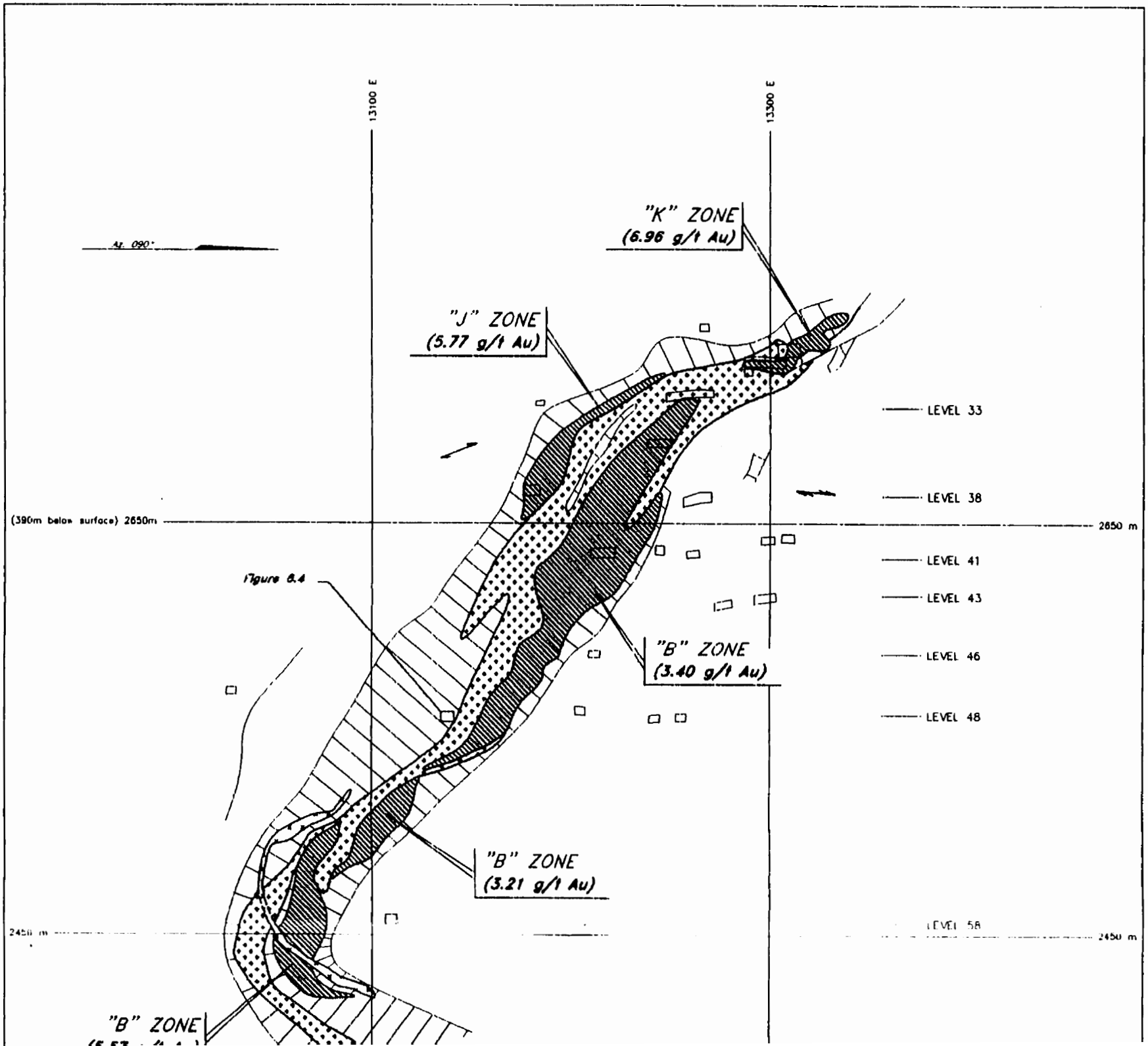
13100 E
13300 E
Az. 090°
"K" ZONE
(6.96 g/t Au)
"J" ZONE
(5.77 g/t Au)
LEVEL 33
LEVEL 38
(390m below surface) 2650m
2650 m
LEVEL 41
LEVEL 43
Figure 6.4
"B" ZONE
(3.40 g/t Au)
LEVEL 46
LEVEL 48
"B" ZONE
(3.21 g/t Au)
LEVEL 58
2450 m
"B" ZONE

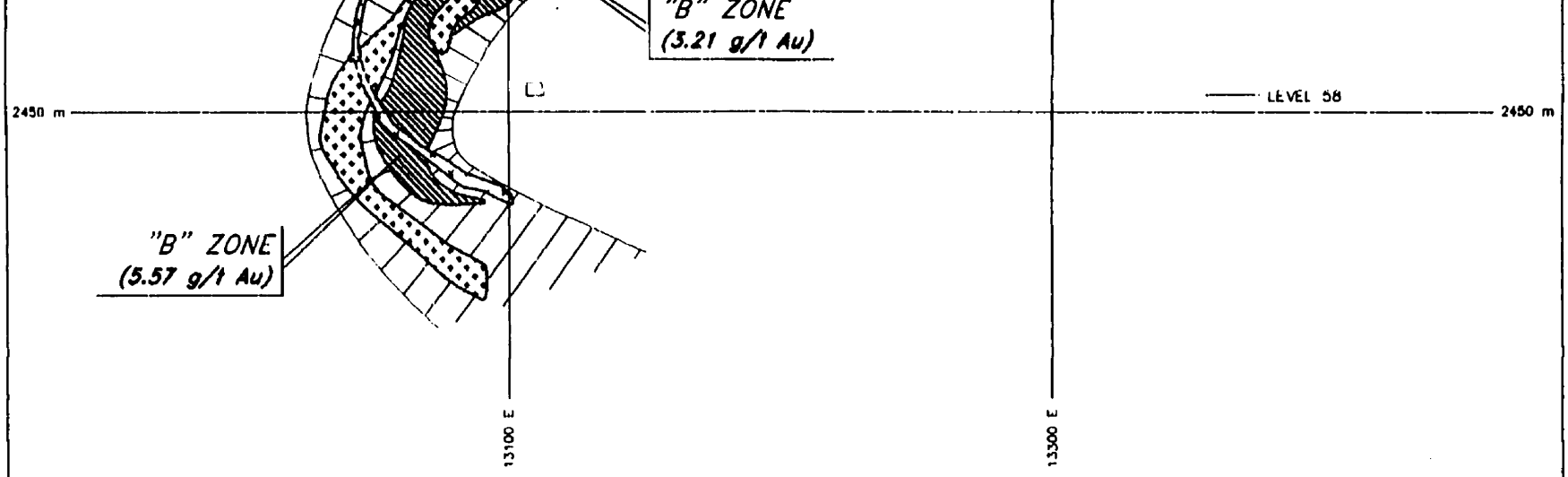

MAIN ORE ZONES	STWK CB--QZ-PY(PO) ± AB--AU	BRECCIA 1	BRECCIA 2
"K" Zone	100 %	-	-
"J" Zone	65 %	30 %	5 %
"B" Zone	30-45 %	15-25 %	15-30 %

- Main ore zones (Part albitite dike) — $\bar{x}$ = average grade for this section
- Ak(Dm)-Qz-Py-Au stockwork vein alteration — $\bar{x}$ = 0.94 g/t Au , 0.34 - 2.40 g/t Au
- **Intermineral granodiorite dike** — $\bar{x}$ = Not available
- **Intermineral feldspar porphyry dike** — $\bar{x}$ = Not available
- Magnesian (West) and iron (East) tholeiites — $\bar{x}$ = 0.18 g/t Au (Bourgel A , 1986)
- Cb-Chl-Tc-(Ab) schist ± boudinaged "Albitite" dike inclusions (Dm stwk vein-altered) — $\bar{x}$ = Not available
- Intersection of deposit's main schistosity with section Sn
- Intersection of crenulation cleavage with section: Sn+1

LES MINES D'OR KIENA LTEE.

SECTION 12636.5 N

COMPILED BY : S. Morasse
DATE : 04/20/94
COMPUTER DRAFTING BY : S. Tremblay

SCALE 1 : 2 500
0m 25m 50m

KIENA MINE - SECTION 12697.5 N

Schematic east-west vertical cross-section 12697.5N, looking north, across the lower-grade ore shell of Kiena's orebody (see **Figure 3.2**), *showing the orebody and its relationships to country rocks, pre-mineral albitite dikes, intermineral granodiorite dike, and the deposit's outer gold alteration halo. Ore zone composition is given in relative percentages of the three ore types encountered at Kiena. The main orebody is dismembered into smaller ore zones by the intermineral granodiorite dike. Ore zones "J North", "K" and "K North" are gold-ore xenoliths of the granodiorite dike. The ore-dike complex and the main schistosity are deformed by a gently (30–40 °) north-northwest-plunging fold and overprinted by a gently east-dipping crenulation cleavage. Traces of the intersection between the main schistosity and crenulation cleavage with the section, appears west and east of the orebody, respectively.*

Représentation schématique de la section verticale **12697.5N**, *orientée est-ouest avec regard vers le nord, à travers le minerai à basse teneur du corps minéralisé de la Mine Kiena (voir* **Figure 3.2**), *montrant la relation spatiale entre le corps minéralisé, les roches encaissantes, les dykes d'albitite pré-minéralisation, le dyke de granodiorite interminéralisation, et le halo d'altération aurifère autour du gisement. La composition de chacune des zones minéralisées est donnée en fonction du pourcentage relatif des trois types de minerai rencontrés à Kiena. Le corps minéralisé est découpé en plusieurs petites zones minéralisées par le dyke de granodiorite interminéralisation. Celui-ci renferme des xénolithes de minerai, représentés par les zones minéralisées "J Nord", "K" et "K Nord". Le minerai, les dykes et la schistosité principale sont déformés par un pli plongeant 30–40 ° vers le nord-nord-ouest, et recoupés par un clivage de crénulation pendant faiblement vers l'est. La trace de l'intersection entre la schistosité principale et la section, ainsi qu'entre le clivage de crénulation et la section, apparaissent à l'ouest et à l'est, respectivement, du corps minéralisé.*

Abbreviations: *Stwk Cb-Qz-Py(Po)±Ab-Au = carbonate-quartz stockwork veins with albite-pyrite (pyrrhotite)-Au in vein alteration halos (1st ore type); Breccia 1 = ankerite-pyrite-Au replacement veins (2nd ore type); Breccia 2 = albite-pyrite-chalcopyrite-scheelite-Au stockwork veins (3rd ore type); Ak = ankerite; Dm = dolomite; Qz = quartz; Au = gold; Cb = carbonate; Chl = chlorite; Tc = talc; Ab = albite; g/t = gram per tonne.*

Abréviations: *Stwk Cb-Qz-Py(Po)-±Ab-Au = stockwork de veines à carbonate et quartz avec halos d'altération à albite-pyrite (pyrrhotine)-Au (1er type de minéralisation); Breccia 2 = veine de remplacement à ankérite-pyrite-Au (2ième type de minéralisation); Breccia 2 = stockwork de veines à albite-pyrite-chalcopyrite-scheelite-Au (3ième type de minéralisation); Ak = ankérite; Dm = dolomie; Qz = quartz; Au = gold; Cb = carbonate; Chl = chlorite; Tc = talc; Ab = albite; g/t = gramme la tonne.*

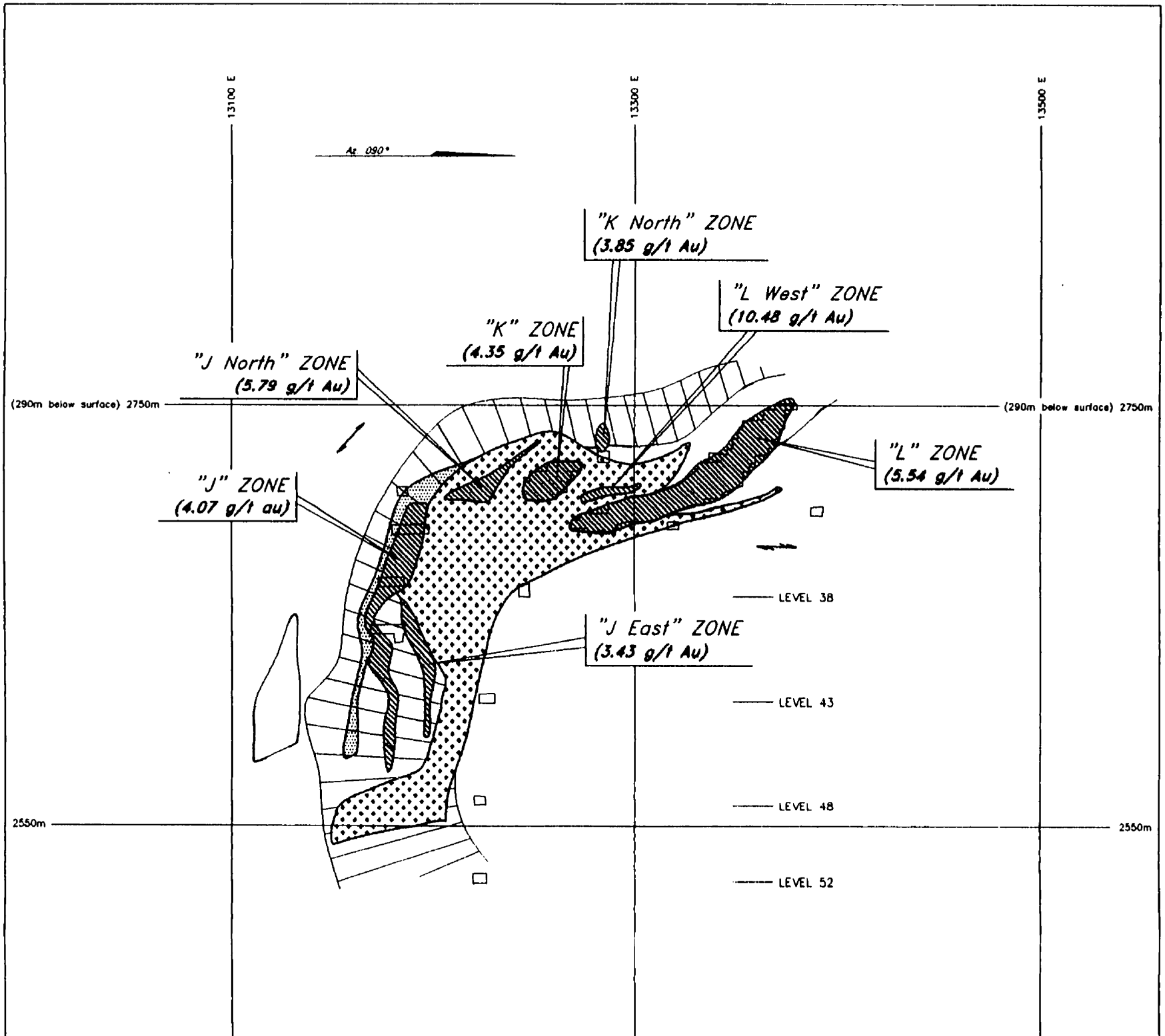
13100 E
13300 E
13500 E
At 090°
"K North" ZONE
(3.85 g/t Au)
"L West" ZONE
(10.48 g/t Au)
"K" ZONE
(4.35 g/t Au)
"J North" ZONE
(5.79 g/t Au)
(290m below surface) 2750m
(290m below surface) 2750m
"L" ZONE
(5.54 g/t Au)
"J" ZONE
(4.07 g/t au)
LEVEL 38
"J East" ZONE
(3.43 g/t Au)
LEVEL 43
LEVEL 48
2550m
2550m
LEVEL 52

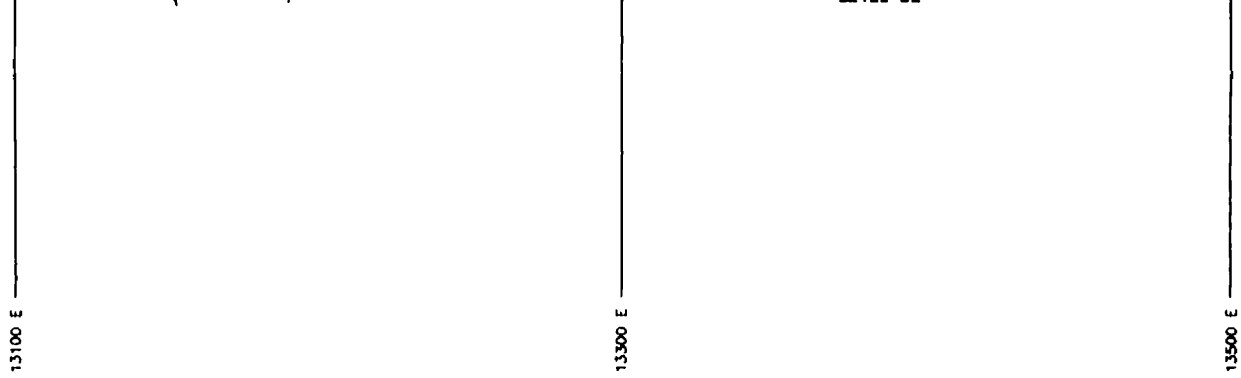

MAIN ORE ZONES	STWK CB-QZ-PY(PO) ± AB-AU	BRECCIA 1	BRECCIA 2
"L" Zone	100 %	-	-
"L West" Zone	100 %	-	-
"K North" Zone	100 %	-	-
"K" Zone	100 %	-	-
"J North" Zone	100 %	-	-
"J" Zone	65 %	30 %	5 %
"J East" Zone	65 %	30 %	5 %

	Main ore zones (Part albitite dike)	$\bar{x}$ = average grade for this section
	Ak(Dm)-Qz-Py-Au stockwork vein alteration	$\bar{x}$ = 0.86 g/t Au , 0.34 - 2.40 g/t Au
	"Albitite" dike	$\bar{x}$ = 1.07 g/t Au
	Intermineral granodiorite dike	$\bar{x}$ = Not available
	Magnesian (West) and Iron (East) tholeiites	$\bar{x}$ = 0.18 g/t Au (Bourget A , 1986)
	Cb-Chl-Tc-(Ab) schist ± boudinaged "Albitite" dike inclusions (Dm stwk vein-altered)	$\bar{x}$ = Not available
	Intersection of deposit's main schistosity with section: Sn	
	Intersection of crenulation cleavage with section : Sn+1	

LES MINES D'OR KIENA LTEE.

SECTION 12697.5 N

COMPILED BY : S. Morasse
DATE : 04/20/94
COMPUTER DRAFTING BY : S. Tremblay

SCALE 1 : 2 500
0m 25m 50m

KIENA MINE - 27 LEVEL MAP

*Schematic geological plan map of **level** 27 of the Kiena Mine (see **Figure** 3.2), showing the orebody and its relationships to country rocks, pre-mineral albitite dikes, intermineral granodiorite and feldspar porphyry dikes, the deposit's outer gold alteration halo, and the main schistosity. Ore zone composition is given in relative percentages of the three ore types encountered at Kiena. At this level, the orebody consists predominantly of breccia ore. Fragments of albitite dikes are distributed alongside the shallowly northwest-dipping orebody (see section 12514.6 N). The ore-dike complex is folded and cut by an axial planar schistosity dipping north.*

*Représentation schématique du plan géologique du **niveau** 27 de la Mine Kiena (voir **Figure** 3.2), montrant la relation spatiale entre le corps minéralisé, les roches encaissantes, les dykes d'albitite pré-minéralisation, les dykes de granodiorite et de porphyre feldspathique interminéralisation, le halo d'altération aurifère autour du gisement, et la schistosité principale. La composition de la zone minéralisée est donnée en fonction du pourcentage relatif des trois types de minerai rencontrés à Kiena. A ce niveau, le corps minéralisé est composé principalement de minerai de type brèche. Notez la présence de lambeaux de dykes d'albitite, distribués le long du corps minéralisé, lequel pend faiblement vers le nord-ouest (voir section 12514.6N). Le complexe minerai-dyke est déformé par un pli et recoupé par une schistosité de plan axial à pendage nord.*

Abbreviations: ***Stwk Cb-Qz-Py(Po)±Ab-Au** = carbonate-quartz stockwork veins with albite-pyrite (pyrrhotite)-Au in vein alteration halos (1st ore type); **Breccia 1** = ankerite-pyrite-Au replacement veins (2nd ore type); **Breccia 2** = albite-pyrite-chalcopyrite-scheelite-Au stockwork veins (3rd ore type); **Ak** = ankerite; **Dm** = dolomite; **Qz** = quartz; **Au** = gold; **Cb** = carbonate. **Chl** = chlorite; **Tc** = talc; **Ab** = albite; **g/t** = gram per tonne.*

Abréviations: ***Stwk Cb-Qz-Py(Po)-±Ab-Au** = stockwork de veines à carbonate et quartz avec halos d'altération à albite-pyrite (pyrrhotine)-Au (1er type de minéralisation); **Breccia 2** = veine de remplacement à ankérite-pyrite-Au (2ième type de minéralisation); **Breccia 2** = stockwork de veines à albite-pyrite-chalcopyrite-scheelite-Au (3ième type de minéralisation). **Ak** = ankérite; **Dm** = dolomie; **Qz** = quartz; **Au** = gold; **Cb** = carbonate; **Chl** = chlorite; **Tc** = talc; **Ab** = albite; **g/t** = gramme la tonne.*

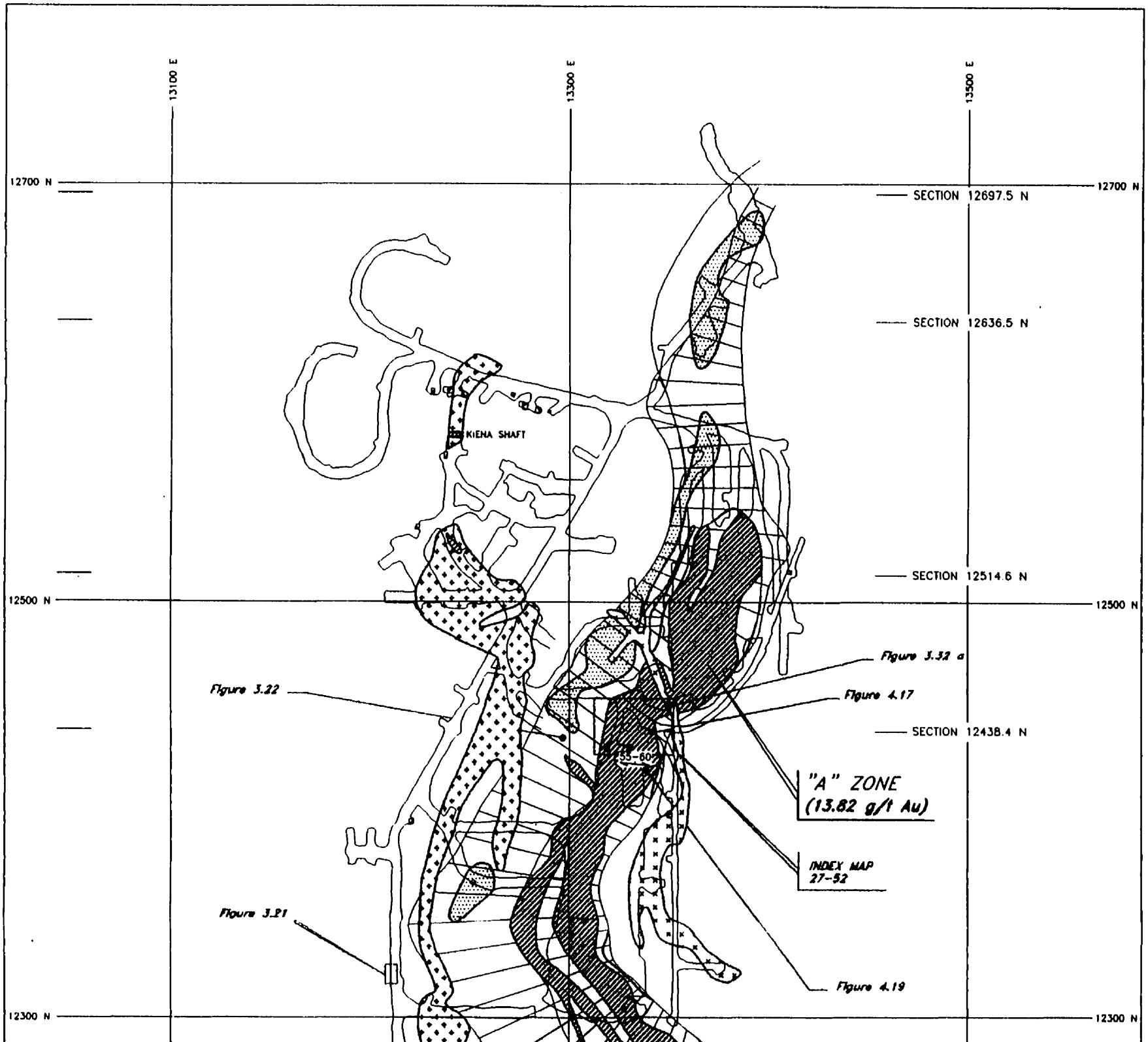
13100 E
13300 E
13500 E
12700 N
12500 N
12300 N
SECTION 12697.5 N
SECTION 12636.5 N
SECTION 12514.6 N
SECTION 12438.4 N
KIENA SHAFT
55-60
Figure 3.22
Figure 3.32 a
Figure 4.17
"A" ZONE
(13.82 g/t Au)
INDEX MAP
27-52
Figure 3.21
Figure 4.19

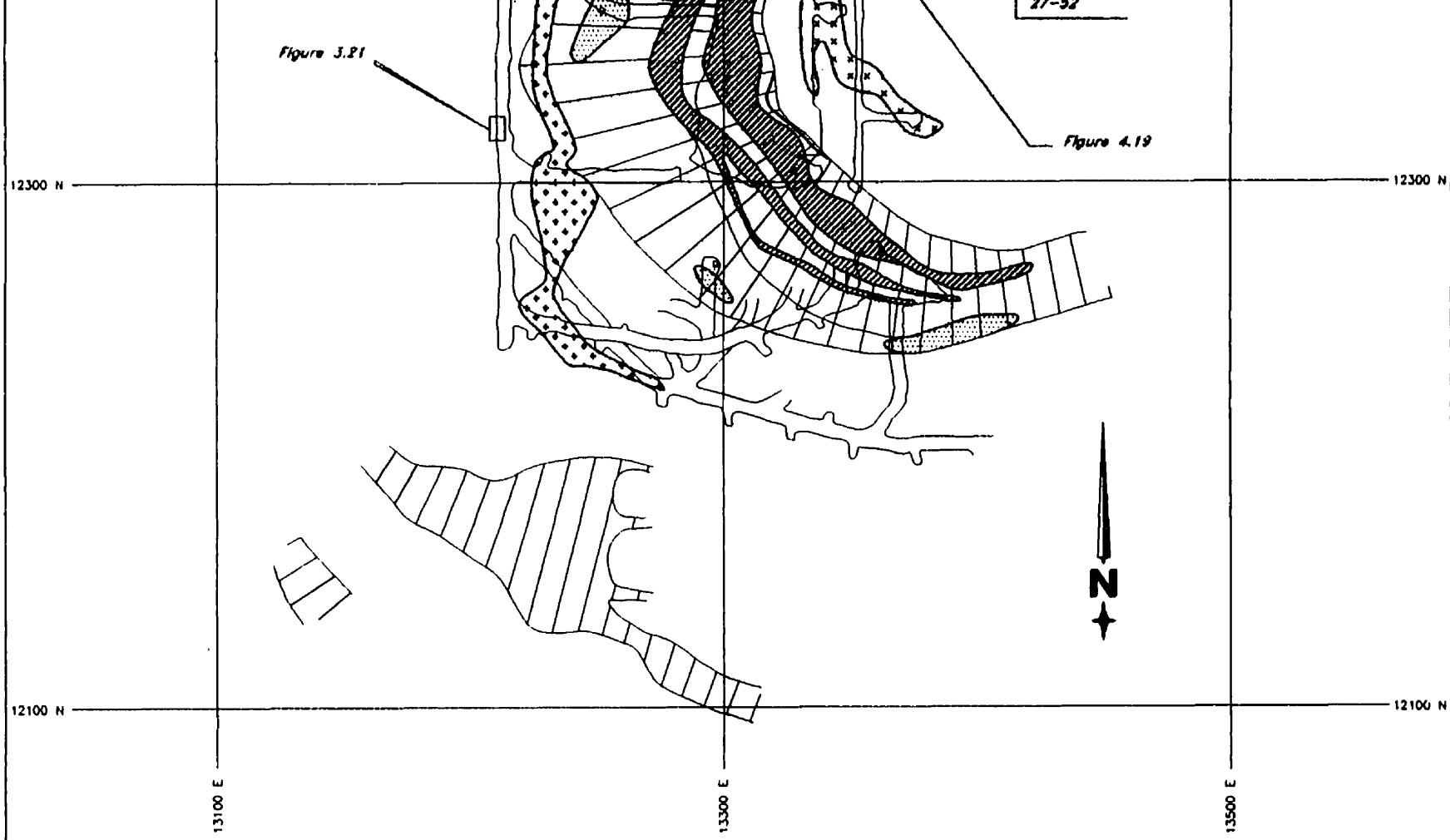

MAIN ORE ZONES	STWK CB-QZ-PY(PO) ± AB-AU	BRECCIA 1	BRECCIA 2
"A" Zone	2-10 %	20-40 %	50-70 %

	Main ore zones (Part albitite dike)	$\bar{x}$ = average grade for this plan
	Ak(Dm)-Qz-Py-Au stockwork vein alteration	$\bar{x}$ = 1.34 g/t Au , 0.34 - 2.98 g/t Au
	"Albitite" dike	$\bar{x}$ = 0.68 g/t Au
	Intermineral granodiorite dike	$\bar{x}$ = Not available
	Intermineral feldspar porphyry dike	$\bar{x}$ = Not available
	Magnesian (West) and iron (East) tholeiites	$\bar{x}$ = 0.18 g/t Au (Bourget A , 1986)
	Cb-Chl-Tc-(Ab) schist ± boudinaged "Albitite" dike inclusions (Dm stwk vein-altered)	$\bar{x}$ = 0.61 g/t Au
40	Main schistosity: Sn	

LES MINES D'OR KIENA LTEE.

27 LEVEL MAP

COMPILED BY : S. Morasse
DATE : 04/20/94
COMPUTER DRAFTING BY : S. Tremblay

SCALE 1 : 2 500
0m 25m 50m

KIENA MINE - 33 LEVEL MAP

Schematic geological plan map of ***level 33*** *of the Kiena Mine (see* ***Figure 3.2****), showing the orebody and its relationships to country rocks, pre-mineral albitite dikes, intermineral granodiorite and feldspar porphyry dikes, the deposit's outer gold alteration halo, the main schistosity, and late-stage faults. Ore zone composition is given in relative percentages of the three ore types encountered at Kiena. The orebody, which dips moderately west (see section 12514.6 N), is predominantly hosted by albitite dikes. The "K" zone is an ore xenolith of the intermineral granodiorite dike. The ore-dike complex is deformed by an asymmetric z-shaped fold and cut by an axial planar schistosity dipping north. Late-stage, oblique-slip faults cut the deformed ore-dike complex as well as the main schistosity. The faults dip steeply to the west and have a right-hand, normal movement.*

Représentation schématique du plan géologique du ***niveau 33*** *de la Mine Kiena (voir* ***Figure 3.2****), montrant la relation spatiale entre le corps minéralisé, les roches encaissantes, les dykes d'albitite pré-minéralisation, les dykes de granodiorite et porphyre feldspathique interminéralisation, le halo d'altération aurifère autour du gisement, la schistosité principale, et des failles tardives. La composition des zones minéralisées est donnée en fonction du pourcentage relatif des trois types de minerai rencontrés à Kiena. Le corps minéralisé pend modérément vers l'ouest (voir section 12514.6 N). La minéralisation est principalement encaissé par les dykes d'albitite. La zone "K" est un xénolithe de minerai au sein du dyke de granodiorite interminéralisation. Le complexe minerai-dyke est déformé par un pli asymétrique en forme de "z" et recoupé par une schistosité de plan axial à pendage nord. Des failles normales à décrochement dextre, recoupent la schistosité principale ainsi que le pli.*

Abbreviations: ***Stwk Cb-Qz-Py(Po)±Ab-Au*** *= carbonate-quartz stockwork veins with albite-pyrite (pyrrhotite)-Au in vein alteration halos (1st ore type);* ***Breccia 1*** *= ankerite-pyrite-Au replacement veins (2nd ore type);* ***Breccia 2*** *= albite-pyrite-chalcopyrite-scheelite-Au stockwork veins (3rd ore type);* ***Ak*** *= ankerite;* ***Dm*** *= dolomite;* ***Qz*** *= quartz;* ***Au*** *= gold;* ***Cb*** *= carbonate;* ***Chl*** *= chlorite;* ***Tc*** *= talc;* ***Ab*** *= albite;* ***g/t*** *= gram per tonne.*

Abréviations: ***Stwk Cb-Qz-Py(Po)-±Ab-Au*** *= stockwork de veines à carbonate et quartz avec halos d'altération à albite-pyrite (pyrrhotine)-Au (1er type de minéralisation);* ***Breccia 2*** *= veine de remplacement à ankérite-pyrite-Au (2ième type de minéralisation);* ***Breccia 2*** *= stockwork de veines à albite-pyrite-chalcopyrite-scheelite-Au (3ième type de minéralisation);* ***Ak*** *= ankérite;* ***Dm*** *= dolomie;* ***Qz*** *= quartz;* ***Au*** *= gold;* ***Cb*** *= carbonate;* ***Chl*** *= chlorite;* ***Tc*** *= talc;* ***Ab*** *= albite;* ***g/t*** *= gramme la tonne.*

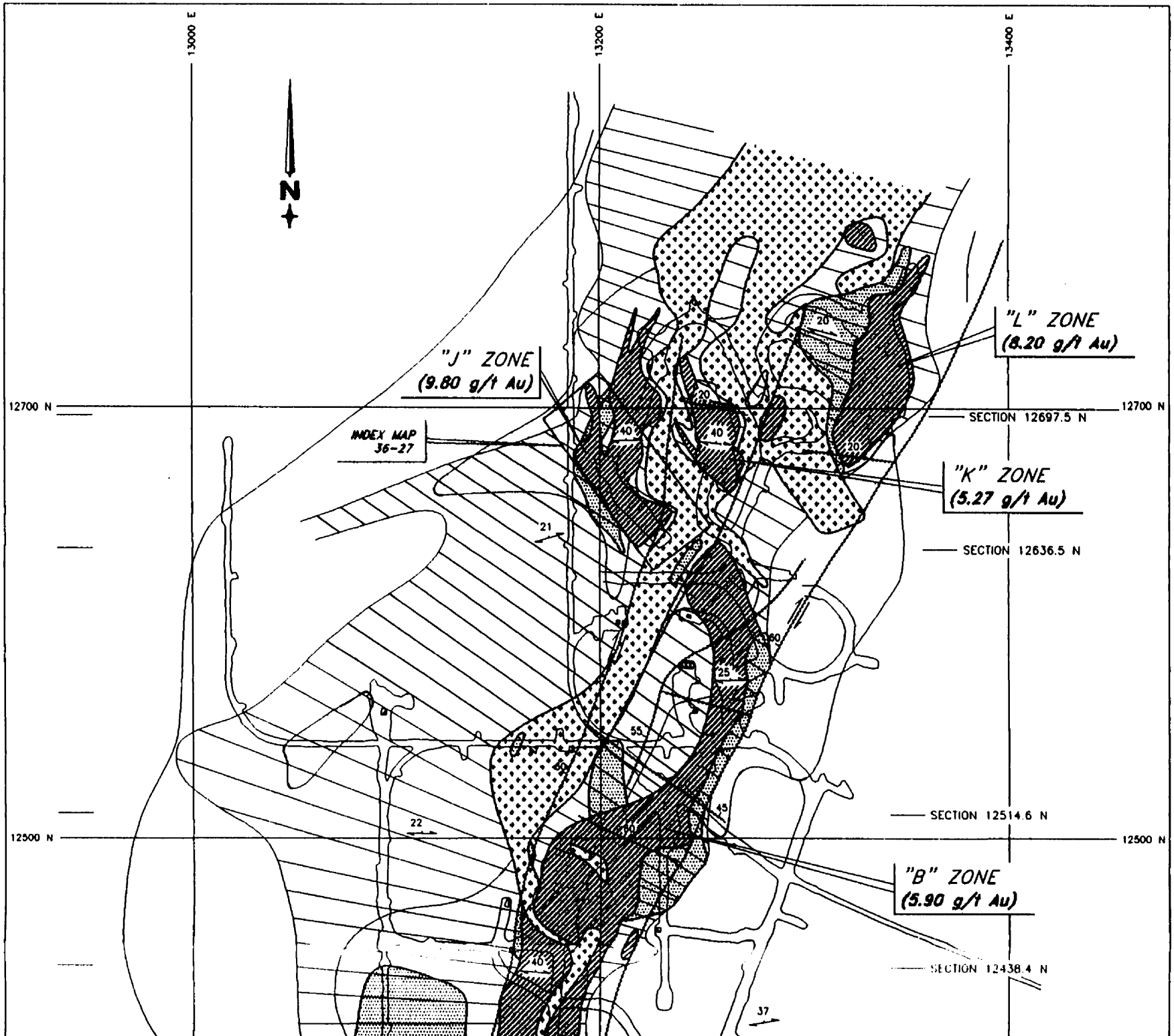
13000 E
13200 E
13400 E
N
"J" ZONE
(9.80 g/t Au)
"L" ZONE
(8.20 g/t Au)
"K" ZONE
(5.27 g/t Au)
"B" ZONE
(5.90 g/t Au)
INDEX MAP
36-27
12700 N
12500 N
SECTION 12697.5 N
SECTION 12636.5 N
SECTION 12514.6 N
SECTION 12438.4 N
20
40
21
60
25
55
45
22
37

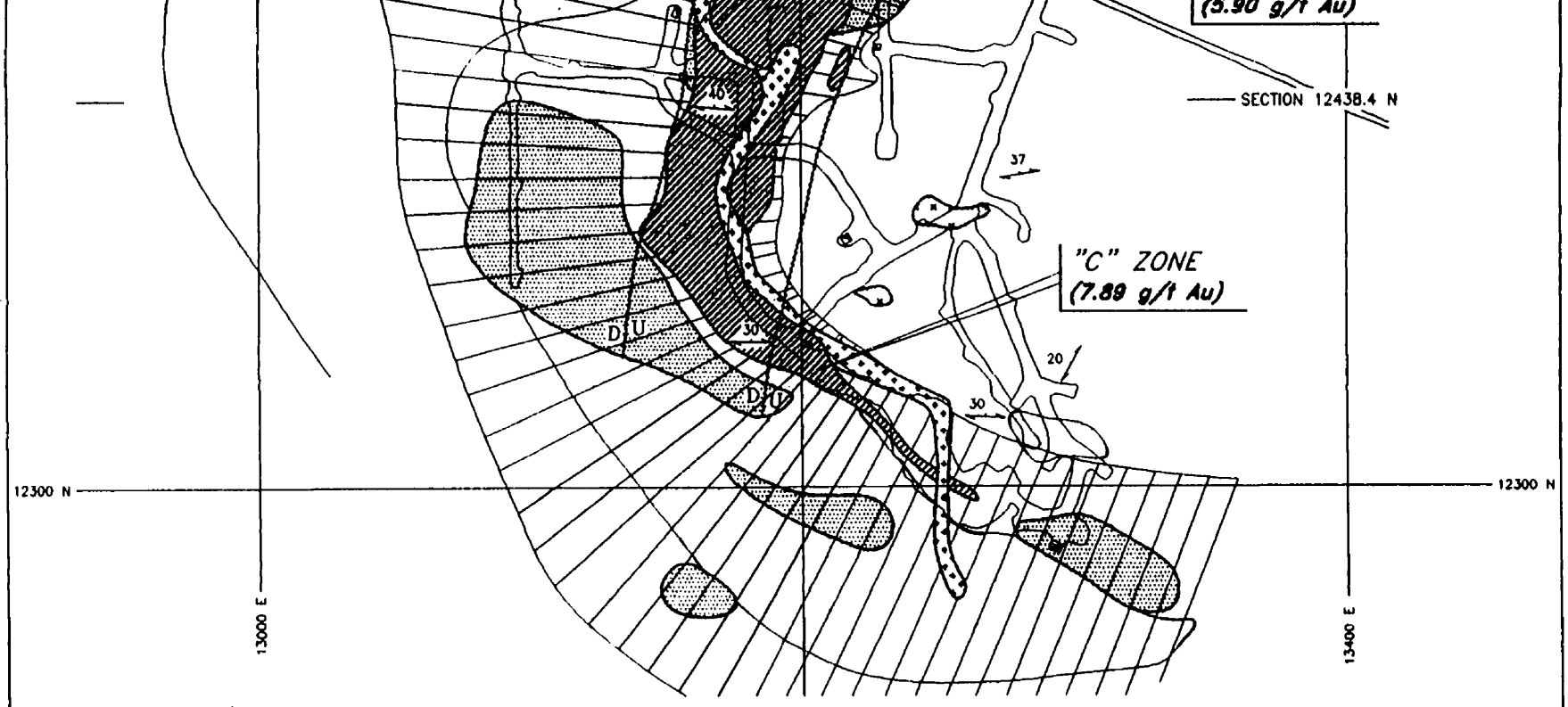

MAIN ORE ZONES	STWK CB-QZ-PY(PO) ± AB-AU	BRECCIA 1	BRECCIA 2
"B" Zone	25-30 %	30-35 %	40-45 %
"C" Zone	75-80 %	15-20 %	0-5 %
"J" Zone	90-95 %	0-5 %	0-5 %
"K" Zone	90-95 %	0-5 %	0-5 %
"L" Zone	90-95 %	0-5 %	0-5 %

	Main ore zones (Part albitite dike)	$\bar{x}$ = average grade for this plan
	Ak(Dm)-Qz-Py-Au stockwork vein alteration	$\bar{x}$ = 1.166 g/t Au
	"Albitite" dike	$\bar{x}$ = 0.82 g/t Au , 0.34-2.40 g/t Au
	Intermineral granodiorite dike	$\bar{x}$ = 630 ppb Au (Stope 30-25)
	Intermineral feldspar porphyry dike	$\bar{x}$ = Not available
	Magnesian (West) and iron (East) tholeiites	$\bar{x}$ = 0.18 g/t Au (Bourget A , 1986)
	Cb-Chl-Tc-(Ab) schist ± boudinaged "Albitite" dike inclusions (Dm stwk vein-altered)	$\bar{x}$ = 0.34 g/t Au
40	Main schistosity: Sn	
30 D U	Brittle ductile , oblique-slip fault (deformation zone averages 0-1 metre) D: Down U: Up	
	Horizontal component of movement	

LES MINES D'OR KIENA LTEE.

33 LEVEL MAP

COMPILED BY : S. Morasse
DATE : 04/20/94
COMPUTER DRAFTING BY : S. Tremblay

SCALE 1 : 2 500
0m 25m 50m

KIENA MINE - 41 LEVEL MAP

Schematic geological plan map of ***level 41*** *of the Kiena Mine (see* ***Figure 3.2****), showing the orebody and its relationships to country rocks, pre-mineral albitite dikes, intermineral granodiorite and feldspar porphyry dikes, the deposit's outer gold alteration halo, the main schistosity, and late-stage faults. Ore zone composition is given in relative percentages of the three ore types encountered at Kiena. The dip of the orebody has changed from moderately west-dipping at upper mine levels, to steeply west-dipping (see section 12514.6 N). Fragments of albitite dikes occur in the hangingwall schist alongside the main orebody, and as xenoliths of the granodiorite dike. The ore mainly consists of "Breccia 2" and "Stwk Cb-Qz-Py(Po)±Ab-Au" vein ore types. The "J" zone is a gold-ore xenolith of the granodiorite dike. The feldspar porphyry dike cuts the ore and the granodiorite dike. The ore-dike complex is deformed by an asymmetric z-shaped fold and cut by an axial planar schistosity dipping north. Late-stage, oblique-slip faults cut the main schistosity and the fold.*

Représentation schématique du plan géologique du ***niveau 41*** *de la Mine Kiena (voir* ***Figure 3.2****), montrant la relation spatiale entre le corps minéralisé, les roches encaissantes, les dykes d'albitite pré-minéralisation, les dykes de granodiorite et porphyre feldspathique interminéralisation, le halo d'altération aurifère autour du gisement, la schistosité principale, et des failles tardives. La composition des zones minéralisées est donnée en fonction du pourcentage relatif des trois types de minerai rencontrés à Kiena. L'inclinaison du corps minéralisé est passée de modéré vers l'ouest aux niveaux supérieurs de la mine, à sub-verticale (voir section 12514.6 N). Des lambeaux de dykes d'albitite apparaissent au sein du schiste de l'éponte supérieure et le long du corps minéralisé, ainsi que sous forme de xénolithe au sein du dyke de granodiorite. Le corps minéralisé est composé principalement de minerai de type "Breccia 2" et "Stwk Cb-Qz-Py(Po)±Ab-Au". La zone minéralisée "J" est un xénolithe du dyke de granodiorite. Le dyke de porphyre feldspathique recoupe le minerai ainsi que le dyke de granodiorite. Le complexe minerai-dyke est déformé par un pli asymétrique en forme de "z" et recoupé par une schistosité de plan axial à pendage nord. Des failles de décrochement à mouvement vertical inverse, recoupent la schistosité ainsi que le pli.*

Abbreviations: *Stwk Cb-Qz-Py(Po)±Ab-Au = carbonate-quartz stockwork veins with albite-pyrite (pyrrhotite)-Au in vein alteration halos (1st ore type);* ***Breccia 1*** *= ankerite-pyrite-Au replacement veins (2nd ore type);* ***Breccia 2*** *= albite-pyrite-chalcopyrite-scheelite-Au stockwork veins (3rd ore type); Ak = ankerite; Dm = dolomite; Qz = quartz; Au = gold; Cb = carbonate; Chl = chlorite; Tc = talc; Ab = albite; g/t = gram per tonne.*

Abréviations: *Stwk Cb-Qz-Py(Po)-±Ab-Au = stockwork de veines à carbonate et quartz avec halos d'altération à albite-pyrite (pyrrhotine)-Au (1er type de minéralisation);* ***Breccia 2*** *= veine de remplacement à ankérite-pyrite-Au (2ième type de minéralisation);* ***Breccia 2*** *= stockwork de veines à albite-pyrite-chalcopyrite-scheelite-Au (3ième type de minéralisation); Ak = ankérite; Dm = dolomie; Qz = quartz; Au = gold; Cb = carbonate; Chl = chlorite; Tc = talc; Ab = albite; g/t = gramme la tonne.*

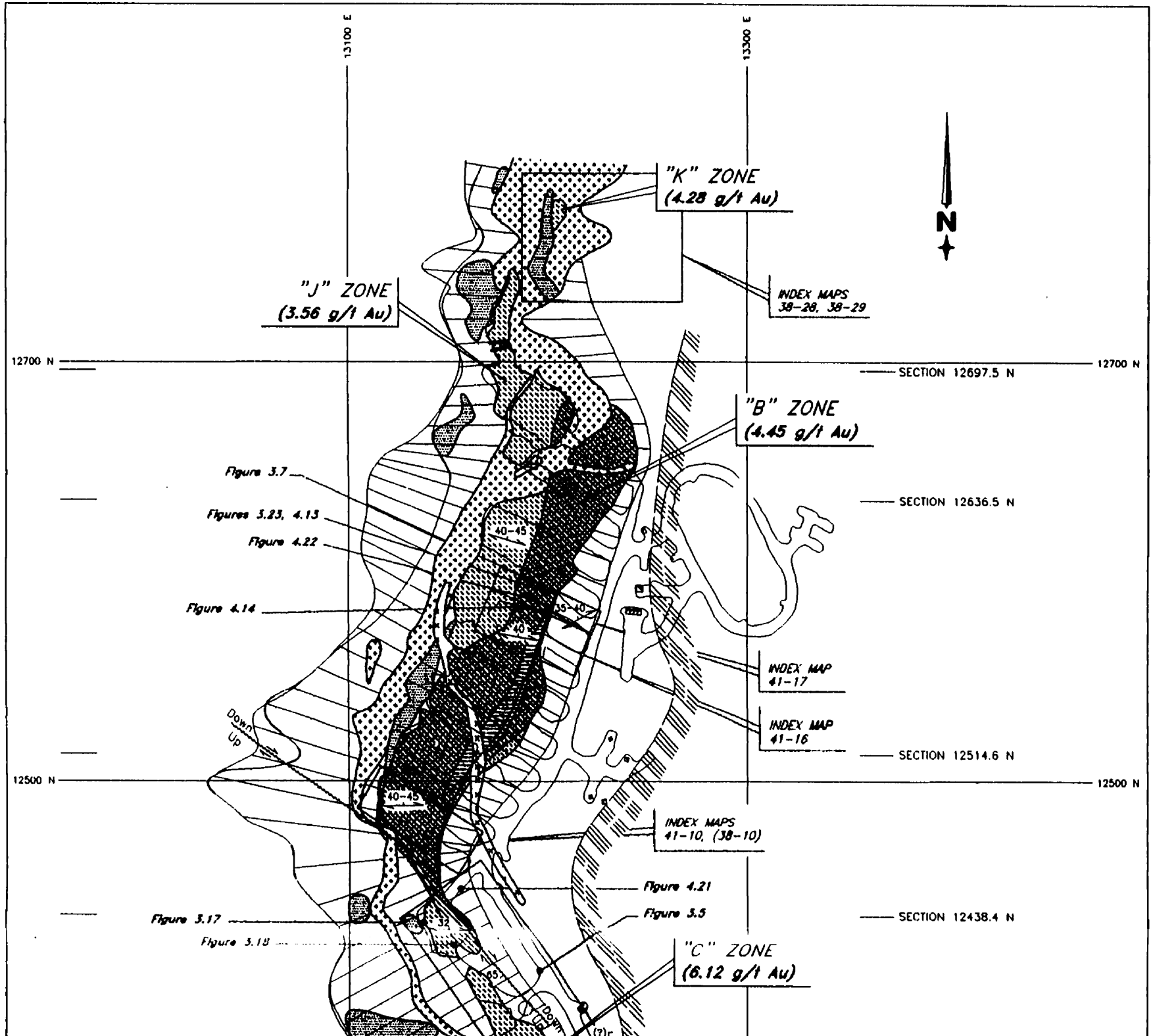
13100 E
13300 E
"K" ZONE
(4.28 g/t Au)
N
"J" ZONE
(3.56 g/t Au)
INDEX MAPS
38-28, 38-29
12700 N
SECTION 12697.5 N
"B" ZONE
(4.45 g/t Au)
Figure 3.7
Figures 3.23, 4.13
Figure 4.22
SECTION 12636.5 N
40-45
Figure 4.14
35-40
40
INDEX MAP
41-17
INDEX MAP
41-16
Down
Up
SECTION 12514.6 N
12500 N
40-45
INDEX MAPS
41-10, (38-10)
Figure 4.21
Figure 3.5
Figure 3.17
SECTION 12438.4 N
Figure 3.19
32
"C" ZONE
(6.12 g/t Au)
45
Down
Up
(?)

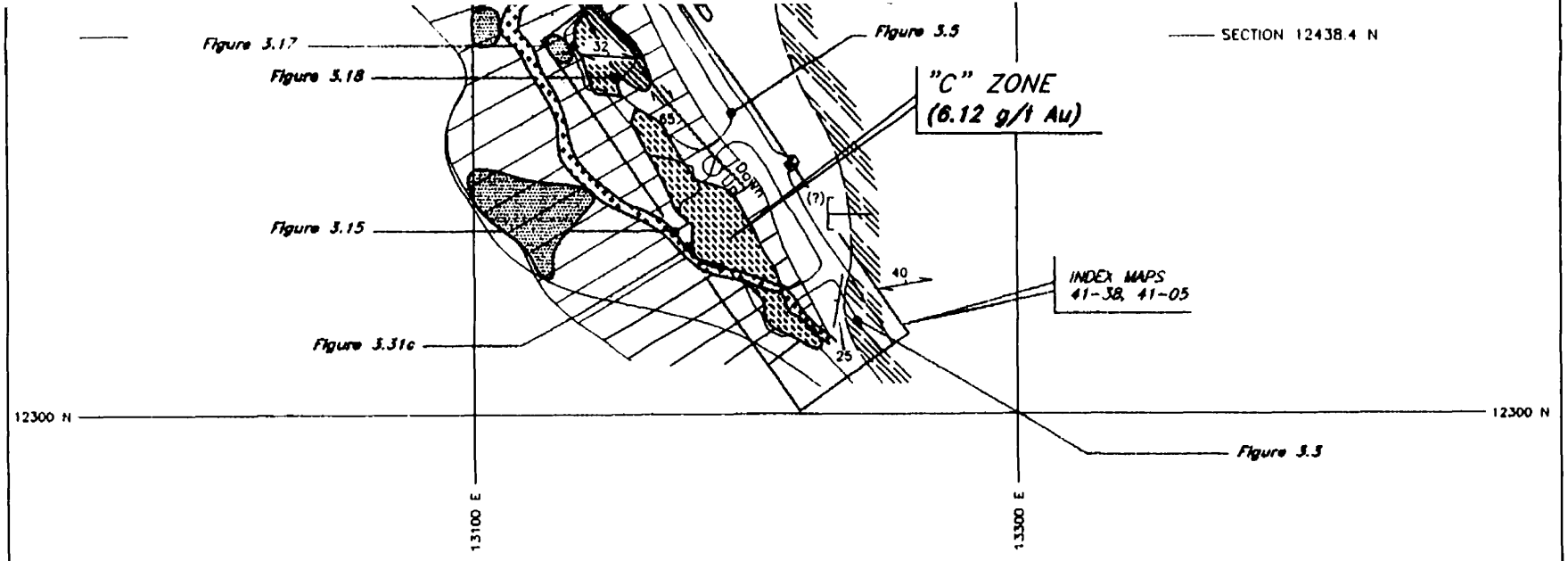

MAIN ORE ZONES (PART ALBITITE DIKE) — $\bar{x}$ = average grade for this plan

- Breccia 2 — $\bar{x}$ = 5.47 g/t Au
- Breccia 1 — $\bar{x}$ = 5.20 g/t Au
- Stwk Cb-Qz-Py(Po) ± Ab-Au — $\bar{x}$ = 4.08 g/t Au

ALTERATION ENVELOPE

- Ak(Dm)-Qz-Py-Au Stockwork vein alteration (Non economic) — $\bar{x}$ = 0.85 g/t Au

INTRUSIVE ROCKS

- "Albitite" dike — $\bar{x}$ = 0.67 g/t Au, 0.34-2.40 g/t Au
- **Intermineral granodiorite dike** — $\bar{x}$ = Not available
- **Intermineral feldspar porphyry dike** — $\bar{x}$ = Not available

VOLCANIC ROCKS

- Magnesian Tholeiite (West) — $\bar{x}$ = 0.18 g/t Au (Bourget A , 1986)
- Iron Tholeiite (East) — $\bar{x}$ = 0.18 g/t Au (Bourget A , 1986)
- Pillowed Magnesian Tholeiite and flow top breccia — $\bar{x}$ = Not available
- Cb-Chl-Tc-(Ab) schist ± boudinaged "Albitite" dike inclusions (Dm-Qtz Stockwork vein-altered) — $\bar{x}$ = Not available

- 45 — Main schistosity :Sn
- 65 — Brittle-ductile, oblique slip fault (deformation zone averages 0-1 metre)
- Horizontal component of movement
- 40 — Bedding and dip
- Stratigraphic younging direction

LES MINES D'OR KIENA LTEE.

41 LEVEL MAP

COMPILED BY : S. Morasse
DATE : 04/20/94
COMPUTER DRAFTING BY : S. Tremblay

SCALE 1 : 2 500
0m 25m 50m

KIENA MINE - 43 LEVEL MAP

*Schematic geological plan map of level 43 of the Kiena Mine (see **Figure 3.2**), showing the orebody and its relationships to country rocks, pre-mineral albitite dikes, intermineral granodiorite and feldspar porphyry dikes, the deposit's outer gold alteration halo, the main schistosity, crenulation cleavage, and late-stage faults. Ore zone composition is given in relative percentages of the three ore types encountered at Kiena. The main orebody is steeply west-dipping to subvertical (see section 12514.6 N). Fragments of albitite dikes can still be observed, but are less common than at upper mine levels. The "B" zone high-grade breccia ore gradually tapers off into the "C" zone Stwk Cb-Qz-Py(Po)±Ab-Au ore type. The main schistosity, which is deformed together with the ore-dike complex by an open fold plunging 30 °to 40 ° to the north-northwest(see section 12514.6 N), is now dipping to the north-northeast (compare with the main schistosity's orientation at level 33). A late-stage, dextral fault cuts the main schistosity and the fold.*

*Représentation schématique du plan géologique du **niveau 43** de la Mine Kiena (voir **Figure 3.2**), montrant la relation spatiale entre le corps minéralisé, les roches encaissantes, les dykes d'albitite pré-minéralisation, les dykes de granodiorite et de porphyre feldspathique interminéralisation, le halo d'altération aurifère autour du gisement, la schistosité principale, le clivage de crénulation, et des failles tardives. La composition des zones minéralisées est donnée en fonction du pourcentage relatif des trois types de minerai rencontrés à Kiena. Le corps minéralisé pend fortement vers l'ouest ou est sub-horizontal (voir section 12514.6 N). Un lambeau de dyke d'albitite peut encore être observé à ce niveau, mais ils deviennent de plus en plus rare avec l'accroissement de la profondeur. Le minerai haute teneur de type brèche de la zone "B" s'amincie en direction du minerai de type Stwk Cb-Qz-Py(Po)±Ab-Au de la zone "C". Le complexe minerai-dyke et la schistosité principale sont déformés par un large pli ouvert plongeant 30 ° à 40 ° vers le nord-nord-ouest (voir la section 12514.6 N), de sorte que la schistosité pend maintenant vers le nord-nord-est (comparer avec l'attitude de la schistosité principale au niveau 33). Une faille tardive à décrochement dextre, recoupe la schistosité principale ainsi que le pli.*

Abbreviations: ***Stwk Cb-Qz-Py(Po)±Ab-Au** = carbonate-quartz stockwork veins with albite-pyrite (pyrrhotite)-Au in vein alteration halos (1st ore type); **Breccia 1** = ankerite-pyrite-Au replacement veins (2nd ore type); **Breccia 2** = albite-pyrite-chalcopyrite-scheelite-Au stockwork veins (3rd ore type); **Ak** = ankerite; **Dm** = dolomite; **Qz** = quartz; **Au** = gold; **Cb** = carbonate; **Chl** = chlorite; **Tc** = talc; **Ab** = albite; **g/t** = gram per tonne.*

Abréviations: ***Stwk Cb-Qz-Py(Po)-±Ab-Au** = stockwork de veines à carbonate et quartz avec halos d'altération à albite-pyrite (pyrrhotine)-Au (1er type de minéralisation); **Breccia 2** = veine de remplacement à ankérite-pyrite-Au (2ième type de minéralisation); **Breccia 2** = stockwork de veines à albite-pyrite-chalcopyrite-scheelite-Au (3ième type de minéralisation); **Ak** = ankérite; **Dm** = dolomie; **Qz** = quartz; **Au** = gold; **Cb** = carbonate; **Chl** = chlorite; **Tc** = talc; **Ab** = albite; **g/t** = gramme la tonne.*


13000 E
13200 E
13400 E
N
12800 N
12800 N
SECTION 12697.5 N
SECTION 12636.5 N
"J" ZONE
(5.14 g/t Au)
Figure 3.13
SECTION 12514.6 N
12600 N
12600 N
"B" ZONE
(5.14 g/t Au)
KIENA SHAFT
INDEX MAP
43-17
Figures 4.12, 4.15
SECTION 12438.4 N
45
75
50
30
15

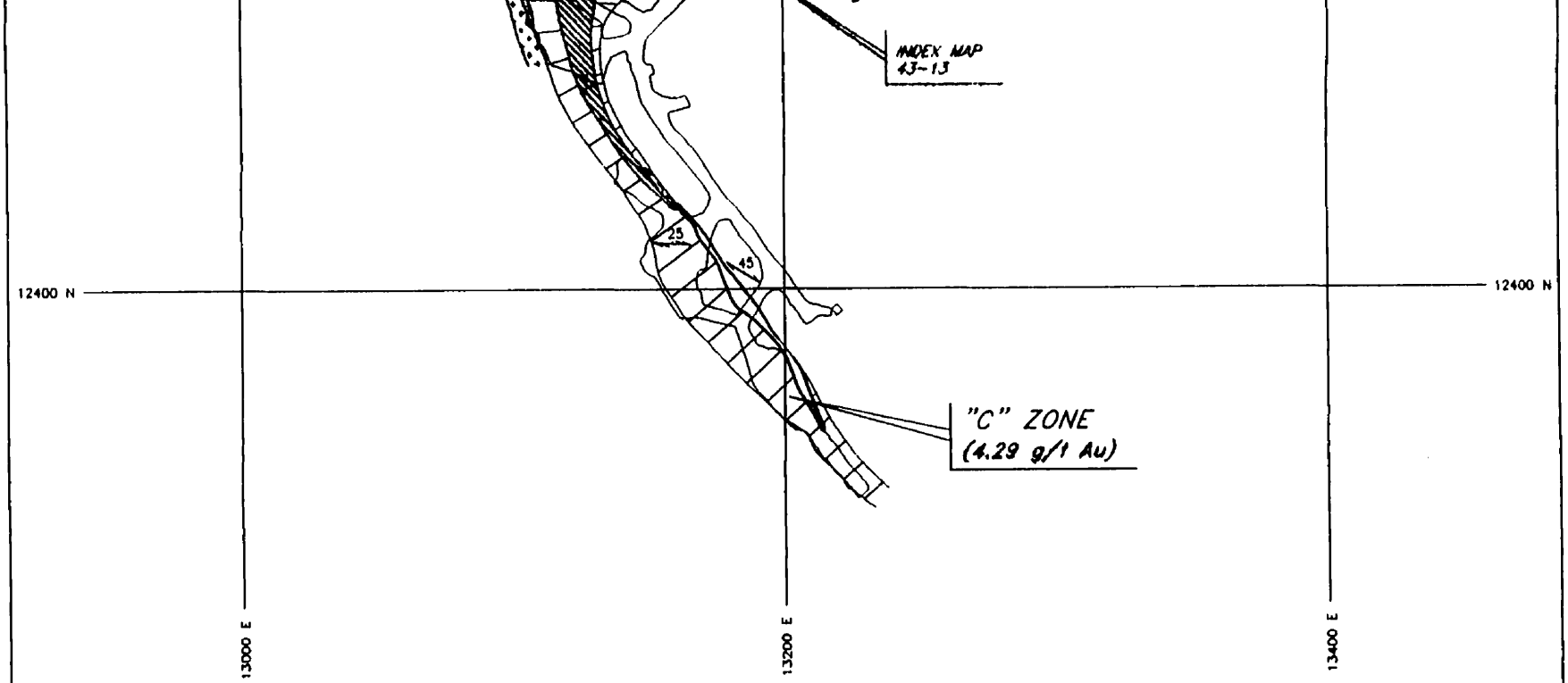

MAIN ORE ZONES	STWK CB-QZ-PY(PO) ± AB-AU	BRECCIA 1	BRECCIA 2
"J" Zone	93-97 %	2-5 %	1-2 %
"B" Zone	45-50 %	25-30 %	25-30 %
"C" Zone	93-97 %	2-5 %	1-2 %

	Main ore zones (Part albitite dike)	$\bar{x}$ = average grade for this plan
	Ak(Dm)-Qz-Py-Au stockwork vein alteration	$\bar{x}$ = 1.03 g/t Au , 0.69 - 2.40 g/t Au
	"Albitite" dike	$\bar{x}$ = 0.81 g/t Au
	Intermineral granodiorite dike	$\bar{x}$ = Not available
	Intermineral feldspar porphyry dike	$\bar{x}$ = Not available
	Magnesian (West) and iron (East) tholeiites	$\bar{x}$ = 0.18 g/t Au (Bourget A , 1986)
	Cb-Chl-Tc-(Ab) schist ± boudinaged "Albitite" dike inclusions (Dm stwk vein-altered)	$\bar{x}$ = 0.80 g/t Au
40	Main schistosity: Sn	
22	Crenulation cleavage: Sn+1	
65	Brittle-ductile , oblique-slip fault (deformation zone averages 1-2 metre)	

LES MINES D'OR KIENA LTEE.

43 LEVEL MAP

COMPILED BY : S. Morasse
DATE : 04/20/94
COMPUTER DRAFTING BY : S. Tremblay

SCALE 1 : 2 500
0m 25m 50m

Geology, Structure and Timing of Gold Mineralization at the Kiena Deposit - Back pocket

S. Morasse 1997

KIENA MINE - 57 LEVEL MAP

*Schematic geological plan map of **level 57** of the Kiena Mine (see **Figure 3.2**), showing the orebody and its relationships to country rocks, pre-mineral albitite dikes, intermineral granodiorite and feldspar porphyry dikes, and the deposit's outer gold alteration halo. The ore-dike complex, which is sub-vertical between levels 48 and 54, has been rotated counter-clockwise during folding, and now dips 65 ° east (see section 12514.6 N). At this depth, the ore consists of an anastomosing network of strongly foliated to schistose albitite dikes mineralized by the "Stwk Cb-Qz-Po(Py)±Ab-Au" vein ore type. The intermineral feldspar porphyry dike cuts the ore and the granodiorite dike. The ore and porphyry dikes are strongly schistose.*

*Représentation schématique du plan géologique du **niveau 57** de la Mine Kiena (voir **Figure 3.2**), montrant la relation spatiale entre le corps minéralisé, les roches encaissantes, les dykes d'albitite pré-minéralisation, les dykes de granodiorite et de porphyre feldspathique interminéralisation, et le halo d'altération aurifère autour du gisement. Le complexe minerai-dyke, lequel est sub-vertical entre les niveaux 48 et 54, a subit une rotation anti-horaire pendant le plissement et pend maintenant à 65 ° vers l'est (voir section 12514.6 N). A cette profondeur, le minerai est essentiellement de type "Stwk Cb-Qz-Po(Py)±Ab-Au" et encaissé par des dykes d'albitite faiblement anastamosés. Le dyke de porphyre feldspathique interminéralisation recoupe le minerai et le dyke de granodiorite. Le minerai et les dykes sont fortement schistosés.*

*Abbreviations: **Stwk Cb-Qz-Py(Po)±Ab-Au** = carbonate-quartz stockwork veins with albite-pyrite (pyrrhotite)-Au in vein alteration halos (1st ore type); **Breccia 1** = ankerite-pyrite-Au replacement veins (2nd ore type); **Breccia 2** = albite-pyrite-chalcopyrite-scheelite-Au stockwork veins (3rd ore type); **Ak** = ankerite; **Dm** = dolomite; **Qz** = quartz; **Au** = gold; **Cb** = carbonate; **Chl** = chlorite; **Tc** = talc; **Ab** = albite; **g/t** = gram per tonne.*

*Abréviations: **Stwk Cb-Qz-Py(Po)-±Ab-Au** = stockwork de veines à carbonate et quartz avec halos d'altération à albite-pyrite (pyrrhotine)-Au (1er type de minéralisation); **Breccia 2** = veine de remplacement à ankérite-pyrite-Au (2ième type de minéralisation); **Breccia 2** = stockwork de veines à albite-pyrite-chalcopyrite-scheelite-Au (3ième type de minéralisation); **Ak** = ankérite; **Dm** = dolomie; **Qz** = quartz; **Au** = gold; **Cb** = carbonate; **Chl** = chlorite; **Tc** = talc; **Ab** = albite; **g/t** = gramme la tonne.*

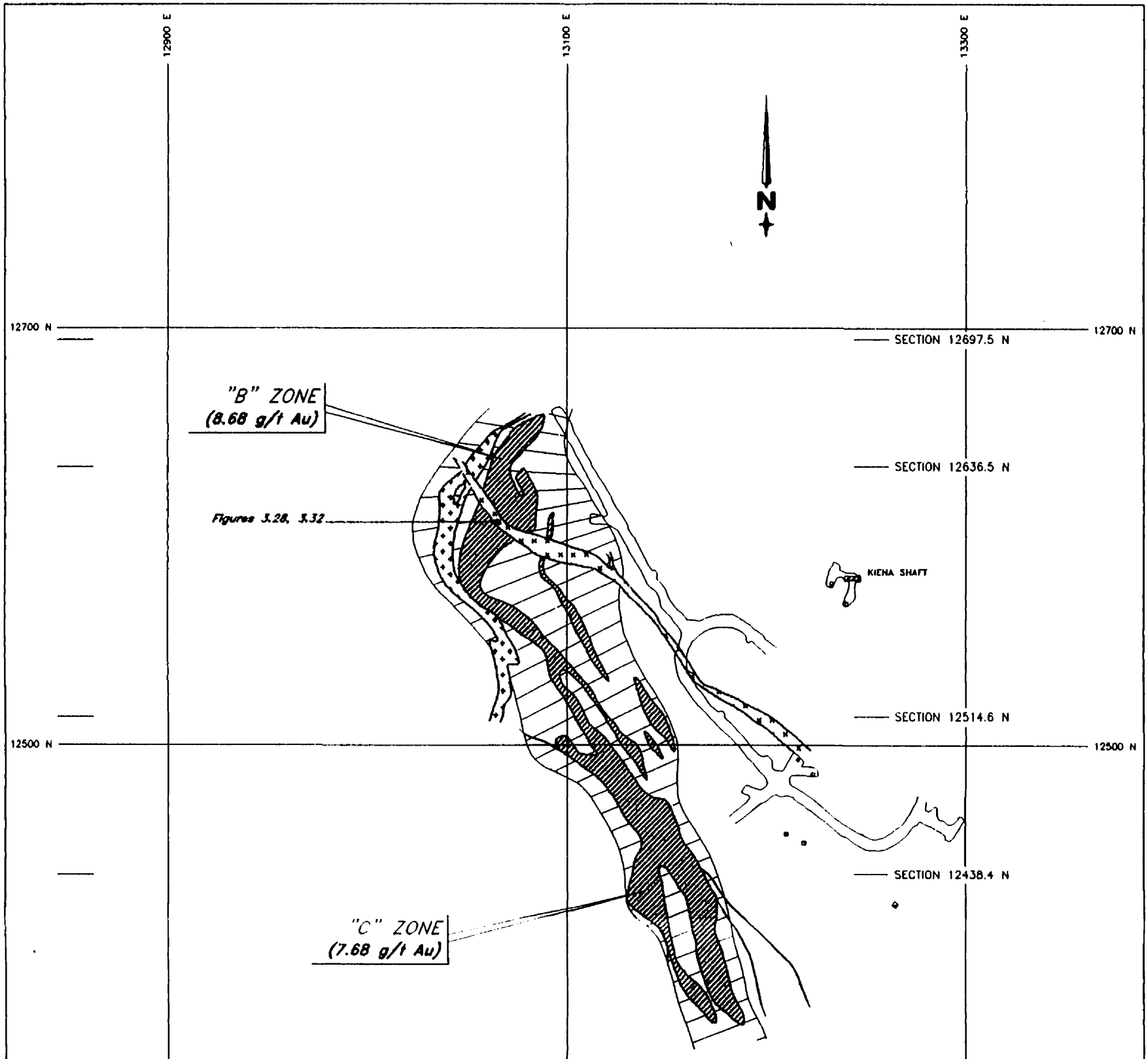
12900 E
13100 E
13300 E
N
12700 N
SECTION 12697.5 N
"B" ZONE
(8.68 g/t Au)
SECTION 12636.5 N
Figures 3.28, 3.32
KIENA SHAFT
SECTION 12514.6 N
12500 N
SECTION 12438.4 N
"C" ZONE
(7.68 g/t Au)

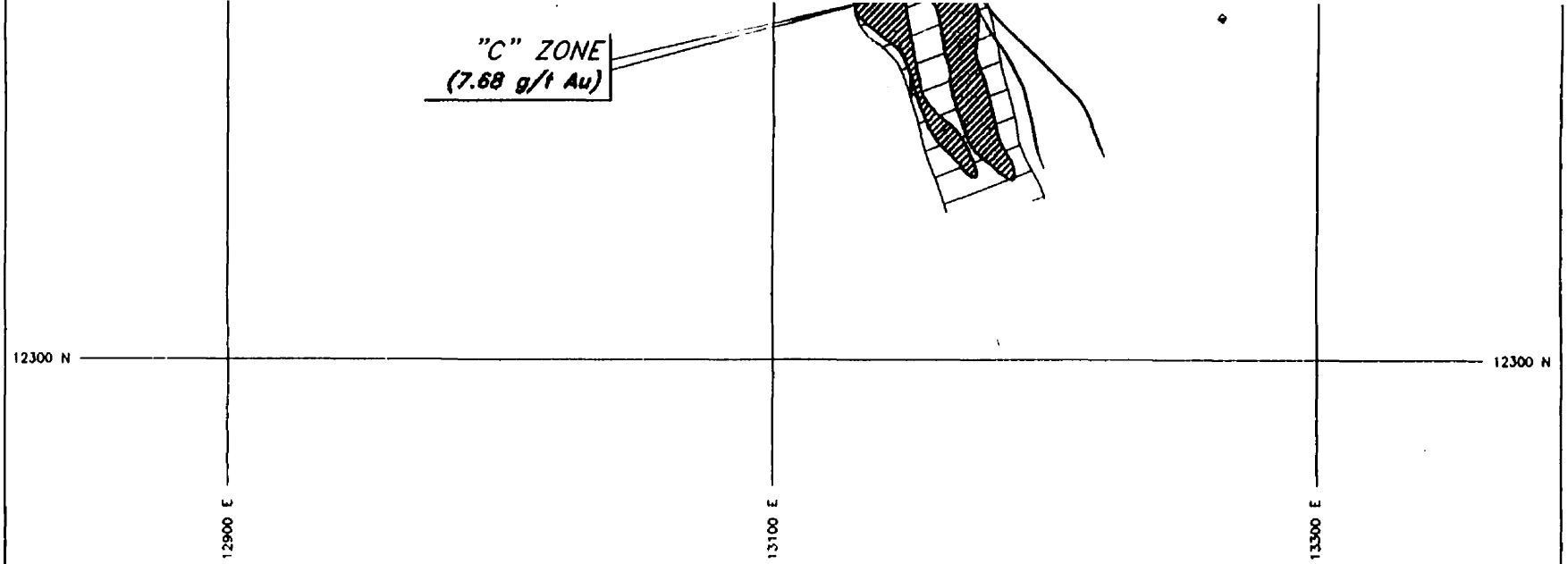

MAIN ORE ZONES	STWK CB-QZ-PY(PO) ± AB-AU	BRECCIA 1	BRECCIA 2
"B" Zone	N/A	N/A	N/A
"C" Zone	100 %	-	-

	Main ore zones (Part albitite dike)	$\bar{x}$ = average grade for this plan
	Ak(Dm)-Qz-Py-Au stockwork vein alteration	$\bar{x}$ = 0.57 g/t Au , 0.14 - 2.67 g/t Au
	Intermineral granodiorite dike	$\bar{x}$ = Not available
	Intermineral feldspar porphyry dike	$\bar{x}$ = Not available
	Magnesian (West) and iron (East) tholeiites	$\bar{x}$ = 0.18 g/t Au (Bourget A , 1986)
	Cb-Chl-Tc-(Ab) schist + boudinaged "Albitite" dike inclusions (Dm stwk vein-altered)	$\bar{x}$ = Not available

LES MINES D'OR KIENA LTEE.

57 LEVEL MAP

COMPILED BY : S. Morasse
DATE : 04/20/94
COMPUTER DRAFTING BY : S. Tremblay

SCALE 1 : 2 500
0m 25m 50m

KIENA MINE - 64 LEVEL MAP

Schematic geological plan map of ***level 64*** *of the Kiena Mine (see* ***Figure 3.2****), showing the orebody and its relationships to country rocks, pre-mineral albitite dikes, intermineral granodiorite and feldspar porphyry dikes, the deposit's outer gold alteration halo, the main schistosity and crenulation cleavage. Breccia ore types no longer exist at this depth. The ore consists of an anastomosing network of strongly foliated to schistose albitite dikes mineralized by the "Stwk Cb-Qz-Po(Py)±Ab-Au" vein ore type. At this level, the network of mineralized albitite dikes is much tighter than at level 57, suggesting that deformation increases with depth. The main planar fabric has evolved from a moderately north-dipping schistosity (or spaced cleavage) at upper mine levels (e.g. 33 Level Map), to a steeply northeast-dipping schistosity at depth. The ore-dike complex and the main schistosity are overprinted by a gently, northeast-dipping crenulation cleavage.*

Représentation schématique du plan géologique du ***niveau 64*** *de la Mine Kiena (voir* ***Figure 3.2****), montrant la relation spatiale entre le corps minéralisé, les roches encaissantes, les dykes d'albitite pré-minéralisation, les dykes de granodiorite et porphyre feldspathique interminéralisation, la schistosité principale et le clivage de crénulation. Il n'y a plus de minerai de type brèche à cette profondeur. Le minerai est essentiellement de type "Stwk Cb-Qz-Po(Py)±Ab-Au" et encaissé par des dykes d'albitite. Le réseau de dykes s'est considérablement reserré depuis le niveau 57, ce qui suggère que le taux de déformation augmente avec la profondeur. La schistosité principale (ou clivage d'espacement) pendant modérément vers le nord aux niveaux supérieurs de la mine (e.g. niveau: 33) est maintenant passé à une schistosité pendant fortement vers le nord-est. La schistosité principale, qui recoupe à la fois le minerai et les dykes interminéralisation, est affectée d'un clivage de crénulation à faible pendage nord-est.*

Abbreviations: ***Stwk Cb-Qz-Py(Po)±Ab-Au*** *= carbonate-quartz stockwork veins with albite-pyrite (pyrrhotite)-Au in vein alteration halos (1st ore type).* ***Breccia 1*** *= ankerite-pyrite-Au replacement veins (2nd ore type);* ***Breccia 2*** *= albite-pyrite-chalcopyrite-scheelite-Au stockwork veins (3rd ore type);* ***Ak*** *= ankerite;* ***Dm*** *= dolomite;* ***Qz*** *= quartz;* ***Au*** *= gold;* ***Cb*** *= carbonate;* ***Chl*** *= chlorite;* ***Tc*** *= talc;* ***Ab*** *= albite;* ***g/t*** *= gram per tonne.*

Abréviations: ***Stwk Cb-Qz-Py(Po)-±Ab-Au*** *= stockwork de veines à carbonate et quartz avec halos d'altération à albite-pyrite (pyrrhotine)-Au (1er type de minéralisation);* ***Breccia 2*** *= veine de remplacement à ankérite-pyrite-Au (2ième type de minéralisation);* ***Breccia 2*** *= stockwork de veines à albite-pyrite-chalcopyrite-scheelite-Au (3ième type de minéralisation);* ***Ak*** *= ankérite;* ***Dm*** *= dolomie,* ***Qz*** *= quartz;* ***Au*** *= gold;* ***Cb*** *= carbonate;* ***Chl*** *= chlorite;* ***Tc*** *= talc;* ***Ab*** *= albite;* ***g/t*** *= gramme la tonne.*

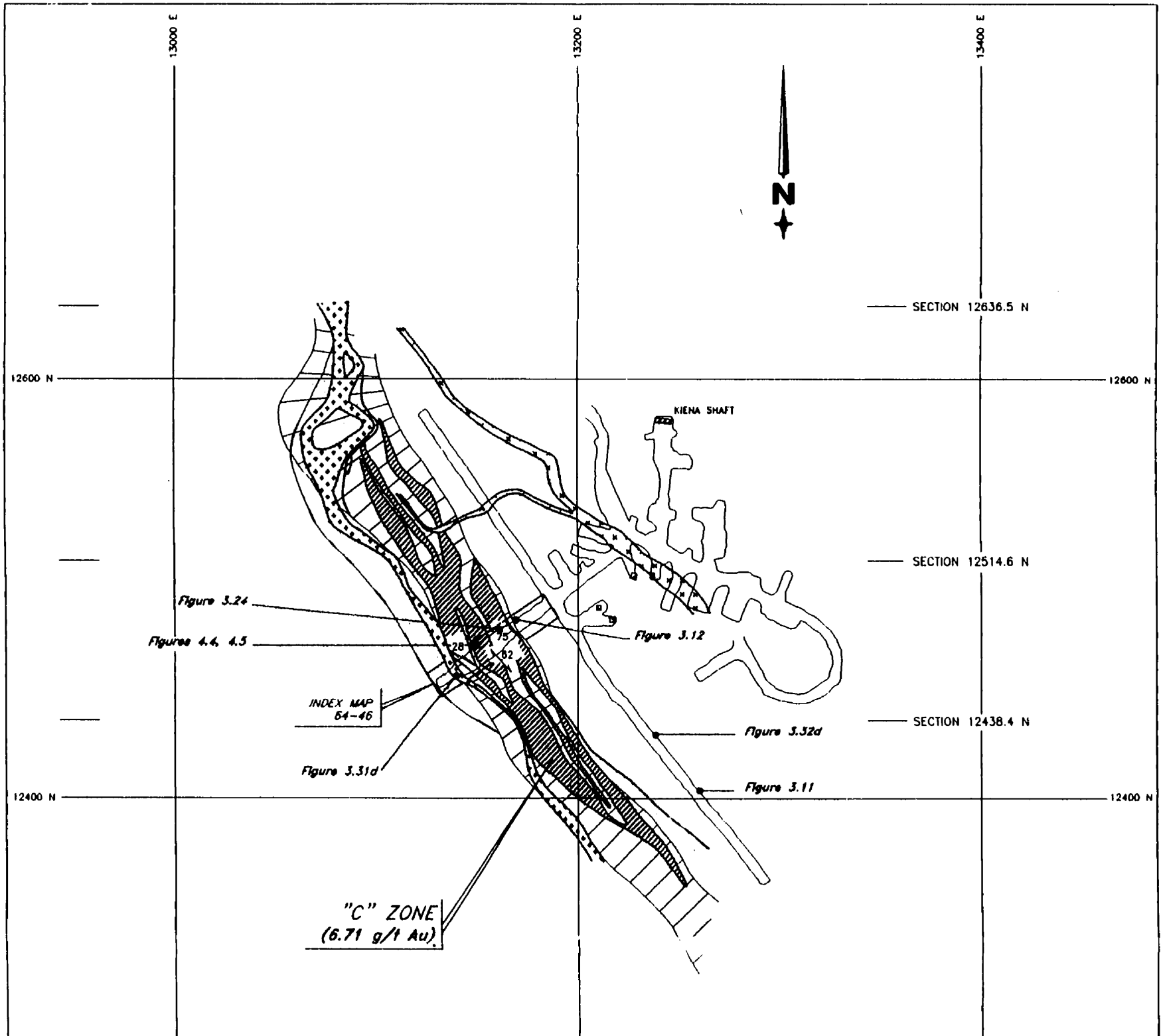
13000 E
13200 E
13400 E
N
SECTION 12636.5 N
12600 N
12600 N
KIENA SHAFT
SECTION 12514.6 N
Figure 3.24
Figures 4.4, 4.5
Figure 3.12
75
28
82
INDEX MAP
64-46
SECTION 12438.4 N
Figure 3.32d
Figure 3.31d
Figure 3.11
12400 N
12400 N
"C" ZONE
(6.71 g/t Au)

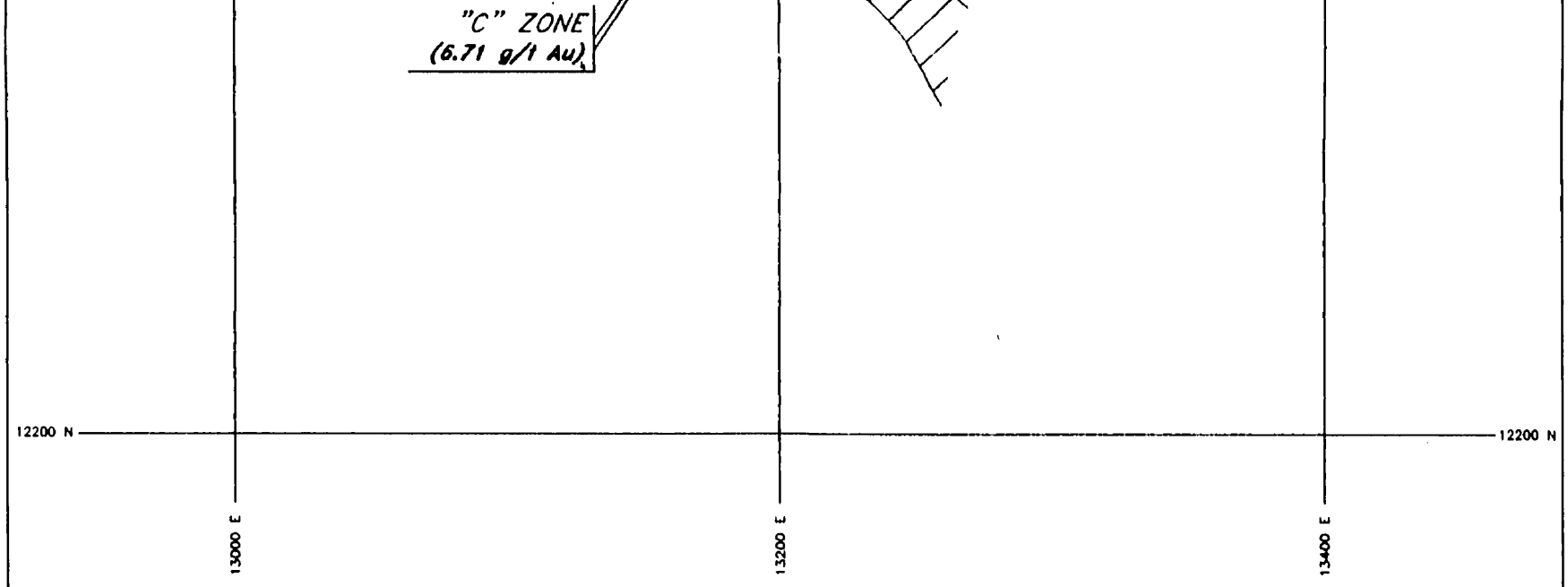

MAIN ORE ZONES	STWK CB-QZ-PO(PY) ± AB-AU	BRECCIA 1	BRECCIA 2
"C" Zone	100 %	-	-

	Main ore zones (Part albitite dike)	$\bar{x}$ = average grade for this plan
	Ak(Dm)-Qz-Po(Py)-Au stockwork vein alteration	$\bar{x}$ = 1.43 g/t Au , 0.34 - 2.98 g/t Au
	Intermineral granodiorite dike	$\bar{x}$ = 70 ppb Au (Stope 64-46)
	Intermineral feldspar porphyry dike	$\bar{x}$ = Not available
	Magnesian (West) and iron (East) tholeiites	$\bar{x}$ = 0.18 g/t Au (Bourget A , 1986)
	Cb-Chl-Tc-(Ab) schist ± boudinaged "Albitite" dike inclusions (Dm stwk vein-altered)	$\bar{x}$ = Not available
60	Main schistosity: Sn	
25	Crenulation cleavage Sn+1	
75	Dextral oblique-slip fault	

LES MINES D'OR KIENA LTEE.

64 LEVEL MAP

COMPILED BY : S. Morasse
DATE : 04/20/94
COMPUTER DRAFTING BY : S. Tremblay

SCALE 1 : 2 500
0m 25m 50m

PLEASE NOTE:

Oversize maps and charts are filmed in sections in the following manner:

LEFT TO RIGHT, TOP TO BOTTOM, WITH SMALL OVERLAPS

The following map or chart has been refilmed in its entirety at the end of this dissertation (not available on microfiche). A xerographic reproduction has been provided for paper copies and is inserted into the inside of the back cover.

Black and white photographic prints (17" x 23") are available for an additional charge.

University Microfilms International

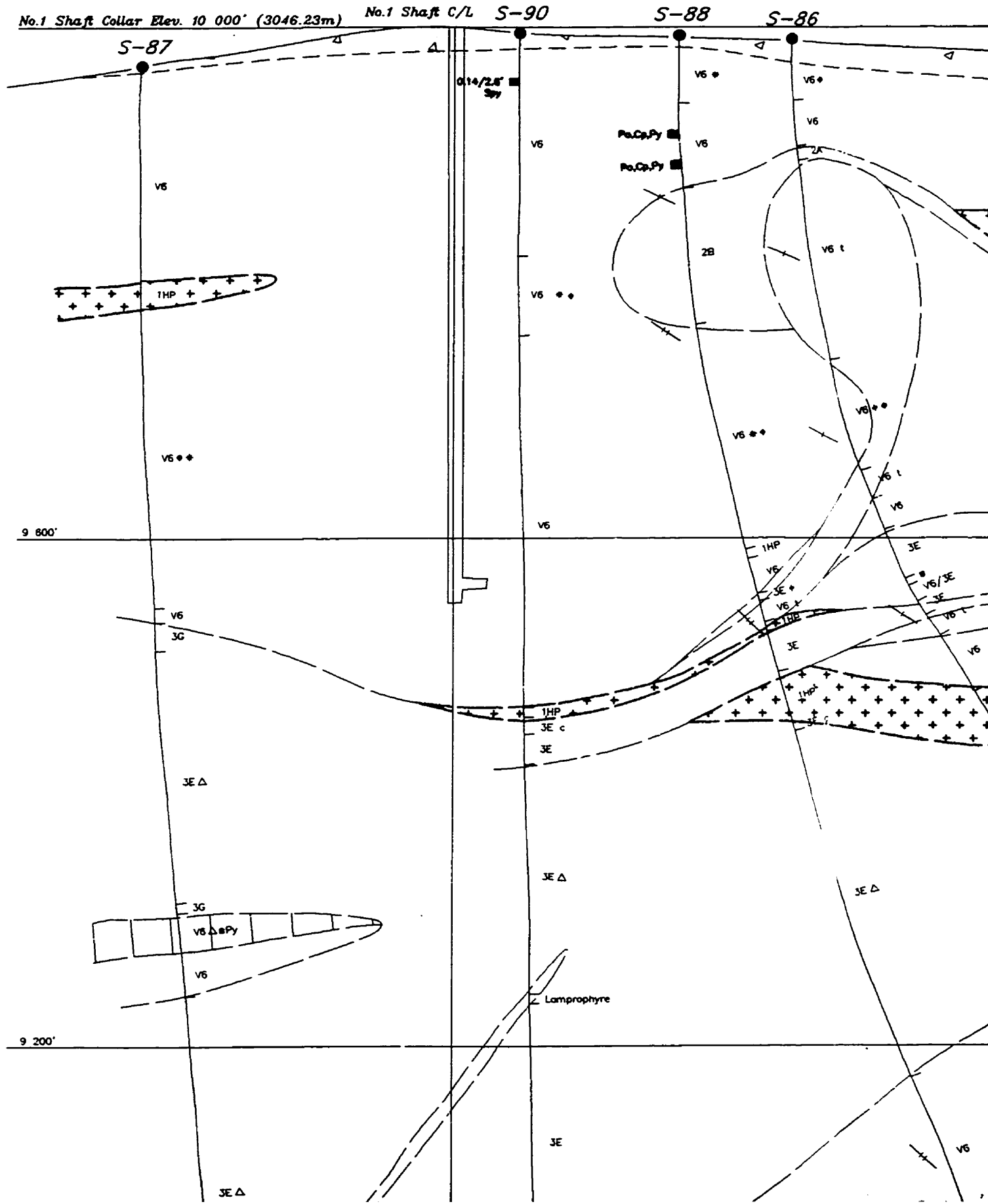
No.1 Shaft Collar Elev. 10 000' (3046.23m)
No.1 Shaft C/L
S-90
S-88
S-86
S-87
0.14/2.6' Spy
Po,Cp,Py
Po,Cp,Py
V6
1HP
2A
2B
V6 t
3E
3E c
3G
V6 Δ sPy
Lamprophyre
9 600'
9 200'

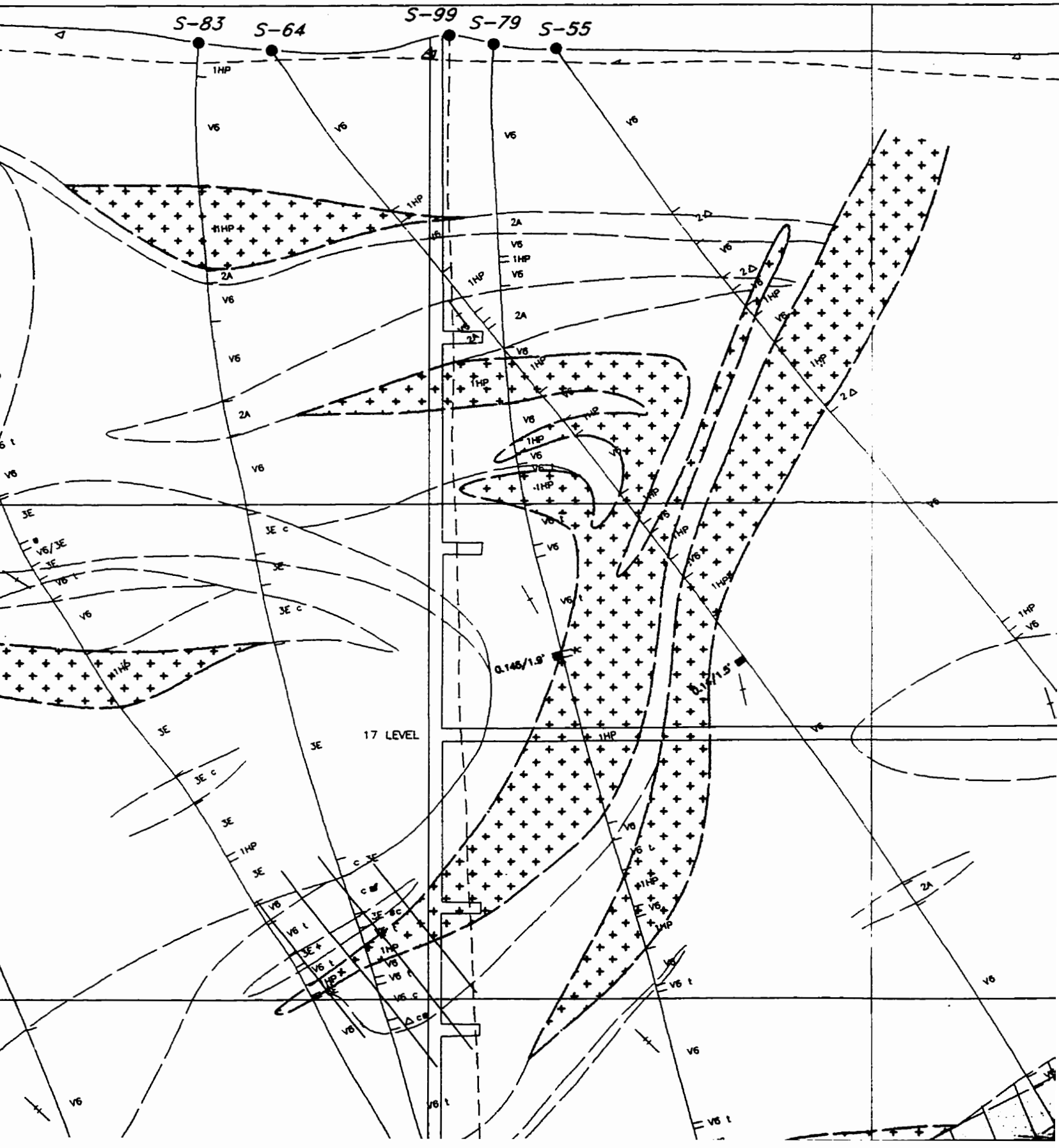
S-83
S-64
S-99
S-79
S-55
17 LEVEL

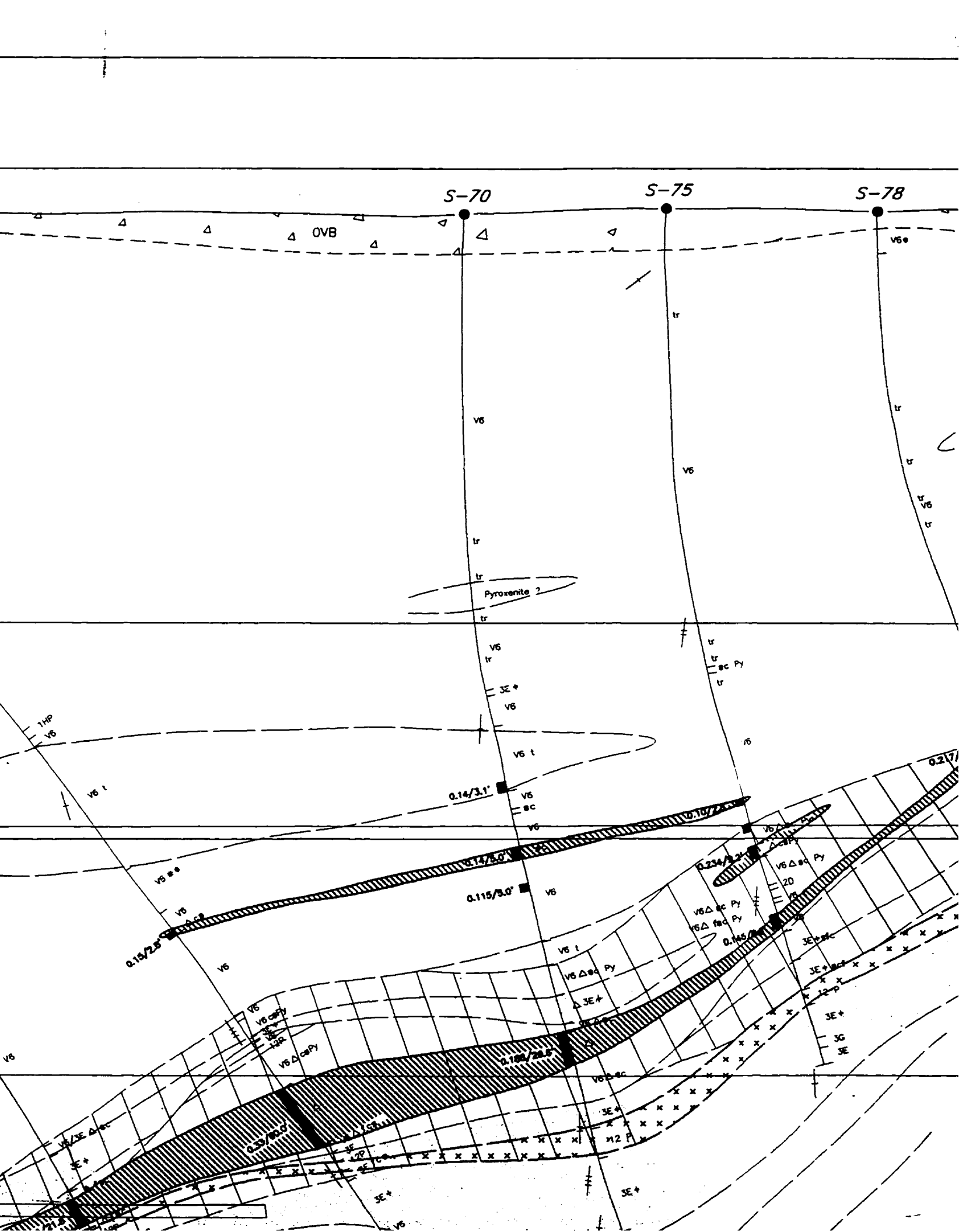
S-70
S-75
S-78
OVB
Pyroxenite 2
0.14/3.1'
0.115/3.0'
0.15/2.8'
0.33/10.0'
0.188/28.6'
0.10/2.4'
0.234/3.2'
0.145/3.8'
0.14/5.0'

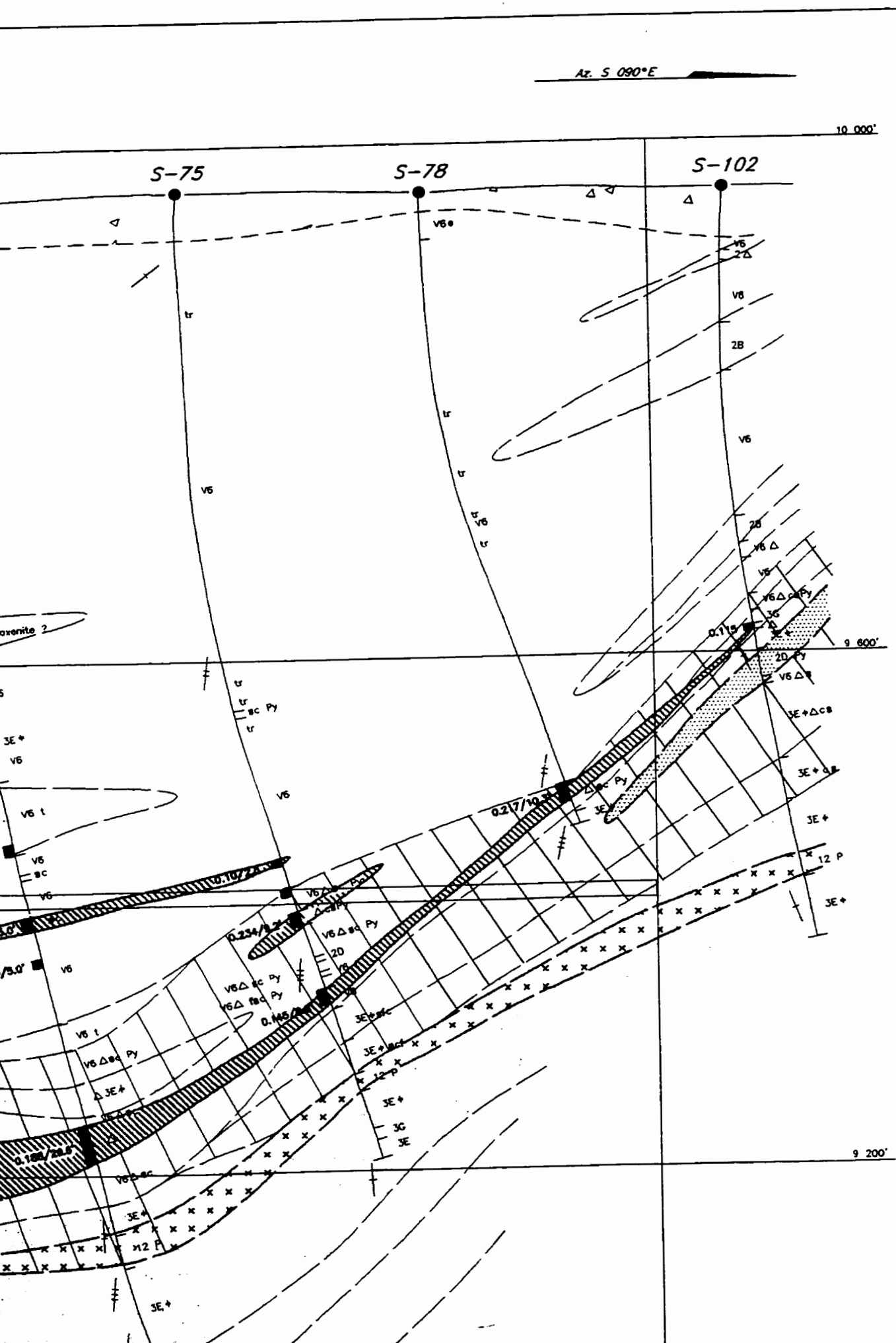
Az. S 090°E
10 000'
S-75
S-78
S-102
9 600'
9 200'
tr
V6
2B
2D
3E+
12 P
3G
3E

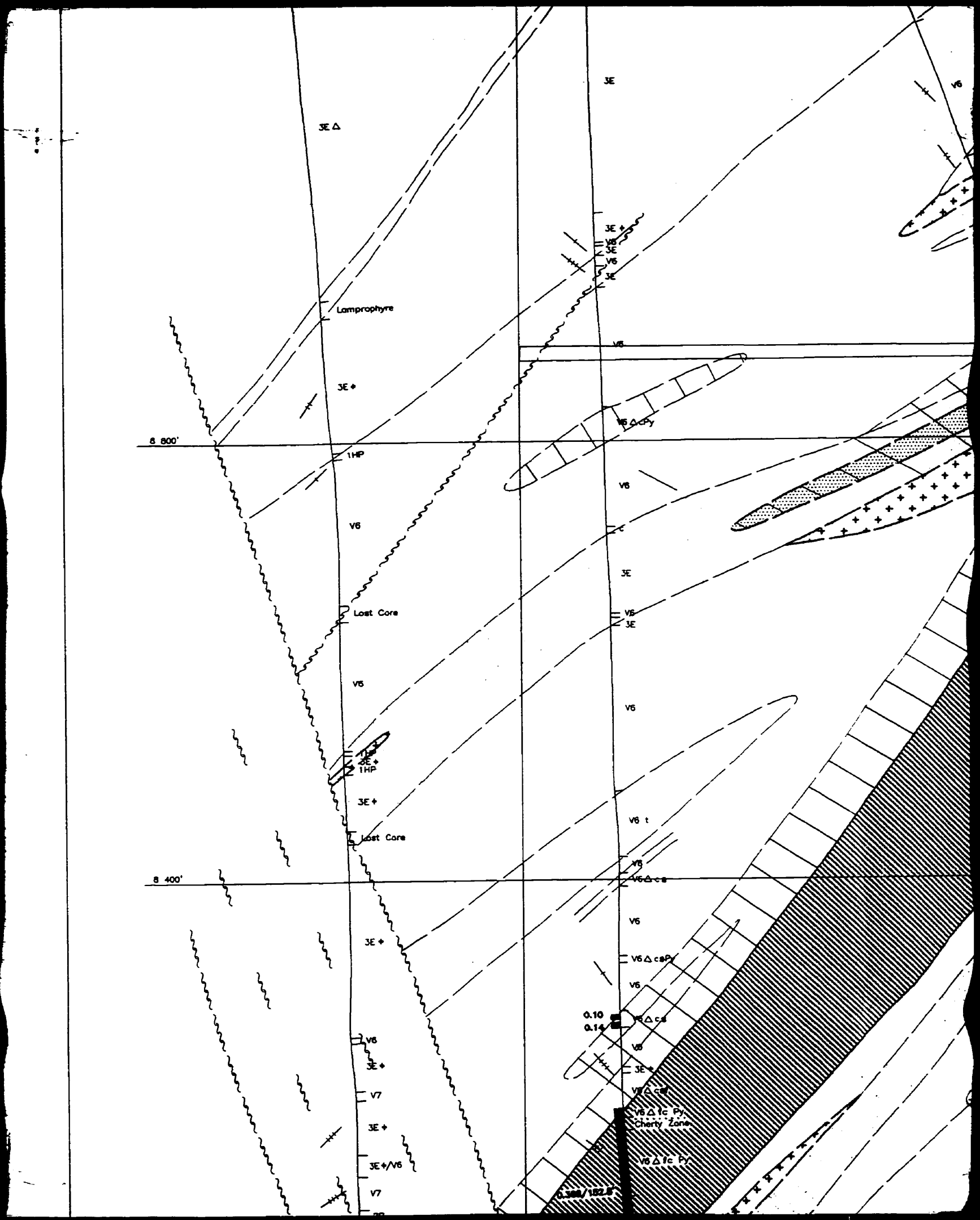
3E Δ
3E
V6
3E +
V6
3E
V6
3E
Lamprophyre
V6
3E +
V6 Δ cPy
S 800'
1HP
V6
V6
3E
Lost Core
V6
V6
3E
V6
3E +
1HP
3E +
Lost Core
V6 t
S 400'
V6
V6 Δ cs
V6
3E +
V6 Δ csPy
V6
0.10
0.1
V6 Δ cs
V6
3E +
V6 Δ csPy
V6 Δ fc Py
Charty Zone
V6
3E +
V7
3E +
3E +/V6
V7
V6 Δ fc Py

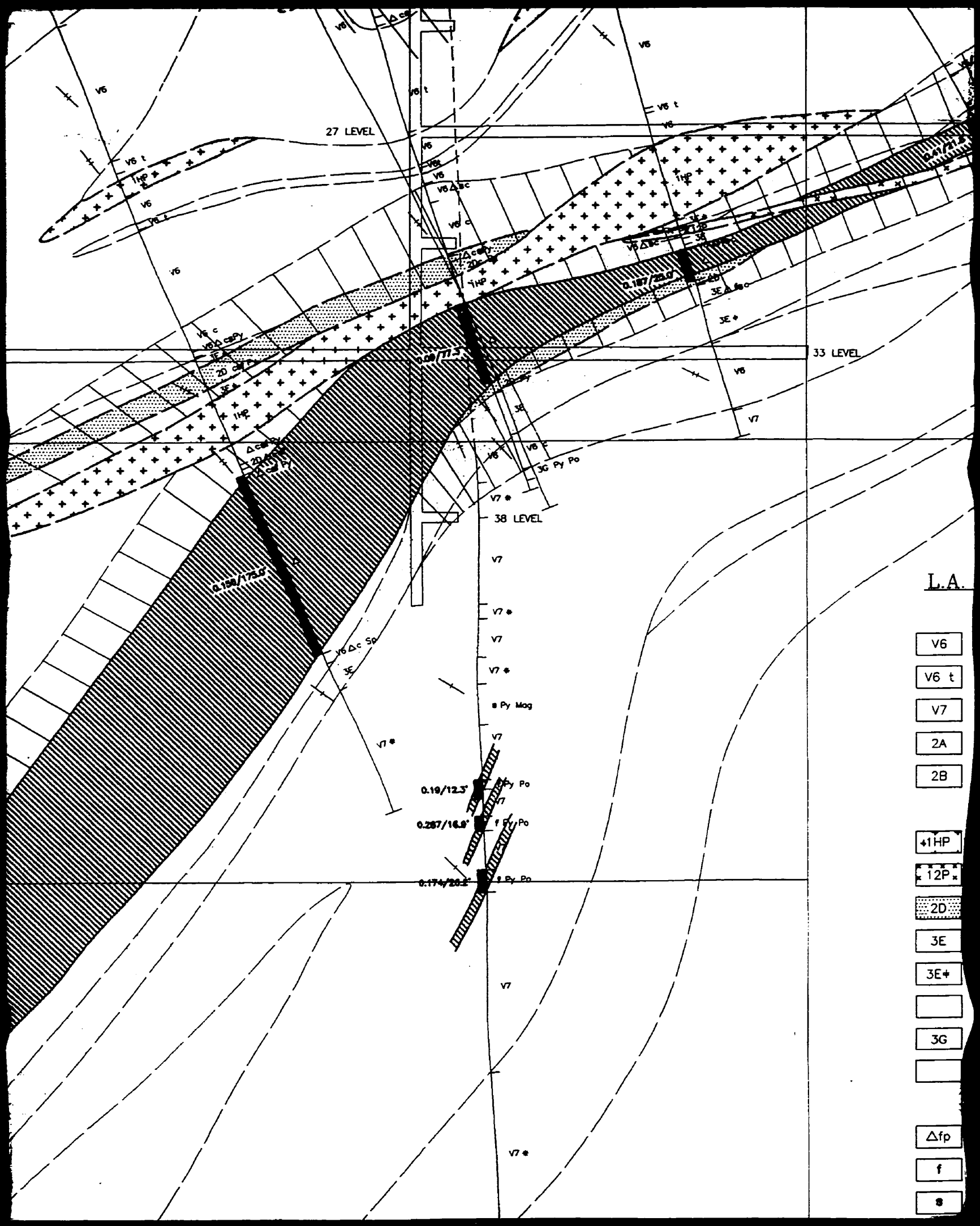
27 LEVEL
33 LEVEL
38 LEVEL
V6
V6 t
V7
2A
2B
1HP
12P
2D
3E
3E*
3G
Δfp
f
s
L.A.

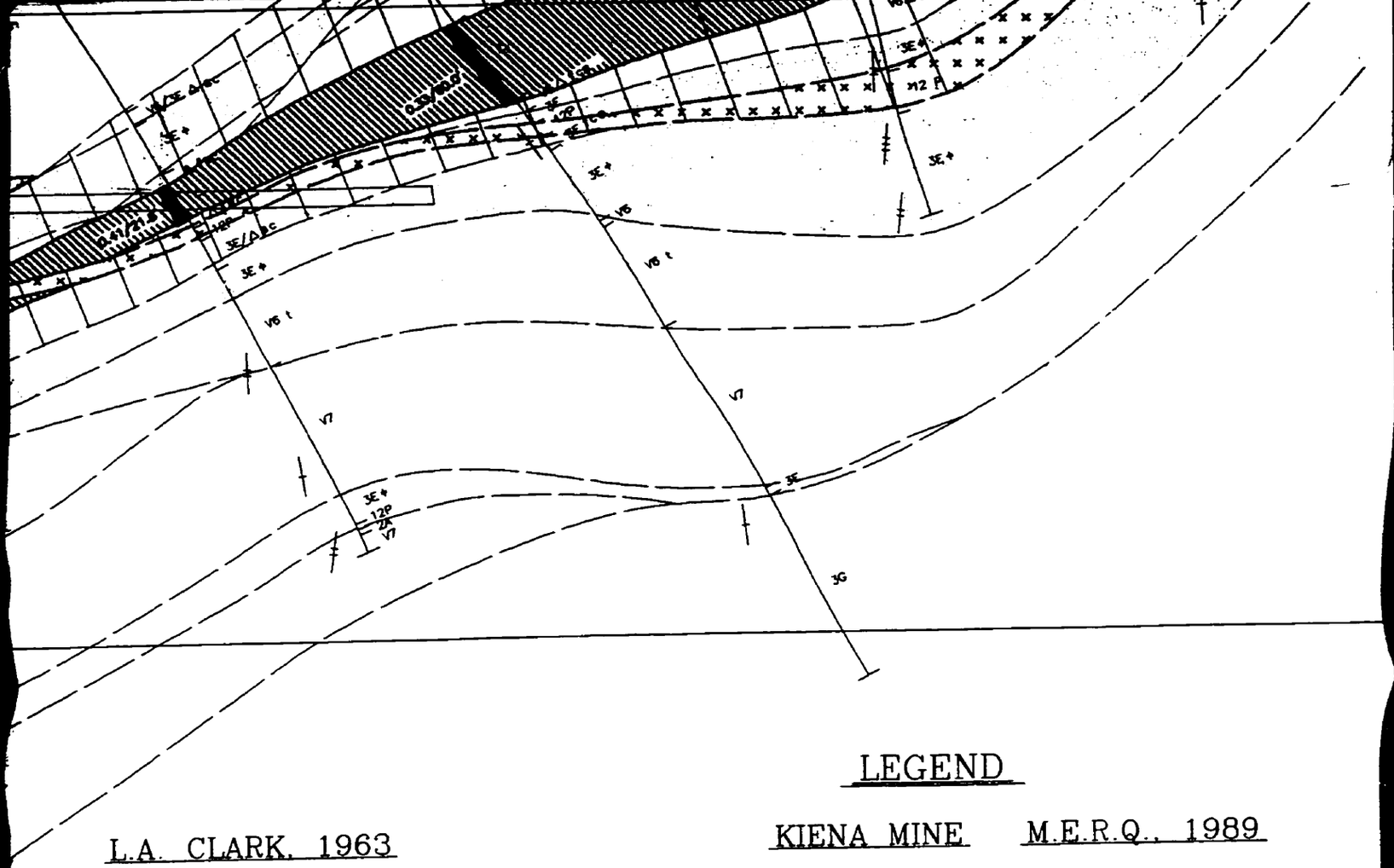

LEGEND

L.A. CLARK, 1963		KIENA MINE	M.E.R.Q., 1989	
VOLCANICS ROCKS				**VOLCANICS R**
V6	Andesite	V6	V3B(MG)	Magnesian Th
V6 t	Andesitic Tuff	V6 t	V3B (MG)	Magnesian Th
V7	Basalt	V7	V3B (FE)	Iron Tholeiite
2A	Green Diorite (Feeder Dikes)	?	12J	Diorite (green
2B	Gabbro (Feeder Dikes)	3G	13A	Gabbro
INTRUSIVES ROCKS				**INTRUSIVES**
+1HP	Syenite Porphyry – Granodiorite	+1D-	+11C+	Granodiorite
12P	Monzonite Porphyry – (Qtz) Feldspar Porphyry	1P	11, PG	Feldspar Porp
2D	Diorite (Grey)	2D	12B, AB	Albitite dike/S
3E	Peridotite	V13	V4C	Peridotitic Kon
3E+	Sheared Peridotite	M13	M8 CL CB TC (AB)	Sheared Perid
	Actinolite Peridotite	V13 Act	V4 AC	Actinolite Per
3G	Gabbro (Qtz–Gabbro)	3G	13E	Gabbro (Qtz–
	Lamprophyre	—	14O	Lamprophyre
MINERALIZATION–ALTERATION				**MINERALIZATI**
Δfp	Ore–Zone Breccia	Breccia	—	S–50 Zone
f	Feldspathization		AB	Albite alterati
	Silicification	S	QZ	Silicification

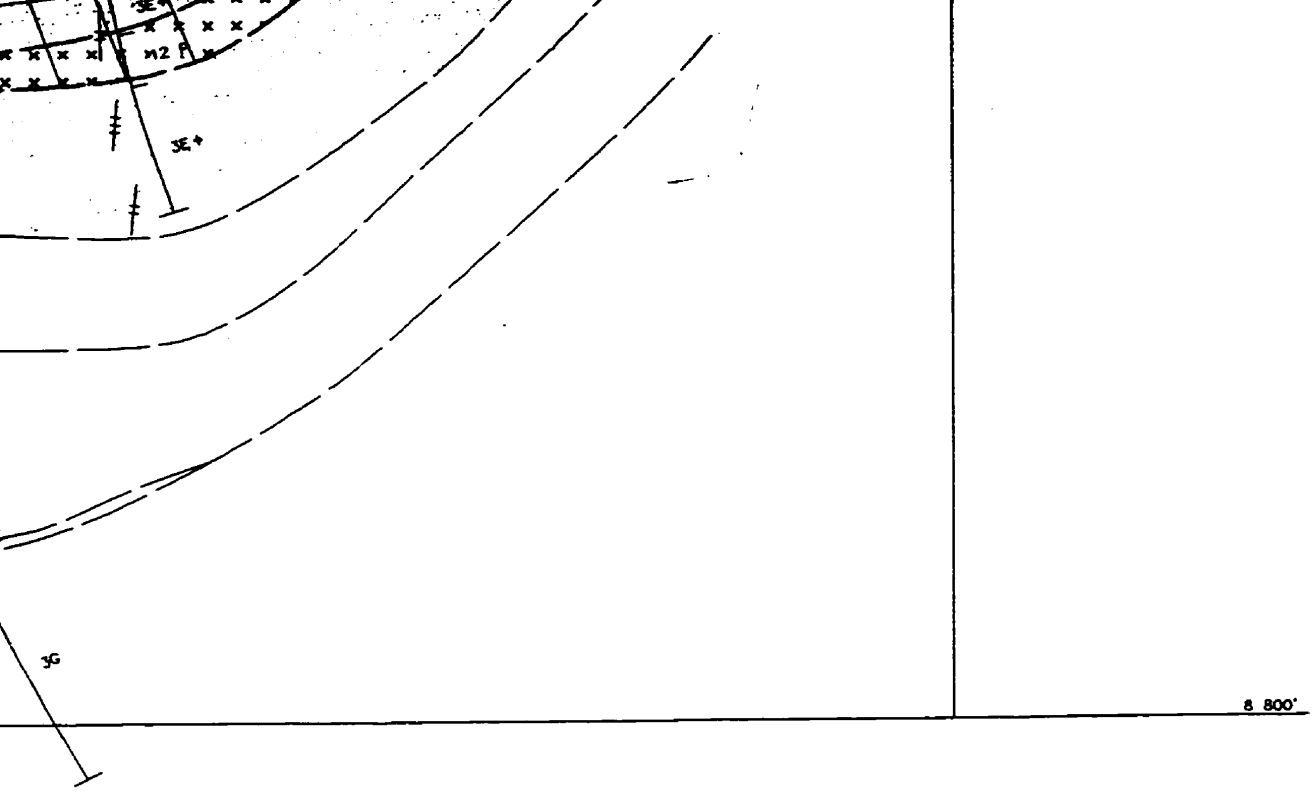

LEGEND

...IENA MINE M.E.R.Q., 1989

VOLCANICS ROCKS

V6	V3B(MG)	Magnesian Tholeiite
V6 t	V3B (MG)	Magnesian Tholeiite flow top breccia
V7	V3B (FE)	Iron Tholeiite
?	I2J	Diorite (green)
3G	I3A	Gabbro

INTRUSIVES ROCKS

+ 1D +	+ I1C +	Granodiorite – Intermineral Granodiorite dike
1P	I1 PG	Feldspar Porphyry (Qtz)–Intermineral feldspar porphyry dike
2D	I2B, AB	Albitite dike/Sill
V13	V4C	Peridotitic Komatiite
M13	M8 CL CB TC (AB)	Sheared Peridotite
V13 Act	V4 AC	Actinolite Peridotite
3G	I3E	Gabbro (Qtz–Gabbro)
—	I4O	Lamprophyre

MINERALIZATION–ALTERATION

Breccia	—	S–50 Zone
	AB	Albite alteration
S	QZ	Silicification

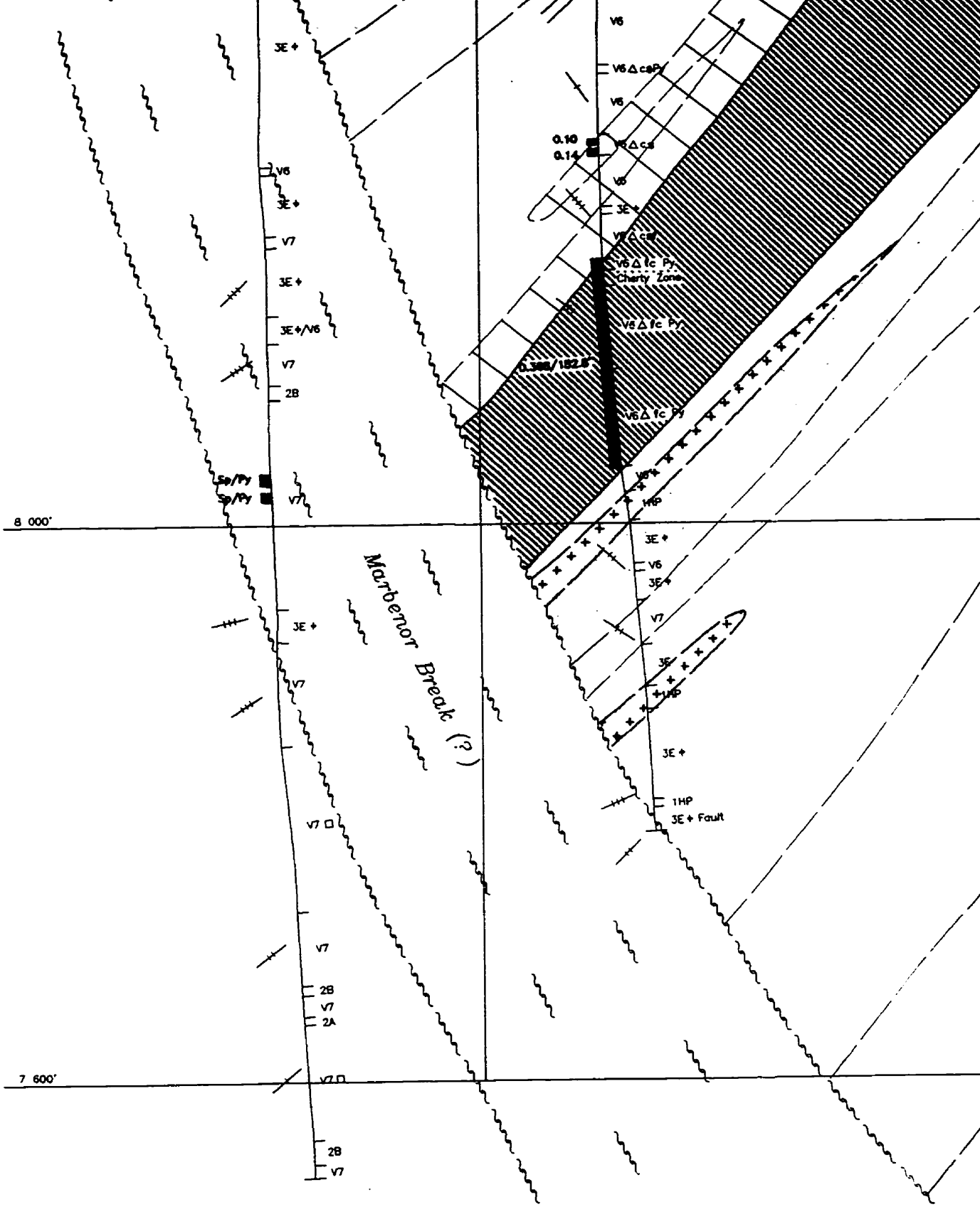

Geology, Structure and Timing of Gold Mineralization at the Kiena Deposit – Back pocket

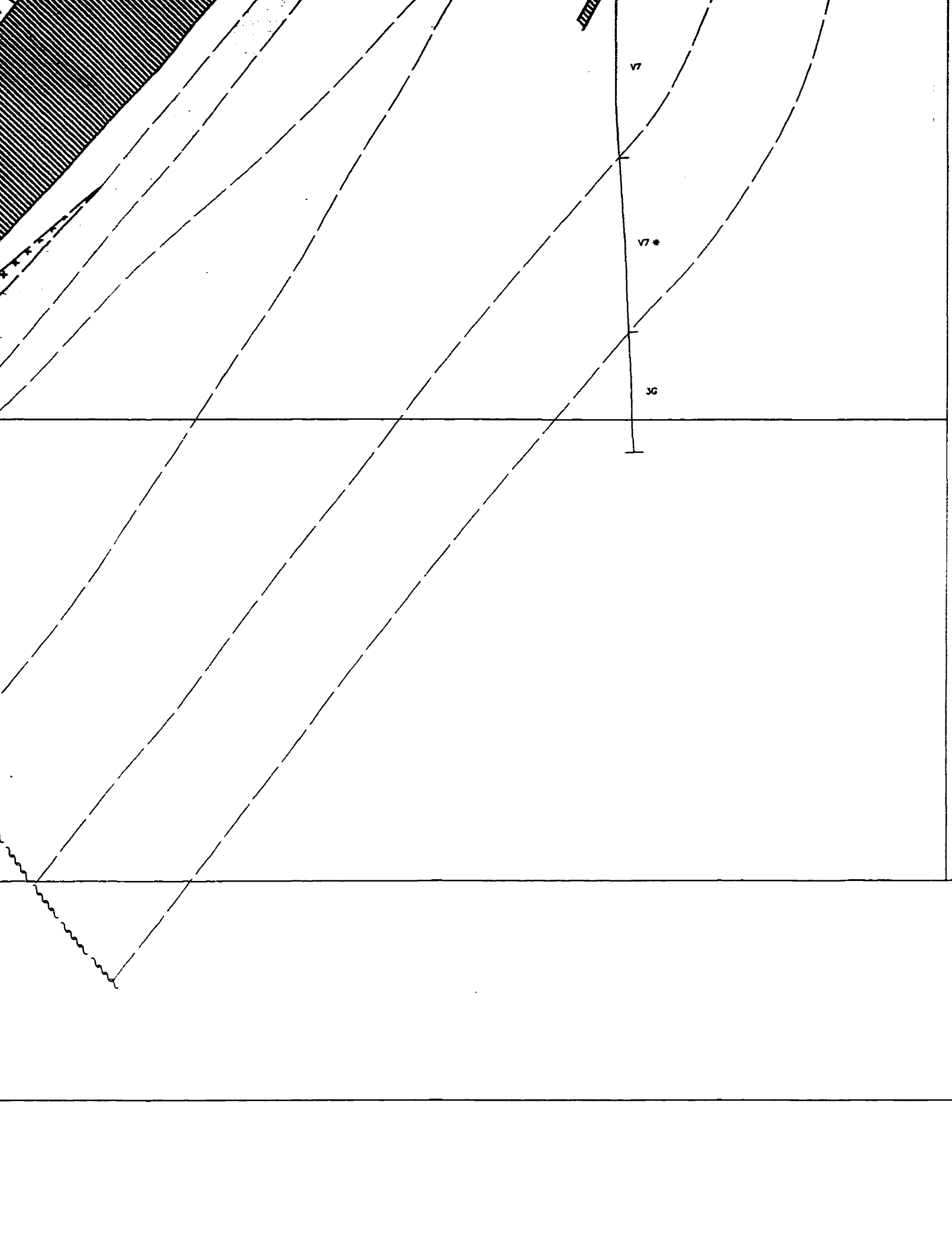
V7
V7 *
JG

12P	*Monzonite Porphyry – (Qtz) Feldspar Porphyry*	1P	11B, PG
2D	*Diorite (Grey)*	2D	12B, AB
3E	*Peridotite*	V13	V4C
3E+	*Sheared Peridotite*	M13	M8 CL CB TC (AB)
	Actinolite Peridotite	V13 Act	V4 AC
3G	*Gabbro (Qtz–Gabbro)*	3G	13E
	Lamprophyre	—	140

MINERALIZATION–ALTERATION

Δfp	*Ore–Zone Breccia*	Breccia	—
f	*Feldspathization*		AB
s	*Silicification*	s	QZ
Py	*Pyrite*	Py	PY
c	*Carbonatization*	—	AK, DM
Po	*Pyrrhotite*	Po	PO
tr	*Tourmaline*	w	TL
Cp	*Chalcopyrite*	Cp	CP
Sp	*Sphalerite*	Sp	SP

SYMBOLS

Ore	*Ore*		
	Rocks altered similarly to Ore–Zone		
0.14/23.0'	*Oz. Au/t / Feet*		Au
ϕ	*Pillowed*		Cb
*	*Amygdaloidal*		S–70
	Sheared		
□	*porphyritic*		
#	*Fractured*		
△	*Brecciated*		

7 60

2D	I2B, AB	*Albitite dike/Sill*
V13	V4C	*Peridotitic Komatiite*
M13	M8 CL CB TC (AB)	*Sheared Peridotite*
V13 Act	V4 AC	*Actinolite Peridotite*
3G	I3E	*Gabbro (Qtz–Gabbro)*
—	I4O	*Lamprophyre*

MINERALIZATION–ALTERATION

Breccia	—	*S–50 Zone*
	AB	*Albite alteration*
s	QZ	*Silicification*
Py	PY	*Pyrite*
—	AK, DM	*Ankerite, Dolomite alteration*
Po	PO	*Pyrrhotite*
w	TL	*Tourmaline*
Cp	CP	*Chalcopyrite*
Sp	SP	*Sphalerite*

SYMBOLS

		Stwk Cb–Qz–Py(Po)–Au ± Ab , Breccia 1 , Breccia 2
		Stwk Cb–Qz–Py(Po)–Au ± Ab (non economic)
	Au	*Gold*
	Cb	*Carbonate*
	S–70	*Diamond drill hole*

LES MINES D'OR KIENA LTEE.

7 600'

COMPOSITE SECTION 11

COMPILED BY : Clark L.A.,1963
EDITED BY : Morasse S., 1993
DATE : 04/20/94
COMPUTER DRAFTING BY : S. Tremblay

SCALE 1" = 100'

0' 50' 100'

S. Morasse 1997

PLEASE NOTE:

Oversize maps and charts are filmed in sections in the following manner:

LEFT TO RIGHT, TOP TO BOTTOM, WITH SMALL OVERLAPS

The following map or chart has been refilmed in its entirety at the end of this dissertation (not available on microfiche). A xerographic reproduction has been provided for paper copies and is inserted into the inside of the back cover.

Black and white photographic prints (17" x 23") are available for an additional charge.

University Microfilms International

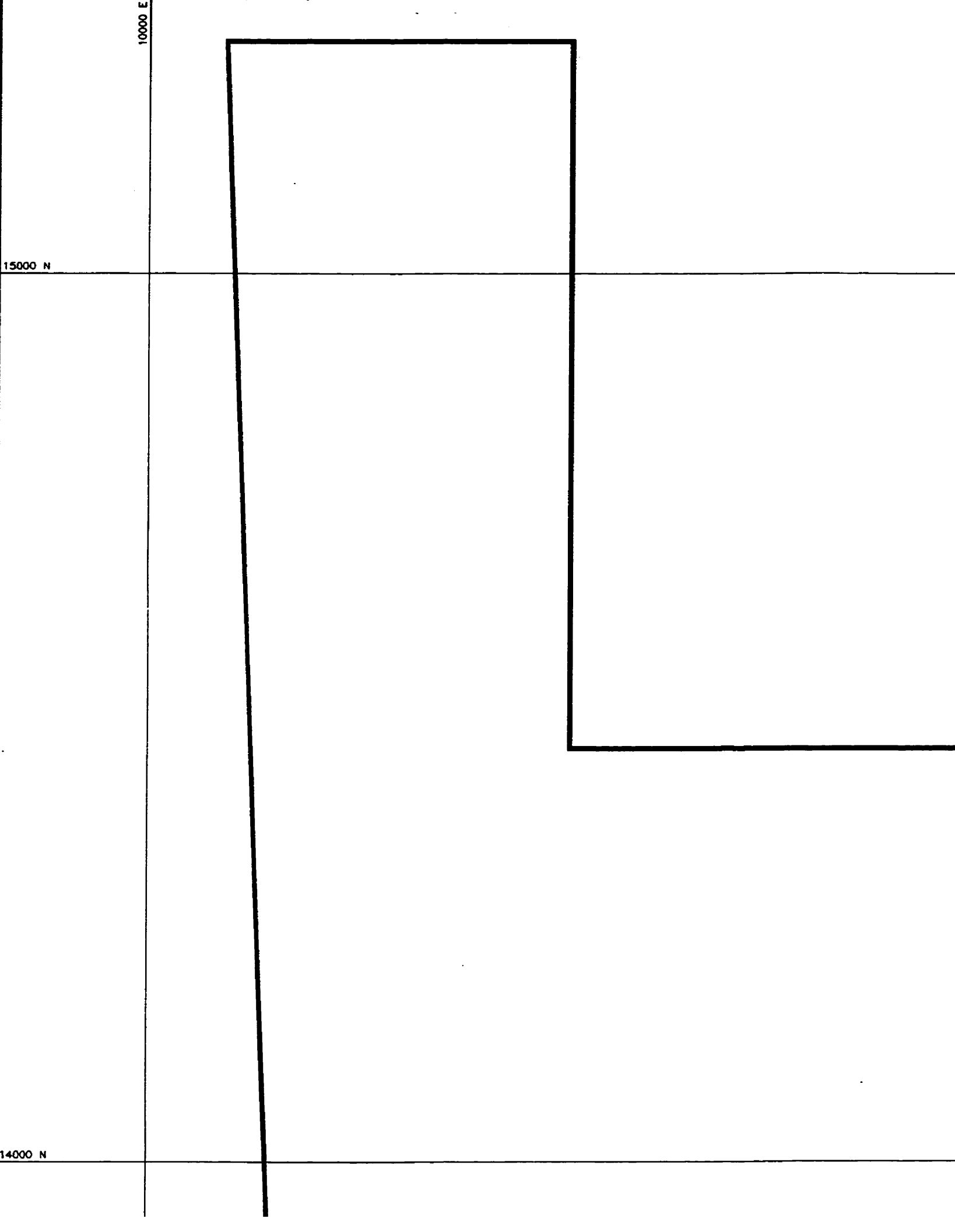
10000 E
15000 N
14000 N

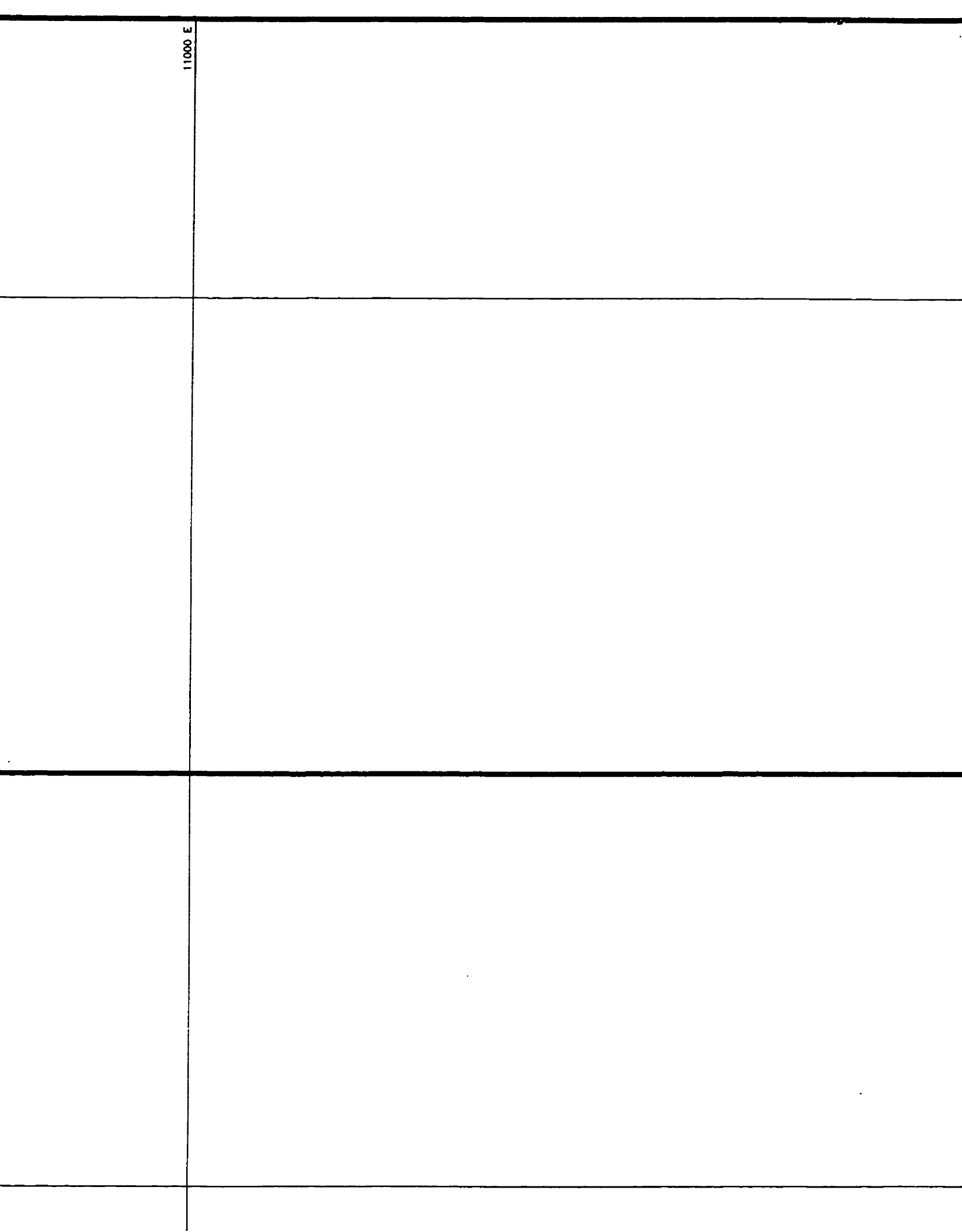
11000 E

12000 E

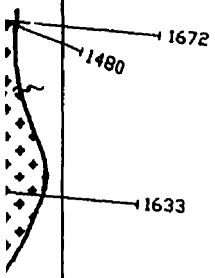

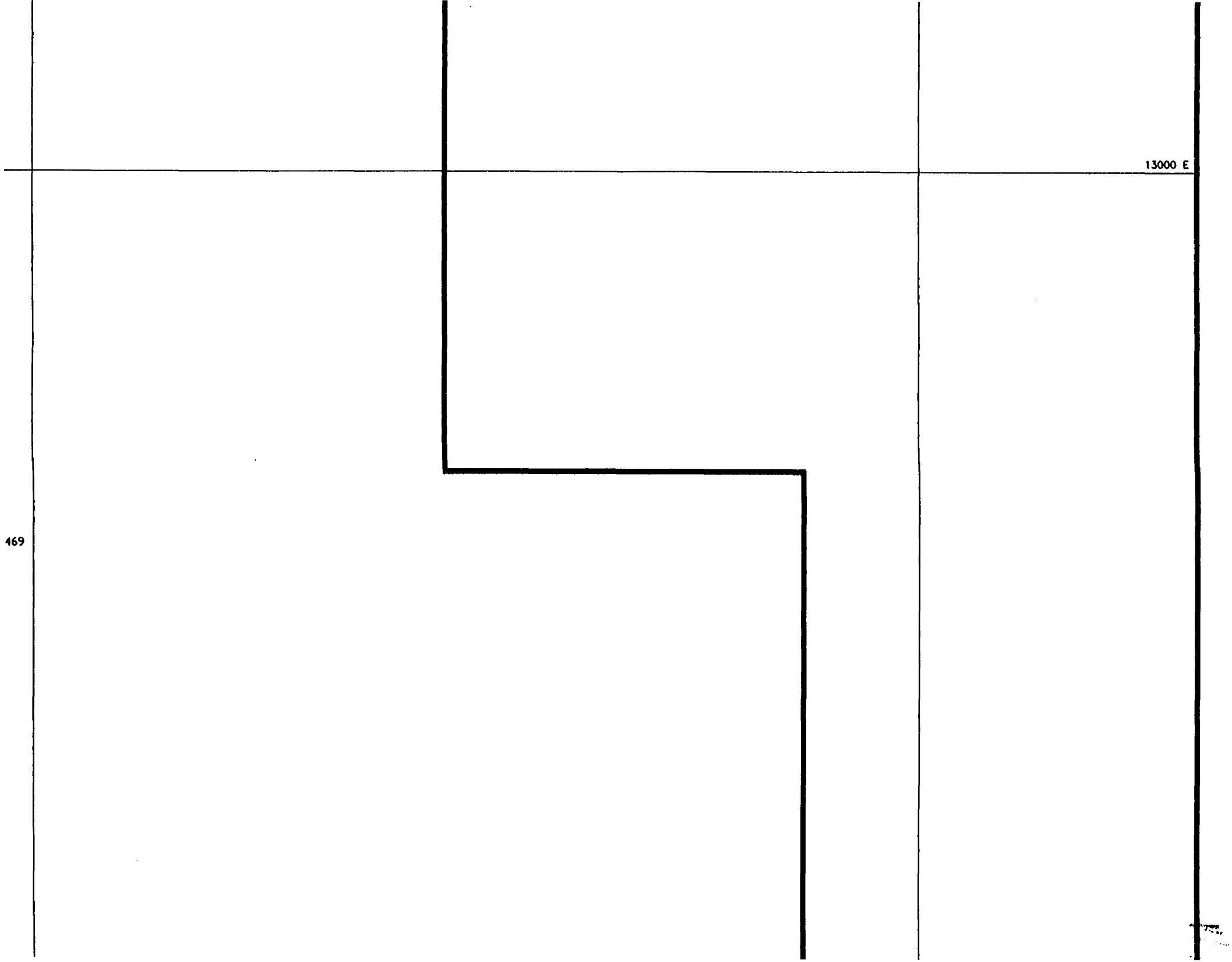
13000 E
469

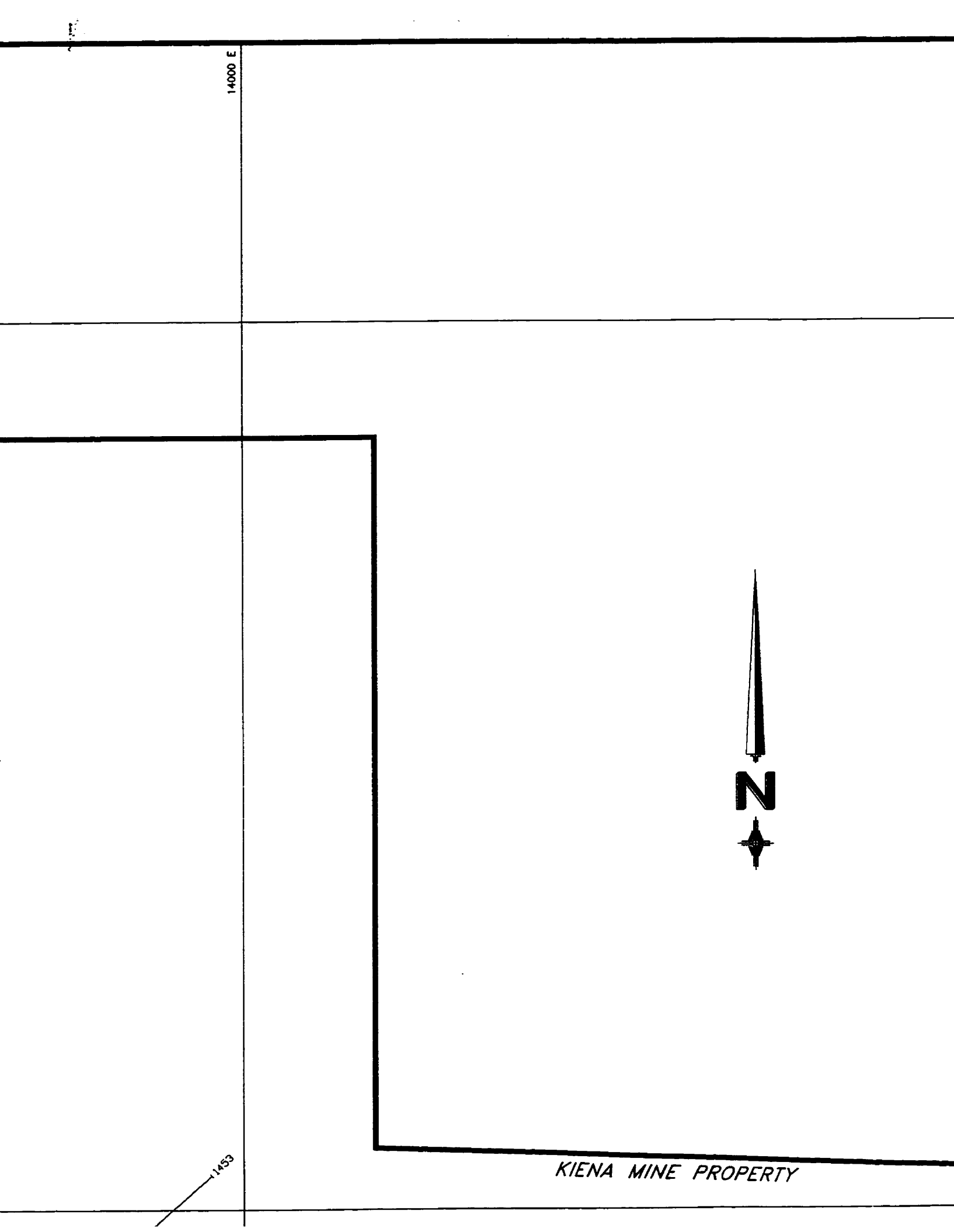
14000 E
N
1453
KIENA MINE PROPERTY

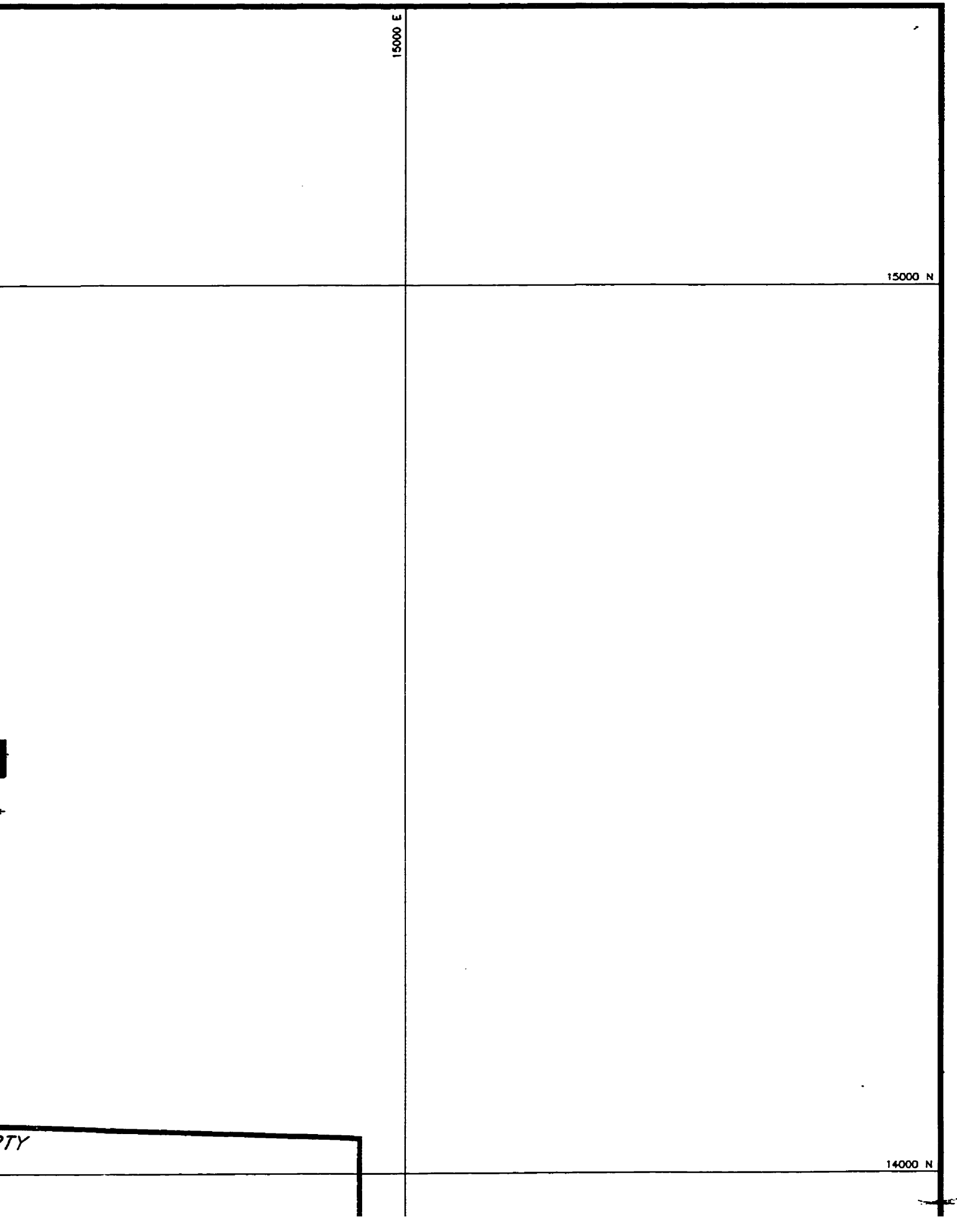
15000 E
15000 N
14000 N
PTY

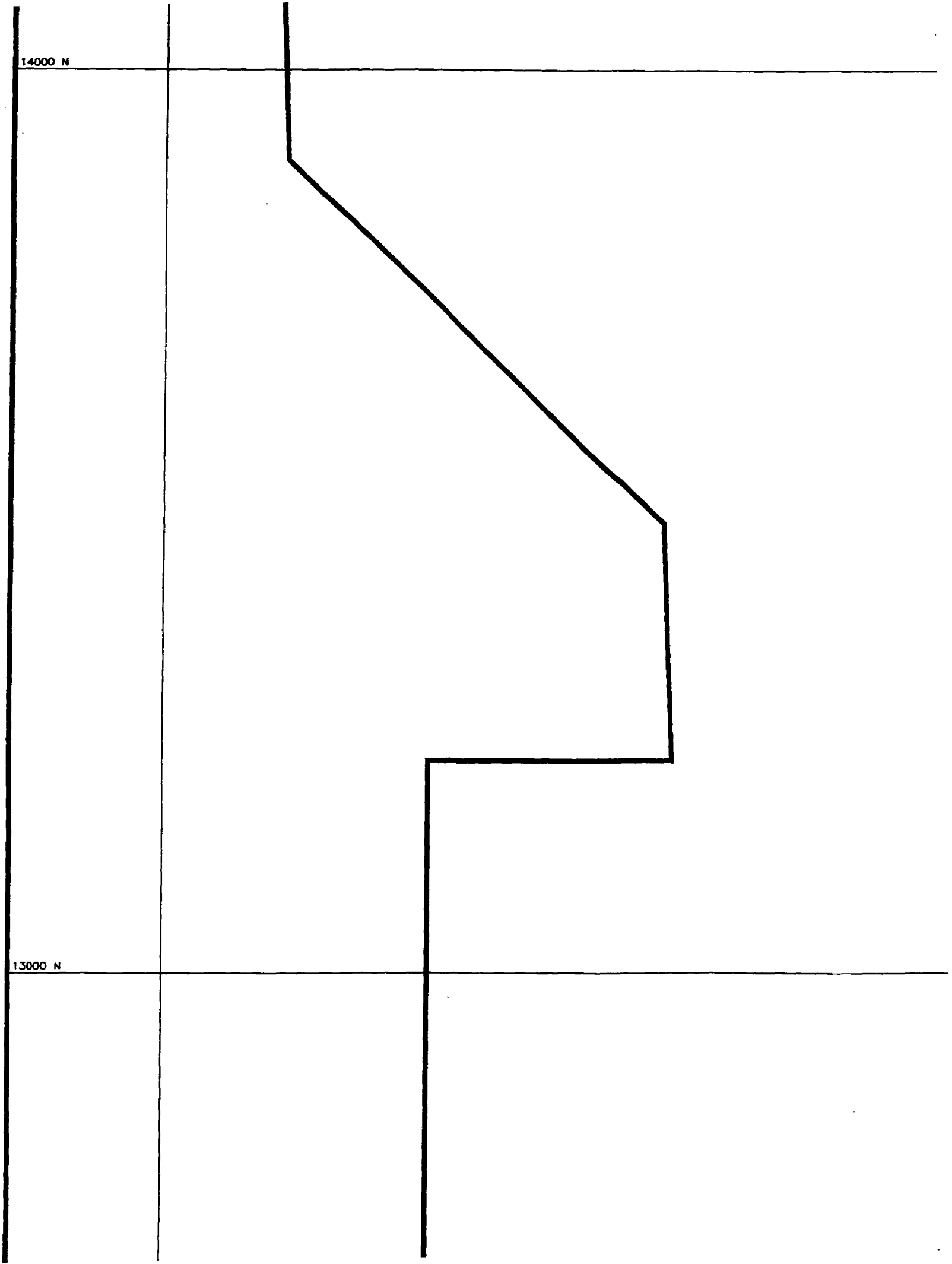
14000 N
13000 N

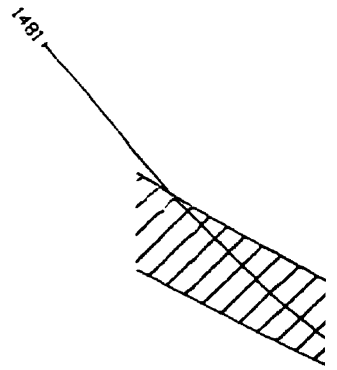
1481

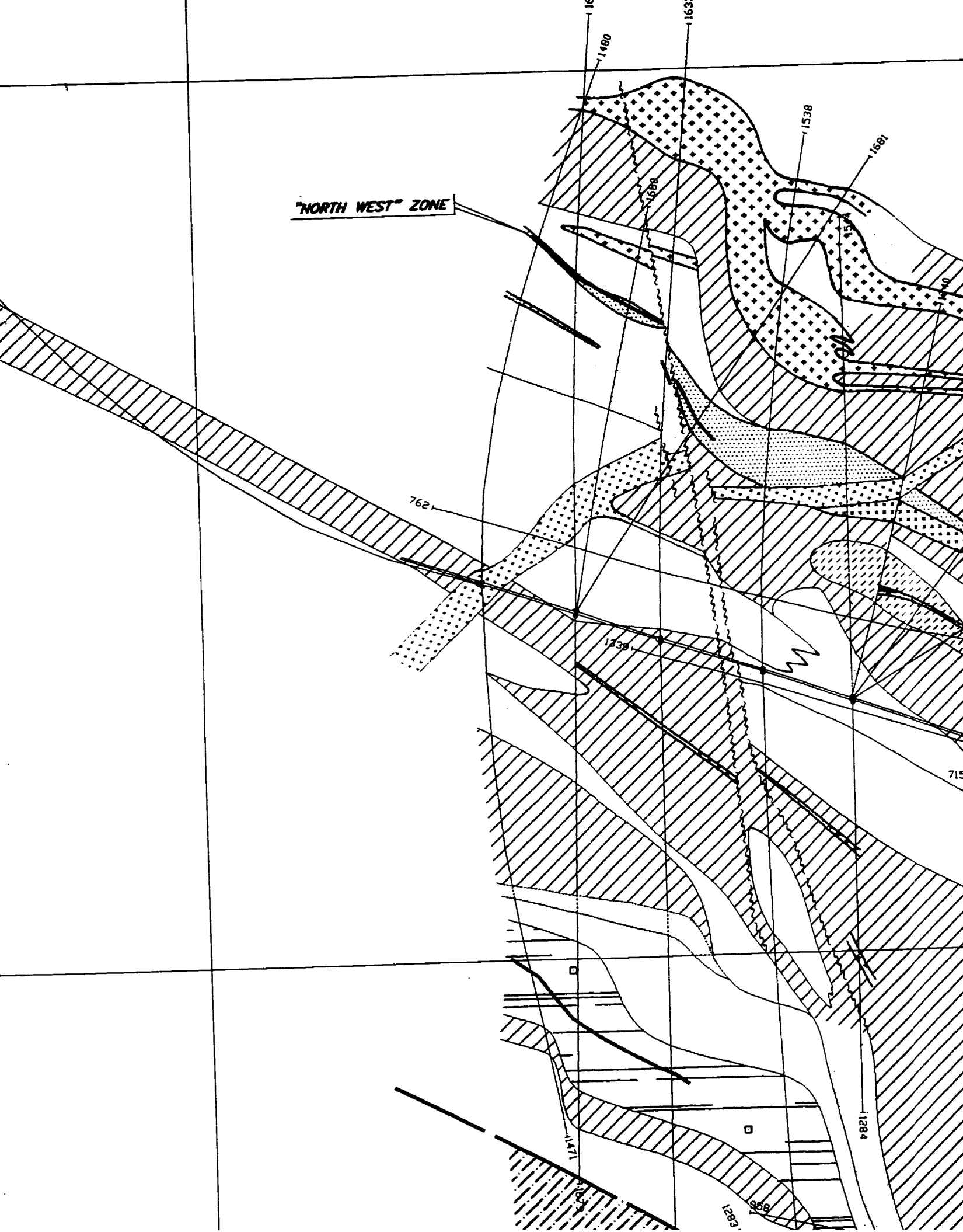
"NORTH WEST" ZONE
1480
1538
1681
762
1239
1471
1284

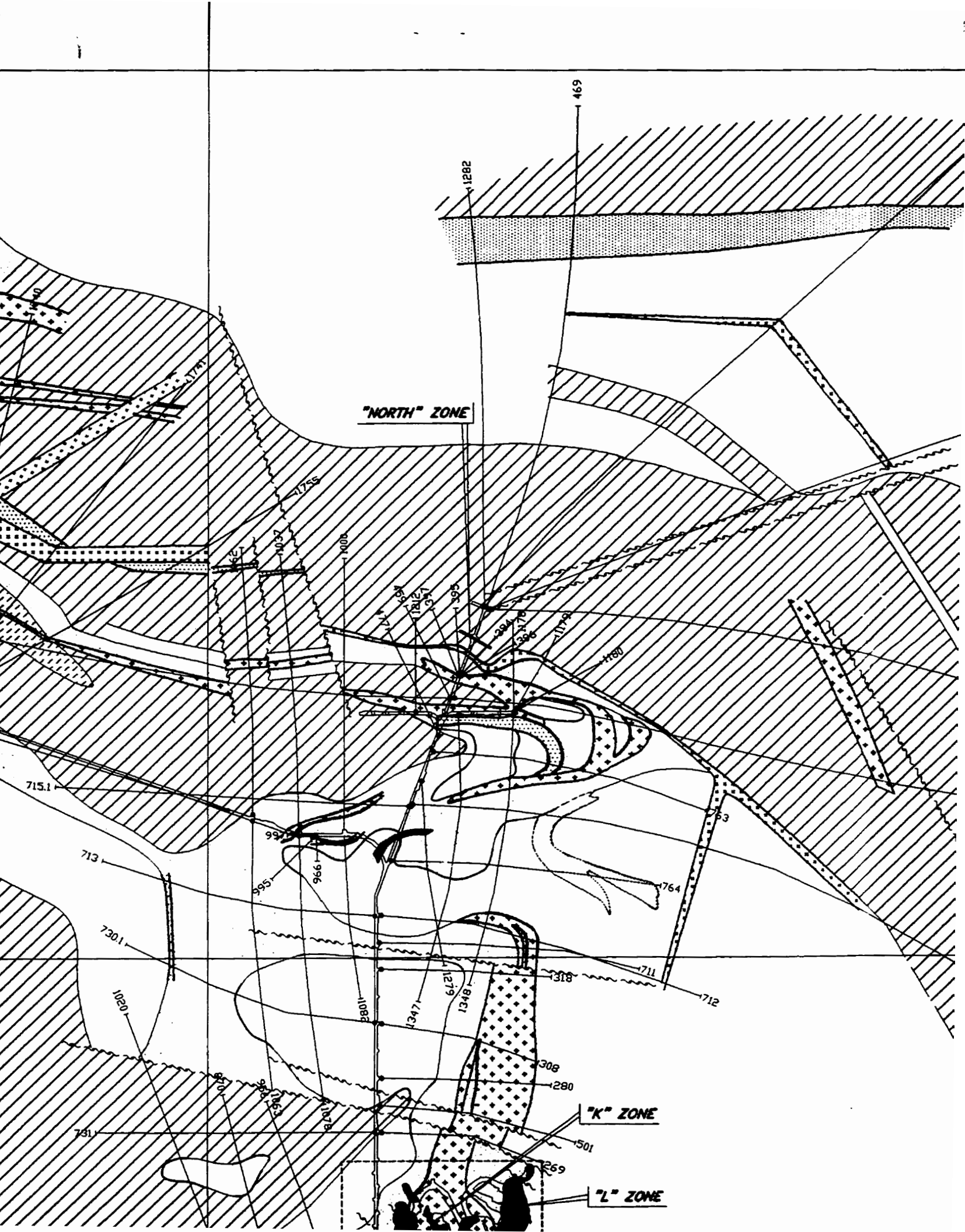
"NORTH" ZONE
"K" ZONE
"L" ZONE
469
1282
1755
1747
1000
1212
1180
715.1
713
995
966
764
730.1
711
712
1318
1279
1348
1347
1088
1020
308
280
501
269
731

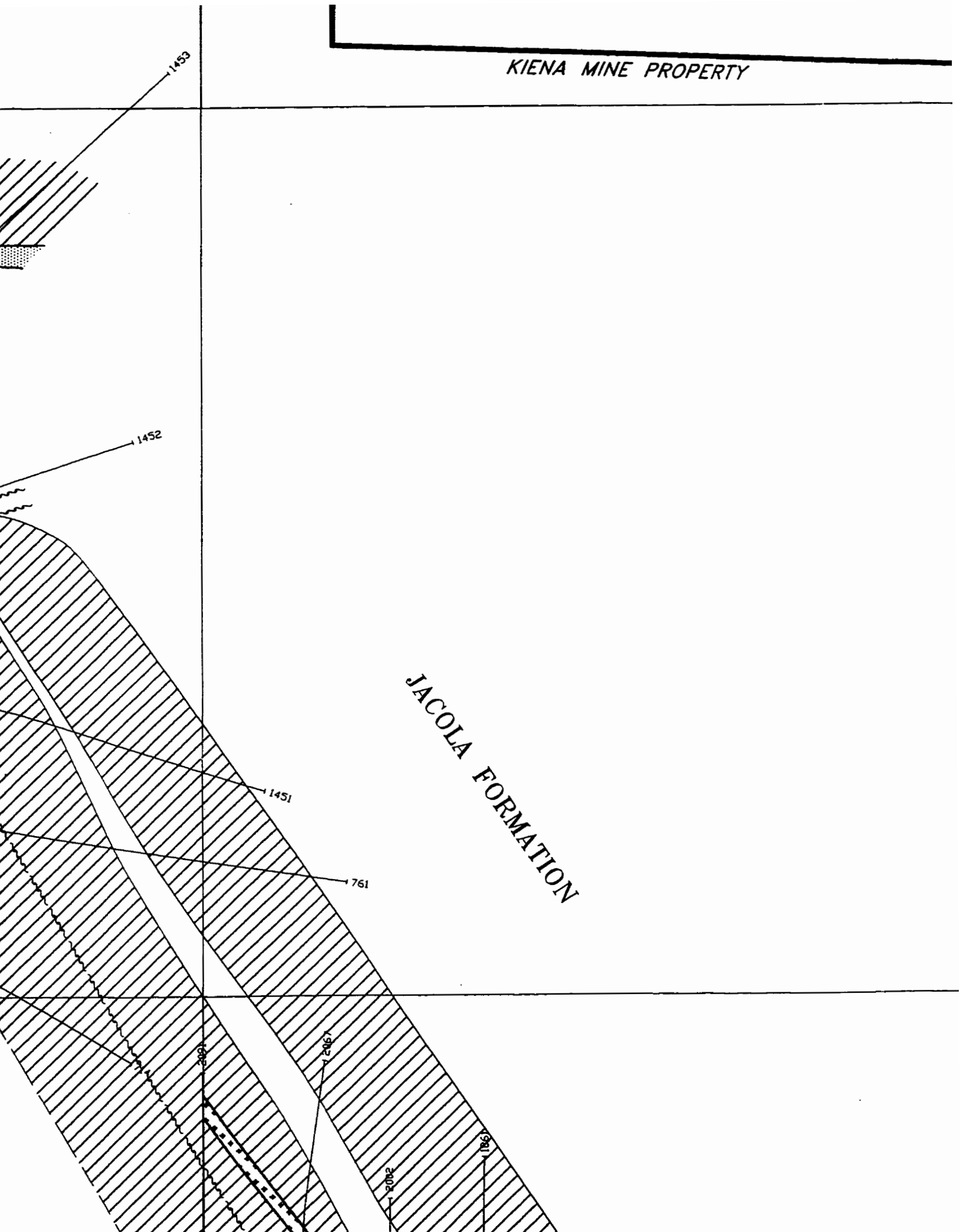
KIENA MINE PROPERTY
1453
1452
1451
761
JACOLA FORMATION
1962
1962
1961
2002
2002

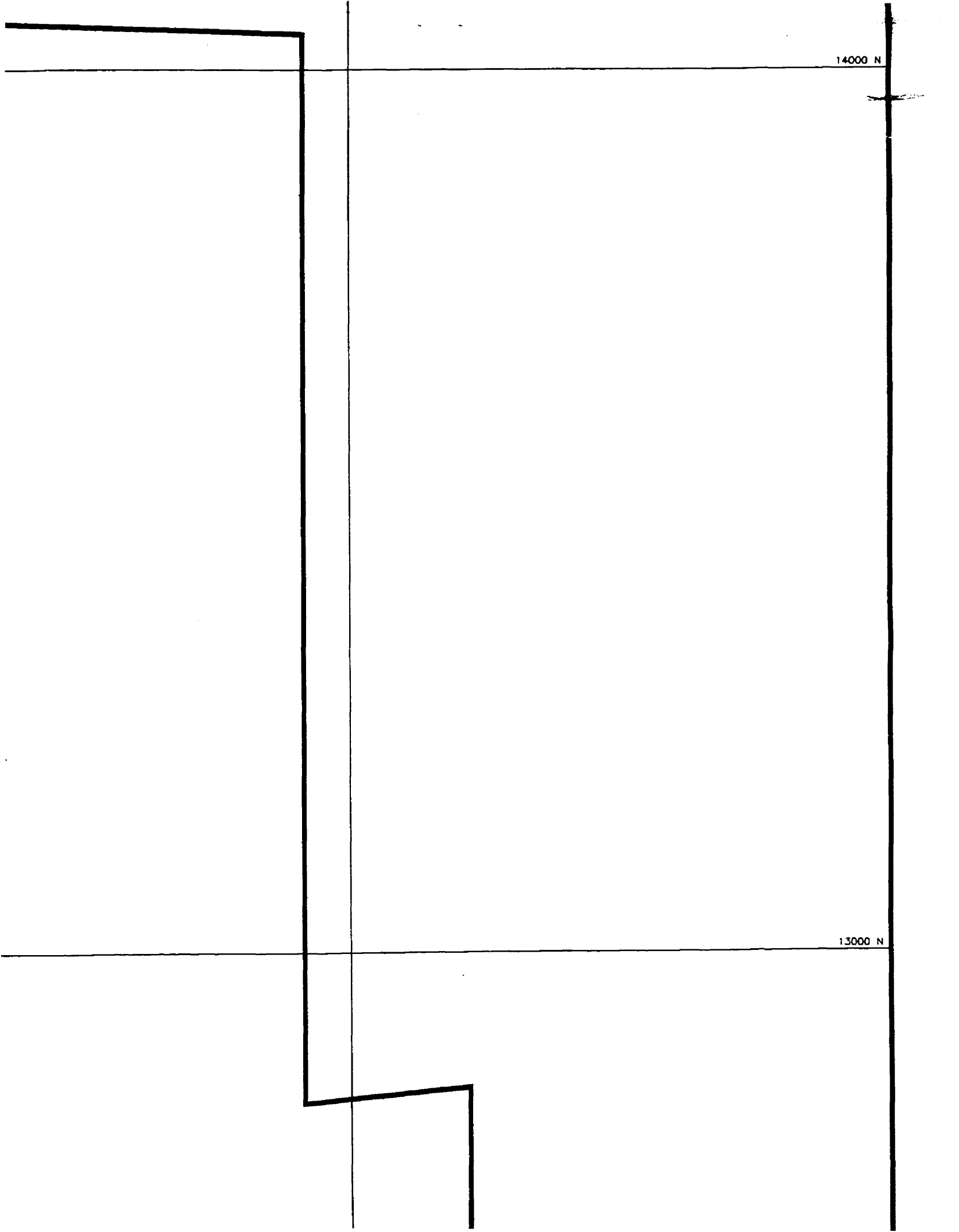
14000 N
13000 N

12000 N

LEG

JACOLA FORMATION

- Tholeiitic basalt : massive, pillowed, schistose
- Tholeiitic basalt : porphyritic
- Coarse – grained tholeiitic basalt
- Tholeiitic flow top breccia
- Komatiitic flow : spinifex, cumulate textures, schistose
- Chlorite – carbonate – talc (Ab) schist
- Amphibolite

HEVA FORMATION

- Basalt : massive, pillow flow
  Volcaniclastic rocks : basaltic to dacitic

INTRUSIVE ROCKS

- Feldspar porphyry : porphyritic, schistose
- Granodiorite : medium – grained, massive, porphyritic, schisto
- Albitite : very fine – grained, massive, schistose
- Aplite
- Diabase

KIENA MINE PROPERTY

EGEND

MINERALIZATION / ALTERATION

- Main mineralized zone (part albitite dike)
- Au-mineralized veins
- 1543 Diamond drill hole
- Intense carbonate alteration

STRUCTURAL SYMBOLS

- Post-ore, strike slip fault
- 1st cleavage : spaced cleavage
- Stratigraphic younging direction

chistose

11000 E

12000 E

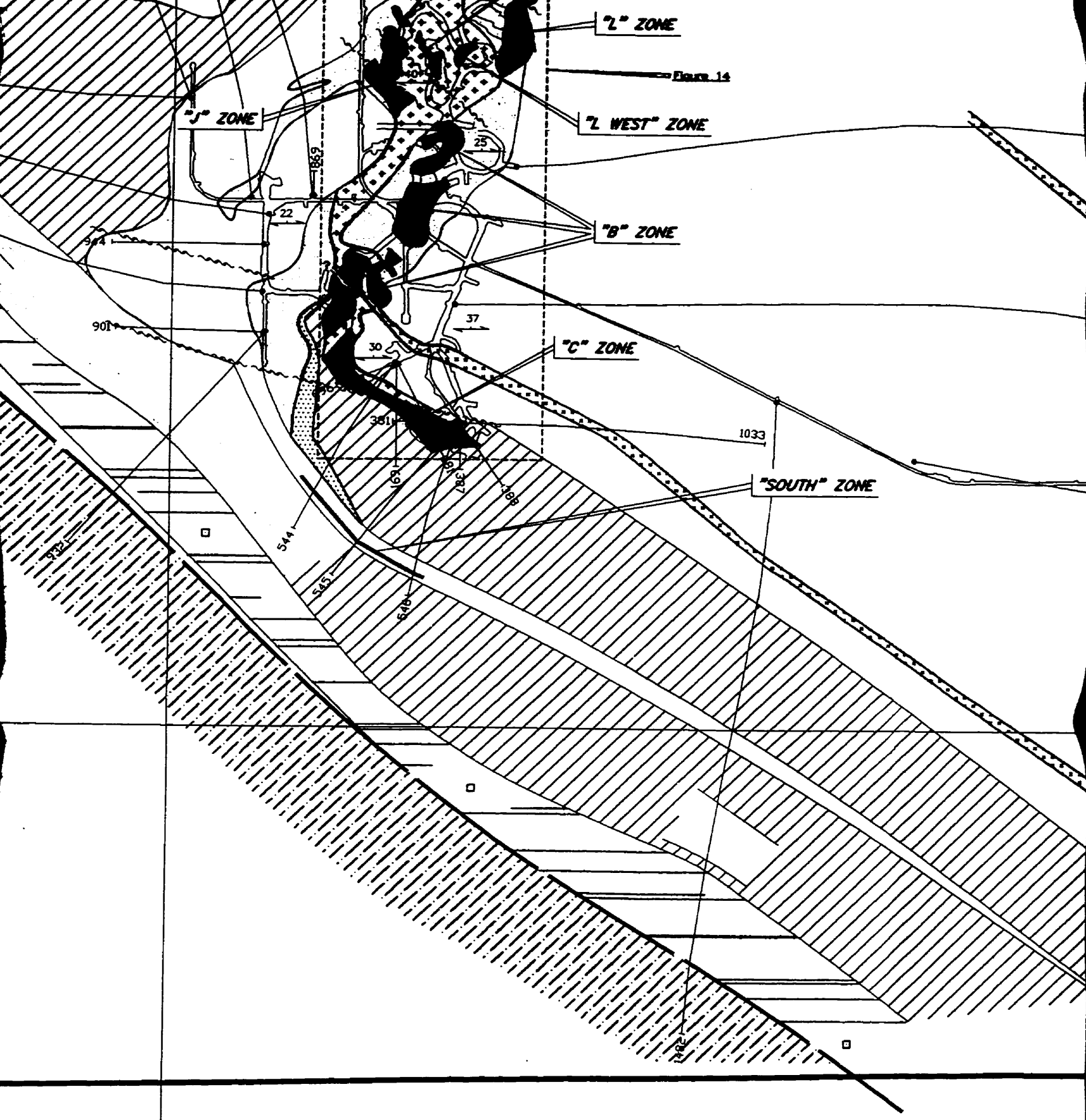
"L" ZONE
Figure 14
"J" ZONE
"L WEST" ZONE
"B" ZONE
"C" ZONE
"SOUTH" ZONE
1033
13000 E

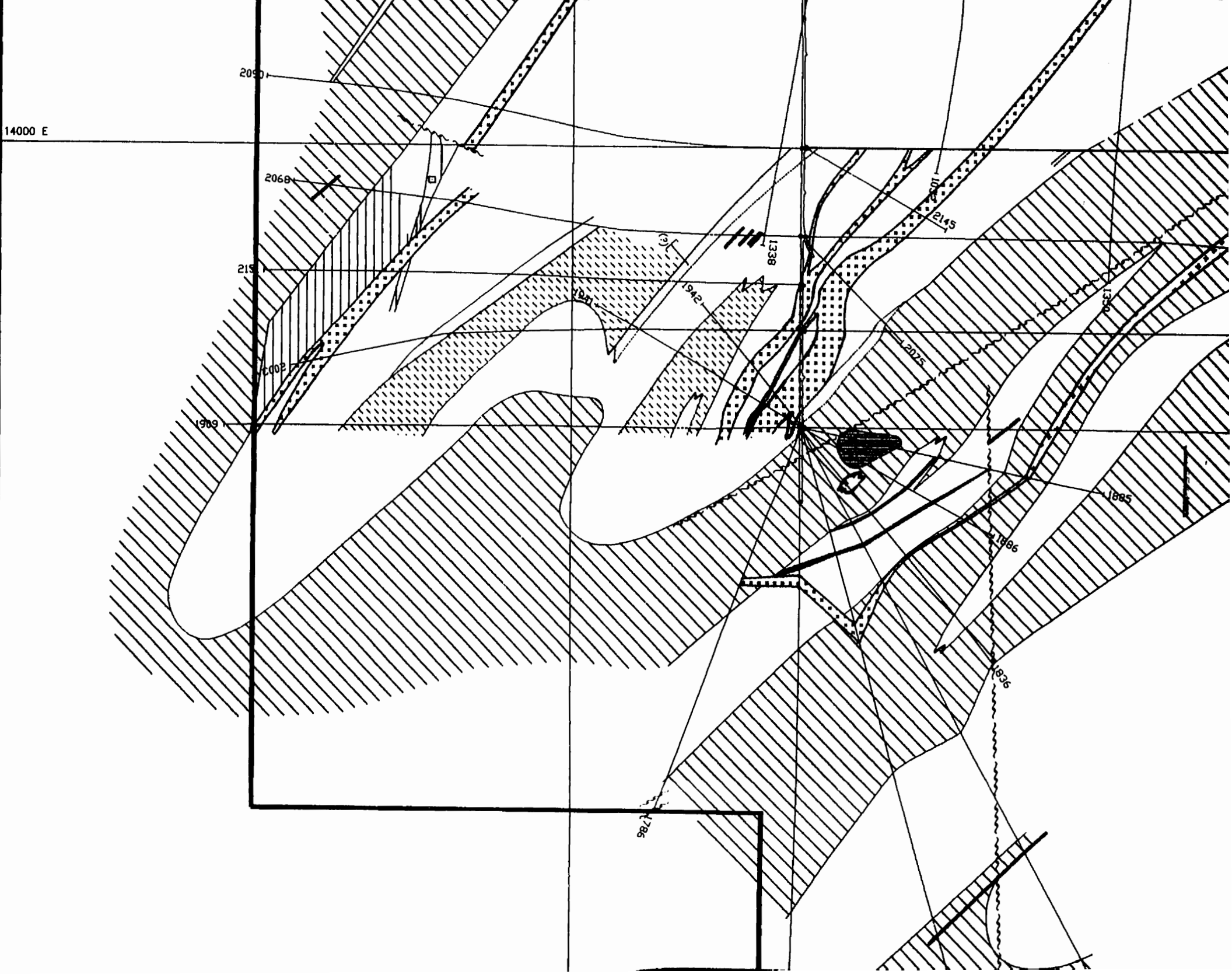
14000 E
2068
2145
1338
1942
1350
2075
1885
1986
1836
1786
1909

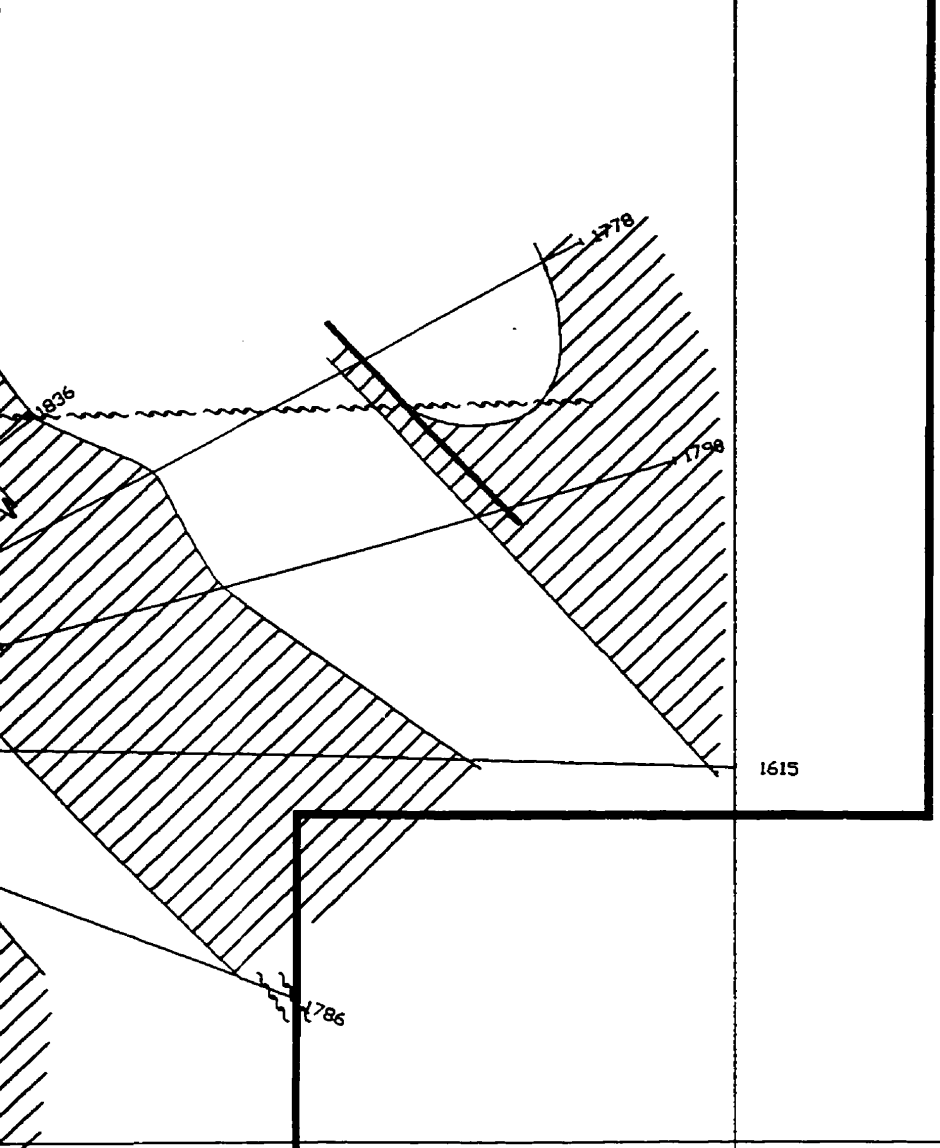

12000 N

5000 E

LES MINES D'OR KIENA LTEE.

EXPLORATION DIAMOND DRILLING
COMPILATION PLAN MAP LEVEL 33

COMPILED BY : Jeansonne P., 1992
EDITED BY : Morasse S., 1993
DATE : 04/20/94
COMPUTER DRAFTING BY : S. Tremblay

SCALE 1 : 5 000
0m 50m 100m 150m 200m

S. Morasse 1997

PLEASE NOTE:

Oversize maps and charts are filmed in sections in the following manner:

LEFT TO RIGHT, TOP TO BOTTOM, WITH SMALL OVERLAPS

The following map or chart has been refilmed in its entirety at the end of this dissertation (not available on microfiche). A xerographic reproduction has been provided for paper copies and is inserted into the inside of the back cover.

Black and white photographic prints (17" x 23") are available for an additional charge.

University Microfilms International

REGIONAL SEQ

***PRE-D_1 VOLCANISM AND ASSOCIATED SUB-VOLCANIC EVENTS* - > 2706 to 2700 Ma**

LOWER MALARTIC GROUP
(LA MOTTE–VASSAN Fm – DUBUISSON Fm)

VAL D'OR CENTRAL VOLCANIC COMPLEX – ZIRCON COLOMBIERE "RHYOLITE" – 2704.7± 1.1 Ma ; 2706± 3 Ma
(INCLUDING JACOLA Fm) (Wong et al., 1991 – Machado et al., 1992)

Au MINERALIZATION AKASABA MINE (?) – (EPIGENETIC VOLCANOGENIC SULPHIDE ORE)
(Sauvé et al., 1985b)

SIGMA MINE SUB-VOLCANIC PORPHYRITIC DIORITE – 2703.7 ± 2.5 Ma
("C" PORPHYRY) (Wong et al., 1991)

BLAKE RIVER GROUP – 2701 ± 2 TO 2696 ± 1 Ma
(Mortensen, 1987 – Corfu et al., 1989)

CADILLAC FAULT ZONE (Dimroth et al., 1982)

BOURLAMAQUE DIORITE – TRONDHJEMITE SILL COMPLEX – 2698.8 ±1Ma
(Compiglio and Darling, 1976 ; Wong et al., 1991)

***D_1 REGIONAL DEFORMATION AND TILTING OF VOLCANIC STRATA* - 2700 to 2694 Ma**

FIRST INTRUSIONS EMPLACED AFTER THE TILTING OF VOLCANIC STRATA – SIGMA MINE FELDSPAR PORPHYRY DIKES 2694 2.2 Ma
(Daigneault et al., 1983; Robert and Brown, 1986; Morasse and Wasteneys,1994)

KIENA MINE FAULT ZONE

***POST-D_1 PLUTONIC EVENTS* - 2694 (?) to 2680 Ma**

SNOWSHOE GRANODIORITE – 2694 ± 3 Ma
(Morasse et al., 1993; Morasse et al. 1995)

SIGMA–LAMAQUE No. 2 FELDSPAR PORPHYRY DIKE SWARM ("G" DIKES) – 2694 ± 2.2 Ma
(Daigneault et al., 1983 – Wong et al., 1991)

MALARTIC GOLDFIELDS–BARNAT–EAST MALARTIC–CANADIAN MALARTIC–SLADEN MINES "DIORITE", "GREY" AND "PINK PORPHYRY DIKES"
(Sansfaçon et al., 1987; Trudel and Sansfaçon, 1987; Sansfaçon and Hubert, 1990)

NORLARTIC MINE "MICRODIORITE" DIKE – KIENA MINE ALBITITE DIKES (?)
(Sauvé et al., 1993 – Pilote et al., 1993 – Morasse et al., 1993)

NORLARTIC MINE TONALITE – 2692 ±2 Ma
(Pilote et al., 1993)

LAMAQUE No. 2 QUARTZ–FELDSPAR PORPHYRY DIKES – Post-feldspar porphyry dikes but pre-F_2 (?)
(Daigneault et al., 1983)

KIENA MINE INTERMINERAL GRANODIORITE DIKE – 2686 ± 2 Ma
(Morasse et al., 1993 ; Morasse and Wasteneys, 1994 ; Morasse et al., 1995)

LAMAQUE MINE DIORITE–TONALITE – 2685 ±3 Ma
(Jemielita et al., 1989)

CAMFLO MINE MONZONITE – 2685 ±6 to 2683 ± 3 Ma
(Zweng and Mortensen 1989–Jemielita et al., 1990)

CAMFLO MINE APLITE DIKE SWARM – Post-monzonite stock and pre-ore
(Zweng, 1994)

***POST-D_1 GOLD MINERALIZATION EVENTS* - 2694 to 2677 (?) Ma**

MALARTIC GOLDFIELDS–BARNAT–EAST MALARTIC–CANADIAN MARLARTIC–SLADEN MINES – Post-F_1 S_1 but pre-F_2 S_2
(Sansfaçon et al., 1987; Trudel and Sansfaçon, 1987; Sansfaçon and Hubert, 1990)

BRAS D'OR MINE – 2693 ± 2 Ma and 2688 ± 7 Ma
(Kerrich and Kyser, 1994)

NORLARTIC MINE – > 2692 ± 2 Ma
(Pilote et al., 1993)

KIENA MINE – > 2686 ± 2 Ma – Post-F_1 S_1 but pre-F_2 S_2
(Morasse et al., 1993 ; Morasse and Wasteneys, 1994 ; Morasse et al., 1995)

LAMAQUE MINE – < 2685 ±3 Ma ; Post-F_1 but pre-F_2 S_2 (this study)
(Karvinen, 1985; Jemielita et al., 1989)

SIGMA MINE – 2682 ± 8 Ma – Post-F_1 but pre-D_2 S_2 (this study)
(Clausé–Long et al., 1990 ; 1992)

CAMFLO, ORION, GOLDEX, SISCOE MINES – Post F_1 but pre– F_2 S_2 (this study)
(Trudel and Sauvé, 1992; Trudeau and Raymond, 1992; Stills and Mason, 1995)

CAMFLO MINE – 2625 ± 6 to 2615 ± 10 Ma
(Jemielita et al., 1989 – Zweng, 1990, 1993)

SIGMA MINE – 2602 ± 20 to 2578 ± 5 Ma
(Anglin, 1990 – Hanes et al., 1992)

LAMAQUE MINE – 2593 ± 7 Ma
(Jemielita et al., 1989)

***REGIONAL THERMAL METAMORPHISM RELATED TO POST-D_1 PLUTONISM (?)* - 2693 TO 2671 Ma**

CORE OF AMPHIBOLE SIGMA MINE "C" PORPHYRY – 2693 ±11 Ma
(Hanes et al., 1989 ; 1992)

RUTILE COLOMBIERE RHYOLITE – 2684 ± 7 Ma
(Wong et al., 1991)

RIM OF AMPHIBOLE SIGMA MINE "C" PORPHYRY – 2671 ± 17 Ma
(Hanes et al., 1989 ; 1992)

***POST-D_1 LOCAL UPLIFT AND SEDIMENTATION EVENTS* - <2695 TO 2683 Ma**

LAC CASTE FORMATION – <2695 Ma – ?
(Feng and Kerrich, 1991)

CADILLAC GROUP WACKES – <2688 ± 3 Ma – ?
(Davis, 1991)

KEWAGAMA GROUP WACKES – <2687 ± 3 Ma to 2682 ± 3 Ma ; >2683 ± 3 Ma
(Davis, 1991 – Mortensen, 1993 – Jemielita, 1990)

***POST-D_1 PONTIAC GROUP SEDIMENTATION EVENT* - <2683 Ma**
(Mortensen and Card, 1993)

***D_2 REGIONAL PENETRATIVE DEFORMATION AND METAMORPHISM* - 2677 (?) TO 2645 Ma**

COEVAL DEVELOPMENT OF PENETRATIVE TECTONIC FABRIC AND METAMORPHISM – 2677 (?) – 2645 Ma
(Powell et al., 1993; 1994 – Corfu et al., 1991 – Feng and Kerrich, 1991)

PEAK METAMORPHISM ALONG LARDER LAKE – CADILLAC DEFORMATION ZONE, KIRKLAND LAKE AREA – 2665 ± 4 Ma
(Wilkinson et al., 1997)

PEAK METAMORPHISM CLERICY SYENITE (PORCUPINE–DESTOR AND PARFOURU FAULTS AREA) – 2657 ± 3 Ma
(Powell, 1994)

***LATE- TO POST-D_2 PLUTONIC EVENTS* - 2675, and 2645 TO 2632 Ma**

LACORNE BATHOLITH MONZO–DIORITE – GRANODIORITE – 2675 ± 24
(Feng and Kerrich, 1991)

S–TYPE GRANITES IN SOUTHERN ABITIBI BELT – 2663 TO 2611 Ma
(Feng and Kerrich, 1991)

S–TYPE GRANITE IN PREISSAC–LACORNE BATHOLITH – 2643 ± 4 Ma
(Feng and Kerrich, 1991)

S–TYPE GRANITES PONTIAC SUBPROVINCE – 2645 TO 2632 ± 3 Ma
(Feng and Kerrich, 1991 – Machado et al., 1991)

***CAMFLO DEPOSIT K–MICA AND BIOTITE COOLING AGES* – 2660 ± 7 TO 2602 Ma**
(Zweng, 1991)

***KIENA DEPOSIT VEIN BIOTITE* – 2313 ±14.9 Ma**
(Wallace, Groen's [illegible] 1994)

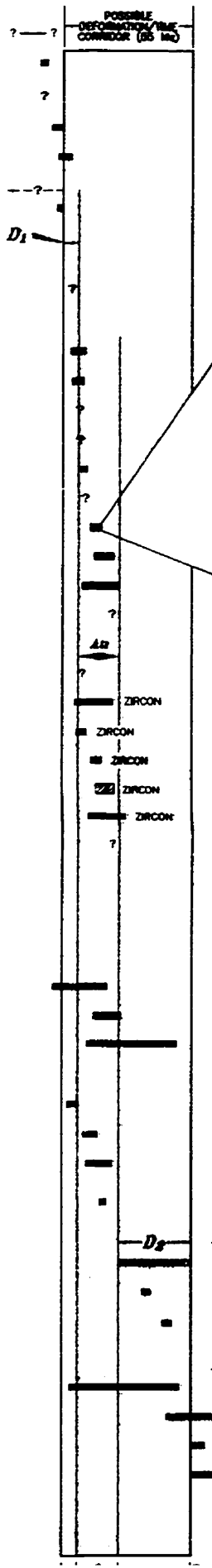

REGIONAL SEQUENCE OF EVENTS

06 to 2700 Ma

t 3 Ma
lochado et al., 1992)

L., 1991)

700 to 2694 Ma

HYRY DIKES 2694 2.2 Ma
Robert and Brown, 1986; Morasse and Wasteneys,1994)

Wang et al., 1991)

ND "PINK PORPHYRY DIKES"
nsfaçon, 1987; Sansfaçon and Hubert, 1990)

94 ; Morasse et al., 1995)

Ma

but pre-S_2
on, 1987; Sansfaçon and Hubert, 1990)

Bills and Mason, 1995)

2693 TO 2671 Ma

2683 Ma

t, 1995)

2677 (?) TO 2645 Ma

1994 – Corfu et al., 1991 – Feng and Kerrich, 1991)

2665 ± 4 Ma
3 Ma
1994)

2632 Ma

Ma

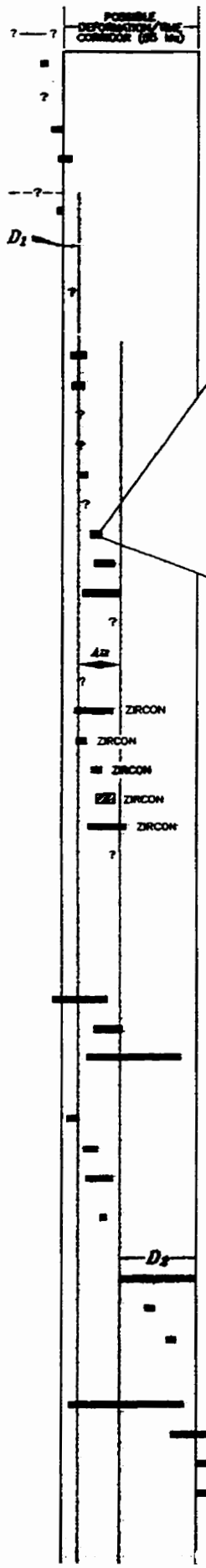

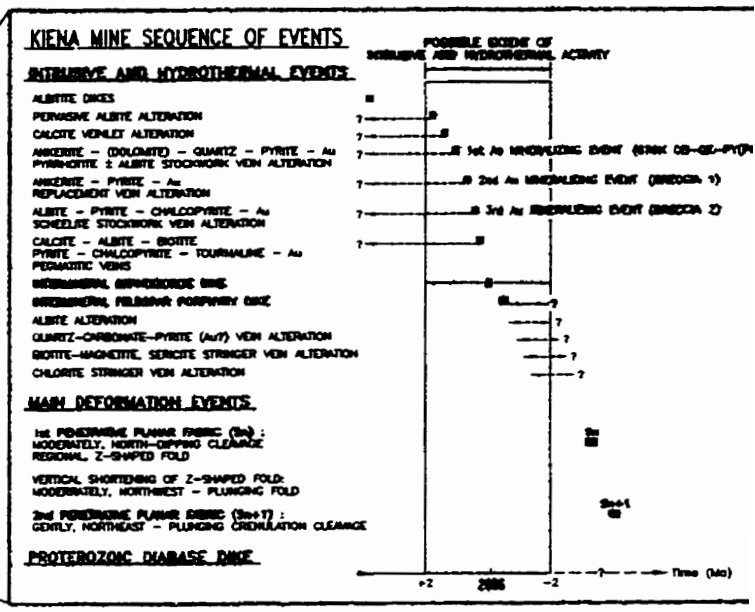

ISOTOPIC DISTURBANCE :

AGES REFLECTING DECREASING CLOSURE TEMPERATURES OF MINERALS FOLLOWING MULTIPLE, POST-METAMORPHIC, HYDROTHERMAL EVENTS. (?)

THERMAL RESETTING RELATED TO EMPLACEMENT OF S-TYPE GRANITES BETWEEN 2663 – 2611 Ma (?) (FENG AND KERRICH, 1991)

E OF EVENTS

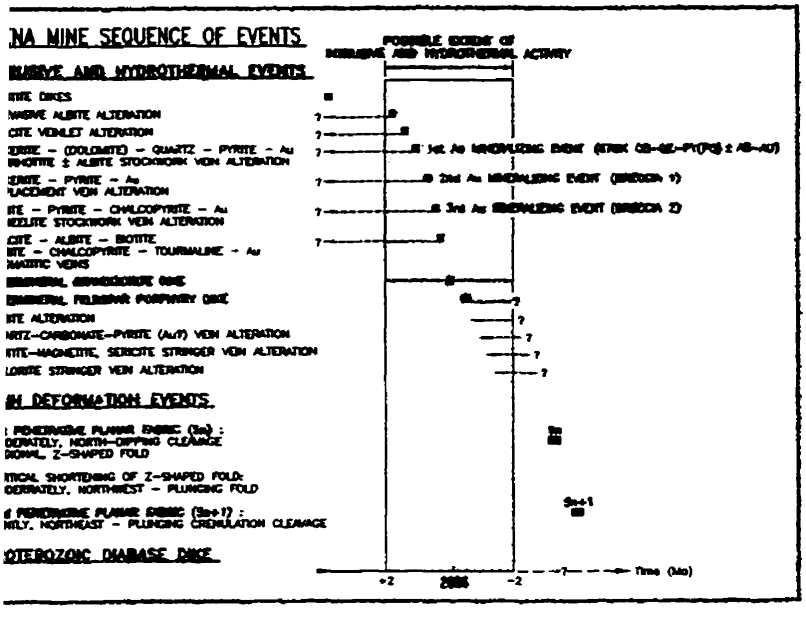

E

BIOTITE + RUTILE + MUSCOVITE

ISOTOPIC DISTURBANCE :

AGES REFLECTING DECREASING CLOSURE TEMPERATURES OF MINERALS FOLLOWING MULTIPLE, POST–METAMORPHIC, HYDROTHERMAL EVENTS. (?)

THERMAL RESETTING RELATED TO EMPLACEMENT OF S–TYPE GRANITES BETWEEN 2643 – 2611 Ma (?) (FENG AND KERRICH, 1991)

South Shears)

K–MICA+BIOTITE

RESETTING OF KIENA DEPOSIT

("C" PORPHYRY) (Wong et al., 1991)

BLAKE RIVER GROUP – 2701 ± 2 TO 2698 ± 1 Ma
(Mortensen, 1987 – Corfu et al., 1989)

CADILLAC FAULT ZONE (Dimroth et al., 1982)

BOURLAMAQUE DIORITE – TRONDHJEMITE SILL COMPLEX – 2688.8 ±1Ma
(Campiglio and Darling, 1976 ; Wong et al., 1991)

D_2 REGIONAL DEFORMATION AND TILTING OF VOLCANIC STRATA – 2700 to 2694 Ma

FIRST INTRUSIONS EMPLACED AFTER THE TILTING OF VOLCANIC STRATA – SIGMA MINE FELDSPAR PORPHYRY DIKES 2684 2.2 Ma
(Daigneault et al., 1983; Robert and Brown, 1986; Morasse and Wasteneys, 1994)

KIENA MINE FAULT ZONE

POST-D_2 PLUTONIC EVENTS – 2694 (?) to 2680 Ma

SNOWSHOE GRANODIORITE – 2694 ± 3 Ma
(Morasse et al., 1993; Morasse et al. 1995)

SIGMA–LAMAQUE No. 2 FELDSPAR PORPHYRY DIKE SWARM ("G" DIKES) – 2694 ± 2.2 Ma
(Daigneault et al., 1983 – Wong et al., 1991)

MALARTIC GOLDFIELDS–BARNAT–EAST MALARTIC–CANADIAN MALARTIC–SLADEN MINES "DIORITE", "GREY" AND "PINK PORPHYRY DIKES"
(Sansfaçon et al., 1987; Trudel and Sansfaçon, 1987; Sansfaçon and Hubert, 1990)

NORLARTIC MINE "MICRODIORITE" DIKE – KIENA MINE ALBITITE DIKES (?)
(Sauvé et al., 1993 – Pilote et al., 1993 – Morasse et al., 1993)

NORLARTIC MINE TONALITE – 2692 ±2 Ma
(Pilote et al., 1993)

LAMAQUE No. 2 QUARTZ–FELDSPAR PORPHYRY DIKES – Post–feldspar porphyry dikes but pre–F_2 (?)
(Daigneault et al., 1983)

KIENA MINE INTERMEDIAL GRANODIORITE DIKE – 2688 ± 2 Ma
(Morasse et al., 1993 ; Mordasse and Wasteneys, 1994 ; Morasse et al., 1995)

LAMAQUE MINE DIORITE–TONALITE – 2685 ±3 Ma
(Jemielita et al., 1989)

CAMFLO MINE MONZONITE – 2685 ±? to 2683 ± 3 Ma
(Zweng and Mortensen 1989–Jemielita et al., 1990)

CAMFLO MINE APLITE DIKE SWARM – Post–monzonite stock and pre–ore
(Zweng, 1994)

POST-D_2 GOLD MINERALIZATION EVENTS – 2694 to 2677 (?) Ma

MALARTIC GOLDFIELDS–BARNAT–EAST MALARTIC–CANADIAN MARLARTIC–SLADEN MINES – Post–F_2 S_1 but pre–F_2 S_2
(Sansfaçon et al., 1987; Trudel and Sansfaçon, 1987; Sansfaçon and Hubert, 1990)

BRAS D'OR MINE – 2693 ± 2 Ma and 2688 ± 7 Ma
(Kerrich and Kyser, 1994)

NORLARTIC MINE – > 2692 ± 2 Ma
(Pilote et al., 1993)

KIENA MINE – > 2688 ± 2 Ma – Post–F_1 S_1 but pre–F_2 S_2
(Morasse et al., 1993 ; Morasse and Wasteneys, 1994 ; Morasse et al., 1995)

LAMAQUE MINE – < 2685 ±3 Ma ; Post–F_1 but pre–F_2 S_2 (this study)
(Karvinen, 1985; Jemielita et al., 1989)

SIGMA MINE – 2682 ± 6 Ma – Post–F_1 but pre–D_2 S_2 (this study)
(Claoué–Long et al., 1990 ; 1992)

CAMFLO, ORION, GOLDEX, SISCOE MINES – Post F_1 but pre– F_2 S_2 (this study)
(Trudel and Sauvé, 1992; Trudeau and Raymond, 1992; Stills and Mason, 1995)

CAMFLO MINE – 2625 ± 6 to 2615 ± 10 Ma
(Jemielita et al., 1989 – Zweng, 1990, 1993)

SIGMA MINE – 2608 ± 20 to 2578 ± 3 Ma
(Anglin, 1990 – Hanes et al., 1989)

LAMAQUE MINE – 2587 ± 7 Ma
(Jemielita et al., 1989)

REGIONAL THERMAL METAMORPHISM RELATED TO POST-D_2 PLUTONISM (?) – 2693 TO 2671 Ma

CORE OF AMPHIBOLE SIGMA MINE "C" PORPHYRY – 2693 ±11 Ma
(Hanes et al., 1989 ; 1992)

RUTILE COLOMBIERE RHYOLITE – 2684 ± 7 Ma
(Wong et al., 1991)

RIM OF AMPHIBOLE SIGMA MINE "C" PORPHYRY – 2671 ± 17 Ma
(Hanes et al., 1989 ; 1992)

POST-D_2 LOCAL UPLIFT AND SEDIMENTATION EVENTS? – <2695 TO 2683 Ma

LAC CASTE FORMATION – <2695 Ma – ?
(Feng and Kerrich, 1991)

CADILLAC GROUP WACKES – <2688 ± 3 Ma – ?
(Davis, 1991)

KEWAGAMA GROUP WACKES – <2687 ± 3 Ma to 2682 ± 3 Ma ; >2683 ± 3 Ma
(Davis, 1991 – Mortensen, 1993 – Jemielita, 1990)

POST-D_2 PONTIAC GROUP SEDIMENTATION EVENT – <2683 Ma

(Mortensen and Card, 1993)

D_3 REGIONAL PENETRATIVE DEFORMATION AND METAMORPHISM – 2677 (?) TO 2645 Ma

COEVAL DEVELOPMENT OF PENETRATIVE TECTONIC FABRIC AND METAMORPHISM – 2677 (?) – 2648 Ma
(Powell et al., 1993; 1994 – Corfu et al., 1991 – Feng and Kerrich, 1991)

PEAK METAMORPHISM ALONG LARDER LAKE – CADILLAC DEFORMATION ZONE, KIRKLAND LAKE AREA – 2685 ± 4 Ma
(Wilkinson et al., 1994)

PEAK METAMORPHISM CLERICY SYENITE (PORCUPINE–DESTOR AND PARFOURU FAULTS AREA) – 2657 ± 3 Ma
(Powell, 1994)

LATE– TO POST-D_3 PLUTONIC EVENTS – 2675, and 2645 TO 2632 Ma

LACORNE BATHOLITH MONZO–DIORITE – GRANODIORITE – 2675 ± 24
(Feng and Kerrich, 1991)

S–TYPE GRANITES IN SOUTHERN ABITIBI BELT – 2663 TO 2611 Ma
(Feng and Kerrich, 1991)

S–TYPE GRANITE IN PREISSAC–LACORNE BATHOLITH – 2643 ± 4 Ma
(Feng and Kerrich, 1991)

S–TYPE GRANITES PONTIAC SUBPROVINCE – 2645 TO 2632 ± 3 Ma
(Feng and Kerrich, 1991 – Machado et al., 1991)

CAMFLO DEPOSIT K–MICA AND BIOTITE COOLING AGES – 2660 ± 7 TO 2602 Ma

(Zweng, 1991)

KIENA DEPOSIT VEIN BIOTITE – 2313 ± 14.9 Ma

(McBride, Queen's University, 1992)

NE PREISSAC DIABASE DIKE SWARM – 2150 ± 25 Ma
(Hanes and York, 1987)

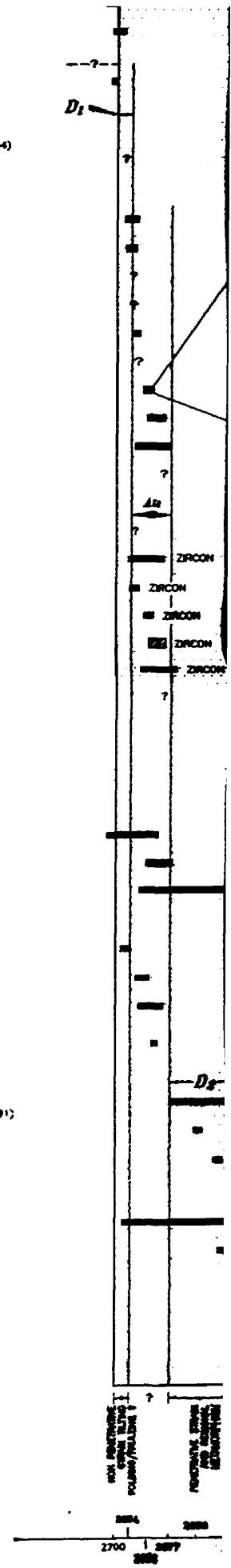

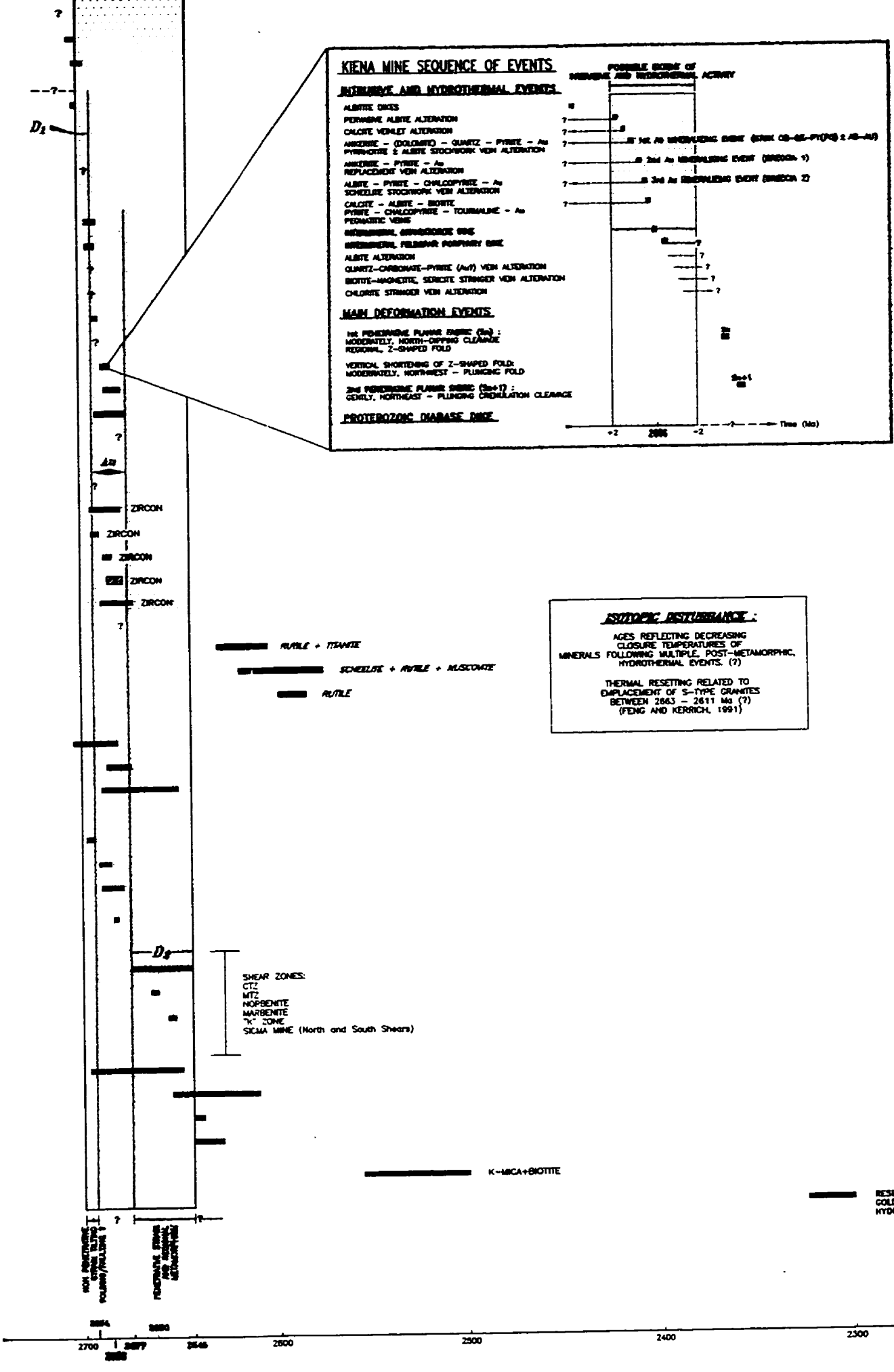
KIENA MINE SEQUENCE OF EVENTS
INTRUSIVE AND HYDROTHERMAL EVENTS
ALBITITE DIKES
PERVASIVE ALBITE ALTERATION
CALCITE VEINLET ALTERATION
ANKERITE – (DOLOMITE) – QUARTZ – PYRITE – Au PYRRHOTITE ± ALBITE STOCKWORK VEIN ALTERATION
ANKERITE – PYRITE – Au REPLACEMENT VEIN ALTERATION
ALBITE – PYRITE – CHALCOPYRITE – Au SCHEELITE STOCKWORK VEIN ALTERATION
CALCITE – ALBITE – BIOTITE PYRITE – CHALCOPYRITE – TOURMALINE – Au PEGMATITIC VEINS
ALBITE ALTERATION
QUARTZ–CARBONATE–PYRITE (Au?) VEIN ALTERATION
BIOTITE–MAGNETITE, SERICITE STRINGER VEIN ALTERATION
CHLORITE STRINGER VEIN ALTERATION
MAIN DEFORMATION EVENTS
PROTEROZOIC DIABASE DIKE
Time (Ma)
ZIRCON
ZIRCON
ZIRCON
ZIRCON
ZIRCON
RUTILE + TITANITE
SCHEELITE + RUTILE + MUSCOVITE
RUTILE
ISOTOPIC DISTURBANCE :
AGES REFLECTING DECREASING CLOSURE TEMPERATURES OF MINERALS FOLLOWING MULTIPLE, POST-METAMORPHIC, HYDROTHERMAL EVENTS. (?)
THERMAL RESETTING RELATED TO EMPLACEMENT OF S-TYPE GRANITES BETWEEN 2663 – 2611 Ma (?) (FENG AND KERRICH, 1991)
SHEAR ZONES:
CT1
MT2
NOPBENITE
MARBENITE
"K" ZONE
SICMA MINE (North and South Shears)
K-MICA+BIOTITE
2700
2600
2500
2400
2300

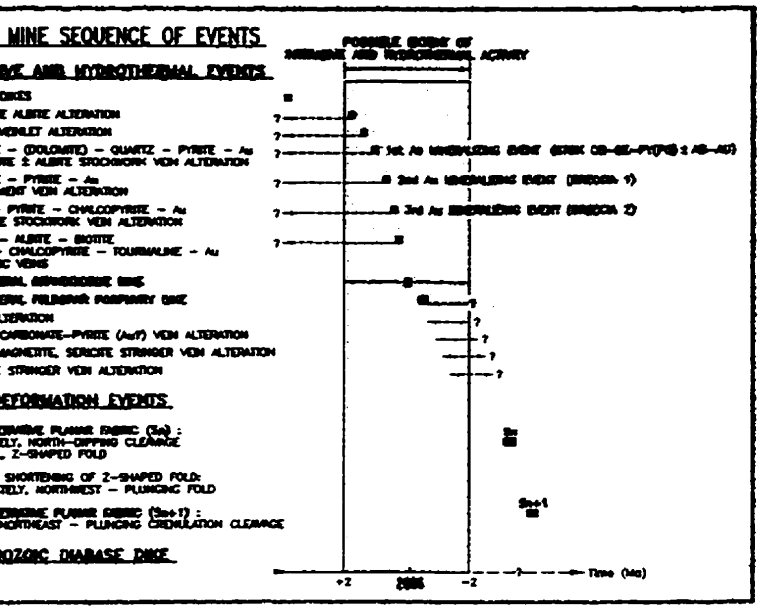

+ RUTILE + MUSCOVITE

ISOTOPIC DISTURBANCE :

AGES REFLECTING DECREASING CLOSURE TEMPERATURES OF MINERALS FOLLOWING MULTIPLE, POST–METAMORPHIC, HYDROTHERMAL EVENTS. (?)

THERMAL RESETTING RELATED TO EMPLACEMENT OF S–TYPE GRANITES BETWEEN 2643 – 2611 Ma (?) (FENG AND KERRICH, 1991)

hears)

K–MICA+BIOTITE

RESETTING OF KIDENA DEPOSIT GOLD–RELATED HYDROTHERMAL BIOTITE

2500 2400 2300 2200 2100 Time (Ma)

S. Morasse, 1997

SIGMA MINE SUB-VOLCANIC PORPHYRITIC DIORITE – 2703.7 ± 2.5 Ma
("C" PORPHYRY) (Wong et al., 1991)

BLAKE RIVER GROUP – 2701 ± 2 TO 2698 ± 1 Ma
(Mortensen, 1987 – Corfu et al., 1989)

CADILLAC FAULT ZONE (Dimroth et al., 1982)

BOURLAMAQUE DIORITE – TRONDHJEMITE SILL COMPLEX – 2688.8 ±1Ma
(Campiglio and Darling, 1976 ; Wang et al., 1991)

D_1 REGIONAL DEFORMATION AND TILTING OF VOLCANIC STRATA – 2700 to 2694 Ma

FIRST INTRUSIONS EMPLACED AFTER THE TILTING OF VOLCANIC STRATA – SIGMA MINE FELDSPAR PORPHYRY DIKES 2694 2.2 Ma
(Daigneault et al., 1983; Robert and Brown, 1986; Morasse

KIENA MINE FAULT ZONE

POST-D_1 PLUTONIC EVENTS – 2694 (?) to 2680 Ma

SNOWSHOE GRANODIORITE – 2694 ± 3 Ma
(Morasse et al., 1993; Morasse et al. 1995)

SIGMA–LAMAQUE No. 2 FELDSPAR PORPHYRY DIKE SWARM ("G" DIKES) – 2694 ± 2.2 Ma
(Daigneault et al., 1983 – Wang et al., 1991)

MALARTIC GOLDFIELDS–BARNAT–EAST MALARTIC–CANADIAN MALARTIC–SLADEN MINES "DIORITE", "GREY" AND "PINK PORPHYRY DIKES"
(Sansfaçon et al., 1987; Trudel and Sansfaçon, 1987; Sansfaçon and H

NORLARTIC MINE "MICRODIORITE" DIKE – KIENA MINE ALBITITE DIKES (?)
(Sauvé et al., 1993 – Pilote et al., 1993 – Morasse et al., 1993)

NORLARTIC MINE TONALITE – 2692 ±2 Ma
(Pilote et al., 1993)

LAMAQUE No. 2 QUARTZ–FELDSPAR PORPHYRY DIKES – Post–feldspar porphyry dikes but pre–F_2 (?)
(Daigneault et al., 1983)

KIENA MINE INTERMINERAL GRANODIORITE DIKE – 2686 ± 2 Ma
(Morasse et al., 1993 ; Morasse and Wasteneys, 1994 ; Morasse et al., 1995)

LAMAQUE MINE DIORITE–TONALITE – 2685 ±3 Ma
(Jemielita et al,. 1989)

CAMFLO MINE MONZONITE – 2685 $\pm^{7}_{6}$ to 2683 ± 3 Ma
(Zweng and Mortensen 1989–Jemielita et al., 1990)

CAMFLO MINE APLITE DIKE SWARM – Post–monzonite stock and pre–ore
(Zweng, 1994)

POST-D_1 GOLD MINERALIZATION EVENTS – 2694 to 2677 (?) Ma

MALARTIC GOLDFIELDS–BARNAT–EAST MALARTIC–CANADIAN MARLARTIC–SLADEN MINES – Post–F_1 S_1 but pre–F_2 S_2
(Sansfaçon et al., 1987; Trudel and Sansfaçon, 1987; Sansfaçon and Hubert

BRAS D'OR MINE – 2693 ± 2 Ma and 2688 ± 7 Ma
(Kerrich and Kyser, 1994)

NORLARTIC MINE – > 2692 ± 2 Ma
(Pilote et al., 1993)

KIENA MINE – > 2686 ± 2 Ma – Post–F_1 S_1 but pre–F_2 S_2
(Morasse et al., 1993 ; Morasse and Wasteneys, 1994 ; Morasse et al., 1995)

LAMAQUE MINE – < 2685 ±3 Ma ; Post–F_1 but pre–F_2 S_2 (this study)
(Karvinen, 1985; Jemielita et al., 1989)

SIGMA MINE – 2682 ± 8 Ma – Post–F_1 but pre–D_2 S_2 (this study)
(Claoué–Long et al., 1990 ; 1992)

CAMFLO, ORION, GOLDEX, SISCOE MINES – Post F_1 but pre– F_2 S_2 (this study)
(Trudel and Sauvé, 1992; Trudeau and Raymond, 1992; Stills and Mason, 1995)

CAMFLO MINE – 2625 ± 8 to 2615 ± 10 Ma
(Jemielita et al., 1989 – Zweng, 1990, 1993)

SIGMA MINE – 2602 ± 20 to 2579 ± 3 Ma
(Angéli, 1990 – Hanes et al., 1989)

LAMAQUE MINE – 2593 ± 7 Ma
(Jemielita et al., 1989)

REGIONAL THERMAL METAMORPHISM RELATED TO POST-D_1 PLUTONISM (?) – 2693 TO 2671

CORE OF AMPHIBOLE SIGMA MINE "C" PORPHYRY – 2693 ± 11 Ma
(Hanes et al., 1989 ; 1992)

RUTILE COLOMBIERE RHYOLITE – 2684 ± 7 Ma
(Wong et al., 1991)

RIM OF AMPHIBOLE SIGMA MINE "C" PORPHYRY – 2671 ± 17 Ma
(Hanes et al., 1989 ; 1992)

POST-D_1 LOCAL UPLIFT AND SEDIMENTATION EVENTS – <2695 TO 2683 Ma

LAC CASTE FORMATION – <2695 Ma – ?
(Feng and Kerrich, 1991)

CADILLAC GROUP WACKES – <2688 ± 3 Ma – ?
(Davis, 1991)

KEWAGAMA GROUP WACKES – <2687 ± 3 Ma to 2682 ± 3 Ma ; >2683 ± 3 Ma
(Davis, 1991 – Mortensen, 1993 – Jemielita, 1990)

POST-D_1 PONTIAC GROUP SEDIMENTATION EVENT – <2683 Ma
(Mortensen and Card, 1993)

D_2 REGIONAL PENETRATIVE DEFORMATION AND METAMORPHISM – 2677 (?) TO 264

COEVAL DEVELOPMENT OF PENETRATIVE TECTONIC FABRIC AND METAMORPHISM – 2677 (?) – 2645 Ma
(Powell et al., 1993; 1994 – Corfu et al., 1991 – I

PEAK METAMORPHISM ALONG LARDER LAKE – CADILLAC DEFORMATION ZONE, KIRKLAND LAKE AREA – 2665 ± 4 Ma
(Mortensen et al., 1993)

PEAK METAMORPHISM CLERICY SYENITE (PORCUPINE–DESTOR AND PARFOURU FAULTS AREA) – 2657 ± 3 Ma
(Powell, 1994)

LATE- TO POST-D_2 PLUTONIC EVENTS – 2675, and 2645 TO 2632 Ma

LACORNE BATHOLITH MONZO–DIORITE – GRANODIORITE – 2675 ± 24
(Feng and Kerrich, 1991)

S–TYPE GRANITES IN SOUTHERN ABITIBI BELT – 2663 TO 2611 Ma
(Feng and Kerrich, 1991)

S–TYPE GRANITE IN PREISSAC–LACORNE BATHOLITH – 2643 ± 4 Ma
(Feng and Kerrich, 1991)

S–TYPE GRANITES PONTIAC SUBPROVINCE – 2645 TO 2632 ± 3 Ma
(Feng and Kerrich, 1991 – Machado et al., 1991)

CAMFLO DEPOSIT K–MICA AND BIOTITE COOLING AGES – 2660 ± 7 TO 2602 Ma
(Zweng, 1991)

KIENA DEPOSIT VEIN BIOTITE – 2313 ± 14.9 Ma
(McBride, Queen's University, 1992)

14000 N

13000 N

KIENA MINE PROPERTY

LEGEND


S-86
S-83
S-64
S-99
S-79
S-55
S-70
S-75
OVB
17 LEVEL
Pyroxenite 2
0.14S/1.9'
0.14/3.1'
0.11S/8.0'